Investigations into aquatic pheromones *and* the palladised iron transformations of halo-organics

Thesis submitted for the degree of Doctor of Philosophy

Susan M. Godwin
School of Chemistry
Cardiff University
2004

ProQuest LLC
789 East Eisenhower Parkway
P.O. Box 1346
Ann Arbor, MI 48106-1346

Summary

The first three chapters investigate the identification of spawning readiness pheromones used by two species of fish, rainbow trout and roach. Tissue samples from rainbow trout were extracted using both solvents and solid phase techniques and analysed by GC-MS, with mainly fatty acids and related compounds identified. Urine samples from rainbow trout were also extracted and analysed by GC-MS and NMR to identify potential pheromones, and a tentative identification of free testosterone and conjugated androgens from female trout urine is made. Egg and milt samples from a second species, roach, were collected during spawning, extracted and analysed using the same techniques, and a prostaglandin pheromone which is released with the eggs is suggested.

The next three chapters investigate the identification of a larval hatching pheromone in the mud crab, *Rhithropanopeus harrisii* (Gould). Animals were collected from Cardiff Docks and a breeding colony established. Samples of hatch water were analysed by ultrafiltration, HPLC and bioassay to give active fractions which were subject to electrospray mass spectrometry to yield molecular masses. A tripeptide with the composition, Tyr/Met/Arg is suggested as the candidate.

The last three chapters describe the study of the degradation characteristics of halogenated organic compounds in aqueous solution with palladium doped onto an iron surface. Degradation rate constants were determined for a number of halo- compounds. Investigations with radical clock compounds exclude a radical intermediate with a half life $>1.8 \times 10^{-6}$ sec. Two novel bromo- compounds, *trans*-1-bromo-2-(*n*-hexyloxy)-cyclohexane and *trans*-1-bromo-2-(*n*-octyloxy)cyclopentane were synthesised to give mechanistic information akin to that from radical clocks. We term these new compounds "anion clocks" and their reactions, octanol production faster than hexanol production and both alcohols rate of formation significantly faster than the rates of formation of the hexyloxycyclohexane and octyloxycyclopentane, suggest a short lived anionic intermediate. Finally, a "dual" clock compound is proposed which could give up to three products depending on whether the intermediate is a short lived radical, a long lived radical or an anion.

Acknowledgments

My thanks must first go to my supervisor, Dr David Kelly for all his help and guidance, especially late into the evening with mass spectra spread all over the desk. I would also like to thank my employer, Bristol Water Plc and especially my Laboratory Manager, Dr. Michael Brighton, for all his enthusiasm and encouragement, without which none of this would have been possible. I am also deeply indebted to all my colleagues at work whose support kept me going, and yes, Scott, I am still blaming you.

I would like to thank my parents, Pauline and David, for their patience when I turned their house into a study, and am grateful to my Mum for the best definition of pheromones yet - fairy phones.

Finally, the biggest acknowledgment has to go to my husband, Oisin Clancy, who was ever patient and tolerated all the late nights, piles of files and moments of despair with quiet stoicism and always seemed to know when a glass of something alcoholic was needed. Thank you.

Oisin and Aidan, this is for you.

Table of Contents

Chapter 1, Fish Pheromones 1
1.0 Introduction 1
1.1 Definitions 1
1.2 Chemical cues in an aqueous environment 5
1.2.1 The fright reaction 5
1.3. How do fish detect pheromones? 6
1.3.1 Structure of the olfactory organ in teleost fish 6
1.3.2. Structure and mechanism of gustation in teleost fish 6
1.3.3 Olfaction versus gustation for pheromone detection 7
1.4. Pheromones in reproduction 7
1.4.1. Endocrine changes and pheromone release in goldfish 8
1.4.2 African Catfish sex pheromones 11
1.4.3 Sex pheromones in salmonids and trout 12
1.4.4 Other fish pheromones 14
1.5 Methods of analysis 15

Chapter 2, Fish Experimental Section 16
2.1 Instrumentation 16
2.1.1 Gas chromatography-mass spectrometry 16
2.1.2 High performance liquid chromatography 17
2.1.3 Standard methods 17
2.2 Analysis of standards 17
2.2.1 GC-MS retention time standards 18
2.2.2 Preparation of fatty acid standard 19
2.2.3 Calibration curve for GC-MS response to testosterone 26 21
2.3 Solid phase extraction of testosterone 26 22
2.3.1 Extraction procedure 1, based on Schoonen and Lambert[71] 22
2.3.2 Extraction procedure 2 23
2.4 Steroid standards 23
2.4.1 Kovats Indices determination 23
2.4.2 Derivatisation of steroid standards 24
2.4.3 Solid phase extraction of steroid mixes 25

2.5 Fishery samples 26
2.5.1 Extraction of spiked fishery samples 26
2.5.2 Extraction of fish holding tanks at Blagdon site 27
2.6 Extraction of rainbow trout tissue 28
2.6.1 Extraction of set 1 28
2.6.2 Extraction of set 2 29
2.6.3 Re-analysis of some of the skin scrape and extracted skin samples 30
2.7 Repeat of fish extraction 32
2.7.1 Neutral tissue extraction 32
2.7.2 Acidification of dichloromethane extracts from section 2.7.1 35
2.7.3 Basification of dichloromethane fish extract samples from section 2.7.1 37
2.7.4 Bicarbonate treatment of dichloromethane fish extract samples from section 2.7.1 39
2.8 Trout urine 43
2.8.1 Direct injection of trout urine 43
2.8.2 Dichloromethane extractions of trout urine 43
2.8.3 NMR analysis of freeze-dried urine 45
2.8.4 HPLC of trout urine 45
2.8.5 Solvent extract and deconjugation of female trout urine 46
2.8.6 Electrospray analysis of female trout urine 48
2.9 Roach samples 49
2.9.1 Extraction of roach samples 49
2.9.2 Derivatisation of roach samples 50
2.9.3 Deconjugation and derivatisation of roach samples 54
2.9.4 Solid phase extraction and derivatisation of roach samples 56

Chapter 3, Fish Discussion 60
3.1 Introduction 60
3.2 Analysis of standards 60
3.2.1 Kovats Indices standards 60
3.2.2 Testosterone 26 calibration curve 60
3.3 Solid phase extraction 60

3.4 Steroid Standards 61
3.5 Fishery samples 62
3.5.1 Extraction of raw water samples 62
3.5.2 Extraction of fish holding tanks at Blagdon site 62
3.6 Extraction of rainbow trout tissue 63
3.6.2 Re-analysis of the skin scrape and extracted skin samples 67
3.7 Repeat of fish extraction 68
3.7.1 Standard tissue extraction 68
3.7.2 Acidification of dichloromethane extracts 70
3.7.3 Alkali treatment of fish extract samples 71
3.7.4 Bicarbonate treatment of fish extract samples 72
3.8 Trout urine 73
3.8.1 Direct injection of trout urine 73
3.8.2 Dichloromethane extractions of trout urine 74
3.8.3 NMR analysis of freeze-dried urine 74
3.8.4 HPLC of trout urine 75
3.8.5 Solvent extract and deconjugation of female trout urine 75
3.8.6 Electrospray analysis of female trout urine 77
3.9 Roach samples 77
3.9.1 Extraction of roach samples 78
3.9.2 Derivatisation of roach samples 79
3.9.3 Deconjugation and derivatisation of roach samples 80
3.9.4 Solid phase extraction and derivatisation of roach samples 81
3.10 Conclusions 82

Chapter 4, *Rhithropanopeus harrisii* Hatching Pheromone 83
4.1 Distribution 83
4.2 Breeding cycle 84
4.3 Larval release 84
4. 4 Larval development and distribution 85
4.5 Synchronised swimming? 86
4.6 Peptide mediated marine behaviour 89
4.7 Characterisation of the hatching pheromone 91
4.8 Aims of this project 94

Chapter 5, *Rhithropanopeus harrissi* Hatching Pheromone - Experimental Work 95
5.1 Introduction 95
5.2 Collection of the animals 95
5.3 Collection and storage of the hatch water 96
5.4 Standard methods 97
5.4.1 HPLC Analysis of peptide standards 97
5.5 Analysis of the first hatch water sample 98
5.5.1 Ultrafiltration of the hatch water sample 98
5.5.2 HPLC analysis of the filtered samples 99
5.5.3 Bioassay of 1000 - 500 D fraction 99
5.5.4 Ultrafiltration of hatch water - a repeat experiment 99
5.6 Stability of sample to freeze-drying 100
5.7 Analysis of crab holding water 100
5.8 Direct analysis of hatch water 101
5.9 Analysis of samples from 10-11/10/97 101
5.9.1 Samples from 10/10/97 101
5.9.2 Stability of frozen samples 102
5.9.3 Ultrafiltration of hatch water samples 103
5.9.4 Fractionation of sample on HPLC 104
5.9.5 Electrospray analysis of fractions 104
5.10 Holding water samples - a rerun 105
5.11 Bioassay of previous fractions 106

Chapter 6, *Rhithropanopeus harrissi* Hatching Pheromone -- Discussion and Conclusions 107
6.1 Introduction 107
6.2 Animal stocks 107
6.2.1 Collection 107
6.2.2. Maintenance and Colony Establishment 107
6.3 Collection and storage of the hatch water 108
6.4 HPLC Analysis of peptide standards 109
6.5 Analysis of the first hatch water sample 109
6.5.1 Ultra-filtration of the hatch water sample 109

6.5.2 HPLC analysis of the filtered samples 111
6.5.3 Bioassay of the 1000 - 500 D fraction 113
6.5.4 Repeat analysis of the first hatch water sample - Filtration and HPLC 114
6.6 Determination of effect on activity by freeze-drying 115
6.7 Analysis of crab holding water 115
6.8 Direct analysis of hatch water 116
6.9 Analysis of samples from 10-11/10/97 118
6.9.1 Samples from 10/10/97 118
6.9.2 Stability of frozen samples 120
6.9.3 Size filtration and HPLC analysis of freeze-dried hatch water samples 121
6.9.4 Fractionation of the sample on HPLC 125
6.9.5 Electrospray analysis of fractions 125
6.10 Holding water samples - a rerun 127
6.11 Bioassay of fractions collected from Section 5.9.3 128
6.12 Conclusions 128

Chapter 7, Halo-compound Degradation on Iron and Palladium/Iron Surfaces 131
7.0 Introduction 131
7.1 Metals and VOCs. 132
7.1.1 Zero-valent metals 132
7.1.2 Iron compounds 132
7.1.3 Bacteria and microflora 133
7.2 Compound rates and fates 136
7.2.1 Zero valent iron and reaction mechanisms 136
7.2.2 Palladised iron 139
7.2.3 Surface effects 140
7.2.4 Effect of solvent on degradation rates 141

Chapter 8, Halo-compound Degradation on Iron and Palladium/Iron Surfaces, Experimental Work 143
8.0 Introduction 143
8.1 Instrumentation 145

8.1.1 Gas Chromatography-Mass Spectrometry 145
8.1.2 General methods & Abbreviations 146
8.1.3 Preparation of iron reagents 148
8.1.4 Analysis of chlorine isotope data 149
8.2 Experimental details 150
Degradation of $CHCl_3$ on activated iron and Pd/Fe (Expt. 1 & 2) 150
Comparison of the rate of degradation of $CHCl_3$ on activated iron and Pd/Fe in aqueous sodium carbonate (Expt. 3) 151
Degradation of $CDCl_3$ on Pd/Fe (Expt. 4) 151
Degradation of $CHCl_3$ in D_2O on Pd/Fe in the presence of chromatography glass beads (Expt. 5) 151
Determination of the products of degradation of $CDCl_3$ in water and $CHCl_3$ in D_2O with palladised iron (Expt. 6) 152
Determination of the degradation products of a $CDCl_3$ and $CHCl_3$ mixture with Pd/Fe in water and D_2O (Expt. 7) 153
Determination of the degradation products of $CDCl_3$ with Pd/Fe in water (Expt. 8) 153
Determination of the products of $CHCl_3$ incubated with D_2O and Pd/Fe in the presence of glass chromatography beads (Expt. 9) 154
Incubation of $CDCl_3$ with glass chromatography beads in water (Expt. 10) 155
Measurement of the pH of chromatography glass beads in water (Expt. 11) 155
Determination of the carbon content of iron filings by dissolution in 6 M HCl (Expt. 13) 156
Comparison of the reaction rates and products of $CHCl_3$ and $CDCl_3$ in D_2O and water respectively (Expt. 14) 156
Comparison of reaction rates for differing initial concentrations of $CHCl_3$ (Expt. 15) 156
Determination of the rate of degradation of $CDCl_3$ in D_2O by Pd/Fe (Expt. 16) 157
Confirmation of the reaction rate for $CDCl_3$ in D_2O in the absence of airborne dichloromethane contamination (Expt. 17) 158
Calibration curve using MSD software and cyclohexane as internal standard

(Expt. 19) 160
Quantification of chloroform degradation (Expt. 20) 160
Confirmation of the quantification of the chloroform degradation (Expt. 21) 161
Quantification of dichloromethane degradation (Expt. 22 -24) 161
Comparison of the rate of degradation vials spiked with dichloromethane and chloroform versus vials spiked with chloroform only (Expt. 25) 162
Calibration curve for chloroform and dichloromethane using 1,4-dioxane as internal standard (Expt. 26, 27) 163
Comparison of the rate of degradation of chloroform with 1,4-dioxane as internal and surrogate standard (Expt. 28, 29) 163
Quantification of chloroform degradation and dichloromethane quantification and monitoring of dichloromethane in controls (Expt. 30) 165
Degradation of $CDCl_3$ by Pd/Fe in water (Expt. 31) 165
Degradation of 6-bromohex-1-ene on Pd/Fe (Expt. 32) 167
Degradation of 6-bromohex-1-ene and chloroform in a mixed system on Pd/Fe (Expt. 33) 167
6-bromohex-1-ene and hex-1-ene calibration curve (Expt. 35) 168
Degradation of bromoethyl ethyl ether on a Pd/Fe (Expt. 34) 168
Degradation of bromoethyl ethyl ether on Pd/Fe run on a thick film column (Expt. 36) 169
Bromoethyl ethyl ether, ether and ethanol calibration curve (Expt. 37) . 170
Ethanol calibration curve (Expt. 38) 170
Degradation of bromoethyl ethyl ether on a Pd/Fe (Expt. 39) 171
Methylcyclopentane, cyclohexane and hexene calibration curve in the presence of iron filings (Expt. 40) 171
Methylcyclopentane, cyclohexane and hexene adsorption on Pd/Fe (Expt. 41) 172
Degradation of bromoform on a Pd/Fe (Expt. 42 & 43) 173
Degradation of bromohexane on a Pd/Fe (Expt. 44 & 45) 173
Degradation of *cis*- and *trans*- dichloroethylene on a Pd/Fe (Expt. 46) . 174
Degradation of carbon tetrachloride and tetrachloroethylene on Pd/Fe (Expt. 47) 174

Degradation of carbon tetrachloride on a Pd/Fe, a fast reaction (Expt. 48) 175
Degradation of bromomethylcyclopropane on a Pd/Fe (Expt. 49) 175
Comparison of the activity of freshly prepared and aged Pd/Fe (Expt. 50) 176
Comparison of the activity of normal and hyper-Pd/Fe (Expt. 51) 176
Comparison of the activity of Pd/Fe and activated iron (Expt. 52) 177
Degradation of (2-bromoethyl)benzene aqueous THF (Expt. 54) 178
Degradation of (2-bromoethyl)benzene in various concentrations of THF (Expt. 55) 178
Degradation of (2-bromoethyl)benzene in 25 % THF solution (Expt. 56) 179
Degradation of (2-bromoethyl)benzene in 10 % methanol solution (Expt. 57) 180
Degradation of (2-bromoethyl)benzene in various concentrations of methanol (Expt. 58) 180
Degradation of 10, 100, 500 fold increase in (2-bromoethyl)benzene (Expt. 59) 181
Comparison of the degradation of benzyl bromide on palladised and activated iron in methanol (Expt. 60) 183
Degradation of bromophenetole (Expt. 61) 184
Preparative scale degradation of benzyl bromide in methanol (Expt. 62) 184
Preparative degradation of benzyl bromide, tentative conditions (Expt. 63) 185
Large scale degradation of benzyl bromide in methanol and THF with use of a sonic bath (Expt. 64) 186
Phenol, ethoxybenzene and bromoethoxybenzene calibration (Expt. 65) 187
Quantification of bromophenetole degradation (Expt. 66) 188
Degradation of benzyl bromide in D_2O (Expt. 67) 188
Degradation of benzyl bromide in the presence of CD_3OD (Expt. 68) .. 189
Degradation of benzyl bromoethyl ether (Expt. 69) 191
Degradation of two anion clocks, benzyl bromoethyl ether and

bromoethoxybenzene (Expt. 70) 192
Degradation of 1-bromo-2-*n*-hexyloxycyclohexane (Expt. 71) 193
Degradation capacity of Pd/Fe with benzyl bromide(Expt.72) 193
Small scale degradation capacity of Pd/Fe, a small scale reaction (Expt.73) 194
Repeated dosing of a small quantity of Pd/Fe with benzyl bromide and fresh solvent (Expt. 74) 195
Incubation of alcohols with Pd/Fe and water (Expt. 75) 196
8.3 Preparation of anion clocks, Introduction 197
Preparation of *trans*-1-bromo-2-(*n*-hexyloxy)cyclohexane 105 (Expt. 76a DRK 832) 198
Preparation of *trans*-1-bromo-2-(*n*-octyloxy)cyclopentane 107 (Expt. 76) 198
Reduction of *trans*-1-bromo-2-(*n*-hexyloxy)cyclohexane 105 to *n*-hexyloxycyclohexane 106 (Expt. 77) 199
Reduction of *trans*-1-bromo-2-*(n*-octyloxy)cyclopentane 107 to octyloxycyclopentane 108(Expt. 78) 200
Degradation of *trans*-1-bromo-2-(*n*-hexyloxy)cyclo-hexane 105 and *trans*-1-bromo-2-*(n*-octyloxy)cyclopentane 107 (Expt. 79) 201
Combined degradation of *trans*-1-bromo-2-(*n*-hexyloxy)-cyclohexane 105 and *trans*-1-bromo-2-(*n*-octyloxy)cyclopentane 107 (Expt. 80) 202
Calibration curve for hexanol, octanol, *trans*-1-bromo-2-(*n*-hexyloxy)-cyclohexane 105, *trans*-1-bromo-2-(*n*-octyloxy)cyclopentane 107, 2-*n*-hexyloxycyclohexane 106 and 2-*n*-octyloxycyclopentane 108 using naphthalene as internal standard (Expt. 81) 203
Degradation of *trans*-1-bromo-2-(*n*-hexyloxy)-cyclohexane 105, and *trans*-1-bromo-2-(*n*-octyloxy)cyclopentane 107 with naphthalene internal standard (Expt. 82) 204
Degradation of *trans*-1-bromo-2-(*n*-hexyloxy)-cyclohexane 105, and *trans*-1-bromo-2-(*n*-octyloxy)cyclopentane 107 with naphthalene internal standard (Expt. 84) 205
Degradation of benzyl bromide on Pd/Fe using hexane as the bulk solvent (Expt. 86) 206

Chapter 9, Halo-compound Degradation on Iron and Palladium/Iron Surfaces, Discussion and Conclusions 208
9.0 Introduction 208
9.1 Degradation of chlorinated compounds 208
9.1.1 Comparison of activated and Pd/Fe and pH on the degradation rate of chloroform. 208
9.1.2 Comparison of the activity of activated iron, palladised iron, aged palladised iron and hyper-palladised iron (Expt. 50, 51, 52) 212
9.1.3 Degradation capacity of palladised iron (Expt. 60, 72-74) 215
9.1.4 Degradation of carbon tetrachloride, tetrachloroethylene and *cis*- and *trans*- dichloroethylene on palladised iron (Expt. 46-48). 218
9.1.5 Degradation of bromoform on palladised iron (Expt 42,43) 219
9.2 Degradation of deuterated compounds - isotopic composition of products .. 219
9.2.1 Degradation of deuterated chloroform on activated and palladised iron (Expt. 4) 220
9.2.2 Degradation of chloroform in deuterium oxide on a palladised iron in the presence of chromatography glass beads (Expt 5) 221
9.2.3 Chloroform and deuterated chloroform hydrogen exchange with deuterium oxide or water in the presence of glass chromatography beads (Experiment 9, 10) 222
9.2.4 Examination of the effect on the pH water of chromatography glass beads 224
9.2.5 Comparison of the products of degraded deuterated chloroform in water and chloroform in deuterium oxide (Expt 16, 17, 8, 31, 6) 226
9.2.6 Comparison of the degradation rates of chloroform in deuterium oxide and deuterated chloroform in water (Expt, 14, 16, 17, 31, 7) ... 228
9.2.7 Degradation of benzyl bromide in deuterium oxide (Expt. 67,68, 75a) 230
9.3 Factors affecting reaction rates 232
9.3.1 Comparison of reaction rates for differing initial concentrations (Expt 15, 59) 232
9.4 Quantification of reactions, with internal and surrogate standards. 236
9.4.1 Internal standards (Expt. 18) 236
9.4.2 Calibration using MSD software and cyclohexane as internal standard

(Expt. 19) 236
9.4.3 Quantification of the degradation of chloroform with Pd/Fe (Expt. 20, 21) 237
9.4.4 Quantification of dichloromethane degradations (Expt 22, 23, 24) 238
9.4.5 Comparison of the rate of degradation of chloroform in the presence and absence of exogenous dichloromethane (Expt. 25) 239
9.4.6 Comparison of the rate of degradation of chloroform (Expt. 28, 29) with 1,4-dioxane as a surrogate standard (Expt. 26, 27) 240
9.4.7 Quantification of the degradation of chloroform and formation of dichloromethane using dioxane as an internal standard (Expt 30) 242
9.5 Use of solvent 243
9.5.1 Degradation of (2-bromoethyl)benzene in various concentrations of aqueous THF (Expt. 54, 55, 56) 243
9.5.2 Degradation of (2-bromoethyl)benzene in various aqueous methanol concentrations (Expt. 57, 58) 245
9.5.3 Degradation of benzyl bromide in aqueous methanol and THF solutions (Expt. 62, 63, 64) 246
9.6 Radical clocks 248
9.6.2 Degradation of 6-bromohex-1-ene alone and mixed with chloroform on a palladised iron (Expt. 32, 33) 250
9.7 Anion clocks 252
9.7.1 Degradation of bromophenetole, anion clock 1 (Expt. 61, 66) ... 253
9.7.2 Degradation of bromoethyl ethyl ether on palladised iron, anion clock 2 (Expt. 34, 36, 39) 256
9.7.3. Degradation of benzyl 2-bromoethyl ether on palladised iron, anion clock 3 (Expt. 69, 70) 260
9.7.4 *trans*-1-Bromo-2-(*n*-hexyloxy)-cyclohexane 105 and *trans*-1-bromo-2-(*n*-octyloxy)cyclopentane 107, anion clocks 4 and 5 262
9.8 Conclusions 266
9.8.1 The catalytic cycle 266
9.8.2 Future work 267

Abbreviations

Some abbreviations and symbols have been used in this thesis and are listed below:

δ	Chemical shift (NMR)
μ	Micron
μM	Micromolar
μmol	Micromole
11-KT	11-Keto-testosterone
15-kPGF$_{2\alpha}$	15-keto-prostaglandin F$_{2\alpha}$
17α,20β-P	17α,20β-dihydroxy-4-pregnen-3-one
17α,20β,21-P	17α,20β,21-trihydroxy-4-pregnen-3-one
Ala	Alanine
amu	Atomic mass units
APCI	Atomospheric pressure chemical ionisation
app. dt	Apparent doublet of triplets
Arg	Arginine
Asn	Asparagine
Asp	Aspartic acid
AUFS	Absorption units full scale
BnOH	Benzyl alcohol
Br	Bromo
CD_2Cl_2	Di-deuterated dichloromethane
$CDCl_3$	Deuterated chloroform
$CHDCl_2$	Mono- deuterated dichloromethane
CMC	Critical micelle concentration
conc.	Concentration
conv	Conversion
Cys	Cysteine
d	Doublet
D	Daltons
D_2O	Deuterium oxide
DCM	Dichloromethane
dd	doublet of doublets

ddd	Double doublet of doublets
DEFRA	Department for environment, food and rural affairs
EI(+)	Electron impact
EI(+)-MS	Eelctron impact mass spectrometry
EOG	Electro-olfactogram
EPA	Eicosapentaenoic acid
EPA	Environment Protection Agency
eV	Electron volts
FAMEs	Fatty acid methyl esters
For. fit	Forward (library) fit
GC	Gas chromatograph
GC-MS	Gas chromatograph - mass spectrometer
Gln	Glutamine
Gly	Glycine
GtH	Gonadotropin
His	Histidine
HPLC	High performance liquid chromatography
hr	Hours
Hz	Hertz
Ile	Isoleucine
inj.	Injector
J	Coupling constant (NMR)
k_1	Rate constant
KI	Kovats Indices
LC-MS	Liquid chromatograph - mass spectrometer
Leu	Leucine
ln	Natural log
Lys	Lysine
m	multiplet
m/z	Mass to charge ratio
M, M^+	Molecular ion
M	Molar
MAFF	Ministry for agriculture, fisheries and food

MeOH	Methanol
Met	Methionine
min	Minutes
mM	Millimolar
mmol	Millimole
MS	Mass spectrometer
MSD	Mass selective detector
n/m	Not measured
n/c	Not calculated
n/a	Not applicable
n	Nano
n/r	No result
n/i	No library fit, not integrated
n/d	Nil detected
NAD	Nicotinamide adenine dinucleotide
NBS	*N*-Bromosuccinamide
nm	Nanometer
NMR	Nuclear magnetic resonance
P&T	Purge and trap
PCB	Polychlorinated biphenyl
PCE	Perchloroethylene (tetrachloroethene)
Pd/Fe	Palladised iron
PFTBA	Perfluorotributylamine
PG	Prostaglandin
$PG_{2\alpha}$	Prostaglandin 2α
PGF	Prostaglandin F
$PGF_{1\alpha}$	Prostaglandin $F_{1\alpha}$
$PGF_{2\alpha}$	Prostaglandin $F_{2\alpha}$
Ph	Phenyl
Phe	Phenylalanine
Pro	Proline
psi	Pounds per square inch
R^2	Correlation coefficient for line of best fit

Ret. time	Retention time
Rev. fit	Reverse (library) fit
RIA	Radioimmunoassay
s	singlet
s	Second
SDS	Sodium dodecyl sulphate
sec.	Seconds
Ser	Serine
SIC	Single ion chromatogram
SPE	Solid phase extraction
spltls	Splitless
t	triplet
TCE	Trichloroethylene (trichloroethene)
tert	*tertiary*
TFA	Tirfluoroacetic acid
THF	Tetrahydrofuran
TIC	Total ion current
TLC	Thin layer chromatography
TMS	Trimethylsilyl
Trp	Tryptophan
Tyr	Tyrosine
$t_{½}$	Half life
UV	Ultra violet
v/v	Volume for volume
Val	Valine
VOC	Volatile organic compound
Vol.	Volume
w/v	Weight for volume

Chapter 1, Fish Pheromones

1.0 Introduction

1.1 Definitions

Pheromones are used throughout nature, "from microbes to man"[1] to transfer information between members of the same species. The original term for this type of chemical was "ectohormone" as defined by Bethe[2] in 1932, but this is not accurate as "ecto" means "external" and "hormone" with its traditional meaning of "an organic compound secreted by an endocrine (ductless) gland, whose products are released into the circulating fluid"[3]. The term 'pheromone' was proposed by Peter Karlson and Martin Lüscher[4] in 1959 and is derived from the Greek "pherein" meaning "to transfer" and "hormon" meaning "to excite". It is defined as "a chemical signal emitted from one member of a species and received by another member of the same species". Pheromones are therefore defined as "intraspecific" (*i.e.* between members of the same species) as opposed to interspecific (between members of different species) and in a strict interpretation the chemical should be produced only for communication, although this latter part of the distinction is becoming blurred with the discovery of metabolic byproducts which also act as communicants.

Pheromones can convey a wide variety of information such as location of a food source, readiness of a partner to mate and avoidance of an area because of predation. Pheromones can be subdivided into two categories, "releaser" pheromones which cause an immediate behaviour response in the receiver, *e.g.* the fright reaction of a school of minnows to an injured conspecific, and "primer" pheromones which cause physiological changes in the recipient, *e.g.* the spawning readiness cue exercised by the female goldfish.

Pheromones are part of a larger class of chemicals called semiochemicals. Semiochemicals are defined as substances produced by organisms for communication. The term is derived from the Greek word "semeion" meaning "to signal"[5]. The other subclass of semiochemical is the allelochemics which act between members of different species, and can be further subdivided into two groups, allomones and kairomones. Allomones, (from the Greek "of one another") and are defined as inducing a response in an individual of another species that is beneficial to the sender, for example the unpleasant odour of a skunk which deters attack. Kairomones are defined as inducing a response in another species that is beneficial to the receiver, for example a predator attracted by the mating pheromone of an insect. In some instances the semiochemical may fall into both categories. For example, the

scent of a flower attracts bees to pollinate it and volatile compounds such as jasmone released by plants suffering aphid attack attract aphid predators[6] which benefits both plant and predator. In this instance, the signal is termed a synomone[7]. Many metabolites act as semiochemicals in addition to their original function[8,9].

The vast majority of the work done to date has been on terrestrial pheromones, most notably those of butterflies and moths, the lepidopteran pheromones. The main reason for this is the economic impact these animals have on agriculture as a number of them are regarded as pests. The first pheromone to be characterised was that of the silk moth (*Bombyx mori*) in 1959 by Butenandt et al. The work lasted over 20 years and used over 1 million females to yield just 11.2 mg of a derivative of the active substance, Bombykol **1**[10].

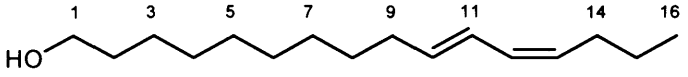

1 Bombykol, 10*E*,12*Z*-hexadecadien-1-ol

By modern standards this identification used an enormous quantity of material. With the instrumentation available today, for instance the gas chromatograph-mass spectrometer (GC-MS), only μg-ng quantities are required for identification[11]. Insect pheromones also lend themselves to mass spectral analysis because, by necessity, they are volatile. The vast majority of insect pheromones are alcohols, aldehydes or ethanoic acid esters derivatives.

Pheromones have been identified across the animal, plant and microbial kingdoms. One of the most widely studied systems is that of the yeast species *Saccharomyces cerevisiae*. This yeast has a two pheromone system using a- and α-factors secreted by a- and α-cells respectively[12]. Both pheromones act in a similar way on their target cells[13], for example, the tridecapeptide α-factor identified as Trp-His-Trp-Leu-Gln-Leu-Lys-Pro-Gly-Gln-Pro-Met-Tyr[14] binds to a protein coupled receptor on the cell surface[15] which activates a kinase cascade starting a signal transduction pathway that arrests cell division and engages polarity establishment proteins which organise the actin cytoskeleton and enable polarised growth up the concentration gradient leading to cell fusion with the alpha cell[16]. Similarly, the dodecapeptide Tyr-Ile-Ile-Lys-Gly-Val-Phe-Trp-Asp-Pro-Ala-Cys-(farnesyl)OCH_3, "a-factor", which has undergone post-translational modification with a farnesyl isoprenoid and carboxymethyl group[17], again binds to a receptor on the alpha cell initiating polarised growth and ultimately cell fusion with the emitting a cell. These types of peptide hormones have been identified for a variety of fungal species[18,19].

Another well documented use of semiochemicals is that of the Western Pine beetle,

Dendroctonous brevicomis, which uses myrcene **2** released by distressed trees for host selection. The female finds the host tree, then releases *exo*-brevicomin **3** which attracts males. The males arrive and release frontalin **4** during mating. The combination of all three compounds in turn acts as a mass attack pheromone to attract more beetles. When the tree is fully colonised, the beetles release the deterrent pheromones verbenol **5**, verbenone **6** and (*S*)-(+)- ipsdienol **7**, produced from the myrcene **2** that attracted them in the first instance[20].

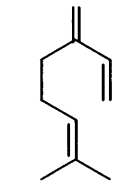

2 Myrcene

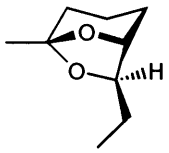

3 *exo*-Brevicomin

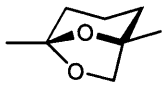

4 Frontalin

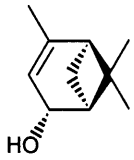

5 *trans*-(1*S*)-(-)-Verbenol

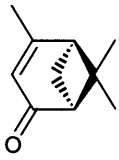

6 Verbenone

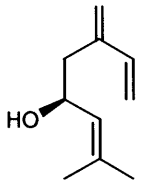

7 (*S*)-(+)-Ipsdienol

Other pheromones identified from the insect kingdom include attraction pheromones *cis*-7,8-epoxy-2-methyloctadecane **8** (Disparlure) from the female gypsy moth, and 7,11-hexadecadienyl acetate **9** (Gossyplure) from the female pink bollworm moth[21], the sex pheromone **10** (Periplanone B) of the American cockroach and the aggregation pheromone of the German cockroach **11**, **12**.

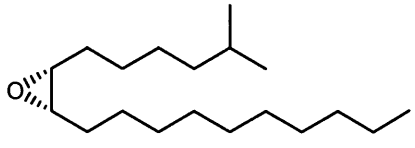

8 Disparlure, (7*R*,8*S*)-epoxy-2-methyloctadecane

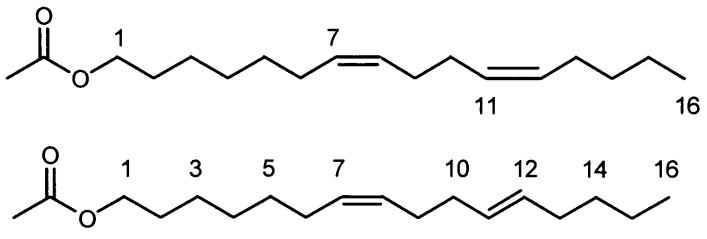

9 Gossyplure, a mixture of *Z*, *Z* and *Z*, *E* -7,11-hexadecadienyl acetate

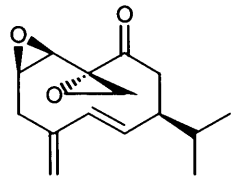

10 Periplanone B

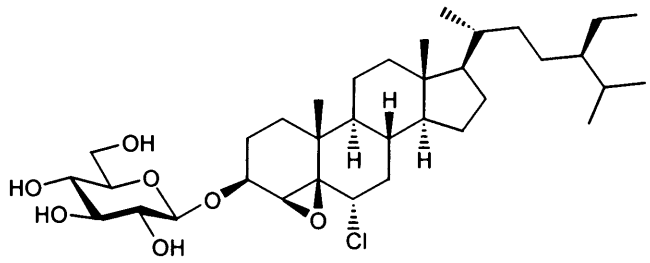

11 Blattellastanoside A

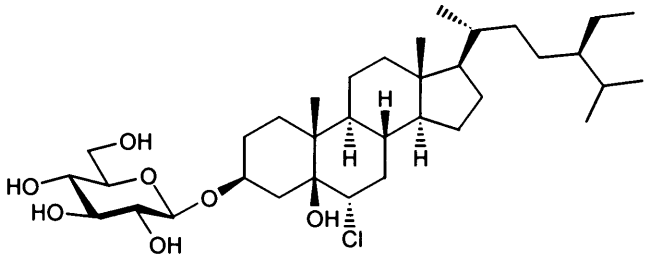

12 Blattellastanoside B

Pheromones identified in mammals include the attack deterrent of the striped skunk containing 3-methyl-1-butanethiol **13** and (2*E*)-butene-1-thiol **14**, the androstenol **15** and androstenone **16** mixture used as a mating pheromone by boars and the ovulation signalling pheromone of Asian elephants, (7 *Z*)-dodecenyl acetate **17**, which, coincidentally, is also used by at least 120 species of Lepidoptra[22].

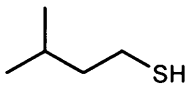

13 3-Methyl-1-butanethiol

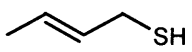

14 (2*E*)-Butene-1-thiol

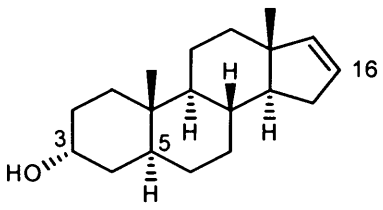

15 Androstenol, 5α-Androst-16-en-3α-ol

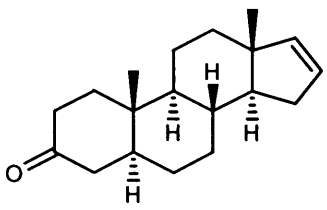

16 Androstenone, 5α-Androst-16-en-3-one

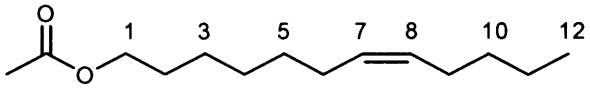

17 (7*Z*)-Dodecenyl acetate

1.2 Chemical cues in an aqueous environment

Many animals in an aqueous environment rely heavily on chemical cues for information. This information may be about many things such as food, other group members, predators and, of course, potential mates. Chemical cues become increasingly important in this environment as audio and visual cues can easily be lost or distorted. Perfect eyesight is of little use in very turbid conditions. Many pheromones have been proposed for fish. They have been implicated in schooling (groups stay together at night)[23,24], salmon migration[25,26], parenting skills[17], reproduction and predator avoidance[24,27,28]. The latter is more commonly referred to as a fright reaction and was discovered by accident in 1938.

1.2.1 The fright reaction

The fright reaction was first observed by Von Frisch when working with European minnows, *Phoxinus phoxinus*. When an individual which had undergone a small surgical procedure was returned to the holding tank, the school retreated and moved closer together, *i.e.* retreat and aggregation[29]. This behaviour was also observed when an injured fish trapped by a metal feeding tube was released. These observations prompted further investigation and it was demonstrated that mechanical rupture of skin cells released the alarm substance[28]. The alarm substance for this minnow is thought to be hypoxanthine-3-(*N*)-oxide[29]**18**, as minnows respond to purine based nitrogen containing compounds, and this one in particular[30], and at low concentrations[31]. It is also interesting to note that in this instance, other species such as fathead minnows and sticklebacks[32] can respond to the alarm substance[33] exhibiting what is now known as classic behaviour by fleeing and schooling at the stream bed. Predators such as pike which have recently eaten minnows can also elicit the fright reaction[34,35],and this is thought to occur by the alarm substance being excreted as a digestion waste product.

18 Hypoxanthine-3(*N*) oxide

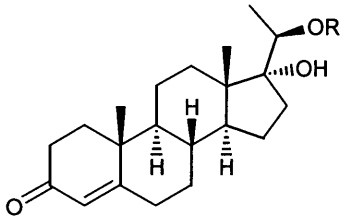

19
a R = H; 17α,20β-Dihydroxy-4-pregnen-3-one, 17α,20β-P
b R = SO_3; 4-Pregnen-17α,20β-diol-3-one 20-sulphate, 17α,20β-P sulphate

1.3. How do fish detect pheromones?

Having established that fish rely heavily on chemical cues, the next question is how are they detected? There are two main methods of detection, smell and taste, *i.e.* olfaction and gustation.

1.3.1 Structure of the olfactory organ in teleost fish

Teleost (or bony) fish have a pair of organs containing the olfactory epithelium on the dorsal side of the head. Water enters the anterior nares, passes over the epithelium and leaves through the posterior nares. Water movement through the nares is caused by the fish swimming.

The olfactory epithelium is folded into lamellae which form a rosette. The epithelium is covered in mucus and contains two types of receptor cells, ciliated and microvillar[36,37]. Odorant molecules enter the nares, dissolve in the mucus and bind to the appropriate receptor cells. The volume of the nares can be increased in some species like flounder by a spontaneous jaw protrusion, termed "coughing" which allows enhanced sampling, analogous to vertebrate sniffing.

Electrical measurements of the epithelium may be made using an electro-olfactogram (EOG) which is analogous to an insect electro-antenneagram. In an EOG, electrodes are placed on the surface of the epithelium and odorants or test solutions flushed through the nasal passages. There are four main classes of compounds which have been shown to induce an olfactory response. They are amino acids, bile acids/salts, sex steroids and prostaglandins. The first two groups are usually associated with feeding behaviour and the last two with mating. These groups were found to be active in all fish species studied[36]. Bile salts have also been implicated in migration and homing in salmonids and eels[25,38].

1.3.2. Structure and mechanism of gustation in teleost fish

Gustation is largely a matter of taste. Taste buds may be internal, for example within the mouth, or external on gills, barbels and fins. Some salmonids have been reported to have up to 4,000 buds on their palates. The taste bud is comprised of receptor, basal and supporting cells. The receptor cells have microvilli, in common with the olfactory epithelium. Electrical measurement similar to the EOG may be made by placing the electrode on the palatine nerve innervating the anterior palate and inside the upper lip[36].

The main group of compounds studied is amino acids, again mainly associated with a feeding behaviour, although certain amino acids induce a sexual response in the Rose

bitterling[39]. Amino acids can induce a response over a wide concentration range. Other classes of compounds studied include bitter substances, bile acids (effective for salmonids), carbon dioxide, some aquatic toxins (*e.g.* the puffer toxin tetrodotoxin), carboxylic acids and nucleotides.

1.3.3 Olfaction versus gustation for pheromone detection

Olfaction has been shown to play a crucial part in pheromone detection and mating for many fish species. It has been demonstrated for several species, that fish with wax blocked or surgically sectioned nasal passages do not respond to primer or releaser pheromones. In addition the olfactory epithelium taken from a mixed sex group of goldfish was shown to specifically/preferentially bind 17α-20β-dihydroxy-4-pregnen-3-one (17α,20β-P, **19a**) from a solution of seven steroids. 17α,20β-P **19a** is a reputed goldfish pheromone[40]. Olfaction for the detection of prostaglandins has also been demonstrated[41,42]. Many experiments have demonstrated the presence of specific pheromone receptors in the olfactory epithelium.

The importance of olfaction for reproduction has also been demonstrated for the African Catfish. When the medial olfactory tracts in ovulated females were severed, it was found that they were not significantly attracted to the part of the tank containing a mixture of steroidal glucuronides, whereas intact females showed a marked preference for this part of the tank[43]. Steroid glucuronides are the proposed male pheromone for spawning readiness.

1.4. Pheromones in reproduction

As previously mentioned, pheromones play a huge role in fish reproduction. It has been shown for many species that fish with impaired olfaction do not respond to chemical cues to initiate spawning. There are many reviews on the role of hormones as pheromones in fish reproduction[44,45,9,46,47,48,49,50,51,52,53], as well as chemical communication in general[54,55,17,18].

The method of pheromone release has also been extensively studied. The urine of sexually mature fish in a spawning situation has been found to be attractive to mature members of the opposite sex. For example, female sea lamprey during the spawning run are attracted to the urine of mature males[42] and male goldfish are attracted to the urine of ovulated females. The release of pheromones is not restricted to one sex, both sexes may release pheromones at different stages of the reproductive/spawning cycle[56,50,44].

The pheromones that have been proposed are mainly steroidal hormones and prostaglandins[49,50,57,8]. In females, the steroidal hormones are associated with egg formation and maturation, and prostaglandins with ovulation, ie follicle rupture and release of the eggs from

the ovary. In males, steroidal hormones either free or conjugated, are implicated in sperm motility and spawning readiness cues[46]. Conjugation, (*e.g.* glucuronides, sulphates) is thought to be necessary to make the steroid water soluble[48] and also for rapid release in urine. There are some exceptions to the steroid and prostaglandins hypothesis, for example male rose bitterling demonstrate sexual "pecking" behaviour and sperm release in response to a dialysis tube containing amino acids[39]. As previously mentioned, more usually, amino acids produce a feeding response. The role of amino acids and peptides as pheromones in an aquatic environment is discussed elsewhere in this thesis.

The use of hormonal steroids and prostaglandins as pheromones raises the question of whether they were primarily for communication or if this function evolved because they were there. It is suggested that the primary role of these compounds is to make the fish ready for spawning and the communication aspect developed around their presence. Sørenson and Scott suggest the evolution of a "spying" mechanism, the chance appearance of a hormone receptor in the olfactory epithelium which became incorporated and specialised for cue recognition[9]. Although they tested twenty one C_{21} and C_{19} steroids, only four were detected when measured by EOG. They also found that there was no difference between the sexes in the detection of the C_{21} steroids. They suggest that these findings, coupled with the rapid release rate support the idea that the pheromonal aspect developed to take advantage of a metabolic process. Free steroids were found to be released from the gills and conjugated steroids from the urine[47].

1.4.1. Endocrine changes and pheromone release in goldfish

The most widely studied fish sex pheromone system is that of the goldfish, *Cariasus auratus*[9]. The regulation of the spawning behaviour in female goldfish was first reported in 1974[58] and the presence of pheromones in 1976[53]. In this early work, it was clearly shown that males responded to an unidentified odorant. Intact males were seen to chase ovulated females for some hours, repeatedly nudging against her ovipore. The incidence of this pattern of behaviour decreased markedly in anosmic fish. The behaviour is similar to that seen in spawning. In this study the use of only one pheromone was suggested, released when females had undergone ovulation. This pheromone acts as a "releaser", *i.e.* induces spawning behaviour in males. As an obvious change in behaviour is induced, the effect is much easier to detect. A "primer" pheromone was also suggested. As the primer acts on the endocrine system, the behavioural effects are not always immediately obvious and therefore harder to detect.

Follicles form in the ovaries and the oocytes are induced to mature by the steroid

17α,20β-P[59] **19a**. Ovulation then occurs as the follicles rupture and the eggs are forced into the oviduct. Prostaglandins have been implicated in follicle rupture. It has been suggested that two pheromones may be involved. The first (associated with oocyte maturation) which causes a gonadotropin (GtH) surge and ultimately an increase in milt volume. The second initiates the male chasing behaviour and results in actual spawning and sperm release. The first pheromone readies the male reproductive system and the second tells it when to act.

Early studies suggested that 17α,20β-P **19a** might be the primer pheromone as it was found that the olfactory epithelium was particularly sensitive to this compound[59,60]. After exposure, milt volumes were found to increase[61]. Interestingly, it was also found that milt volume increased significantly 6 hours after exposure, which coincides with the usual time of ovulation. Water-borne levels of 17α,20β-P **19a** as low as 10^{-10} M were found to increase milt volume[40,49,60]. However, as already described, the nudging behaviour of males around the genital opening may expose them to higher local concentrations. The response of the endocrine system by increasing blood levels of GtH is rapid, within 15 minutes.

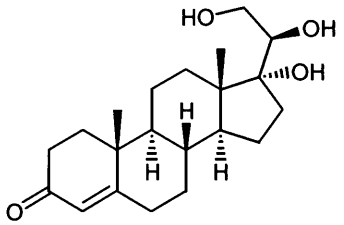

20 17α,20β,21-Trihydroxy-4-pregnen-3-one, 17α,20β,21-P

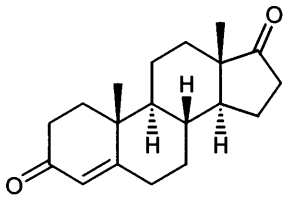

21 Androstenedione

Further studies have suggested that the primer pheromone may be a mixture of compounds, comprised of steroidal hormones in free and conjugated form[62,63]. It has been shown that mature goldfish ovaries produce a variety of steroids in three main forms, either free or conjugated as glucuronides or sulphates. Other steroids implicated as having pheromonal activity are 17α,20β,21-trihydroxy-4-pregnen-3-one (17α,20β,21-P, **20**), another oocyte maturation steroid, and 17α,20β-P sulphate **19b**, which has similar effects on the male endocrine system to 17α,20β-P[56] **19a**. Although both of these compounds are potent odorants to goldfish, they are not as potent as 17α,20β-P **19a**. In addition, steroids such as androstenedione **21** are released which inhibit the endocrine action of 17α,20β-P **19a**. The hypothesis is that 17α,20β-P **19a** and androstenedione **21** are released together and the action of 17α,20β-P **19a** is blocked. As the ratio of 17α,20β-P **19a** to androstenedione **21** increases, the priming action of 17α,20β-P **19a** over rides some threshold and starts to take effect. The

reasoning behind this is that non-ovulated females also release 17α,20β-P **19a** at levels that would affect males, and this override mechanism eliminates sperm and energy wastage.

The releaser pheromone implicated in goldfish spawning is associated with follicle rupture[64] and ovulation. When the oocytes have matured, a prostaglandin (PG) causes ovulation and the eggs are deposited in the oviduct. At the same time, both males and females become sexually receptive and begin spawning behaviour. If eggs are stripped from one female and inserted into the reproductive tract of an unovulated female, the latter female spawns normally. This indicates that spawning is induced by the presence of the eggs rather than the process of follicle rupture. This reaction to the inserted eggs may be stopped by injection of a prostaglandin synthesis inhibitor, such as indomethacin. This effect can, in turn, be reversed by PG injection. PG injection can also induce spawning behaviour in females with no eggs in their reproductive tracts[44].

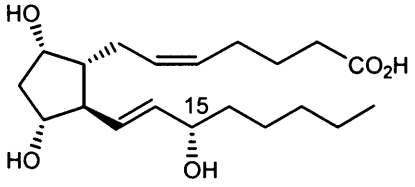

22 $PGF_{2\alpha}$

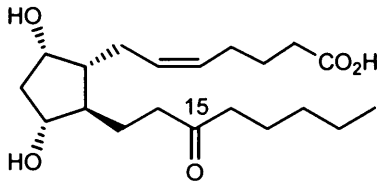

23 13,14-Dihydro-15-oxo-$PGF_{2\alpha}$,15-keto-$PGF_{2\alpha}$

Other studies have suggested that the pheromone may be an F type of prostaglandin. Levels of PGF in blood and ovaries increase at the time of ovulation. $PGF_{2\alpha}$ **22** has been demonstrated to induce female spawning behaviour by its action on the brain[65] and females injected with $PGF_{2\alpha}$ **22** also induce spawning behaviour in males. When preference tests between $PGF_{2\alpha}$ **22** solution, $PGF_{2\alpha}$ **22** injected females and ovulated females were performed, it was found that males only responded to the injected or ovulated females[44]. $PGF_{2\alpha}$ **22** itself did not elicit any courtship or spawning behaviour at the concentration tested[57,50]. This finding implies that $PGF_{2\alpha}$ **22** undergoes some form of metabolism before any pheromonal activity is possible. Analysis of tank water revealed high levels of PGF from ovulated and $PGF_{2\alpha}$ **22** injected fish. EOG also revealed that olfactory epithelium is extremely sensitive to all the prostaglandins tested in the study, but acutely so for $PGF_{2\alpha}$, **22** at 10^{-10} M[65]. This is a typical level for a pheromone and is comparable to that of 17α,20β-P **19a**. EOG studies also found that the detection limit for 15-keto-prostaglandin $F_{2\alpha}$ (15-k$PGF_{2\alpha}$, **23**), a metabolite of $PGF_{2\alpha}$ **22** was 10^{-12} M, a factor of 100 times lower than $PGF_{2\alpha}$ **22**[4,49,42,66]. Although PGF can be found in washings from eggs, the exact route of release was not identified, although urine is likely

to be involved. Urine can act as a physical mover by pushing the eggs out of the genital pore. Studies in other fish species have shown it to be a powerful odorant in its own right[38, 42].

In summary, the primer pheromone for goldfish is thought to be a mixture of approximately five progesterone metabolites, of which 17α,20β-P **19a** is the most potent at inducing an EOG response. The releaser pheromone is thought to be a mixture of F prostaglandins, of which the 15-keto metabolite **23** is the most potent at inducing an EOG response.

Carp are closely related to goldfish, and as expected, similarities exist. EOG studies have shown that carp, *Cyprinus carpio*, have identical response patterns to aqueous steroids as goldfish, and recent studies have shown that milt volume is increased after exposure to 17α,20β-P **19a**[67,68]. A variety of teleosts have been tested with a variety of sex steroids, and it has been found that different species are sensitive to different steroids[68,49]. Closely related species may respond to the same steroids if, at some evolutionary stage, they shared a common ancestor.

1.4.2 African Catfish sex pheromones

After goldfish, the African Catfish, *Clarias gariepinus* must have the most widely studied pheromone system. The main reason for this is the economic importance of this species in aquaculture. The method of pheromone detection has again been shown to be by olfaction[33]. However, in this species, the majority of the work has been carried out on male pheromones attracting ovulated females[8] and inducing ovary maturation. When seminal vesicles were incubated with tritiated pregnenolone **24** and androstenedione **21**, six glucuronides were formed, but none were detected in identical experiments using testes[69,48]. Castrated males, in which the seminal vesicle is enlarged, attracted more females than intact males, which suggests that the seminal vesicle is the source of the pheromone. Studies demonstrated the sensitivity of the female olfactory epithelium to these glucuronides, in particular 5β-pregnane-3α,17α-diol-20-one 3α-glucuronide **25**[43]. When "active" samples were treated with β-glucuronidase, the activity was lost. Gas chromatography-mass spectrometry studies[70,71,48,72] were performed, after initial sample cleanup by solid phase extraction. The free steroids were first removed by solvent extraction then the glucuronides were deconjugated by incubation with β glucuronidase. The steroids were then converted to either their trimethylsilyl (TMS) or oxime-TMS derivative. The GC-MS investigation of seminal vesicle fluid identified seven glucuronides at 10^{-8} M levels. Only four of the glucuronides were present at detectable

levels in male holding water[72]. Of the four detected, only 5β-pregnane-3α,17α-diol-20-one 3α-glucuronide **25** was above the threshold level, all the rest were below. It therefore seem likely that a steroid glucuronide or some combination of these glucuronides acts as a pheromone for the female African catfish.

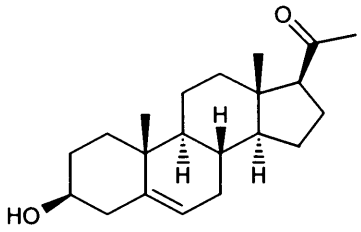

24 Pregnenolone

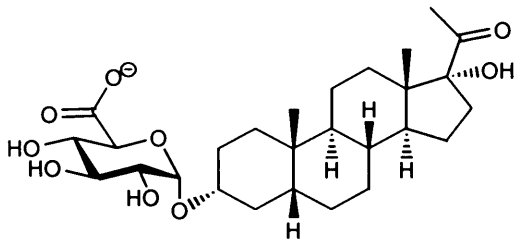

25 5β-Pregnane-3α,17α-diol-20-one 3α-glucuronide

1.4.3 Sex pheromones in salmonids and trout

Pheromones have been implicated in several aspects of salmon behaviour. As previously discussed, olfaction is thought to be vital for migration and homing. Studies have shown that skin mucus, intestinal content and urine all provoke an olfactory response[38]. The attraction of urine has already been discussed for other species, such as goldfish.

The role of urine as a carrier for sex pheromones in Atlantic salmon, *Salmo salar L.*, has only recently been studied. Urine from ovulated females has a priming effect on males similar to the goldfish model. EOG studies have shown that testosterone **26** at levels as low as 10^{-10} M is a potent odorant to mature males[73] and induces prespawning behaviour. It is suggested that females release testosterone **26** some time prior to spawning to the correct locale, as sensitivity is lost some two weeks before spawning actually commences.

The oocyte maturation steroid, 17α,20β-P **19a**, is again implicated in pheromone activity. Ovulated female urine contains conjugated 17α,20β-P sulfate **19b**[74], and negligible amounts of free testosterone **26**[75] which is known to be a potent odorant for male salmon. However, mature males do not give an EOG response to 17α,20β-P sulfate **19b** unless the olfactory epithelium has previously been exposed to ovulated female urine. This is a very important finding as it suggests that there is some other, as yet unidentified, factor in the urine which is needed to render the epithelium capable of 17α,20β-P sulfate **19b** detection. Other potent odorants were found to be $PGF_{1\alpha}$ **27** and $PGF_{2\alpha}$, **22** and the response was not dependent on pre-exposure. It is worth noting that although a compound may be a potent odorant, this alone does not render it a pheromone.

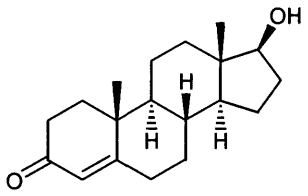

26 Testosterone

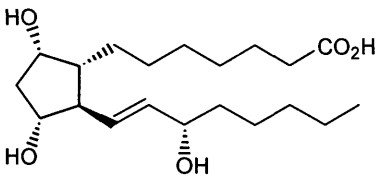

27 PGF1α

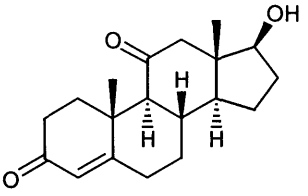

28 11-Ketotestosterone

The first report of a chemical cue for spawning readiness in rainbow trout (*Salmo gairdneri, Oncorhynchus mykiss*) was published in 1973[76]. The study demonstrated that fish of both sexes were attracted to water that had held spawning conspecifics. Further studies refined the hypothesis and showed that mature males were attracted to water containing ovarian fluid, obtained when females were hand-stripped of their eggs[77,78]. The eggs themselves did not contain a source of attraction. Thin layer chromatography of ether soluble basic substances obtained from egg washings produced three spots. Although the spots were ineffective when tested singularly, a positive attractive result was obtained when two of the three were combined. No further attempt at characterisation was made at this stage. Again, the role of olfaction in pheromone detection was clearly demonstrated[77,76,78].

Studies on the endocrine changes and sex steroid levels in plasma associated with spawning showed an increase in C_{21} steroids for both males and females[79]. This pattern of steroid production was also seen in the goldfish. The steroid 17α,20β-P **19a** (oocyte maturation steroid) was detected in both sexes[80,79]. It was suggested that 17α,20β-P **19a** occurs in sperminated males because the conversion to C_{19} steroids by desmolase is inhibited. The role of 17α,20β-P **19a** in males was suggested to be controlling the potassium ion concentration and hence sperm motility. Examples of C_{21} steroids controlling both potassium and sodium ion transport across membranes have previously been reported.

The seasonal variation of the sex steroid levels has major implications for work on spawning pheromones in any species, as the pheromone will only be active and induce a behavioural response if it is the spawning season[80,81,82]. Some social effects on plasma steroid levels were also reported[83,79]. Ovulated females exposed to courtship behaviour retained elevated levels of 17α,20β-P **19a** compared to those in isolation. In comparison, males exposed to courting ovulated females had elevated levels of GtH, 11-keto-testosterone (11-KT, **28**), 17α,20β-P **19a** and increased milt volumes[84,83]. Anosmic males placed with ovulated females spawned, but plasma steroid levels and milt decreased in contrast to the maintained levels in

the control group. This was taken as evidence of a primer pheromone.

Studies on the composition of female trout urine identified the presence of 17α,20β-P sulphate **19b**[85,86], which was thought to be a good pheromone candidate for two major reasons. Firstly, the route of excretion is in urine; conjugated steroids tend to be removed via urine whereas free steroids tend to excreted via the gills[87]. Secondly, 17α,20β-P sulphate **19b** is a potent odorant in both Atlantic salmon and (possibly a primer for) goldfish. Males exposed to synthetic 17α,20β-P sulphate **19b** at 10^{-8} - 10^{-9} M had elevated GtH and 17α,20β-P **19a** plasma levels, but milt volumes were unaffected. Males exposed to female urine had the highest plasma levels of all. It was also found that males had no preference for water containing 17α,20β-P sulphate **19b**. In addition, unovulated female urine which contains very low levels of 17α,20β-P sulphate **19b** also has a priming effect on males. The results of these studies make is seem unlikely that 17α,20β-P sulphate **19b** is the primer pheromone for rainbow trout.

As prostaglandins are a putative goldfish releaser pheromone (cf. **22**. **23**), four mixtures of commercially available standards were tested. The mixtures comprised of A_1, A_2, B_1; B_2, D_2, E_1; E_2, B_1; B_2, D_2; and A_1, A_2, E_1, E_2, $F_{1\alpha}$, $F_{2\alpha}$. None of these mixtures gave any rise in plasma 17α,20β-P **19a** levels.

It has also been noted that some males have a larger (and therefore better) endocrine response. Some studies have screened for this effect[88], which raises questions as to whether this may have influenced the final results. Moreover, there is a wide variation in results obtained for many of these studies, which has been attributed to seasonal factors. To date the exact identity of both the primer and releaser pheromone in trout spawning behaviour remains unknown.

1.4.4 Other fish pheromones

Pheromones have been implicated in the spawning behaviour of a number of other fish species. These include sea lamprey[89,42], yellowfin Baikal sculpin[90], blue gourami[91], rose bitterling[92,39], loach[93,94], paradise fish[95], bleeker[96], herring[97,98], plaice[47], zebrafish[69] and dab[99,100]. The current status of chemical communication in general[55,54,23], and pheromones in particular[18,46,9,45,44,27,51,50,49,64,53] have been extensively reviewed, although few identifications have been made.

By understanding the role and identity of these pheromones, the possibility for management of fish populations moves a step closer. This management could either be for

commercially important species, such as African Catfish, trout and salmon, or as a means of "pest control" for species such as lamprey.

1.5 Methods of analysis

Methods and techniques in pheromone research can be split into two broad classes. One is based on observation or measurement of some specific animal response. When the behaviour is used to determine if a sample contains any active component, it is termed a bioassay. The other side of pheromone research tends to analytical methods for identification. Both classes are equally important as the bioassay gives information about the activity of the target compound and the analytical techniques give some characterisation. There is no clear division, however, and increasingly bioassay relies on analytical techniques and vice versa. For example, an increase in plasma steroid levels is a behaviour response (bioassay) but the steroids need to be quantified (analytical).

A behavioural response tends to be most easily identified with a releaser pheromone. For example, with the Y choice maze, a positive result is given when the fish spends significantly more time in the arm containing the test sample, or after exposure, the volume of expressible milt increases. Although EOG uses electrodes to record the response of the olfactory epithelium, again a behavioural response is being monitored. Another example of an overlap between the two classes is that of the radioimmunoassay (RIA). This technique can be used to quantify sex steroids in a variety of matrices. This is achieved by raising antibodies to target compounds and using a radio label (either on the target compound or to bind to any free antibodies). The uptake can then be measured. This technique is very specific, although some cross binding can occur with closely related compounds. The main drawback to this technique is that some idea of the likely candidates is required to raise the specific antibodies.

Chemical identification of a unknown pheromone, typically requires separation of a mixture followed by identification using spectroscopic techniques. This typically requires concentration and preliminary "cleanup" using techniques such as conventional solvent or solid phase extraction (SPE)[71]. Final separation is usually by GC-MS[101,70,71,72], HPLC[94,93,102,98] and occasionally by TLC[90,91]. Mass spectrometry is the pre-eminent technique for the identification of pheromones, because it can easily be linked directly to GC and with a little more difficulty to LC. This enables routine compounds to be identified directly from library comparisons, particularly for EI(+)-MS.

Chapter 2, Fish Experimental Section

2.1 Instrumentation

2.1.1 Gas chromatography-mass spectrometry

The gas chromatograph-mass spectrometer system used for this study was an HP-5890 gas chromatograph (GC) interfaced to a VG Trio-1 mass spectrometer (MS). The GC used scrubbed helium as the carrier gas at a column head pressure of 8 psi, to give a column flow rate of 4 ml/min. The septum purge was 0.6 ml/min and injections were performed in the splitless mode, with the split vent for septum purge closed for 1 minute. The capillary column was connected to the inlet without a guard column, and interfaced to the mass spectrometer through a heated interface, set at 10° C above the final temperature of the oven programme.

The MS was used in the electron impact (EI+) mode, at 10^{-4} atmospheres source pressure. In this mode, electrons are emitted from a filament at 70 eV and collide with analyte molecules in the ionisation chamber, heated to 210° C. An electron trap (cathode) set at 250 μA, situated opposite the filament, controlled the filament energy to 70 eV. The resultant ions are ejected through the exit plate by a repeller plate set at 2.0 - -6.0 V into the quadrupole. The ions were separated according to their mass/charge ratio (*m/z*) by the quadrupole. The Trio-1 has an 18 cm quadrupole mass filter with pre and post filters. The full possible scan range is from 2 - 1023 atomic mass units (amu) and mass selection was achieved by diagonally matched poles which vary current or radio frequency. The mass range scanned was 33 - 700 amu in 0.9 seconds with an interscan time of 0.1 seconds. A solvent delay of 3 min was used to preserve the filament. During the solvent delay, the filament current was reduced and no data was collected so that the large solvent peak did not blow the filament. The ions were detected by a impact onto a phosphor screen, enhanced by a photomultiplier and a conversion dynode. The vacuum within the source and analyser was maintained by a 240 L/s and a 60 L/s Balzer turbomolecular pump respectively. The backing pump was an Edwards 2 stage rotary pump. The MS was tuned with heptacosa FC43, using peaks at *m/z* 69, 219, 264 and 502 with relative intensities of 100%, 31%, 7% and 1%.

The system control and data acquisition was performed by a computer running Lab Base II software. "70 eV"-spectra are the standard for mass spectral libraries. The Lab Base software contains the NBS library of 54,000 entries which is matched by the computer to the analyte spectra. In the initial screen analyte and library spectra are matched using the eight most abundant peaks. Candidate library spectra are then ranked by a forward or reverse fit

process. A reverse fit matches the ions in the library to the unknown spectrum, whereas a forward fit matches the ions in the unknown to the library. The degree of "goodness of fit" or matching is scored out of 1000, with a reasonable match scoring >800. Reverse fit is best used when analytes are likely to be impure and this mode was used throughout the current work.

The injection volume was 1 µl and this volume was used for all work unless otherwise stated. Gas Chromatograph-Mass Spectrometer (GC-MS) operating conditions were as follows: 40 °C held for 3 minutes then ramp of 25 °C per minute to 260 °C held for 15 minutes. The column was a DB-17 phase, 30 m, 0.25 µm film column and the injector was run in the splitless mode at 220 °C. The source was held at 210 °C.

This is summarised in the following form throughout this thesis:

40(3) x 25 to 260(15) inj220 spltls 1 min

The source temperature remained constant throughout this work unless otherwise stated

2.1.2 High performance liquid chromatography

The high performance liquid chromatograph (HPLC) system used for this work was a Dionex 300 system, comprising of a AS3500 autosampler, advanced gradient low pressure mixing (AGP) tertiary pump and variable wavelength UV (VDM-II) detector. The system was fitted with a Vydac C18 5µm 25 x 4.6 mm guard cartridge and 150 x 4.6 mm analytical column. The sample was drawn into the 250 µl sample loop by syringe through a Rheodyne valve and injected onto the column. The injection volume was 100 µl, the mobile phase was methanol/water (70 %, *v/v*) and the UV detector was set at 254 nm unless stated otherwise. The system control and data acquisition was performed by a computer running Dionex AI 450 software.

2.1.3 Standard methods

Flow evaporation (50 °C) indicates that the samples were evaporated to incipient dryness under a gentle stream of nitrogen at 50 °C. Flow evaporation shown without a temperature was run at ambient temperatures.

All water was deionised from a Millipore Milli-Q deioniser fitted with ICP-MS grade exchange pack.

2.2 Analysis of standards

Identification by MS

Some materials such as siloxanes and phytane **33b** were identified in many samples. These

were identified by retention time and characteristic ions [*m/z* (abundance)].

Cholesterol **32a**: 386 (100), 368 (35), 301 (30),145 (34),105 (38),

Bis(2-ethylhexyl) phthalate **34**: 279 (7), 167(29), 149(100), 104 (5)

Phytane **33b**: 57 (100), 71 (73), 85 (43), 99 (16).

Siloxanes: 73 (40), 147(25), 207 (100)

Testosterone **26**: 288 (79), 246 (50), 203 (24), 147 (35), 124 (100), 105 (23)

2.2.1 GC-MS retention time standards

A series of fatty acids and alkane standards were analysed by GC-MS (30(3) x 5 to 260(35) inj 275) to determine standard retention times and Kovats Indices (Table 2.1). These conditions are identical to those used for the analysis of trout urine (Sections 2.8.2) and are linear in the range 3-49 min.

Table 2.1: Retention time standards and Kovats's Indices

Peak identity	Retention time min,	Predicted Kovats Index	Calculated Kovats Index	Difference
Fatty acid std, TIC =23061304, sample identity = sue335				
Dodecanoic acid	24.42	n/a	1616	n/a
Tetradecanoic acid	28.37	n/a	1792	n/a
Hexadecanoic acid	31.64	n/a	1948	n/a
Octadecanoic acid	34.92	n/a	2117	n/a
Cholesterol **32a**	51.00	n/a	Not calculated	n/a
C9 - C30,C10, C16, C18 - C30, squalene **35** standard, TICs = 50098392, 57506528, 51454992, sample				
Nonane	4.32	900	909	+9
Decane	7.20	1000	995	-5
Undecane	10.37	1100	1094	-6
Dodecane	13.43	1200	1195	-5
Tridecane	16.32	1300	1297	-3
Tetradecane	19.15	1400	1402	+2
Pentadecane	21.65	1500	1501	+1
Hexadecane	24.02	1600	1599	-1
Heptadecane	26.40	1700	1702	+2
Octadecane	28.65	1800	1805	+5
Nonadecane	30.69	1900	1902	+2
Eicosane	32.72	2000	2002	+2
Heneicosane	34.55	2100	2097	-3
Docosane	36.47	2200	2200	0
Tricosane	38.30	2300	2302	+2
Tetracosane	39.92	2400	2396	-4
Pentacosane	41.52	2500	2491	-9
Hexacosane	43.15	2600	2592	-8
Octacosane	46.10	2800	2782	-18
Tricosane	49.44	3000	3011	+11
Squalene **35**	49.14	n/a	Not calculated	n/a

The alkane series was used to construct a time versus Kovats indices plot (Fig 2.1) and the equation from the third order fitted line was then used to calculate Kovats Indices for some of the other compounds detected.

Fig 2.1: Kovats Indices calculated using the alkane series with 3rd order fit

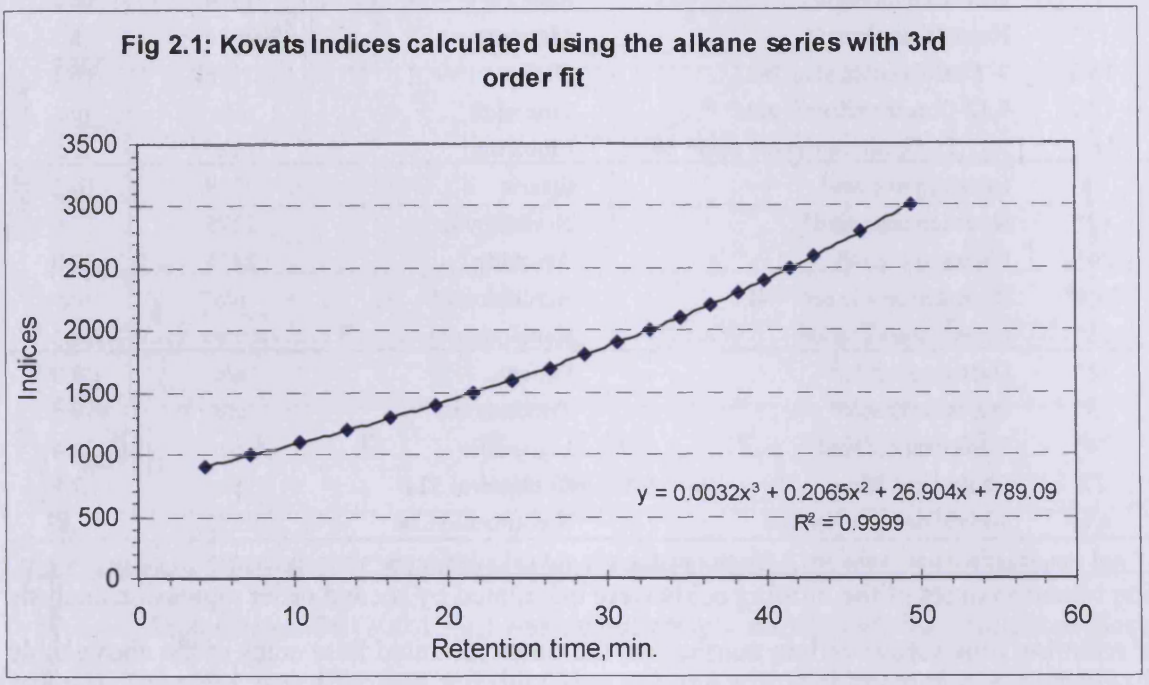

2.2.2 Preparation of fatty acid standard

An eight component standard was prepared containing hexanoic acid, octanoic acid, decanoic acid, dodecanoic acid, hexadecanoic acid, octadecanoic acid, octadecenoic acid **38a** and cholesterol **32a** (approximately 20 mg of each) dissolved in dichloromethane (100 ml). The standard was injected onto the GC-MS to obtain the retention times of the various components. A nicotinamide **36** standard was also run to confirm retention time and spectra. The samples were analysed by GC-MS (40(3)x15 to 260(15)).

The resulting chromatogram showed only seven peaks instead of the expected eight. On examination of the spectra, it was discovered that both C_{18} acids were co-eluting. The non-systematic names and retention times are shown in the following table (Table 2.2):

Table 2.2: Retention time standards and Kovats's Indices

carbon number	Systematic name	Non-systematic name	Kovats Index	Ret. time, min
6	Hexanoic acid	Caproic	n/c	6.4
7*	Heptanoic acid	Enanthic	n/c	7.8
8	Octanoic acid	Caprylic	691	8.5
9*	Nonanoic acid	Pelargonic	1048	9.4
10	Decanoic acid	Capric	1290	10.2
11*	Undecanoic acid*	Undecylic	1457	10.9

12	Dodecanoic acid	Lauric	1620	11.8
13*	Tridecanoic acid	Tridecylic	1703	12.4
14*	Tetradecanoic acid	Myristic	1792	13.2
15*	Pentadecanoic acid	Pentadecylic	1872	14.0
16	Hexadecanoic acid	Palmitic	1949	14.8
17*	Heptadecanoic acid	Margaric	2026	15.5
18:1	9- Octadecenoic acid **38a**	Oleic†	2118	16.2
18:2	9,12-Octadecadienoic acid*	Linoleic†	n/c	n/c
18:3	9,12,15-Octadecatrienoic acid* **39**	Linolenic†	n/c	n/c
18	Octadecanoic acid	Stearic	2118	16.2
19*	Nonadecanoic acid*	Nonadecylic	2275	17.0
20*	Eicosanoic acid*	Arachidic	2435	17.8
20:4*	Eicosatetraenoic acid* **41**	Arachidonic†	n/c	n/c
21*	Heneicosanoic acid*	Heneicosanoic	n/c	18.6
22*	Docosanoic acid*	Behenic	n/c	19.0
23*	Tricosanoic acid*	Tricosanoic	n/c	19.7
24*	Tetracosanoic acid*	Lignoceric	n/c	20.4
27	Cholesterol **32a**	Cholesterol **32a**	n/c	27.9
n/a	3-Pyridine carboxamide	Nicotinamide **36**	1752	12.83

* not run, standard not available, † unsaturated, n/c = not calculated, n/a = not applicable

The retention times of the missing acids were calculated by second order regression analysis of retention time versus carbon number for the other saturated fatty acids in the above table (Fig 2.2). The Kovats Indices for the fatty acids were then calculated from the appropriate plot (Fig 2.3).

Fig 2.2: Carbon number versus retention time for fatty acid series

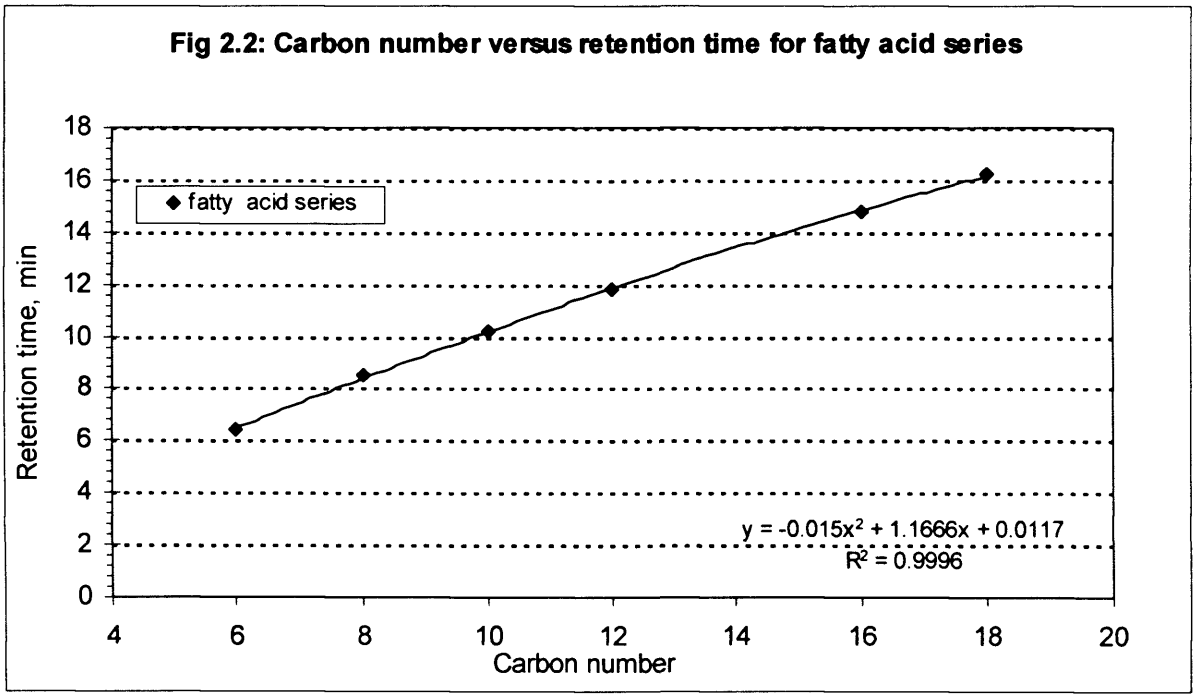

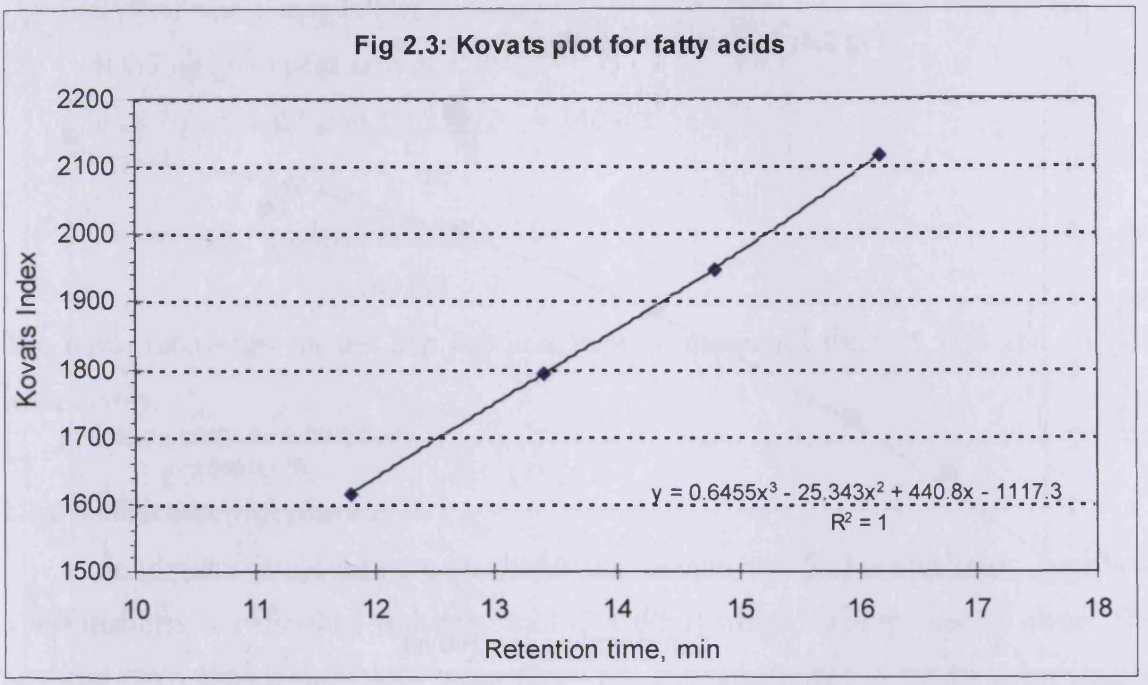

2.2.3 Calibration curve for GC-MS response to testosterone 26

Testosterone **26** (100.1 mg) was quantitatively transferred to a volumetric flask (100 ml). The solid was dissolved and diluted to volume with dichloromethane. A series of calibration standards were prepared by diluting varying aliquots (Table 2.3) of the stock standard as appropriate to volume in a series of volumetric flasks (10 ml). Duplicate samples were analysed by GC-MS (40(3) x 25 to 260(15)), retention time was 21.3 min. The calibration curve was obtained by plotting mean peak TIC (Total Ion Current) against concentration (Fig 2.4).

Table 2.3: Calibration curve data for testosterone **26**.

Standard concentration, mg/100 ml	Aliquots of stock solution, ml	Sample 1 TIC	Sample 2 TIC 2	Mean TIC	% Mean deviation
0	0.0	0	0	0	n/a
10	1.0	1748387	1273813	1511100	31.4
20	2.0	2248732	2392941	2320836.5	6.2
40	4.0	3972975	3942057	3957516	0.8
60	6.0	5010498	5121946	5066222	2.2
80	8.0	5453640	5203997	5328818.5	4.7
100	10.0	6891984	6041346	6466665	13.2

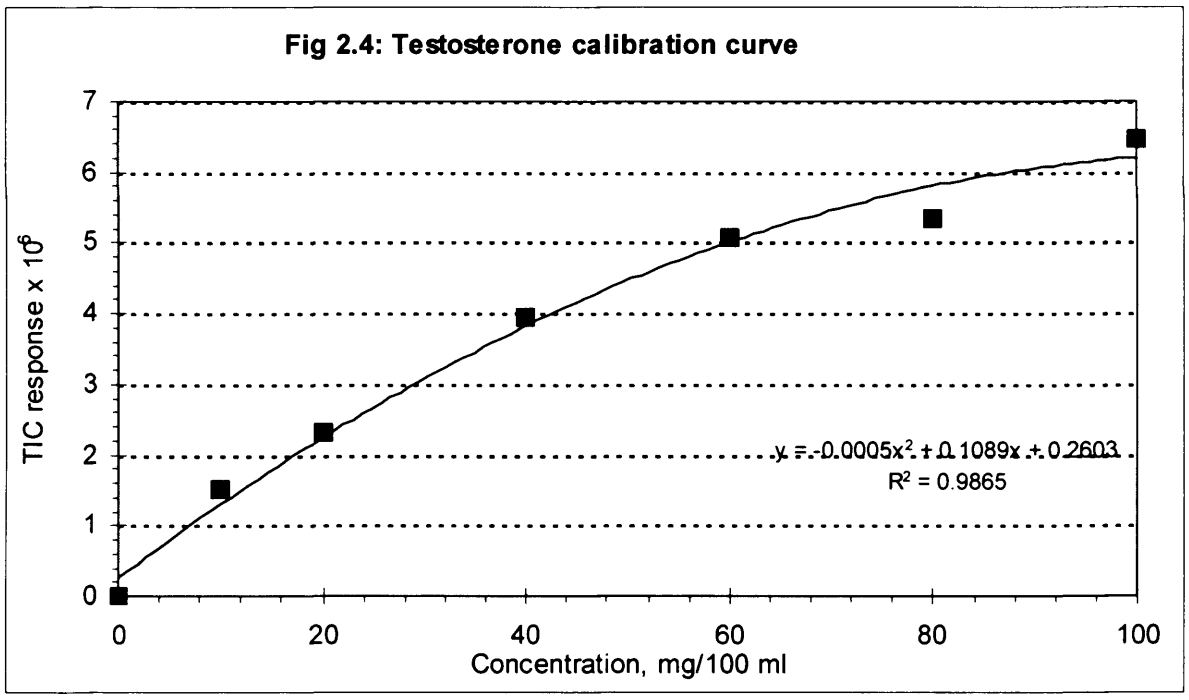

2.3 Solid phase extraction of testosterone 26

2.3.1 Extraction procedure 1, based on Schoonen and Lambert[71]

Solid phase cartridges (Sep Pac C18 and C18 Environ Clean) were attached to the top of a vacuum manifold. The cartridges were washed with methanol (2 x 2 ml) and water (2 x 2 ml) which was aspirated to waste. The flow controllers were closed as soon as the water was seen to reach the top of the bed to prevent the cartridges "running dry". The testosterone **26** samples were prepared in duplicate by spiking testosterone **26** solution (200 µl, 1mg/100 ml in methanol) into water (250 ml, 8 ng/ml), and were applied using Teflon lines and a cartridge adapter. The cartridges were washed with water (10 ml) and eluted with ethanol (4 x 2 ml) and ethanol/water (50 % *v/v*, 3 x 2 ml). The samples were flow evaporated (70 °C) , reconstituted in methanol/ water solution (70% *v/v*, 100 µl) by vortex mixing (20 sec) and injected onto the HPLC using methanol/ water mobile phase. The testosterone **26** peak (Table 2.4) eluted at 8.3 min.

Table 2.4: Peak areas from standards and extracts

Sample identity	Injection volume (µl)	Peak area 1	Peak area 2	Mean peak area	% Mean deviation
1 mg/100 ml	50	35225	34958	35092	0.8
Sep Pac S1,S2	100	18698	24949	21824	28.6
Supelco S3, S4	100	92511	120769	106640	26.5

The recovery was calculated by comparison with the standard mean peak area and correction for the differing on-column concentration, as detailed in the following equations:

50 µl of 1 mg/100 ml solution contains 0.5 µg

250 ml water sample contains 2 μg

if 0.5 μg gives peak area of 35092,

then 2 μg should give $\frac{2 \times 35092}{0.5} = 140368$

$$\% \text{ recovery} = \frac{\text{mean peak area}}{140368} \times 100$$

The mean recoveries for the Sep Pac and Supelco cartridges were 15.5 % and 76.0 % respectively.

2.3.2 Extraction procedure 2[103]

Solid phase cartridges were attached to the vacuum manifold as previously described. The cartridges were washed with methanol (2 x 6 ml) which was aspirated to waste. The cartridges were then washed with water (2 x 6 ml) and not allowed to run dry as previously described. The testosterone **26** samples, prepared as previously described (250 ml, 8 ng/ml) were applied using the Teflon lines. The cartridges were washed with methanol/ water (2/3 *v/v*, 2 x 3 ml), eluted with methanol/ water (6/4 *v/v*, 3 x 2 ml) and methanol/ water (4/1 *v/v*, 2 x 2 ml). The samples were flow evaporated (70° C), reconstituted in methanol (70% *v/v*, 100 μl) and analysed using the HPLC conditions previously described (Table 2.5).

Table 2.5: Peak areas from HPLC

Sample identity	Injection volume (μl)	Peak area 1	Peak area 2	Mean peak area	% Mean deviation
1 mg/100 ml	25	36914	35478	36196	4.0
Sep Pac B1,B2	100	22481	22921	22701	1.9
Supelco B3,B4	100	111227	110952	111090	0.2

The recoveries were calculated as described above. The mean recoveries for the Sep Pac and Supelco cartridges were 15.5 % and 76.0 % respectively.

2.4 Steroid standards

2.4.1 Kovats Indices determination

A series of fatty acids and steroids (tetradecanoic acid, hexadecanoic acid, octadecanoic acid, squalene **35**, testosterone **26**, 5β-androstan-3,17-dione **29**, 17α-hydroxyprogesterone **30a**, 4-pregnen-17α, 20α-diol-3-one **31** and cholesterol **32a**) were dissolved in dichloromethane and analysed by GC-MS (30(4) x 5 to 300(20) inj 310) to determine retention times and Kovats Indices (Table 2.6a). These conditions are similar to those used for the analysis of dichloromethane extracted trout urine (section 2.8.7)

Table 2.6a: Retention time standards and Kovat's Indices for steroids

Peak identity	Retention time, min	Kovats Index
Fatty acid standard		
Tetradecanoic acid	31.81	1792
Hexadecanoic acid	34.63	1948
Octadecanoic acid	38.19	2117
Squalene **35**	48.19	2670
Steroid standard		
Testosterone **26**,	50.92	2826
5β-Androstan-3,17-dione **29**	48.56	2690
17α-Hydroxyprogesterone **30a**	55.24	n/c
4-Pregnen-17α, 20α-diol-3-one **31**	57.17	n/c
Cholesterol **32a**	53.56	2981

n/c = not calculated

The fatty acids and squalene were used to construct a Kovats Indices plot (Fig not shown) with a second order fit ($y = 0.2152x^2 + 36.082x + 430.88$, $R^2 = 0.9997$). This equation was used to calculate the Indices for the steroids, except those which were not on the linear part of the temperature program.

2.4.2 Derivatisation of steroid standards

A series of steroids (testosterone **26**, 5β-androstan-3,17-dione **29**, 17α-hydroxyprogesterone **30a**, 4-pregnen-17α, 20α-diol-3-one **31** and Reichstein's Substance **30b**, approx 2 mg) were taken and individually dissolved in a minimum volume of dichloromethane. Vials containing various proportions of the standards were taken and flow evaporated. Hydroxylammonium chloride (2% *w/v*) in pyridine (10 ml) was prepared and an aliquot (200 µl) added to each vial. The vials were capped and placed on a hotplate (100°C, 1 hour). The vials were removed and after cooling, decapped and placed on a vacuum line to remove the pyridine. *N,O bis*(trimethylsilyl)acetamide (900 µl) and trimethylsilyl chloride (100 µl) was freshly prepared and added (100 µl) to the vials. The vials were again placed on the hotplate (70°C, 1 hour). A colour change from colourless to black was noted. The samples were removed and excess reagent removed on the vacuum line. The black residue was dissolved in hexane (2 ml) and extracted with acetonitrile (2 x 200 µl), the acetonitrile was discarded. The samples were evaporated to dryness under a gentle stream of nitrogen at room temperature. The acetonitrile cleanup step was repeated once more. The samples were finally reconstituted in hexane (250 µl) and analysed by GC-MS (100(3.5)x15to190(1)x2to280(15), inj 260)(Table 2.6b).

Table 2.6b: Derivatised steroid standards, retention times, TICs and significant ions

Ret. time min	TIC	Rev. fit	For. fit	Significant ions *m/z*	Identity
Testosterone **26** & 5β-androstan-3,17-dione **29**, sample identity = sue244					
31.58	4161536	n/i	n/i	447,417,358,268,211,183	Unidentified contaminant, TMS ester
32.59	4079616	n/i	n/i	447,432,358,252,211,183	Testosterone, TMS ester
34.27	4096000	n/i	n/i	462,447,432,373,342,283	5β-Androstane-3,17-dione, TMS ester
Reichstein's substance **30b**, 17α-hydroxyprogesterone **30a**, 4-pregnen-17α, 20α-diol-3-one **31**, sample identity = sue245					
38.62	4161536	n/i	n/i	472,460,373,358,307,279	Unidentifed contaminant, TMS ester
42.24	4177920	n/i	n/i	576,487,432,355,331,246	Reichstein's Substance, TMS ester
44.50	4177920	878	93	664,575,486,433,396,330	4-Pregnene-17α,20-diol-3-one, TMS ester
51.95	3047424	n/i	n/i	592,503,395,375,357,283	17α-Hydroxy-progesterone, TMS ester
n/i = no library fit available					

2.4.3 Solid phase extraction of steroid mixes

A stock solution of testosterone **26**, 17α-hydroxyprogesterone **30a**, Reichstein's Substance **30b** and cholesterol **32a** (100 mg respectively) in methanol (100 ml) was prepared. Working samples were prepared by diluting the stock solution (250 µl) into water (250 ml). The samples were extracted through 2 brands of SPE cartridges (Sep Pac C18 and Bakerbond C18). The cartridges were washed with methanol (2 x 5 ml) and water (2 x 5 ml). The sample was applied using vacuum and a Teflon line. After the samples had been aspirated, the cartridges were air dried (15 min.) The steroids were eluted with methanol (3 x 5 ml). The samples were concentrated to a low volume, transferred to ½ dram vials, flow evaporated (40°C), derivatised as previously described and analysed (Table 2.7).

Table 2.7: Derivatised steroid standards, retention times, TICs and significant ions

Ret. time min	TIC	Rev fit	For fit	Significant ions *m/z*	Identity
Steroid mix, sample identity = sue247					
30.00	12288	n/i	n/i	447,432,357,211,183,129	Testosterone, TMS ester
33.64	12928	n/i	n/i	373,358,282,236,211,129	Unidentified TMS ester
41.74	602112	863	561	459,369,330,247,213,129	Cholesterol TMS ester
Baker SPE, sample identity = sue248					
6.22	405504	905	692	243,174,154,147,130,73	4-*bis*(Trimethylsilyl) amino-butanoic acid, TMS ester
30.49	11328	n/i	n/i	448,432,374,342,268,211	Testosterone TMS ester
33.65	8448	n/i	n/i	105,91,75,73,55	Unidentified TMS ester

Sep Pac SPE, sample identity = sue249					
11.73	700416	740	578	385,173,148,133,119,73	9,12,15-Octatrienoic acid, TMS ester
30.24	9472	n/i	n/i	433,358,343,316,248,73	Testosterone TMS ester

n/i = no library fit available

Recoveries of testosterone **26** were calculated based on the TIC of the steroid mix and were 92 % and 77 % for the Baker and Sep Pac cartridges respectively. The other steroids in the mixture were not detected.

2.5 Fishery samples

2.5.1 Extraction of spiked fishery samples

Extraction procedure 2 was used for subsequent work with one minor modification. The solvent used in the elution step was allowed to soak into the cartridges (3 min) before being aspirated through the cartridges. Samples (1 .0 L) were obtained from the hatcheries run by Bristol Water Plc. The samples used were from the following sites: Horseshoe Pond, Blagdon Lake, Mill Leat, River Yeo Gauging Weir, Langford Spring, Eel Grid and Rickford Spring. A water sample (1.0 L) was spiked with testosterone **26** standard (500 µl, 100 µg/ml in methanol). The extraction was as previously described. The samples were evaporated to incipient dryness (Turbovap, 50°C). The samples were reconstituted in dried methanol (100 µl) and analysed by GC-MS (40(3) x 20 to 260(45)).

The samples gave the following results; non-extracted testosterone **26** std (10 mg/100 ml), one peak: 21.2 minutes (TIC 76800, testosterone **26**) The 50 µg testosterone **26** std showed two peaks: 16.4 (TIC 675840, rev. fit 949, *bis*(2-ethylhexyl) phthalate **34**) and 21.2 minutes (TIC 186368, testosterone **26**). The recovery was calculated using the following equations:

non-extracted standard contained 0.1 µg/µl, extracted standard contained 0.5 µg/µl

$$\therefore \text{expected response} = \frac{0.5 \times 76800}{0.1}$$

$$= 384000$$

$$\text{recovery} = \frac{186368}{384000} \times 100$$

$$= 48.5\%$$

All the fishery samples gave two peaks at 10.8 min (phytane **33b**) and 16.4 min (*bis*(2-ethylhexyl) phthalate **34**). No other peaks were detected.

2.5.2 Extraction of fish holding tanks at Blagdon site

Fish holding tanks at Blagdon site were hand dipped and the samples (1.0 L) were stored in brown glass bottles with refirgeration until extracted the following day. The samples extracted were as follows:

Sample identity	Site description
Samples 1 & 2	Tank 1 holding approximately 30 000 x 325 g rainbow trout.
Samples 3 & 4	Tank 2 contained water flowing through from tank 1 and holding approximately 10 500 x 1 kg rainbow trout
Samples 5, 6, 7	Outlet from the 4 stew ponds connected to the outlet of tank 2, holding approximately 2500 x 5 kg rainbow trout.

In summary, the water flowed in through tank 1, on through tank 2 and finally out through the stew ponds.

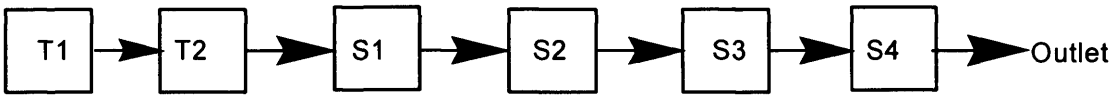

Fig 2.5 Fish farm sampling schematic

Extractions were performed by either solid phase extraction as previously described (Section 2.3.2), or by liquid/liquid extraction. For the liquid/liquid extraction, dichloromethane (30 ml) was added to the bottle and shaken (5 min) and the contents transferred to a separating funnel. The sample bottle was rinsed with dichloromethane (10 ml), which was added to the separating funnel. The funnel was shaken (5 min), the contents were allowed to settle and the lower organic layer run off into a flask. The aqueous phase was extracted with dichloromethane (2 x 20 ml). The aqueous layer was discarded and the separating funnel rinsed with dichloromethane (20 ml). The combined dichloromethane extracts were dried over anhydrous sodium sulphate, filtered and flow evaporated (40°C) and reconstituted with dried methanol (100 µl). Samples were analysed by GC-MS (40(3) x 15 to 260(10).

Samples 1, 3, 5 and 7 were extracted using the solid phase method. A water sample and sample 7 were spiked with testosterone **26** std (250 µl, 0.1 mg/ml) prior to extraction. Samples 2, 4, 6 were extracted using the liquid/liquid technique. Blanks were also extracted using the same conditions.

The non-extracted standard contained 8 peaks: 10.7, 11.9, 12.9, 13.8, 14.5, 15.4, 16.1 min (7 x siloxanes from the column lining), 24.2 min (TIC 12224, testosterone **26**).

The SPE water standard gave 2 peaks: 19.5 min (*bis*(2-ethylhexyl) phthalate **34**) and 24.3 min (TIC 52736, testosterone **26**). The recovery was 86.3% (calculated as previously described). The water blank gave 4 peaks: 12.7, 14.4, 16.1 (3 x siloxanes) and 19.5 min (*bis*(2-ethylhexyl)phthalate **34**). The TIC for the testosterone **26** peak in sample 7 was 34048 and the

recovery was 55.7%.

The SPE fishery samples were compared against the water blank, and corresponding peaks excluded. Sample 1, one peak: 10.7 min (phytane **33b**). Samples 3, 5 and 7 contained this peak, and a further peak at 28.4 min (cholesterol **32a**). No other peaks were detected.

The water blank, liquid/liquid extract contained a peak at 19.5 min (*bis*(2-ethylhexyl) phthalate **34**) as seen previously. No other peaks were detected.

2.6 Extraction of rainbow trout tissue

A farmed rainbow trout (age and sex unknown) was purchased from a local fishmonger. The parts of the fish subject to extraction were the mucus scraped from the skin (samples 1 & 2), the contents emitted from the abdomen after application of gentle pressure (sample 3), part of the abdominal organs (samples 4 & 9), skin (samples 5 & 6), water blanks (samples 7 & 8) and testosterone **26** spiked standards (samples 10 & 11). The samples were split into two sets (set 1 consisted of samples 1, 3, 5, 7, 9, 11 and set 2 consisted of 2, 4, 6, 8, 10).

2.6.1 Extraction of set 1

Set 1 were extracted by grinding the tissue sample with saturated ammonium sulphate (1 ml, pH 1 with HCl). The sample was extracted with diethyl ether/ethanol (2 x 4 ml, 80/20 *v/v*) solution in an ultrasonic bath (2 min). The organic layers were combined, dried over anhydrous sodium sulphate, decanted into clean test tubes and the sodium sulphate washed with a further aliquot of the diethyl ether/ethanol solution (4 ml). The extracts were flow evaporated and reconstituted by addition of dichloromethane (500 µl). The samples were analysed by GC-MS (40(3)x15 to 260(45)).

The extracted water blank produced peaks at 7.22, 7.57 (2 x reagent extractables), 12.87, 13.77, 14.60, 15.38, 16.00, 16.77 (6 x siloxanes) min. Testosterone **26** recovery check: unextracted, TIC 468473; extracted, TIC 358861; recovery 76.6 %. Table 2.8 shows the peaks identified with calculated Kovats Indices in the linear range of the temperature program (3-18 min).

Table 2.8: Ammonium sulphate, diethyl ether/ ethanol trout extracts, retention times, TICs and significant ions

Ret. time, min	Peak TIC	Rev. fit	Significant ions *m/z*	Kovats Index	Identity
Sample 1, skin mucus, TIC =4867048, sample identity = sue073					
11.50	102400	946	148,104,76,61,50,38	1580	Phthalic anhydride
15.48	146432	939	139,125,111,97,83,69	2017	Hexadecene
20.80	115712	n/i	368,247,213,145,105,81	n/c	Cholesterol, ester 1 **32b**
22.24	36096	n/i	368,314,255,145,105,81	n/c	Cholesterol, ester 2 **32b**
22.87	220160	n/i	368,247,213,147,105,81	n/c	Cholesterol, ester 3 **32b**
28.70	29952	889	386,353,301,275,213,107	n/c	Cholesterol† **32a**
Sample 3, stomach contents, TIC = 62759700, sample identity = sue074					
13.58	1884160	956	228,185,143,129,97,73	1816	Tetradecanoic acid†
15.18	2457600	860	256,213,185,157,129,73	1989	Hexadecanoic acid†
16.40	2490368	805	284,241,185,129,97,73	2148	Octadecanoic acid†
17.90	2211840	n/i	166,133,119,105,91,79	2454	C_{24} Aliphatic hydrocarbon
18.97	749568	n/i	185,131,119,105,91,79	n/c	$>C_{24}$ Aliphatic hydrocarbon
19.42	1818624	851	173,131,119,105,91,79	n/c	$>C_{24}$ Aliphatic hydrocarbon
22.87	33280	918	368,326,283,247,213,147	n/c	Cholesterol, ester 3 **32b**
24.27	32256	n/i	366,281,253,213,171,145	n/c	Dehydrocholesterol derivative
29.17	175104	866	386,353,301,275,255,213	n/c	Cholesterol† **32a**
31.62	108544	840	369,300,271,213,159,105	n/c	Desmosterol
Sample 5, trout skin, TIC = 21609182, sample identity = sue075					
9.25	327680	n/i	102,89,74,56,45	993	Benzoyl containing compound
10.28	417792	n/i	268,113,99,85,71,57	1314	Pristane **33a**
11.85	3178496	n/i	282,183,113,99,85,71,57	1624	Phytane **33b**
13.63	177152	899	278,179,123,109,95,81	1836	Dodecanol
14.90	303104	916	256,227,213,129,97,73	1959	Hexadecanoic acid†
15.52	152576	825	242,227,133,108,91,79	2028	6,9,12-Octatrienoic acid methyl ester
16.28	89088	n/i	284,264,213,129,103,73	2130	Octadecanoic acid†
20.02	26368	886	188,147,119,105,91,79	n/c	8,11,14-Eicosatrienoic acid **40**
20.87	104448	n/i	136,121,95,81,69	n/c	Squalene **35**
22.85	2592	n/i	368,255,213,161,147,105	n/c	Cholesterol ester 3 **32b**
28.84	93184	895	386,301,275,213,159,145	n/c	Cholesterol† **32a**

n/i = no library fit available, ♯related compounds† confirmed by comparison to authentic standard n/c = not calculated

2.6.2 Extraction of set 2

The tissue was ground with a pestle and mortar in water (2 ml) and extracted by sonication (2 min) in dichloromethane (4 ml). Samples 2 and 4 formed an emulsion which was broken by centrifugation (2000 rpm, 5 min). The organic layer was set aside and the residue re-extracted by sonication (2 min) in dichloromethane (4 ml). The organic layers were combined and dried over anhydrous sodium sulphate sparged with dichloromethane (4 ml). The samples were flow evaporated and reconstituted with dichloromethane (250 μl). GC

program 40(3)x15 to 260(45)

The extracted water blank produced peaks at 6.05 and 8.43 minutes (reagent extractable material). The following peaks were detected (Table 2.9):

Table 2.9: Dichloromethane trout extracts, retention times, TICs and significant ions

Ret. time, min	Peak TIC	Rev. fit	Significant ions *m/z*	Kovats Indices	Identity
Unextracted testosterone **26** std, TIC = 462993, sample identity = sue077					
13.02	33024	875	242,211,199,143,87,74	1777	Methyl tetradecanoate
14.43	77824	n/i	270,227,199,143,87,74	1913	Methyl hexadecanoate
15.77	20224	913	264,152,111,97,83,74	2062	Methyl octadecenoate
24.2	1584	611	288,246,228,203,124,91	n/c	Testosterone **26** *
Sample 2, skin mucus, TIC = 47875, sample identity = sue080					
10.93	4132	709	180,151,124,91,77,38	1460	1-Methyl-4-(1-methylpropyl)thio benzene
12.83	7808	825	122,106,78,51,44	1749	Nicotinamide† **36**
28.75	2800	n/i	91,67,55,44	n/c	Cholesterol† **32a**
Sample 4, internal organs TIC = 4673406, sample identity = sue082					
8.42	38912	929	154,125,111,97,83,69	655	2-Propyl 2-heptanal
11.83	720896	966	268,183,127,113,99,85	1621	Phytane **33b**
13.50	81920	919	228,185,143,129,97,73	1826	Tetradecanoic acid†
14.98	376832	917	256,213,185,129,97,73	1968	Hexadecanoic acid†
16.25	176128	917	264,213,185,97,83,69	2128	*cis*-9-Octadecenoic acid† **38a**
28.9	79872	878	386,301,275,213,145,105	n/c	Cholesterol† **32a**
Sample 6, skin extract, TIC = 6061761*, sample identity = sue083					
6.08	74752	930	86,71,58,43	n/c	3-Penten-2-ol
8.43	52224	930	154,125,107,97,83,69	659	2-Propyl-2-heptenal
10.33	77824	924	113,99,85,71,57,43	1314	Pristane **33a**
11.87	1179648	960	268,183,127,113,99,85	1627	Phytane **33b**
12.27	25088	903	126,111,97,83,69,56	1685	3-Octadecene
13.63	15232	n/i	278,167,123,109,95,81	1832	Dodecanol
22.35	52992	n/i	386,353,301,275,213,105	n/c	Cholesterol ester 2 **32b**
28.89	36096	879	386,368,301,275,213,105	n/c	Cholesterol† **32a**

n/i = no library fit available, n/c = not calculated, *not reconstituted in dichloromethane, liquid sample† confirmed by comparison to authentic standard

2.6.3 Re-analysis of some of the skin scrape and extracted skin samples

These samples had been stored frozen and were re-analysed to confirm the earlier findings (Table 2.10). A fatty acid standard comprising C_6-C_{18} with cholesterol **32a** and a nicotinamide **36** standard were also run to confirm retention times and spectra (Table 2.2). GC program 40(3)x15 to 260(13).

Table 2.10: Reanalysis of some trout extracts, retention times, TICs and significant ions

Ret. time, min	TIC	Rev fit	Significant ions *m/z*	Kovats Index	Identity
Sample 6, skin extract, TIC = 21528028, sample identity = sue102					
5.88	87040	n/i	86,71,58,53,43	n/c	2-Penten-2-ol
8.25	77824	961	154,125,111,107,83,69	n/c	2-Propyl-2-heptenal
10.15	244736	968	127,113,99,85,71,57	1266	Pristane **33a**
11.68	3276800	956	183,155,127,113,85,71	1405	Phytane **33b**
12.08	139264	940	173,140,126,111,97,83	1660	3-Octadecene
13.45	262144	889	278,137,123,109,95,81	1815	Dodecanol
15.33	323584	n/i	242,227,119,108,91,79	2005	Unsaturated C_{16} fatty acid methyl ester
20.48	238592	865	410,149,136,121,95,81	n/c	Squalene **35**
27.92	90112	846	386,301,275,213,145,105	n/c	Cholesterol† **32a**
Sample 5, skin extract, TIC = 43418220, sample identity = sue104					
3.53	1835008	757	119,103,91,75,56,44	n/c	2,2-Dimethoxy-*N*-methyl-ethanamine
8.23	88064	939	166,154,125,109,83,69	565	2-Propyl-2-heptenal
9.08	491520	n/i	145,102,89,74,56,45	930	Mixed component peak
10.03	606208	714	145,127,117,89,71,43	1242	Diethyl malate
11.67	4161536	943	183,127,113,99,85,71	1596	Phytane **33b**
12.07	215040	n/i	140,126,111,97,83,69	1656	3-Octadecene
13.30	3293184	n/i	256,213,157,129,101,88	1803	Ethyl tetradecanoate*
13.68	95232	n/i	270,227,157,115,101,88	1840	Ethyl pentadecanoate*
13.98	256000	n/i	270,227,157,115,101,88	1871	C_{16} Fatty acid ethyl*
14.68	4112384	n/i	284,241,157,115,101,88	1937	Ethyl hexadecanoate*
15.33	258048	n/i	242,227,133,119,108,91	2005	Methyl-5,1,14,17-eicosatetraenoate type ester, likely C_{18}
15.97	1802240	913	310,264,222,180,110,97	2079	>C_{18} Poly unsaturated fatty acid
16.30	344064	n/i	208,161,147,108,91,79	2130	Methyl eicosa-5,8,11,14,17-pentaenoate type ester, likely C_{19}
17.12	1261568	n/i	292,250,208,137,111,101	2276	Nonadecenoic type acid
17.45	1114112	935	215,133,119,105,91,79	2346	Methyl eicosa-5,8,11,14,17-pentaenoate*
18.20	544768	892	320,278,236,155,111,97	n/c	*cis*-9-Octadecenoic acid type ethyl ester
18.68	835584	n/i	201,159,131,119,105,91	n/c	Methyl eicosa-5,8,11,14,17-pentaenoate* type compound
20.40	130048	864	368,353,255,247,145,121	n/c	Cholesterol ester 1♯ **32b**
21.75	25600	892	368,353,314,255,213,145	n/c	Cholesterol ester 2♯ **32b**
22.29	95232	945	368,353,247,213,147,105	n/c	Cholesterol ester 3♯ **32b**
27.77	9728	n/i	386,301,275,213,145,107	n/c	Cholesterol† **32a**
Sample 1, skin scrape, TIC = 8598629, sample identity = sue108					
10.02	91136	852	56,55,45,43	1242	3-Methyl-4-pentenol
10.27	17920	948	135,108,91,82,69,63	1312	Benzothiazole
13.67	10112	875	228,185,129,97,83,73	1839	Tetradecanoic acid†
14.77	626688	900	256,213,185,157,129,73	1945	Hexadecanoic acid†
15.35	129024	n/i	224,125,111,97,83,69	2005	Hexadecene
16.07	344064	938	264,213,185,129,111,97	2096	*cis*-9-Octadecenoic acid† **38a**
16.70	45312	n/i	239,129,111,101,82,73	2200	Unsaturated C_{19} fatty acid ester
17.90	51456	n/i	248,149,135,121,95,81	2454	Polyunsaturated acid likely C_{20}

20.48	22272	883	368,353,247,213,159,145	n/c	Cholesterol, ester 1♯ **32b**
21.85	3024	n/i	368,353,314,255,213,105	n/c	Cholesterol, ester 2♯**32b**
22.40	21504	942	368,353,247,213,147,105	n/c	Cholesterol, ester 3♯**32b**
28.00	6464	n/a	386,275,255,213,159,145	n/c	Cholesterol† **32a**
Sample 2, skin scrape, TIC = 342235, sample identity = sue109					
6.10	11008	903	136,121,93,91,79,77	n/c	β-Phellandrene
7.70	10560	897	123,109,95,84,79,67,55	315	7-Methyl-3,4-octadiene
10.77	9024	805	180,151,124,91,79	1412	1-Methyl-4-(1-methylpropyl)thio-benzene
11.68	1952	n/i	113,97,85,71,57	1592	Phytane **33b**
12.68	24832	923	122,106,94,78,51	1732	Nicotinamide† **36**
15.35	17152	961	154,139,125,111,97,83	2005	Hexadecanol
28.00	664	n/a	368,353,301,255,213,163	n/c	Cholesterol† **32a**

*,♯,‡ homologous series of compounds, †confirmed by comparison to authentic standard, n/i = no library fit available, n/c = not calculated, Similar types of compounds were reported for both extraction procedures and sample types.

2.7 Repeat of fish extraction

2.7.1 Neutral tissue extraction

A small farmed rainbow trout (approx. 1 kg) was purchased. Various parts of the fish were divided and subject to the two extraction procedures as described in section 2.6.2 and 2.6.1. The second extraction procedure used ammonium acetate in place of ammonium sulphate as this was unavailable. The samples extracted with water were centrifuged (2000 rpm, 5 min) to break the emulsion formed. The combined extracts were dried over anhydrous sodium sulphate, flow evaporated, reconstituted in dichloromethane (250 µl) and analysed by GC-MS (Tables 2.11, 2.12). GC program (40(3)x15 to 260(13)).

Table 2.11: Dichloromethane trout extracts, retention times, TICs and significant ions

Ret. time, min	TIC	Rev fit	For fit	Significant ions *m/z*	Kovat Index	Identity
Sample 4, skin scrape, TIC = 17323672, sample identity = sue121						
12.6	n/i	n/i	n/i	122,106,94,78,51	1725	Nicotinamide† **36**
13.37	111616	930	909	228,185,171,129,115,73	1805	Tetradecanoic acid†
14.83	1294336	883	854	256,213,185,171,129,73	1955	Hexadecanoic acid†
15.35	524288	941	923	224,153,125,111,83	2006	Cyclohexadecane
16.12	847872	822	783	264,222,123,111,97,83	2106	*cis*-9-Octadecenoic acid† **38a**
17.85	31744	n/i	n/i	429,371,355,315,117,83	2441	Polyunsaturated acid likely C_{20}
28.60	9344	751	622	386,353,301,275,213,145	n/c	Cholesterol† **32a**
Sample 2, stomach contents, TIC = 29365340, sample identity = sue122						
13.38	327680	935	915	228,185,129,73,60	1805	Tetradecanoic acid†
14.90	2490368	884	865	256,213,129,73,60	1959	Hexadecanoic acid†
15.45	50432	858	814	270,256,129,83,73,69	2018	Heptadecanoic acid
16.13	1572864	878	822	284,129,97,83,73,69	2106	Octadecanoic acid†
17.48	122880	n/i	n/i	284,264,79,69,67,57	2354	Linolenic acid
17.68	199680	893	800	213,119,93,91,79,67	2399	8,11,14-Eicosatrienoic acid **40**

18.87	177152	884	833	299,239,134,98,84,74	n/c	1-Glyceryl hexadecanoate
19.08	222208	828	651	256,119,105,97,79,67	n/c	Methyl eicosa-5,8,11,14,17-pentaenoate
20.68	22784	812	744	284,267,185,129,98,57	n/c	1-Glyceryl octadecanoate
28.74	8576	816	679	386,368,353,301,275,255	n/c	Cholesterol† **32a**
Sample 6, internal organs, TIC = 40104984, sample identity = sue123						
13.47	1589248	934	914	228,185,129,73,60	1818	Tetradecanoic acid†
15.00	2195456	870	855	256,213,129,73,69,60	1968	Hexadecanoic acid†
15.28	144384	795	700	256,129,79,67,55,41	2000	Hexadecenoic acid
15.55	205824	n/a	n/a	270,256,250,227,213,129	2031	Heptadecanoic acid
16.27	1802240	n/a	n/a	284,264,111,97,83,69	2129	Octadecanoic acid†
16.60	1146880	859	751	207,180,119,108,91,79	2178	Polyunsaturated C_{18} acid ester
16.97	372736	715	520	285,211,203,190,130,117	2246	1-Hexadecyl-2,3-dihydro-1H-indene
17.75	1081344	848	762	175,133,119,105,91,79	2416	1,4-Methano-benzocyclodecene
19.07	74752	n/a	n/a	264,256,221,213,171,129	n/c	Methyl eicosa-5,8,11,14,17-pentaenoate
28.24	30208	687	570	386,368,353,301,275,255	n/c	Cholesterol† **32a**
Sample 8, skin extract, TIC = 20054076, sample identity = sue124						
10.17	199680	n/i	n/i	212,141,121,99,85,71	1268	Pristane **33a**
11.72	3096576	n/i	n/i	183,155,141,127,113,71	1604	Phytane **33b**
12.10	126976	n/a	n/a	266,196,140,126,111,97	1666	C_{16} type alkene
12.63	379312	916	894	122,106,78,51	1732	Nicotinamide† **36**
12.87	97280	924	901	242,211,199,185,143,74	1756	Methyl tetradecanoate
13.48	140288	881	849	278,228,185,123,95,81	1818	Dodecanol
14.28	487424	885	801	270,227,143,87,74,55	1898	Methyl hexadecanoate
14.80	270336	879	858	256,213,129,73,60,43	1955	Hexadecanoic acid†
15.37	67584	n/i	n/i	256,242,227,119,109,91	2010	C_{17} Unsaturated fatty acid
15.62	137216	913	882	264,222,180,97,83,74	2039	Methyl octadecenoate
16.13	86016	n/i	n/i	264,256,98,85,55,43	2112	*cis*-9-Octadecenoic acid **38a**
16.82	31488	952	904	292,250,208,137,111,97	2223	Methyl 11-eicosenoate
17.92	29696	881	810	320,291,278,236,131,111	2460	Methyl 10-nonadecenoate
18.40	99328	910	841	206,159,131,119,105,91	n/c	Methyl eicosa-5,8,11,14,17-pentaenoate
20.58	126976	883	835	203,191,136,95,81,69	n/c	Squalene **35**
28.20	19968	555	434	386,368,301,255,213,135	n/c	Cholesterol† **32a**

n/i = no library fit available, n/c = not calculated, †confirmed by comparison to authentic standard

Table 2.12: Ammonium acetate trout extracts, retention times, TICs and significant ions

Ret. time, min	TIC	Rev fit	For fit	Significant ions *m/z*	Kovat Index	Identity
Sample 9, internal fatty strip, TIC = 7528919, sample identity = sue125						
9.33	62208	881	683	152,137,124,109,96,82	n/c	Cyclodecene
11.70	1605632	n/i	n/i	183,155,141,127,113,99	1603	Phytane **33b**
13.38	209920	927	896	228,199,185,129,73,60	1808	Tetradecanoic acid†
14.28	14400	834	679	316,270,227,185,143,129	1898	Methyl hexadecanoate
14.85	188416	n/i	n/i	256,213,185,171,129,111	1955	Hexadecanoic acid†
16.10	185344	935	916	264,185,129,111,97,83	2137	*cis*-9-Octadecenoic acid† **38a**

17.37	7680	n/i	n/i	292,264,221,185,129,111	2337	11-Eicosenoic acid
17.70	17152	n/i	n/i	256,207,185,157,129,91	2304	8,11,14-Eicosatrienoic acid **40**
28.09	25856	861	759	386	n/c	Cholesterol† **32a**
Sample 3, skin scrape, TIC = 43037988, sample identity = sue130						
6.20	356352	860	791	101,83,74,73,57,43	n/c	4-Methyl pentanoic acid
10.34	528384	n/i	n/i	99,82,70,55,42	1314	Furanone type compound
11.30	1753088	946	918	150,104,91,77,65,51	1423	Phenylpropanoic acid
13.60	1949696	935	916	228,185,129,73,60	1833	Tetradecanoic acid†
14.20	552960	897	885	242,199,182,129,73,60	1889	Pentadecanoic acid
15.12	1720320	817	790	256,213,182,129,73,60	1986	Hexadecanoic acid†
15.52	262144	n/i	n/i	268,256,213,185,69,55	2034	Heptadecenoic acid
16.30	2310144	n/i	n/i	284,264,241,185,129,97	2130	Octadecanoic acid†
17.39	299008	922	874	292,111,97,83,69,55	2330	8,11,14-Nonadecatrienoic acid
Sample 1, stomach contents, TIC = 22400652, sample identity = sue131						
4.20	671744	721	682	88,73,66,55,42	n/c	Butanoic acid
5.00	577536	730	724	87,74,57,41	n/c	2-Methylbutanoic acid
6.47	761856	868	860	101,87,83,74,57,43	n/c	4-Methylpentanoic acid
10.29	933888	928	899	136,91,65,51,39	1314	Phenylethanoic acid
11.30	1884160	947	935	150,131,104,91,77,65,51	1528	Phenylpropanoic acid
12.39	2162688	793	748	137,107,91,77	1702	4-Hydroxyphenylethanol
13.49	59904	910	876	228,185,129,91,73,60	1822	Tetradecanoic acid†
14.92	1867776	915	907	256,213,129,73,60,57	1959	Hexadecanoic acid†
16.17	319488	n/i	n/i	284,264,256,185,129,73	2118	*cis*-9-Octadecenoic acid† **38a**
Sample 5, internal organs, TIC = 53795900, sample identity = sue132						
4.37	1556480	730	698	88,73,60,55,42	n/c	Butanoic acid
6.10	315392	972	990	101,87,83,74,73,60,57	n/c	4-Methylpentanoic acid
8.80	917504	n/i	n/i	129,114,86,73,60,56	768	1,5-Pentadiamine
10.3	1212416	923	892	136,92,91,77,65	1314	Phenylpropanedioic acid
11.13	1622016	n/i	n/i	150,117,90,63	1504	Indole type derivative
13.73	2080768	894	878	228,185,129,73,60	1896	Tetradecanoic acid†
14.28	978944	902	891	242,199,185,171,129,73,	1898	Pentadecanoic acid
15.25	2260992	751	726	256,213,185,129,97,73	1938	Hexadecanoic acid†
15.60	188416	n/i	n/i	268,256,213,129,97,73	2039	Heptadecanoic acid
16.05	491520	n/i	n/i	320,264,237,194,123,97	2096	1-Glyceryl hexadecanoate
16.35	2244608	734	677	284,264,129,111,97,69	2149	Octadecanoic acid†
17.42	483328	n/i	n/i	292,250,185,129,97,83	2335	Nonadecatrienoic acid
18.57	121856	n/i	n/i	320,264,111,97,83,69	n/c	Glyceryl hexadecanoate
19.18	139264	n/i	n/i	320,256,213,152,119,79	n/c	Glyceryl hexdecanoate
28.42	3456	565	424	386,368,353,275,107,95	n/c	Cholesterol† **32a**
Sample 7, skin extract, TIC = 45464344, sample identity = sue133						
3.47	339968	n/i	n/i	88,73,60,45,43	n/c	Short chain fatty acid
5.02	536576	850	769	87,74,57,41	n/c	2-Methylbutanoic acid
11.13	1835008	n/i	n/i	150,117,90,63,59	1504	Indole type derivative
11.75	1844160	919	895	183,155,141,127,113,99	1604	Phytane **33b**
13.63	2342912	932	909	228,185,129,97,85,73	1833	Tetradecanoic acid†
14.23	339968	901	879	242,228,213,199,185,73,	1893	Pentadecanoic acid
15.12	2146304	834	816	256,213,129,83,73,69	1986	Hexadecanoic acid†

16.28	1916928	n/i	n/i	264,222,111,97,83,69	2130	*cis*-9-Octadecenoic acid† **38a**
17.45	14400	902	745	292,264,213,185,129,111	2352	Nonadecatrienoic acid
19.15	38424	n/i	n/i	256,129,111,91,79,69	n/c	1-Glyceryl hexadecanoate
28.5	na	n/i	n/i	386,368	n/c	Cholesterol† **32a**

nd = not detected, †confirmed by comparison to authentic standard, na = not applicable, n/i = no library fit available, n/c = not calculated

2.7.2 Acidification of dichloromethane extracts from section 2.7.1

Dichloromethane (200 µl) was added to the samples 2 and 4 to obtain sufficient sample volume. An aliquot of the diluted sample (100 µl) and dichloromethane (100 µl) were placed in a vial and thoroughly mixed. Dilute hydrochloric acid solution (500 µl, 10 % *v/v*) was added and the mixture warmed gently on a hot plate (setting 1, 20 minutes). The samples were cooled to room temperature and the dichloromethane layer transferred to a clean vial. The acid fraction was washed with dichloromethane (2 x 200 µl) and the organic extracts combined. The samples were flow evaporated to approximately half the original volume. Diluted and acidified samples were analysed by GC-MS(Table 2.13), GC program (40(3.5)x15 to 260(13)). The comparison of the extracted blanks did not reveal any significant peaks.

Table 2.13: Trout extracts, retention times, TICs and significant ions

Ret. time, min	TIC	Rev fit	For fit	Significant ions *m/z*	Kovats Index	Identity
Sample 2, stomach contents, TIC = 3672653, sample identity = sue145						
13.88	6848	907	837	228,185,129,87,73	1788	Tetradecanoic acid†
15.27	319488	894	866	256,213,185,129,115,73	1953	Hexadecanoic acid†
16.55	123904	n/i	n/i	264,151,111,97,83,69	2111	Octadecanoic acid†
17.93	4352	869	717	129,115,99,83,69,55	2333	1-Glyceryl hexadecanoate
18.25	19456	n/i	n/i	372,315,239,117,130,101	n/c	Long chain fatty acid cinnamate type ester
19.23	8320	888	804	257,239,185,129,112,98	n/c	1-Glyceryl hexadecanoate
28.75	4480	361	220	387,354,302,275,145	n/c	Cholesterol† **32a**
Sample 2a, acidified stomach contents, TIC = 795271, sample identity = sue146						
13.98	888	n/i	n/i	97,83,71	1805	Tetradecanoic acid†
15.20	42496	871	825	256,213,185,129,97,73	1944	Hexadecanoic acid†
16.55	9280	n/i	n/i	284,256,185,157,97,73	2116	Octadecanoic acid†
18.25	5952	n/i	n/i	315,239,130,117,101,75	n/c	Long chain fatty acid cinnamate type ester
28.4	12544	n/i	n/i	387,354,302,275213,145	n/c	Cholesterol† **32a**
Sample 4, skin scrape, TIC = 5585008, sample identity = sue147						
7.28	112640	n/i	n/i	86,56,42	n/c	γ-Butyrolactone
13.30	116736	n/i	n/i	171,111,97,83,69,55	1720	Methyl 2-hydroxy-dodecanoate
13.88	12288	929	840	228,185,143,129,87,73	1788	Tetradecanoic acid†
15.25	446464	915	883	256,213,185,157,129,73	1953	Hexadecanoic acid†
15.78	144384	n/i	n/i	125,111,97,83,69,55	2016	1-Hexadecanol
16.53	286720	959	913	284,264,241,151,129,97	2111	*cis*-9-Octadecenoic acid† **38a**

18.25	7744	n/i	n/i	372,315,239,130,117,101	n/c	Long chain fatty acid cinnamate type ester
18.92	28416	827	359	198,155,134,109,91,69	n/c	Benzenesulphonamide derivative
23.37	22528	873	795	351,274,197,154,120,77	n/c	Hydroxytriphenyl stannane
28.65	27648	n/i	n/i	387,354,302,255,213,119	n/c	Cholesterol† **32a**
Sample 4a, acid skin scrape, TIC = 762263, sample identity = sue148						
7.20	32256	637	625	86,56,42	n/c	γ-Butyrolactone
13.30	64768	n/i	n/i	171,111,97,83,69,55	1720	Methyl 2-hydroxy-dodecanoate
15.78	9536	n/i	n/i	154,125,111,97,83,69	2016	1-Hexadecanol
16.57	5760	n/i	n/i	377,280,196,182,126,113	2116	1-8(3-Octyloxiranyl)-1-oxooctyl pyrrolidine
28.14	14400	759	626	387,354,302,275,213,145	n/c	Cholesterol† **32a**
Sample 6, internal organs, TIC = 14569057, sample identity = sue150						
13.88	352256	945	890	228,185,143,129,87,73	1788	Tetradecanoic acid†
15.38	860160	881	840	256,213,157,129,115,73	1964	Hexadecanoic acid†
15.95	54016	930	857	250,227,129,111,97,83	2031	Heptadecenoic acid
16.70	618496	848	806	284,264,241,129,111,97	2137	*cis*-9-Octadecenoic acid, **38a** Octadecanoic acid†
16.95	81920	n/i	n/i	278,222,135,121,108,95	2173	Methyl octadecadienoate
17.78	315392	915	840	292,125,111,97,83,69	2304	Eicosenoic acid
18.22	802816	n/i	n/i	166,147,133,119,105,91	n/c	8,11,14-Eicosatrienoic acid **40**
18.90	36864	n/i	n/i	320,166,133,111,97,91	n/c	Unsaturated C_{21} fatty acid
19.53	147456	812	730	147,119,105,91,79,67	n/c	Methyl eicosapentaenoate type compound
28.75	4672	574	399	387,328,275,213,145,109	n/c	Cholesterol† **32a**
Sample 6a, acid internal organs, TIC = 6194415, sample identity = sue151						
13.30	15744	908	707	171,111,97,83,69,55	1720	Dodecanol
13.92	26112	931	866	228,185,129,115,87,73	1797	Tetradecanoic acid†
15.27	286720	868	821	256,213,157,129,83,73	1953	Hexadecanoic acid†
16.58	512000	911	844	264,151,123,111,97,83	2111	*cis*-9-Octadecenoic acid, **38a** Octadecanoic acid†
16.92	43264	895	837	280,264,180,108,91,79	2173	Methyl octadecadienoate
17.73	13824	916	794	292,264,185,123,97,83	2303	Eicosenoic acid
18.10	41216	897	831	166,119,105,91,79,67	2369	8,11,14-Eicosatrienoic acid **40**
28.28	4416	567	393	387,301,275,213,145,107	n/c	Cholesterol† **32a**
Sample 8, skin, TIC = 6668608, sample identity = sue152						
12.15	499712	945	936	183,127,113,85,71,57	1558	Phytane **33b**
13.32	589824	n/i	n/i	171,111,97,83,67,55	1720	Dodecanol
13.92	19968	864	689	278,199,137,123,109,81	1797	Tetradecanoic acid & unsaturated C_{15} acid methyl ester
14.43	67584	n/i	n/i	203,176,158,130,104,75	1858	Unidentified indole type compound
15.00	122880	n/i	n/i	216,190,174,144,128,117	1919	Unidentified
15.25	278528	872	824	256,213,171,129,97,73	1953	Hexadecanoic acid†
16.53	187392	945	891	284,264,185,111,97,83	2110	*cis*-9-Octadecenoic acid, **38a** Octadecanoic acid†
20.92	55552	n/i	n/i	149,136,121,95,81,69	2473	Squalene **35**
28.32	14976	745	623	386,369,301,275,231,105	n/c	Cholesterol† **32a**
Sample 8a, acid treated skin, TIC = 794749, sample identity = sue153						
12.13	155648	965	938	183,127,113,99,85,71	1558	Phytane **33b**
13.32	6528	n/i	n/i	111,97,83,69,55,43	1720	Dodecanol

13.98	19200	n/i	n/i	196,138,124,109,96,82	1805	Mono-unsaturated C_{14} fatty acid ester
15.40	24320	n/i	n/i	248,135,121,111,98,83	1970	Mono-unsaturated C_{16} fatty acid ester
16.85	440	n/i	n/i	129,96,81,61	2155	*cis*-9-Octadecenoic acid **38a**
28.20	3088	694	542	387,354,301,275213,159	n/c	Cholesterol† **32a**
Sample 9, internal fatty strip, TIC = 2922144, sample identity = sue154						
12.13	143360	948	945	183,141,127,113,99,85	1558	Phytane **33b**
13.83	29696	941	903	228,185,171,129,87,73	1788	Tetradecanoic acid†
15.25	252928	847	800	256,227,213,171,129,73	1953	Hexadecanoic acid†
16.53	157696	n/a	n/a	264,222,123,11197,83	2110	*cis*-9-Octadecenoic acid, **38a** Octadecanoic acid†
28.20	5312	n/a	n/a	387,354,302,213,159,105	n/c	Cholesterol† **32a**
Sample 9a, acid treated internal fatty strip, TIC = 434889, sample identity = sue155						
11.22	1072	n/a	n/a	86,85,70,67,57,55	1388	Unidentified
12.13	50432	946	939	183,127,113,9985,71	1558	Phytane **33b**
13.98	5632	n/i	n/i	125,111,96,82,71	1805	Tetradecanoic acid† & unsaturated fatty acid ester
15.28	28160	864	830	256,213,185,129,97,73	1953	Hexadecanoic acid†
16.63	3152	n/a	n/a	111,97,83,73,55	2127	*cis*-9-Octadecenoic acid, **38a** Octadecanoic acid†
28.20	1472	656	446	387,302,275,213,159,107	n/c	Cholesterol† **32a**
†confirmed by comparison to authentic standard, n/i = no library fits available, n/c = not calculated						

2.7.3 Basification of dichloromethane fish extract samples from section 2.7.1

The samples prepared by dichloromethane extraction detailed in section 2.7.1 were taken and an aliquot (200 µl) flow evaporated. Aqueous sodium hydroxide (10% *v/v*, 500 µl) was added to each and mixed. The samples were warmed on a hotplate (setting 8, 30 min) with periodic shaking to ensure thorough mixing. The samples were cooled and extracted with dichloromethane (3 x 200 µl). The samples were flow evaporated to approximately half volume and analysed by GC-MS (Table 2.14), GC program (40 (3.5) x 15 to 260(12.5) inj. 220).

Table 2.14: Trout extracts, retention times, TICs and significant ions

Ret. time, min	TIC	Rev fit	For fit	Significant ions *m/z*	Kovats Index	Identity
Sample 2, stomach contents, TIC = 2101524, sample identity = sue159						
13.85	7168	932	859	228,185,171,143,129,73	1857	Tetradecanoic acid†
15.32	194560	894	869	256,213,129,115,73	1958	Hexadecanoic acid†
16.57	84992	925	865	285,241,185,157,83	2116	*cis*-9-Octadecenoic acid, **38a** Octadecanioc acid†
18.13	2736	894	780	133,119,105,95,91,79	2369	C_{20} Polyunsaturated fatty acid ester
28.42	1744	n/a	n/a	387,369,354,302,277,159	n/c	Cholesterol†¶ **32a**
Sample 2b, base stomach contents, TIC = 41950, sample identity = sue160						
17.57	3408	n/i	n/i	239,185,129,116,98,84	2268	C_{19} type unsaturated fatty acid derivative

18.77	1520	n/i	n/i	129,116,98,83,69,55	n/c	C_{20} type di-unsaturated fatty acid derivative
28.34	380	n/i	n/i	95,93,81	n/c	Cholesterol†¶ **32a**
Sample 4, skin scrape, TIC = 257899, sample identity = sue161						
13.07	2496	779	779	122,106,78,51	1690	Nicotinamide† **36**
13.88	1552	728	717	129,97,83,73	1792	Tetradecanoic acid†
15.23	22784	864	819	257,213,185,129,115,73	1950	Hexadecanoic acid†
16.53	4160	n/i	n/i	129,111,97,83,69,55	2110	*cis*-9-Octadecenoic acid, **38a** Octadecanoic acid†
28.50	n/a	n/a	n/a	386,95,93,81	n/c	Cholesterol†¶ **32a**
Sample 4b, base skin scrape, TIC = 121272, sample identity = sue162						
15.80	10816	928	916	125,111,97,83,69,55	2016	3-Eicosene
28.34	520	n/i	n/i	107,95,91,83,79,71	n/c	Cholesterol†¶ **32a**
Sample 6, internal organs, TIC = 1044394, sample identity = sue163						
13.83	12864	920	858	228,185,143,129,97,73	1785	Tetradecanoic acid†
15.28	86016	864	824	256,213,185,129,115,73	1955	Hexadecanoic acid†
16.57	65536	n/a	n/a	265,165,138,123,111,97	2116	*cis*-9-Octadecenoic acid† **38a**
17.60	4928	820	735	145,133,119,105,97,79	2270	Methyl eicosa-5,8,11,14,17-pentaenoate
28.25	1024	n/a	n/a	387,276,213,145,107,95	n/c	Cholesterol†¶ **32a**
Sample 6b, base internal organs, TIC = 402584, sample identity = sue164						
10.63	4480	868	853	99,85,71,57,43	1275	Pristane **33a**
12.15	83968	942	907	183,155,141,127,113,99,	1558	Phytane¶ **33b**
14.07	6400	898	848	124,109,95,85,71,58	1814	6,10,14-Trimethyl-2-pentadecanone
28.38	1664	na	n/a	388,354,302,213,145,105	n/c	Cholesterol†¶ **32a**
Sample 8, skin, TIC = 2406819, sample identity = sue165						
6.95	19968	840	785	110,95,81,65,53	n/c	3-Ethyl-1,4-hexadiene
9.73	10496	n/i	n/i	152,137,124,109,96,82	1052	Unidentified
11.58	12544	n/i	n/i	166,138,123,110,95,68	1463	Unsaturated fatty acid likely C_{11}
12.17	475136	947	924	183,141,127,113,99,85	1560	Phytane **33b**
12.93	13952	n/i	n/i	161,147,133,117,108,91	1671	Aromatic cyclic type compound
13.30	25600	896	838	242,199,143,129,87,74	1719	Methyl tetradecanoate
13.93	10112	884	837	137,123,109,95,81,68	1797	14-Methyl-8-hexadecen-1-ol
14.73	103424	935	886	271,227,185,143,129,74	1890	Methyl 12-(acetyloxy)-octadecenoate
15.23	854	801	984	257,213,185,129,115,73	1948	Hexadecanoic acid†
16.05	37888	941	904	265,222,143,123,111,96	2047	Methyl octadecenoate
16.53	25856	881	755	265,171,129,111,97,83	2111	*cis*-9-Octadecenoic acid, **38a** Octadecanoic acid†
18.80	8384	890	795	173,145,133,117,105,91	n/c	Methyl eicosa-5,8,11,14,17-pentaenoate
28.38	1504	n/a	n/a	387,370,302,229,159,95	n/c	Cholesterol†¶ **32a**
Sample 8b, base skin, TIC = 2229854, sample identity = sue166						
12.17	471040	952	929	183,127,113,99,85,71	1560	Phytane¶ **33b**
13.3	7616	890	844	137,123,109,95,81,68	1720	14-Methyl-8-hexadecen-1-ol¶
28.37	1840	n/a	n/a	387.355.303.276.133.105	n/c	Cholesterol†¶ **32a**
Sample 9, internal strip, TIC = 655639, sample identity = sue167						
6.93	9216	826	795	110,95,81,67,53	n/c	3-Ethyl-1,4-hexadiene¶

10.62	7232	n/i	n/i	99,85,71,57	1272	Pristane **33a**
12.15	151552	946	900	183,141,113,85,71,57	1558	Phytane¶ **33b**
12.55	4864	n/i	n/i	126,111,97,83,71,56	1618	7-Methyl-6-tridecene
12.80	9472	n/i	n/i	180,137,124,111,83,55	1654	Propyl thio type compound
12.93	6016	n/i	n/i	136,133,117,108,105,91	1671	*cis,cis*-1,3,5-Octatriene¶
13.87	5824	930	867	228,185,143,129,73	1780	Tetradecanoic acid†
15.28	9216	n/a	n/a	257,199,157,123,111,97	1954	Hexadecanoic acid†
16.53	11328	873	741	265,151,129,111,97,83	2110	*cis*-9-Octadecenoic acid, **38a** Octadecanoic acid†
28.35	1280	n/a	n/a	387,369,302,276,199,159	n/c	Cholesterol†¶ **32a**
Sample 9b, base treated internal strip, TIC = 1714205, sample identity = sue168						
6.72	13568	n/i	n/i	132,117,91,79,66,54	n/c	Dicyclopentadiene
6.92	30976	851	795	110,95,81,67,65	n/c	2,4 Heptadienal¶
7.75	7488	866	825	114,98,95,82,69,57	368	Nonanal
7.95	5056	n/i	n/i	124109,95,81,53	451	3,5-Octadien-2-one
9.60	11456	908	806	121,111,97,83,70,57	1016	7-Tetradecene
10.27	19200	n/i	n/i	150,136,121,107,91,81	1195	Terpenoid type compound 1¶
11.15	10688	n/i	n/i	154,137,124,111,83,55	1383	Terpenoid type compound 2
12.17	372736	940	899	183,127,113,99,85,71,57	1560	Phytane¶ **33b**
12.93	21504	n/i	n/i	161,147,133,117,108,91	1671	Unidentified¶
20.97	4000	n/i	n/i	109,99,95,85,81,69	n/c	Squalene **35**
28.45	1712	n/a	n/a	388,370,327,302,213,105	n/c	Cholesterol†¶ **32a**

†confirmed by comparison to authentic standard ¶ occurs in both treated and untreated sample, n/a = not applicable, n/i = no library fit available, n/c = not calculated

2.7.4 Bicarbonate treatment of dichloromethane fish extract samples from section 2.7.1

The ether/ethanol extracts prepared in section 2.7.1 were taken and an aliquot (250 µl) taken from each. The samples were flow evaporated and sodium bicarbonate (2M, 500 µl) was added to each. The samples were warmed on a hot plate (30 min), cooled and hydrochloric acid (10 % *v/v*, 4 drops) added to neutralize the solution. The samples were extracted with dichloromethane (3 x 200 µl), flow evaporated to approximately half volume and analysed by the GC-MS (Table 2.15), GC program (40(3.5)x15 to 260(13)).

Table 2.15: Trout extracts, retention times, TICs and significant ions

Ret. time, min	TIC	Rev fit	For fit	Significant ions *m/z*	Kovats Index	Identity
Sample 2, stomach contents, TIC = 5358050, sample identity = sue173						
4.65	98304	n/i	n/i	88,73,60,44	n/c	Octanoic acid
5.50	67584	807	594	91,87,74,57	n/c	2-Methylbutanoic acid
7.02	97280	770	750	117,101,87,83,73,60	32	4-Methylpentanoic acid
10.73	368640	934	919	136,91,77,65,51	1290	Phenylpropanedioic acid
11.72	737280	892	872	150,105,104,91,77	1488	Phenylpropanoic acid
12.78	143360	805	670	138,107,91,77,65	1651	4-Hydroxy-phenylethanol¶
13.42	95232	n/i	n/i	137,127,109,99,91,81	1735	Pyrrolidine type derivative¶
13.90	10304	788	552	228,171,150,104,91,73	1797	Tetradecanoic acid†¶
15.35	421888	610	560	256,213,157,129,115,73	1958	Hexadecanoic acid†¶

16.02	4096	749	627	270,227,185,129,98,74	2047	Heptadecanoic acid
16.60	257024	919	841	284,241,213,185,129,97	2126	*cis*-9-Octadecenoic acid, **38a** Octadecanoic acid†¶
17.40	25856	n/i	n/i	131,120,107,91,71	2240	Phenyl amino type compound¶
18.78	12224	n/i	n/i	256,198,156,142,129,114	n/c	Cinnamic acid type compound¶
19.52	21504	814	729	227,192,117,105,91,79	n/c	8,11,14-Eicosatrienoic acid¶**40**
28.75	1568	523	374	387,369,314,275,145,109	n/c	Cholesterol†¶ **32a**
Sample 2c, bicarb treated stomach contents, TIC = 3528510, sample identity = sue174						
7.97	33024	892	862	109,107,90,79,63	451	4-Methylphenol
10.98	69632	915	865	117,90,74,63	1327	3-Methylbenzonitrile
11.43	10944	n/i	n/i	147,127,104,99,83	1423	Ketone/pyrrolidine type derivative
12.32	4608	893	655	138,107,91,77,62	1598	3H-Hydroxy-phenylethanol¶
12.92	76800	n/i	n/i	137,127,109,99,81,55	1671	Pyrrolidine/imidazole type compound¶
13.47	5760	822	691	228,185,143,129,85,73	1757	Tetradecanoic acid†¶
14.82	303104	877	826	256,213,171,129,115,73	1904	Hexadecanoic acid†¶
16.08	120832	941	872	284,241,213,185,129,97	2047	*cis*-9-Octadecenoic acid, **38a** Octadecanoic acid†¶
16.90	20736	n/i	n/i	182,154,140,120,107,91	2155	Benzamine type derivative 1¶
17.47	12480	n/i	n/i	193,175,133,121,105,91	2254	Benzamine type derivative 2¶
18.28	9408	n/i	n/i	326,256,184,142,129,114	n/c	1-Glyceryl hexadecanoate¶
19.03	37120	n/i	n/i	192,131,117,105,91,79		8,11,14-Eicosatrienoic acid¶ **40**
19.82	4416	n/i	n/i	352,212,184,156,142,114	n/c	1-Glyceryl ocatdecanoate
28.30	1184	n/a	n/a	372,314,275,231,159,145	n/c	Cholesterol†¶ **32a**
Sample 4, skin scrape, TIC = 9309619, sample identity = sue175						
3.37	131072	693	642	91,78,73,61,45	n/c	Inositol cf **51**
6.13	28672	824	802	101,83,73,60,57	n/c	4-Methylpentanoic acid
10.38	149504	921	888	136,123,105,91,77,65	1235	Phenylpropanedioic acid
11.13	667648	919	898	150,104,91,77,65	1382	Phenylpropanoic acid
13.47	389120	908	832	228,185,171,129,115,73	1757	Tetradecanoic acid†
13.78	15488	839	756	242,199,171,143,129,73	1779	C_{15} fatty acid
14.08	46336	849	780	242,199,171,143,129,73	1815	Pentadecanoic acid
14.98	360448	n/a	n/a	256,213,185,171,157,129	1919	Hexadecanoic acid†
15.48	35072	n/a	n/a	270,213,171,129,111,97	1993	Heptadecanoic acid
16.28	176128	n/a	n/a	264,220,151,111,97,83	2077	*cis*-9-Octadecenoic acid, **38a** Octadecanoic acid†¶
16.53	121856	n/i	n/i	180,147,119,105,91,79	2110	C_{18} Fatty acid ester
17.05	54272	859	797	264,222,180,137,111,97	2185	Methyl *cis*-9-octadecenoate¶
17.38	204800	n/i	n/i	292,249,138,125,111,97	2237	Methyl octadecatrienoate¶
17.68	262144	895	804	166,133,119,105,91,79	2290	Methyl eicosa-5,8,11,14,17-pentaenoate¶
18.73	26880	n/i	n/i	321,277,152,124,111,97	n/c	Unsaturated C_{20} fatty acid ester¶
19.22	18432	n/i	n/i	284,187,159,133,105,91	n/c	Unsaturated C_{20} fatty acid ester
20.15	9728	856	772	241,176,147,133,108,91	n/c	Ethyl eicosa-5,8,11,14,17-pentenoate
28.20	2608	n/a	n/a	369,330,301,255,107,95	n/c	Cholesterol†¶ **32a**
Sample 4c, bicarb. treated skin scrape, TIC = 7762206, sample identity = sue176						
10.03	65280	n/i	n/i	100,99,70,58	1132	Unidentified

13.42	239616	942	877	228,185,143,129,115,73	1735	Tetradecanoic acid†¶
14.12	11008	844	765	242,199,185,143,129,73	1820	Pentadecanoic acid¶
14.88	376832	775	732	256,213,157,129,97,73	1904	Hexadecanoic acid†¶
15.47	13504	937	860	270,227,171,129,111,73	1993	Heptadecenoic acid¶
16.18	335872	n/a	n/a	284,264,151,111,97,83	2062	*cis*-9-Octadecenoic acid, **38a** Octadecanoic acid†¶
16.47	114688	n/i	n/i	180,133,119,105,93,79	2094	Fatty acid C_{18} ester¶
17.05	36096	874	793	264,222,180,137,111,97	2185	Methyl *cis*-9-Octadecenoate
17.32	164864	n/i	n/i	292,249,138,125,111,97	2225	Methyl octadecatrienoate
17.65	154624	n/a	n/a	166,133,119,105,91,79	2308	Methyl eicosa-5,8,11,14,17-pentaenoate¶
18.53	44288	n/i	n/i	321,277,152,124,111,97	n/c	Unsaturated C_{20} fatty acid ester¶
19.08	84992	n/i	n/i	159,133,119,105,91,79	n/c	Unsaturated C_{20} fatty acid ester
28.14	1680	n/a	n/a	387,354,301,275,145,95	n/c	Cholesterol†¶ **32a**
Sample 6, internal organs, TIC = 14037429, sample identity = sue177						
4.15	110592	n/i	n/i	86,73,60	n/c	Octanoic acid
4.72	98304	760	635	128,87,74	n/c	2-Methylbutanoic acid
6.07	32000	815	773	101,83,74,57	n/c	4-Methylpentanoic acid
10.20	311296	934	890	136,91,65	1177	Phenylpropanedioic acid
10.95	197632	935	907	150,104,91,77	1321	Phenylpropanoic acid
13.57	495616	n/i	n/i	228,185,171,143,129,115	1757	Tetradecanoic acid†
14.13	211968	837	776	242,199,185,143,129,73	1821	Pentadecanoic acid
14.18	23040	n/i	n/i	243,222,171,157,129,111	1827	C_{15} Fatty acid
14.38	65536	n/i	n/i	256,211,185,128,101,73	1864	C_{16} Fatty acid
15.18	1310720	503	407	256,213,185,157,129,97	1938	Hexadecanoic acid†
15.60	194560	908	827	250,206,151,125,111,97	1993	Unsaturated C_{17} fatty acid¶
15.92	120832	767	651	310,265,236,194,152,97	2031	Unsaturated C_{17} fatty acid glyceride
16.23	236544	n/i	n/i	285,264,207,133,112,97	2062	*cis*-9-Octadecenoic acid, **38a** Octadecanoic acid†
17.10	238592	n/i	n/i	338,285,265,222,123,97	2196	*cis*-9-Octadecenoic acid ester¶
17.50	794624	n/i	n/i	249,193,175,152,133.91	2254	Fatty acid glyceride ¶
18.33	76800	798	731	292,256,180,133,129	n/c	2-Glyceryl hexadecanoate ¶
18.55	31488	866	813	322,292,256,201,147,131	n/c	1-Glyceryl hexadecanoate ¶
18.70	10240	n/i	n/i	341,321,291,277,145,131	n/c	2-Glyceryl octadecanoate ¶
19.45	17664	n/i	n/i	338,278,171,131,91,79	n/c	1-Glyceryl octadecanoate ¶
28.22	2800	473	329	387,369,301,275,145,119	n/c	Cholesterol†¶ **32a**
Sample 6c, bicarb. treated internal organs, TIC = 15550322, sample identity = sue178						
12.98	66560	n/i	n/i	163,133,117,104,91,79	1680	5-Phenylpentanone
13.63	247808	671	541	228,185,157,143,129,115	1757	Tetradecanoic acid†¶
13.87	103424	827	783	242,199,185,143,129,73	1788	C_{15} fatty acid¶
14.15	278528	852	818	242,213,199,143,129,73	1821	Pentadecanoic acid¶
14.57	134144	n/i	n/i	284,229,211,129,116	1864	C_{15} Fatty acid ester
15.00	40960	n/a	n/a	256,213,171,157,129,97	1939	C_{16} Fatty acid¶
15.25	1409024	n/a	n/a	256,213,185,82,72	1939	Hexadecanoic acid†¶
15.52	307200	n/i	n/i	268,168,153,138,110,97	1993	Unsaturated C_{17} fatty acid
15.65	323584	900	828	250,206,151,125,111,97	1993	Heptadecanoic acid
15.93	319488	786	681	311,264,236,194,152,97	2031	methyl hexadecenoate ¶
16.25	458752	n/i	n/i	222,165,151,127,111,83	2077	*cis*-9-Octadecenoic acid† **38a**
16.87	294912	n/i	n/i	298,280,241,222,135,108	2155	C_{19} Fatty acid

17.13	434176	n/i	n/i	338,285,265,222,123,97	2196	*cis*-9-Octadecenoic acid ester¶
17.52	1523712	n/i	n/i	249,193,175,152,133.91	2254	Fatty acid phenyl ester¶
17.90	872448	744	681	166,147,131,119,91,79	2326	Methyl eicosa-5,8,11,14,17-pentaenoate
18.37	130048	n/i	n/i	320,256,180,131,129,91,	n/c	Unsaturated fatty acid glyceride¶
18.57	86016	n/i	n/i	289,201,147,133,119,79	n/c	8,11,14-Eicosatrienoic acid ester 1¶
18.85	58112	n/i	n/i	321,207,138,125,97	n/c	8,11,14-Eicosatrienoic acid ester 2¶
18.97	61184	n/i	n/i	320,304,276,151,123,111	n/c	8,11,14-Eicosatrienoic acid ester 3
19.42	36096	n/i	n/i	338,278,171,131,91,79	n/c	8,11,14-Eicosatrienoic acid ester 4
20.18	69632	n/i	n/i	338,278,171,131,91,79	n/c	8,11,14-Eicosatrienoic acid ester 5
28.25	4288	n/a	n/a	387,369,301,275,145,119	n/c	Cholesterol†¶ **32a**
Sample 8, skin, TIC = 17879860, sample identity = sue179						
4.82	47360	n/i	n/i	101,85,69,60,45	n/c	Butanoic acid ester
10.23	60416	893	792	136,129,91,65	1176	Phenylpropanedioic acid
10.97	1163264	n/i	n/i	150,117,104,91	1321	Terpenoid type compound
11.67	327680	962	956	183,127,113,99,85,71	1476	Phytane **33b**
12.98	140288	924	799	163,127,104,91,72,65	1680	5-Phenyl-2-pentanone
13.57	618496	n/a	n/a	228,184,143,129,115,97	1757	Tetradecanoic acid†¶
13.84	47616	854	813	242,199,143,129,115,73	1787	C_{15} Fatty acid mixed peak
14.14	238592	886	891	242,199,143,129,115,73	1821	Pentadecanoic acid¶
15.00	42752	n/a	n/a	256,213,157,129,115,73	1938	C_{16} Fatty acid¶
15.17	1376256	n/a	n/a	256,213,129,115,73	1938	Hexadecanoic acid†¶
15.45	145408	n/i	n/i	268,212,153,138,123,97	1970	Mono unsaturated C_{17} fatty acid¶
15.58	129024	n/i	n/i	250,208,151,123,111,97	1993	C_{17} Fatty acid
15.92	83968	901	859	312,264,108,123,101,88	2031	Ethyl *cis*-9-Octadecenoate
16.24	405504	n/i	n/i	284,264,129,111,97,83	2077	*cis*-9-Octadecenoic acid, **38a** Octadecanoic acid†¶
17.38	248832	n/i	n/i	310,292,208,151,125,97	2237	Monounsaturated C_{19} fatty acid ester¶
17.70	413696	907	838	166,133,119,105,91,79	2290	Methyl eicosa-5,8,11,14,17-pentaenoate
18.62	52736	n/i	n/i	320,278,170,125,110,97	n/c	8,11,14-Eicosatrienoic acid¶**40**
19.15	135168	n/i	n/i	167,149,117,105,91,79	n/c	C_{20} Unsaturated fatty acid ester¶
28.20	1520	538	342	386,354,301,212,145,105	n/c	Cholesterol†¶ **32a**
Sample 8c, bicarb. treated skin, TIC =13720884, sample identity = sue180						
10.97	315392	896	872	117,90,53	1321	3-Methylbenzonitrile¶
11.67	108544	959	947	183,141,113,99,85,71	1475	Phytane¶ **33b**
13.45	724992	950	929	228,185,143,129,115,73	1735	Tetradecanoic acid†¶
14.13	44032	878	851	242,199,143,129,115,73	1821	Pentadecanoic acid¶
14.90	307200	n/a	n/a	256,213,185,157,129,73	1904	Hexadecanoic acid†¶
15.50	23296	n/i	n/i	270,256,227,171,129,73	1993	C_{17} Fatty acid¶
16.20	643072	n/i	n/i	284,264,129,111,97,83	2062	*cis*-9-Octadecenoic acid, **38a** Octadecanoic acid†¶
16.47	160768	859	788	355,147,119,105,91,79	2094	Methyl octadecatrienoate

17.32	57344	n/i	n/i	310,292,208,151,125,97	2225	Mono unsaturated C_{19} fatty acid ester¶
17.63	70656	n/i	n/i	355,147,119,105,91,79	2279	Methyl eicosa-5,8,11,14,17-pentaenoate
18.48	8064	n/i	n/i	280,235,178,123,111,83	n/c	Unsaturated C_{20} fatty acid ester¶
19.00	19200	n/i	n/i	320,255,199,133,119,105	n/c	Unsaturated C_{20} fatty acid ester¶
28.20	n/a	n/a	n/a	386	n/c	Cholesterol†¶ **32a**

n/i = no library fit available, n/a = not applicable , n/c = not calculated, † confirmed by comparison to authentic standard ¶ occurs in both treated and untreated samples, ♯ late runner from last sample

2.8 Trout urine

Urine samples were collected by catheterizing trout and pooling the urine. The female urine was subject to bioassay and known to be active. Male urine was also collected in the same fashion. The trout stocks, urine collection and bioassay were all maintained by Dr. Alexander Scott, DEFRA (formerly MAFF) at Lowestoft.

2.8.1 Direct injection of trout urine

Frozen urine samples were thawed, thoroughly mixed and portions (4 ml) were freeze dried (4 millibar, 3.5 hours). Native and freeze dried samples were directly injected (5 µl) onto the GC-MS, DBWax column, (30(3) x 5 to 260(35), inj 275, interface 280).

Both the male and female direct injection samples were found to contain only 1 peak, which was identified as *N*-methyl-methanamine. The freeze-dried samples of both the male and female urine were found to contain two peaks, the dimethylamine as in the previous samples and also trimethylamine. The female direct injection also contained peaks at 3.33, 7.05, 15.42, 43.95, 50.47 min, but the TIC was too low to identify. The direct injection male urine sample contained peaks at 14.17, 18.50, 58.35, 64.37, 65.95. The freeze-dried samples contained peaks at 3.22, 3.40, 27.50, 46.44, 51.92, 66.40 min for the female and at 17.67, 26.44, 29.29, 29.69, 30.40, 34.89, 35.37, 55.84. Again, the TIC counts were too low to permit identification.

2.8.2 Dichloromethane extractions of trout urine

Portions of the trout urine (2 ml) were treated with sodium hydroxide or hydrochloric acid to give a pH of either 12 or 1. These samples plus an untreated urine were extracted with dichloromethane (3 x 1 ml). The organic layers were filtered through a plug of glass wool to break the emulsion formed. The samples were concentrated (200 µl) under a gentle stream of nitrogen at room temperature. The samples were analysed by GC-MS (30(3) x 5 to 260(35),

inj 275, interface 280) on the standard DB17 column (Table 2.16).

Table 2.16: Trout urine, retention times, TICs and significant ions

Ret. time, min	TIC	Rev fit	For fit	Significant ions *m/z*	Kovat Index	Identity
Neutral extract of female trout urine, TIC = 1887458, sample identity = sue328						
34.50	16256	n/i	n/i	281,256,154,129,111,97	2096	3-Decanol
37.54	38656	n/i	n/i	194,128,111,97,83,72,59	2264	9-Octadecenamide **38b**
38.70	2960	873	642	281,184,129,114,86,72	2333	Hexadecanamide
40.65	27136	930	528	140,112,97,83,72,59	2453	C_{17} amine
43.57	10944	783	520	292,253,212,126,114,97	2647	2,6-Dimethylnonanedioic acid type compound
44.74	110592	886	767	175,136,121,95,81,69	2730	Squalene **35**
46.60	61952	930	599	337,140,113,97,83,72,59	2868	2-Hydroxy-cyclopentadecanone
51.39	1968	n/i	n/i	386,353,301,275,213,105	n/c	Cholesterol **32a**
77.87	1648	n/i	n/i	377,331,315,253,157,129	n/c	Cholesterol derivative
79.37	2464	n/i	n/i	377,316,269,185,145,111	n/c	Cholesterol derivative
Acid extract of female trout urine, TIC = 108921, sample identity = sue331						
30.67	3632	n/i	n/i	129,107,95,81,69,55	1901	Squalene type derivative
37.87	4416	n/i	n/i	113,97,81,69,55,43	2284	Squalene type derivative
39.35	5248	n/i	n/i	113,97,85,69,57,43	2372	Squalene type derivative
40.84	5056	n/i	n/i	113,97,85,69,57,43	2465	Squalene type derivative
42.30	4864	886	619	111,85,69,57,43	2561	17-Pentatriacontene
44.87	5248	n/i	n/i	149,137,121,11,95,81	2740	Squalene **35**
Base extract female urine, TIC = 84903, sample identity = sue332						
37.94	2816	n/i	n/i	97,85,71,69,57,43	2285	Squalene type derivative
39.44	2592	n/i	n/i	113,97,85,69,57,43	2373	Squalene type derivative
44.82	11776	n/i	n/i	149,136,121,107,81,69	2736	Squalene type derivative
47.65	3136	n/i	n/i	335,234,195,159,111,94	2950	Squalene type derivative
Neutral extract of male trout urine, TIC = 3536034, sample identity = sue329						
18.15	25600	872	619	138,135,107,94,77,66	1353	Phenylphosphonic acid
24.52	7488	913	284	287,169,153,143,126,101	1621	1,2:3,4:5,6-*tri-O*-Isopropylidene-D-glucitol#
25.14	5568	924	272	287,257,229,157,143,115	1648	1,2:3,6:4,5-*tri-O*-Isopropylidene-D-mannitol#
31.99	20992	n/i	n/i	147,97,91,85,83,71,57	1966	C_{19} alkane
35.95	6656	n/i	n/i	253,228,169,141,113,85,	2174	C_{22} alkane
36.52	7296	797	589	213,199,170,145,127,100	2206	1-Methyltridecyl octanoate
37.17	15488	n/i	n/i	213,194,166,124,96,70	2243	Unidentified
39.10	14656	n/i	n/i	281,141,113,99,85,71	2357	C_{24} alkane
40.59	16384	n/i	n/i	225,149,113,99,85,71,57	2449	C_{24} alkane
42.04	16640	n/i	n/i	279,155,140,127,99,85	2543	C_{25} alkane
43.47	12864	n/i	n/i	283,197,171,127,112,85	2640	C_{26} alkane
44.70	700416	901	797	148,136,121,95,81,69	2727	Squalene **35**
45.44	8064	882	595	219,179,117,93,79,67	2781	Methyl 9,12,15-octadecatrien-oate
46.49	23808	n/i	n/i	341,270,154,113,97,85	2860	C_{28} alkane
47.49	12608	868	616	278,277,201,183,152,77	2937	Acetic acid (triphenylphosphor-anylidene), methyl ester#
51.19	1744	879	580	386,301,275,231,213,145	3000	Cholesterol **32a**

Acid male trout urine, TIC = 42384, sample identity = sue333						
44.87	6272	n/i	n/i	137,121,107,95,81,69	2739	Squalene **35**
57.20	2080	n/i	n/i	520,506,475,367,334,290	n/c	Lanostan-11-one type compound
72.91	2320	n/i	n/i	793,730,608,528,407,249	n/c	Unidentified
73.34	2592	n/i	n/i	488,411,393,280,264,93	n/c	Unidentified
Base male trout urine, TIC = 77641, sample identity = sue334						
44.75	5504	n/i	n/i	137,121,107,95,81,69	2731	Squalene type derivative
46.54	7296	n/i	n/i	136,126,112,97,83,72	2864	9-Octadecenamide type compound **38b**

Likely contaminants, n/i = no library fit available, n/c = not calculated

2.8.3 NMR analysis of freeze-dried urine

Female trout urine (1 ml) was freeze dried (2 hr), and azeotroped twice with D_2O (2 x 1.5 hr). The remaining yellow solid was dissolved in a minimum volume of D_2O and submitted for NMR analysis. Peaks were present at δ 5.24 (d *J* 4 Hz) and δ 4.66 (d *J* 8 Hz), which are consistant with the α- and β-anomers of glucose. Residual water and impurity peaks did not allow full interpretation and so this procedure was repeated with a larger volume.

Female trout urine (60 ml) was freeze dried as above. ^{1}H-NMR spectra were measured on a solution in D_2O and the same sample after the addition of $CDCl_3$.

^{1}H-NMR (D_2O) The ^{1}H-NMR spectra of this sample contained a complex mixture and hence reliable integrations could not be made. However it was a apparent that there were major and minor components with the ratio of approx 5-10:99-95. δ 5.23 (minor, d *J* 3.8); 4.65 (minor, d *J* 7.9); 4.27 (minor, dd, *J* 7.0, 4.5); 4.08 (minor, s); 3.95 (major, s); 3.68 (major, d *J* 6.6); 3.4 (major, t *J* 6.6); 3.3 (major, s); 3.25 (major, t *J* 6.5); 3.05 (major, s); 1.48 (minor, d *J* 7.2); 1.32 (minor, d *J* 6.9)

^{1}H-NMR ($CDCl_3$) Broad hydrocarbon peaks at δ 1.3 & 0.9.

2.8.4 HPLC of trout urine

The female trout urine was subject to solid phase extraction, the cartridges (Sep Pac C18) were conditioned with methanol (2 x 4 ml) and washed with water (5 ml). The sample (5 ml) was loaded onto the cartridge using a syringe. The cartridges were soaked (2 min) and eluted with methanol (3 x 1 ml). The methanol extract was subject to HPLC using the standard system as described in section 2.1.2. The mobile phase was run at 0.5 ml/min, as a gradient, 20 % *v/v* acetonitrile for 10 min, rising to 70 % *v/v* acetonitrile in 50 min then isocratically at the final composition for 15 min. The sample volume was 200 µl. The eluant from the column was collected as four fractions (0 - 20, 20 - 40, 40 - 60, 60 - 75 min) These samples were intended for bioassay, but due to an exceptionally short spawning season, this was not

possible. A total of 8 peaks were observed at the following times: 9, 18, 20, 22, 29, 49, 64, 66 min.

Trout urine is dilute and possibly containing sugars, so a solution of acetic chloride in pyridine (5% *v/v*, 250 µl) was added to a portion (75mg) of the freeze-dried sample (section 2.8.3), the samples were capped, gently shaken and left overnight at room temperature. The samples were flow evaporated (40°C) and reconstituted in aqueous acetonitrile (80% *v/v*, 200 µl). The samples were analysed by HPLC (section 2.1.2), the mobile phase gradient was 20% acetonitrile for 10 min, rising to 70% over 50 min, isocratic for 15 min then rising to 95% over 5 min. The flow rate was 0.5 ml/min and UV detection was at 254 nm. A water blank and steroid standards containing Reichstein's Substance **30b**, 4-pregnen-17α, 20α-diol-3-one **31**, 17α-P **30a**, testosterone **26** $PG_{2\alpha}$ (10 mg in 100 ml methanol respectively) were derivatised and analysed under identical conditions.

The blank sample displayed a small peak (0.02 AU) at 1.5 minutes. The remaining chromatogram did not show any further peaks. The steroid standards, Reichstein's Substance **30b**, 4-pregnen-17α, 20α-diol-3-one **31**, 17α-P **30a**, testosterone **26** and $PG_{2\alpha}$ had retention times at 10.0, 12.5, 15.0, 20.0, 22.9 minutes respectively. The derivatised urine sample contained a total of 25 peaks at the following retention times, 9.2, 9.5, 10.3, 11.4, 11.9, 12.7, 13.5, 16.5, 17.6, 20.8, 23.2, 26.2, 27.6, 28.9, 31.1, 34.3, 35.7, 40.5, 42.2, 43.5, 46.5, 48.9, 53.8, 61.6 and 66.5. The chromatography produced broad, tailing peaks, so it was not possible to get reliable integration for peak area information.

2.8.5 Solvent extract and deconjugation of female trout urine

A large volume (25 ml) of female trout urine was subject to solvent extraction with dichloromethane (3 x 2.5 ml). The remaining aqueous layer was deconjugated using glucuronidase solution (1 ml) at 37°C as previously described and re-extracted with dichloromethane (3 x 2.5 ml). The dichloromethane extracts were concentrated (approx. 50 µl) and analysed by GC-MS (Table 2.17), GC program (30(4) x 5 to 280 (20) inj 300 interface 300, vol 2µl).

Table 2.17: Large volume trout urine, retention times, TICs and significant ions

Ret. time, min	TIC	Rev fit	For fit	Significant ions *m/z*	Kovats Index	Identity
Large volume trout urine extract for free steroids, TIC = 1467879, sample identity = sue356						
12.05	27136	866	833	128,104,103,73,59	n/c	1-(2-Methoxy-1-methyl ethoxy)-2-propanol

12.37	49408	799	691	134,105,91,73,59	n/c	1-(2-Methoxypropoxy)-2-propanol*
12.67	23296	931	860	134,28,119,105,91,77	n/c	1,2,3,4-Tetramethyl benzene
13.45	17920	906	825	134,120,119,105,91,77	n/c	1-Ethyl-2,4-dimethyl-benzene
19.13	8832	772	636	199,130,110,109,81,54	n/c	1-Methyl 1H imidazole-2-carboxaldehyde
20.95	77824	906	685	138,107,94,77,66,51	n/c	2-Phenoxyethanol
21.80	52480	838	713	100,99,98,70,55,42	1730	5-Butyldihydro-4-methyl-2(3*H*)-furanone
29.90	25856	832	431	356,281,223,180,127,99	1762	Dimethyl 1-methylpropenyl ester of phosphoric acid
31.02	1888	796	600	228,185,129,116,85,73	1792	Tetradecanoic acid†
35.02	11712	789	648	256,213,185,129,73	1935	Hexadecanoic acid†
36.85	35072	n/i	n/i	168,140,125,97,70	2016	4-Hydroxy-3-methoxy benzoic acid type compound
38.75	11072	n/i	n/i	284,264,241,222,185,129	2108	*cis*-9-Octadecenoic acid† **38a**
39.95	47104	n/i	n/i	195,167,154,139,125,86	2170	Acetamide type compound
40.55	8704	880	619	295,253,224,183,127,95	2201	3,7,11,15-Tetramethyl-1-hexadecanol
41.70	166912	n/i	n/i	194,166,138,124,96,70	2262	Acetoxymethoxy cinnamic acid type derivative
43.19	34560	953	694	284,264,206,185,166,91	2343	Methyl eicosa-5,8,11, 14,17-pentaenoate
45.54	106496	819	397	189,172,171,158,127,99	2471	1H-Pyrido 3,4-indole, 2,3,4,9-tetrahydro-1-(1-methylethyl)
45.95	95232	817	618	297,252,224,145,127,97	2493	1,3-Dioxolane-4-methanol, 2-pentadecyl acetate
48.30	4608	n/i	n/i	386,371,293,273,260,191	2619	Cholesterol derivative
49.27	8128	861	603	378,341,220,191,137,121	2669	Squalene **35**
49.59	7360	n/i	n/i	327,277,249,207,178,129	2685	Benzene 1,1'-(2-methyl-2-phenylthio) cyclopropylidene
52.07	4672	819	435	327,288,274,246,203,191	2804	17α-Hydroxy-androst-4-en-3-one **44**
53.49	15360	830	544	398,309,263,191,177,163	2866	28-Nor-17β-(H)-hopane*** **45**
54.57	14272	n/i	n/i	412,317,231,191,163,137	n/c	28-Nor-17β-(H)-hopane type derivative*** **45**
55.42	10240	n/i	n/i	386,368,353,273,213,159	n/c	Cholesterol **32a**
Large volume female trout urine - deconj'ted steroids, TIC = 6074475, sample identity = sue357						
4.08	29696	795	725	87,78,71,69,55,41	n/c	2,3-Dimethyl 2-butene
15.53	22016	833	803	109,108,107,90,77,65	n/c	4-Methyl phenol
20.97	430080	849	588	138,107,94,77,66	n/c	Phenylphosphoric acid
21.87	12480	n/i	n/i	208,141,99,70,56	1730	2-Butyldihydro-4-methyl 2(3H) furanone
31.02	23040	865	767	228,185,171,143,129,73	1792	Tetradecanoic acid†
33.04	8896	790	667	264,242,199,171,143,129	1857	Pentadecanoic acid
35.34	83968	779	699	256,227,213,185,171,157	1948	Hexadecanoic acid†
36.97	42496	n/i	n/i	261,217,205,168,140,125	2022	4-Hydroxy-3-methoxy benzoic acid type of compound
38.92	41472	849	727	284,264,241,199,185,129	2110	Octadecanoic acid†
40.27	6336	n/i	n/i	284,264,200,185,169,124	2200	*cis*-9-Octadecenoic acid† **38a**
41.72	96256	818	414	195,194,166,138,124,70	2262	Acetoxymethoxy cinnamic acid type compound
42.22	11392	927	634	310,292,249,208,165,139	2290	9-Octadecenyl 9-hexadecenoate

43.24	40704	958	736	273,206,166,145,133,119	2345	Methyl eicosa-5,8,11,14,17-pentaenoate
45.54	128000	820	412	189,172,171,158,127,99	2471	1H-Pyrido 3,4-B indole, 2,3,4,9-tetrahydro-1-(1-methylethyl)
46.72	35584	940	724	241,192,152,131,119,91	2535	Methyl eicosa-5,8,11,14,17 pentaenoate type compound
49.10	23552	n/i	n/i	331,243,223,197,140,125	2660	Cholestane derivative
49.27	11136	504	719	357,341,218,137,81,69	2669	Squalene **35**
49.35	7616	803	621	286,292,277,233,215,165	2672	3α,5α,17β-Androstane-3,17-diol **47**
49.55	10688	776	530	357,316,290,257,247,220	2683	5β, 17β-Hydroxy-androstan-3-one **48**
50.34	36884	n/i	n/i	290,231,185,155,153,139	2722	3-Octylmethyloxirane octanoate
50.72	39168	n/i	n/i	337,294,240,18,154,126	2741	9-Octadecenamide type compound **38b**
55.57	8128	n/i	n/i	386,353,276,229,213,171	3080	Cholesterol† **32a**

*,**,*** related compounds, † confirmed by comparison to authentic standard, n/i = no library fit available, n/c = not calculated

2.8.6 Electrospray analysis of female trout urine

A sample of freeze-dried urine was submitted for electrospray analysis by direct injection and produced ions at *m/z* 549, 533, 413, 285, 263, 204, 171, 141 and 132 which corresponds to masses of 548, 532, 412, 284, 262, 203, 170, 140 and 131.

Thawed urine (15 ml) was extracted with dichloromethane (3 x 2 ml) and subject to SPE as previously described. The cartridges were eluted with methanol (2 x 3 ml) and acetonitrile (2 x 2 ml). The methanol/acetonitrile extracts were flow evaporated (40°C) to a limited volume (approx. 300 µl) . An LC-MS system was configured in APCI mode. The system consisted of a Vydac C18 5µ 150x4.2 column, two isocratic pumps, one to produce the gradient (Perkin Elmer, 1 ml/min) and the other (Jasco 1 ml/min) connected to the analytical column. The column eluant was monitored by a UV detector (Spectrophysics) at 254 nm prior to MS analysis. The gradient was produced by low pressure mixing of the starting mobile phase (12.5 % *v/v* acetonitrile/water containing 0.1 % acetic acid) with acetonitrile. The injection volume was 100 µl. A combined nicotinamide **36** and testosterone **26** standard run under these conditions gave peaks which eluted at 2.6 and 19.8 min respectively. The identity of these peaks was confirmed by extracting the ions of these peaks which corresponded to M+1 (molecular ion increased by 1, as species are protonated in APCI). A water blank extracted and analysed under identical conditions did not produce any peaks.

The chromatogram of the extracted urine showed 7 peaks at 1.6, 2.2, 5.2, 6.2, 14.1, 15.1, 15.6, 47.8 minutes. The peak at 1.6 min is the solvent front and the peak at 2.2 min elutes on its tail. None of these peaks produced a mass spectrum as the responses were all very low.

The mass spectrum of the peak at 47.8 min gave fragments at *m/z* 411, 179, 161, corresponding to masses at 410, 178, 160: the TIC for this peak after background subtraction was 5.51 x 10^3, still a low response.

2.9 Roach samples

2.9.1 Extraction of roach samples

Samples of eggs and milt were obtained by handstripping from ripe mature roach fish located in Titlesworth Reservoir, near Keele. Dr Mark Williams (Keele University) identified the fish as roach (*Rutilus rutilus*) and performed the sample collection. The samples were stored frozen until required for analysis.

Egg fluid (500 µl), eggs (5 g) and milt (500 µl) were extracted with dichloromethane (3 x 500 µl, 3 x 2.5 ml and 3 x 250 µl respectively). The samples were transferred to silanised test tubes, flow evaporated and reconstituted in dichloromethane (100 µl). The samples were analysed by GC-MS (Table 2.18), GC program (30(3) x 2.5 to 200(1) x 10 to 280(5), inj 280, interface 300).

Table 2.18: Roach samples, retention times, TICs and significant ions

Ret. time, min	TIC	Rev fit	For fit	Significant ions *m/z*	Identity
egg fluid, TIC = 562455, sample identity = sue255					
55.89	1184	n/i	n/i	313,145,124,117,97,71	Hexadecanoic acid TMS ester
64.20	544	632	390	340,145,129,117,99,73	*cis*-9-Octadecenoic acid TMS ester
75.44	16384	703	568	340,284,177,161,149,127	2,2'-Methylene *bis* 6-(1,1-dimethylethyl)-4-methyl phenol
80.29	1088	654	413	459,370,330,248,215,161	3β, 5-*bis*(Trimethylsiloxy)-5α-cholestane
82.10	2336	n/i	n/i	387,302,274,159,145,105	Cholesterol derivative
Eggs, TIC = 1404002, sample identity = sue256					
48.02	3664	732	500	286,258,201,145,117,73	Tetradecanoic acid TMS ester
50.19	1216	n/i	n/i	300,145,129,117,75,71	C_{15} fatty acid TMS ester
51.82	3648	n/i	n/i	300,201,145,129,117,73	C_{15} fatty acid TMS ester
55.54	22528	613	280	314,195,132,115,73,71	Hexadecanoic acid TMS ester
56.15	11520	n/i	n/i	314,257,201,145,117,73	C_{16} fatty acid TMS ester
59.77	2240	n/i	n/i	329,271,208,145,129,75	C_{17} fatty acid TMS ester
63.67	4992	n/i	n/i	356,282,242,233,129,97	*cis*-9-Octadecenoic acid TMS ester
70.14	2624	n/i	n/i	384,172,134,117,105,91	C_{20} fatty acid TMS ester
71.32	12160	835	644	220,166,147,133,119,79	Methyl eicosa-5,8,11,14,17-pentaenoate
75.36	7744	n/i	n/i	185,145,119,105,79,73	Methyl eicosa-5,8,11,14,17-pentaenoate type compound
77.14	6912	800	626	215,178,131,117,105,91	Methyl eicosa-5,8,11,14,17-pentaenoate type compound
77.60	10560	755	626	231,136,121,93,81,69	Squalene **35**

80.40	20736	736	579	458,369,330,248,160,129	3β-(Trimethylsiloxy)-5α-cholestane
83.22	43008	n/i	n/i	386,369,302,276,213,145	Cholesterol **32a**
Milt, TIC = 1472526, sample identity = sue257					
56.54	2320	n/i	n/i	329,314,255,132,115,73	Hexadecanoic acid TMS ester
63.05	3424	n/i	n/i	340,242,170,129,99,73	*cis*-9-Octadecenoic acid TMS ester
71.70	16384	801	548	248,220,192,166,145,91	Methyl eicosa-5,8,11,14,17-pentaenoate
77.59	38656	826	711	191,136,121,107,81,69	Squalene **35**
78.62	2720	n/i	n/i	369,354,248,213,147,105	Cholesterol derivative
80.20	7296	729	573	460,369,330,248,159,129	3β-(Trimethylsiloxy)-5α-cholestane
83.36	7744	n/i	n/i	388,354,302,255,133,105	Cholesterol type derivative
83.44	7168	n/i	n/i	387,300,276,245,213,145	Cholesterol type derivative
84.32	6016	n/i	n/i	388,354,302,274,145,107	Cholesterol type derivative
84.40	6784	n/i	n/i	387,355,276,230,213,105	Cholesterol type derivative
n/i = no library fit available					

2.9.2 Derivatisation of roach samples

The samples obtained from section 2.13.1 were subject to the derivatisation procedure detailed in section 2.4.1. A steroid mix containing testosterone **26**, 17α-hydroxyprogesterone **30a**, Reichstein's Substance **30b** and cholesterol **32a** was subject to the same procedure. The samples were analysed by GC-MS (Table 2.19), GC program (75(3)x5to190(1)x2to(280(20)).

The steroid standard was found to contain the following compounds; ethanedioic acid *bis*(TMS) ester, (4-methoxyphenoxy)trimethylsilane, an unidentified carboxylic acid TMS ester, *bis*(trimethylsilyloxy)lacetic acid TMS ester, 2,2-dimethyl-3-(trimethylsilyloxy) butanoic acid TMS ester, glycerol TMS ester and 3-*bis*(trimethylsilyl)amino-2-methyl propanoic acid TMS ester. These peaks were discounted from all other samples.

Table 2.19: Derivatised roach samples, retention times, TICs and significant ions

Ret. time, min	TIC	Rev fit	For fit	Significant ions *m/z*	Identity
Steroid standard, TIC = 48716500, sample identity = sue257					
45.62	765952	n/i	n/i	447,432,342,211,129,73	Testosterone TMS ester
53.90	2736128	891	683	458,368,329,145,129,73	Cholesterol TMS ester
58.84	344064	n/i	n/i	487,433,329,246,147,73	17α-Hydroxy-progesterone TMS ester
62.30	270336	n/i	n/i	458,331,147,103,84,73	Reichstein's Substance TMS ester
Derivatised egg fluid, TIC = 11409298, sample identity = sue260					
3.18	76800	n/i	n/i	233,218,190,147,103,73	Short chain, C_4 type acid TMS ester
3.22	194560	n/i	n/i	295,233,218,190,147,73	Short chain C_4 type acid TMS ester
4.80	227328	n/i	n/i	204,188,146,104,73	Short chain, C_4 type acid TMS ester
5.48	442368	733	613	232,217,191,147,75,73	Glyoxime *bis*(TMS) ester
6.32	54272	n/i	n/i	158,147,142,116,75,73	Amino acid TMS derivative
6.82	56320	762	417	231,147,132,116,75,73	L-Asparagine tris(TMS) derivative
8.45	610304	n/i	n/i	323,220,193,147,103,73	Glycerol TMS derivative§
8.83	214016	n/i	n/i	220,193,177,147,103,73	C_8 type acid TMS ester
9.15	27648	n/i	n/i	203,188,160,145,116,73	Unsaturated C_8 type acid TMS ester

9.55	96256	n/i	n/i	247,232,147,117,75,73	C_{10} type acid TMS ester
11.30	130048	n/i	n/i	206,174,147,130,00,73	Cadaverine TMS ester cf **50**
12.48	46080	n/i	n/i	190,179,164,150,136,107	2-Imino-3-ethyl benzothiazoline type compound
13.97	107520	n/i	n/i	191,147,130,103,75,73	Carboxylic acid TMS ester
14.73	43008	n/i	n/i	333,244,217,188,147,73	Amino acid TMS derivative
15.20	48896	n/i	n/i	357,254,191,147,131,73	Carboxylic acid TMS ester
15.72	106496	n/i	n/i	147,143,112,86,73	Unidentified
18.30	55040	n/i	n/i	243,233,218,147,128,73	Unidentified amino acid TMS derivative
19.00	41472	877	755	285,241,145,132,117,73	Tetradecanoic acid TMS ester
19.18	78848	848	748	317,201,153,129,117,73	Azelaic acid *bis*TMS ester
20.20	119808	827	742	319,218,205,147,103,73	Glucitol TMS ester
22.78	561152	869	781	329,313,145,132,117,73	Hexadecanoic acid TMS ester
23.78	49664	808	726	342,327,145,132,117,73	Heptadecanoic acid TMS ester
24.57	21760	n/i	n/i	387,203,191,147,117,73	Saturated C_{17} fatty acid TMS ester
26.25	114688	n/i	n/i	341,221,152,129,75,73	Octadecanoic acid TMS ester
30.77	17664	798	589	205,147,133,117,91,73	9,12,15-Octadecatrienoic acid TMS ester
31.54	17920	825	540	175,133,117,91,75,73	Methyl eicosa-5,8,11,14,17-pentaenoate type compound
36.44	28672	n/i	n/i	393,213,171,155,129,73	cis, *cis*-1,5,8-undecatriene-3,7-diol *bis* TMS ester
36.70	133120	n/i	n/i	484,427,249,233,177,73	Unidentified TMS derivative
52.57	61184	746	631	458,368,329,159,145,75	α-(Trimethylsiloxy)-cholest-5-ene
58.15	6912	n/i	n/i	486,396,358,275,159,120	Cholesterol TMS ester
Derivatised egg extract, TIC = 32560990, sample identity = sue261					
4.87	188416	n/i	n/i	204,188,146,104,73	C_4 type acid TMS ester
5.55	339968	720	561	232,217,191,147,75,73	Glyoxime *bis*(TMS) ester
6.38	221184	n/i	n/i	158,147,142,116,75,73	Amino acid TMS ester
6.97	221184	900	803	314,300,211,193,133,73	Tris (trimethylsilyl) phosphate
8.85	303104	n/i	n/i	220,193,177,147,103,73	C_8 type acid TMS ester
9.60	716800	n/i	n/i	247,232,147,117,75,73	C_8 type acid TMS ester
11.33	274432	929	735	191,174,155,147,100,73	Cadaverine tetra TMS cf **50**
14.70	154624	n/i	n/i	333,244,217,188,147,73	Amino type TMS ester
15.67	557056	n/i	n/i	147,112,86,73	Amine type TMS ester
18.25	155648	750	558	357,299,233,147,117,73	Phosphoric acid 2,3-*bis* (TMS) ester
18.98	847872	917	866	300,285,145,132,117,73	Tetradecanoic acid TMS ester
19.17	434176	846	n/i	317,217,201,152,129,73	Azelaic acid *bis*(TMS) ester
20.27	1540096	860	793	319,217,205,147,103,73	Glucitol, TMS ester
20.88	303104	899	753	314,299,145,132,117,73	1H-indole-2-carboxylic acid 1-(TMS)-5-(TMS) ester
21.95	112640	873	767	328,313,145,132,117,73	C_{16} fatty acid TMS ester
22.82	364544	n/i	n/i	328,313,109,89,75	C_{16} fatty acid TMS ester
23.05	2654208	900	808	328,313,145,132,117,73	Hexadecanoic acid TMS ester
23.15	516096	955	n/i	311,236,145,129,117,73	Palmitelaidic acid TMS ester
23.37	73728	753	613	309,234,147,129,117,73	Palmitoleic acid TMS ester
23.80	593920	942	897	327,201145,132,117,73	C_{17} fatty acid TMS ester
24.02	421888	938	839	342,327,145,132,117,73	Heptadecanoic acid TMS ester
24.55	250880	n/i	n/i	387,327,191,147,132,73	*cis*-9-Octadecenoic acid TMS ester
25.47	31488	649	477	401,341,244,147,129,73	Nonadecanoic acid TMS ester

26.34	348160	n/i	n/i	355,339,222,199,129,75	*cis*-9-Octadecenoic acid TMS ester
26.52	462848	743	622	354,339,264,145,129,117	C_{18} monounsaturated acid TMS ester
26.64	458752	n/i	n/i	337,262,145,121,109,95	C_{18} monounsaturated acid TMS ester
26.92	53760	889	775	178,145,129,117,93,75	9,12,15-Octadecatrienoic acid TMS ester
27.10	147456	944	845	335,163,145,129,117,75	9,12,15-Octadecatrienoic acid type TMS ester
27.35	123904	n/i	n/i	355,129,111,103,83,75	C_{20} type acid TMS ester
28.24	33536	n/i	n/i	413,355,236,203,117,86	C_{20} type acid TMS ester
28.74	197632	903	818	387,315,299,217,147,73	*myo*-1,2,4,5,6-*Pentakis*-*O*-(TMS)-inositol-3- phosphate cf **51**
30.87	540672	n/i	n/i	387,299,217,175,150,117	C_{20} type acid TMS ester
31.62	839680	n/i	n/i	369,173,147,129,117,73	C_{20} type acid TMS ester
35.65	307200	n/i	n/i	225,171,147,129,117,73	C_{22} type acid TMS ester
36.10	34304	n/i	n/i	217,161,147,133,117,73	Methyl eicosa-pentaenoate type compound
36.57	240640	756	471	393,171,147,129,117,73	Unidentified benzylic TMS ester
37.20	544768	n/i	n/i	215,173,131,117,105,91,	Methyl eicosa-pentaenoate type compound
41.05	107520	n/i	n/i	261,171,147,129,117,73	C_{22} fatty acid TMS ester
42.37	397312	n/i	n/i	419,171,155,129,117,73	Glyceryl docosahexaenoate TMS ester
42.99	36864	n/i	n/i	261,171,131,117,91,73	C_{22} polyunsaturated fatty acid TMS ester
45.32	251904	740	559	287,171,129,117,75,73	4-Trimethylsiloxycyclo-hexylacetate, TMS ester
53.90	16384	944	818	367,329,274,171,133,95	3β-*bis*(Trimethylsiloxy) 5α cholestane
55.52	44544	879	647	368,329,213,147,129,73	3α-(TMS) cholest-5-ene
60.89	31232	n/i	n/i	361,217,204,147,129,73	Cholesterol type TMS ester
Derivatised milt extract, TIC = 21592624, sample identity = sue262					
3.93	643072	727	550	323,220,193,147,119,73	2-Phenyllactic acid *bis*(TMS) ester
4.62	111616	787	n/i	260,245,188,147,133,73	2-Butanedioic acid *bis*(TMS) ester
4.83	171008	n/i	n/i	226,204,191,147,119,73	Short chain carboxylic acid TMS ester
5.52	380928	n/i	n/i	232,217,191,147,73	Glyoxime *bis*(TMS) ester
5.93	79872	735	467	292,221,174,147,86,93	Propanedioic acid (TMS)oxy-*bis*(TMS) ester
6.33	138240	n/i	n/i	158,144,116,102,73	Amino acid TMS ester
6.60	64256	n/i	n/i	216,172,147,128,112,73	Butanoic acid 4-*bis*(TMS) amino-TMS ester
6.92	174080	890	813	314,299,283,211,133,73	Tris (trimethylsilyl) phosphate
8.83	376832	n/i	n/i	220,193,177,147,103,73	C_4 carboxylic acid TMS ester
9.12	20224	n/i	n/i	245,203,188,146,116,75	Monounsaturated C_4 fatty acid TMS ester
9.58	438272	n/i	n/i	247,232,172,147,117,73	Trimethylsilyl 2,2-dimethyl-3-(trimethylsilyloxy) butanoate
10.60	13504	n/i	n/i	329,306,216,190,147,117	C_6 type carboxylic acid TMS ester
11.33	204800	953	741	229,174,155,131,100,73	Cadaverine tetra-TMS ester cf **50**
11.60	11008	n/i	n/i	237,209,188,170,146,73	Amino acid TMS ester
13.05	18432	n/i	n/i	257,201,174,147,143,73	Phenylethanediamine TMS ester
13.97	92160	767	651	191,164,147,131,103,73	*bis*(TMS)oxyl-carboxylic acid TMS ester

14.25	29696	783	n/i	230,217,189,147,100,73	Glyoxime *bis*(TMS) ester
14.48	23296	n/i	n/i	307,232,180,142,134,73	C_8 type carboxylic acid TMS ester
14.72	71680	n/i	n/i	217,203,156,147,101,73	C_8 type carboxylic acid TMS ester
15.22	73728	n/i	n/i	254,191,147,130,73	C_{10} type carboxylic acid TMS ester
18.23	142336	851	715	357,315,233,147,101,73	Tetra (TMS) glycerol-1-*O*-phosphate
18.47	47616	n/i	n/i	299,219,191,172,100,73	C_{12} carboxylic acid TMS ester
18.67	38144	n/i	n/i	256,214,191,132,73	C_{12} carboxylic acid TMS ester
18.95	104448	929	870	285,145,132,117,73	Tetradecanoic acid TMS ester
19.17	102400	820	n/i	317,201,147,129,117,73	Azelaic acid *bis*(TMS) ester
20.03	16192	n/i	n/i	299,244,145,129,117,73	C_{14} carboxylic acid TMS ester
20.40	16384	n/i	n/i	244,181,149,124,117,73	C_{15} carboxylic acid TMS ester
20.88	30976	n/i	n/i	310,299,145,132,117,73	C_{15} carboxylic acid TMS ester
22.85	1490944	941	841	328,313,145,132,117,73	Hexadecanoic acid TMS ester
23.02	36096	839	n/i	311,216,185,129,117,73	Monounsaturated C_{16} fatty acid TMS ester
23.42	16640	n/i	n/i	427,191,129,105,91,73	Palmitelaidic acid TMS ester
23.75	68608	905	820	342,327,145,132,117,73	Heptadecanoic acid TMS ester
23.99	25344	789	n/i	370,327,201,145,129,117	C_{17} acid TMS ester
24.07	27648	n/i	n/i	217,167,147,130,117,73	Riboic acid 2,3,5 *tris* TMS γlactone
24.54	137216	n/i	n/i	387,327,145,132,117,73	C_{18} fatty acid TMS ester
26.37	1114112	941	844	341,201,145,132,117,73	cis-9-Octadecenoic acid TMS ester
26.42	62976	n/i	n/i	354,339,264,222,180,96,	Monounsaturated C_{18} fatty acid TMS ester
26.55	83968	950	n/i	337,262,220129,117,73	9,12-Octadecadienoic acid TMS ester
27.05	64000	910	793	335,129,117,108,93,79	9,12,15-Octadecatrienoic acid TMS ester
27.64	10752	n/i	n/i	249,205,147,131,115,73	C_{19} fatty acid TMS ester
28.22	15488	n/i	n/i	355,202,145,132,117,75	C_{19} fatty acid TMS ester
28.72	41728	719	n/i	315,299,217,147,73	1,2,4,5,6-*Pentakis-O*-(TMS) inositol, phosphate cf **51**
30.94	577536	n/i	n/i	249,175,129,117,105,91	C_{19} polyunsaturated acid TMS ester
31.72	454656	860	717	201,173129,117,105,91	Methyl eicosa-5,8,11,14,17-pentaenoate type compound
34.42	46592	851	n/i	371,239,205,147,129,73	1-Glyceryl hexadecanoate TMS ester
35.78	27392	n/i	n/i	205,147,132,111,95,73	11-Eicosaenoic acid TMS ester
37.12	319488	875	709	201,133,129,117,105,91	Methyl eicosa-5,8,11,14,17-pentaenoate
38.64	17920	n/i	n/i	311,191,147,97,85,73	Polyunsaturated C_{20} fatty acid TMS ester
39.19	19968	907	669	218,190,147,129,91,73	2-(Trimethylsilyl)oxy-1-(trimethylsilyl)-9,12,15-octadecatrienoic acid
39.97	35584	877	671	399,205,147,129,73	Glyceryl octadecanoate TMS ester
44.04	45056	n/i	n/i	147,136,109,91,81,69	Squalene **35**
45.69	17408	785	n/i	147,129,103,91,79,73	11,14-Eicosadienoic acid TMS ester
52.07	11648	n/i	n/i	459,274,247,157,120,93	Cholesterol type TMS ester
53.05	262144	928	n/i	458,368,329,145,129	3β,5-*bis*(TMS)-5α-cholestane
54.12	192512	810	595	458,368,329,247,159,129	Cholesterol TMS ester
56.00	26880	918	n/i	368,329,213,145,129,73	3α-(TMS) cholest-5-ene
57.30	17152	n/i	n/i	368,329,247,146,129,73	Cholesterol type TMS ester
57.97	14336	n/i	n/i	368,329,247,146,129,73	Cholesterol type TMS ester

n/i = no library fit available

2.9.3 Deconjugation and derivatisation of roach samples

The aqueous layer from the samples obtained from section 2.9.1 were treated with an aliquot (2 ml) of β-glucuronidase stock solution (β-glucuronidase, type HP-2 from *Helix pomatia*, 20 μg, in sodium acetate buffer, 10 ml, 0.1 M, pH 6.5). The samples were heated (37°C, 30 min), extracted with dichloromethane (3 x 10 ml), derivatised as previously described and analysed by GC-MS (Table 2.20), GC program (75(3)x5to190(1)x2to280(10).

A sample of water was subjected to the procedure described above and produced a series of 20 peaks (3.85, 5.25, 6.32, 6.82, 7.97, 8.43, 8.80, 9.55, 10.42, 11.30, 12.13, 13.90, 14.65, 18.88, 22.68, 26.18, 38.40, 41.35, 43.87, 44.35, 47.39, 50.40, 53.42 min respectively). Any peaks found in the test samples at these times were examined and if the spectra corresponded with the peak in the blank, were deemed to be an artifact of the derivatisation procedure and not considered further.

Table 2.20: Deconjugated, derivatised roach samples, retention times, TICs and significant ions

Ret. time, min	TIC	Rev fit	For fit	Significant ions *m/z*	Identity
Derivatised fatty acid & cholesterol **32a** standard, TIC = 95502648, sample identity = sue272					
3.87	1097728	n/i	n/i	218,203,187,147,113,73	Hexanoic acid TMS ester
10.89	1064960	n/i	n/i	244,229,185,132,117,73	Decanoic acid TMS ester
15.63	1490944	823	726	272,257,145,132,117,75	Dodecanoic acid TMS ester
20.10	2293760	741	666	300,285,201,145,129,117	Tetradecanoic acid TMS ester
23.88	3145728	712	627	328,313,201,145,129,117	Hexadecanoic acid TMS ester
24.84	901120	892	762	387,327,191,145,132,117	Heptadecanoic acid TMS ester¥
27.02	1851392	836	700	356,341,145,132,117,73	Octadecanoic acid TMS ester
54.02	4161536	n/i	n/i	458,367,328,145,129,73	Cholesterol TMS derivative
Deconjugated derivatised egg fluid, TIC = 289994528, sample identity = sue265					
8.57	667648	642	397	321,219,177,146,102,73	Glycine TMS ester
17.30	397312	n/i	n/i	306,291,250,216,201,73	Cinnamic acid type TMS ester
19.08	741376	657	537	299,284,145,131,116,73	Tetradecanoic acid TMS ester†
23.14	4177920	477	385	326,311,201,146,131,118	Hexadecanoic acid TMS ester†
23.94	1081344	593	452	340,326,145,131,116,73	Heptadecanoic acid TMS ester†
24.17	749568	657	480	341,326,201,145,131,116	C_{17} acid TMS ester†
24.69	385024	n/i	n/i	388,340,325,145,131,116	C_{17} carboxylic acid TMS ester
26.65	2949120	n/i	n/i	354,339,146,133,116,73	*cis*-9-Octadecenoic acid TMS ester†
26.72	634880	n/i	n/i	355,340,199,132,109,95	C_{18} fatty acid TMS ester
27.55	749568	622	235	368,355,353,129,102,75	Unidentified TMS ester
31.07	417792	n/i	n/i	385,206,175,128,116,91	Polyunsaturated C_{19} fatty acid TMS ester
31.87	765952	n/i	n/i	306,237,199,131,116,91	Polyunsaturated C_{20} fatty acid TMS ester
37.45	851968	n/i	n/i	412,385,199,161,128,116	Unidentified
54.47	4177920	n/i	n/i	456,441,366,327,274,245	Cholesterol type TMS ester■
54.75	4177920	n/i	n/i	458,369,329,274,145,130	Cholesterol type TMS ester

54.94	790528	505	288	499,458,366,327,160,128	Cholesterol TMS ester†
Deconjugugated derivatised eggs, TIC =298347200, sample identity = sue267					
4.02	1622016	533	344	324,221,192,160,146,73	2-Methyl-2,3-*bis*(TMS)oxy propanoic acid TMS ester
4.85	737280	n/i	n/i	294,217,204,148,116,73	Gluconic acid 2-methoximine TMS ester
7.57	1032192	n/i	n/i	298,292,190,148,102,73	Amino acid type TMS ester
8.65	1753088	n/i	n/i	324,221,177,148,102,73	C_8 type acid TMS ester
19.15	937984	n/i	n/i	299,284,144,133,118,73	Tetradecanoic acid TMS ester†
23.67	4177920	n/i	n/i	326,313,269,202,131,116	Hexadecanoic acid TMS ester†
24.42	552960	n/i	n/i	342,328,242,157,116,73	C_{17} acid TMS ester
24.95	186368	n/i	n/i	384,327,203,190,147,117	Heptadecanoic acid TMS ester†
27.02	1015808	n/i	n/i	354,342,227,187,132,117	C_{18} fatty acid TMS ester
27.35	4161536	647	428	356,342,339,133,117,75	Octadecanoic acid TMS ester†
27.77	323584	n/i	n/i	350,334,145,131,116,107	Monounsaturated C_{18} acid TMS ester
31.52	499712	n/i	n/i	375,364,206,147,129,116	Polyunsaturated C_{18} acid TMS ester
32.25	540672	612	284	367,236,187,162,129,73	Prost-13-en-1-oic acid 9,11,15-*tris* TMS ester
35.32	831488	n/i	n/i	456,369,238,175,146,116	C_{18} glyceride TMS ester
37.99	585728	n/i	n/i	468,410,383,145,116,73	Polyunsaturated C_{20} type acid TMS ester
53.75	112640	n/i	n/i	458,368,354,327,245,129	Cholesterol type TMS ester
54.27	253952	n/i	n/i	457,368,327,159,129,73	Cholesterol TMS ester†
54.42	4161536	635	364	456,441,366,354,274,121	24-Nor-22,23-methylenecholest-5-en-3β-ol TMS ester■
54.80	4096000	519	222	458,369,330,255,130,73	3β,5α-Cholest-7-en-3-yloxy TMS ester
54.85	4177920	558	229	458,368,353,327,255,130	3β,5β,6β-Cholestane-3,6-diyl *bis*(oxy) TMS ester■
55.05	4177920	718	434	499,456,441,366,351,327	3β,5α-Cholesta-8,24-dien-3-yl oxy TMS ester■
55.20	294912	n/i	n/i	456,366,327,214,145,128	Cholesterol type TMS ester
55.32	4177920	628	374	499,459,366,352,327,121	3β,5α-*bis*(TMS) 5α-Cholestane■
55.49	4177920	651	399	499,456,368,327,160,121	24-Nor-22,23-methylenecholest-5-en-3β-ol type TMS ester■
55.69	4177920	589	320	499,459,369,352,327,129	3β,5α-*bis*(TMS) 5α-cholestane type compound■
55.72	4177920	n/i	n/i	502,458,368,327,255,130	Cholesterol type TMS ester■
55.92	4177920	n/i	n/i	500,455,369,327,147,130	Cholesterol type TMS ester■
56.35	421888	n/i	n/i	503,457,367,326,158,129	Cholesterol type TMS ester
Deconjugated derivatised milt, TIC = 66705828, sample identity = sue264					
3.97	2523136	n/i	n/i	321,219,192,148,115,73	Succinic acid type TMS ester
6.05	278528	n/i	n/i	292,260,220,187,173,147	Unknown TMS ester
7.05	663552	698	400	312,300,297,212,147,132	Tris (trimethylsilyl) phosphate
7.55	647168	564	335	291,268,221,190,146,129	Butanoic acid 4-ethylthio-2(TMS)-amino, TMS ester
8.63	1392640	n/i	n/i	321,221,193,175,147,102	1,1,1 Trimethyl-2,4-TMS oxyphenyl silamine
9.02	1196032	n/i	n/i	221,194,176,146,102,73	Unknown TMS ester
9.20	311296	675	515	233,192,159,148,127,74	Hexanoic acid 2-(TMS)oxy-TMS ester
9.95	239616	n/i	n/i	320,302,228,159,147,117	Unknown TMS ester
11.10	135168	n/i	n/i	328,292,248,220,147,73	C_8 type acid TMS ester
14.12	815104	n/i	n/i	348,256,190,148,130,73	2-Methoxy phenylpentanoic acid TMS ester

15.10	417792	649	350	347,308,256,231,216,147	Tris (trimethylsilyl)-2-ketogluconic acid oxime
16.02	225280	n/i	n/i	264,243,207,163,150,136	Triethoxy ethyl silane
17.83	1605632	n/i	n/i	276,261,245,161,130,73	Cyclopropanecarbonitrile, (dimethylamino) phenyl
19.10	892928	n/i	n/i	299,284,145,131,116,73	Tetradecanoic acid TMS ester†
21.02	148480	n/i	n/i	338,310,298,204,131,116	Pentadecanoic acid TMS ester
23.90	201728	n/i	n/i	341,326,201,145,131,116	Hexadecanoic acid TMS ester†
24.67	352256	774	503	388,341,326,145,132,116	Heptadecanoic acid TMS ester†
26.63	3129344	661	448	354,339,201,144,131,116	*cis*-9-Octadecenoic acid TMS ester†
31.14	839680	725	347	359,248,175145,129,116	11-Eicosenoic acid TMS ester
31.90	610304	n/i	n/i	372,264,162,145,128,116	Docosahexaenoic acid TMS ester
33.29	397312	900	712	367,167,140,112,98,84	Decanedioic acid didecyl ester
33.97	132096	749	340	374,280,255,240,212,185	Abietic type acid TMS ester
34.40	1245184	n/i	n/i	372,355,253,238,171,128	Unidentified
36.12	438272	872	686	278,239,205,125,112,96	Decanedioic acid didecyl ester type compound
37.37	356352	n/i	n/i	411,385,223,173,116,91	$>C_{24}$ Polyunsaturated fatty acid TMS ester
39.09	548864	837	628	393,196,167,140,112,84	Decanedioic acid didecyl ester type compound
42.19	458752	n/i	n/i	406,350,280,209,168125	Triglyceride type compound
43.12	565248	n/i	n/i	234,220,190,156,142,119	Unidentified aromatic
44.52	121856	n/i	n/i	448,433,359,211,182,129	Androsta-3,5-dien-17-one *bis* (TMS) type compound
53.30	226240	n/i	n/i	458,368,327,156,130,119	Cholestane TMS ester
53.84	3080192	n/i	n/i	458,367,327,245,145,128	Cholesterol, TMS ester
73.76	2834432	n/i	n/i	529,488,310,206,124,110	Octadecyloxypropoxy octadecane
74.16	1769472	n/i	n/i	516,474,310,206,166,110	Unidentified
75.72	160768	n/i	n/i	490,310,251,219,140,111	Unidentified

¥ contaminant in fatty acid standard †corresponds to standard retention time and similar spectrum
■detector overloaded, n/i = no library fit available

2.9.4 Solid phase extraction and derivatisation of roach samples

Eggs and milt were thawed and samples (10 ml and 2 ml respectively) taken from the bulk. The samples were diluted with an equal volume of water. Two solid phase cartridges (Sep Pac, C18, 1g) were taken and conditioned with methanol (2 x 2ml, 5 min resting). The cartridges were washed with water (2 x 5 ml) and were not allowed to dry out at this stage. The milt and aqueous fraction from the eggs was loaded onto the cartridges. The cartridges were washed with water (5 ml) and eluted with ethanol (3 x 2ml) then aqueous ethanol (50/50 *v/v*, 3 x 2 ml). The samples were flow evaporated, reconstituted by mixing with water (5 ml) and extracted with dichloromethane (2 x 10 ml) to remove the free steroids. The dichloromethane was flow evaporated and reconstituted by vortex mixing with a further aliquot of dichloromethane (200 µl). The samples were injected directly onto the GC-MS. The samples were then derivatised as previously described and re-analysed by GC-MS. The

aqueous layer was deconjugated as previously described, extracted with dichloromethane (2 x 10 ml), concentrated and reconstituted as previously described. The samples were analysed by GC-MS (Table 2.21), GC program (100(3) x 5 to190 (0.5) x 2.5 to 280(15), inj 280, interface 300).

Table 2.21: SPE and derivatisation of roach samples, retention times, TICs and significant ions

Ret. time, min	TIC	Rev fit	For fit	Significant ions *m/z*	Identity
Milt SPE extracted free steroid, TIC = 4255604, sample identity = sue275					
11.52	101376	915	707	140,113,97,83,73,55	6-Tridecene
14.00	9472	n/i	n/i	228,185,129,117,87,73	Tetradecanoic acid†
18.12	157696	816	697	256,213,129,115,97,73	Hexadecanoic acid†
20.84	11648	n/i	n/i	281,256,157,133,101,88	Methyl 2,4,6-trimethyl-11-dodecenoate
21.54	33536	879	698	264,125,111,97,83,69	*cis*-9-Octadecenoic acid† **38a**
23.87	61696	907	714	150,133,119,105,91,79	Methyl 5,8,11-heptadecatrienoate
24.50	98304	915	695	161,131,119,105,91,79	Methyl eicosa-5,8,11,14,17-pentaenoate type compound
25.07	12416	906	702	207,175,133,119,105,91	8,11,14-Eicosatrienoic acid* **40**
26.25	89088	n/i	n/i	166,150,133,119,105,91	Methyl eicosa-5,8,11,14,17-pentaenoate type compound
27.04	153600	n/i	n/i	166,147,133,119,105,91	Methyl eicosa-5,8,11,14,17-pentaenoate type compound
29.29	67584	n/i	n/i	159,131,119,105,91,79	Methyl eicosa-5,8,11,14,17-pentaenoate type compound
30.59	18176	n/i	n/i	173,159,146,131,119,105	Methyl eicosa-5,8,11,14,17-pentaenoate type compound
33.39	75776	804	712	109,91,79,71,58	Unidentified
36.17	53760	n/i	n/i	136,121,109,95,81,69	Squalene **35**
46.49	12544	n/i	n/i	386,368,301,213,145,121	Cholesterol **32a**
Milt SPE extracted derivatised free steroid, TIC =38242428, sample identity = sue278					
3.43	48640	707	459	246,231,217,147,117,72	Trimethylsilyl 2,2-dimethyl-3-(trimethylsilyloxy) butanoate
17.67	847872	691	424	314,270,201,131,116,72	Hexadecanoic acid TMS ester†
18.40	51712	n/i	n/i	328,295,221,147,117,73	Heptadecanoic acid TMS ester
21.10	121856	756	490	356,341,201,145,132,117	*cis*-9-Octadecenoic acid TMS ester†
21.74	84992	887	641	335,189,145,129,108,93	9,12,15-Octatrienoic acid TMS ester
25.82	219136	n/i	n/i	278,238,175,145,129,117	Methyl eicosa-5,8,11,14,17-pentaenoate type compound
26.55	876544	n/i	n/i	221,175,145,129,117,91	Methyl eicosa-5,8,11,14,17-pentaenoate type compound
27.72	33792	897	671	267,203,175,147,133,105	Methyl eicosa-5,8,11,14,17-pentaenoate type compound
29.78	16192	818	403	295,252,204,147,83,73	Tritetracontane
31.04	389120	n/i	n/i	201,175,145,129,107,91	Unidentified aromatic
31.82	48896	911	741	155,127,113,97,85,71,57	Tritetracontane
34.24	46848	n/i	n/i	141,126,111,85,71,57	Unidentified >C_{30} alkane
36.27	125952	805	668	149,136,121,95,81,69	Squalene **35**
36.79	14464	n/i	n/i	221,147,111,97,85,71	Unidentified >C_{30} alkane

37.59	22272	n/i	n/i	281,237,146,129,103,73	Monopalmitin TMS ester
39.50	20736	n/i	n/i	280,252,148,97,85,71,57	Unidentified >C_{30} alkane
42.59	12864	n/i	n/i	307,252,149,113,97,85	Unidentified >C_{30} alkane
44.57	1753088	924	453	502,458,368,329,237,129	Cholesterol TMS ester
Milt SPE extracted deconjug'd derivatised steroid, TIC = 30844432, sample identity = sue282					
3.52	140288	n/i	n/i	160,146,116,104,74	Indole type derivative 1
7.18	121856	n/i	n/i	185,131,116,100,75	Indole type derivative 2
12.52	294912	n/i	n/i	270,194,147,89,73	Benzeneacetic acid α-methyl-3-phenoxy TMS ester
17.48	593920	901	790	328,313,201,145,132,117	Hexadecanoic acid TMS ester†
21.00	442368	854	877	356,341,201,145,132,117	*cis*-9-Octadecenoic acid TMS ester†
25.05	145408	916	589	249,205,147,129,117,91	Eicosa-5,8,11,14-tetraenoic acid TMS ester
25.70	72704	925	593	187,145,129,117,105,91	Methyl eicosa-5,8,11,14,17-pentaenoate
26.94	64256	n/i	n/i	256,239,147,112,83,70	Pyran-5-carboxylic acid derivative, TMS ester
34.35	55296	950	715	167,149,111,99,85,71	Tritetracontane
34.77	66560	958	848	253,225,113,97,85,71	Pentatriacontane
39.32	63488	n/i	n/i	197,149,127,99,85,71	Unidentified >C_{30} alkane
40.80	35840	n/i	n/i	280,215,155,112,95	Cyclododecanone type derivative
42.05	31232	n/i	n/i	217,183,167,111,95,85	Unidentified >C_{30} alkane
43.79	14912	n/i	n/i	458,368,329,217,145	Cholesterol TMS ester
Egg SPE extracted free steroid, TIC = 3653633, sample identity = sue276					
11.53	13440	n/i	n/i	140,127,112,97,83,73	Dodecanol
14.08	34048	n/i	n/i	227,185,129,97,87,73	Tetradecanoic acid†
16.08	16640	n/i	n/i	271,241,143,126,100,87	Methyl 14-Methyl hexadecanoate
18.58	116736	827	502	255,213,157,129,115,97	Hexadecanoic acid†
19.08	50688	n/i	n/i	271,185,153,129,106,97	C_{17} Monounsaturated acid methyl ester
19.82	14784	n/i	n/i	271,185,143,126,109,97	C_{18} Acid methyl ester
21.77	22528	n/i	n/i	285,208,129,111,96,83	*cis*-9-Octadecenoic acid† **38a**
23.92	27136	892	622	175,150,133,119,105,91	Methyl 4,7,10-hexadecatrienoate*
24.57	29440	n/i	n/i	180,146,119,105,91,79	Polyunsaturated C_{17} acid methyl ester
26.32	32000	n/i	n/i	166,150,133,119,105,91	Polyunsaturated C_{18} acid methyl ester
27.02	29952	n/i	n/i	180,166,133,119,105,91	Polyunsaturated C_{19} acid methyl ester
29.40	82944	n/i	n/i	173,145,131,117,105,91	Polyunsaturated C_{20} acid methyl ester
38.60	47872	n/i	n/i	131,117,105,91,79,71,58	Aromatic alkane
46.47	4992	n/i	n/i	387,369,302,248,158,107	Cholesterol **32a**
Egg SPE extracted derivatised free steroid, TIC = 46860060, sample identity = sue279					
5.02	246784	913	847	143,142,141,140,115,89	1-Methyl naphthalene
5.58	120832	n/i	n/i	170,147,142,141,129,115	2- Methyl naphthalene
13.70	544768	791	629	285,201,145,132,117,73	Tetradecanoic acid TMS ester†
14.72	124928	n/i	n/i	314,299,243,145,132,117	Pentadecanoic acid TMS ester
15.55	155648	880	693	314,299,145,132,129,117	1H-Indole-2-carboxylic acid 1-(trimethylsilyl)-5-(TMS) ester
18.08	2801664	909	854	328,313,269,145,129,117	Hexadecanoic acid TMS ester†
18.62	544768	922	796	342,327,185,145,132,117	Heptadecanoic acid TMS ester
19.33	274432	898	663	387,327,191,145,129,117	Octadecanoic acid TMS ester
21.42	802816	867	613	341,201,145,132,117,73	*cis*-9-Octadecenoic acid TMS ester
21.95	565248	968	788	355,173,145,129,108,95	9,12,15-Octatrienoic acid TMS ester

23.32	176128	819	678	318,299,221,191,147,73	Inositol, 1,2,4,5,6-*pentakis-O-bis*(trimethylsilyl) ester cf **51**
25.45	454656	n/i	n/i	238,150,106,95,79,73	Polyunsaturated C_{20} fatty acid TMS ester
26.30	851968	n/i	n/i	369,215,175,147,117,91	Polyunsaturated C_{20} fatty acid TMS ester
27.67	49920	894	675	267,203,147,133,105,91	Methyl eicosa-5,8,11,14,17-pentaenoate
31.34	1228800	n/i	n/i	201,161,132,108,91,75	Polyunsaturated C_{22} fatty acid TMS ester
34.88	290816	788	519	147,129,91,75,73	*cis*-1,8- Undecadien-5-yne 3,7-*bis*-TMS ester
35.54	157696	902	652	173,145,129,117,91,73	Methyl eicosa-5,8,11,14,17-pentaenoate type compound
36.89	33792	n/i	n/i	308,261,197,147,103,85	Unidentified
37.67	39424	803	508	419,203,171,147,129,103	9-Octadecenoic acid 2-TMSoxy-1-TMS ester
38.47	11968	n/i	n/i	392,287,219,171,131,103	Unidentified
39.49	41984	n/i	n/i	140,129,111,85,71,57	Unidentified $>C_{30}$ alkane
43.62	65536	757	453	458,368,255,159,129,105	3α-(Trimethylsiloxy) cholest-5-ene
44.45	557056	742	499	458,368,329,159,129,105	Cholesterol TMS ester
Egg SPE extracted deconjug'd derivatised steroid, TIC = 27387120, sample identity = sue281					
17.63	1343488	896	778	328,313,201,145,129,117	Hexadecanoic acid TMS ester†
20.98	262144	779	624	354,339,264,145,116,75	*cis*-9-Octadecenoic acid TMS ester†
25.12	319488	n/i	n/i	175,150,129,117,105,91	Polyunsaturated C_{20} acid TMS ester
25.77	225280	n/i	n/i	175,150,129,117,105,91	Polyunsaturated C_{20} acid TMS ester
26.97	118784	n/i	n/i	256,239,129,112,83,70	Phosphonic acid [1-((2,2-dimethylpropylidene)amino)ethyl] TMS ester
36.80	133120	962	852	141,111,97,85,71,57	Tritetracontane
39.37	76800	n/i	n/i	182,113,99,85,71,57	Unidentified $>C_{30}$ alkane
40.90	46592	n/i	n/i	357,215,129,112,93,83	Unidentified $>C_{30}$ alkane
43.42	66560	630	436	458,368,255,159,129,105	3α-(Trimethylsiloxy) cholest-5-ene
44.67	20992	n/i	n/i	458,368,329,159,129,105	Cholesterol TMS ester

*,** similar spectra, likely to be related compounds, †= confirmed by comparison to authentic standard, n/i = no library fit available

Chapter 3, Fish Discussion

3.1 Introduction

The aim of this project was to try and identify the pheromone associated with rainbow trout spawning. Fatty acids and amines are common volatile components found in fish and standards were run so that these could be excluded from the analysis. Testosterone **26** is potent salmon odorant and was selected as an initial target for detection and quantification.

3.2 Analysis of standards

3.2.1 Kovats Indices standards

A series of alkane standards were analysed by GC-MS under a standard temperature program to determine retention times. Plots of the known Kovats indices (KI) of the alkanes (carbon number x 100) against retention time (Fig 2.1), yielded the equation of the regression line which was used to calculate the KIs of unknowns. Similarly a sequence of fatty acids were run, the KI determined and these used to calculate the KI and retention times of homologues (Fig 2.2, 2.3).For example the index for tetradecanoic acid is 1792, the KI for hexadecanoic acid is 1948 so the index for pentadecanoic acid is approximately 1870 and can be used as an extra confirmatory test with the spectral information. Excellent regression lines were obtained and typical errors in KI were ± 5. Unfortunately, under this set of run conditions, both C_{18} acids, stearic and oleic, co-eluted, but they could be distinguished by differences in their mass fragmentation spectra.

3.2.2 Testosterone 26 calibration curve

The testosterone **26** standards were analysed by GC-MS and the detector response plotted to produce a calibration curve (Fig 2.4) which was fitted to a second order equation (R^2 = 0.9865).

3.3 Solid phase extraction

To concentrate small amounts of hydrocarbons, such as steroids we elected to use solid phase extraction with HPLC analysis. The recovery rate was measured using a test solution of testosterone **26** with Sep Pac and Supelco, C18 solid phase extraction cartridges[104], eluted with ethanol and ethanol/water. The recovery rates were 15.5 % and 76.0 % respectively. This experiment was repeated, but the elution solvents were changed to aqueous methanol to try and increase the testosterone **26** recovery, but the recoveries were identical to those before.

3.4 Steroid Standards

A fatty acids standard (C_{14} - C_{18} and squalene) was analysed and used to construct a Kovats Indices plot, the regression data was then used to calculate Kovats Indices for a steroid standard (testosterone **26**, 5β-androstan-3,17-dione **29**, 17α-hydroxy-progesterone **30a**, 4-pregnen-17α, 20α-diol-3-one **31** and cholesterol **32a**). The linear program ran to 50 minutes and cholesterol with a retention time of 51.6 minutes was included in the Kovats calculation to give an approximate value.

A series of steroids (testosterone **26**, 5β-androstan-3,17-dione **29**, 17α-hydroxy-progesterone **30a**, 4-pregnen-17α, 20α-diol-3-one **31** and Reichstein's Substance **30b**) were selected which were structurally representative. Steroids are not particularly amenable to analysis by GC-MS as they are relatively large and involatile, consequently they were derivatised as the more volatile trimethylsilyl derivatives prior to GC-MS analysis[105]. The ketone groups were converted to oximes with hydroxylammonium chloride in pyridine and the hydroxyl groups were converted to silyl ethers with trimethylsilyl chloride and *N,O-bis*(trimethylsilyl)acetamide[71]. Trimethylsilyl reagents react readily with hydroxyl groups to give more volatile and stable derivatives, but must be prepared under dry conditions. All five steroids were successfully derivatised and were identified by GC-MS analysis. The addition of the silyl groups does make identification of compounds more difficult as many are not in commercial libraries, and deduction from first principles is hindered by the loss of the *m/z* 73 silyl groups.

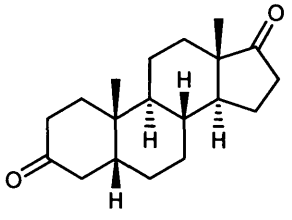

29 5β-Androstan-3,17-dione

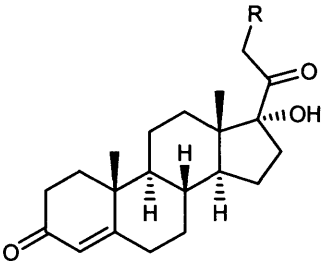

30
a R = H 17α-Hydroxyprogesterone
b R = OH Reichstein's Substance S

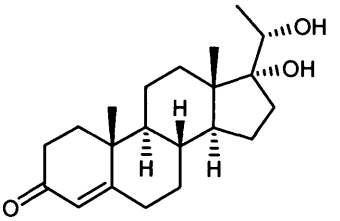

31 4-Pregnen-17α,20α-diol-3-one

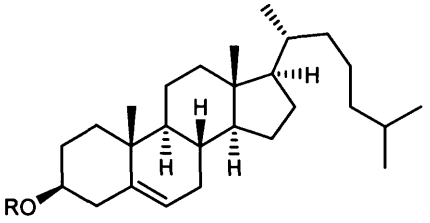

32
a R = H Cholesterol
b R = acyl (fatty acid esters)

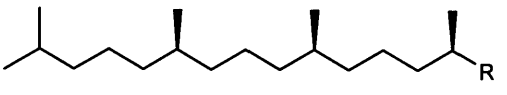

33
a R = CH_3 2,6,10,14- tetramethylpentadecane; pristane
b R = CH_2CH_3 2,6,10,14 tetramethylhexadecane; phytane

3.5 Fishery samples

3.5.1 Extraction of raw water samples

The next step in the program was to determine the types of compounds which are routinely present in natural waters used in the hatcheries and fisheries. The samples were extracted using the SPE procedure described in section 2.3.2, using aqueous methanol as the elution solvent. The samples were obtained from the hatcheries stocked and managed by Bristol Water Plc. The outflow from the hatcheries contained a complex mixture of both organic and inorganic parameters and the presence of such inorganic components and any solid, suspended material can interfere with recovery. A testosterone **26** standard prepared in water was similarly treated and comparison with a non-extracted standard gave a recovery of 48.5%, which was a little lower than those reported earlier.

The samples in this experiment were analysed by GC-MS and two peaks were detected in the chromatogram. The earlier eluting peak was identified as a saturated hydrocarbon, phytane **33b** (2,4,6,10- tetramethylhexadecane, see section 2.2), from the mass spectrum: it is a commonly occurring compound, often found in fish oils, but equally it could have been derived from the pelleted fish food or from plant matter. The other peak in the chromatogram was identified as a *bis*(2-ethylhexyl)phthalate ester **34** a notorious contaminant, used as a plasticiser. The failure to detect more components is probably due to the high flow of water through the fish farm and the consequent dilution of analytes.

3.5.2 Extraction of fish holding tanks at Blagdon site

We next investigated water taken from holding tanks, which was anticipated to contain more metabolites. Samples 1, 3, 5, 7 (Fig. 2.5) were extracted using the solid phase method whereas samples 2, 4, 6 were extracted using the liquid/liquid technique. A water sample and sample 7 were spiked with testosterone **26** std (250 µl, 0.1 mg/ml) prior to extraction. Blanks were also extracted using the same conditions. The testosterone **26** recovery from the fishery sample was found to be 55.7%, a little lower than that found in the previous SPE method, the reduced recovery may be explained by the presence of fine particulate material.

The compounds detected by both methods were very similar, most of which were also detected in the water blanks, and could therefore be attributed to incidental contamination and background. The most likely source for them was the dichloromethane, which was an HPLC grade solvent and when samples of this grade were concentrated, they displayed a similar TIC.

Both extraction methods use a 1.0 L sample and concentrate to 100 µl, of which only 1 µl was injected. This is a concentration factor of 10 000 times, but only an analytical

concentration of 100 fold, which was not sufficient to produce enough material to detect. In studies of steroids and steroid glucuronides from holding water containing adult African Catfish, the sample volume collected was 70 L after 24 hours with no through tank flow, and this was concentrated down to just 2 L by freeze-drying before any form of extraction[72].

The most obvious difference between the SPE and liquid/liquid extracts was that the latter were more highly coloured. The source and nature of the coloured component(s) was not identified, and it is likely to be an organic component as it was solvent extractable. The samples were compared against the appropriate blank, and any peaks appearing in both chromatograms were excluded. The liquid/liquid extracts were found only to contain *bis*(2-ethylhexyl) phthalate **34**. The SPE extracts were found to contain two peaks, which were identified as phytane **33b** and cholesterol **32a**. No other peaks were detected, which confirmed the organic purity of the water discharged through tanks containing 43 000 fish.

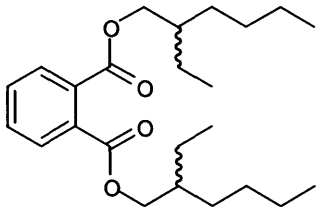

34 *bis*(2-Ethylhexyl)phthalate

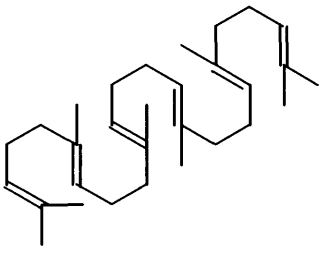

35 Squalene

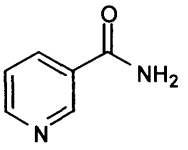

36 Nicotinamide

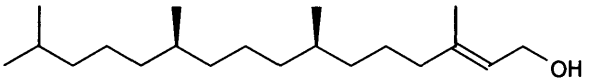

37 Phytol

3.6 Extraction of rainbow trout tissue

It was decided to examine various parts of a fish to determine what types on compounds could be detected. Although the actual sex of the fish was unknown, it is likely that the fish was female because male fish become aggressive and rapidly loose condition with damaged scales and fins during the breeding season, which makes them unattractive to consumers and therefore the majority of farmed fish are female. The fish was separated into 3 duplicate sets of samples, skin mucus, abdominal organs and skin, with an additional single sample of stomach contents.

Fatty acids are major metabolites from fish and we wished to identify the characteristic profile from trout so that we could identify them in further analysis. One set of the samples plus the stomach contents were prepared by extraction with saturated ammonium sulphate at pH 1 with diethyl ether/ethanol solution and reconstituted in dichloromethane. Another set of

samples were ground with water and extracted with dichloromethane. Three main groups of compounds were detected in these samples: fatty acids, cholesterol type derivatives and aliphatic hydrocarbons. The skin mucus sample contained significantly different compounds from the skin and stomach contents with three cholesteryl esters **32b** identified. The stomach contents sample contained three main saturated fatty acids, C_{14}, C_{16} and C_{18}, cholesterol **32a** and cholesterol derivatives **32b** were also found. The skin contained both saturated and unsaturated fatty acids, mainly hexadecanoic and 9-*cis*-octadecenoic acid **38a** (Fig 3.1) and squalene **35**, with lesser amounts of 8,11,14-eicosatrienoic acid **40**. The other major component was dodecanol. Octadecanoic, octadecenoic **38a**, octatrienoic **39** and eicostrienoic **40** acids plus cholesterol **32a** and squalene **35** are all common fish oil constituents.

Fig 3.1: Comparison of fatty acids from acid or neutral solvent extraction of trout tissues

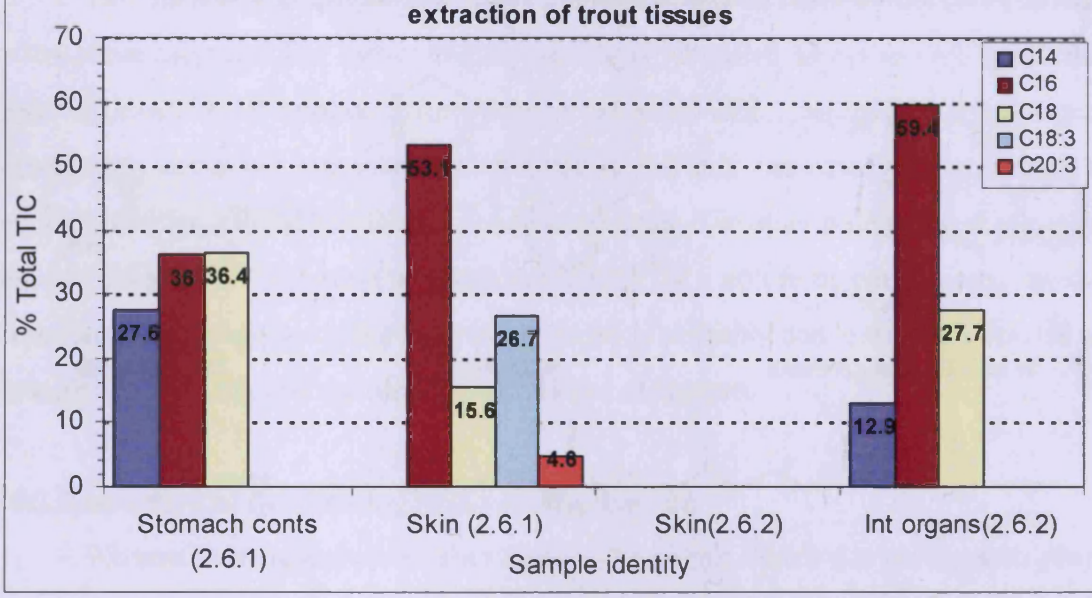

The samples extracted with dichloromethane were found to contain the same classes of compounds as those from the acid/buffer extraction with the exception that the skin mucus sample produced nicotinamide **36** (pyridinecarboxamide or niacinamide), which is not extractable from aqueous acid. This is a naturally occurring derivative of nicotinic acid, is found in plants and animals, usually associated with enzymes and is often in a conjugated form. It has functions in protein and carbohydrate metabolism, lipid metabolism in fish, is a component of coenzyme I and coenzyme II for glycolysis and tissue respiration and is the base in nicotinamide adenine dinucleotide (NAD). The skin sample did not yield any fatty acids at neutral extraction, but did give pristane **33a** and phytane **33b**.

The stomach contents sample contained differing combinations of C_{14}, C_{16} and C_{18} fatty acids, as well as cholesterol **32a**, phytane **33b** and pristane **33a**. Pristane **33a** and phytane **33b**

are found in hydrocarbon fuels as well as fish liver oils; the internal organs contained only phytane **33b** whereas the skin extract contained pristane **33a** as well in the ratio 1:15 in favour of phytane **33b**.

Pristane **33a**, 2,6,10,14-tetramethylpentadecane, is a C_{19} alkane and is derived from phytol **37**, a C_{20} alcohol which is a component of chlorophyll. Phytane **33b**, 2,6,10,14-tetramethyl-hexadecane, is also a phytol derivative and both compounds are isoprenoids. The relative amount of phytane **33b** to pristane **33a** in fish tissue has been suggested as a tool for determining hydrocarbon pollution after an oil spill[106], as have squalene **35** ratios relative to pristane **33a**. Pristane **33a** is reported as being the predominant hydrocarbon in marine salmon. In contrast, in our study of freshwater trout, phytane **33b** was the major hydrocarbon. Squalene **35** has been reported as a major component in trout livers[107], but in these tissue samples it was relatively less abundant.

The range of fatty acids in our study is typical of those routinely determined in this work and also with those reported (by Satué and López) for the fatty acid composition in trout livers who looked at sex based differences. They found that the relative proportion of mono-unsaturated acids to total acid content was much higher in females, whereas the polyunsaturated acids were higher in males. The saturated acids in the range C_{14} - C_{22} were only slightly higher in males. The main unsaturated acids were $C_{16:1}$ n-7, $C_{18:1}$ n-9, $C_{18:1}$ n-7, $C_{18:2}$ n-6, $C_{20:1}$ n-9, $C_{20:2}$ n-6, $C_{20:5}$ n-3, $C_{22:1}$ n-11, $C_{22:5}$ n-3, $C_{22:6}$ n-3. Of these, the predominant male acids were $C_{22:6}$ n-3, $C_{16:0}$, $C_{18:1}$ n-9, $C_{22:5}$ n-3, $C_{18:2}$ n-6 and the predominant female acids were $C_{18:1}$ n-9, $C_{22:6}$ n-3, $C_{16:0}$, $C_{18:0}$, $C_{16:1}$ n-7 (Fig 3.2). The fatty acid which occurred in the highest concentration was octadecenoic acid **38a** and this was also found in the various tissue samples examined in our studies.

6,9,12-Octadecatrienoic acid **39** (γ-linolenic acid, GLA) is the precursor of dihomo-γ linolenic acid, which in turn is a precursor of monenoic prostaglandins (PGA-J_1). 5,8,11,14-Eicosatetraenoic acid **41** (arachidonic acid,) is the precursor of dienic prostaglandins (PGA-J_2). 5,8,11,14,17-Eicosapentaenoic acid **42** is an important polyunsaturated fatty acid of the marine food chain and is a precursor of trienic prostaglandins (PGA-J_3). It differs from arachidonic acid **41** by the extra double bond between C_{17} and C_{18} and is isolated from cod liver oil.

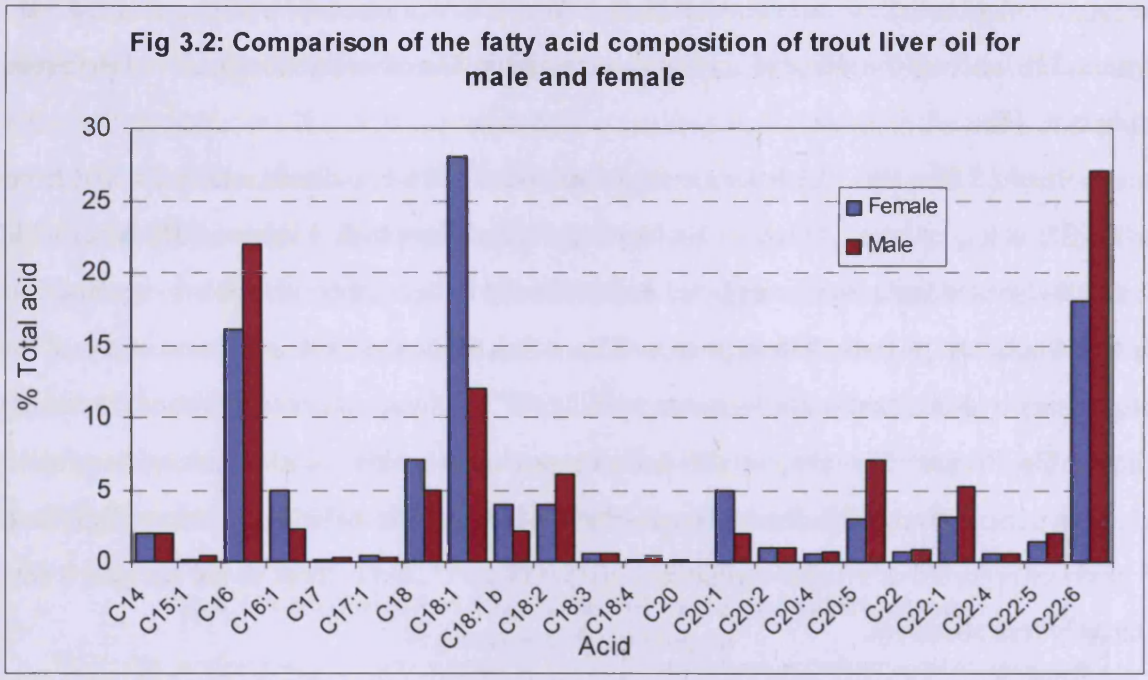

The eicosanoids are a class of biochemically active compounds derived from arachidonic acid **41** which includes prostaglandins, prostacyclin, thromboxanes and leukotrienes. Prostaglandins were first discovered in seminal fluid and accessory genital glands of man and sheep. Prostaglandins are divided into groups: A-J based on the functional groups of the cyclopentane ring. $PGF_{2\alpha}$ **22** has been implicated as a goldfish pheromone released by the female to induce spawning as the eggs are released.

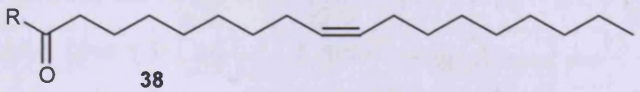

38
a R = OH; (*Z*)-9-Octadecenoic acid, oleic acid
b R = NH_2; (*Z*)-9-Octadecenamide

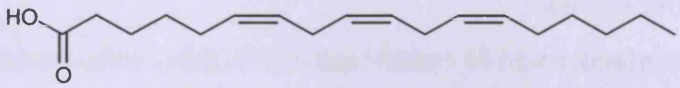

39 (*Z*,*Z*,*Z*)-6,9,12-Octadecatrienoic acid, γ-linolenic acid

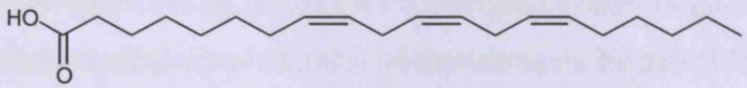

40 (*Z*,*Z*,*Z*)-8,11,14-Eicosatrienoic acid

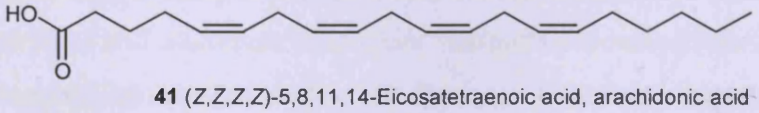

41 (*Z*,*Z*,*Z*,*Z*)-5,8,11,14-Eicosatetraenoic acid, arachidonic acid

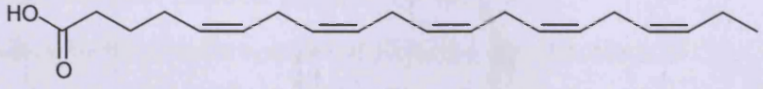

42 (*Z*,*Z*,*Z*,*Z*,*Z*)-5,8,11,14,17-Eicosapentenoic acid

3.6.2 Re-analysis of the skin scrape and extracted skin samples

The samples prepared in sections 2.6.1 and 2.6.2 were stored frozen and reanalysed to compare the components found (Fig 3.3). The pristane **33a** :phytane **33b** ratio of 1:13 in the neutral skin extract again confirmed that phytane **33b** is the major component, with pristane **33a** not detected in the acid extract at all. This was surprising as both pristane **33a** and phytane **33b** are neutral hydrocarbons and should not be affected by the sample pH. The acid skin extract also produced a wide range of fatty acids and cholesteryl esters **32b**. The fatty acids were even numbered acids, with trace amounts of odd numbered acids (C_{15}, C_{17}) which may be naturally occurring, or they may have formed as breakdown products during storage. The fatty acid methyl esters detected were also present in trace amounts and again may be naturally occurring or as a result of sample degradation as they had not previously been detected.

The skin scrape samples produced similar results to the original experiment, nicotinamide **36** and no fatty acids were detected in the neutral extract, but the acid extracted sample contained the fatty acids and cholesteryl esters **32b** as previously seen. The acid extract also produced a chromatogram with a TIC an order of magnitude higher than the neutral method.

Fig 3.3: Comparison of fatty acid ratios from reanalysed samples

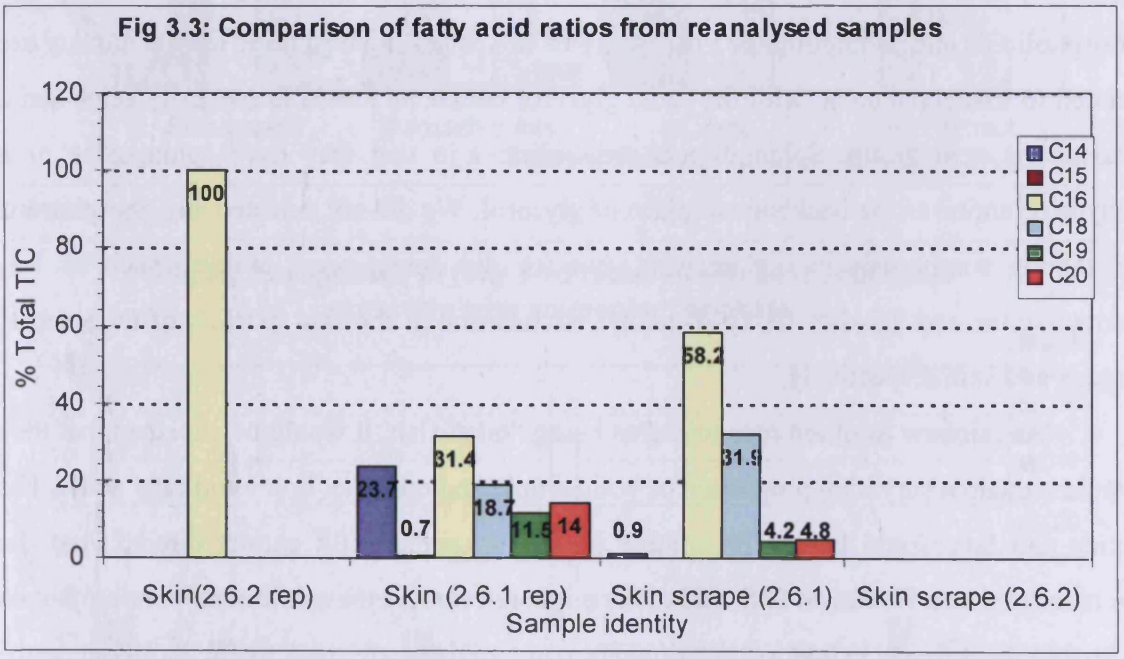

Some of the compounds could not be identified and this is due to a number of factors, including low TIC counts (total ion current) and hence crucial ions may be missing, and, despite the large number of entries in the library, no matching spectra. In this latter case it is sometimes possible to work out the structure from first principles, but as compounds become increasing complex this becomes almost impossible and it is only possible to identify the broad

class to which the compound belongs by identifying specific parts of the structure.

3.7 Repeat of fish extraction

3.7.1 Standard tissue extraction

A fresh fish was subjected to the same extraction and analysis as before ie two sets of samples comprising of skin mucus, stomach contents, internal organs and skin were subject to extraction at either neutral pH with dichloromethane or extraction at pH 1 with ammonium acetate and diethyl ether/ethanol solution. This produced a duplicate set of extracts which, after initial analysis, could be further manipulated.

The results for the samples extracted with ammonium acetate produced a wide range of fatty acids and glycerides. Complex lipids such as those found in fats and waxes would have high melting and boiling points so would be difficult to analyse by GC-MS and are usually converted to more volatile esters such as the methyl esters, FAMEs, for analysis. Complex lipids have ester linkages and typically are triacylglycerols, comprised of a glycerol backbone with long chain carboxylic acids attached by these ester links. The ester bonds can be readily hydrolysed to yield smaller molecules. Cholesterol **32a** is classed as a simple lipid and has no ester bonds, so cannot be hydrolysed in this fashion. Other important groups of lipids are phospholipids and sphingolipids. Phospholipids are esters of phosphoric acid and many are related to triacylglyercols, with the same glycerol backbone joined to two fatty acids and a phosphoric acid group. Sphingolipids are different in that they have sphingosine or a dihydroxyamine as the backbone in place of glycerol. We did not detected any phosphorous containing compounds in our analysis, but we did detect some amines, such as 1,5-pentadiamine and 2,2-dimethoxy-*N*-methyl ethanamine in the acid extracts of the internal organs and skin respectively.

As rainbow trout are recognised as being "oily" fish, it would be expected that they would contain a very high proportion of both simple and complex lipids and fatty acids. The lipids and fats would be readily soluble in solvent and should extract directly into the dichloromethane. However, fatty acid esters might not survive the acidic conditions employed with the ether/ethanol extraction and would be converted to their respective acids and alcohols. The acid conditions would ensure that most species would be fully protonated and therefore more amenable to solvent dissolution. A wide range of fatty acids was identified for both extraction techniques (Figs 3.4, 3.5).

Naturally occurring fatty acids whether saturated or unsaturated, all have an even number of carbon atoms, and is a feature of the biosynthetic pathway. This observation raises

questions over the identities of the odd numbered acids suggested by the library searches, *i.e.* their source and even accuracy of the library matches. It is also unusual to find branched fatty acids, the majority being straight chain, again irrespective of degree of saturation. These identifications should be regarded as tentative, especially when the "goodness of fit" is low.

The samples extracted under neutral conditions confirmed earlier findings of a series of C_{14} - C_{20} fatty acids, cholesterol **32a** and nicotinamide **36** in the skin extract. Pristane **33a** and phytane **33b** in the ratio of 1:15 were only detected in the skin sample. The neutral extracts produced a narrower range of fatty acids than the ammonium sulphate extracts.

Fig 3.4: Comparison of fatty acid ratios from trout tissue, repeat neutral extraction

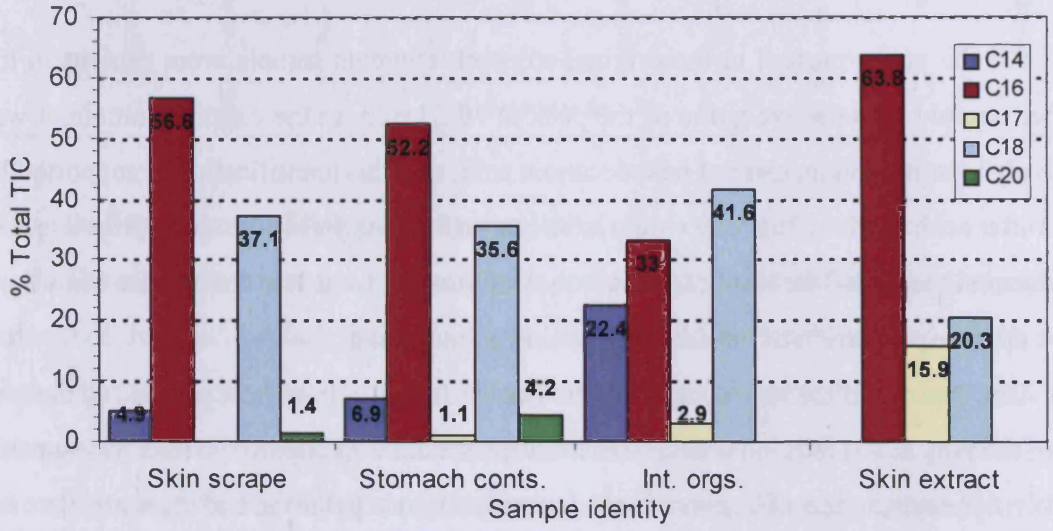

Fig 3.5: Comparison of fatty acid ratios after repeat trout tissue extraction with ammonium sulphate

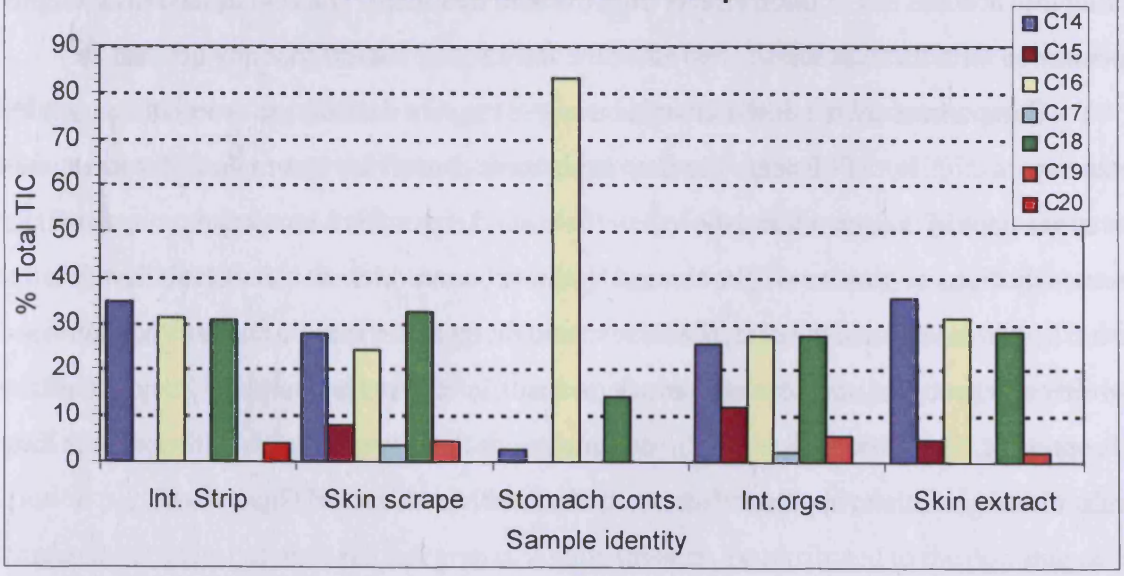

The carboxylic acids detected were heavily influenced by the pH at extraction. The samples extracted at neutral pH tended to produce large fatty acids in the range C_{14} - C_{20}, whereas the acid extracts produced some very small acids, *e.g.* 2-methylbutanoic acid, as well as the larger acids.

3.7.2 Acidification of dichloromethane extracts

The neutral extracts prepared in Section 2.7.1 were treated with dilute hydrochloric acid and re-extracted with dichloromethane. The acid treatment was designed to ensure that any basic material would not extract. The samples were compared pre- and post acid treatment (Fig 3.6).

All the peaks present in the original stomach contents sample were present in the acidified sample with the exception of the peak at 19.23 min. In the original sample, it was tentatively identified as an ester of hexadecanoic acid, and this identification is supported by its loss after acidification. The ester would have been cleaved to yield both the appropriate acid (hexadecanoic acid) and the alcohol. The alcohol has not been detected under these conditions but the relative proportion of hexadecanoic acid has increased.

Comparison of the skin scrape sample before and after treatment resulted in the loss of all of the fatty acids, the cinnamate, benzenesulphonamide and hydroxytriphenyl stannane. Hydroxytriphenylstannane is a pesticide used to treat blight in potatoes, and the acetate is used as an algicide. The dodecanoate ester was unaffected as was the hexadecanol and cholesterol **32a**. The fatty acid loss was unexpected, as was the order of magnitude drop in TIC, even taking into account any dilution effects from the acid treatment. The acid treated skin sample, in common with the skin scrape, lost all of the fatty acids, but left the fatty acid esters.

Comparison of the internal organ samples again showed an order of magnitude reduction in TIC, but in this case the fatty acids were conserved. The main differences were the appearance of dodecanol, and the loss of the methyl eicosapentaenoate type compound. As previously discussed, esters will be cleaved by this process which would account for this latter loss. The conservation of the octadecadienoic acid methyl ester may be due to either increased stability and hence resistance to acid attack, or insufficient acid to completely degrade all the ester present. The internal fatty strip in common with the internal organs conserved the fatty acids, although with an apparent decrease in the relative amount of C_{18}.

Fig 3.6: Comparison of fatty acids from various fish tissues with and without acid treatment

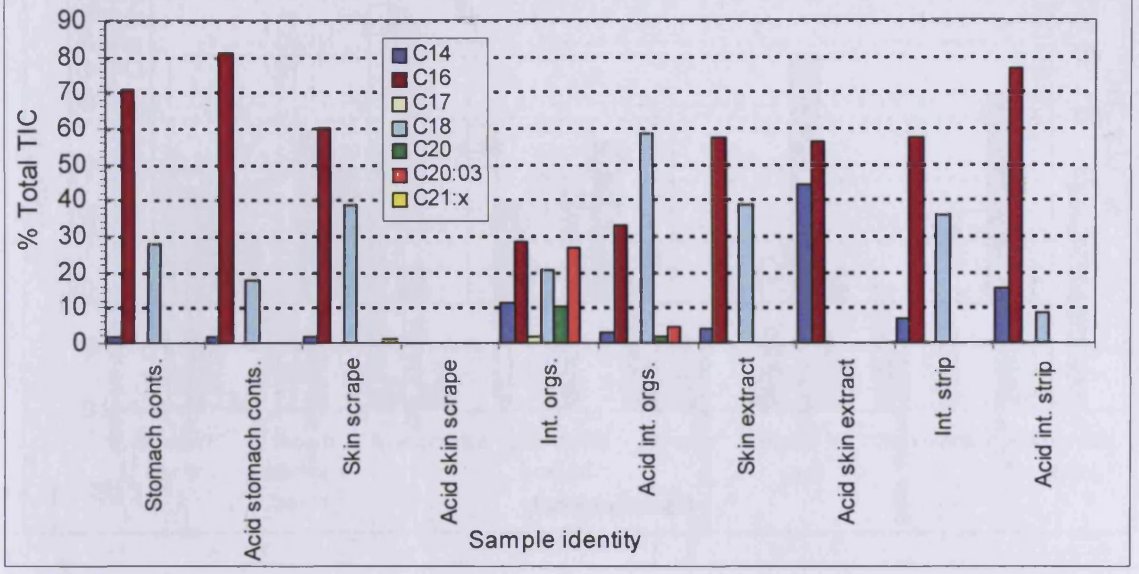

3.7.3 Alkali treatment of fish extract samples

The alkali treatment used a strong base, sodium hydroxide, and it was anticipated that compounds such as the fatty acids and glycerides would be much reduced which would enhance the detection of basic compounds and components obscured by the huge acid peaks in previous samples. However, it was found that any basic compound peaks were very small and mainly unidentified. The alkanes, cholesterol **32a**, pristane **33a** and phytane **33b** were not affected. Pristane **33a** and phytane **33b** were detected in the base internal organs at the ratio of 1:19, and in the internal fatty strip at the ratio of 1:21, which were comparable to those reported previously.

Generally, the base treated samples had a lower overall TIC than the untreated samples and this was due to the presence of huge fatty acid peaks in the untreated samples. The fatty acids were completely removed from the base treated samples (Fig 3.7), but the corresponding esters were not detected, although 6,10,14-trimethyl-2-pentadecanone (dihydrofarnesyl acetone) was identified in the base treated internal organs. 6,10,14-trimethyl-2-pentadecanone is commonly found in natural products (723 reports in *Chemical Abstracts*, 160904) and is usually derived from a sesquiterpene by 3 carbon chain extentension. Nicotinamide **36** was again lost from the skin scrape sample, suggesting it is extremely sensitive to changes in solution pH. Some peaks which were identified in treated samples were also present in the untreated samples, but were not integrated. Again, this may be attributed to the dominance of the fatty acids.

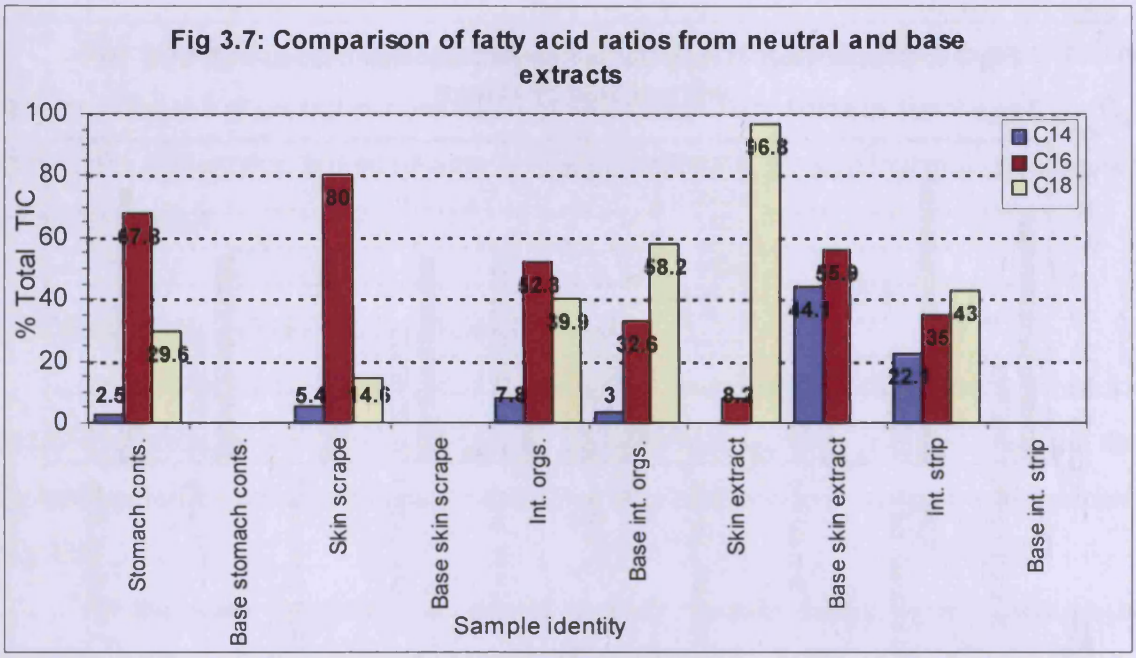

3.7.4 Bicarbonate treatment of fish extract samples

The bicarbonate treatment was a milder form of basification than that used in the previous section. Although the long chain acids (>C_{14}) were reduced in the bicarbonate treated samples, they were not completely removed. For many of the samples the compounds were the same in the bicarbonate treated and untreated samples. The most changes were seen at the lower retention times, with some of the short chain fatty acids absent in the bicarbonate treated samples. The larger fatty acids *e.g.* tetradecanoic acid seem to be immune to bicarbonate treatment, which is presumably a consequence of the low solubility of the carboxylic acid in the aqueous phase and hence a very slow reaction with base. The glycerides detected in the stomach contents were also reduced, but still detectable. Cholesterol **32a** was not obviously affected by this treatment. Comparison of the relative proportions of the long chain acids (Fig 3.8) shows identical patterns for both the treated and non-treated samples, with C_{16} being the dominant acid in the majority of cases.

The fatty acid esters, *e.g.* methyl eicosapentaenoate were enhanced in the treated samples, because bicarbonate is sufficiently basic to convert carboxylic acids to water soluble salts, but not sufficiently basic to hydrolyse esters.

Fig 3.8: Comparison of fatty acid ratios from neutral and bicarbonate extracts

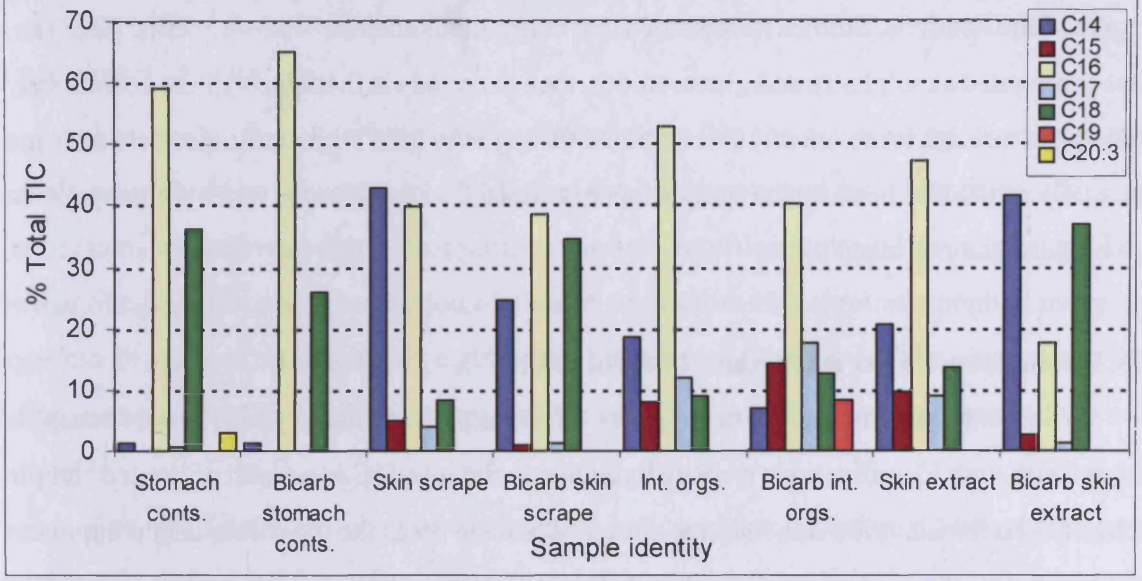

Comparing the results of this experiment with the previous, harsher base treatment showed that more components were removed under the harsher regime, and the bicarbonate was used because the hydroxide was too strong. It was intended that the acids would be removed and esters retained. The hydroxide experiment produced an order of magnitude reduction in the TICs recorded, probably as a result of the fatty acid removal, whereas this degree of TIC reduction was not seen with the bicarbonate treatment, at most a reduction of a factor of 1.5 was seen, which corresponds to the fatty acids retention.

3.8 Trout urine

Urine samples were collected by catheterizing trout and pooling the urine. The female urine was subject to bioassay and known to be active. Male urine was also collected in the same fashion. The trout stocks, urine collection and bioassay were all maintained by Dr. Alexander Scott, DEFRA (formerly MAFF) at Lowestoft. Having analysed various parts of the fish, the next step was to obtain samples of the urine for analysis. Urine is thought to be the route of pheromone release. Urine has been shown to be a potent odorant for several fish species, including salmon and goldfish. Collaborators based at MAFF, Lowestoft, were able to maintain a population of rainbow trout and collected the urine direct from their bladders using a catheter system. The pooled male and pooled female urine was received for analysis.

3.8.1 Direct injection of trout urine

Direct injection of both regular and freeze-dried urine on a DB-Wax column produced

only two identifiable peaks, dimethylamine (*N*-methylmethanamine) and trimethylamine. Although other peaks were detected in the concentrated samples, the amounts were too low to give identifications. Studies have shown that compounds such as benzo-a-pyrene (BaP) are first conjugated as sulphates and glucuronides, then excreted via the urine[108]. Fish excrete only some urea through urine, mostly it is excreted through the gills with ammonia. Teleost urine is usually dilute and because the samples were collected *via* a catheter, water reabsorption in the bladder had not taken place.

3.8.2 Dichloromethane extractions of trout urine

Solvent extraction of the urine under different pH conditions yielded more complex results, although identifications were difficult due to the low TIC as a result of limited sample volume. The female urine was found to contain squalene **35** as the most abundant component and associated derivatives in all fractions. The basic fraction contained nothing other than squalene and the acid extract showed only one other peak, a monounsaturated long chain (C_{30}) alkene. The neutral extract was found to contain amides and an amine, an alcohol, and also cholesterol **32a** and cholesterol derivatives.

All the male trout urine samples again contained squalene **35**. The basic sample also gave a compound tentatively identified as 9-octadecenamide **38b** and the acid sample gave a lanostanone type compound. A series of C_{19} - C_{28} alkanes was identified, and the C_8 and C_{18} fatty acids were not detected in any of the other samples.

3.8.3 NMR analysis of freeze-dried urine

The freeze dried and deuterium oxide azeotroped urine gave a ^{1}H-NMR spectrum in D_2O which indicated the presence of two components in the ratio circa 90:10, plus other minor peaks. Signals from the minor component at δ 5.24 (d 3.8 Hz) and δ 4.66 (d 7.9 Hz) indicated the α- and β-anomers of a pyranose with an equatorial group at the 2-position. There was also a methyl doublet at δ 1.32 (d 6.9 Hz). The spectrum was not identical to 6-deoxyglucose, which leaves the alternatives of 6-deoxy-allose and -galactose (cf **53**). From comparison with published data the minor component appears to be 3-*O*-methyl-6-deoxygalactose (3-*O*-methyl-fucose, digitalose) **52**, which is a common component of steroidal glycosides. The major component only showed three peaks 3.68 (d *J* 6.6); 3.4 (*J* 6.6); 3.25 (t *J* 6.5). The absence of aldehydic, acetal or hydrate signals excluded a sugar and the simplicity of the couplings indicated a symmetrical molecule. Comparison with authentic material showed the material was mannitol **54**.

When $CDCl_3$ was added to the NMR tube, no signals were seen other than hydrocarbons, therefore no organic material in a solvent extractable form was present.

3.8.4 HPLC of trout urine

The aim of this experiment was to demonstrate that the active component from the female urine could be separated by HPLC, and the bioassay would have identified which of the fractions was active so that further purification and identification could be undertaken. The methanol eluant from SPE extraction of female trout urine was chromatographed using an acetonitrile gradient and produced eight peaks between 9 - 66 minutes. The eluant from the HPLC was collected in 4 time fractions, but due to a short breeding season, bioassay was not possible.

The NMR data from the previous section indicated that sugars might be present, so a portion of the freeze-dried urine was acetylated and subject to HPLC. The urine sample produced 25 peaks with retention times between 9 - 66 min, as seen in the SPE extract. Although identification was not possible, this clearly demonstrates that female trout urine contains many components.

3.8.5 Solvent extract and deconjugation of female trout urine

The HPLC results showed that many compounds are present in trout urine, but gave no structural information so the presence of steroids could not be confirmed A solvent extraction was performed to remove organic material, then the aqueous layer was treated with glucuronidase solution and extracted with dichloromethane. This extract and the initial dichloromethane extract were both analysed by GC-MS. Compounds which were found in both extracts were suspected to be contaminants. The first solvent extract yielded two alkoxyalcohols, an alkyl phosphate, an acetamide, an alkylthio cyclopropylidene, two 28-nor-17β-(H) hopane derivatives **45ab** and 17α-hydroxy-androst-4-en-3-one (17-*epi*-testosterone) **44** as assigned from reverse library fit.

Hopanoids are produced by aerobic bacteria from the cyclization of squalene **35** to a pentacyclic triterpenoid with a hopane skeleton. Prokaryote cells use hopanes in the cell walls where eukaryotes use sterols[109]. Hopanes are frequently found in oil spills, in association with pristane **33a** and phytane **33b**, and are often used as pollution markers.

The identification of 17-*epi*-testosterone **44**, was very significant given that testosterone **26** is described as a potent odourant in salmon and plausibly could have a biological role with trout. The Kovats Index for 17-*epi*-testosterone **44** was 2804, which is

comparable to that for testosterone **26** (KI 2826). The time difference is 26 seconds. The forward and reverse fits for 17-*epi*-testosterone **44** were 435 and 819 respectively and the initial assignment was made on the basis of the reverse match. The second entry in the list of spectral matches was for testosterone **26**, with a forward and reverse match of 471 and 782 respectively and although the reverse match for 17-*epi*-testosterone **44** is slightly higher, the forward match for testosterone **26** is better. The spectra of both isomers are virtually identical with the same major fragments and intensities, the matches are almost identical and testosterone **26** is a known fish hormone, thus 17-*epi*-testosterone **44** is likely to be a misidentification and the correct assignment is testosterone **26**.

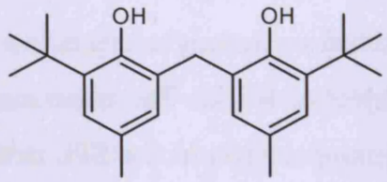

43 2,2'-Methylene-*bis*-6-(1,1-dimethylethyl)-4-methylphenol

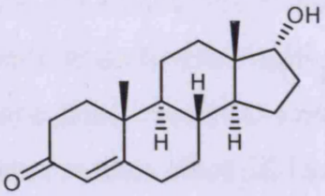

44 17α-Hydroxyandrost-4-en-3-one, 17-*epi*-testosterone

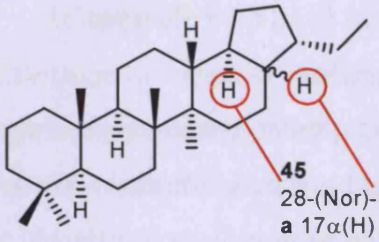

$C_{30}H_{52}$ parent hopane
$C_{29}H_{50}$ for nor-compounds
$C_{28}H_{48}$ for *bis*-nor-compounds

45
28-(Nor)-17(H)hopane
a 17α(H)
b 17β(H)

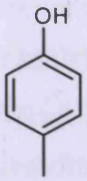

46 4-Methylphenol, *p*-cresol

The deconjugated extract gave 4-methylphenol (*p*-cresol) **46**, 3α,5α,17β-androstane-3,17-diol **47** and 5β,17β-hydroxy-androstan-3-one **48** with Kovats Indices of 2683 and 2722 respectively, which again compare favourably with the Index of 2690 for 5β-androstane-3,17-dione **29**. Two further peaks with retention times of 50.3 and 50.7 min were tentatively identified as an alkyl ester of an oxirane acid and 9-octadecenamide, but despite high TIC counts, the matches were poor leading to doubt over the assignments and it is more probable that at least the oxirane acid may be a steroid. 9-Octadecenamide (oleamide) is a known sleep inducing lipid in mammals and is rapidly hydrolysed to ammonia and 9-octadecenoic acid[110, 111] **38a**. All the steroids identified in the urine were androgens, rainbow trout release sulphated steroids through urine[112] and testosterone **26** is a potent odorant in precocious male Atlantic salmon[73].

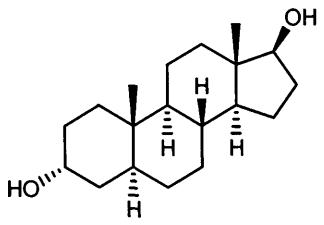

47 3α,5α17β-Androstan-3,17-diol

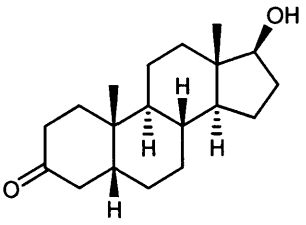

48 5β,17β-Androstan-3-one

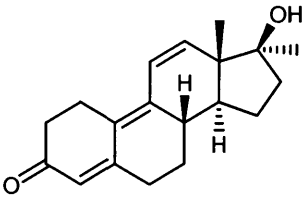

49 17β-hydroxy-17-methylestra-4,9,11-trien-3-one

3.8.6 Electrospray analysis of female trout urine

The freeze-dried urine direct injection analysis will give masses for all components in the sample. The HPLC results indicated at least eight components were present, rising to 25 after acetylation. The electrospray produced 9 peaks with an abundance over 20 % ranging in mass from 131 - 548. The androgens identified in the previous experiment have masses in the range of 288 - 292 as free steroids, and 384 - 388 as sulphates, but there are no direct matches with the electrospray masses. A survey of the masses of C_{19}, C_{21} and C_{27} steroids and prostaglandins produced one match for the 284 mass, a synthetic anabolic steroid, 17β-hydroxy-17-methylestra-4,9,11-trien-3-one; methyltrienolone **49**.

The HPLC separation prior to electrospray produced a series of peaks which did not give mass spectra as the response was too low. The final peak in the chromatogram gave also gave a low response, but a spectrum was obtained and gave the molecular mass as 410, which is tentatively identified as squalene **35**.

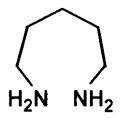

50 Cadaverine

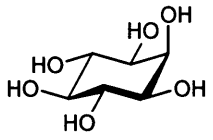

51 *myo*-Inositol

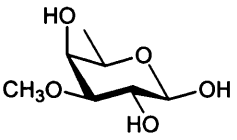

52 3-O-Methyl-6-deoxygalactose, 3-O-methyl-fucose, digitalose

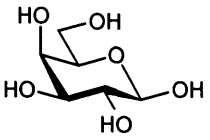

53 D-Galactose

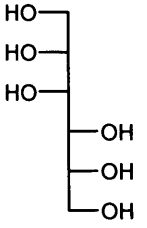

54 D- Mannitol

3.9 Roach samples

As time constraints had not permitted any further work with rainbow trout, a second fish species was examined. The roach spawning season takes place in the summer, during July. We again faced the problem of not having an accessible fish population for bioassay, so were not able to obtain this type of information. However, we were able to obtain both milt and egg samples. A releaser pheromone, $PGF_{2\alpha}$ **22** has been identified as the spawning cue in goldfish, so we hoped to demonstrate the presence of a similar compound for roach. By extracting whole eggs and milt, it was hoped to minimise the amount of lipids detected which would aid

the detection and identification of any minor components. In relative terms, the amount of fatty acids to pheromone candidates (*e.g.* steroids, prostaglandins) would be huge, several orders of magnitude, so any steps to reduce these tiny peaks from being obscured were considered.

3.9.1 Extraction of roach samples

The eggs and milt were handstripped and collected straight into polyethylene containers. It was crucial that the eggs did not come into contact with water as they then become very sticky (to anchor them for incubation) and harden. The eggs, egg fluid and milt were subject to liquid/liquid extraction using dichloromethane at the pH of collection. The solvent extracts were collected in elution tubes which had been treated with a commercially available silanising agent. The silanising agent had been used to "cap" the reactive silanol groups present on the surface of the glass and prevent compound loss. However, a reaction between these silanyl groups and some components in the extracts occurred as some of the compounds detected are present as their silyl derivatives.

The egg fluid (*i.e.* the liquid surrounding the eggs) was found to contain C_{16}, C_{18} fatty acids, cholesterol type compounds and 2,2'-methylene *bis* 6-(1,1-dimethylethyl)-4-methyl phenol **43** and is a commercial antioxidant. Although the likely source was the original sample collection vessel, it was not detected in any of the other samples.

The eggs were extracted whole in order to reduce the amount of lipids obtained. This was only partially successful as the majority of the components identified were saturated and unsaturated C_{14} - C_{20} fatty acids (Fig 3.9). Squalene **35** and two cholesterol type compounds were also detected, but there was no evidence of any steroidal or PG type material. If any of these compounds were present, it is likely that the concentrations are too low to be detected. Two peaks were detected in the latter part of the chromatogram where steroids and PGs would be expected to elute, but they were too small to give adequate spectra for identification. PGs are associated with follicle rupture and may be released with the eggs and fluid, making them likely pheromone candidates. Female roach studied over the course of a year were found to have higher concentrations of circulating oestradiol than male conspecifics, but testosterone **26** levels were similar in both sexes[113], prior to spawning females had elevated levels of 17 β-oestradiol and during spawning, had elevated levels of 17α,20β-P **19a**[114].

Handstripping milt from some species of fish can contaminate the sample with urine as it is released at the same time and mixes with the milt when expressed. A study which examined milt and urine samples collected from some marine species as well as goldfish and rainbow trout found that the milt samples from rainbow trout alone were free from urine

contamination and that urine samples from all species studied contained high levels of conjugated steroids[97]. Thus, the milt samples obtained from the roach are almost certainly contaminated with urine. Male roach also have high levels of circulating androgens such as 11-keto-testosterone **28** during the spawning season, which may be present in their urine[115]. The milt sample also contained some C_{16} and C_{18} acids, in addition to cholesterol **32a** and squalene **35** as previously seen. In addition, there were four peaks which were cholesteryl esters **32b** between 83 and 85 min, but complete spectral identification was not possible. There were also two peaks detected at about 70 min which again were too small to yield identifiable spectra, although both contained fragments at *m/z* 91, 105 and all six peaks are derived from cholesterol **32a**.

Fig 3.9: Comparison of fatty acid ratios from Roach eggs and milt

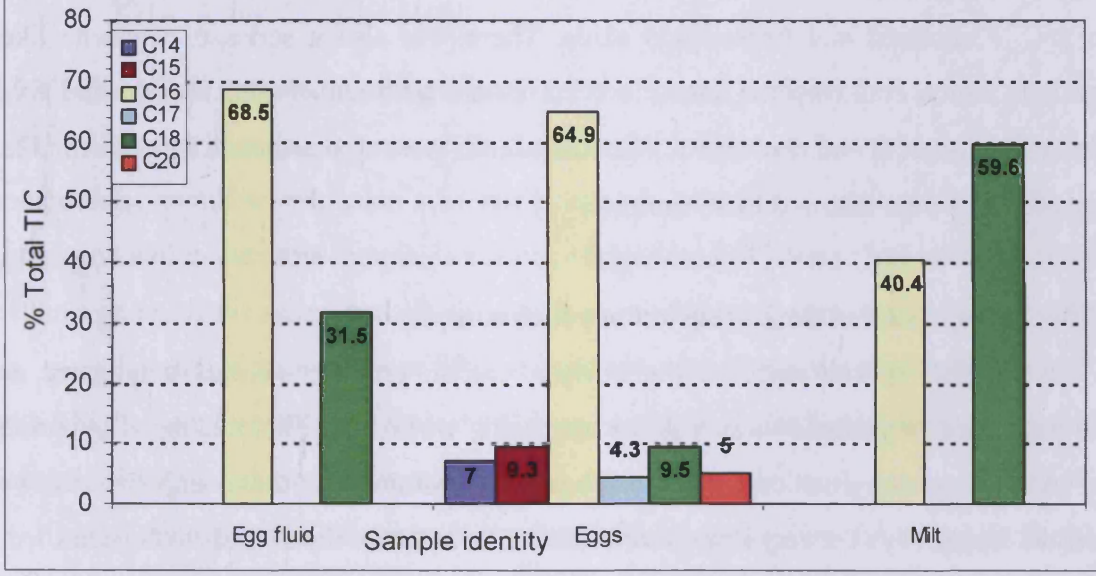

3.9.2 Derivatisation of roach samples

The dichloromethane extracts from Section 2.9.1 were derivatised as described in section 2.4.1 and analysed by GC-MS. The majority of tentative identifications were for carboxylic acids, some cholesterol type compounds were identified. Some derivatives which had relatively long retention times were detected, which are typical of steroids. It seems probable that we have detected some steroids from these samples, even if total identification is not possible.

The number of components detected after derivatisation was increased, for the egg fluid it rose from five to 28. Once again, the main classes of compounds detected were the carboxylic acids and cholesterol **32a**, although some sugars and amino acids were tentatively

identified. A peak with a retention time of 36.7 min was unidentified, but it had an area of the same order of magnitude as the C_{16} and C_{18} acids and did not occur in either the egg or milt sample.

The egg sample contained similar components to the egg fluid. The range of fatty acids was from C_{14} - C_{22}, and unsaturated acids appeared at C_{16}. Some odd C atom acids were detected, but only in trace amounts compared to the even ones and fatty acid esters were also detected. Three phosphate compounds, trimethylsilanol phosphate, trimethylsilylphosphonic acid, inositol-3-phosphate (cf **51**) and indole-2-carboxylic acid. After the fatty acids had eluted, a series of three relatively small peaks (max. TIC 37000) eluted between 45 and 50 min. These peaks may be steroidal in nature, although too small to give identifiable spectra.The milt sample also contained a wide variety of fatty acids, more than either of the two egg samples, and included both short chain acids eluting between 11 - 20 min, and long chain ($>C_{14}$) saturated and unsaturated acids. There was also a series of squalene like compounds which could not be identified, but eluted between 40 and 50 min and five cholesterol derivatives and cholesterol like compounds were also detected. Cholesterol **32a** and squalene **35** were detected in all samples.

3.9.3 Deconjugation and derivatisation of roach samples

Some fish species such as the African catfish produce steroids conjugated as glucuronides and sulphates as a means for increasing water solubility, making elimination easier and in spawning situations, it has also been demonstrated that these conjugates can be powerful odorants, even at very low concentrations. In order for the steroids to be identified, these conjugates were first broken down using a glucuronidase enzyme, the free steroids were solvent extracted and derivatised. The enzyme (snail "juice") used was from *Helix pomatia* and was capable of cleaving sulphates and glucuronides.

Once again, all 3 samples produced a wide range of $\geq C_{14}$ acids of varying degrees of saturation. The egg fluid sample produced identical compounds to those found in the previous experiment.

The egg sample produced some extra peaks which eluted after 30 min, between polyunsaturated C_{18} (31.5 min) and squalene **35** (44 min). Tentative identification (32.2 min) suggested a prostenoic type of compound, *tris* TMS ester of 9,11,15 - prost-13-en-1-oic acid, eg $PGF_{2\alpha}$, **22**,which has been identified as a pheromone for spawning goldfish. The peak at 38.0 min was not identified, but the library search results included possible steroidal type compounds, such as androstanes. Deconjugation produced 13 peaks with retention times

similar to cholesterol **32a**, in comparison to the 4 detected in the conjugated sample. These were all tentatively identified as cholesterol deriviatives.

The milt sample produced the same range of fatty acids as previously seen. However, the compounds potentially released by deconjugation were quite different from those in the egg samples with no evidence of the tentative prostenoic acid type compound. The number of cholesterol type derivatives was also much smaller, only two compared with the 13 for the egg sample and six in the conjugated milt sample. The peak at 44.5 min was tentatively identified as an androstane type compound, and a further two peaks at 45.1 and 48.9 min were detected but could not be identified. In contrast to the egg samples, three peaks were detected between 73 and 76 min which were tentatively identified as triglycerides. The cholesterol derivatives in the egg sample were also large peaks in comparison to those from all other samples, including the conjugated samples.

3.9.4 Solid phase extraction and derivatisation of roach samples

SPE was intended to remove the fatty acids, but due to the high amounts of these compounds, complete exclusion was not achieved. Multiple identifications of the same compound within the same sample, is a result of mis-identification of individual compounds within a homologous series, usually as a result of missing molecular and higher mass ions.

Milt extracts obtained from SPE and solvent extraction gave similar compounds but with a higher concentration of cholesterol based compounds in the solvent extracts, and the derivatised extracts showed the same pattern.

The deconjugated milt extract produced fewer peaks than the comparable solvent extract and cholesterol **32a** was again identified. The SPE extract also produced four peaks with an alkane type fragmentation pattern, and a compound tentatively assigned as TMS ester of α-methyl-3-phenoxybenzene acetic acid.

The SPE free steroid egg extract showed C_{14} - C_{18} acids and methyl esters of acids in a profile similar to that of the comparable milt sample and the solvent egg extract. There was no evidence of steroidal type material in any of these samples. Dodecanol was only detected in the SPE free steroid egg extract.

The derivatised free steroid egg extract again produced a variety of fatty acid and fatty acid ester peaks. Both SPE and solvent egg fluid extract had what appeared to be a related C_{11} compound; in the solvent extract it was identified as *cis, cis*-1,5,8-undecatrien-3,7-diol-*bis* TMS ester and in the SPE extract as *cis,cis*-1,8-undecadien-5-yne-3,7-diol-*bis* TMS ester and both the SPE and solvent egg extracts were found to contain an indole-2-carboxylic acid and

inositol per TMS esters cf **51**. The deconjugated SPE extract contained fewer peaks than the conjugated extract, once again fatty acids were detected with hexadecanoic acid being the predominant acid.

3.10 Conclusions

We have demonstrated that female trout urine contains a different range of compounds to male trout urine, and have tentatively identified free testosterone **26** and conjugates of 3α, 5α, 17β- androstane-3,17-diol **47** and 5β, 17β- hydroxy-androstan-3-one **48** in the female urine. Bioassay data is needed to determine if these compounds are active.

Analysis of roach eggs have also identified a prostaglandin as a potential spawning pheromone candidate, and again, bioassay data is needed to determine if prostaglandins are acting as pheromones in this species.

Chapter 4, *Rhithropanopeus harrisii* Hatching Pheromone

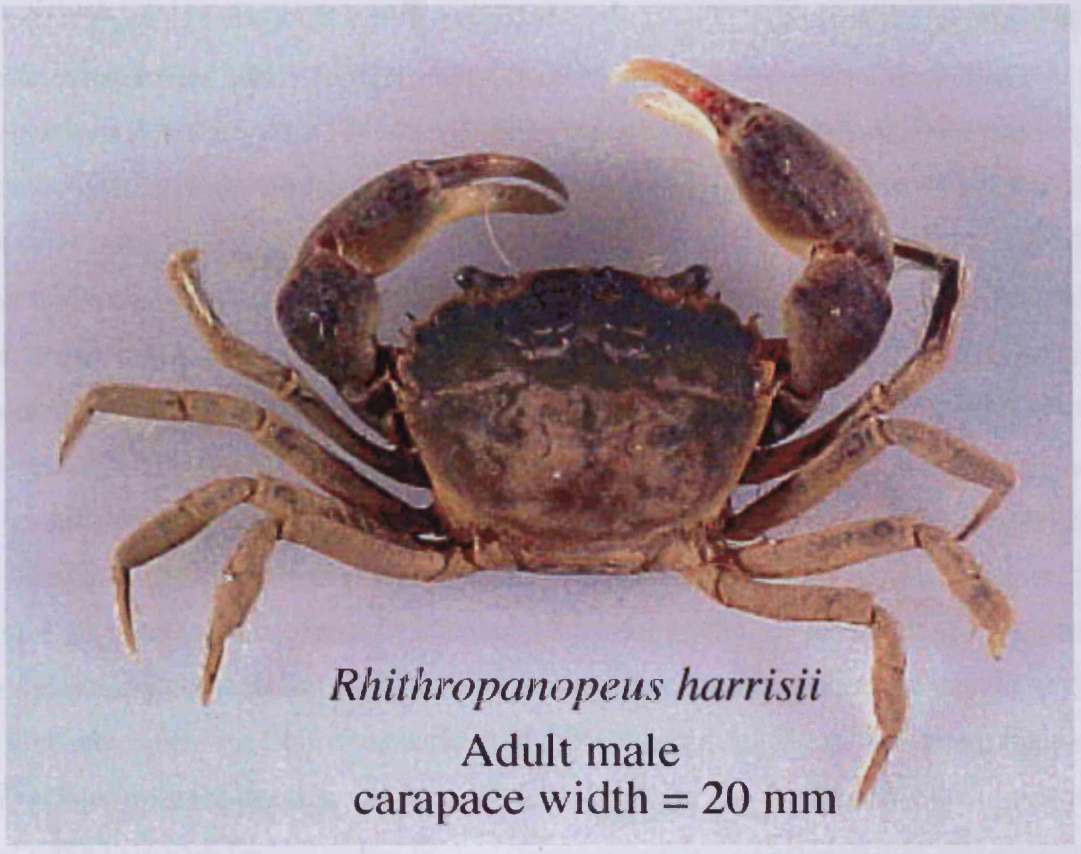

Fig. 4.1 : from http://www.tarleton.edu/~biology/MudCrab.html with permission of Prof. D. E. Keith, Dept. of Biological Sciences, Tarleton State University, Texas, USA.

4.1 Distribution

The dwarf mud crab *Rhithropanopeus harrisii* (Gould, 1841) (Brachyura: Xanthidae) is a small, brown/green crab with a carapace typically 1.5 cm long (Fig 4.1). It is found in estuaries and can survive in both salt and fresh water (euryhaline), which is typical of conditions found in upper estuarine waters. It was originally found along the North American Atlantic coastline, from Canada down to Mexico, but now enjoys a far wider distribution, probably as a result of accidental introduction from imported shellfish stocks and discharged bilge or ballast water from transatlantic shipping. The first reported sighting in Europe was in the Netherlands in 1874[116,117] and it is known as the Zuiderzee crab. It is now found throughout Europe, much of the rest of the world and even in the freshwater Possum Kingdom Lake, in North Central Texas[118]. The crabs are easy to collect, readily maintainable, hardy and fecund and this makes them one of the most widely studied crab species with respect to environmental factors. It has only been reported in the UK at Cardiff docks (first report 1996) and its presence

there may be due to the comparatively low salinity of the Severn estuary[119].

4.2 Breeding cycle

The breeding cycle of the crabs has been widely studied and is dependent on water temperature rather than extended light cycle[117]. The animals mate after the female has moulted her old shell and the new shell has hardened. The breeding season for the crabs in their original environment is from mid-April until the end of September[120], although this can be extended under laboratory conditions by maintaining an elevated water temperature. The breeding period in one study was extended by inducing the crabs to begin breeding earlier in the year and finish in early November, although the number of egg producing females declined throughout October. The crabs then entered a refractory or resting period until the following spring and breeding patterns in the wild follow this pattern. In warmer waters, the season is far longer than in the colder waters found in more northerly areas, for example, crabs in Florida breed from May to November, whereas in Poland they have a season lasting from June until September[116] and although the spawning season could be artificially extended, the broods were largest at the beginning of the season[121].

Other factors which were found to affect spawning were stocking density and the sex ratio. Although wild populations tend to a sex ratio of 1:1, under laboratory conditions it was found that more clutches were spawned with a greater population density and higher proportion of females to males. A probable explanation is that males are more aggressive than females and will kill both sexes, and one male can mate with many females[120].

The *R. harrisii* are also capable of multiple ovipositions from a single mating[121] and it is possible for the females to oviposit within three days of hatching a brood or dropping their egg mass. When the eggs are laid they are attached to the abdomen and are incubated for approximately 17 days before hatching into plankton.

4.3 Larval release

The development of the larvae within the eggs can be monitored by observing the yolk consumption and state of eye development. Eggs which are close to hatching are almost black in colour, as opposed to the grey shade of less developed eggs, but this is very difficult to determine with the naked eye because the eggs are so small (<1 mm diameter).

The actual time of release of larvae is itself subject to environmental factors. Tides, lunar phase and time of day have all been found to influence crustaceans[122,123] . In laboratory studies, a population of crabs from an estuary with no regular tides were found to have a

circadian rhythm and to release their larvae in a two hour interval after the onset of darkness. With crab populations taken from estuaries with semi-diurnal tides, larval release occurred near the time of high tide, indicating a circatidal rhythm. Crabs exhibiting a circatidal rhythm could be entrained under laboratory conditions to respond to a circadian rhythm after a minimum period of six days, and crabs displaying a circadian rhythm could be retrained to a circatidal rhythm with no preference for light or dark high tide although crabs displaying a natural circatidal rhythm also display a significant dark high tide preference. A circadian pattern is normally defined as a pattern which has a period of nearly 24 hours and occurs for 5-10 cycles in an individual. With larval release taking place over a maximum of two nights, this definition is not literally fulfilled, however, if the overall pattern of larval release is considered, the conditions can be said to be satisfied[123].

Night time release has been reported for a number of other crustaceans and is probably attributable to the avoidance of predators, of both the larvae and the adults, which rely on visual cues. The preference for a circatidal rhythm is more difficult to explain, but the reason may be associated with the effect of salinity and osmoregulation[124]. The crab's normal environment is near the head of estuaries and during the tidal cycle the salinity of the water will decrease with the ebb tide, due to the inflow of fresh water. At high tide the water is at its most saline and therefore less stressful to the emerging larvae[123], which is in part why crabs in a non-tidal environment modify their behaviour when placed in a tidal estuary. Some crustaceans use the tidal flow as a means of distribution to transport the larvae away from the adult population and out to sea where the conditions may be more favourable for the larval development, but in *R. harrisii* the larvae are retained in the estuary and remain in close proximity to the adult population[125,126].

4. 4 Larval development and distribution

The larvae go through four zoeal stages before becoming megalopa. The time spent in the planktonic form is again influenced by temperature and salinity, with temperature the dominant factor, and may last for many months. The larvae hatch into prezoea but quickly moult into zoea which are tiny, shrimp like creatures which have only the first two thoracic appendages. The rest may be present as limb buds and the heads are fully functional. The zoea moult several times more before emerging as megalopa, the final stage before adulthood. Zoea swim rapidly and may migrate vertically in the water column and in the migration studies, all 4 larval stages and the megalopa form could be found in the same section of the water column in the area of lowest water flow[125,126]. The explanation proposed is that the plankton migrate

vertically to stay near the area of least water flow to avoid being washed out to sea, they also remain at a depth where it is dark so that the risk from predators is reduced. However, it was also noted that the first larval stage was strongly influenced by light, exhibiting a phototactic response and the pattern of vertical migration showed a striking similarity to that of larval release; larvae that hatched in tidal waters showed a circatidal migration pattern whereas larvae released in non-tidal estuaries tended to show a circadial rhythm during which they migrated upward in dark periods and downwards in light periods, ie phototaxis. When comparison and training studies were performed, the circatidal rhythm overrode a circadial response.

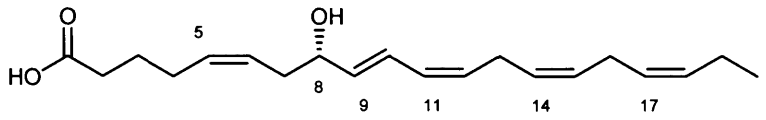

60 (5*Z*,8*S*,9*E*,11*Z*,14*Z*,17*Z*)-8-Hydroxyeicosapentaenoic acid

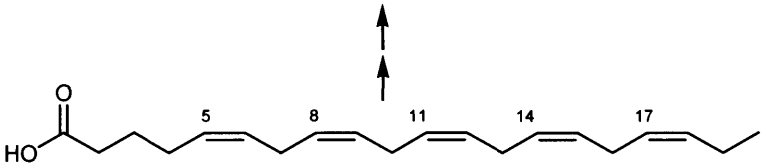

42 (5*Z*,8*Z*,11*Z*,14*Z*,17*Z*)-Eicosapentaenoic acid, EPA, Timnodonic acid

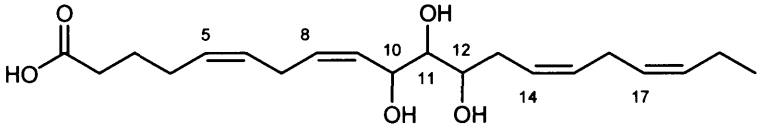

61 (5*Z*,8*Z*,14*Z*,17*Z*)-10,11,12-Trihydroxy-eicosatetraenoic acid

4.5 Synchronised swimming?

The timing of larval release is dependent on environmental factors such as time of day and high tide, whereas chemical cues control the hatching once it has been initiated. These cues for synchronised hatching have been reported for a variety of marine species. Corals and crustaceans frequently use eicosanoids as allelochemicals and pheromones[127]. In the barnacle *Elminius modestus* the hatching event is controlled by the adult. The cue, which was identified as 8-hydroxyeicosapentaenoic acid **60**, causes movement in the mature larvae and mechanical rupture of the eggs, which expels the larvae from the mantle into the sea[128]. The structure was established by unambiguous synthesis from mannitol **54** and this remains the only barnacle hatching factor for which the structure has been definitively determined[129]. Another fatty acid, 10,11,12-trihydroxy-5,8,14,17-eicosatetraenoic acid **61**, a prostaglandin precursor, has been reported as the hatching cue for the circumboreal barnacle, *Balanus balanoides*[130,131]. Both are

probably formed biosynthetically from (5*Z*,8*Z*,11*Z*,14*Z*,17*Z*)-eicosapentaenoic acid (EPA) **42** by the action of lipoxygenases.

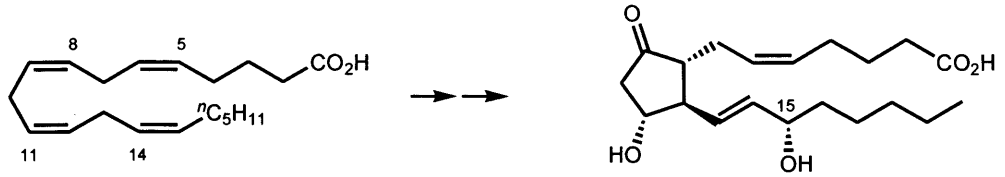

41 (5Z,8Z,11Z,14Z)-Eicosatetraenoic acid, Arachidonic acid

62 PGE_2

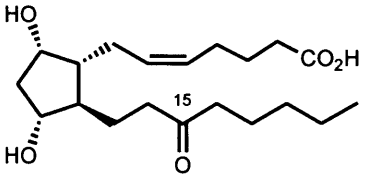

23 13,14-Dihydro-15-oxo-$PGF_{2\alpha}$

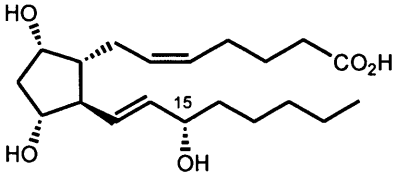

22 $PGF_{2\alpha}$

Both male and female *R. harrisii* could be induced to perform abdominal "pumping", a typical behaviour associated with copulation and spawning, when exposed to prostaglandins-E_2 **62** and -$F_{2\alpha}$ **22**. $PGF_{2\alpha}$ **22** is the spawning readiness pheromone of postovulatory goldfish[65] and is implicated as a sex pheromone of paradise fish[95], bleeker[96] and other teleost fish[64]. 13,14-Dihydro-15-oxo-$PGF_{2\alpha}$ **23** is the female released sex pheromone of the loach[94]. The "3-series" PGs are derived biosynthetically from EPA **42**, and the "2-series" PGs from arachidonic acid **41** (cf section 1.4.1). Some furan fatty acids **63,** also formed by biosynthesis from fatty acids, were isolated from *R. harrisii*[132], but their function is currently unknown and as they have different physical properties from the putative larval release pheromone, it is not likely that this group of compounds is the pheromone in question.

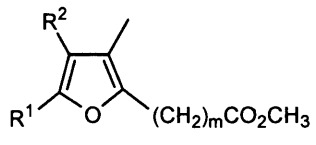

63	R^1	R^2	m	Name	Chain length
a	$^nC_5H_{11}$	H	8	F2	C18
b	$^nC_5H_{11}$	CH_3	8	F2	C18
c	C_2H_5	CH_3	10	F4	C20
d	$^nC_5H_{11}$	H	10	F5	C20
e	$^nC_5H_{11}$	CH_3	10	F6	C20

When egg carrying females were collected from the field they were found to release their larvae in a short burst, usually a 15 minute interval, during the 2 hours after sunset[123], although in a few instances not all the larvae were released at the same time. In this case, a proportion of the larvae were initially released on the first evening and the remainder on the second evening and this was also seen in wild populations.

To determine whether the female or the eggs control the start of the hatching process, a series of experiments was set up to monitor the hatching of larvae from eggs detached from the females and kept in isolation. It was found that detached eggs do hatch at the same time as attached eggs, which suggests that the larvae are controlling the moment of hatching. The detached eggs were found to hatch over several hours whereas the attached eggs hatched over a much shorter time period, probably as a result of mechanical assistance from the female. It was also found that the length of time which elapsed between egg removal and hatching affected the synchronicity of the larval release, with a longer time period giving rise to less uniformity in hatching[122].

Females carrying eggs that were exposed to larval hatch water exhibited behaviour observed during larval release. The females rise up on their walking legs, probe the egg mass and flex the abdomen in a rhythmic "pumping" action which is therefore classed as the pumping response. This response was observed in females carrying eggs at all stages of development, and also those infected with a rhizocephalon parasite, *Loxothylacus panopei*[133]. This typical behaviour was later used as the bioassay response. Although all egg carrying females responded, larvae were not released at earlier stages of development. The females were also observed to respond directly to "change" in concentration of hatch water and also to homogenised eggs. It was found that larvae holding water did not provoke a response, but the crushed egg solutions did and with the egg solutions, an embryo development dependence was observed, *i.e.* the oldest eggs produced the most vigorous response. This pumping response was not found to be daylight dependent as it could be induced at any time. In the case of *R. harrisii*, the larvae initiate hatching and are then assisted by the female[122,134].

It is proposed that under field conditions, a few of the eggs hatch and release the chemical cue which induces the female to perform this pumping response. The flexing of the abdomen and probing with the legs helps to mechanically rupture the remaining eggs and the larvae are flushed away by the circulating water. This method of mass release has advantages for both the female and the larvae, the female is exposed to predation for a minimum amount of time whilst the eggs are hatching and the planktonic larvae have a "safety in numbers" factor.

Experiments to determine the chemical and physical nature of the hatching cue showed that it was retained on an Amberlite XAD resin column and could be eluted with methanol, would not dissolve in dichloromethane and could be destroyed by incubation with a Subtilopeptidase A (alkaline protease). The solubility properties and susceptibility to protease actions suggest a short peptide. It was found to have a molecular weight of approximately 500

Daltons, as activity was both retained and passed through a 500 Dalton dialysis filter[135]. This retained and unretained activity is probably due to the variability of the pore size of the filter and the similar size of the cue to the pores, or if the cue is a mixture of small and large compounds, activity of the individual components. The concentrated sample was then analysed for amino acids by *O*-phthalaldehyde derivatisation and reversed phase high performance liquid chromatography (HPLC) with fluorescence detection.

The amino acid HPLC analysis showed the presence of five unidentified peaks and five amino acids, lysine **64**, leucine **65**, arginine **66**, asparagine **67** and glutamine **68** which were identified by matching retention times with authentic standards. After hydrolysis, the five unidentified peaks disappeared and an increase of nearly 300 % in free amino acids was noted, nearly half of which was arginine **66**.

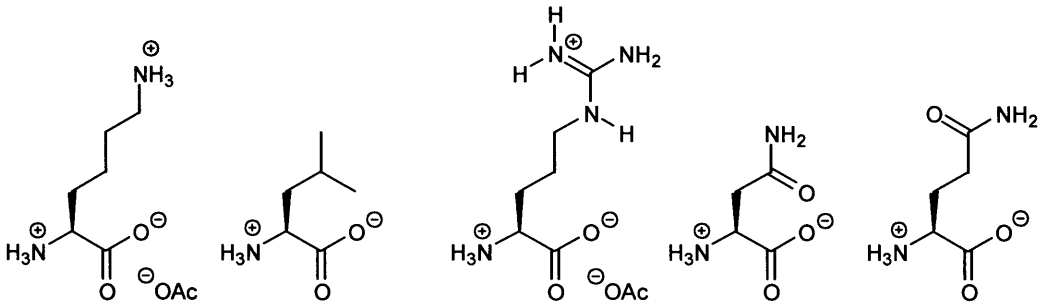

64 L-Lys. AcOH **65** L-Leu **66** L-Arg. AcOH **67** L-Asn **68** L-Gln

Testing of individual amino acids by bioassay showed no response but bioassay of mixtures of arginine **66** and glycine **77a**, although at much higher concentrations than those detected by HPLC, did give a pumping response. No other types of compounds appear to have been tested. Peptides were found to be more "active" than amino acid mixtures which in turn were more "active" than individual acids. Hence the cue was likely to be a peptide containing arginine **66**.

4.6 Peptide mediated marine behaviour

Peptides have been reported to mediate behaviour of other marine organisms[136]. Chemical cues for synchronised hatching have been reported for other crab species. Hatch water for the crab *Neopanope sayi* was collected and subject to reversed phase HPLC with precolumn derivatisation with phenylisothiocyanate[137] to determined the amino acid composition. The four most abundant amino acids were found to be cysteine, glycine **77a**, isoleucine and methionine **82**. These are not the same acids as those found in the *R. harrisii*

hatch water, although *N. Sayi* did respond to the *R. harrisii* hatch water.

Fig 4.2: Hydrolysis of *N. Sayi* Hatching Factor

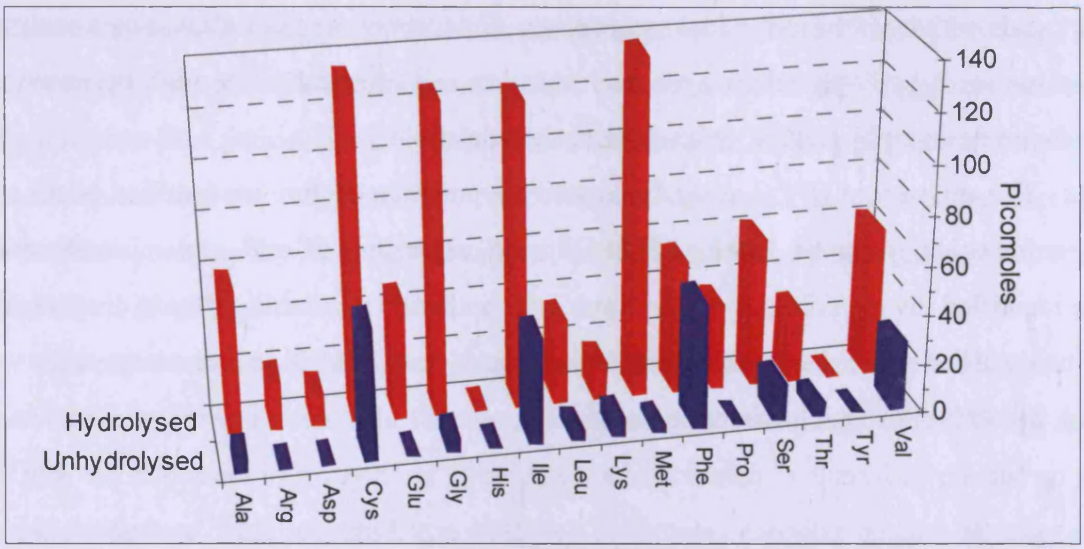

Amino acids are known to be feeding stimulants in some fish, for example a synthetic mixture of the aromatic and basic amino acids to rainbow trout[138] and for the pigfish when combined with betaine **77b**[139].They have also been found to induce a sexual response in one species of fish; the mature male rose bitterling[39]. Dialysis tubes were filled with either an amino acid solution or distilled water and placed in a tank under dark conditions. The tubes containing the amino acid solution attracted rose bitterling and a "pecking" behaviour was observed. As the light level was increased, sperm release was also noted. A total of twenty amino acids were tested of which five, cysteine, serine **80**, alanine **79**, lysine **64** and glycine **77a** had high activity, a further five, threonine, isoleucine, glutamine **68**, methionine **82** and arginine **66** had medium activity and the remaining ten had little activity. Juveniles and female fish did not exhibit the pecking action at all. The explanation proposed is that proteins could be hydrolysed during egg maturation and ovulation and would therefore be released by the female. This can be compared with the steroidal hormones and prostaglandins released during maturation and ovulation in other fish species, such as salmon and goldfish respectively. The rose bitterling study does not report whether steroidal hormones and prostaglandins also produced a response.

As previously mentioned, peptides and amino acids can act as feeding stimulants in some fish. They are also used to locate prey by predatory snails[140], new shells by hermit crabs[141] , and as alarm responses in gastropods[142]. In these instances the peptides and amino

acids are acting as semiochemicals. Peptides and amino acids are thought to act as pheromones for crab larval release for several species, location and settlement of a larval group and also control metamorphosis of marine invertebrates. Again, the hypothesis is that the peptides and amino acids are released by protein breakdown and are then "recycled" and used as a means of communication. This secondary use of metabolic byproducts for communication has also been proposed for goldfish, in the terms of "chemical spying" rather than a primary means of communication[9].

4.7 Characterisation of the hatching pheromone

Based on the hydrolysis study previously discussed, the next stage in the characterisation was to subject a series of peptides to bioassay to determine which would elicit a recognisable response. The purpose of this exercise was twofold, to eliminate peptides which did not provoke an appropriate response and to study those that do, with a view to gaining structural information about the cue. The peptides used in this exercise were di and tri-peptides which encompassed acidic, neutral and basic character at both the carboxy and amino terminals and the test peptides were based on the amino acids determined by the hydrolysis of the pumping factor. The bioassay itself was performed by placing a succession of test animals in the peptide solution and monitoring for the pumping response. The conclusions were that only peptides with a neutral residue at the amino terminus and a basic residue at the carboxy terminus produced a "significant" response. All others tested failed to elicit a pumping response. The concentration could also affect the response of the crab to the mixtures, the pumping action was observed over a 100 fold concentration range and then the response declined. The effective concentration range was dependent on the peptide under examination, for example, the dipeptides Leu-Arg **69** and Gly-Lys **70** had response ranges of 10^{-10} - 10^{-7} and 10^{-7} - 10^{-5} M respectively.

In the structure-function work carried out concurrently, compounds containing arginine **66** in conjunction with various side groups were used to determine the size of the peptide, size of hydrophobic group and the requirement to have free amino acid groups present. The study determined that a large hydrophobic side chain in a small peptide molecule with no primary amino side chains provoked a response at the lowest concentration. The measure used to determine an active compound was this threshold concentration, the more "active" the component, the lower the threshold concentration needed to trigger a pumping response.

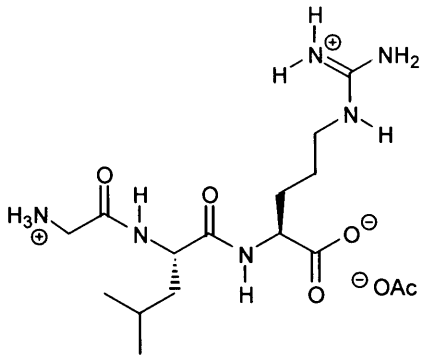

71 L-Gly-L-Leu-L-Arg. AcOH

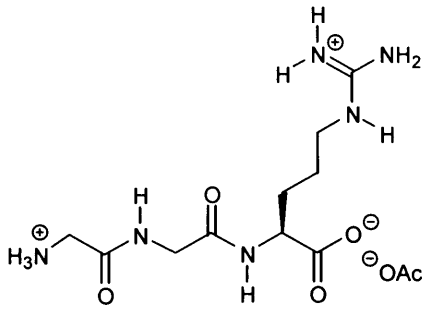

72 L-Gly-L-Gly-L-Arg. AcOH

The conclusions drawn from these studies were that the hatching cue was likely to be a small peptide or group of small peptides, as there was less activity with increasing molecular size, although this was contadicted by a later study [143]. The 500 Dalton filter work suggests that the active compound(s) are small, and given that the average mass of an amino acid is 120, this is consistent with the mass of a tetrapeptide (480), or a tripeptide of arginine **66** (486). Peptides containing lysine **64** at the carboxy terminus were discounted as the cue because although active, the threshold concentration needed was considerably more than the quantities of free acid produced from the hydrolysis and the reason for their activity may be the structural similarity to arginine **66**. Although no actual peptide identity was proposed, the two most active peptides tested were Gly-Leu-Arg **71** and Gly-Gly-Arg **72**. The threshold concentrations for both these peptides at 10^{-13} and 10^{-9} M respectively, were well below the maximum concentrations found by the hydrolysis study.

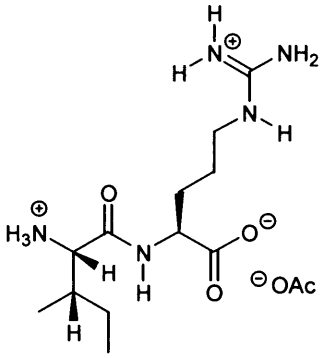

73 L-Ile-L-Arg. AcOH

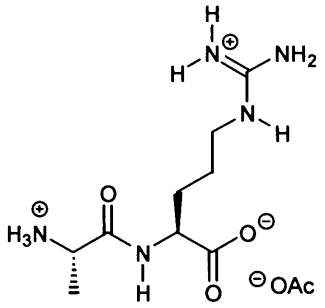

74 L-Ala-L-Arg. AcOH

A further study of the structure and function of peptides concentrated on peptides containing arginine **66** at the carboxy terminus and demonstrated that all combinations of di and tripeptides tested elicited a response, although at differing threshold concentrations[143]. The dipeptides with the lowest concentration thresholds and therefore the most active were Ile-Arg

73 and Aln-Arg **74** at 10^{-11} M, and the most active tripeptide of the group tested was Ile-Gly-Arg **75** at 10^{-15} M.

The acids identified by the hydrolysis study were constituents of the peptides tested for threshold concentrations, although no comparison of free acid concentrations was made, so it is not possible to identify a pheromone candidate. The structure study also demonstrated that altering the order of the first two amino acids in the tripeptides could have a profound affect on the threshold concentration[144], for example Ile-Gly-Arg **75** at 10^{-15} M and Gly-Ile-Arg **76** at 10^{-17} M. Some insect pheromones have been identified which are active in this concentration range, and although a peptide may provoke a response at a very low concentration, the actual localised concentration experienced when the eggs hatch is likely to be orders of magnitude higher, so the lowest threshold peptide may not be the pheromone.

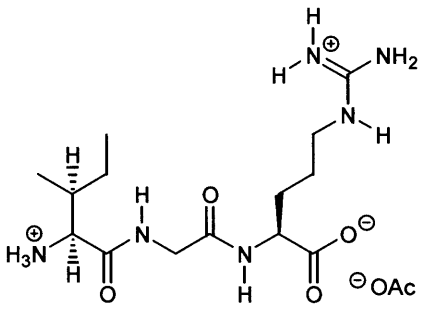

75 L-Ile-L-Gly-L-Arg. AcOH

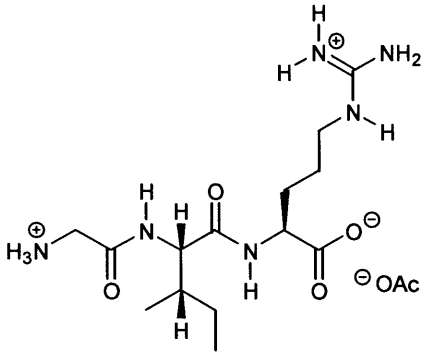

76 L-Gly-L-Ile-L-Arg. AcOH

The peptides with very low concentration thresholds were used to obtain information about the pheromone receptor. In the first of the structure/function studies it was found that side chain length did not affect responsiveness, although this study concluded that the optimum size would be that of a large dipeptide. Bulky side groups were not as effective, probably as a result of steric hindrance. Free amino acids were inhibitory at high concentrations, probably as a result of competitive inhibition of the binding sites which suggested that only 1 receptor type was being utilised which contains a hydrophobic part that interacts with the hydrophobic part of the peptide side chain, and an acidic area which binds with the basic arginine **66** moiety. The structure/function study which used superpotent mimics of the larval release pheromone confirmed that although the actual pheromone had not yet been identified, tripeptides with arginine **66** at the carboxy terminus could invoke a pumping response at femtomole levels[144]. At this low level, the response is being generated by only a few molecules (approx 6 million molecules/ml).

4.8 Aims of this project

The object of this project was to attempt further characterisation and identification of this larval release pheromone. The techniques employed included HPLC and mass spectrometry.

Chapter 5, *Rhithropanopeus harrissi* Hatching Pheromone - Experimental Work

5.1 Introduction

The majority of the prior work on this subject was based on two main observations. The first was the relatively large increase in the concentration of free amino acids (especially arginine **66**) in hydrolysed hatch water. The second was the typical "pumping" response of egg bearing females to some solutions of short chain peptides. So, although no actual identification had been proposed, the involvement of peptides was suspected. Peptides are known to mediate some aspects of behaviour of marine species such as predatory snails. A peptide hatching pheromone has also been proposed for another crab species, *Neopanope Sayi*. The amino acids detected after hydrolysis were different to those detected for *R. harrisii*, although hatch water from the latter did induce a pumping response.

The main aim of this project was to isolate and identify the hatching pheromone. The techniques used were based on HPLC, size filtration, and mass spectrometry (MS). The samples analysed were also subject to bioassay during storage and purification.

5.2 Collection of the animals

The first set of animals were collected from the Cardiff Bay at the end of June 1997 (Fig 5.1). This was done using a large net with a serrated edge on the end of an extending pole. At maximum extension, the pole was in the region of 2 m long. The serrated edge of the net was scraped up the stone wall of the dock and the contents of the net transferred to a carrying box for transport back to the laboratory. The contents of the box were transferred to a sorting table and the female crabs that were carrying eggs (20) were placed individually in collecting jars containing sea water (3 ml, 5% salinity). The remaining crabs and the rest of the material, which included eels, barnacles, mussels and worms were returned to the docks.

This procedure was labour intensive and only provided one set of crabs with eggs at a time. It was decided to set up a laboratory breeding colony, in collaboration the School of Biological Sciences, at Cardiff. At the beginning of September 1997, a further collection of animals took place and these were placed in a recirculating sea water tank. The system was maintained and monitored by Piers Meynell, working with Drs. Jorge Hardege and Chris Mettam of the School of Biological Sciences.

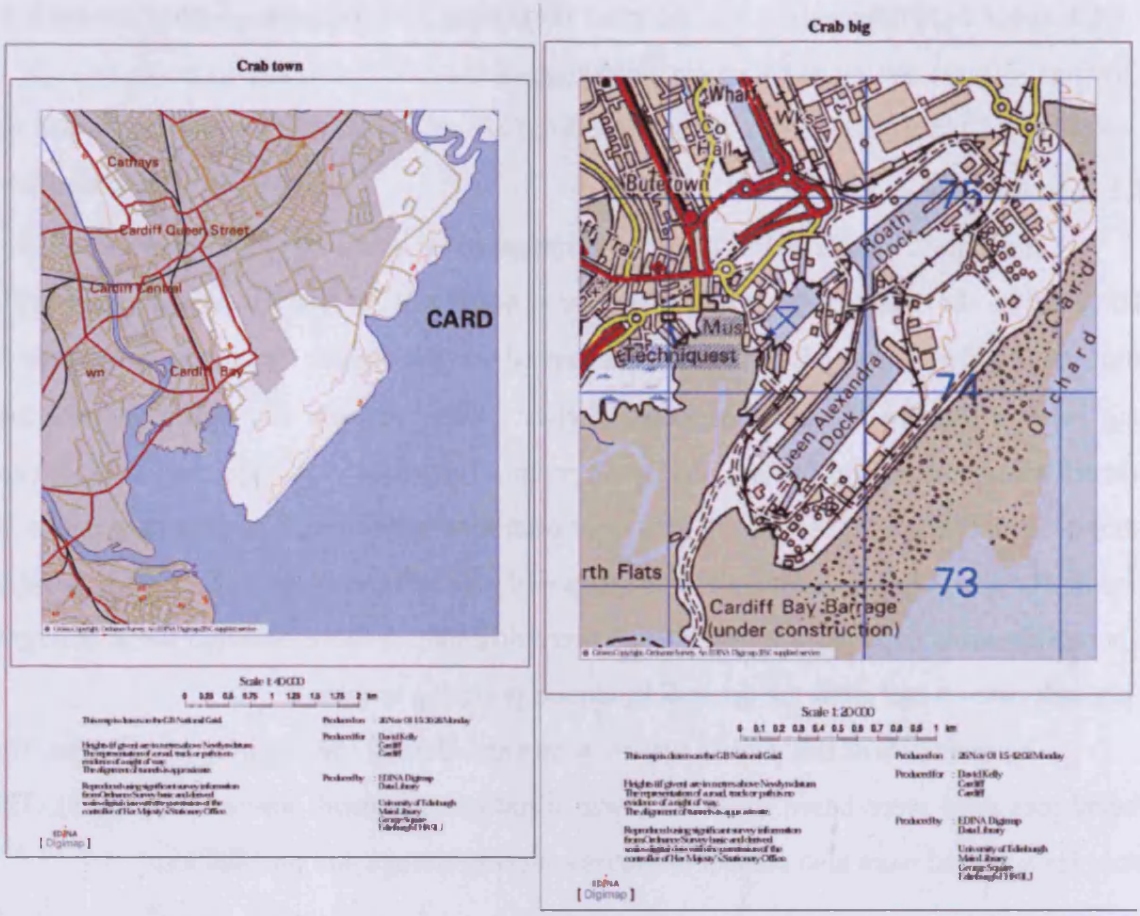

Longitude: 3° 20' Latitude 51°23'

Fig 5.1 Maps of Cardiff Bay from EDINA

By elevating the temperature of the seawater and extending daylight hours, the breeding season was extended to 11th October 1997, rather than the end of September. The winter refractory period was also reduced, so that the first hatch water collection in the new breeding season took place on 14th February 1998, rather than mid-April as is usual. The final sample was collected on 14th March 1998.

5.3 Collection and storage of the hatch water

The animals are known to release their larvae in the two hour period after the onset of darkness. When the females were found to have released their larvae, they were transferred to another collecting jar. The hatch water sample was then filtered (0.45 μ filter) and stored in a glass bottle (Duran bottle, -20°C) until required for analysis. Some hatch water from the collected animals was obtained and pooled, and three individual hatch waters were obtained from the cultured population.

5.4 Standard methods

Ultrafiltration was performed by fitting the appropriate sized filter to the apparatus and forcing the sample through the filter under nitrogen pressure (55 psi). All filters were washed prior to use.

Storage was in glass containers at -20° C unless otherwise stated.

All water was deionised from a Millipore Milli-Q deioniser fitted with ICP-MS grade exchange pack.

Two HPLC systems were employed for analysis of standards and analytes. System 1 consisted of an isocratic pump (Perkin Elmer 100 series) fitted with a Rheodyne injector and a sample loop (100 µl), a guard and an analytical column (Vydac 201TP5415 C18 5 µ, 15 x 4.6 mm and 150 x 4.6 mm respectively) and a Perkin Elmer LC90UV UV detector (214 nm, 0.05 absorption units full scale deflection [AUFS]). The flow rate was 1 ml/min. The data was recorded on a chart recorder (Phase Sep linear chart recorder 10 mV input, 0.5 cm/min). System 2 consisted of a Spectraphysics SP8000 ternary pump fitted with a Rheodyne injector (100 µl loop), an analytical column (Hypersil ODS 5 µ, 250 mm x 4.6 mm column) and a Spectraphysics Spectra 100 UV detector (200 nm, 0.2 AUFS, rise time 0.1 AUFS/sec). The flow rate was 1.5 ml/min. The data was recorded on a Lloyd chart recorder,1.0 cm/min). Both systems were eluted with TFA/ water (0.1%, *v/v*).

5.4.1 HPLC Analysis of peptide standards

Solutions of Leu-Arg **69** (acetate salt, Sigma, 9.3 mg, 1ml TFA/ water 0.1%, *v/v*) and Gly-His-Gly (acetate salt, Sigma, 2.12 mg, 1.25 ml 0.1% TFA/ water *v/v*) were analysed by HPLC. Leu-Arg **69** eluted at 4.8 min using System 1 and at 3.7 min using System 2. Gly-His-Gly eluted at the edge of the solvent front in both systems. A calibration curve over the range 0.0093 - 9300 µg/ml (0.03 µM - 30 mM) for Leu-Arg **69** was measured on both Systems 1 and 2 (Table 5.1). The peak height was obtained by comparison to the chart paper scale and then corrected with the AUFS scale used, *e.g.* a peak height of 10 squares on a range of 2.0 AUFS gives a response of 1.0 AUFS.

Table 5.1: Calibration curve data for Leu-Arg **69**

Concentration µg/ml	Peak height AUFS	
	System 1, 214 nm	System 2, 200 nm
0	0	0
0.0093	0	0.0008
0.093	0	0.0032
0.93	0	0.008
9.3	0.0125	0.0189
93.0	0.0465	0.168
930.0	0.28	1.24
9300.0	1.39	over range

A plot of log concentration versus log response for both systems was constructed (Fig 5.2), the regression analysis for System 1 gave $y = 0.0313x^2 + 0.5371x - 2.4673$, with $R^2 = 0.9982$, and for System 2, $y = 0.0224x^3 + 0.0317x^2 + 0.4565x - 2.0894$, with $R^2 = 0.9947$.

Fig 5.2: Log plot of UV detector response for Leu-Arg 69 at 214 and 200 nm

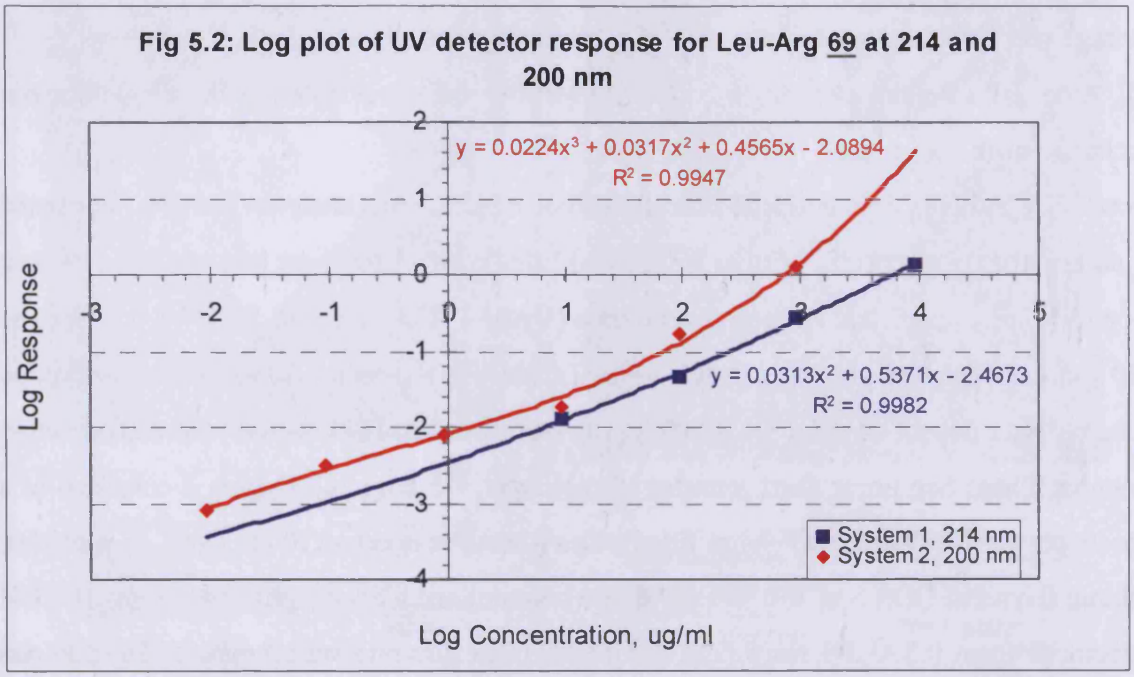

5.5 Analysis of the first hatch water sample

5.5.1 Ultrafiltration of the hatch water sample

A hatch water sample (300 ml) was divided into portions (2 x 150 ml) and freeze-dried. The solids were removed (1.7744 g and 1.5298 g respectively) and the bottles rinsed with a minimum volume of water. One portion (1.7744 g) was reconstituted with water and the bottle washings added (final volume 22 ml). This was ultrafiltered through a 1 kD filter and the combined supernatant and filter washings reserved. An aliquot of the filtrate (5 ml) was subject to HPLC analysis and the rest of the sample ultrafiltered through a 500 D filter. The combined supernatant and washings were reserved. The samples were designated as follows:

1. Water blank filtered through 1 kD filter.
2. 1 kD filter washing after sample filtration (1000 D+ fraction).
3. Water blank filtered through 500 D filter (500 D blank).
4. Hatch water sample after 500 D filtration (<500 D fraction).
5. Washings from 500 D filter (1000 - 500 D fraction).

The water blank filtered more quickly than the hatch water sample, which suggested that material had been retained by the filter.

5.5.2 HPLC analysis of the filtered samples

The samples were injected in the order 1-5 onto HPLC system 1. The chromatograms of the samples contained a small peak at 6.6 minutes (peak areas 2, 6, 3, 20, 0.5 mm^2 respectively). This peak was detected in all the samples except the 1000 - 500 D fraction, where a peak at 6.2 minutes eluted over the same retention window. The only sample which displayed any other peaks was sample 5, the 1000 - 500 D fraction (Table 5.2), which was subjected to bioassay (Section 5.5.3) The areas were calculated using 0.5 x width x height. The peak at 20.5 minutes had a shoulder on the leading edge at 19.0 minutes, but this was not resolved and therefore the combined area was calculated.

Table 5.2:Retention time and peaks areas for sample 5, 1000 – 500 D fraction

Retention time, min	1.8	2.2	2.4	3.0	3.9	5.5	6.2	7.8	10.0	14.4	20.5	23.2
Peak area, mm	77	24	279	10	3	1	94	4	5	9	108	20
Peak area, %	12	4	44	1.6	0.47	0.16	15	0.63	0.79	1.4	17	3.2

5.5.3 Bioassay of 1000 - 500 D fraction

Sample 5, the 1000 - 500 D fraction (Section 5.5.1) was bioassayed in the School of Biosciences. Aliquots of the sample (10 ml) and filtered sea water (10 ml) were placed in identical jars and the test crab was placed in one of the solutions. The number of pumps and other behaviour was noted over two minutes (Table 5.3), the animal was returned to its holding jar and allowed to recover for a minimum time period (5 minutes) before testing in the other solution.

Table 5.3: Bioassay Results for sample 5 (1000 - 500 D fraction) showing number of pumps and other activity

Crab identity	Sea water control	Sample 5, 1000 - 500 D fraction
a1	0, A	39, A, R
a3	2, A	10, A
a8	0	33, R, A
b1	0	12, A
b3	0, A	0, A
b4	0, A	0, A
b8	0	0
b10	0	56
b12	0	27, A
b15	1, Ch,Cp	0, A
mean ($\bar{x}$)	0.30	17.7
standard deviation (σ_{n-1})	0.68	20.0
degrees of freedom (n)	9	9
Student's t test value	n/a	2.610

Activity codes: A = active; R = raised up on legs; Ch = checking egg mass with legs; Cp = checking egg mass with pinchers. Student's paired t test value at 95% confidence level = 2.262[145]

5.5.4 Ultrafiltration of hatch water - a repeat experiment

Hatch water (50 ml, collected 7/8/97) was filtered through 1 kD and 500 D filters to give five samples as described previously (Section 5.5.1), which were subjected to HPLC analysis on System 1 and the samples were injected in the order 1-5 as before. No peaks were apparent in any of the chromatograms, other than trace contaminants.

5.6 Stability of sample to freeze-drying

A sample of pooled hatch water (60 ml), containing a fraction which was previously shown to have bioassay activity, and a sample of seawater (60 ml) were spilt into two portions (30 ml), one portion of each was freeze dried and reconstituted in water (1.5 ml). The samples were bioassayed (Table 5.4) as previously described (Section 5.5.3).

Table 5.4: Number of pumps elicited by freeze dried hatch water and controls

Crab identity	Sea water	Pooled hatch water	Seawater freeze-dried	Pooled hatch water freeze-dried
a1	0	52	0	9
a3	0	1	0	0
a5	0	25	nm	nm
a4	nm	nm	0	23
a8	0	0	0	4
b3	0	0	0	0
b4	0	0	0	0
b10	0	0	0	22
b12	1	40	nm	nm
b13	0	41	nm	nm
b14	nm	nm	1	32
b15	nm	nm	0	0
b18	0	0	nm	nm
mean ($\bar{x}$)	0.10	15.9	0.11	10.0
standard deviation (σ_{n-1})	0.32	21.3	0.33	12.4
degrees of freedom (n)	9	9	8	8
Student's t test value	n/a	2.225	n/a	2.256

nm = Not Measured, Student's paired t test value at 95% confidence level for 9 degrees of freedom = 2.262, t test value at 95% confidence level for 8 degrees of freedom = 2.306

5.7 Analysis of crab holding water

A sample of blank holding water was obtained for males only, females only and females carrying eggs. The crabs had been resting in the holding water for 1 hour and also overnight (17.5 hours). The samples were analysed by HPLC Systems 1 and 2 to determine if any UV visible compounds were released which might interfere with later analyses. System 1 showed a peak at 2.4 minutes for all crabs, which increased with length of holding time (Table 5.5).The results for System 2 showed only the solvent front in all cases.

Table 5.5: Increase in peak area with length of holding time

Sample	Peak area, mm^2	
	1 hour	17.5 hour
Female only	10	36
Females with eggs	4	128
Males only	1	64

5.8 Direct analysis of hatch water

A female was observed to release some of her larvae late in the afternoon. A series of samples were taken and analysed using HPLC System 2 (Table 5.6).

Table 5.6: Retention time and peak areas for various hatch and holding water samples

Sample no	Sample identity	Retention time, min	Peak area, % total
1	Blank sea water	10	105 (58)
		13	75 (42)
2	Holding water containing female and initial release of larvae	5.5	671 (97)
		10	10 (1.4)
		16	9 (1.3)
3	Holding water of female carrying eggs but no larval release	6.5	140 (70)
		14	60 (30)
4	Holding water after female removed and larvae filtered off	6	210 (93)
		10	4 (1.8)
		11.5	5 (2.2)
		16	7 (3.1)
5	Water into which the remaining larvae were released	4.5	48 (48)
		7	3 (3.0)
		10	18 (18)
		15.5	32 (32)

The peak eluting at 10 minutes occurs in all samples and is likely to be system contamination. Only the female carrying eggs produced a peak at 6 minutes. The rest of the samples were not subject to bioassay.

5.9 Analysis of samples from 10-11/10/97

5.9.1 Samples from 10/10/97

Two female crabs were found to be carrying eggs, one of which was seen to begin releasing larvae (Sample 10/10/97a). They were transferred to glass vials (30 ml volume) containing sea water (10 ml) and allowed to acclimatise (90 minutes). An aliquot (100 µl) from a series of samples (1-7, Table 5.7) was injected onto HPLC System 2. The females were removed from the vials and the samples stored in the freezer until required for further analysis (Section 5.9.2 , 3 & 4). The female released the rest of her larvae the following day. This sample was filtered free of larvae and also frozen (Sample 11/10/97b)

Table 5.7: Retention time and peak areas for various hatch and holding water samples

Sample no.	Samples of holding water	Equilibration time, min.	Retention time, min	Peak area, mm^2 (% Total)
1	Sea water	NA	nil	nil
2	Female hatching larvae	90	2.6	20 (28)
			4.8	15 (21)
			5.3	36 (51)
3	Female hatching larvae	110	3.0	20 (23)
			3.6	44 (50)
			5.4	24.5 (28)
4	Female hatching larvae	130	3.0	13.5 (9.7)
			3.6	80 (58)
			5.3	45 (32)
5	Female carrying eggs	150	2.8	10.5 (3.3)
			3.3	50 (16)
			3.7	108 (34)
			4.5	13.75 (4.3)
			5.4	77 (24)
			7.9	56 (18)
			10.0	2 (0.63)
6	Female carrying eggs	200	3.3	78 (24)
			3.7	108 (33)
			5.4	66 (20)
			7.9	76 (23)
			10.0	2 (0.60)
7	Female without eggs	180	3.9	81 (84)
			5.8	15 (16)

5.9.2 Stability of frozen samples

The hatch water samples collected from the previous experiment (10/10/97a, 11/10/97b) were thawed and analysed using HPLC System 2 (Table 5.8).

Table 5.8: Analysis to check the stability of frozen stored samples

Sample description	Retention time, min	Peak area, mm^2 (% Total)
Sea water blank	nil	nil
Hatch water 10/10/97a rep 1	3.0	352.5 (80)
	5.2	45 (10)
	9.1	18 (4.1)
	12.0	3 (0.68)
	17.0	22 (5.0)
Hatch water 10/10/97a rep 2	2.9	345 (66)
	5.2	95 (18)
	9.1	30 (5.8)
	12.0	11 (2.1)
	17.0	40 (7.7)
Hatch water 11/10/97b	5.2	24 (83)
	9.1	5 (17)

The second hatch water sample (11/10/97b) was freeze-dried (~2.5 ml), and analysed using HPLC

System 2. The concentrate was freeze-dried to completion, reconstituted in water (1 ml) and analysed using HPLC System 2 (Table 5.9).

Table 5.9:Analysis to check the stability of freeze dried samples

Sample	Retention time, min	Peak area, mm^2 (% Total)
Mobile phase blank	nil	nil
Hatch water (11/10/97b) replicate 1	4.8	12.5 (68)
	6.0	6 (32)
Hatch water (11/10/97b) replicate 2	4.8	18 (72)
	6.0	7 (28)
Hatch water (11/10/97b) freeze-dried to ~2.5 ml	3.85	10 (4.8)
	4.7	85 (41)
	6.0	21 (10)
	8.5	25 (12)
	9.1	16 (7.7)
	10.6	10 (4.8)
	13.0	40 (19)
Hatch water (11/10/97b) freeze-dried, reconstituted to 1 ml	2.6	226 (26)
	2.95	120 (14)
	3.8	30 (3.4)
	4.45	215 (24)
	6.0	48 (5.4)
	7.0	7 (0.80)
	7.9	76.5 (8.7)
	9.1	30 (3.4)
	10.5	24 (2.7)
	12.35	104 (12)

5.9.3 Ultrafiltration of hatch water samples

A hatch water sample (10/10/97a) was thawed, ultrafiltered through 1000 D and 500 D filters and an aliquot from each procedure analysed on HPLC System 2. An aliquot (2 ml) of the <500 D fraction was shaken diethyl ether (500 µl), the ether layer discarded and the aqueous phase analysed using HPLC System 2. A water blank (2 ml) was similarly treated with ether (Table 5.10).

Table 5.10: Analysis of hatch water (10/10/97a) ultrafiltration and ether extracted samples

Sample description	Retention time, min	Peak area, mm^2 (Total%)
Water blank	nil	nil
No treatment	2.7	350 (67)
	4.3	80 (15)
	5.2	6 (1.2)
	6.7	17.5 (3.4)
	8.6	24 (4.6)
	10.4	42 (8.1)
<1000 D fraction	2.7	40.5 (51)
	4.2	24.5 (31)
	6.6	5 (6.2)
	10.4	10 (12)

>1000 D fraction	3.5	14 (58)
	4.3	10 (42)
<500 D fraction	2.3	52.5 (42)
	4.4	56 (45)
	5.4	4 (3.2)
	6.0	2.2 (1.8)
	6.8	10.5 (8.4)
1000 - 500 D fraction	3.2	5 (13)
	4.4	27 (71)
	5.4	6 (16)
Diethyl ether extracted water blank	nil	nil
Diethyl ether extracted fraction	2.7	30 (26)
	4.3	45 (39)
	5.2	36 (31)
	6.8	5 (4.3)

5.9.4 Fractionation of sample on HPLC

Hatch water sample 11/10/97b, which had previously been freeze-dried and reconstituted in water, was analysed using standard HPLC system 2, except a larger sample loop (500 µl) was installed. Three aliquots (250 µl) were injected and the eluant collected in glass vials. The fractions were combined by collecting identical time points from each run into the same vial. In one run, fraction 5 showed a small addition peak (peak 6) However repetition of the HPLC analysis only showed a single peak (Table 5.11). The fractions were freeze-dried to remove excess mobile phase.

Table 5.11: Fractions collected

Fraction number	Retention time, window min	Peak no. collected
1	2.0-3.0	1 + 2
2	4.2 - 4.8	3
3	4.8 - 5.4	4
4	6.0 – 9.0	5
5	10.7 - 11.5	6 + 7
6	15.0 – 20.0	8
7 (injection 3 only)	9.7 - 10.5	8

5.9.5 Electrospray analysis of fractions

Three of the fractions (4, 5, 6 section 5.9.4) were reconstituted in aqueous acetonitrile/formic acid solution (1 ml, 50 % *v/v* with 1 % formic acid *v/v*) and analysed by electrospray-MS (Table 5.12). The system used was a Fisons Platform II mass spectrometer run in the positive electrospray mode, fitted with a Rheodyne injector and sample loop (10 µl). The source temperature was 70 °C, the cone voltage was 20 V and the nitrogen head pressure was 7 bar. The mobile phase was acetonitrile/water (50% *v/v*) containing formic acid (1% by volume) and the flow rate was 0.1 ml/min

Table 5.12: Electrospray analysis of the major HPLC fractions

Fraction	Response x 10^5	Molecular ion	Significant ions, *m/z*
4	1.17	396	294, 119, 83
5	2.29	396	294, 119, 83
6	2.87	396	119, 83

All the above fractions showed a fragment at *m/z* 397.4. As the samples are all protonated, this implies the molecular weight is 396.4 D. An acceptable response from this type of analysis is in the range of 10^4 units and the responses of all three samples was above this minimum threshold .

The remaining peak fractions (section 5.9.4) were freeze-dried and reconstituted in aqueous acetonitrile (1 ml, 50 % *v/v* acetonitrile/water) acidified with formic acid (1 % *v/v*). The system was set up as previously described and the samples analysed (Table 5.13).

Table 5.13: Electrospray analysis of the remaining HPLC fractions

Fraction	Response x 10^4	Mol. ion	Significant ions *m/z*
1	1.06	468	469, 312, 217, 204, 186, 176, 119, 118, 104
2	3.66	396	397, 146, 119, 83
3	7.61	396	397, 119, 104, 95
4*	5.89	654	654, 600, 521
5*	9.54	626	627, 521, 397
6*	1.36	624	No fragments detected
7	2.36	500	No fragments detected

* = sample reanalysed

The threshold response of the instrument was 1 x 10^4, therefore some of the signals were difficult to discern.

5.10 Holding water samples - a rerun

Samples of holding water were collected from female crabs with eggs in various stages of larval release. They were concentrated on a freeze-drier to approximately one quarter of their original volume. The samples were analysed on System 2 with the UV detector set to 200 nm and then rerun with the detector set to 214 nm (Table 5.14).

Table 5.14: HPLC analysis of water samples at 200 and 214 nm

Sample description	Retention time, min	Peak area, mm^2 200 nm	214 nm
Water blank	nil	-	-
Sea water blank	5	10	-
Female holding water, some pumping but no release	2.3	33	7
Female holding water, 9 larvae released	2.6	1470	965
Female hatch water	5	48	8
	7.4	42	30
	11	18	60
Sea water blank, plastic container	nil	-	-
24 Hour hatch water, 27 larvae released, plastic	2.3	621	262.5

container			
24 Hour holding water, plastic container	2.3	438	378

5.11 Bioassay of previous fractions

Three female crabs with eggs three female crabs without eggs were used for the bioassay. The crabs without eggs were used as the control animals and those with eggs as the test animals. Female eggs 1 was carrying eggs, female eggs 2 was likely to release larvae soon and female eggs 3 had released about half the larvae.

Beakers (250 ml) were rinsed and filled with sea water (100 ml), the crabs with eggs were transferred into the beakers and allowed to settle for 30 seconds. Their behaviour was monitored for 5 minutes and any pumps recorded. At the end of the time, the crabs were returned to their holding jars. The beakers were cleaned, rinsed, and fresh sea water added. The procedure was repeated with the control animals. The assay was repeated with hatch water containing larvae released by crab 3 (larvae water), HPLC fraction 4 (Section 5.9.4), <500 D fraction (Section 5.9.3), the 1000 - 500 D fraction (Section 5.9.3) and frozen hatch water (Section 5.5.1), (Table 5.15). HPLC fraction 4 (Section 5.9.4) was freeze-dried prior to bioassay to remove the TFA.

Table 5.15: Number of pumps elicited by hatch water, various HPLC fractions and controls

Sample	Crabs carrying eggs			Crabs not carrying eggs (control)		
	1	2	3	1	2	3
Sea water	0	0	0	0	0	0
Larvae water	0	0	4	0	0	0
HPLC fraction 4 (Section 5.9.4)	0*	0*	0*	0	0	0
< 500 D fraction (Section 5.9.3)	0	0	0	0	0	0
1000 - 500 D fraction (Section 5.9.3)	0*	1	0*	0	0	0
Hatch water (Section 5.5.1)	0*	2	5	0	0	0
mean ($\bar{x}$)		0.67			0	
standard deviation (σ_{n-1})		1.50			0	
degrees of freedom (n)		17			17	
t value		1.812			n/a	

*more agitated than controls, *i.e.* moved around the beaker, probed egg mass.
Crabs carrying eggs 1 and 2, which had been exposed to HPLC fraction 4 were seen to repeatedly pump their abdomens, when replaced in the holding jars.
Student's paired t test value at 95% confidence level for 17 degrees of freedom = 2.110

Chapter 6, *Rhithropanopeus harrissi* Hatching Pheromone -- Discussion and Conclusions

6.1 Introduction

The work on this project was centred around three sets of hatch water samples. The samples were examined using four main techniques. Initially, the samples were concentrated by freeze-drying, subject to size filtration to retain small molecules and analysed by both HPLC and electrospray to obtain an insight into the mass and structure of the pheromone cue.

6.2 Animal stocks

6.2.1 Collection

The first collection took place in Cardiff docks in June 1997. The crabs were plentiful and in the egg laying season (May - September), consequently they were sorted on the basis of whether they were carrying eggs or not. This collection yielded twenty egg-bearing females; about a quarter of the individuals examined. Crabs were collected a further three times during the course of the study. These occurred in August and September 1997, and March 1998. In later collections, males were sorted from females using the abdominal markings. Both genders have an inverted "v" shape to the rear of the carapace, but it is much narrower on the males.

In the early part of the study, only egg bearing females were kept as the breeding season was well underway, so stocks were easy to replenish. However, it soon became obvious that repeated animal collections were too time consuming to be continued. Although multiple ovipositions from a single mating are documented, this did not occur with any of the females we collected, possibly as a result of the stress of changing environment. In collections during September, *i.e.* towards the end of the breeding season, some males were retained for breeding purposes.

6.2.2. Maintenance and Colony Establishment

The short breeding season (June - September) and the availability of caught specimens were a limitation on the progress of the project. It was envisaged that creation of a colony would enable the breeding season to be extended which would increase availability of hatch water samples and also the number of females bearing eggs for the bioassays. Moreover, when crabs bearing eggs were collected from the wild, it was not possible to predict when they would hatch their eggs.

The bioassay for this work relies on a response from a statistically significant population of egg carrying females. At the start and end of the season this is very difficult to achieve because there are few egg carrying females and during the winter refractory period, samples can neither be collected nor assayed. For example, samples obtained in October would have to be stored for at least four months before the bioassay could be performed. In this case, the long-term storage of the samples would also have to be examined.

A colony of circa 50 crabs was maintained in a recirculating seawater tank. During the shortened refractory period the water was maintained at 14 °C. This is cooler than normal summer temperatures, but warmer than normal winter water temperatures (8 - 10 °C). Then, by artificially increasing the water temperature and the light part of their light/dark cycle to the norms for summer, the breeding seasons was induced to commence early. This regime enabled hatch water to be collected from one female on the 10 - 11th October 1997 and from two others on the 14th February and the 9th March 1998 respectively. However the mortality rate was high and no samples were collected from other individuals outside the normal breeding season and attempts to maintain the colony were abandoned.

6.3 Collection and storage of the hatch water

In studies of crab populations with no observable tide, larval release is under a circadial rhythm and tends to occur in a two hour interval after the onset of darkness. The incubation period for the eggs is approximately two weeks, so it was possible to predict when they would hatch from the first observation of eggs appearing and this was successfully done with the female who laid eggs in February.

At the beginning of the study, the intention was to retrain the crabs under artificial light/dark cycles, so that larval release could be timed to coincide with daytime. Although there was some initial success, this proved to be impractical in the long-term and was abandoned during the overwintering phase. The females which did release larvae tended to do so in the early evening, so careful observation around the predicted hatch date was maintained.

It was important to remove the hatch water as quickly as possible to preserve the highest concentration of active components, as if females remained in the water, the cue would bind to the appropriate receptors and be metabolised[146]. The crab was removed and the water filtered through various pore sized filters, primarily to remove larvae and other large particulates and ultimately through a membrane (0.45 μ) to remove bacterial contamination. The use of plastic containers was avoided as far as practical, as it is possible for compounds of interest to migrate into and be retained by the pores of the plastic. The samples were transferred to Duran® glass bottles and

stored in the freezer to minimize sample degradation.

6.4 HPLC Analysis of peptide standards

HPLC Systems 1 and 2 were set up with different columns and different wavelengths. System 1 used a Vydac 201TP5415 C18 5μ column which is a type routinely used for protein and peptide analysis, whereas System 2 was fitted with a Hypersil ODS C18 5μ column, again a C18 column of silica particle size 5μ, and routinely used for uron and triazine (herbicide) analysis and although the stationary phases are similar, there may be significant differences in their retention characteristics.

HPLC Systems 1 and 2 were calibrated and the lower limits of detection determined using commercial Leu-Arg.AcOH **69**. The calibration curves were run over a concentration range of 6 orders of magnitude, and the lowest standard was approximately 3 μmol, which is comparable to the reported levels of free amino acids detected in hydrolysed hatch water. System 1 using a detector at 214 nm was only able to detect the peptide down to 3 mmol, whereas System 2 using the detector set at 200 nm was able to detect the peptide down to 3 μmol.

Lower wavelength settings for HPLC detectors are generally viewed as less selective and less desirable because more compounds adsorb in this region. However in the current work, where the peptides and amino acids are only likely to contain basic and hydrophobic groups, the lower wavelength setting will favourably discriminate against aromatic compounds, which are less likely to be pheromone candidates.

The 214 nm wavelength was chosen as it was suggested in the literature for protein and peptide analysis[147] and was used in Sections 5.4 through 5.10 as appropriate. Although the absorbance characteristics of each peptide are different, the proposed peptide contains amino acids common to the test peptides. The UV absorbance of the amino acids will be similar in either of these peptides, so it is possible to detect the theoretical peptide under our HPLC conditions. The retention times of the peptides were 2.5 and 3.5 minutes respectively and small (tri- and tetra-) peptides should have similar retention times to these. The exact retention time will depend on the amino acids in the peptide and their interaction with the stationary phase of the column and as the test peptides contain the candidate pheromone amino acids, the retention times should be comparable.

6.5 Analysis of the first hatch water sample

6.5.1 Ultra-filtration of the hatch water sample

The main aim of the experiment was to separate the bulk sample into easily defined

subsamples. In the long term, this would enable us to perform a simple, reproducible sample clean up on a relatively large sample volume, typically up to several hundred millilitres, and discard the non-active portions. The sample was freeze-dried to remove the bulk of the water and hence concentrate any active material, although this also concentrated the salt which made up most of the dried material in the bottle, 1.77 g from 150 ml hatch water sample. The solid was redissolved in 22 ml water which gave a concentration factor of approximately 7 fold, or, assuming the solid was 100 % salt, an increase in concentration from 0.2 to 1.4 M.

The main benefits in using ultra-filtration are twofold; if the active compounds were not retained on any of the filters, then any retained material would not interfere with further analysis, and if the active compounds were retained, they could be concentrated relatively quickly and easily with the large amounts of salt in the matrix also being removed. High levels of salt can cause problems with both instrumental analysis (*i.e.* crystallising out in parts of the instrument) and the bioassay as the crabs are sensitive to salinity levels and this could affect the behavioural response to the cue.

Ultra-filtration was the cleanup technique of choice because it had previously been shown that the active cue was both retained and transferred through a 500 D filter[133]. It is suggested that the cue is a small peptide, possibly a tri- or tetra-peptide as it is readily soluble in polar solvents. Monosaccharides, which are also soluble in polar solvents, were discounted on the basis of HPLC analysis which identified 5 peaks, which after hydrolysis disappeared and lead to a large increase in free amino acids, the majority of which was arginine **66**. The actual pore size of the filters is within a defined range and is not absolute, for example, the 500 D filter might have a pore range of 400 - 600 D. This range can also be affected by previous usage with the smaller pores becoming blocked more quickly than the larger ones which will then restrict the passage of molecules of this size, leading to retention which would not occur on a fresh filter. This has implications when considering the 500 D and 1000 - 500 D fractions, as potentially there is a crossover area where compounds close to the smallest pore size may be partially retained on the filter. Therefore, if the active component is close to the pore size, it may be possible for activity to be found in both the supernatant and the filtrate.

The sample was applied to the filter and the gas pressure forced the liquid through the pores. The ultrapure blank passed through the 500 D filter at a similar rate to the 1000 D filter, but the hatch water filtration through the 500 D filter was considerably slower than either the blank or through the 1000 D filter. This increased filtration time suggested that material was being retained on the 500 D filter, and the size was in the 1000 - 500 D range, consistent with a tetra-peptide containing amino acid residues of an average molecular weight of 120.

6.5.2 HPLC analysis of the filtered samples

The samples were injected onto the HPLC using water as the mobile phase. All the chromatograms were found to contain a small peak at 6.5 minutes, probably leachate from the injector, and was therefore not considered significant. This peak co-eluted with a larger peak (94 mm^2) in the 1000 - 500 D fraction.

The 1000 - 500 D fraction was found to contain 12 peaks at 214 nm (Fig 6.2). Previous studies identified 10 peaks from 500 D filtration, five of which were identified as free amino acids, and the remainder yielded free amino acids on hydrolysis[135]. None of the peaks had a retention time which corresponded directly with the test peptides at 2.5 and 3.5 minutes, but the retention window is consistent with the tri-peptides.

The 12 peaks are comprised of components with masses between 500 and 1000 D, but as previously discussed, the size of the pores is not uniform, so the lower size limit may be less than 500 D. Associated water molecules may also affect the relative size of the peptide especially when the peptide contains amino acids with charged groups such as arginine **66** or lysine **64**. The largest peak was that at 2.4 minutes, and had an area of 270 mm^2. Of the 12 peaks detected, the four peaks at 1.8, 2.4, 6.2 and 20.5 minutes had the majority of the total peak area with 88 %. The remaining eight components were considered to be minor constituents with only 12 % of the total area.

Fig 6.2: Retention times and peak areas for 1000 - 500 D fraction

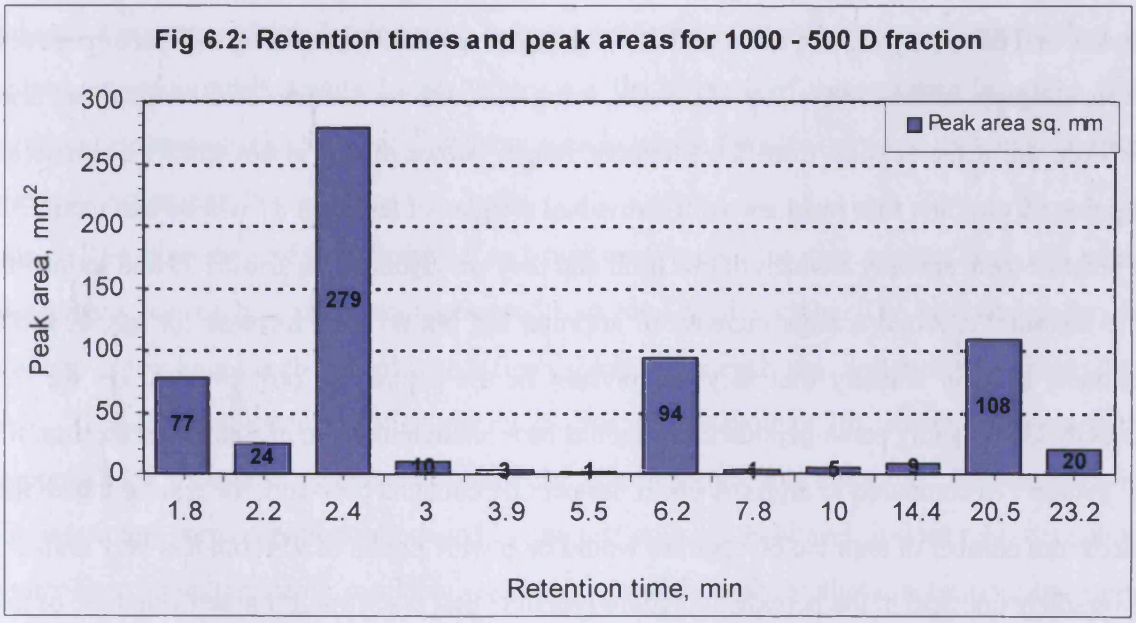

None of the other samples contained any detectable material, so hatch water contains components with a limited size range between 1000 - 500 D. The molecular weight of the peptide suggested in the literature is between 308 - 520. If an average weight of 120 is taken for a "consensus" amino acid weight, then the suggested literature range would correspond to a tri- or

tetra-peptide. However, the actual amino acids range from glycine **77a** at 75 up to tryptophan **78** at 204 . It has been suggested that arginine **66** is at least one of the residues within the peptide and it is one of the heavier acids with a weight of 174. The relative weights of peptides containing increasing numbers of glycine **77a**, tryptophan **78** or consensus residues with or without an arginine **66** residue were compared (Fig 6.3). This compares the lightest with the heaviest and thus encompasses the whole weight range possible.

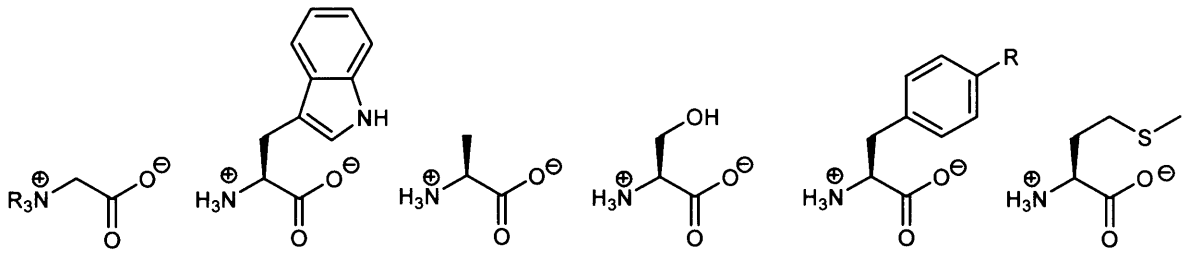

77
a R = H Gly
b R = CH_3

78 L-Trp

79 L-Ala

80 L-Ser

81
a R = H L-Phe
b R = OH L-Tyr

82 L-Met

The peptide is small, so if we limit the range to penta-peptides, it can be seen that the range runs from the di-peptide, Trp/Trp with a weight of 390 up to the penta-peptide Arg/Gly/Gly/Gly/Gly with a weight of 402. If we assume that the peptide contains arginine **66** based on the ~150 % increased reported after hatch water hydrolysis, we can discount the di-peptide and have only the tri-, tetra- and penta-peptides to consider. Although all penta-peptides in our example fit the 1000 - 500 D criteria, using the consensus amino acid line, we can also discount the penta-peptide from the literature range. Although this is not strictly accurate as arginine **66** plus any four residues with individual weights of less than 87 will be less than 520, in practice there are only 3 which fit this limit and they are glycine **77a**, alanine **79** and serine **80**. The literature reported a huge increase in arginine **66**, but no such increase for any of these residues, so it is unlikely that they are present in the peptide as polyresidues, *i.e.* for the Arg/Gly/Gly/Gly/Gly penta-peptide there should be a relative increase of four times the amount of glycine **77a** compared to arginine **66**. If the peptide contains poly-arginine residues, then the maximum number of arginine **66** residues would be 6 with a mass of 954, but it is very unlikely to be solely one acid in the peptide, it is more probable that one, two or maybe even three of the residues would be arginine **66**.

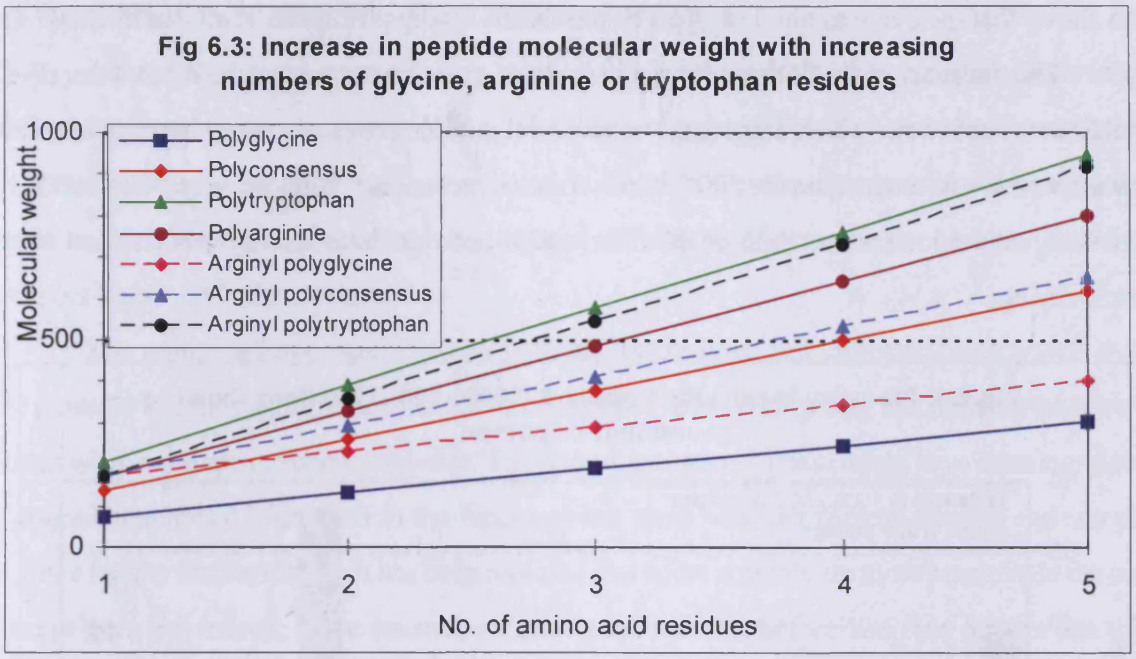

6.5.3 Bioassay of the 1000 - 500 D fraction

The bioassay is based on the behaviour displayed during larval release. The crabs rise up on their walking legs, probe the attached egg mass with their pinchers and flex the abdomen in a "pumping" action to aid mechanical rupture of the eggs and flush the larvae away. The abdomen flexing gives rise to the "pumping response" name for the procedure. This behaviour can be induced at any stage of egg development, by using either water into which larvae have hatched, or water containing crushed eggs. In this latter case, the strength of the response increases with increased embryonic development[120]. It is not seen in barren females or males, making it an ideal bioassay response.

The bioassay used ten animals and two portions of the test mixture and sea water respectively, *i.e.* each solution was presented to a total of five crabs. The best design for the bioassay is to present each animal with a fresh solution for each test, and preferably more than once. This eliminates concentration decreases due to metabolism (to generate the pumping response) and thus false negative results if the cue becomes sub threshold. This design also eliminates any contamination introduced by the test animals. However, it does rely on copious quantities of solution being available, which is possible with synthetic solutions, but more problematic with natural ones and in practice, the limited volume of the 1000 - 500 D fraction precluded this approach.

The results from the bioassay (Fig 6.4) gave a significant response at the 95 % confidence level using a paired Student's T test. This demonstrates the presence of the active cue in this sample, which was the only one to show any peaks in the chromatogram run at 214 nm. This result

also shows that the cue was not destroyed by the freeze-drying process so is not volatile.

The summary of the findings from this series of experiments are that the hatch water does contain some active cue which triggers the behavioural pumping response in egg bearing females. The active cue was retained on the 500 D filter, so has a molecular weight between 500 - 1000 D, depending on the lower mass limit of the filter, and is not volatile as activity was retained after freeze-drying.

Fig 6.4: Bioassay results for sample 5 (1000 - 500 D fraction) showing number of pumps

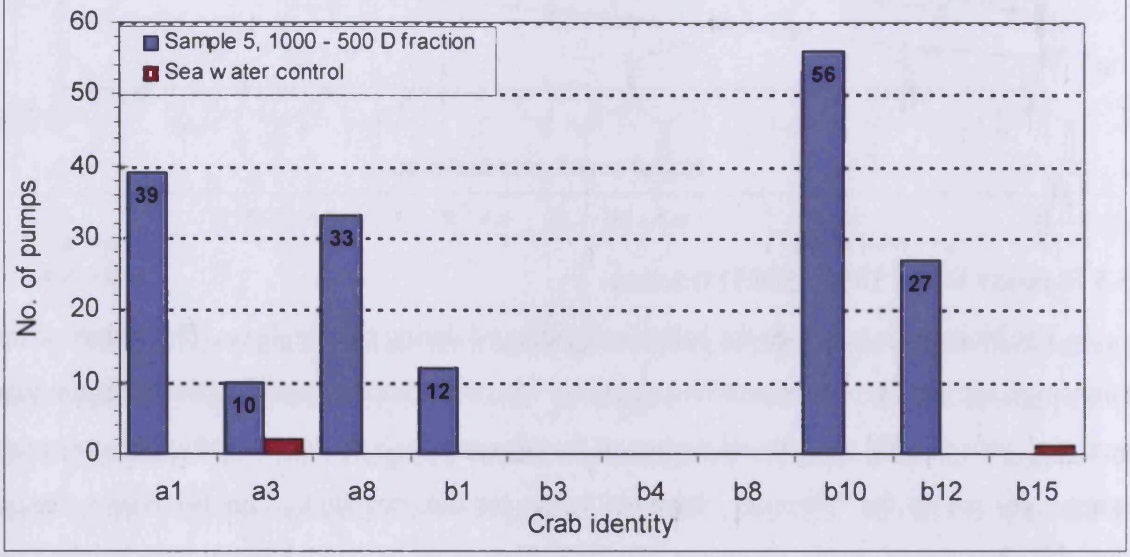

6.5.4 Repeat analysis of the first hatch water sample - Filtration and HPLC

This hatch water sample was not freeze-dried prior to the ultra-filtration to see in this concentration step was necessary. The filters should still trap out components of the appropriate molecular weight, even though the solution is more dilute, although filtration times would be increased. The main benefit would be the time saved from the freeze-drying stage as this typically took overnight.

Although the filtration rate for the hatch water through the 500 D filter was again much slower than through the 1000 D filter and the blank water through the 500 D filter, there were no peaks detected in the HPLC analysis. The slow filtration rate again suggests that some material is being retained, but it was not visible at 214 nm, possibly the sample was too dilute as the initial volume was only 50 ml as compared to 150 ml in the previous experiment and the final volume for the 1000 - 500 D fraction was 15 ml as compared to 5 ml, *i.e.* a 6 fold difference in concentration.

6.6 Determination of effect on activity by freeze-drying

Although the previous experiment (section 6.5.3) demonstrated that the active hatch water had retained its activity after freeze-drying, it has been suggested that some samples are not stable to frozen storage or freeze-drying[148], so although still active, these samples would not be as potent as fresh hatch water. This experiment compared the degree of response by bioassay to active samples before and after treatment.

The pumping response elicited by both the freeze-dried and untreated hatch waters over the controls was only significant at the 90 % confidence level, confirming that both samples were active when compared to blank sea water. The pumping response result might have been increased if more animals had been used in the bioassay, but there was insufficient animals and sample volume for any further testing. It has been reported that some animals are more sensitive to the cue than others, and indeed, some researchers screen the animals before use. We did not use this approach as there is the chance that the results are artificially enhanced by screening.

The freeze-dried and untreated hatch waters results were not significantly different at the 95 % confidence level (t_{calc} = 1.43, table value 2.306), clearly demonstrating that freeze-drying did not affect the activity of the cue as it was neither increased nor decreased (Fig 6.5). This experiment confirms that the active cue is not significantly diminished by freeze-drying and therefore the active component(s) are not volatile, in accordance with the literature findings and the peptide hypothesis.

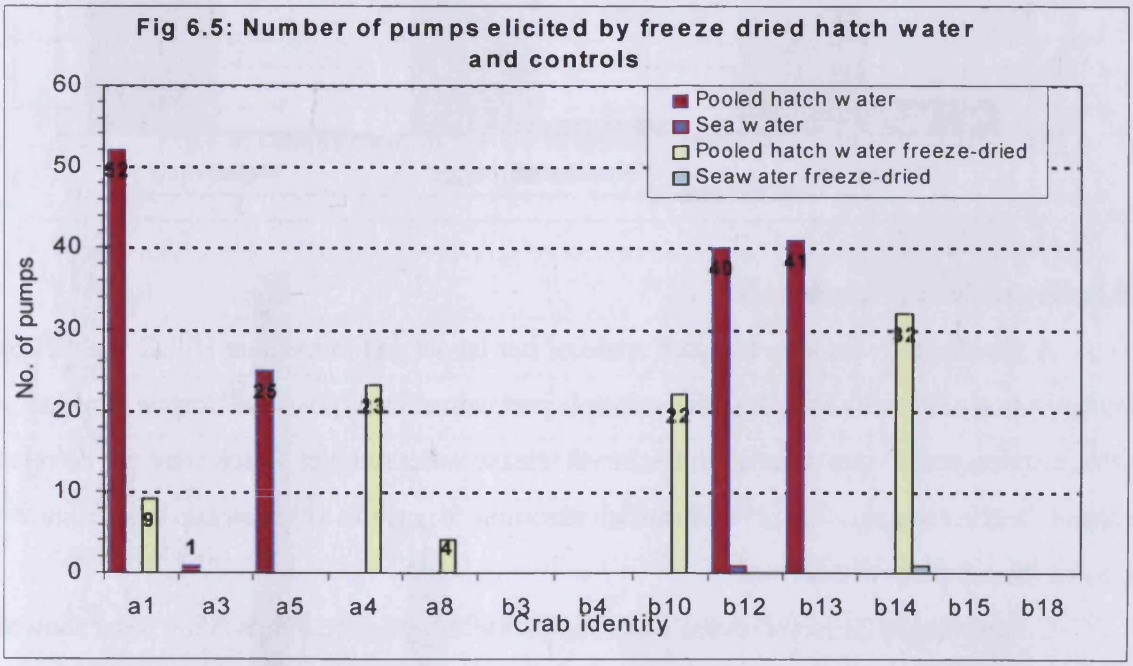

6.7 Analysis of crab holding water

The previous experiments demonstrated that larval release water contains several components which could be detected by UV absorption at 214 nm. The next step was to examine

the holding water of male, female and egg bearing females to see if any other UV visible compounds were released, and if so, compare their retention times and peak areas with those reported for the hatch water (Section 5.5). The animals were placed in jars containing sea water and allowed to rest there overnight, with samples being taken after 1 and 17.5 hours. The samples were analysed directly with no pretreatment on the two HPLC systems at 214 and 200 nm respectively.

Although only 14 nm apart, the only peak detected at 214 nm was the solvent front, whereas at 200 nm, a new peak at 2.4 minutes was seen for all the crabs which increased with length of holding time (Fig 6.6) and therefore this peak was attributed to waste products from metabolism. Although the peak from the egg bearing female was the largest, it was not associated with the hatching cue as no pumping response was observed and there was no larval release.

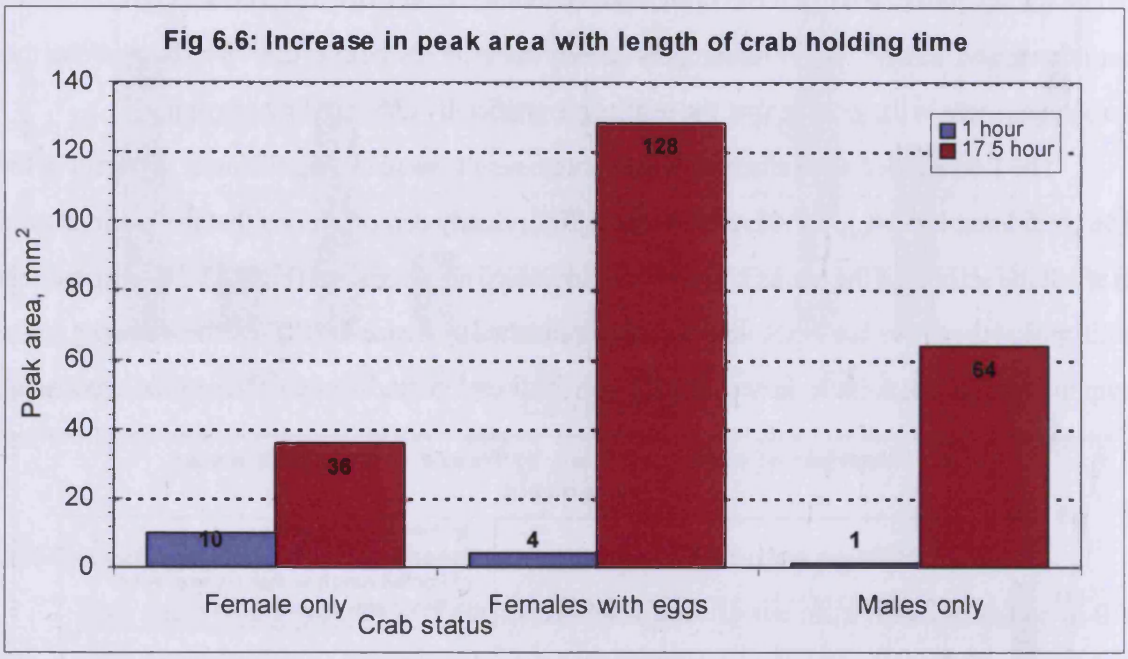

6.8 Direct analysis of hatch water

A female crab was seen to hatch some of her larvae and immediate HPLC analysis by direct injection of the bulk sample with no sample pretreatment was possible. Despite the dilution of the samples, peaks were detected in the larval release water samples which were not detected in any of the other samples. There was insufficient sample to perform a bioassay, so it is not known if any of the samples were active.

Comparison of the larval release water samples with the egg bearing holding water showed clear differences, the holding water produced two peaks of total area 200 mm^2 whereas the larval release water samples produced an average of 3 peaks with a mean total area of 149 mm^2. Although the mean area is less than the holding water area, this is explained by the relatively small area of the first peak in the larval release samples. The last sample was collected the following

morning after the remaining larvae had hatched, and the peak area decrease is consistent with metabolism of the cue. The final larval release sample showed three main differences to the other release samples, the first was that the peak area of the first peak (4.5 min) was significantly less than the corresponding peak (5.5 and 6.5 min) in the other samples. The other two observations were the emergence of a small peak (area 3 mm^2) at 7 minutes and an increase in the area of the last peak at 16 minutes, which could be due to the larval or cue metabolism, but was not further investigated (Fig 6.7, Fig 6.8).

Fig 6.7: Comparison of HPLC response of various hatch waters

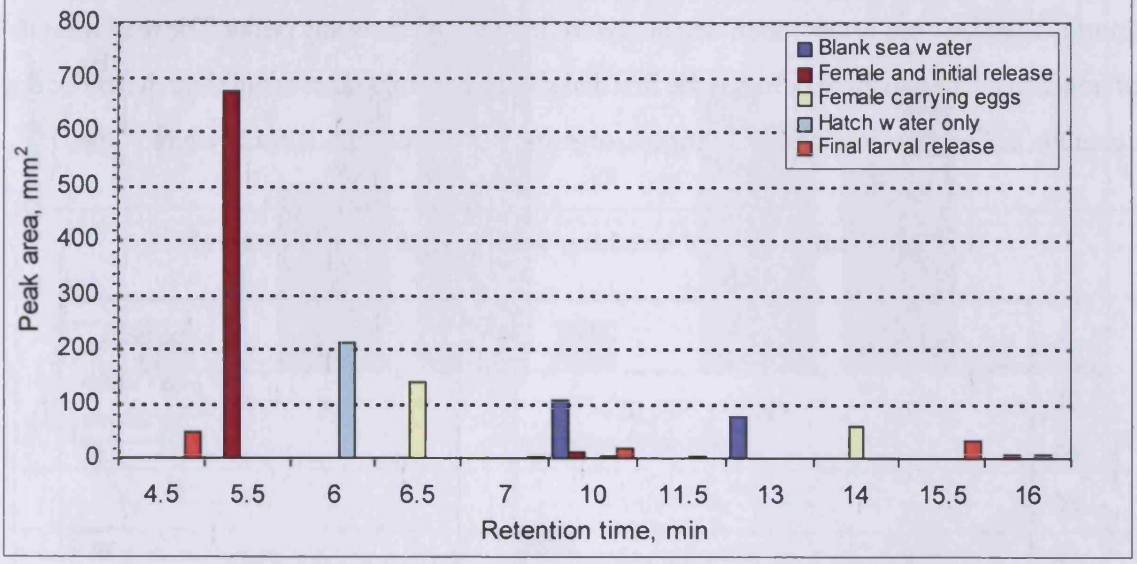

Fig 6.8: Comparison of the UV response to the three hatch water samples

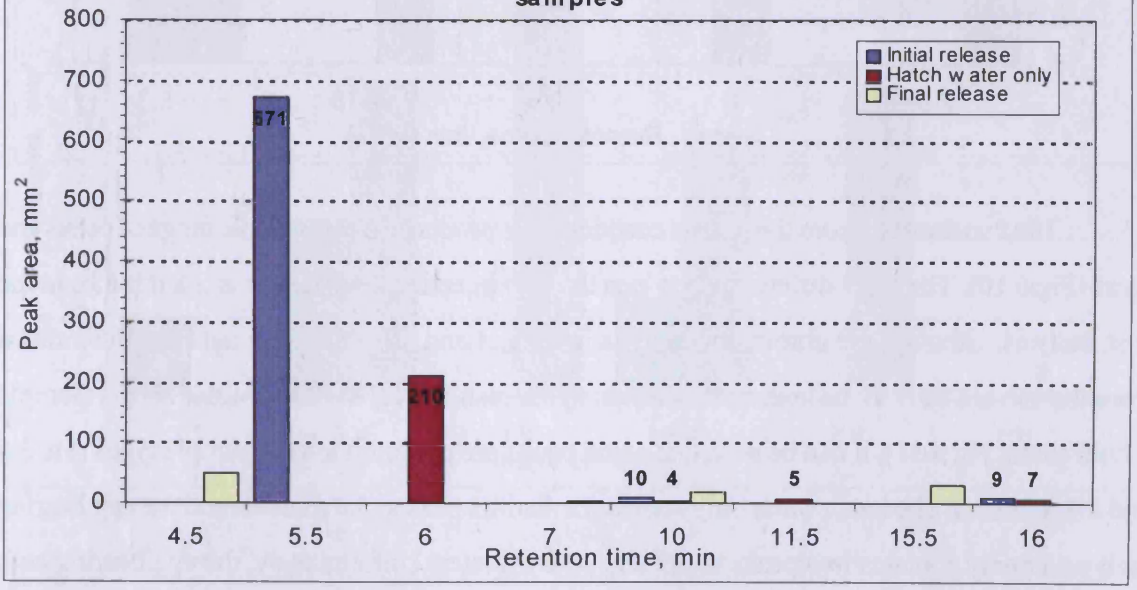

6.9 Analysis of samples from 10-11/10/97

6.9.1 Samples from 10/10/97

Three injections were performed at 20 minute intervals during actual larval release, the hatching female was allowed to acclimatise for 90 minutes prior to the first injection. All three injections produced three peaks (Fig 6.9), but injection one had slightly different retention times (2.6, 4.8 min) to the other two (3.0, 3.6 min), with the peak at 5.4 minutes consistent throughout. The peak pattern for injection 1 was also slightly different to the other two injections with a clear single peak at 2.6 minutes and two joined peaks at 4.8 - 5.4 minutes, whereas the other chromatograms showed two overlapping peaks at 3.0 - 3.6 minutes and a single peak at 5.4 minutes. The blank sea water which was analysed first did not show any peaks. The reason for the difference in the peak pattern between the first and subsequent injections is not clear, it may be due to genuine differences between the samples, or some effect from the HPLC system.

Fig 6.9: Comparison of hatching waters at 20 minute intervals

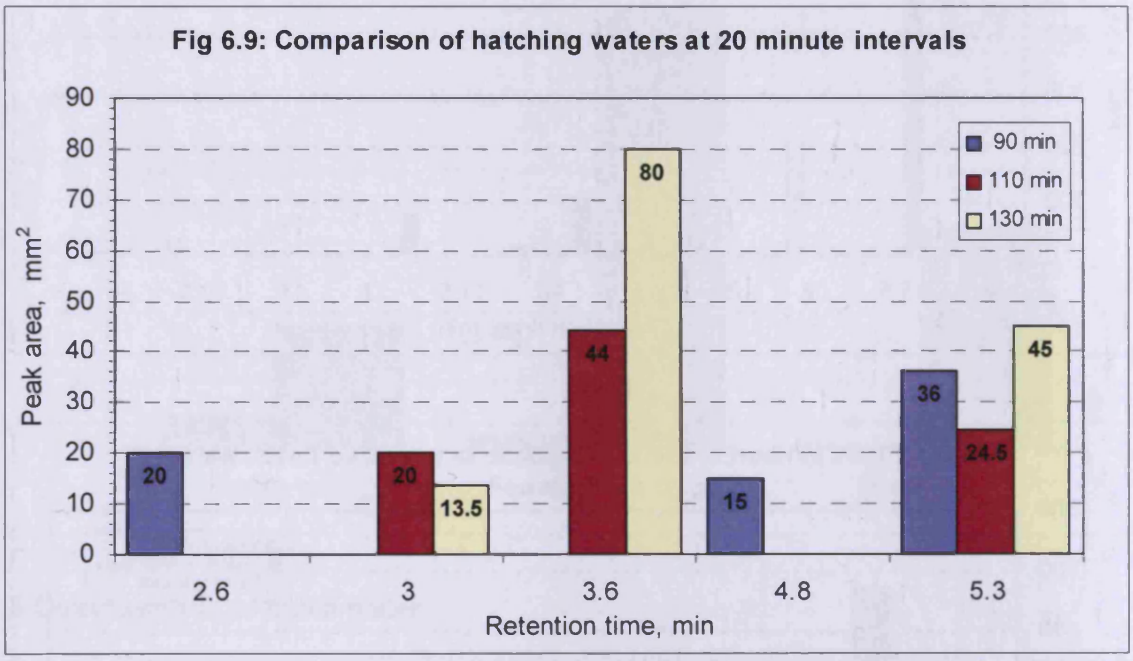

The two samples from the female carrying eggs produced a comparable range of peaks and areas (Fig 6.10). The main difference between the two injections was a peak at 2.8 minutes in the first analysis, although the chromatography is indistinct and this peak may not be differentiated from the solvent front in the later run. Comparing the results with the hatch water results (sample 2 both cases, Fig 6.11), it can be seen that some peaks are common to both sample types (*i.e.* 3.4 and 5.4 minutes). The hatch water only contains a distinct peak at 3.0 minutes and the egg bearing crab water only contains two peaks at 7.9 and 10.0 minutes. Unfortunately, the egg bearing crab died during the night, so it was not possible to tell if she was about to release her larvae, and therefore to highlight or exclude any of the peaks detected as potential cue candidates. If larval

release was imminent, it is possible that some hatching cue had already been released but environmental factors (such as the vial or the crab's health) may have prevented a pumping response and hence full release. The reason for this hypothesis is the holding water from the barren female showed only two broad peaks at 3.9 and 5.8 minutes, in contrast to those seen for both egg bearing and hatching females.

Fig 6.10: Holding water of females carrying eggs, comparison of peak times and areas

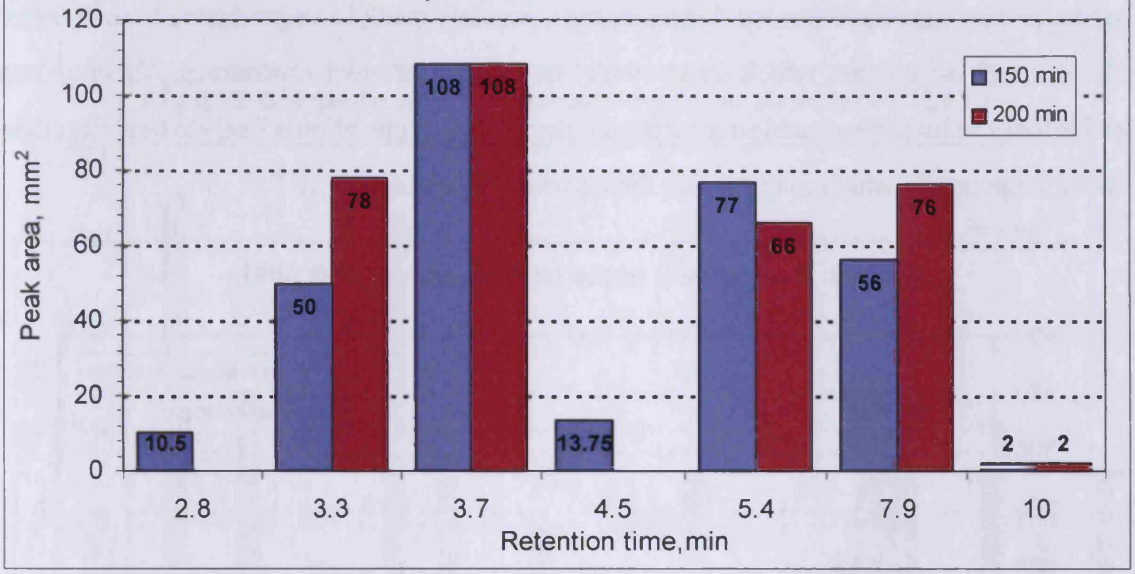

Fig 6.11: Comparison of hatching and holding waters

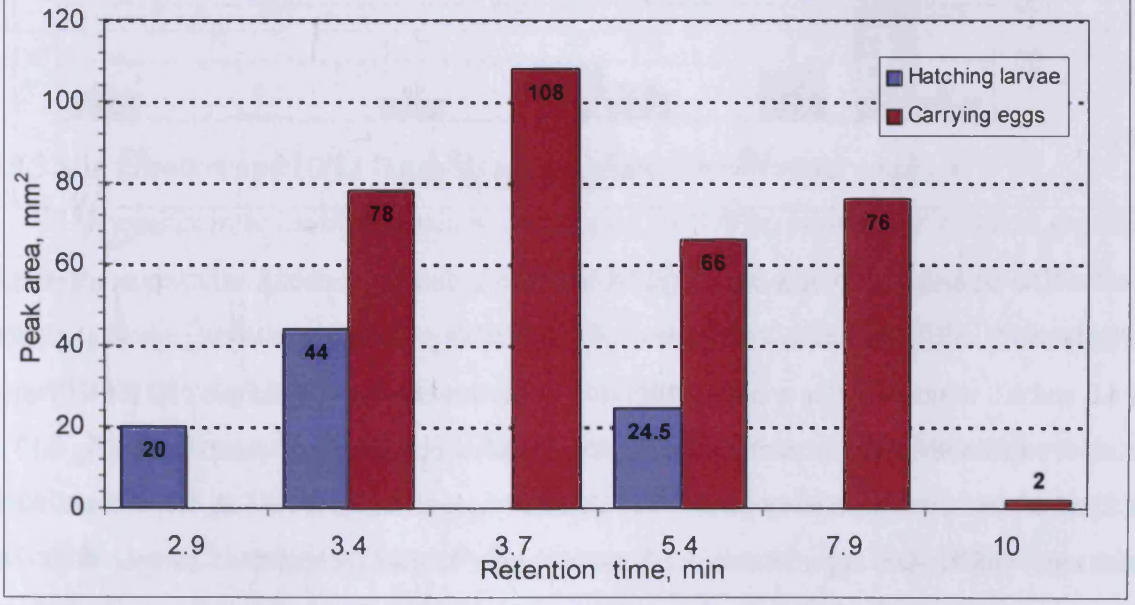

6.9.2 Stability of frozen samples

The hatch water samples collected in the previous experiment were stored frozen for a week, then thawed, mixed and analysed by HPLC to see if any significant changes were taking place in the samples. The analysis of the first hatch water sample (10/10/97a) produced five peaks (3.0, 5.2, 9.1, 12.0, 17.0 min) compared to the three (3.0., 3.6, 5.4 min) previously detected (Section 6.10.1), of which only two were consistent with the first analysis (Fig 6.12), three new peaks have emerged. It is possible that they were present previously but undifferentiated from the baseline, or they may have formed during storage, possibly breakdown products of much larger molecules such as proteins, which are known to be unstable at low temperatures. Although it is possible for samples to be unstable during frozen storage, the degradation is likely to be slower than at room temperature, which may explain the occasional loss of activity[149].

Fig 6.12: Comparison of the two injections of 10/10/97a

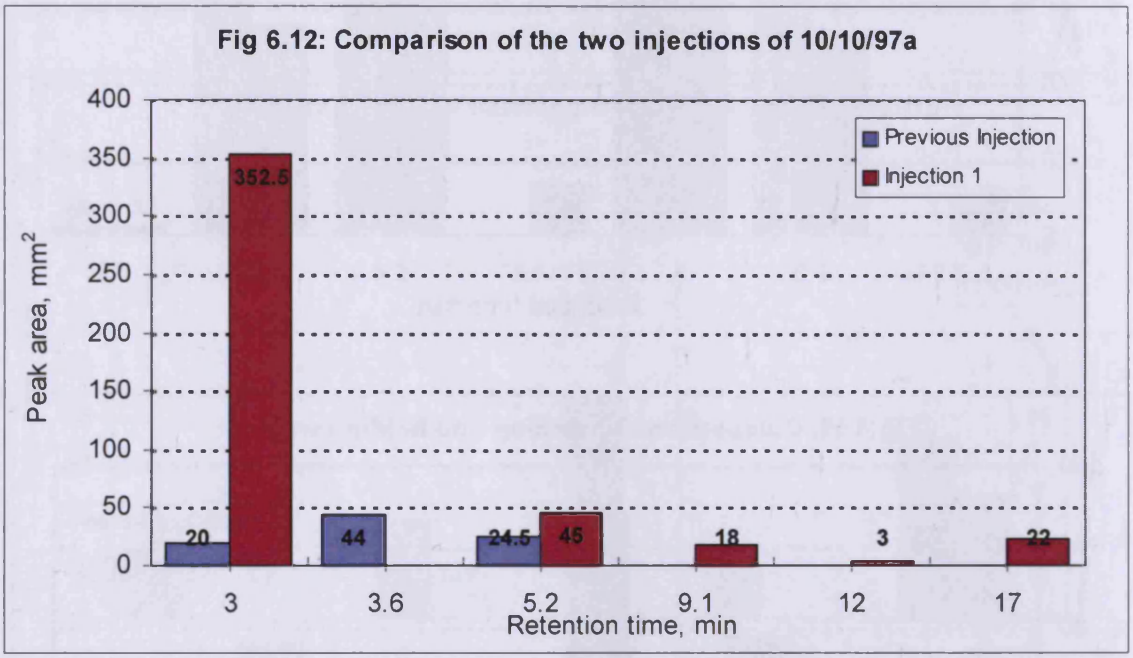

The second hatch water sample (11/10/97b) was found to contain only two small peaks initially at 5.2 and 9.1 minutes. Re-injection of the fraction prior to freeze-drying gave two peaks at 4.8 and 6.0 minutes. After concentration to 2.5 ml, this hatch water sample (11/10/97b) was found to contain seven components, and after drying and reconstitution, 10 components (Fig 6.13). In four instances, corresponding peaks were detected in both samples (at 3.8, 6.0, 9.1 and 10.5 minutes), which were approximately 2.5 times larger in the reconstituted sample than the concentrated one, as would be expected. Three peaks at 4.7, 8.5 and 13 minutes in the 2.5 ml concentrate seem to have disappeared from the reconstituted sample, although there are new peaks at 4.45, 7.9 and 12.35 minutes in the latter sample. It is not clear from the chromatography whether these peaks are related, but overloading components onto a column will reduce their retention times

and the high concentration of salt may modify the column properties, or if freeze-drying has actually destroyed the peaks. The relative ratios of the peaks at 4.45:4.7, 7.9:8.5 and 12.35:13 minutes is 2.5, 3 and 2.6 respectively, which does suggest that they are related, if so, then the reconstituted sample only actually has three new peaks at 2.6, 2.95 and 7 minutes, with the 7 minute peak being relatively minor with an area of only 7 mm^2. Although the activity of this sample had not been determined, this exercise clearly demonstrates that the hatch water is actually a complex mixture of very dilute components, which is consistent with the free amino acid levels of 10^{-6} M .

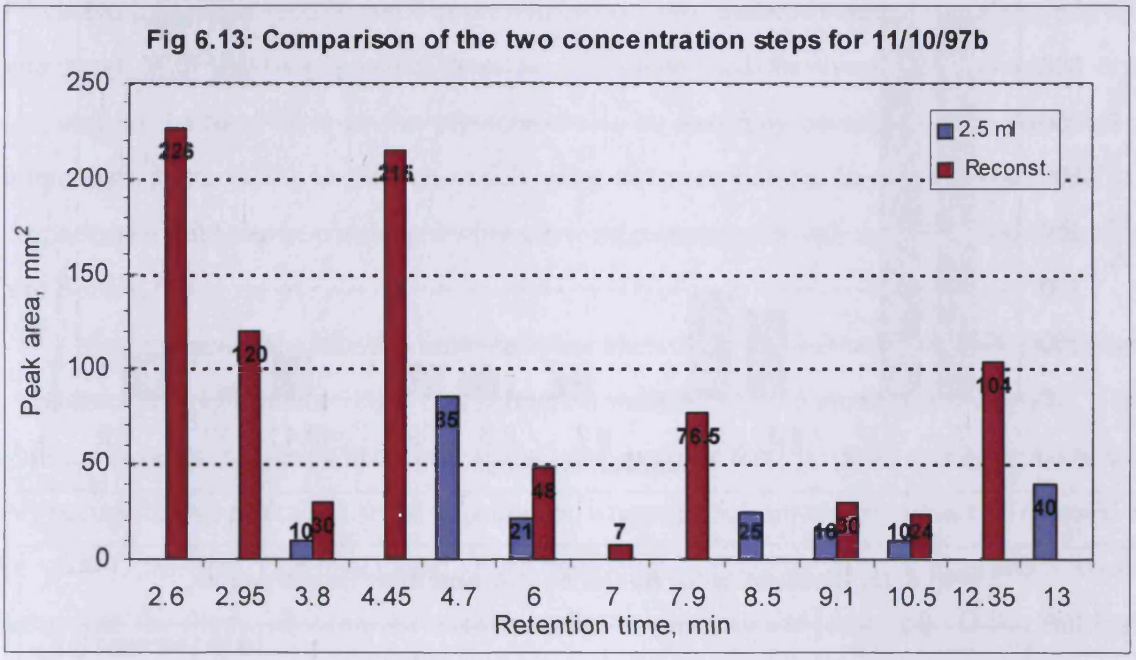

6.9.3 Size filtration and HPLC analysis of freeze-dried hatch water samples

The initial injection of the hatch water sample (10/10/97a) prior to any treatment gave six peaks as compared to five in the previous experiment (Fig 6.14), two of which were at identical retention times. This was attributed to slight changes in the sensitivity of the HPLC system and is supported by the small peak areas of the new peaks detected.

The hatch water sample (10/10/97a) was thawed, subject to ultrafiltration and the various fractions analysed by HPLC (Fig 6.15). The sample prior to treatment produced 6 peaks ranging in area from 6 - 350 mm^2, with the majority between 20 - 80 mm^2. The 1000 D filtration had a marked effect on the components in this experiment, the peak areas were all reduced by at least 50 %, and two of the peaks (5.3 and 8.6 min) were removed completely, which despite thorough washing of the filter, could not be recovered. This peak removal had not previously been occurred, and may be due to irreversible binding of the components to the filter surface. In addition, two

peaks (3.5 and 4.3 min) were detected in the filter washings which had also not been seen previously. However, as the cue is suspected to be a small peptide, it is unlikely that either of these components is the active candidate. The peak at 5.4 minutes was also not detected in the <1000 D fraction, but was detected in both the 1000 - 500 D and <500 D fractions, but as it was a very small peak it is possible it was obscured by other components eluting near the same time.

Fig 6.14: Comparison of two injections of sample 10/10/97a on different days

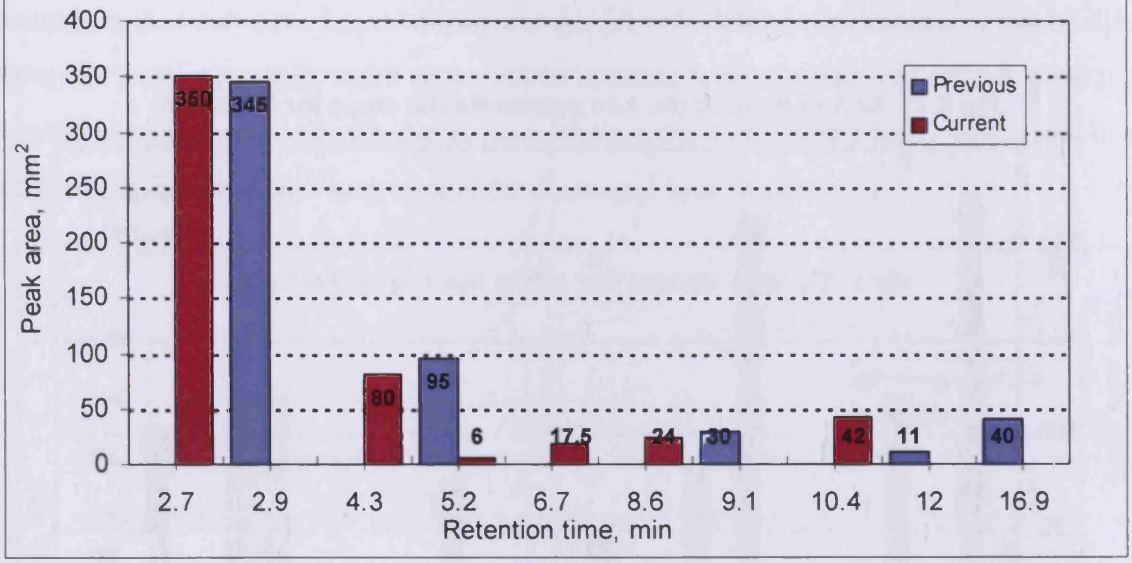

Fig 6.15: Distribution of peaks before and after fractionation

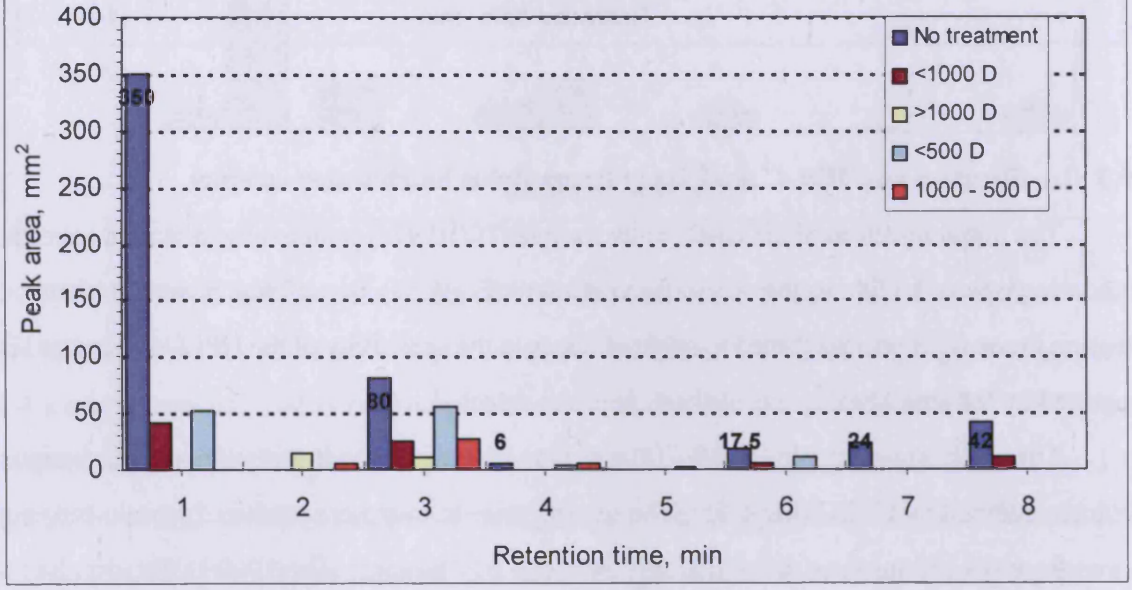

The combined 1000 D supernatant and filter washings produced two small peaks (14 and 10 mm^2 respectively) at 3.5 and 4.3 min. The peak at 4.3 min was seen in all samples, except the water blank, with varying areas, and may well be a genuine component of the samples, although

how it can apparently pass through and be retained by all the filters is not clear.

The <500 D fraction was found to contain five peaks, four of which were found in the untreated sample. The very small peak (2.2 mm^2) at 6.0 min was not seen in the untreated sample, but could have easily been obscured by interference from other components. Once again, a peak, at 10.4 minutes, was lost after filtration and could not be recovered, as seen with the 8.6 min peak in the 1000 D fraction. In addition, its area had already been reduced from 42 to 10 mm^2 by the 1000 D filtration, suggesting a large molecule.

In previous work (Section 5.5), the 1000 - 500 D fraction was the only fraction to contain UV visible components at 214 nm. The presence of retained material was again confirmed in this experiment, with three components detected. The filter used for this work was a new one, compared to the used filter in the previous work, so this may account for the presence of components in the <500 D fraction which were not seen before. In this case, the <500 D components should also be considered when drawing comparisons with the 1000 - 500 D fraction from Section 5.5.

Comparison of the retention times and peak areas of the <500 D and 1000 - 500 D fractions from this experiment and the 1000 - 500 D fraction from Section 5.5 are shown in Fig 6.16. If the same components are present in the both of the latter samples, then the peaks should coincide, this only occurs for two peaks, at 3.0 and 5.4 minutes, where the 5.4 minute peak was also detected in the <500 D fraction. This may already have been explained by the relative ages and previous histories of the filters, so it may be of more value to compare the 1000 - 500 D fraction from Section 5.5 with the current <500 D fraction. In this case, three peaks coincide at 2.4, 5.4 and 6.0 minutes. As the 1000 - 500 D fraction from Section 5.5 was found to be active, it was anticipated that the coincident peak(s) from either the 1000 - 500 D or <500 D fractions would be the active component. It was hoped to bioassay these fractions to confirm this theory, but due to the lack of egg bearing females, this was not possible.

Treatment with the diethyl ether did not result in the loss of any significant peaks from the <500 D fraction, the 6.0 minute peak was very small in the initial sample and difficult to distinguish from the baseline (Fig 6.17). When the diethyl ether was evaporated to dryness and the residue redissolved in water, the HPLC analysis did not reveal any peaks. This confirms the hypothesis that the cue is a small (<1000 D), polar molecule and not a lipid like compound.

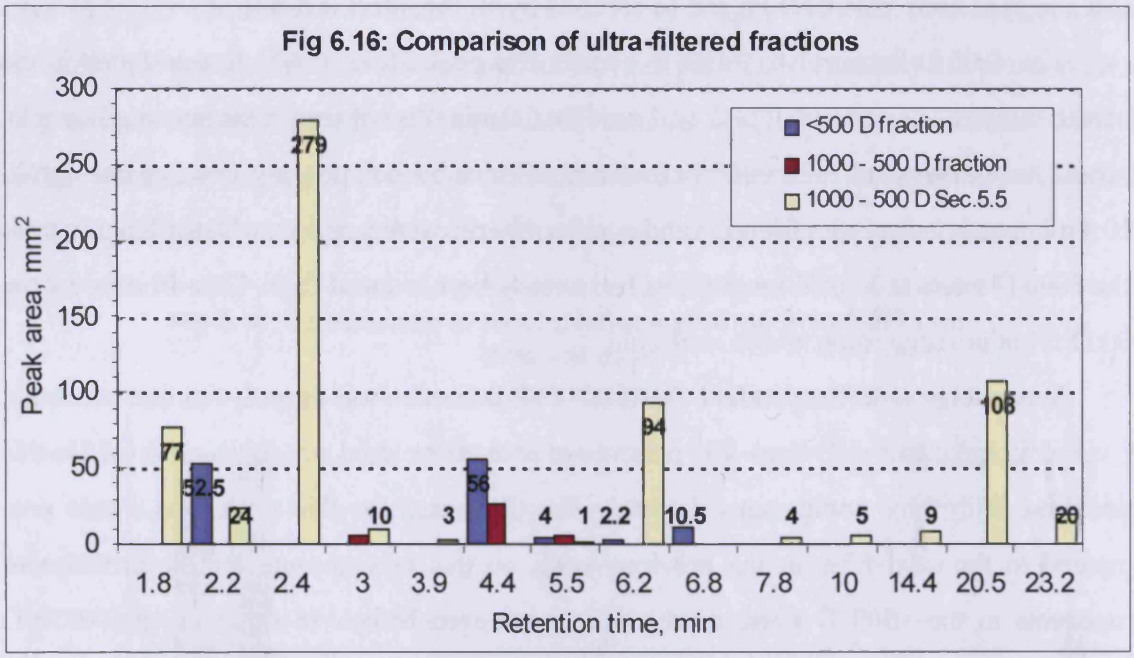

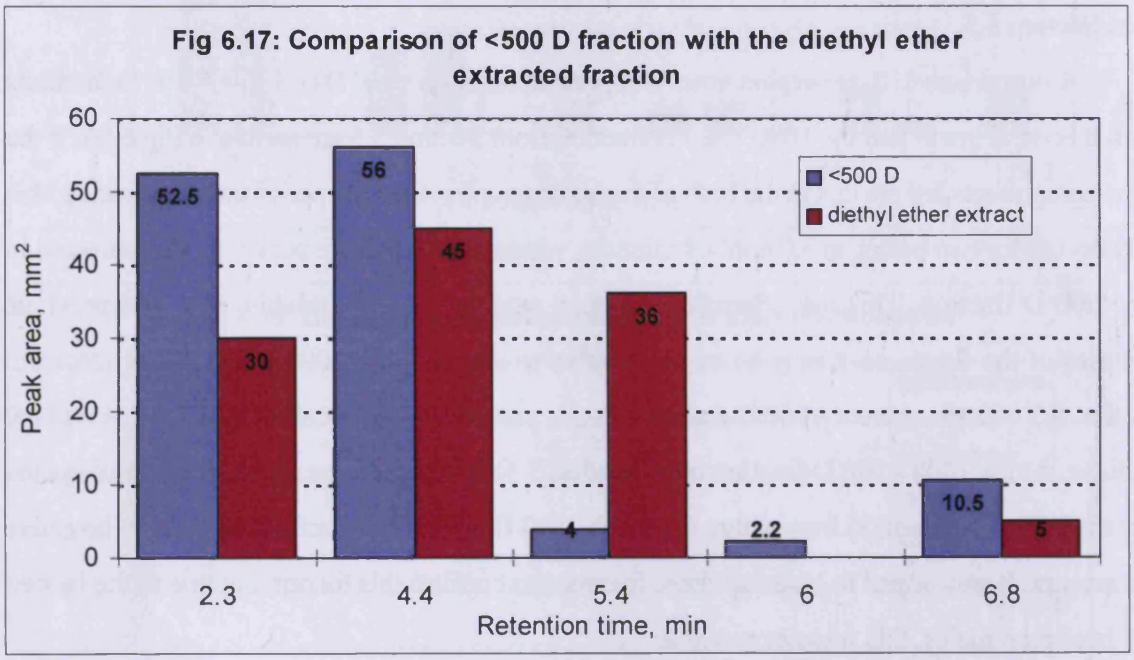

Ideally, after each filtration and HPLC analysis, a bioassay should be performed to check whether activity has been retained in any fraction. In practice, it was not possible to do this for two reasons: the analysis was carried out during the refractory period so there were no egg bearing females available and there was insufficient sample volume to test. The refractory period was kept as short as possible by artificial manipulation of water temperature and light/dark cycle. The sample volume could only be increased by keeping a far larger crab population, which was not possible as there was insufficient tank space and manpower.

6.9.4 Fractionation of the sample on HPLC

Having demonstrated the presence of UV visible compounds which are unique to hatch water, and shown that the hatch water contained the active cue, the next step was to fractionate a sample by HPLC. The advantages are that selected peaks and the intervening mobile phase can be collected and combined from different runs, so a relatively large sample volume can be easily divided into its constituent peaks. The dilution effect from the mobile phase was overcome by freeze-drying. Hatch water sample 11/10/97b was used because it had already been concentrated to 1 ml and was known to contain a minimum of eight peaks, the actual number was difficult to determine as the sample was so concentrated and the injection volume such that the column became overloaded. The main aim of the exercise was to produce series of discrete UV visible components which could then be further analysed by electrospray MS. The sample was split into seven fractions by time, with fractions 1 and 5 containing two peaks and the rest containing one.

6.9.5 Electrospray analysis of fractions

Electrospray was chosen to analyse the HPLC fractions. It is well suited to peptide analysis because ionisation occurs with minimal fragmentation. 1% formic acid in acetonitrile was used as mobile phase because it is volatile and miscible with water, but this does produce solvent clusters at *m/z* 101,119,142 from acetonitrile.

Initially, the three fractions which were known to contain significant HPLC-UV active peaks (fractions 4,5,and 6) were analysed. All three samples showed a fragment at *m/z* 397.4. As the samples are protonated, this fragment is actually M+1 (where M is the molecular ion), so the actual molecular mass is 396.4. Although discrete UV peaks had been collected, the spectra of all three fractions were similar, suggesting a common component and this did give a tentative molecular mass at a reasonable response, as the average molecular mass of the common amino acids is 120, this would be within the range of a tri-peptide.

The responses for the rest of the fractions were below the threshold response, making it difficult to distinguish between signal and noise and hence if any of the other samples produced any significant results. However, two of the fractions produced a fragment at *m/z* 397.6, which is consistent with the previous results. The fractions which gave a response on the first analysis did not do so on the second analysis because the bulk of the sample had already been used, so the initial result could not be verified.

A computer program was written to compare the masses of all possible combinations of tri-peptides and to report only those of the appropriate mass. Out of a possible 8000 permutations, a list of nine candidates was produced (Table 6.1), although the exact amino acid order is not

implied. The possible fragmentation ions were derived from the losses of the various residue masses; in addition, some amino acids readily form immonium ions[150] (H_2N^+=CHR) and these are also noted.

Table 6.1: Tri-peptides with masses of 396 and possible amino acid residue ions.

Tri-peptide	Single residue ions	Di-peptide ions	Immonium ions
Asp/Thr/Tyr	114, 101, 163	233, 282, 295	Tyr, 136
Cys/Phe/Gln	103, 128, 147	247, 268, 293	Phe, 120
Ser/Tyr/Gln	87, 163, 128	233, 268, 309	Tyr, 136
Gln/Leu/His	128, 113, 137	259, 268, 283	His, 110, Leu, 86
Gln/Ile/His	128, 113, 137	259, 268, 283	His, 110, Ile, 86
Lys/Leu/His*	n/a	n/a	n/a
Lys/Ile/His*	n/a	n/a	n/a
Cys/Phe/Lys	103, 147, 128	293, 268, 249	Phe, 120
Ser/Tyr/Lys	87, 163, 128	309, 268, 233	Tyr, 136

n/a = not applicable

The combinations marked with an asterisk contain two basic acids, both of which would be protonated by the formic acid. Therefore, these tri-peptides would have $(M + 2H)^{2+}$ at 396/2, *i.e.* 198. Even with the instrument configured to give only molecular ion data, this peak would be seen, but examination of the spectra did not reveal the presence of such a fragment. Therefore, if the compound is a tri-peptide with this mass, is does not contain any of these dibasic combinations. Examination of the spectra also failed to detect any of the possible amino acid residue masses listed in the table, but as the instrument was set up for maximum sensitivity, only molecular ion masses and not fragmentation patterns are obtained. The literature also reported a large increase in arginine **66** after hydrolysis[6], but none of the above peptides contained arginine **66**, so if the hatching cue does contain arginine **66**, then it is not one of these tri-peptides.

The same computer program was modified to search for tri-peptide combinations with a mass of 468. This mass was suggested from the results obtained on analysis of the second set of fractions analysed. The possible combinations was surprisingly small, only three, and they are listed (Table 6.2), again with possible ions.

Table 6.2: Tri-peptides with masses of 468 and possible amino acid residue ions.

Tri-peptide	Single residue ions	Di-peptide ions	Immonium ions
Met/Tyr/Arg	131, 163, 156	337, 312, 305	Met, 104, Tyr, 136
Phe/Phe/Arg	147, 156	321, 312	Phe, 120
Thr/Trp/Tyr	101, 186, 163	367, 305, 282	Trp, 159, Tyr, 136

Now there are two combinations that contain arginine **66**. In addition, tyrosine **81b**, phenylalanine **81a** and tryptophan **78** will also have an appreciable UV absorbtion, giving rise to a relatively large peak. Examination of the spectra did not identify fragments which could be reliably differentiated from background noise, so it is not possible to rule out any of the above as

hatching cue candidates. The computer exercise was extended to look for tetra-peptides with masses of 396 and 468, which yielded 15 and 49 candidates respectively out of a possible 160 000 possible permutations, many of which contained duplicate residues but none contained arginine **66**, and hence these peptides were not considered pheromone candidates.

Although commercial peptide sequencers are available, they are not effective on small molecules, because the technique involves sequential removal and identification of a terminal peptide. This is very difficult to achieve with tri- and tetra- peptides as so few bases are present and the peptide is easily destroyed.

6.10 Holding water samples - a rerun

Holding water samples were collected from females with eggs at varying stages of development, concentrated by freeze-drying and analysed by HPLC. The results from this experiment were twofold, and initially confirmed earlier findings (Section 6.7) of a peak close to the solvent front (2.3 min) which increased with length of holding time, from 33 to 438 mm^2.

The female holding water, the 24 hour hatch water (plastic) and the 24 hour holding water (plastic) produced a peak at 2.3 min in all chromatograms and the holding water with 9 larvae released again showed a peak at 2.6 min in both chromatograms. This is consistent with earlier work (reported above) which demonstrated the emergence of a peak close to the solvent front and was attributed to products of metabolism. The hatch water produced three peaks which were not seen in any of the other samples, as has also previously been demonstrated. Although it has previously been shown that 200 nm is more sensitive for many compounds, this experiment allowed a direct comparison as the same hardware was used for both injections, so all optical

Fig 6.18: Comparison of peak areas for hatch water at 200 and 214 nm: (2.6 min data reduced x 10)

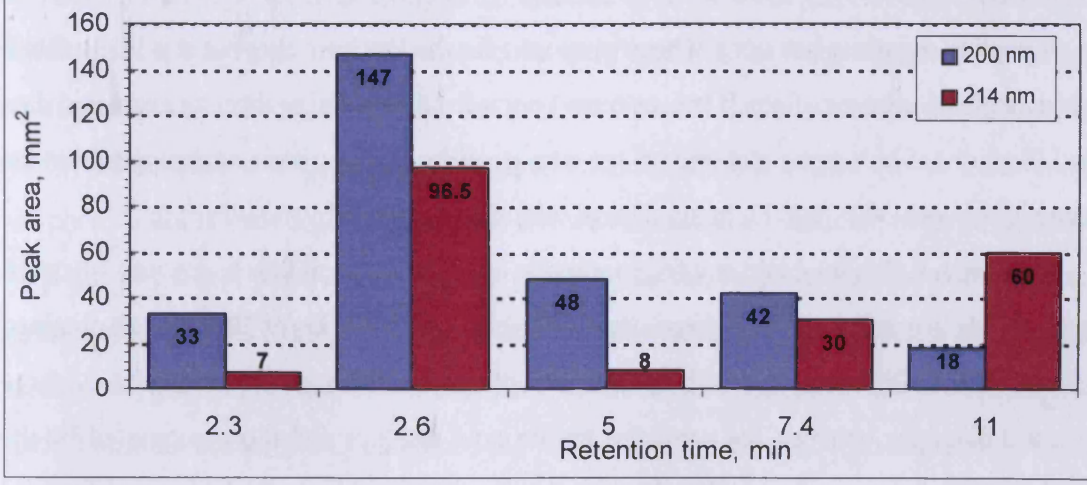

properties aside from wavelength were the same. The comparison of response (Fig 6.18) show that the differences are not constant, ranging from a maximum of 6:1 response ratio at 5 mins, but reversing completely to 1:3 at 11 minutes.

6.11 Bioassay of fractions collected from Section 5.9.3

This bioassay confirmed that under our conditions, females without eggs do not respond to the hatch water cue whereas egg bearing females do. Due to the small numbers of test animals and limited sample volume, it was not possible to produce a statistically significant result, but the other aspects of behaviour observed indicate that the active cue was present.

The most significant result for this study is the agitation caused by the five minute fraction from the HPLC runs. If the response was due to some contamination (*e.g.* mobile phase) then all crabs would be affected to the same degree and as this is not seen, it is likely that the hatching cue is operating. The full response was not seen, and this may be due to several factors, such as sub-threshold levels of the cue, environmental stress or simply unresponsive crabs.

6.12 Conclusions

This project encountered several practical difficulties, the major one being animal availability. We were not able to collect enough hatch water for source material, or keep enough crabs for reliable bioassay.

Despite these setbacks, we were able to demonstrate that larval release produces some cue which elicits a typical behaviour in response, but only with egg-bearing females and we were also able to demonstrate that the active cue is a relatively small molecule, with a size in the 500 D range, which confirms the findings of an earlier study[121]. We found that hatch water produced UV absorbing compounds which were absent from holding water and that it may be fractionated on an HPLC system.

A peptide sequence has not yet been proposed for the hatching cue, but it is likely that it is either a single or mixture of small (tri- or tetra-) peptides. Considering the size exclusion data obtained (Section 6.5) we agree that only tri- or tetra-peptides fit the criteria, and suggest that the size range is between 300 - 600 D, in agreement with that proposed by the literature[121].

We were not able to obtain any fragmentation information from the electrospray analysis, but we were able to confirm the size range suggested above, with masses of 396 and 468 obtained for different HPLC fractions. When the possible peptide combinations were calculated, some significant differences between the predicted amino acid residues and those suggested by the hydrolysis analysis became apparent. The literature suggests ten residues which increase after acid

hydrolysis, the largest increase being arginine **66**. Some amino acids are sensitive to acid hydrolysis, tryptophan **78** is completely destroyed and serine **80**, threonine and tyrosine **81b** are affected depending on the hydrolysis time and conditions. Base hydrolysis was not reported, which means that it is not possible to determine if tryptophan **78** was liberated or if the other labile acids were affected. When the possible tri-peptides generated by our computer exercise are compared with those in the literature, the suggested amino acids are different (Fig 6.18).

Fig 6.18: Comparison of the computer and literature suggested amino acids for residues of mass 396 and 468 D

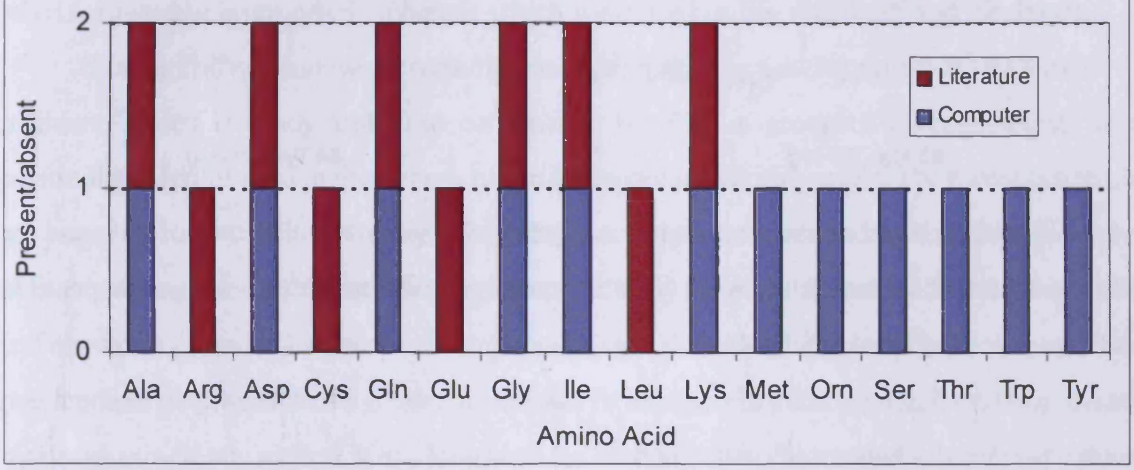

The computer exercise has given 12 possible amino acids, the hydrolysis data gave 10 likely acids, and four acids, valine, histidine, asparagine **67** and phenylalanine **81a**, are missing completely. Of these, six match and they are Asp, Ser **80**, Arg **66**, Ile, Leu **65** and Lys **64**. We have already established that peptides containing two basic amino acid residues would produce the $(M + 2H)^{2+}$ ions at either *m/z* 198 or 234, neither of which were seen, so this limits the possible combinations, especially if the peptide must contain arginine **66**, as it is a basic amino acid. We would therefore not expect to see peptides which contain histidine and/or lysine **64** with arginine **66**. The literature reported a relatively small increase in lysine **64** of 25 % over the base value, and histidine was not reported at all. At a molecular weight of 396, the computer searches did not give any tri-peptides containing arginine **66**, but some of the combinations contained acids found in the hydrolysed sample. At 468, two of the searches contained arginine **66**, one of which also contained two phenylalanine residues. This combination was excluded a candidate because the literature study did not detect phenylalanine in the pumping factor, and it should have been present at significant quantities if present as two residues. The other computer search result contained threonine, tryptophan **78** and tyrosine **81b**, none of which were detected in the hydrolysed pumping factor. The literature study only examined the <500 D fraction even though some activity remained

on the filter surface, so it is possible that the combinations reported here are part of the larval release cue and due to retention, were not detected in the previous work.

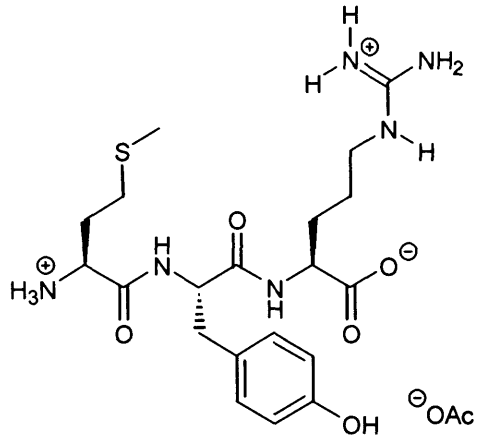

83 Met-Tyr-Arg

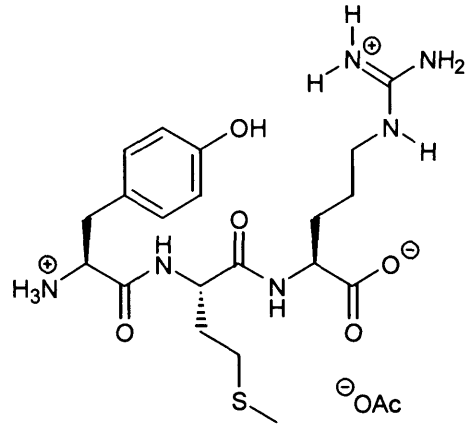

84 Tyr-Met-Arg

Therefore, based on the electrospray analysis yielding a molecular mass of 468, and the literature report of increased arginine **66** after hydrolysis, we are able to suggest a possible candidate. It is Met/Tyr/Arg **83, 84**.

Chapter 7, Halo-compound Degradation on Iron and Palladium/Iron Surfaces

7.0 Introduction

Chlorinated solvents such as dichloromethane, perchloroethylene, trichloroethylene and carbon tetrachloride (VOCs, volatile organic compound) are used as degreasing and cleaning agents in commercial and industrial processes. This has lead to widespread problems, especially in the USA, where they cause contamination to groundwater sources, together with pesticides such 1,2-dibromoethane (ethane dibromide, EDB) or 1,2-dibromo-3-chloro-propane (DBCP) and polychlorinated or brominated biphenyls which were used as fire retardants and insulators.

Traditionally, groundwater remediation requires that the water is pumped to the surface for treatment, which is costly and time consuming. In 1990, a group of hydrogeologists were examining materials used in the casings of ground water monitoring wells. They were concerned that sampling bias might be caused by adsorption onto plastic surfaces, but they found that problems were caused by the steel fittings instead[151]. They found that galvanised steel (a bimetallic Zn/Fe system) degraded halogenated compounds faster than aluminium which in turn was faster than stainless steel, and that the greater the number of halogens in the compound, the faster the rate of degradation on any surface. It had long been known that when chlorinated solvents were stored in steel drums, the drums became corroded and when used as degreasing agents, they even attacked the metal surfaces they were supposed to be cleaning[152].

The earliest reports of dechlorination were on iron surfaces, and as iron is a cheap and readily available material, much of the work has focussed on it, especially with a view to groundwater remediation. As long ago as 1972, patents were granted for the use of zero-valent metals in dechlorination schemes[153]. Compounds which have been shown to be degraded range from halomethanes, through halobenzenes and chlorophenols to polychlorinated biphenyls[154]. Nitrobenzene **97**[155] is degraded by zero-valent iron *via* nitrosobenzene **98** and phenylhydroxylamine **99**[156] to yield aniline **100**. This is also toxic, but is fairly readily degraded by ground microflora. Nitrobenzenes are important contaminants because they are constituents of explosives, pesticides, pharmaceuticals and dye intermediates.

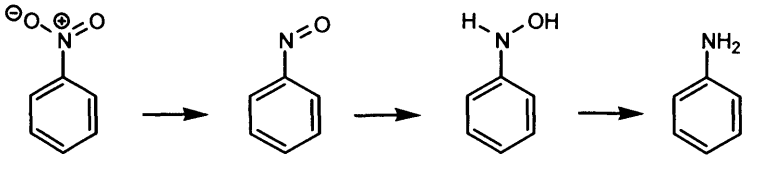

97 Nitrobenzene **98** Nitrosobenzene **99** Phenylhydroxylamine **100** Aniline

Fig. 7.1: Reduction of nitrobenzene **97**

7.1 Metals and VOCs.

7.1.1 Zero-valent metals

The use of metals in aqueous solution as reagents is not new, zinc has been used in the presence of cetyl trimethylammonium bromide (a phase transfer reagent) to reduce various organohalides[157]. Indium catalysed reactions can be used to prepare α-methylene-γ-lactones[158] and the allylation of carbonyl compounds[159,160] whilst Barbier-Grignard reactions are the mainstay of the undergraduate laboratory practical[161,162]. Work with groundwater remediation has looked at systems comprising of iron and manganese[163,152], copper and brass[164,165,166], zinc[167,168] plus more exotic and expensive platinum-ruthenium catalysts[169], palladium electrodes[170], palladium on alumina or graphite[171] and palladium doped onto an iron surfaces[154,172]. The latter is known as palladised iron and a wide variety of compounds have been shown to degrade on this surface, including chlorinated alkanes[173], trichloroethylene[174], tetrachloroethylene[154], chlorophenols[172] and polychlorinated biphenyls[154].

7.1.2 Iron compounds

Dechlorination occurs on some minerals and zeolite[175]; iron minerals such as biotite, vermiculite, pyrite and marcasite degrade carbon tetrachloride and hexachloroethane. Biotite and its weathered product, vermiculite, are iron containing 2:1 sheet silicates comprising of an aluminium hydroxide layer between silicon dioxide and have the general formula $K(MgFe)_3(AlFe)Si_3O_{10}(OH)_2$[176], whilst pyrite and marcasite are iron sulfides with the general formula of FeS_2. When hexachloroethane was degraded on biotite and vermiculite, tetrachloroethene was formed. Addition of sulfide in the form of HS^- produced a dramatic increase in the degradation rate, a half life reduction of 290 fold for biotite at 0.65 days and a 100 fold reduction for vermiculite at 0.45 days. When carbon tetrachloride was degraded on the sulfide containing minerals, pyrite and marcasite, the half lives were similar to those for hexachloroethane at 0.44 and 0.85 days respectively, although the products were not reported[177]. A second study of carbon tetrachloride with biotite and vermiculite demonstrated complete degradation to carbon dioxide *via* a carbon disulfide intermediate. Chloroform was also formed, but as a relatively minor product[178]. Chlorinated alkanes are also degraded by iron bearing clays and Portland cement slurries. Portland cement typically has a composition of approximately 75% di- and tri- calcium silicates, 12% tricalcium aluminate, 3.5% gypsum and 8% tetracalcium aluminoferrite, $4CaO.Al_2O_3Fe_2O_3$, the iron source for the degradation reactions. The degradation rate for carbon tetrachloride by cement was comparable to that using zero-valent iron and the major products were chloroform and dichloromethane which was not transformed further[179], whereas with clay,

pentachloroethane gave tetrachloroethene as the major product[180]

Fenton's reagent (Fe(II), H_2O_2) is a strong oxidising agent and also uses iron to degrade VOCs. The hydrogen peroxide reacts with the iron to form the extremely reactive hydroxyl radical which is scavenged by the VOC or hydrogen peroxide (Fig. 7.2). When trichloroethylene was treated with Fenton's reagent, the hydroxyl radicals reacted with the trichloroethylene rather than hydrogen peroxide and consequently the degradation rate of hydrogen peroxide decreased relative to the control. Trichloroethylene was completely oxidised to carbon dioxide, chloride and hydrogen ions with no intermediates detected[181] and this degradation occurred in both aqueous solution and soil samples.

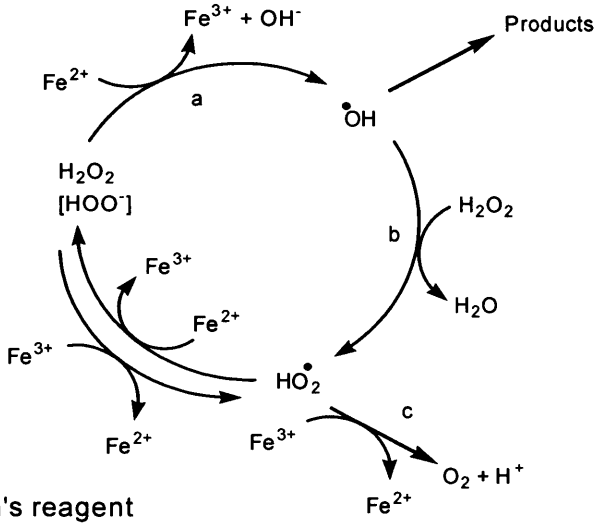

Fig 7.2: Action of Fenton's reagent

Iron bound in other forms has also been suggested to be capable of catalysing dehalogenation reactions. It was even claimed to be responsible for a potentially lethal reaction involving the generation of phosgene from chloroform preserved with amylene and stored in a brown glass bottle. In this instance, the source of the metal catalyst was the glass colorant and when iron (II) was added to another, older bottle of chloroform, the phosgene content doubled overnight[182].

7.1.3 Bacteria and microflora

Microflora and bacteria also play a vital role in organic contamination clean-up as bioremediators and have been shown to completely degrade benzene, toluene and chlorobenzene in a contaminated aquifer[183], whilst a second study at a disused gasification plant demonstrated that benzene, toluene, xylene, oil, grease and polycyclic aromatic hydrocarbons (PAH) were reduced, by up to 86%[184]. Microbial degradation can occur either aerobically or anaerobically, depending on the type of microorganism and a mixture of both processes is required for complete degradation of tetrachloroethene mixed with benzene. In a contaminated aquifer, anaerobic bacteria successfully

removed all of the tetrachloroethene to give ethane and ethylene as the final products, whereas benzene contamination was not completely removed. Aerobic bacteria were then required to complete the cleanup. This highlights the need for mixed cultures and also both aerobic and anaerobic conditions at the same site for complete groundwater remediation. This degradation was carried out under sulphate reducing conditions, and when sulphate was withheld from the groundwater, the level dropped due to microbial use and concentrations of methane increased to over twenty times normal background levels[185].

Interest in the area of bioremediation has grown recently and a number of microorganisms capable of degrading VOCs have been identified. Microorganisms can link the reductive dehalogenation of the VOCs to respiration *via* electron transport coupled phosphorylation (halorespiration). Respiration occurs via an electron transport chain in which NADH is oxidised to NAD^+ with the hydrogen being accepted by FAD to $FADH_2$ which is in turn oxidised by cytochromes which ultimately act as the electron dump[186]. Bacteria which have been identified include *Dehalococcoides ethenogenes* strain 195, the only one found so far that will completely degrade tetrachloroethene to ethene, *Dehalococcoides* sp. strain CBDB which degrades PCBs, *Desulfitobacterium* sp. strain Y51 which also degrades tetrachlorethene, but only as far as *cis*-1,2-dichloroethene, as well as other polychlorinated ethanes but a genetically modified *Pseudomonas* strain is capable of degrading *cis*-1,2-dichloroethene[187]. It has been reported that these bacteria use tetrachloroethene as an electron acceptor by converting it to *cis*-1,2-dichloroethene *via* radical process. Interestingly, the enzyme catalysing this reaction is postulated to contain a metal corrinoid[188] and hence may be another example of a metal catalysed halo-degradation (cf vitamin B_{12} **101**).

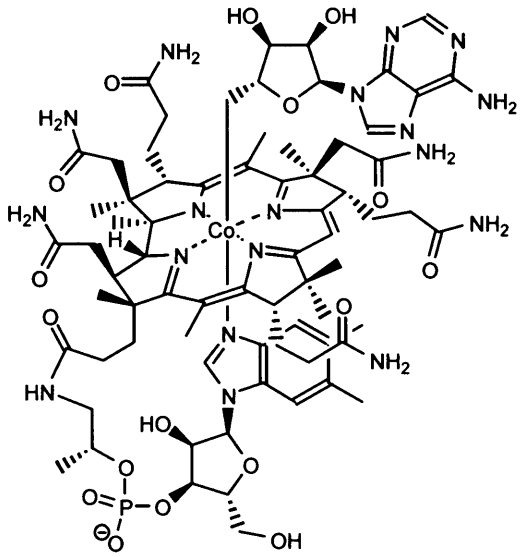

Coenzyme B_{12} **101**

Although bioremediation has been demonstrated to be effective in VOC clean up, it is by

no means a simple technique to use because a consortium of both aerobes and anaerobes are required for complete VOC degradation. Some of the products are also toxic or inhibitory to the bacteria. *Dehalococcoides ethenogenes* strain 195 did not degrade commercially supplied *cis*-dichloroethene as it was found to contain low levels (approx. 0.4%) of chloroform which acted as an inhibitor, but biologically produced *cis*-dichloroethene was consumed even at high concentrations (0.65 mM). In addition, the vinyl chloride produced from this degradation could only be further degraded if another chloroethene such as PCE or TCE was present to act as an electron acceptor; high concentrations of these chloroethenes are inhibitory for vinyl chloride degradation as the chloroethenes are preferentially consumed[189].

Ethoprophos **102**

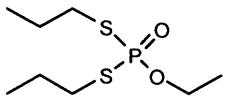

Many factors can affect the success of bioremediation. One of the most obvious is microbe density of an appropriate type; whether the density is artificially increased by innoculation or naturally enhanced by population increase which can occur with a ready supply of a suitable electron donor for halorespiration. *Pseudomonas putida* strain epI was used to degrade the nematicide, Ethoprophos **102**. Soil samples containing 1.9 x 10^6 cells/g completely degraded Ethoprophos **102** within 4 days whereas samples containing 1.9 x 10^5 cells/g took 9 days and 1.9 x 10^4 cells/g took 16 days[190]. Population density was also the dominant environmental factor when 1,1,1-trichloroethane was incubated with 0.56 mg-VSS/l or 1.7 mg-VSS/l obtained from anaerobic digester sludge at a sugar waste water facility. The 1.7 mg-VSS/l system degraded the 1,1,1-trichloroethane to 50% initial concentration in 110 days compared with 130 days for the 0.56 mg-VSS/l system when using acetate as the electron donor. The choice of electron donor was less clear cut, with glucose in the 0.56 mg-VSS/l system seeming to have no effect (*i.e.* no reduction in 1,1,1-trichloroethane concentration), whereas in the 1.7 mg-VSS/l system the addition of glucose caused a 50% reduction in initial concentration in 65 days[191]. The electron donor effect was examined in a separate study using differing concentrations of acetate over the range 150 - 1500 mg/l with trichloroethene as the halocarbon source and a methanogenic culture (exact species not reported). At relatively low acetate concentrations, the dechlorination rate increased rapidly with increasing acetate concentration, but this effect became less significant as the concentration rose, thus the dechlorination rate is not enhanced by increasing electron donor concentration once the electron donor concentration reaches a certain level[192].

Another factor affecting dechlorination rates is bioavailability of the contaminant versus other potential food sources. With the *Pseudomonas putida* strain epI used to degrade Ethoprophos

102, fresh applications of the pesticide were rapidly and completely degraded, but the degradation of aged residues was slower, suggesting that a portion of the Ethoprophos **102** was sequestered away from the bacteria. Degradation rates were also much slower in soil samples containing relatively high organic material than soils which were had low levels of organic matter (organic matter not defined) suggesting competition between the organic matter and the pesticide as the food source.

Temperature has also been found to have a significant impact on degradation rates, with *Pseudomonas putida* strain epI able to almost fully degrade Ethoprophos **102** at temperatures between 20 - 35 °C within 2 days, but the degradation rate was significantly reduced at 5 °C, which took 13 days. A similar pattern was seen with the dechlorination of tetrachloroethylene where the rate of degradation increased by a factor of ten between 5 °C and 15 °C, it then increased steadily up to 35 °C and fell at 45 °C, leading to the conclusion that the optimum temperature for bioremediation in this system was 35 °C, a temperature not normally encountered in a temperate zone.

One of the consequences of any type of remediation is the formation of the products and the effect they can have on the local environment, for example pH. Bacteria have a pH range at which they are most effective, and outside of this, degradation rates will decrease and may cease entirely. The dechlorination of tetrachloroethene was monitored over the range 4 - 9.5 pH units and the maximal dechlorination was recorded in the 6.8 - 7.6 range. The products were also affected, with predominantly vinyl chloride and *cis*-dichloroethylene produced in this range, vinyl chloride was not seen outside of this range, but the transformation to *cis*-dichloroethylene was largely unaffected. The effective pH range was the same for the Ethoprophos **102** degradation and up to pH 8.5 for the carbon tetrachloride and chloroform degradation by *Methanosarcina thermophila.* There is an increase in corrinoid activity at higher pH and *M thermophila* has a high concentration of these corrinoids, hence the extended pH range of its activity. This *M thermophila* study also examined the effect of zero valent iron; under anaerobic conditions Fe^0 is oxidised to Fe^{2+} with the production of hydrogen gas which acts as the electron donor and also raises the pH[193]. This could have important implications for a combined metal/microbial remediation of contaminated groundwaters.

7.2 Compound rates and fates

7.2.1 Zero valent iron and reaction mechanisms

Early studies using zero valent iron showed that degradation of halomethanes proceeded by sequential halogen loss with decreasing rates until some non-reactive species was reached. For carbon tetrachloride, the rate of degradation to chloroform was so fast that the half life could not be determined. The chloroform in turn was degraded and the half life was measured in hours and the dichloromethane produced was not degraded at all[194]. As a remediation process, this is only moderately useful as dichloromethane itself is harmful, but when the bimetallic system of palladium doped onto the iron surface is used, the degradation proceeds much further with dichloromethane finally being degraded to relatively harmless methane (Fig 7.3).

Different mechanisms have been reported for different starting materials, carbon tetrachloride is degraded by a single chlorine loss stepwise reaction, whereas TCE is reported to degrade completely, losing all three chlorines without a free intermediate. The explanation given is that π bonding between the chloroethene and Fe^0 is so strong that the chloroethene is held on the surface until all the chlorines have been removed, then desorbs back into solution.

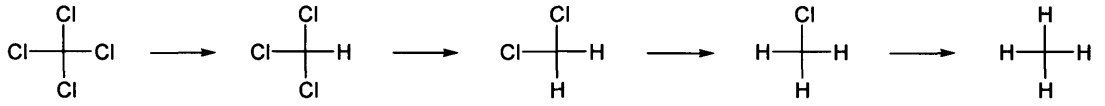

Fig. 7.3: Sequential reduction of carbon tetrachloride to methane

C_1 - C_4 hydrocarbons also reported in this study were accounted for by the formation of carbon chains on the iron surface including the catalytic reduction of CO_2. The main hydrocarbons produced were ethene and ethane, accounting for about 80 % of the hydrocarbons detected in a ratio of 2:1, with the remainder comprising of methane, propene, propane, 1-butene and butane[195]. The formation of hydrocarbons on a metal surface is a well known catalytic process, the Fischer-Tropsch process, in which carbon monoxide and hydrogen are passed over a metal such as iron, cobalt or nickel catalyst at high temperatures and pressure to produce a range of short chain hydrocarbons; it was mainly used to produce synthetic petrol from 1925 - 1945[196]. Experiments comparing the products of simulated ground water and organic free deionised water on commercially available (iron) metal cuttings or electrolytic grade (ultrapure) iron found that methane, ethene and ethane with traces of pentene and butene isomers were detected in all situations. The iron cuttings were found to contain approximately 2.4 % carbon, but the concentration of hydrocarbons produced was similar to electrolytic iron, suggesting that this surface carbon was not the carbon source for the hydrocarbon formation. Pretreating the iron with hydrogen increased the mass of hydrocarbons produced, and both the hydrocarbon concentration and chain length increased with time[197]. These findings were disputed by a study examining the products formed from ^{13}C labelled CO_2. The same range of hydrocarbons were produced here, but the

carbonate concentration in the water was controlled and the carbon concentration was less than the total carbon from the hydrocarbons produced. In addition, when $^{13}CO_2$ was used, no hydrocarbons containing ^{13}C were detected at all, ruling out the aqueous CO_2 as the carbon source. Carbon impurities exist in iron in two forms, as graphite which is discrete carbon crystals or carbide which is single carbon atoms bound to the iron surface. Examination of iron high in carbide showed almost 100 % conversion to hydrocarbons whereas iron high in graphite did not, indicating that carbide carbon is the source for hydrocarbon formation, and this process occurs with and without the presence of chlorinated hydrocarbons[198].

Zero valent iron is a good reducing agent especially when combined with a good proton donor like water, and the general reaction involving an alkyl halide is known as the "dissolving metal" reaction:

$$Fe^0 + RX + H^+ \rightarrow Fe^{2+} + RH + X^-$$

This study reported that the mechanism for carbon tetrachloride reduction proceeded *via* a radical formation from the dissociation of the alkyl halide on the metal surface which then abstracts a proton from the bulk solvent and a second electron transfer from the metal[194].

$$RX + e^- \rightarrow R^\bullet + X$$

$$R^\bullet + H^+ + e^- \rightarrow RH$$

If the second electron donation occurs before reaction with a proton, the carbanion so formed, may undergo α,α-elimination to give a carbene, which reacts with water and ultimately yields carbon monoxide and hydrochloric acid. Generally under the conditions of these metal reductions, reduction occurs in preference to α,α-elimination (Fig 7.4).

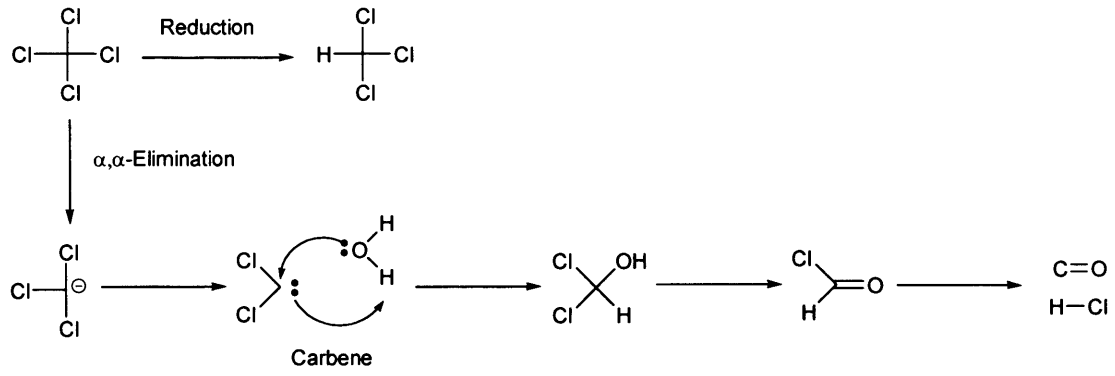

Fig 7.4: Reduction is the preferred route for chloromethanes

For chloroethanes eg hexachloroethane, there are three possible degradation routes, reduction, α,α-elimination and β-elimination. Generally reduction and β-elimination are competing reactions, with the β-elimination predominating (Fig. 7.5). For chloroethenes eg tetrachloroethene, β-elimination and reduction are competitive reactions, and the reduction is now the preferred

pathway. All of these pathways can be rationalised by a radical[199,200] (Fig 7.6) or an equivalent anionic mechanism.

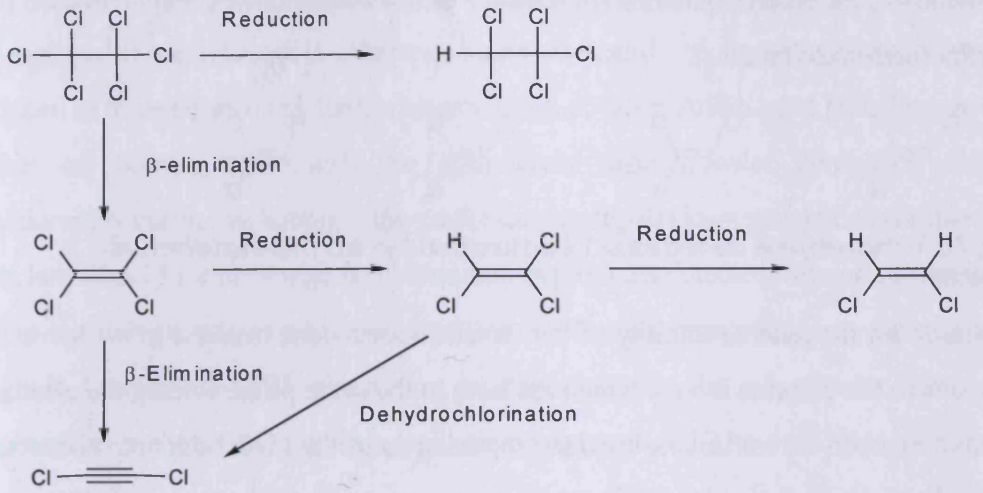

Fig. 7.5: β-Elimination is the preferred route for polychloroethane degradation

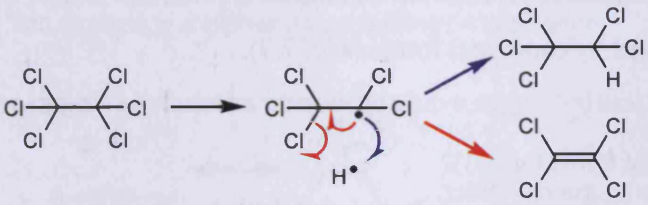

Fig. 7.6: Hydrogenolysis and dihalo-elimination *via* a radical mechanism

7.2.2 Palladised iron

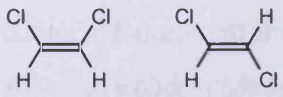

Fig. 7.7: *cis*- and *trans*- Dichloroethylene

The addition of palladium to the system not only affects the degree of degradation, but also the rate of the reaction. When trichloroethylene was degraded on zero-valent iron, the rate constant was reported to be 0.093 hr^{-1}, but when the Pd/Fe system was used, the rate constant increased to 1.17 hr^{-1}, a twelve fold increase[172], moreover in the iron only system, dichloroethylene was seen, but this could not be detected in the Pd/Fe system. The dichloroethylene detected in the Fe only system was found to be the *cis*- isomer, no trace of the *trans*- isomer was detected (Fig. 7.7). It might be expected that the *trans* isomer would be the thermodynamically more stable isomer, as it is with most alkyl substituted alkenes, but in fact *cis*-dichloroethylene is energetically more favourable. A computation study found that the trichloroethylene radical is extremely unstable (Fig. 7.8), and the *cis*-dichloroethen-1-yl radical is 6 kJ mol^{-1} more stable than the *trans*-dichloroethen-1-

yl radical and 21 kJ mol^{-1} more stable than the 1,1-dichloroethen-2-yl radical, with an energy barrier of 30 - 40 kJ mol^{-1} for the interconversion between the *cis*- and *trans*-forms[201]. These energy differences equate to a thermodynamic ratio of 92:8 for the *cis*:*trans* isomers and 99.98:0.02 for the *cis*:1,1-dichloroethen-2-yl radical.

Fig 7.8: Trichloroethylene, *cis*- and *trans*- 1,2-dichloroethen-1-yl- and 1,1-dichloroethen-2-yl radicals

The reason for the relative stability of the *cis*-dichloroethylene over the *trans*-isomer is thought to be due to the chlorine atoms, which are both in the same plane, forcing the electron density towards the carbon-carbon double bond and repelling each other. This both strengthens and shortens the C-X and the C=C bonds, relative to the *trans*- isomer[202]. Collectively, this is known as the *cis* effect. Theoretical calculations at the highest level of theory indicate that the non-bonded interactions between *cis*-halosubstituents result in stabilisation of the *cis*- isomer over the *trans*-. This can be crudely represented by canonical forms (Fig. 7.9).

Fig. 7.9: Canonical forms for bond stabilisation by *the cis*-effect

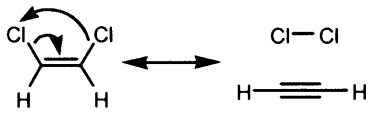

7.2.3 Surface effects

One of the most important factors affecting reaction rates is the surface area available for the degradation to use. Initial studies used varying amounts of iron to solution volume to look for trends and found that the degradation rate of trichloroethylene increased with increasing iron mass, but that increasing the amount of iron also increased the pH of the reaction mixture which was also thought to affect the reaction rate. When 50 g of iron was used, the initial degradation rate was extremely rapid with half the trichloroethylene degraded in 2 minutes, but this rate was not sustained and the degradation rate declined rapidly and even after 7 hours some trichloroethylene remained. The data showed two distinct rates, a rapid rate for the first few hours and then a much slower rate over the remaining experiment time; the pseudo-first order model only fitted the 1 g iron system where the pH did not rise significantly above 7[153]. A review of halogenated organic compounds degraded on iron surfaces looked at various brands and particle sizes (as well as other factors) of the iron used in studies reported in the literature. When the data was normalised for iron surface area (degradation rate / apparent iron surface area), the degradation rates for the various organic compounds were found to be comparable over the majority of studies, within one order of magnitude. The factor which most affected the degradation rates was acid washing which liberates

an unquantified number of reactive surface sites[203]. Surface studies involving direct synthesis particulate iron found that the synthesised iron particles had a surface area of 33.5 m^2/g as compared to 0.9 m^2/g for commercially available iron powder and were able to completely degrade 20 mg/l trichloroethylene in less than two hours whereas the trichoroethylene was not significantly reduced in three hours using the commercial iron powder. Addition of palladium had a dramatic effect on both systems with the commercial iron powder completely degrading the trichloroethylene in two hours but the synthesised iron/palladium system had completely degraded it in less than 15 minutes with no chlorinated byproducts detected. Similar results were reported when the iron powder, synthesised iron and synthesised iron/palladium systems were used to degrade Aroclor 1254 **103** with almost no degradation in the iron powder system to complete degradation in the synthesised iron /palladium system over 17 hours[204].

X = H or Cl

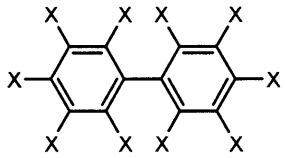

Aroclor 1254 **103**, a mixture of biphenyls containing 54% chlorine

Surface studies using x-ray photoelectron spectra have suggested that Pd(IV) in solution is reduced to Pd(II);

$$PdCl_6^{2-} + Fe^0 \rightarrow Fe^{2+} + Pd^{2+} + 6Cl^-$$

which then forms a Pd-O-Fe bond with the surface hydroxy groups on the iron and as this bond is extremely unstable, the palladium is further reduced to Pd^0 by oxidation of the Fe^0 accessible through the hydroxylated iron oxide film.

$$2FeOH + Pd^{2+} \rightarrow 2FeOPd + 2H^+$$

$$2H^+ + 2FeOPd + Fe^0 \rightarrow Fe^{2+} + 2FeOH + Pd^0$$

The binding energies for the 3d orbitals for palladium were examined and confirmed the presence of the Pd-O-Fe species in the form of a Pd^{2+} species which converted to Pd^0 overnight. It was found that the 3d spectra for palladium was unaffected by either iron or oxygen on the surface and the conclusion drawn was that palladium atoms were randomly dispersed amongst the iron and oxygen atoms in the hydroxylated iron oxide surface and no electronic interaction between any of these atoms was detected.

7.2.4 Effect of solvent on degradation rates

One of the main problems with remediating VOC contaminated ground water is the low solubility of VOC. Chloroform will dissolve in water at about 0.8 g/100 ml, trichloroethylene has a solubility of 0.1 g/100 ml, tetrachloroethylene has a solubility of 0.015 g/100 ml and carbon

tetrachloride has a solubility of 0.1 g/100ml, all at 20° C. Surfactants can help increase the solubility and hence the surface concentration of these types of compounds. It was reported that surface concentration was dependent on the aqueous surfactant concentration and once the critical micelle concentration (CMC), the concentration at which the surfactant molecules conglomerate to form micelles, was reached, competition between the micelles and surface adsorption was evident. It was found that using sodium dodecyl sulphate (SDS) an anionic surfactant, both tetrachloroethylene and trichloroethylene adsorption on an iron surface increased until the CMC was reached and then declined with increasing surfactant concentration. No significant difference in the degradation rates for either compound in deionised water or surfactant system were found below 23.07 g/l SDS, but above this level the rate declined, probably because the VOCs were held by the micelles instead of on the iron surface. Although the surfactant increased the VOC solubility, the degradation rate was unaffected by the aqueous concentration increase. When Triton X-100, a non-ionic surfactant was used, the surface coverage of tetrachloroethylene decreased with increasing Triton X-100 but the degradation rate increased and reached a maximum when the surfactant concentration reached 1.5 g/l, the point at which the surfactant layer on the iron surface stopped forming. Triton X-100 had no effect on the degradation rate of trichloroethylene. Alcohols can also enhance VOC dissolution and the degradation rates were also examined when various concentrations of alcohols were present. When methanol, ethanol and iso-propyl alcohol were present at 57 % *v/v*, the degradation rates for both tetrachlorethylene and trichloroethylene were reduced by a factor of 10, and when the degradation was performed completely in ethanol, the degradation effectively stopped, but at 28% *v/v* ethanol, the trichloroethylene degradation was unaffected[205].

Chapter 8, Halo-compound Degradation on Iron and Palladium/Iron Surfaces, Experimental Work

8.0 Introduction

Halogenated organic compounds are degraded on metal surfaces to less halogenated compounds. The rates of the degradation have also been shown to be faster in a bimetallic system than a mono-metallic system, and also to increase with increasing surface areas. In the study reported here, the system was bimetallic using palladium doped onto iron and the rates of degradation was measured using GC-MS.

The rate of a reaction is given by the slope of the line when some function of concentration is plotted against time. The function of concentration will depend on the order of the reaction. The rate of the reaction is usually a function of concentration of the reactant(s), in our system the excess of iron renders it pseudo first order with respect to the VOC, so for chloroform dechlorination the following rate equation applies:

Reaction rate = $d[CHCl_3]/dt$

ie reaction rate is equal to the rate of change of chloroform concentration with time. For this first order reaction, at time t=0, the concentration of chloroform will be a. At some time t later, the concentration of chloroform will have fallen to (a-x) where x is the change in concentration of the product as the reaction proceeds.

$\therefore$ at time t, $[CHCl_3] = (a-x)$ and $[CH_2Cl_2] = x$

since reaction rate = $d[CHCl_3]/dt$ we can say that

Reaction rate = $-d(a-x)/dt = dx/dt = k_1(a-x)$

rate constant = k_1

$\therefore$ rearranging this expression;

$-d(a-x) = dx = dt\ k_1\ (a-x)$

to obtain x we can simplify;

$dx = dt\ k_1\ (a-x)$

$= dx/(a-x) = k_1\ dt$

integrate the equation;

$\ln (a-x) = k_1\ t + \text{constant}$

To find the constant let time t = 0, so that x = a

$\therefore$ -ln (a-0) = constant

$\therefore$ -ln a - ln (a-x) $\equiv$ ln(a/a-x)= k_1 t

It may be seen that ln (a-x) is a linear function of time and the multiplier is equivalent to the rate constant. The concentration is directly proportional to peak area, hence the peak area may be used in place of the concentration term. In a graph of ln(peak area) vs time, the gradient of the regression line of the data is equal to the rate constant. This procedure was executed in Excel spreadsheets and graphs. Representative graphs are shown in the discussion.

The half life of the reaction is the time at which the concentration of $CHCl_3$ is a/2

$\ln(2a/a) = k_1 t_{½}$

ie $\ln 2 = k_1 t_{½}$

$t_{½} = \ln 2/k_1$

For a first order reaction, the half life depends solely on the rate constant and is therefore independent of the initial concentration.

Percentage conversion (Conv.) was calculated from the first (F) and last (L) peak count measurements in a run as follows: Conv. = 100 x (F - L)/F. It is intended as an easily calculated measure of the efficiency of a degradation and in most cases it will reflect a genuine measure of the degradation efficiency, if the first analysis is at zero time. In some cases conversion has been calculated for formation of products using: Conv. = 100 x (L - F)/L. This indicates the increase in products from the first to the last measurement. It has no significance beyond this, because it depends on how early the first measurement is made in the run, and is not calculable when F = 0 at time = 0.

Multiples Percentage conversion becomes less useful at high conversions and it is more informative to report multiples ie 100 x (F/L) for degradations or 100 x (L/F) for formation. To unambiguously distinguish between these calculations; degradation is reported as 1/Multiple and formation as Multiple.

8.1 Instrumentation

8.1.1 Gas Chromatography-Mass Spectrometry

The gas chromatograph-mass spectrometer system used for this study was an HP6890 gas chromatograph (GC) interfaced to a 5972 mass selective detector (MSD). Helium was used as the carrier gas at constant column flow rate of 1 ml/min, controlled by electronic pneumatic control (EPC) within the GC operating software. Liquid injections were performed in the splitless mode and headspace injections in the split mode with a split ratio of 50:1. The capillary column was connected to the inlet without a guard column, and interfaced to the mass spectrometer through a heated interface, set at 180° C, the instrument maximum.

The purge and trap system was a Hewlett Packard 16 place autosampler unit model G1904A connected to a Hewlett Packard concentrator unit model G1900A fitted with a Vocarb 3000 trap. The liquid samples were loaded onto the autosampler unit using a gas tight syringe. The purge program was based on the EPA conditions used for volatile analysis , method 524.2. The purge conditions were the same in all experiments and were as follows: transfer line 280°C; solvent delay 0.9 min, line temperature 150°C, valve temperature 150° C, MCS temperature 120° C, purge 11 min at room temperature, dry purge time 2 min, desorb pre-heat 245° C for 2 min, desorb temperature 250° C for 2 min, bake temperature 255° C for 10 min. MCS bake temperature 300° C, TPC pressure 8 psi.

The MS was used in the electron impact (EI+) mode, between 50 to 65 mTorr source pressure. In this mode, electrons are emitted from a filament at 70 eV and collide with analyte molecules in the ionisation chamber, heated by the filament. An electron trap (cathode) set at between 1750 to 2200 μA, situated opposite the filament, controlled the filament energy to 70 eV. The resultant ions are ejected through the exit plate by a repeller plate set between 0 to 42.8 V into the quadrupole. The ions were separated according to their mass/charge ratio (*m/z*) by the quadrupole. The 5972 MSD has a hyperbolic fused silica quadrupole mass filter, coated on the inside with a conductive material and connected opposing segments, and also pre and post filters. The full possible scan range is from 2 - 800 atomic mass units (amu) and mass selection was achieved by diagonally matched poles which vary current or radio frequency. The mass range scanned was 33 - 700 amu in 0.9 seconds with an interscan time of 0.1 seconds. A solvent delay of 3 mins was used to preserve the filament. The ions were detected by a impact onto a phosphor screen, enhanced by a photomultiplier and a conversion dynode. The vacuum within the source and analyser was maintained by a diffusion pump and the backing pump was an Edwards RV3 2 stage rotary pump. The MS was tuned with PFTBA, using peaks at *m/z* 69, 219 and 502 with relative intensities of 100%, 61%, 4% using the automated "standard spectra" tune facility within the

instrument operating software.

The system control and data acquisition was performed by a computer running Chemstation software. The filament current of 70 eV is taken as standard for the generation of mass spectral libraries. The Chemstation software contains the NIST library of 75,000 entries which is matched by the computer to the analyte spectra. In the initial library search, analyte and library spectra are matched using the six most abundant peaks. Candidate library spectra are then ranked by a reverse fit process, the degree of "goodness of fit" or matching is scored out of 100, with a reasonable match scoring >80.

The GC-MS and purge conditions were identical in all cases (Table 8.1a). For purge and trap analysis the purge time was 11 minutes (EPA method 524.2) with the transfer line at 280 °C. The GC-MS conditions were 35(4) x 5 to 75 (0), 50:1 split ratio, as described in Section 8.1.1. The liquid injection volume was 1 µl and this volume was used for all work unless otherwise stated. The GC-MS conditions for direct liquid injection were 40(5) x 10 to 200(0) inj 220 unless otherwise stated. The column for all liquid work and some purge and trap work was an HP5MS phase, 30 m, 0.25 µm film column and the rest of the purge and trap work was performed on an HP624 phase, 25 m, 1.12 µm film column, and is noted as appropriate.

Total ion chromatograms (**TIC's**) are created using GC-MS data by summing the ions in a mass scan and plotting on a time axis. Single ion chromatograms (**SIC's**) are created by plotting the data for a single *m/z* value in the same way from full scan data. This is a very selective method for detecting trace constituents. In single ion monitoring (SIM), only a single *m/z* ion is measured by the mass spectrometer, which results in an increase in sensitivity of typically 200-1,000. This technique was not used in the current work.

8.1.2 General methods & Abbreviations

Shaken and analysed (P&T, GC-MS) indicates that the vials were immediately capped with a lid fitted with a rubber septum/Teflon liner and shaken in a plastic box (120 rpm) on a flat bed shaker until required for analysis by purge and trap GC-MS, reactant volumes are given in Table 8.1b.

All water used for making up solutions was deionised prepared using a Millipore, Milli-Q deioniser fitted with a ICPMS pack.

A **surrogate standard** is a substance (usually similar in nature, *i.e.* a deuterated version of the compound of interest) which is added at a concentration to give a peak area similar to that of the compound of interest at the start of the experiment. An **internal standard** is a substance

similar in nature to the compound of interest (again it could be a deuterated analogue) added at a concentration to yield a peak area similar to that of the compound of interest but is added **immediately** prior to the sample analysis.

Controls contain no activated or palladised iron, whereas **blanks** contain no reactant.

Table 8.1a: GC conditions, analytes, and retention times

GC program, injector, column	Analytes	Ret. time, min	Experiment no
35(4) x 5 to 75(0), inj 200, P&T HP624	$CHCl_3$ (& $CDCl_3$), CH_2Cl_2 (& $CDHCl_2$)	4.56, 2.72	1, 2, 3, 4, 5, 6, 7, 8, 9, 10, 12
34(4) x 7.5 to 200(0) inj 220, P&T HP5MS	$CDCl_3$, $CHCl_3$, $CDHCl_2$, CH_2Cl_2	2.91, 2.27	11, 14, 15, 16
35(3) x 20 to 150(0) inj220, P&T, HP5MS	$CDCl_3$ & $CHCl_3$, $CDHCl_2$ & CH_2Cl_2, 1,4-dioxane, cyclohexane, 6-bromo-hexene, hexene, methylcyclopentane, cyclohexane, bromohexane	2.87, 2.26, 4.16, 3.46, 7.00, 2.56, 2.95, 3.39, 7.08	17, 18, 26, 27, 28, 29, 30, 31,19, 20, 21, 22, 23, 24, 25, 32, 33, 35, 40, 41, 44, 45, 50, 51, 52
35(3) x 20 to 250(0) inj260, P&T, HP5MS	Bromoethyl ethyl ether, diethyl ether, ethanol	5.49, 2.15, 2.02	34
35(3) x 20 to 250(0) inj260, P&T, HP624	Bromoethyl ethyl ether, diethyl ether, ethanol	7.83, 2.92, 2.80	36, 37, 38, 39
35(3) x 20 to 175(0) inj220 P&T, HP5MS	Bromoform, carbon tetrachloride, PCE	6.54, 3.45, 5.56	42, 43, 47, 48
35(3) x 20 to 150(0) inj220, P&T, HP624	*cis*- and *trans*-Dichloroethylene	6.02, 4.31	46
35(3) x 20 to 150 (2) inj 220, P&T, HP5MS	Bromomethylcyclopropane, bromocyclobutane	4.87, 4.75	49
35(5) x 20 to 150 (2) inj 220, HP5MS	Bromomethylcyclopropane, bromocyclobutane	2.24, 2.12	49
40(5) x 10 to 110(0) inj 220, HP5MS	Bromohexane, (2-bromoethyl) benzene	8.94, 13.59,	53, 54
40(5) x 10 to 150(0) inj 220, HP5MS	(2-Bromoethyl) benzene, ethyl benzene	14.12, 7.55	55, 56, 57, 58,59
35(5) x 10 to 140(0) x 25 to 200(0), inj 220, HP5MS	Benzyl bromide, toluene, bibenzyl, benzyl alcohol, benzyl methyl ether	12.00, 4.53, 18.05, 10.89, 10.00	60, 62, 63, 64, 67, 68, 72, 73, 74, 86
40(5) x 10 to 200(0) inj 220, HP5MS	Bromophenetole, ethoxybenzene, phenol, benzyl 2-bromoethyl ether, benzaldehyde, benzyl alcohol, ethoxymethyl-benzene	15.23, 10.09, 9.92, 16.41, 9.42, 10.89, 11.37	61, 65, 66, 69
35(5) x 10 to 250(2) inj 260, HP5MS	Benzyl 2-bromoethyl ether, bromophenetole, ethoxybenzene, benzyl ethyl ether, benzyl alcohol, phenol	16.40, 15.25, 10.09, 11.37, 10.89, 9.91	70
35(5) x 10 to 250(2) inj 260, HP5MS	1-Bromo-2-*n*-hexyloxy-cyclohexane, 1-bromo-2-*n*-octyloxycyclopentane, *n*-hexyloxycyclohexane, *n*-octyloxycyclopentane hexanol, octanol,	18.80, 19.72, 15.31,16.60, 7.40, 11.52	71, 75, 79, 80, 81, 82, 84, 85

8.1.3 Preparation of iron reagents

The following procedures are representative, the quantities were altered *pro rata* for other experiments and the weights indicated in both cases are that of the iron, which was subjected to activation.

Activated iron Iron filings (16 g, 80-100 mesh, Fisher) were washed with hydrochloric acid (50 % *v/v*, 4 x 25 ml aliquots) and water (4 x 25 ml aliquots) to remove the acid. The water was decanted and the activated iron used as described subsequently.

Palladised iron (Pd/Fe) Activated iron (12.6 g) was treated with potassium hexachloropalladate (0.05 % *w/w*, 0.06 g) dissolved in the minimum volume of water. The water was decanted and the palladised iron used as described subsequently.

Table 8.1b: Volumes of parameters in the final degradation/control vials

Parameter	Initial volume, µl and diluent volume, ml (A)	Spiking volume (A), µl and solvent volume, ml (B)	Final vial volume (B), nl/ml	Experiment no.
$CHCl_3$	1.0, 1000	7500, 7.5	0.5	1
$CHCl_3$	1.0, 1000	1500, 13.5	0.1	2, 3
$CHCl_3$	1.0, 1000	3750, 11.25	0.25	4,
$CHCl_3$	0.1, 2	25, 10	0.125	5,
$CHCl_3$, $CDCl_3$	0.1, 2 each	5, 2	0.125	6, 7, 8, 14, 16, 17, 28,
$CHCl_3$, $CDCl_3$	0.1, 2 each	5, 1.5	0.17	9, 10, 11
$CHCl_3$	0.2, 2	5, 10, 15, 2	0.25, 0.5, 0.75	15
CH_2Cl_2	0.75, 15	5, 2	0.125	22
CH_2Cl_2	0.1, 2	5,2	0.125	23, 24
$CHCl_3$, CH_2Cl_2	0.1, 2 each	5,2	0.125	25
$CDCl_3$	0.2, 2	5, 2	0.25	31
6-Bromohexene	0.2, 2	10, 2	0.5	32
6-Bromohexene, $CHCl_3$	0.4, 0.2, 2	5, 2	0.5, 0.25 resp.	33
Bromoethylethyl ether	0.3, 2	10, 2	0.75	54
Bromoethylethyl ether, $CHCl_3$	0.4, 0.2, 2	5, 2	0.5, 0.25	36
Bromoethylethyl ether	1.5, 15	100, 15	0.67	39
$CHBr_3$	0.2, 2	5, 2	0.25	42, 43
Bromohexane	0.2, 2	5, 2	0.25	44, 50
Bromohexane	0.2, 2	10, 2	0.5	45, 51, 52
cis and *trans* Dichloroethylene	0.2, 0.2, 2	5, 2	0.25 each	46
CCl_4, $CCCl_2$:CCl_2	0.2, 0.2, 2	10, 2	0.5 each	47, 48
Bromomethyl cyclopropane	0.5, 2	10, 2	1.25	49
Bromohexane	0.2, 2	50, 2	2.5	53
(2-Bromoethyl) benzene	0.4, 2	50, 1	10	54

(2-Bromoethyl)benzene	3, 15	100, 1	20	55, 56
(2-Bromoethyl)benzene	0.2, 2	100, 1	10	57, 58
Bromomethylbenzene	3,15	100, 1	20	60
Bromomethylbenzene	n/a	10000, 1.5	6667	62
Bromomethylbenzene	75, 15	1000, 0	5000	63
Bromomethylbenzene	75, 15	3750, 15	1250	64
Benzyl 2-bromoethyl ether	0.2, 2	10, 1	1	69
(2-Bromoethyl)benzene	0.2, 2	10, 1	1	67
(2-Bromoethyl)benzene	0.2, 0.5	50, 0.45	40	68
1-Bromo-2-*n*-hexyloxy-cyclohexane, 1-bromo-2-*n*-octyloxycyclopentane	3, 3, 15	100, 0.9	20	71, 79

8.1.4 Analysis of chlorine isotope data

The ratios for the Cl_2CH ion were calculated by summing the odd and the even *m/z* ions (cf Section 9.2.3). This was implemented in an Excel spreadsheet and the results and errors are expressed as % ratios for the whole isotopomer cluster.

The ratios for the dichloromethane molecular isotopomers, were calculated by variation of the ratios of CH_2Cl_2, $CHDCl_2$ and CD_2Cl_2 in the range 0 - 1 in increments of 0.005 (ie 0.5 %). The time for the permutation, scales as the cube of the increment, hence the 200 values used here requires 8 million loop cycles and required >83 sec on a 1.2 GHz PC. The key Visual Basic code is shown below, where CalcAbun() is the calculated abundance, ClAbun() is the abundance values for the $CHCl_2$ cluster ions and n1, n2 and n3 are the proportions of CH_2Cl_2, $CHDCl_2$ and CD_2Cl_2 respectively. The function FNMaxDP gives the maximum value of a double precision array and the subroutine NormaliseDP, normalises a double precision array to a proscribed value. All variables are double precision (16 bits).

```
Calc_Diff_Save = 100 (Arbitary value)
Start_Loop = 0#: End_loop = 1#: Step_loop = .005#
For n1 = Start_Loop To End_loop Step Step_loop
For n2 = Start_Loop To End_loop Step Step_loop
For n3 = Start_Loop To End_loop Step Step_loop
    CalcAbun(1) =  ClAbun(1) * n1
    CalcAbun(2) = (ClAbun(2) * n1) + (ClAbun(1) * n2)
    CalcAbun(3) = (ClAbun(3) * n1) + (ClAbun(2) * n2) + (ClAbun(1) * n3)
    CalcAbun(4) = (ClAbun(4) * n1) + (ClAbun(3) * n2) + (ClAbun(2) * n3)
    CalcAbun(5) = (ClAbun(5) * n1) + (ClAbun(4) * n2) + (ClAbun(3) * n3)
    CalcAbun(6) = (ClAbun(6) * n1) + (ClAbun(5) * n2) + (ClAbun(4) * n3)
    CalcAbun(7) = (ClAbun(6) * n2) + (ClAbun(5) * n3)
    CalcAbun(8) = (ClAbun(6) * n3)
```

```
    MaxCalcAbun = FNMaxDP(CalcAbun(), 1, 8) / 100
    Call NormaliseDP(CalcAbun(), 1, 8, MaxCalcAbun) (relative to 100)
    Calc_diff = 0
    For n4 = 1 To 8 (determine absolute sum of errors)
        Calc_diff = Calc_diff + Abs(FoundAbun(n4) - CalcAbun(n4))
    Next n4
    If Calc_diff < Calc_Diff_Save Then
       Calc_Diff_Save = Calc_diff (save best result so far)
          Record result (pseudocode)
    End If
Next n3, n2, n1
```

This routine can also be applied to the $CDCl_2/CHCl_2$ clusters of $CHCl_3$ (n3 = 0).

8.2 Experimental details

Degradation of $CHCl_3$ on activated iron and Pd/Fe (Expt. 1 & 2)

Activated iron (16 g, 1.0 ± 0.1 g portions) was added to a series of clean, oven dried vials. Water (7.5 ml) was added to each vial containing iron and also to a series of identical vials without iron to act as controls. An aliquot (7.5 ml) of $CHCl_3$ stock solution (1 µl in 1 l water, 742.0 μgl^{-1}, prepared immediately prior to use) was added to each vial which was shaken and analysed (P&T, GC-MS). At each sampling point, one vial containing iron and one control was analysed (Table 8.2a). Control vials were prepared with appropriate substrates in all subsequent experiments.

A series of reaction and control vials were prepared with Pd/Fe (12.6 g) as above but the water volume was increased (13.5 ml) and the $CHCl_3$ volume decreased (1.5 ml, 148.4 μgl^{-1}) to avoid overloading the detector (Table 8.2b).

Peak areas for the degradation of $CHCl_3$

Table 8.2a, activated iron			Table 8.2b, Pd/Fe		
Time, hr	Control	Fe	Time, hr	Control	Pd/Fe
0	488604847	nm	0	401172475	nm
0.5	447085106	465807228	0.5	407999980	nr
1.0	493927534	462621734	1.0	405650099	351511189
1.83	477489325	423881968	2.0	381997943	314652920
3.17	nr	344586191	3.0	nr	301905276
4.0	494979786	380237713	5.5	390554139	277368934
5.	482167298	409138359	7.5	384265640	197261681
6.0	472603625	409356933	11.75	nr	95567514
7.0	478607742	369263783	21.75	342265251	14384165
8.0	467003592	370586656	24.0	376598063	14561984
k_1, hr^{-1};$t_{½}$, hr	na	0.0398;17.42	k_1, hr^{-1}; $t_{½}$, hr	na	0.1045; 6.63

nr = no result, nm = not measured, na = not applicable

Comparison of the rate of degradation of $CHCl_3$ on activated iron and Pd/Fe in aqueous sodium carbonate (Expt. 3)

Activated iron (15 g) and Pd/Fe (15 g) were dispensed (1.0 ± 0.1 g) into a series of reaction vials. Aliquots (13.5 ml) of sodium carbonate solution (21.2 g in 1 l, 207 mM CO_3^{2-}) and aliquots (1.5 ml, 148.4 µg/l) of $CHCl_3$ in sodium carbonate (1 µl in 1 l) were added to each vial, which were shaken and analysed (P&T, GC-MS)(Table 8.3). The pH of the samples and controls was measured.

Table 8.3: Peak areas for $CHCl_3$ incubated with water control, activated iron and Pd/Fe in sodium carbonate solution

Time, hr	Control	Fe	Pd/Fe
0	131189287	nm	nm
1	87681905*	121707721	113268658
2	107466738	121736582	106930884
3	nr	nr	89004448
4	nr	15588841	59456233
6	122253133	1017777014	97544105
7	nr	113190657	80491683
10	nr	nr	nr
pH	11.47	11.46	11.47
k_1, hr^{-1}; $t_{½}$, hr	na	0.0440; 15.77	0.1292; 5.36

nr = no result, nm = not measured, na = not applicable, * results excluded from calculations

Degradation of $CDCl_3$ on Pd/Fe (Expt. 4)

Activated iron (10 g) and Pd/Fe (10 g) were dispensed (2.0 ±0.1 g) into two series of vials. An aliquot of water (11.25 ml) and $CDCl_3$ (3.75 ml, 371.0 µg l^{-1}) from a stock solution (1 µl in 1 l water) was added to each vial, plus a series of control vials, which were shaken and analysed (P&T, GC-MS)(Table 8.4).

Table 8.4: Peak areas for $CDCl_3$ incubated with activated or palladised iron.

Time, hours	Control	Fe	Pd/Fe
0	nr	nm	nm
1	286146599	266600412	249437058
2	255386503	267025302	nr
3	277970744	254261506	198328482
4	245081185	244889639	158662026
5	51494014*	226255391	148426846
7	nr	273523491	10854722
k_1, hr^{-1}; $t_{½}$, hr	na	0.04614; 15.02	0.1346; 5.15

nr = no result, nm = not measured, na = not applicable, * results excluded from calculations

Degradation of $CHCl_3$ in D_2O on Pd/Fe in the presence of chromatography glass beads (Expt. 5)

Pd/Fe (1.0 ± 0.1 g) was placed in each of two clean preweighed vials containing glass

chromatography grade beads (80 mesh, 5 ml). The vials were filled to the brim with D_2O. A stock solution of $CHCl_3$ (0.1 µl) in D_2O (2.0 ml) was prepared and an aliquot (25 µl) added to each vial which was shaken and analysed (P&T, GC-MS)(Table 8.5). This was a qualitative experiment, at this stage peak areas and relative compositions were not of paramount importance and these were examined in greater detail in subsequent experiments.

Table 8.5: Degradation products for $CHCl_3$ with D_2O

Vial type	Time, hr	$CHCl_3$?	$CDCl_3$?	CD_2Cl_2?	CH_2Cl_2?	$CHDCl_2$?
Control	4	✓	✓	x	✓	x
Control	7	✓	✓	x	✓	x
Pd/Fe	4	✓	✓	x	x	✓
Pd/Fe	7	✓	✓	x	x	✓

Determination of the products of degradation of $CDCl_3$ in water and $CHCl_3$ in D_2O with palladised iron (Expt. 6)

Pd/Fe (0.25 ± 0.02 g) was added to a series of vials. A set comprising of Pd/Fe and control vials were filled to the brim with water and an identical set filled with D_2O. Stock solutions of $CDCl_3$ (0.1 µl in water 2 ml) and $CHCl_3$ (0.1 µl in D_2O 2ml) were prepared. Aliquots (25 µl) of $CDCl_3$ in water were added to the vials containing water, and aliquots (25 µl) of $CHCl_3$ in D_2O were added to the vials (0.125 nl/ml) containing D_2O, which were shaken and analysed (P&T, GC-MS)(Table 8.6).

Table 8.6: Degradation products for $CDCl_3$ or $CHCl_3$ with either water or D_2O

Vial type	Chloroform			Dichloromethane[a]	
	Peak area	*m/z* 83-88, mm	Ratio $CHCl_3$[b]	*m/z* 84-89, mm	Ratio CH_2Cl_2[c]
D_2O control, 4 hr	132648460	42,7,28,5,6,2	84:16, 6	nd	na
D_2O control, 4 hr	131860901	68,7,45,3,7,1	92:8, 2	nd	na
H_2O control, 4 hr	222563115	3,68,2,44,1,7	5:95, 2	12,3,7,0,1,0	81:19:0, 14
H_2O control, 4 hr	93716975	3,68,2,44,1,7	5:95, 2	nd	na
D_2O control, 6hr	119920635	68,8,45,4,8,1	90:10, 3	53,8,36,3,5,1	85:12:3, 4
D_2O control, 6 hr	150075451	42,6,28,4,7,2	87:13, 8	nd	na
H_2O control, 6 hr	197592474	1,68,3,44,1,7	4:96, 3	7,3,5,2,1,0	67:28:5, 3
H_2O control, 6 hr	191592331	4,68,3,44,1,7	6:96, 2	5,1,4,1,0,0	74:14:12, 14
D_2O Pd/Fe, 4 hr	53165597	68,13,45,7,7,1	85:15, 2	13,22,10,15,3,3	36:60:4, 4
D_2O Pd/Fe, 4 hr	33013364	68,42,43,26,7,5	62:38, 2	19,33,14,21,3,4	36:62:3, 1
H_2O Pd/Fe, 4 hr	79524854	4,68,3,44,1,7	6:94, 2	15,72,11,46,2,10	17:82:1, 2
H_2O Pd/Fe, 4 hr	27639155	3,42,2,27,1,5	8:93, 3	10,75,8,49,2,8	12:87:1, 1
D_2O Pd/Fe, 6 hr	48515726	68,13,45,8,8,1	85:15, 2	30,41,22,26,5,5	41:56:3, 1
D_2O Pd/Fe, 6 hr	ni	42,16,28,10,6,3	72:28, 5	9,14,7,10,2,2	38:58:5, 5
H_2O Pd/Fe, 6 hr	46168802	5,68,4,44,1,8	8:92, 2	10,57,7,37,2,6	15:85:0, 1
H_2O Pd/Fe, 6 hr	98790904	3,68,2,44,1,7	5:95, 2	5,38,4,24,1,4	12:88:1, 1
D_2O Pd/Fe[d]	71 % conv.				38:59:4[e]
H_2O Pd/Fe[d]	60 % conv.				14:86:1[e]

[a] The dichloromethane peaks were below the integration threshold; [b] Ratio $CHCl_3$:$CDCl_3$, % error; [c] Ratio CH_2Cl_2:$CHDCl_2$:CD_2Cl_2; % error; [d] Averages; nd = nil detected; [e] standard deviations 0.5 - 2.5 ± 0.15; ni = not integrated, broad peak; na = not applicable.

Determination of the degradation products of a $CDCl_3$ and $CHCl_3$ mixture with Pd/Fe in water and D_2O (Expt. 7)

Pd/Fe (0.25 ± 0.02 g) was added to a series of vials, which were filled to the brim with D_2O or water. An aliquot (5 µl) of a $CDCl_3$ and $CHCl_3$ stock solution (0.1 µl, 0.1 µl in water 2 ml) was added to each vial (0.125 nl/ml) which was shaken (7 hr) and analysed (P&T, GC-MS)(Table 8.7).

Table 8.7: Degradation products for a combined solution of $CDCl_3$ and $CHCl_3$ with either water or D_2O

Vial type	Chloroform			Dichloromethane[a]	
	Peak area	*m/z* 83-88, mm	Ratio $CHCl_3$[b]	*m/z* 84-89, mm	Ratio CH_2Cl_2[c]
D_2O control	347437801	53,68,34,42,6,7	44:56, 2	23,2,15,2,4,0,0	92:7:1, 5
H_2O control	250138489	62,68,42,43,7,7	48:52, 1	30,4,19,3,3,0,0	89:11:0, 2
Pd/Fe, D_2O	256737617	49,68,32,43,6,7	48:52 2	25,39,47,24,25,4,4	27:41:32, 3
Pd/Fe, D_2O	165402155	51,68,35,43,6,7	44:56, 1	26,40,53,27,26,5,5	26:39:35, 2
Pd/Fe, H_2O	141937415	55,68,31,43,6,7	44:56, 3	40,25,26,16,5,3,0	62:38:0.3, 1
Pd/Fe, H_2O	128877201	57,68,39,42,6,7	47:53, 2	40,31,26,19,4,3,0[d]	57:43:0, 1

[a] Peak areas were below the integration threshold, except for the last run; [b] Ratio $CHCl_3$:$CDCl_3$, % error; [c] Ratio CH_2Cl_2:$CHDCl_2$:CD_2Cl_2; % error; [d] Integration 7512219.

Determination of the degradation products of $CDCl_3$ with Pd/Fe in water (Expt. 8)

Pd/Fe (0.2 ± 0.01g) was added to a series of vials (2 ml) which were filled to the brim with water (pH 6.15). An aliquot (5 µl) of a $CDCl_3$ stock solution (0.1 µl $CDCl_3$ in 2 ml water), was added to each vial (0.125 nl/ml) which was shaken (15 hr) and analysed (P&T, GC-MS)(Table 8.8).

Table 8.8: Degradation products for $CDCl_3$ with water

Vial type	Chloroform			Dichloromethane		
	Peak area	*m/z* 83-88	Ratio $CHCl_3$[a]	Peak area	*m/z* 84-89	Ratio CH_2Cl_2[b]
Control 1	201303960	3,68,3,43,1,7	6:94, 2	6654525	28,6,19,5,7,4	81:16:3, 12
Control 2	263241630	3,68,3,43,1,7	6:94, 2	5739244	43,2,29,1,4,0	94:3:3, 3
Control 3	276781756	3,68,3,43,1,7	6:94, 2	5935706	43,2,29,1,6,0	94:3:3, 2
Average	247109115			6109825		
Pd/Fe 1	55965396[c]	4,68,4,43,1,7	7:93, 7	10983382	40,29,26,19,5,3	58:42:0.3, 1
Pd/Fe 2	86667519[d]	11,68,8,43,2,7	15:85, 2	8067615	23,16,18,11,5,2	55:38:7, 3
Pd/Fe 3	100986094[e]	3,68,3,43,1,7	6:94, 2	9099227	25,21,15,14,3,2	55:45:0, 3
Average	81206336			9383408		
% ratio	67[f]			65[g]		
Library*	$CDCl_3$	3,68,3,43,1,7	6:94, 2	CH_2Cl_2	50,0,33,0,5,0	98:0:2, 2

[a] Ratio $CHCl_3$:$CDCl_3$, % error; [b] Ratio CH_2Cl_2:$CHDCl_2$:CD_2Cl_2; % error; [c, d, e] 77, 65, 59 % degradation respectively based on the average of the controls; [f] Average conversion based on the controls; [g] % of CH_2Cl_2 present based on the ratio of the averages of the areas of the controls and the areas of the degradations;* library spectra

Determination of the products of $CHCl_3$ incubated with D_2O and Pd/Fe in the presence of glass chromatography beads (Expt. 9)

Pd/Fe (0.2 ± 0.01g) and glass beads (chromatography grade, 80-100 mesh, 0.5 ± 0.02 ml) were added to two vials which were then filled to the brim with D_2O. An aliquot (5 µl) of a stock solution ($CHCl_3$ 0.1 µl in D_2O 2 ml) was added to each of the vials which were shaken (7 hr) and analysed (P&T, GC-MS)(Figs 8.9a, 8.9b). Data for the NIST library spectrum of $CDCl_3$ is shown in Table 8.9. Interestingly this material only contains 94% deuterium.

Table 8.9: Degradation and exchange products for $CHCl_3$ with D_2O and chromatography glass beads

Vial type	Chloroform			Dichloromethane		
	Peak area	*m/z* 83-88, mm	Ratio $CHCl_3$[a]	Peak area	*m/z* 84-90, mm	Ratio CH_2Cl_2[b]
Control	885031796	15,68,11,43,2,7	19:81, 1	ni	31,10,25,7,8,2,1	68:21:11, 4
Sample 1	254583597	28,68,19,43,4,7	30:70, 2	31264195	19,72,53,46,30,7,4	15:55:31, 1
Sample 2	309414934	25,68,17,44,3,7	27:73, 1	40309837	17,73,58,48,34,8,5	12:53,:34, 1
Average		26.5,68,18,43.5, 3.5,7	29:71, 1		18,72.5,55.5,47,32,7 .5,4.5	13:54:32, 1
Blank	nd	na	na	13972061	56,16,36,10,6,2,0	78:22:0, 1
$CDCl_3$*	na	3:68:3:43:1:7	6:94, 2	na	na	na

[a] Ratio $CHCl_3$:$CDCl_3$, % error; [b]Ratio CH_2Cl_2:$CHDCl_2$:CD_2Cl_2, % error; nd = nil detected; ni = not integrated, below integration threshold; na = not applicable; *$CDCl_3$ library spectrum

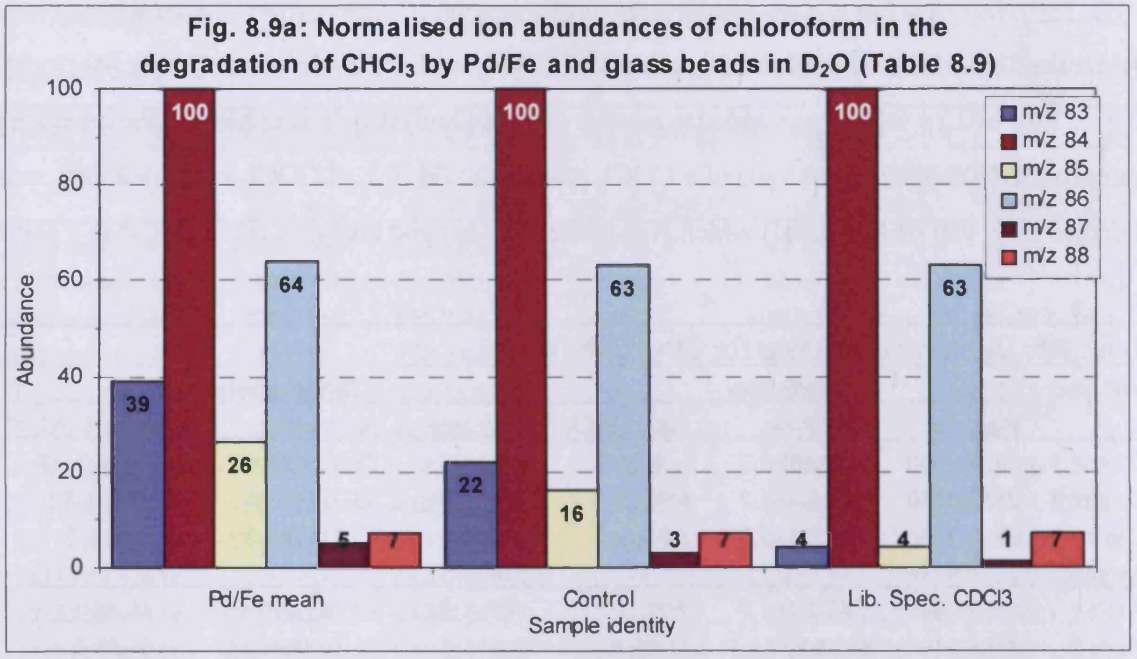

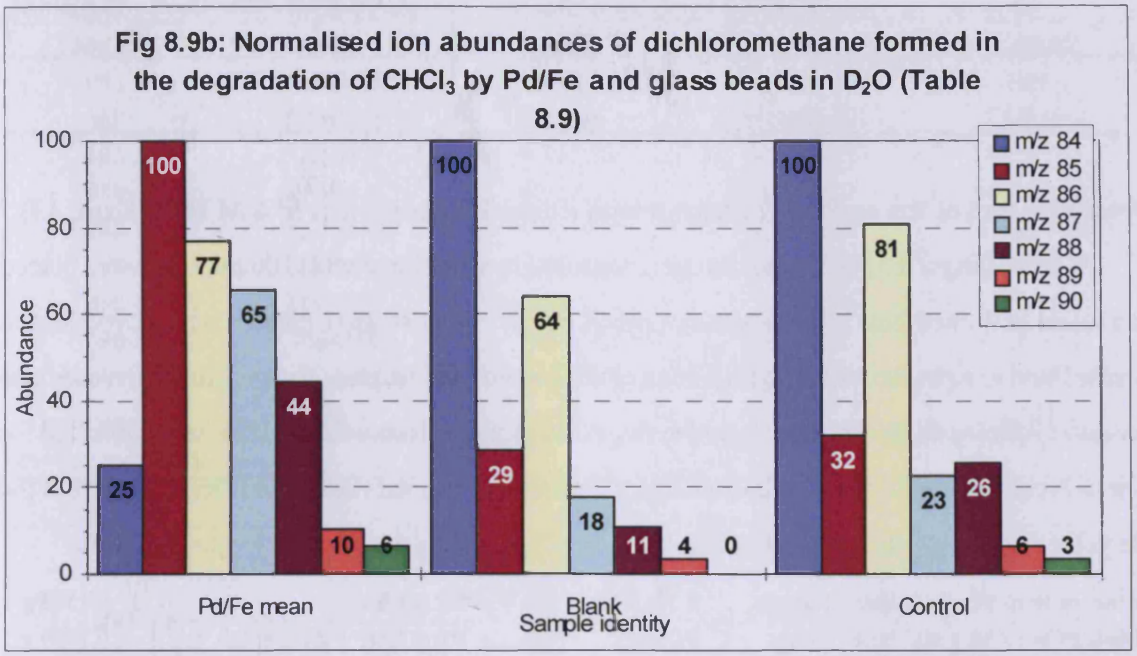

Incubation of $CDCl_3$ with glass chromatography beads in water (Expt. 10)

Chromatography glass beads (80-100 mesh, 0.5 ml) were added to two vials (2 ml) which were filled to the brim with water. An aliquot (5 µl) of a stock solution of $CDCl_3$ (0.1 µl in 2 ml) was added to each vial which was shaken (7 hr) and analysed (P&T, GC-MS)(Table 8.10).

Table 8.10: Exchange products for $CDCl_3$ with water and chromatography glass beads

Vial	Peak area	*m/z* 83-88, mm	$CHCl_3$	$CDCl_3$	Error, %
Sample 1	124672034	68, 25, 43, 15, 7, 2	74	26	1.5
Sample 2	168572323	68, 25, 44, 15, 7, 2	74	26	1.2

Measurement of the pH of chromatography glass beads in water (Expt. 11)

Constant total volume Chromatography glass beads were added to a series of 15 ml glass vials, which were filled to the brim with water and the pH measured. The vials were shaken for 10 min, left to stand for a further 50 min and the pH measured (Table 8.11).

Constant volume of water Portions of glass beads (5 ml), were added with stirring to a glass beaker containing water (20 ml) and the pH measured after each addition.

Beads (10 ml) weighed 17.83 g and hence the density was 1.78.

Table 8.11: pH of different volumes of chromatography glass beads

Constant total volume			Constant volume of water	
Volume of beads, ml	pH at 0 min	pH at 60 min	Volume of beads, ml	pH
0	7.10	7.14	0	6.31
1	8.64	10.08	5	10.49
2	8.94	10.39	10	10.63
5	9.02	10.69	15	10.79
7.5	8.53	10.88	20	10.87

10	8.75	10.96	25	11.00
11	9.14	10.83	30	11.06
12.5	9.26	10.79	35	11.06
14	9.19	10.76	nr	nr

Determination of the carbon content of iron filings by dissolution in 6 M HCl (Expt. 13)

Iron filings (0.5170 g) and nitrogen degassed hydrochloric acid (100 ml, 6M) were placed in a round bottomed flask, which was stoppered with a rubber septum, pierced with a hypodermic needle fitted to a plastic syringe with a latex glove for pressure release. The mixture effervesed and was left to stir for 48 hr. The needle and syringe assembly was removed and the flask sonicated for 6 hr to break up any iron left. The insoluble material, was filtered (cellulose filter, 0.2 μ) from the the yellow solution, washed with water (2 x 20 ml) and the dried in a desiccator for 48 hr.

Mass of tared weighing boat + filings	0.5218 g	Mass of 0.2 μ filter	0.1505 g
Mass of tared weighing boat - filings	0.0048 g	Mass of 0.2 μ filter + dried solids	0.1839 g
Total mass of filings	0.5170 g	Total mass of solids	0.0334 g
		Percentage acid insoluble material	**6.46%**

Comparison of the reaction rates and products of $CHCl_3$ and $CDCl_3$ in D_2O and water respectively (Expt. 14)

Pd/Fe (0.2 ± 0.02 g) was added to a series of vials (2 ml). One set was filled with water and the other filled with D_2O. Aliquots (5 μl) of stock solutions of $CDCl_3$ (0.1 μl in water 2 ml) and $CHCl_3$ (0.1 μl in D_2O 2 ml) were added to vials containing the same solvent. $CDCl_3$ in water was added to the control vials. The vials were shaken (7 hr) and analysed (P&T, GC-MS) (Table 8.14).

Table 8.14: Peak areas for $CDCl_3$ in H_2O and $CHCl_3$ in D_2O

Time, min	$CDCl_3$[a]	$CHCl_3$[b]	Control
30	3376304	13681185	5090742
60	2921309	11562219	4147260
120	1848275	11326552	5114737
180	1382000	6236681	6458978
270	1824496	6173653	5736934
360	891858	4366072	4262871
k_1, min^{-1}, $t_{½}$, min	0.0034, 204	0.0034, 204	na

[a, b] % degradation of $CDCl_3$ & $CHCl_3$, 74%, 68% respectively; na =not applicable

Comparison of reaction rates for differing initial concentrations of $CHCl_3$ (Expt. 15)

Pd/Fe (0.25 ± 0.02 g) was added to a series of vials, which were filled to the brim with water. An aliquot (40 μl) was removed from a stock solution ($CHCl_3$ 0.2 μl in water 2 ml) and sub aliquoted (5 μl, 10 μl, 15 μl, 10 μl) into a set of vials, three of which contained Pd/Fe and the other was the control. A concentration series of a set of vials was thus prepared. The vials were shaken and analysed (P&T, GC-MS) (Fig 8.15, Table 8.15).

Table 8.15: Peak areas for degradation of 5 µl, 10 µl and 15 µl $CHCl_3$

Time, min	5 µl	10 µl	15 µl	Control
0	54200138	143775353	214808710	nm
60	57753293	99857566	165209383	128423484
120	32781876	89709043	165009079	142167422
180	33003656	65818207	138999107	144164651
240	52091618	65956803	69121296	129631696
330	22448466	31826880	39368065	138892802
480	14875921	28561923	27235261	112517028
630	7684853	14045704	9480653	110244603
k_1, min^{-1}; $t_{½}$, min	0.0031; 224	0.0035; 198	0.005; 139	na
Degradation, %	86	90	96	na

nm = not measured

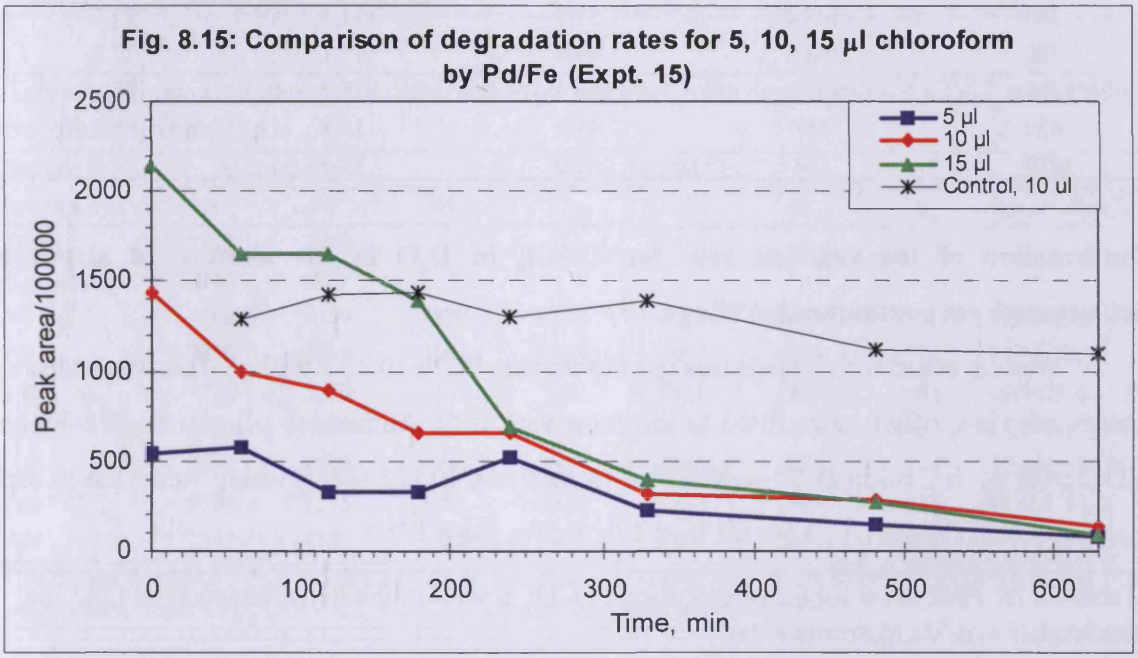

Determination of the rate of degradation of $CDCl_3$ in D_2O by Pd/Fe (Expt. 16)

Pd/Fe (0.25 ± 0.02 g) was added to a series of vials, which were filled to the brim with D_2O. Aliquots (5 µl) of a stock solution ($CDCl_3$ 0.1 µl in 2 ml D_2O) were added to each vial (0.125 nl/ml) which was shaken and analysed (P&T, GC-MS)(Tables 8.16a, 8.16b).

Table 8.16a: Peak areas for the degradation of $CDCl_3$ with D_2O and the formation of dichloromethane.

Time, min	$CDCl_3$	Control	CX_2Cl_2	% Ratio $CDCl_3$[a]	% Ratio CX_2Cl_2[a]
0	nm	34889408*	477586	na	na
60	19005057	25869555	715105	96	4
120	16599630	29287358	644511	96	4
180	10255320	23249142	827118	93	7
240	7080401	27450907	873804	89	11
300	4316075	27647167	1041894	81	19

360	2103676	27618199	863731	71	29
420	2608049	19366598*	904298	74	26
480	3562300[b]	29245271	957974	79	21
k_1, min^{-1}	0.0052	na	na	na	na
$t_{½}$, min	133	na	na	na	na

[a] Based on TIC peak areas; [b] 81% degradation of $CDCl_3$; na = not applicable, * = excluded

Table 8.16b: Proportions of CH_2Cl_2, CD_2Cl_2 and $CDHCl_2$

Time,min	Total A, mm	% CH_2Cl_2	% $CDHCl_2$	% CD_2Cl_2
0	100	100	0	0
60	153.8	65.0	12.7	22.7
120	148.3	67.4	9.7	22.9
180	147.2	53.2	13.7	33.1
240	148.4	51.7	14.8	33.5
300	148.6	45.6	17.1	37.3
360	147.7	49.6	15.2	35.1
420	147	48.4	15.3	36.3
480	144	41.0	16.5	42.5

Confirmation of the reaction rate for $CDCl_3$ in D_2O in the absence of airborne dichloromethane contamination (Expt. 17)

Water sparged with helium was used to prepare Pd/Fe (0.25 ± 0.02 g). This was added to a series of vials, which were filled to the brim with D_2O. Aliquots (5 µl) of a stock solution ($CDCl_3$, 0.1 µl in 2 ml in D_2O) were added to each vial (0.125 nl/ml) which were shaken and analysed (P&T, GC-MS) (Tables 8,17a, 8.17b, 8.17c, Fig 8.17).

Table 8.17a: Peak areas for the degradation of $CDCl_3$ with Pd/Fe in helium sparged D_2O and the formation of dichloromethane

Time, min	$CDCl_3$	Control, $CDCl_3$	CX_2Cl_2
0	nm	9971522	nd
30	7154958	9851720	319094
60	5710115	9775273	373706
120	5813901	9278828	394282
180	4574679	8999230	nr
240	3783522	9222613	303670
330	3372653	8688577	303374
420	2060470[a]	9000852	364599
k_1, min^{-1}; $t_{½}$, min	0.0029; 239	na	na

[a] 71% degradation of $CDCl_3$; nm = not measured, nd = nil detected, nr = no result, na = not applicable

Table 8.17b: Ion abundances[a] for residual $CDCl_3$ in the degradation of $CDCl_3$ with Pd/Fe in helium sparged D_2O and control vials

Time, min	82	83	84	85	86	87	88
30[b]	264	16	10000	108	6357	101	1029
60[b]	253	48	10000	139	6544	125	1067

120[b]	234	44	10000	111	6367	114	1015
180[b]	218	23	10000	40	6498	121	1047
240[b]	254	0	10000	113	6413	80	1092
330[b]	247	0	10000	173	6328	88	1047
420[b]	233	39	10000	126	6489	117	1054
0[c]	255	13	10000	90	6476	109	1053
30[c]	248	55	10000	143	6463	109	1035
60[c]	247	0	10000	44	6397	96	1056
120[c]	261	15	10000	40	6320	95	1022
180[c]	256	0	10000	172	6327	99	1064
240[c]	251	17	10000	172	6348	72	1050
330[c]	237	30	10000	92	6370	80	1035
420[c]	265	0	10000	35	6412	87	1029

[a] All of the clusters show the abundances (100: 1.1: 64: 0.7: 10.2) expected for the $CDCl_2$ ion of $CDCl_3$; *m/z* 82 is due to CCl_2; [b] reaction vials; [c] control vials

Table 8.17c: Ion abundances for dichloromethane found in the degradation of $CDCl_3$ with Pd/Fe in helium sparged D_2O

Sample id	*m/z* control		*m/z* Pd/Fe					Pd/Fe
or time, min	84[a]	86[a]	84	85	86	87	88	Ratio[b] CH_2Cl_2
Blank	3327	1939						
0 control	2949	1515[c]						
30	6300	3579	7679	1280	5405	1178	1518	83:13:5, 6
60	7890	3618	7184	1336	7662	2094	2726	63:11:27, 8
120	9219	5793	7483	988	7321	1311	2262	69:8:23, 6
180	6121	5011	5327	935	8356	2106	2838	48:8:44, 15
240	6044	5398	3094	2099	8366	2431	3118	27:18:55, 17
330	6399	1215	5601	2535	9285	1463	4225	41, 18, 42, 5
420	7341	4783	3600	2005	7781	1275	3968	33:18:50,5

[a] With one exception[c], only the *m/z* 84 and 86 peaks could be measured for the controls, because of low ion abundances; [b]Ratio CH_2Cl_2:$CHDCl_2$:CD_2Cl_2; % error; [c] also peak at *m/z* 88 1066;

Fig. 8.17: % Ratio of dichloromethane isotopomers in the degradation of $CDCl_3$ by Pd/Fe in helium sparged D_2O (Expt 17)

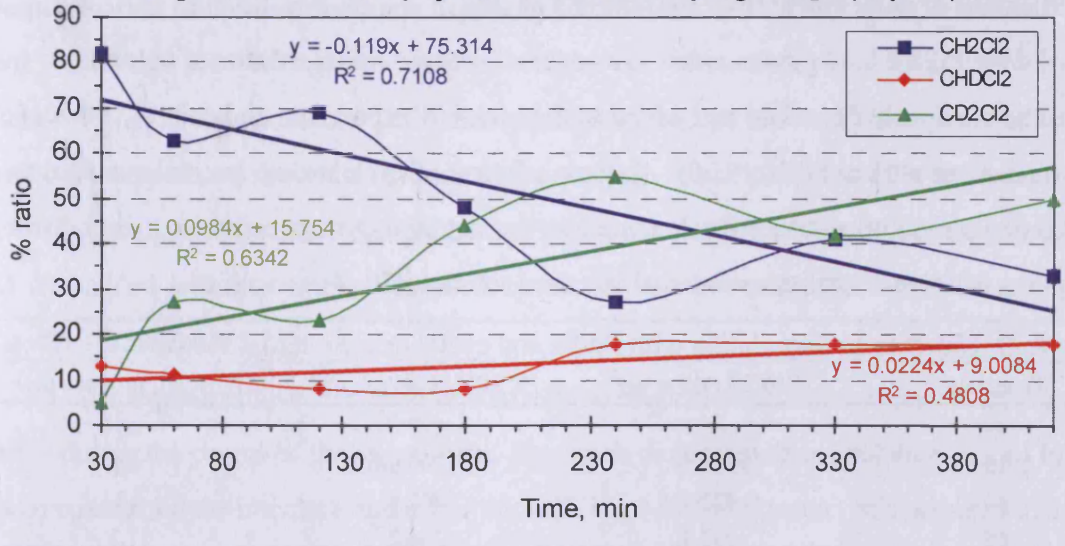

Calibration curve using MSD software and cyclohexane as internal standard (Expt. 19)

A calibration curve for chloroform and dichloromethane using cyclohexane as an internal standard was run. Stock solutions of chloroform (0.5 µl in 15 ml water), dichloromethane (0.5 µl in 15 ml water) and a combined intermediate solution (150 µl of each stock solution diluted to 15 ml with water) were prepared. A series of standards was prepared by varying the volumes of the intermediate (Table 8.19) and immediately the sample was drawn into the sampling syringe the internal standard solution was added (20 µl) using a spiking syringe. This was more effective than trying to add the internal standard before capping (*i.e.* the cyclohexane would have been acting as a surrogate standard rather than an internal standard). The samples were analysed (GC-MS) and the calibration curves constructed using the GC-MS software quantification facility.

Table 8.19: Intermediate volumes for calibration standards. (conc. µg/l)

Nominal conc.	Vol. intermediate, µl	$[CHCl_3]$, µg/l	$[CH_2Cl_2]$, µg/l
0	0	0.0	0.0
1	4	1.0	0.9
2.5	10	2.5	2.2
5	20	5.0	4.4
10	40	9.9	8.9
25	100	24.7	22.1
50	200	49.5	44.2
75	300	74.2	66.4
100	400	98.9	88.5
200	800	197.9	176.9
300	120	296.8	265.4
400	1600	395.8	353.8
500	2000	494.7	442.3
Response		1.03×10^4 x conc. + 3.05×10^4	3.48×10^3 x conc. + 6.02×10^4
R^2		0.999	0.999

Quantification of chloroform degradation (Expt. 20)

Pd/Fe (0.25 ± 0.02 g) was added to a series of vials. A stock solution of chloroform was prepared as previously described and added to the series of experiment and control vials which were which were shaken (Table 8.20). A stock solution of cyclohexane internal standard was prepared (0.5 µl in 2 ml water). After loading into the sampling syringe and prior to introduction to the purge and trap, cyclohexane internal standard solution (20 µl) was added.

Table 8.20: Chloroform degradation with Pd/Fe and cyclohexane internal standard

Time, min	$[CHCl_3]$ Pd/Fe, µg/l	$[CHCl_3]$ Control, µg/l	$[CH_2Cl_2]$ Product, µg/l
0	nm	377.6	nd
10	1523.1*	1290.9*	nd
30	421.4	412.6	6.3
60	272.4	340.2	11.1
90	228.3	274.6	13.9

120	97.6*	180.0	7.1
195	46.4*	324.4	8.5
240	170.3	168.9	22.6
300	122.0	148.9	15.2
360	63.4	144.3	24.5
450 (conversion, %)	46.4 (89)	400.5	15.7 (6)
k_1, min^{-1}; $t_{½}$, min	0.0048; 144	na	na

nm = not measured, nd = nil detected, na = not applicable * excluded

Confirmation of the quantification of the chloroform degradation (Expt. 21)

The chloroform degradation experiment described in expt. 20 was repeated to confirm the original results (Table 8.21).

Table 8.21: Repeat chloroform degradation with cyclohexane internal standard

Time, min	Pd/Fe				Control		
	$CHCl_3$ area	$[CHCl_3]$, µg/l	Int.Std. area	$[CH_2Cl_2]$, µg/l	$CHCl_3$ area	$[CHCl_3]$, µg/l	Int. Std. area
0	nm	nm	nm	nd	2098670	119.8	6843453
10	2372916	150.3	5724865	6.2	nr	nr	nr
30	1716809	55.3	10918870	2.7	2182214	75.1	10423995
60	1869816	53.2	12078282	2.7	2231534	68.8	11799683
90	1578860	46.4	11862318	3.9	2085445	56.8	12444027
120	1486951	49.7	10530592	5.1	2959434	98.0	10714488
180	1529234	62.8	8547540	6.0	2429314	95.7	9087649
240	1079728	52.0	7294350	8.3	2108248	97.4	7840191
320	1106904	63.1	5985867	9.7	1848371	102.3	6417738
360	407323	32.3	4758740	nd	1665641	120.7	5168728
420	743286	60.8	4015042	nd	1568867	128.5	4498105
570	466505	42.8	3485945	16.0	2266057	245.9	3519516

nm = not measured, nr = no result, nd = nil detected; $CHCl_3$ k_1, 0.0041 min^{-1}; $t_{½}$, 170 min; 72 % conv; CH_2Cl_2, 11 % formation

Quantification of dichloromethane degradation (Expt. 22 -24)

Pd/Fe (0.25 ± 0.02 g) was added to a series of vials which were filled with water and aliquots (5 µl) of a stock solution of dichloromethane (0.75 µl in 15 ml water) were added. The vials were capped and shaken until required for analysis. A stock solution of cyclohexane (0.5 µl in 2 ml) was prepared. After loading the sample into the sampling syringe, internal standard (20 µl) was added and the samples analysed by purge and trap using the calibrated method for quantification (Table 8.22).

The experiment was repeated to confirm the original results as the internal standard area varied during the course of the experiment. The stock dichloromethane solution (0.1 µl in 2 ml) was prepared and the internal standard solution (3.75 µl in 15 ml water) was prepared in a larger volume.(Table 8.23)

The experiment was repeated again with fresh stock dichloromethane solution (0.1 µl in 2 ml water) and internal standard solution (0.5 µl in 2 ml water; Table 8.24).

Peak areas for the degradation of dichloromethane with cyclohexane internal standard

Time,	Table 8.22		Table 8.23		Table 8.24	
min	Pd/Fe	Control	Pd/Fe	Control	Pd/Fe	Control
0		1121812		5129615		3242269
10	1285302	1538530			3686153	4417162
15			5665773	5432982		
30	1519806	1241880	5823148	5467296	4813095	4433978
60	1470681	1541210	5346412	5702263	nr	3382941
90	1111167	1053648			4545511	3627130
110			5152799	5918998		
120	987123	1470106			3493098	3909758
140			5605426	5738691		
150					3847577	4739357
180	1263819	1419952				
210			5134733	5400503		
240	1136157	1810316			3085294	3526388
270			5627060	6588167		
300	1107927	1725446	5383358	5281693	3037159	3832644
360	1236285	1168620	5784644	5359574	2806473	3418214
420	1139644	1395049			3135330	2934471
435			5169381	5164142		
480	929805	1207052	5228894	4713242	2886781	3471596
540			4626985	5337712		
k_1, min^{-1}	0.00055	na	0.00021	na	0.00093	na
$t_{½}$	1260	na	3300	na	745	na
Conv. %	28	na	18	na	21	na

nr = no result, na = not applicable

Comparison of the rate of degradation vials spiked with dichloromethane and chloroform versus vials spiked with chloroform only (Expt. 25)

Pd/Fe (0.25 ± 0.02 g) was added to two sets of vials and the vials filled with water. Chloroform solution (0.1 µl in 2 ml) was added to one set of vials and chloroform/ dichloromethane solution (0.1 µl of each in 2 ml water) was added to the other set and to the control vials. A mixed control of chloroform and CH_2Cl_2 was run to monitor the peak areas during the course of the run (Table 8.25). The vials were shaken and analysed (P&T, GC-MS).

Table 8.25: Peak areas for the degradation of chloroform only and chloroform-dichloromethane systems

Time,		$CHCl_3/CH_2Cl_2$		Control	
min	$CHCl_3$	$CHCl_3$	CH_2Cl_2	$CHCl_3$	CH_2Cl_2
0	nm	nm	nm	1934312	5901505
10	5792868	2144675	5434852	2286163	5443229
30	5570873	2229030	5773940	2216623	5957424
60	4385146	1618452	5529253	2126632	6085405

90	851199	1246105	5778426	2056963	5641067
120	1624384	1240509	6277704	2189341	6036274
150	319372*	600321*	4801344	2166484	6787845
180	1235318	814044	6518684	1766491	4644487
240	303729	322417	4379265	2339787	6518986
300	175199	262888	4674133	2087626	5937698
360	242266	132145	5567093	2123024	6026847
k_1, min^{-1}	0.0103	0.0081	0.0017[a]	na	na
$t_{½}$, min	67	86	407[a]	na	na
Conv. %	95	93	-2	7	-10

[a] Calculated from data at 10 min; nm = not measured, na = not applicable, * excluded.

Calibration curve for chloroform and dichloromethane using 1,4-dioxane as internal standard (Expt. 26, 27)

The use of 1,4-dioxane as an internal standard was reinvestigated as the cyclohexane proved to be too variable to use. A series of stock solutions (5µl, 20 µl and 10 µl) were prepared and an aliquot (20 µl) added to a chloroform solution (5 µl in water, 2 ml). The samples were analysed and the stock producing a peak area closest to that of the chloroform was selected for use.

A combined solution of chloroform (100 µl) and dichloromethane (100 µl) was prepared. An aqueous stock solution (1 µl in 2 ml water) was sonicated (5 min) and an aliquot (150 µl to 15 ml) was diluted to give a working intermediate. The calibration standards were then prepared by serial dilution of the intermediate in water (2 ml) as described in Table 8.26. The internal standard was prepared by diluting an aliquot (10 µl in 2 ml) of 1,4-dioxane and sonication (5 min) prior to use.

Table 8.26: Intermediate volumes for calibration standards and peak areas for 1,4-dioxane

Nominal conc., µg/l	Vol. intermediate, µl	$[CHCl_3]$, µg/l	$[CH_2Cl_2]$, µg/l	Peak area
0	0	0	0	11379237
1	4	0.99	0.88	10791412
2.5	10	2.48	2.2	11095074
5	20	4.95	4.4	12161491
10	40	9.9	8.85	10893376
25	100	24.75	22.11	12288195
100	400	99.0	88.46	11661964
200	800	198.0	176.92	11539699
300	1200	297.0	265.84	11846493
400	1600	396.0	35.84	13067177
500	2000	494.7	442.3	11582256

Mean peak area 11664216; σ_{n-1} 664944; cv = (σ_{n-1}/mean)x100 5.7%

Comparison of the rate of degradation of chloroform with 1,4-dioxane as internal and surrogate standard (Expt. 28, 29)

Initially, the degradation of chloroform was analysed with two sets of vials containing

Pd/Fe. 1,4-Dioxane solution (5 µl in 2 ml, sonic bath 5 min) was added to one set of vials and also to the controls. Chloroform solution (0.2 µl in 2 ml sonic bath 5 min) was added to all vials which which were shaken and analysed (P&T, GC-MS) (Table 8.28).

Table 8.28: Peak areas of chloroform and 1,4-dioxane using 1,4-dioxane as surrogate standard

Time, min	$CHCl_3$ only	$CHCl_3$ + dioxane surr.std	1,4-dioxane (With $CHCl_3$)	$CHCl_3$ control	1,4-dioxane control
0	nm	nm	nm	2815198	4291617
10	3077655	3553722	5195585	nm	nm
30	2473369	2750496	5246567	nm	nm
60	2479733	2307169	5718815	3067350	6056921
90	2110386	1926399	5002687	nm	nm
120	1870223	2182708	5272576	3510198	5150864
190	861367	1469712	4666931	nm	nm
240	917683	1480656	4618259	3401612	4619202
300	862130	1444973	4286186	nm	nm
360	898121	928338	4317734	2814163	4635591
420	472738	1170167	3866020	nm	nm
480	723268	987337	3695298	2584979	4498086
k_1, min^{-1}	0.0035	0.0024	na	na	na
$t_{½}$, min	198	289	na	na	na
Conv. %	76	72	na	na	na

nm = not measured, na = not applicable

The experiment was repeated using 3 sets of vials. The first set had only chloroform solution added (5 µl), the second set had chloroform solution added (5 µl) initially and 1,4-dioxane solution (20 µl) added immediately before injection onto the GC-MS and the last set had both chloroform solution (5 µl) and 1,4-dioxane solution (20 µl) added at the start of the experiment. The 1,4-dioxane was used as both an internal and a surrogate standard in this experiment (Table 8.29).

Table 8.29: Peak areas for chloroform and 1,4-dioxane for the chloroform degradation using 1,4-dioxane as surrogate standard and internal standard

Time, min	Chloroform				1,4- dioxane		
	No dioxane	Surrogate standard	Internal standard	Control	Surrogate standard	Internal standard	Control
0	nm	nm	nm	14560374	nm	nm	6683344
10	2771755	3107352	2903431	nm	5712425	nm	nm
30	nm	2673804	nm	nm	5919363	6243645	nm
60	1529746	2485122	1475894	8533781	5470456	6356380	4285269
90	2001979	2262237	1506411	nm	6664399	5927942	nm
120	1404165	3239415	1866448	nm	6123717	6740557	nm
150	1756535	1855162	1176265	8130111	4532672	6440141	4082369
200	1542104	1162515	1146977	nm	5153270	5917995	nm
240	nm	1074906	1018215	nm	4630250	5244502	nm
300	nm	791730	961612	7599834	4389113	5958723	4043265
360	nm	850082	894811	nm	4342950	6296746	nm

420	nm	836143	550374	8501105	5062928	4954528	3694594
480	nm	504531	408582	7368051	4304657	5393549	3307678
k_1, min^{-1}	nm	0.0038	0.0033	na	na	na	na
$t_{½}$, min	nm	182	210	na	na	na	na
Conv. %	44	83	86	na	na	na	na

nm = not measured, na = not applicable

Quantification of chloroform degradation and dichloromethane quantification and monitoring of dichloromethane in controls (Expt. 30)

Pd/Fe (0.25 ± 0.02 g) was added to a set of vials. A stock solution of chloroform (0.2 µl in 2 ml) was sonicated (5 min) to ensure complete dissolution. A stock solution of dichloromethane was also prepared (0.5 µl in 15 ml) sonicated (5 min) and an intermediate was prepared (150 µl diluted to 15 ml). Chloroform solution (5 µl) was added to all vials and dichloromethane solution (40 µl) was added only to the control vials. The vials were shaken until required for analysis. A solution of 1,4-dioxane (5 µl diluted to 2 ml) was prepared and an aliquot (20 µl) added immediately prior to analysis to act as an internal standard.

The nominal dichloromethane concentration was calculated to be 8.8 µg/l. The following table (Table 8.30) summarises the concentrations found at the respective time points for chloroform, dichloromethane generated from the degradation and the control values.

Table 8.30: Concentrations of chloroform and dichloromethane from chloroform degradation and in control solutions

Time, min	Pd/Fe		Control	
	$[CHCl_3]$, µg/l[a]	$[CH_2Cl_2]$, µg/l	$[CHCl_3]$,µg/l	$[CH_2Cl_2]$,µg/l
0	nr	nr	418.1	6.1
10	478.5	nd	507.6	7.0
30	266.7	6.0	413.7	8.2
60[b]	335.0	14.4	448.6	13.
90	142.5	8.8	524.2	7.4
120	113.9	11.8	452.4	7.4
150	147.6	20.7	530.4	7.5
180	70.0	12.3	503.0	7.5

[a] k_1 0.0098 min^{-1}; $t_{½}$, 71 min; 85 % conversion; [b] not used in analysis; nr = no result, nm = not measured, nd = nil detected

Degradation of $CDCl_3$ by Pd/Fe in water (Expt. 31)

Pd/Fe (0.25 ± 0.02 g) was added to a set of vials. A stock solution of $CDCl_3$ (0.2 µl in 2 ml) in water was prepared and an aliquot (5 µl) of added to each vial which were shaken and analysed (P&T, GC-MS) (Tables 8.31a, 8.31b, 8.31c).

Table 8.31a: Peak areas for $CDCl_3$ in the degradation of $CDCl_3$ by Pd/Fe in water

Time, min	Pd/Fe	Control	Time, min	Pd/Fe	Control
0	nm	4461620	180	2022872	4770699

10	4411365	5540721	240	1324809	4465426
30	3855490	5188072	300	870366	4197512
60	3550020	5844415	360	631410	3948976
90	2608800	4708505	420	632002[a]	4383150
120	2278210	6054470	k_1, min^{-1}	0.0051	na
150	2198009	4833313	$t_{1/2}$, min	136	na

[a] 86 % degradation of $CDCl_3$; nm = not measured, not applicable

Table 8.31b: Ion abundances[a] (*m/z* 82-88) for residual $CDCl_3$ in the degradation of $CDCl_3$ with Pd/Fe in H_2O and control vials (Expt 31)

Time, min	82	83	84	85	86	87	88
Degradation							
10	338	1362	10000	1077	6391	202	986
30	302	282	10000	311	6355	68	998
60	284	199	10000	294	6350	64	943
90	257	173	10000	239	6571	91	925
120	300	214	10000	287	6550	87	1094
150	277	73	10000	206	6560	37	1017
180	290	150	10000	262	6478	44	1088
240	245	147	10000	162	6365	0	1048
300	266	1158	10000	824	6355	118	1050
360	169	354	10000	123	6471	0	713
420	311	383	10000	160	6484	0	988
480	186	171	10000	161	6641	0	1134
Controls							
0	288	247	10000	285	6689	90	1063
10	312	306	10000	376	6362	90	1035
30	262	389	10000	360	6522	107	1006
60	283	458	10000	396	6417	112	1008
90	278	101	10000	121	6433	65	1002
120	285	47	10000	210	6561	92	991
150	277	130	10000	207	6391	62	1035
180	287	218	10000	276	6457	83	1032
240	277	313	10000	331	6325	86	1012
300	283	220	10000	263	6231	103	1011
360	268	198	10000	292	6484	85	1007
420	280	357	10000	323	6419	121	1073
480	268	158	10000	259	6449	96	982

[a] All of the clusters show the abundances (100: 1.1: 64: 0.7: 10.2) expected for the $CDCl_2$ ion of $CDCl_3$; *m/z* 82 is due to CCl_2; [b] reaction vials; [c] control vials.

Table 8.31c: Ion abundances[a] (*m/z* 84-87) for dichloromethane in the degradation of $CDCl_3$ with Pd/Fe in H_2O and control vials (Expt 31)

Time, min	Degradation, *m/z*					Controls, *m/z*		
	84	85	86	87	Ratio CH_2Cl_2[b]	84	85	86[c]
60[d]	838	0	0	0	nc	nd	nd	nd
90	1777	1460	0	929	nc	nd	nd	nd
120	502	1871	0	925	nc	nd	nd	nd
150	0	1389	0	532	nc	nd	nd	nd
180	0	1284	0	591	nc	nd	nd	nd
240	1862	3321	821	783	36:63:0, 34	367	0	118[e]
300	909	2431	551	1433	27:73:0, 10	1836	0	914[e]
360	2633	3990	1804	2338	39:60:1, 9	1468	0	1020[e]

420	1771	2561	1091	2198	41:59:0, 14	1386	0	982[e]
480	1121	1596	874	451	39:55:5, 24	4203	0	2246[e]

[a] Dichloromethane peaks were below the integration threshold; [b] ratio CH_2Cl_2:$CHDCl_2$:CD_2Cl_2; % error; [c] *m/z* 87 not detected; [d] no ions were detected in the 0, 10, and 30 min degradation and control vials; [e] the low ion abundances preclude calculation of accurate ratios, however the ratios are consistant with the exclusive presence of CH_2Cl_2; nd = nil detected., nc = not calculated

Degradation of 6-bromohex-1-ene on Pd/Fe (Expt. 32)

Pd/Fe (0.25 ± 0.02 g) was added to a set of vials. A stock solution of 6-bromohex-1-ene (0.2 µl in 2 ml water) was prepared, sonicated (5 min) and an aliquot (10 µl) added to each vial. The vials were shaken and analysed (P&T, GC-MS) (Table 8.32).

Table 8.32: Peak areas for 6-bromohex-1-ene degradation over Pd/Fe

Time, min	Pd/Fe	Control	Time, min	Pd/Fe	Control
0	nm	18894298	360	8119649	20710898
10	13937159	18124683	420	nr	17656546
30	16357252	18393609	480	3669345	12353457
60	9105228	22376739	540	4853259	10232261
90	8441390	16941358	600	2805653	15349096
120	8510949	16501220	660	3045502	15545169
150	7825896	13467870	720	1600641	12816679
180	4387953	12415593	1395	659409	12178159
240	6298948	16255250	k_1, min^{-1}	0.0023	na
300	6169823	17637966	$t_{½}$, min	301	na

nm = not measured, nr = no result, na = not applicable

Degradation of 6-bromohex-1-ene and chloroform in a mixed system on Pd/Fe (Expt. 33)

A stock solution of 6-bromohex-1-ene (0.4 µl) and chloroform (0.2 µl) in water (2 ml) was sonicated (5 min) and aliquots (10 µl) added to a set of vials containing Pd/Fe (0.25 ± 0.02 g). The vials were shaken and analysed (P&T, GC-MS) (Table 8.33).

Table 8.33: Peak areas for 6-bromohex-1-ene and chloroform combined degradation

Time, min	Pd/Fe		Control	
	$CHCl_3$	6-Bromo-hexene	$CHCl_3$	6-Bromo-hexene
0	nm	nm	6770085	878694
10	7563126	1966149	10082773	2722523
30	8634002	2798690	10436393	2989161
60	4284663	883157	10543203	2664364
90	6780750	1672461	10358924	2504745
120	5174350	1423738	8397737	1684589
150	3775378	949259	8447448	1778737
180	2680464	1057830	8926411	1944762
240	2651520	796320	6590460	1397367
300	1382450	711701	10651964	2256485
360	1822616	779599	9125232	2437032
420	1578936	593354	9385032	2324201
480	908220	345717	8579044	1989102

540	1251607	332646	8041653	1759314
k_1, min^{-1}	0.0039	0.0032	na	na
$t_{1/2}$, min	178	217	na	na

nm = not measured, na = not applicable

6-bromohex-1-ene and hex-1-ene calibration curve (Expt. 35)

Stock solutions of 6-bromohex-1-ene (0.5 µl) in methanol (15 ml) and hexene (0.5 µl) in methanol (15 ml) were prepared. A combined working solution of 6-bromohexene (300 µl) and hexene (300 µl) in water (15 ml) was prepared. A calibration series was prepared by diluting varying volumes of the working standard with water to a constant volume (2 ml)(Table 8.35).

Table 8.35: 6-Bromohexene and hexene calibration

Nominal concentration standard	Working solution volume, µl	[6-bromohexene], µg/l	[hexene], µg/l
0	0	0	0
5	12.5	5.1	2.8
10	25	10.1	5.6
25	62.5	25.4	14.0
50	125	50.7	28.0
75	187.5	76.1	42.1
100	250	101.4	56.1
200	500	202.8	112.2
300	750	304.2	168.3
400	1000	405.7	224.4
500	1250	507.1	280.4
600	1500	608.5	336.5
700	1750	709.9	392.6
800	2000	811.3	448.7

The series of calibration standards was run under identical conditions to the actual samples. Initially, the stock solutions were prepared in water, but the insolubility and volatility of the components meant that the standards were irreproducible. By preparing the stock solutions in methanol, the solubility problem is overcome. Methanol is the solvent of choice because it is readily soluble in water, does not purge easily and has a mass which was below the *m/z* cutoff specified in the scan parameters for the mass spectrometer.

Using the quantitation software provided with the instrument operating system, a calibration curve for each parameter was constructed and a linear fit established. The correlation coefficient for 6-bromohexene was found to be 0.962, and for hexene the correlation coefficient was also found to be 0.962. Data files generated from earlier degradations were quantified using this calibration.

Degradation of bromoethyl ethyl ether on a Pd/Fe (Expt. 34)

Pd/Fe (0.25 ± 0.02 g) was added to a set of vials. A stock solution of bromoethyl ethyl

ether (0.4 µl) in water (2 ml) was sonicated (5 min). The vials were filled to the brim with water and an aliquot (5 µl) of the stock solution added to each. The vials were shaken and analysed (P&T, GC-MS) (Table 8.34). A standard of ethanol (0.4 µl) in water (5 ml) was prepared and analysed under identical conditions to identify the mass spectrum and the retention time. The GC-MS run conditions were altered to take into account the possible long retention time. Parameters; 35(3) x 20 to 250(0) inj 275, and low mass cutoff set to *m/z* 30 at 2 min.

Table 8.34: Peak areas for bromoethyl ether degradation on Pd/Fe

Time, min	Pd/Fe	Control	Time, min	Pd/Fe	Control
0	nm	4415623	150	4702485	6124824
10	5704607	5678540	180	5370448	5745563
30	5693518	5836908	240	5336715	6112157
60	5272541	5512552	300	2587457	5216497
90	4798594	5598569	k_1, min^{-1}	0.0018	na
120	4773363	6881953	$t_{½}$, min	385	na

nm = not measured, na = not applicable

Degradation of bromoethyl ethyl ether on Pd/Fe run on a thick film column (Expt. 36)

Pd/Fe (0.25 ± 0.02 g) was added to a set of vials. A stock solution of bromoethyl ethyl ether (0.4 µl) and chloroform (0.2 µl) in water (2 ml) was sonicated (5 min). The vials were filled to the brim with water and an aliquot (5 µl) of the stock solution added to each. The vials were which were shaken and analysed (P&T, GC-MS)(Table 8.36). A standard of ethanol (0.5 µl) and ether (0.2 µl) in water (2 ml) was prepared and analysed under identical conditions to identify the mass spectrum and the retention time. The GC-MS run conditions were altered to take into account the possible long retention time of the parameters; 35(3) x 20 to 200 (0) inj 250, on HP624 thick film column 25 m and low mass cutoff set to *m/z* 30 at 2.5 min.

Table 8.36: Peak areas for bromoethyl ether and chloroform degradation on Pd/Fe run on thick film column

Time, min	Pd/Fe		Control	
	$CHCl_3$	Bromoethyl ethyl ether	$CHCl_3$	Bromoethyl ethyl ether
0	nm	nm	28974171	48681773
10	38585744	25216925	41133732	24541829
30	33028320	21528065	31472162	19705487
60	31809656	20696511	36987001	22296226
90	20512426	15090666	31954331	24895592
120	20656648	16830544	38437009	22297800
150	20720932	19409107	31483321	18574034
180	18389990	18571207	29873936	21135970
240	13875294	15833088	33483481	21272835
300	12208495	15004920	33737116	21642608
360	11029907	17238454	34107102	20884970
420	8946981	12016827	36799836	22427129
480	6687046	17836126	35944893	21433295

540	6014477	14269398	33629151	22581888
600	8629385	14671155	32760949	19607958
660	5475429	11255437	30841585	20183183
780	5486193	14883091	31698957	19952371
1460	1633006	9216075	30378618	19466484
1680	2224960	7207075	nm	nm
k_1, min^{-1}	nm	0.0006	na	na
$t_{1/2}$, min	nm	1155	na	na

nm = not measured, na = not applicable

Bromoethyl ethyl ether, ether and ethanol calibration curve (Expt. 37)

Stock solutions of bromoethyl ethyl ether (0.5 µl) in methanol (15 ml), diethyl ether (0.5 µl) in methanol (15 ml) and ethanol (2.5 µl) in water (15 ml) were prepared. A combined working solution of bromoethyl ethyl ether (300 µl), ethanol (300 µl) and diethyl ether (300 µl) in water (15 ml) was prepared. A calibration series was prepared by diluting varying volumes of the working standard with water to a constant volume (2 ml)(Table 8.37).

Table 8.37: Calibration standards for bromoethyl ether, diethyl ether and ethanol

Nominal conc. standard	Working solution volume, µl	[Bromoethyl ethyl ether], µg/l	[Ethanol], µg/l	[Diethyl ether], µg/l
0	0	0	0	0
5	20	9.1	26.3	4.7
10	40	18.1	52.7	9.5
25	100	45.3	131.7	23.
50	200	90.7	263.3	47.3
75	300	136.0	395.0	71.0
100	400	181.3	526.7	94.7
200	800	362.7	1053.3	189.3
300	1200	5544.0	1580.0	284.0
400	1600	725.3	2106.7	378.7
500	2000	906.7	2633.0	473.3

The calibration lines for both the bromoethyl ethyl ether and the diethyl ether were good, with correlation coefficients >0.9 using a linear fit. The line for ethanol, however, was not good, as it was not possible to detect any ethanol at a concentration less than 500 µg/l, because the ethanol is so water soluble it does not purge well.

Ethanol calibration curve (Expt. 38)

A working standard was prepared by addition of an aliquot (300 µl) of a stock solution (ethanol 25 µl in water 15 ml) to water (15 ml). A calibration series was prepared by diluting varying volumes of the working standard with water to a constant volume (2 ml)(Table 8.38).

Table 8.38: Calibration standards for ethanol

Nominal concentration standard	Working solution volume, µl	[ethanol], µg/l
0	0	0

5	20	263.3
10	40	526.7
25	100	1316.7
50	200	2633.3
75	300	3950
100	400	5266.7
200	800	10533.3
300	1200	15800
400	1600	21066.7
500	2000	26333.3

An acceptable calibration curve was produced, but the limit of detection was confirmed from the previous experiment.

Degradation of bromoethyl ethyl ether on a Pd/Fe (Expt. 39)

Pd/Fe (0.25 ± 0.02 g) was added to a set of vials. A stock solution of bromoethyl ether (1.5 µl) in water (15 ml) was sonicated (5 min). The vials were filled to the brim with water and an aliquot (100 µl) of the stock solution added to each. The vials were shaken and analysed (P&T, GC-MS). The degradation was also monitored for a longer period of time as it was much slower than the chloroform degradation (Table 8.39).

Table 8.39: Peak areas for the large scale bromoethyl ether degradation

Time, min	Pd/Fe	Control	Time, min	Pd/Fe	Control
0	nm	33592375	420	12317245	19191257
10	18572591	20624710	480	11472986	17099723
30	17930320	20208762	540	12367201	17093193
60	18079995	20220332	600	13160442	17207146
90	17607206	19901524	1440	9479246	16659073
120	15553755	19384268	1560	10588788	18513019
150	13711715	19119724	1725	7877480	18619790
180	11863495	19175462	1800	8973646	17931104
240	12190650	19423156	1920	8329541	17471257
300	14399978	18556575	k_1, min^{-1}	0.0003	na
360	14083213	18484900	$t_{½}$, min	2310	na

nm = not measured, not applicable

Methylcyclopentane, cyclohexane and hexene calibration curve in the presence of iron filings (Expt. 40)

Stock solutions of hex-1-ene (0.5 µl) in methanol (15 ml), methylcyclopentane (0.5 µl) in methanol (15 ml) and cyclohexane (0.5 µl) in methanol (15 ml) were prepared. A combined working solution of hex-1-ene (300 µl), methyl cyclopentane (300 µl) and cyclohexane (300 µl) in water (15 ml) was prepared. Pd/Fe (0.25 ± 0.02 g) was added to a set of vials. A calibration series was prepared by diluting varying volumes of the working standard with water to a constant volume (2 ml) (Table 8.40), which were shaken (10 hr) and analysed (P&T, GC-MS).

Table 8.40: Methyl cyclopentane, cyclohexane and hexene calibration in the presence of Pd/Fe

Nominal conc. standard, µg/l	Working solution volume, µl	[Methylcyclo-pentane], µg/l	[Cyclohexane], µg/l	[Hexene], µg/l
0	0	0	0	0
5	12.5	3.1	3.2	2.8
10	25	6.2	6.5	5.6
25	62.5	15.6	16.2	14.0
50	125	31.2	32.5	28.0
75	187.5	46.8	48.7	42.1
100	250	62.4	64.9	56.1
200	500	124.8	129.9	112.2
300	750	187.2	194.8	168.2
400	1000	249.7	259.7	224.3
500	1250	312.1	324.6	280.4
700	1750	436.9	454.5	392.5
800	2000	499.3	519.4	448.6

The calibration curves were all satisfactory with correlation coefficients > 0.9 using a linear fit. The limit of detection for all parameters was approximately 5 µg/l. When the peak area of hexene was compared with an earlier calibration curve, the latter area was found to be approximately 20% lower.

Methylcyclopentane, cyclohexane and hexene adsorption on Pd/Fe (Expt. 41)

Stock solutions of methylcyclopentane, cyclohexane and hexene and a combined intermediate solution were prepared as described in the previous experiment. Pd/Fe (0.25 ± 0.02 g) was added to a set of vials. Standards were prepared at three concentrations by dilution of the combined intermediate in the vials which were shaken and analysed (P&T, GC-MS). The standards were set up 10 times at each level, 5 with Pd/Fe and without. The standards were set up at 10, 62.5 and 500 µg/l. The 10 µg/l standards were analysed after 6 hr, the 62.5 µg/l after 7 hr and the 500 µg/l after 10 hr (Table 8.41).

Table 8.41: Methyl cyclopentane, cyclohexane and hexene incubation with and without Pd/Fe

Std, µg/l	Methylcyclopentane		Cyclohexane		Hexene	
	Pd/Fe	no Pd/Fe	Pd/Fe	no Pd/Fe	Pd/Fe	no Pd/Fe
10	416314	365662	147113	397402	nd	nd
	439383	638892	321198	306343	nd	618733
	490658	623407	514250	399777	497154	395033
	404573	474468	205009	323659	459678	nd
	389874	544252	219863	597498	414114	476760
62.5	1335315	1097005	1453006	926517	974987	703022
	1462001	1107514	1392390	896767	nr	568205
	2544931	1198227	1865832	980423	3272615	707480
	999229	1097821	1123726	996955	743780	897142
500	6051883	9620234	6413615	9536711	3315469	6224915
	6275767	7241364	6876499	7901587	3091733	5319917
	4899060	7581209	5700573	7790083	4484340	8841208
	6358666	8190124	6944388	8982904	2884905	4240381

	6841731	7447870	7817405	8197475	3800220	5318770

nd = nil detected, nr = no result, NB one of the 62.5 µg/l sets was lost on transfer to the instrument.

Degradation of bromoform on a Pd/Fe (Expt. 42 & 43)

Pd/Fe (0.25 ± 0.02 g) was added to a set of vials which were filled to the brim with water and an aliquot (5 µl) of the stock solution of bromoform (0.2 µl in water 2 ml, sonicated 5 min) added to each. The vials were shaken and analysed (P&T, GC-MS) (Table 8.42).

Table 8.42: Peak areas for the bromoform degradation on Pd/Fe

Time, min	Replicate 1		Time, min	Replicate 2	
	Pd/Fe	Control		Pd/Fe	Control
0	nm	4399299	0	nm	8240606
10	3354156	10891249	5	8013315	11137701
30	3928978	8821092	10	6841064	9412773
60	172106	4820918	15	6233529	9669615
90	1016026	7191031	20	3521164	9444354
120	136628	8294435	25	5564369	9536894
150	199644	5293582	30	2361891	6579624
180	nd	5203556	40	659649	11062361
240	nd	4907894	50	330660	7672472
300	nd	6636897			
360	nd	4829691			
420	nd	5434992			
480	nd	5994891			
k_1, min^{-1}	0.0223	na	k_1, min^{-1}	0.0738	na
$t_{½}$, min	31.1	na	$t_{½}$, min	9.4	na

nm = not measured, nd = nil detected, na = not applicable

Replicate 1 was non-linear after 60 min and so the reaction was rerun over a shorter time span. Both runs had similar gradients for the rate *vs* time plot over 50 mins.

Degradation of bromohexane on a Pd/Fe (Expt. 44 & 45)

Pd/Fe (0.25 ± 0.02 g) was added to a set of vials which were filled to the brim with water and an aliquot (5 or 10 µl) of the stock solution of bromohexane (0.2 µl in water 2 ml, sonicated 5 min) added to each. The vials were shaken and analysed (P&T, GC-MS) (Table 8.44).

Table 8.44: Peak areas for the bromohexane degradation on Pd/Fe

Time, min	5 µl		10 µl	
	Pd/Fe	Control	Pd/Fe	Control
0	nm	758821	nm	2222225
10	451595	480546	2048396	2741702
30	608714	942829	1754232	3164749
60	334152	606126	1564312	1691375
90	250627	586696	963263	1321691
120	213648	nr	1139701	1899480
150	310364	481220	601900	2248656

180	141794	402148	707297	1524168
210	209999	502477	244697	2207834
240	213575	389682	307196	1177453
300	nd	368249		
360	nd	322017		
420	nd	652185		
480	nd	412558		
k_1, min^{-1}	0.0044	na	0.0089	na
$t_{1/2}$, min	157.5	na	77.9	na

nm = not measured, nd = nil detected, nr = no result, na = not applicable * excluded from calculations

Degradation of *cis*- and *trans*- dichloroethylene on a Pd/Fe (Expt. 46)

Stock solutions of *cis*-dichloroethylene (0.2 µl in water 2 ml) and *trans*-dichloroethylene (0.2 µl in water 2 ml) were prepared and sonicated (5 min). Pd/Fe (0.25 ± 0.02 g) was added to two sets of vials. These and another two sets of vials were filled to the brim with water. Aliquots of *cis*-dichloroethylene stock solution (5 µl) and *trans*-dichloroethylene stock solution (5 µl) were added to one set each of reaction and control vials. The vials were shaken and analysed (P&T, GC-MS)(Table 8.46) on a 10 m thick film HP624 column, 35(5) x 20 to 150(0), inj 220 split ratio 40:1.

Table 8.46: Peak areas for *cis*- and *trans*-dichloroethylene degradation on Pd/Fe

Time, min	Pd/Fe		Control	
	cis-DCE	*trans*-DCE	*cis*-DCE	*trans*-DCE
0	nm	nm	634582	752787
10	759943	700244	615960	624396
30	637386	536503	571568	669170
60	490349	355264	680539	717380
90	349790	303055	698670	571110
120	433711	159342	718154	659700
150	499683	294627	595691	688273
180	360073	125758	525087	518681
240	326598	110572	622036	602370
300	172819	30366	624377	491088
360	222261	77217	585668	541396
k_1, min^{-1}	0.0035	0.0078	na	na
$t_{1/2}$, min	198	88.9	na	na

nm = not measured, nd = nil detected, nr = no result, na = not applicable * excluded from calculations

Degradation of carbon tetrachloride and tetrachloroethylene on Pd/Fe (Expt. 47)

Stock solutions of carbon tetrachloride (0.2 µl) in water (2 ml) and a separate stock solution of tetrachloroethylene (0.2 µl) in water (2 ml) were sonicated (5 min). Pd/Fe (0.25 ± 0.02 g) was added to two sets of vials. The vials were filled to the brim with water and an aliquot of the carbon tetrachloride stock solution (10 µl) added to one set of vials and to the control vials. An aliquot of the tetrachloroethylene stock solution (10 µl) was added to the other set of vials and also to the

control vials. The vials were shaken and analysed (P&T, GC-MS)(Table 8.47). The results for carbon tetrachloride are not reported because the reaction proceeded so quickly that only 3 results were obtained. The degradation was repeated under a shorter time scale and is reported under experiment 48.

Table 8.47: Peak areas for tetrachloroethylene degradation on Pd/Fe

Time, min	Pd/Fe	Control	Time, min	Pd/Fe	Control
0	nm	8595322	180	1401068	5456484
10	7415936	7046422	240	1585963	3939014
30	5528165	5939364	300	1089129	3938320
60	2524739	6548316	360	1126448	4142648
90	3818444	5509373	k_1, min^{-1}	0.0073	na
120	1145885	5507415	$t_{½}$, min	95.0	na
150	1269741	6247175			

nm = not measured, na = not applicable

Degradation of carbon tetrachloride on a Pd/Fe, a fast reaction (Expt. 48)

A stock solution of carbon tetrachloride (0.2 µl) in water (2 ml) was sonicated (5 min). Pd/Fe (0.25 ± 0.02 g) was added to a set of vials which were filled to the brim with water. An aliquot (10 µl) of the stock solution was added to one of each set of the vials, capped and shaken. After a timed interval (5 min) an aliquot of stock solution (10 µl) was added to the next vial in each of the two sets and also shaken. This aliquot addition after a set time interval continued until all the vials had been spiked and placed on the shaker. A further time period (5 min) elapsed then the samples were removed from the shaker, the liquid fractions removed from the vials and introduced to the purge and trap autosampler by means of a gas tight syringe. The samples were analysed as previously described (Table 8.48).

Table 8.48: Peak areas for carbon tetrachloride degradation on Pd/Fe

Time, min	Pd/Fe	Control	Time, min	Pd/Fe	Control
0	nm	20083179	30	257485	19606574
5	14912334	27025435	35	330666	19023587
10	15466456	27940474	40	nd	15054383
15	10787385	25787589	k_1, min^{-1}	0.0730	na
20	3850012	22728841	$t_{½}$, min	9.5	na
25	158216	21371779			

nm = not measured, nd = nil detected, na = not applicable

Degradation of bromomethylcyclopropane on a Pd/Fe (Expt. 49)

A solution of bromomethylcyclopropane in dichloromethane (0.1 µl in 2 ml) was prepared and diluted 10 fold. An aliquot (1 µl) was injected onto the GC-MS configured with a liquid injector tower to confirm the spectrum of the starting material.

Pd/Fe (0.25 ± 0.02 g) was added to a set of vials, which were filled to the brim with water

and an aliquot (10 µl) of bromomethylcyclopropane stock solution (0.5 µl in water 2 ml) added to each. The vials were shaken and analysed (P&T, GC-MS)(Tables 8.49a, 8.49b).

Table 8.49a GC-MS data for bromomethylcyclopropane and bromomethylcyclopropane

Liquid injection:	Bromocyclobutane	Bromomethylcyclopropane
Retention time, mins	2.12	2.24
Counts	118438	826607
Counts ratio	12	88
P&T retention times, mins	4.75	4.87

Table 8.49b: Peak areas for the degradation of bromomethylcyclopropane on Pd/Fe

Time, min	Bromocyclobutane		Bromomethylcyclopropane
	Pd/Fe	Control	Control
0	nm	4858016	3783038
10	2861877	2652978	0
30	2142532	1597956	0
60	1115747	1031824	0
90	842160	923789	0

Comparison of the activity of freshly prepared and aged Pd/Fe (Expt. 50)

Pd/Fe filings (10 g) used in the previous experiment which had been prepared one week earlier were taken and rinsed with water. Fresh Pd/Fe (0.25 ± 0.02 g) was added to one set of vials and the aged Pd/Fe (0.25 ± 0.02 g) was added to a second set of vials which were filled to the brim with water. An aliquot (5 µl) of a stock solution of 6-bromohexane (0.2 µl in water 2 ml) was added to each vial. The vials were shaken and analysed (P&T, GC-MS)(Table 8.50).

Table 8.50: Bromohexane degradation on freshly prepared and aged Pd/Fe

Time, min	Fresh	Aged	Control
0	nm	nm	1431521
10	1527095	1927285	1969387
30	982947	1491839	1792401
60	605321	926510	1390000
90	750123	1055608	1775083
120	910690	1048657	1600643
150	653281	826085	1521620
180	519560	876837	1391425
240	494945	536705	1429157
300	368514	405310	1459862
360	nd	246303	1369237
420	nd	295757	1516348
k_1, min^{-1}	0.0038	0.0046	na
$t_{½}$, min	182.4	150.7	na

nm = not measured, nr = no result, nd = nil detected, na = not applicable

Comparison of the activity of normal and hyper-Pd/Fe (Expt. 51)

Potassium hexachloropalladate (40 mg) was dissolved in water (80 ml) and aliquots added

(5 ml) to Pd/Fe (5 g) until the colour of the solution persisted. Two identical sets of vials were taken, one set had "normal" Pd/Fe (0.25 ± 0.02 g from 5 g Fe) added to them and the other set had hyper-Pd/Fe (0.25 ± 0.02 g) added to them, both were filled to the brim with water. A stock solution of bromohexane (0.2 µl) in water (2 ml) was prepared as previously described and an aliquot (10 µl) added to each vial. The vials were shaken and analysed (P&T, GC-MS)(Table 8.51).

Table 8.51: Peak areas for bromohexane degradation on normal and hyper-Pd/Fe

Time, min	Normal	Hyper	Control
0	nm	nm	777607
10	1729046	1475637	1918720
30	1383064	1058672	2010141
60	1191503	1069977	1460828
90	842519	nd	1357048
120	572732	216959	1268941
150	697131	nd	1208023
180	715801	nd	1056850
240	385596	nd	1086257
300	nd	nd	864929
360	262921	nd	886580
k_1, min^{-1}	0.0052	0.0171	na
$t_{½}$, min	133.3	40.5	na

nm = not measured, nd = nil detected, na = not applicable

Comparison of the activity of Pd/Fe and activated iron (Expt. 52)

Pd/Fe (0.25 ± 0.02 g from 5g Fe) was added to one set of vials and activated iron (0.25 ± 0.02 g from 5g Fe) to another. All the vials were filled to the brim with water and an aliquot (10 µl) of a stock solution of bromohexane (0.2 µl in water 2 ml) was added to each vial which were shaken and analysed (P&T, GC-MS)(Table 8.52).

Table 8.52: Peak areas for bromohexane degradation on palladised or activated iron

Time, min	Activated	Palladised	Control
0	nm	nm	3986704
10	3563147	4571159	5414770
30	2387593	3095712	4456029
60	2721722	1762933	3346216
90	2297611	807206	3567951
120	1758005	477023	3719557
150	2087955	1051023	3575236
180	1340153	431981	2289819
240	1191991	348610	3092044
300	776133	87750	2316475
360	772149	164260	3315004
420	524727	nd	2582767
480	829549	nd	2208733
k_1, min^{-1}	0.0047	0.0118	na
$t_{½}$, min	147.5	58.7	na

nm = not measured, nr = no result, nd = nil detected, na = not applicable

Degradation of (2-bromoethyl)benzene aqueous THF (Expt. 54)

A stock solution of (2-bromoethyl)benzene (0.4 µl) in water (2 ml) was prepared. Pd/Fe (0.25 ± 0.02 g) was added to two sets of vials. Aqueous THF (5% *v/v* THF/ water, 1 ml) was added to each of the first set of vials. Water (1 ml) was added to each of the other set and the control vials. An aliquot of (2-bromoethyl)benzene solution (50 µl) was added to each vial which was immediately capped. The vials were stored in a plastic box on a flatbed shaker (120 rpm) until required for analysis. Immediately prior to analysis, the samples were removed from the box and extracted with diethyl ether (2 x 200 µl). The organic layer, also containing the THF, was transferred to a clean vial, capped and an aliquot (1 µl) injected onto the GC-MS (Table 8.54).

Table 8.54: Peak areas for (2bromoethyl)benzene degradation on Pd/Fe in 5% aqueous THF or water

Time, min	Water	THF	Control	Time, min	Water	THF	Control
0	nm	2529846	21440750	300	23096	13616	2193877
60	2145945	2537689	3059710	360	22790	19589	2437496
120	1230722	1805205	4054648	k_1, min^{-1}	0.0173	0.0158	na
180	888607	1034268	2376721	$t_{1/2}$, min	40	44	na
240	155851	408401	2231275	Conv., %	99	99	na

nm = not measured

Degradation of (2-bromoethyl)benzene in various concentrations of THF (Expt. 55)

A stock solution of (2-bromoethyl)benzene (3 µl) in water (15 ml) was prepared. Pd/Fe (0.25 ± 0.02 g) was added to a series of vials which were were split into 6 sets. Aqueous THF solutions (0, 10, 25, 50, 75, 100 % *v/v* THF/ water) were prepared. Each set of vials had one concentration of THF solution (1 ml) added and the control vials had water (1 ml) added to them. An aliquot of the (2-bromoethyl)benzene stock solution (100 µl) was added to each vial, which was shaken until required for analysis. Immediately prior to analysis, the vials were extracted with diethyl ether (2 x 200 µl). The (top) organic layer also containing the THF was transferred to a clean vial, capped and injected onto the GC-MS (Table 8.55, Fig 8.55).

Table 8.55: Peak areas for (2-bromoethyl)benzene degradation in varying concentrations of THF

Time, min	0%	10 %	25 %	50 %	75 %	100 %	Control
0	nm	nm	nm	nm	nm	nm	1289445
30	909268	2502771	2929312	nr	1184722	783570	1417765
60	1650238	2086424	2924688	nr	1123463	823099	2017758
90	1942524	2282104	1856630	nr	nr	nr	2518760
120	1600328	1386566	1447795	nr	nr	nr	2309516
180	1156458	814355	1352903	nr	nr	nr	283463
240	131245	424850	1084902	nr	nr	nr	3824794

300	360724	80579	584286	nr	nr	nr	2842893
360	405705	65380	483650	nr	nr	nr	1407689
420	63565	70677	365617	1571147	989967	822978	2153461
480	30803	23390	102107	1462979	nr	990244	2937423
k_1, min^{-1}	0.0080	0.0110	0.0064	0.0012	0.0004	+0.0003†	na
$t_{½}$, min	86.6	63.0	108.3	577.6	1732.9	2310.5	na
Conv. %	98	99	97	7	16	-26	na

nm = not measured, nr = no result, na = not applicable; † positive slope

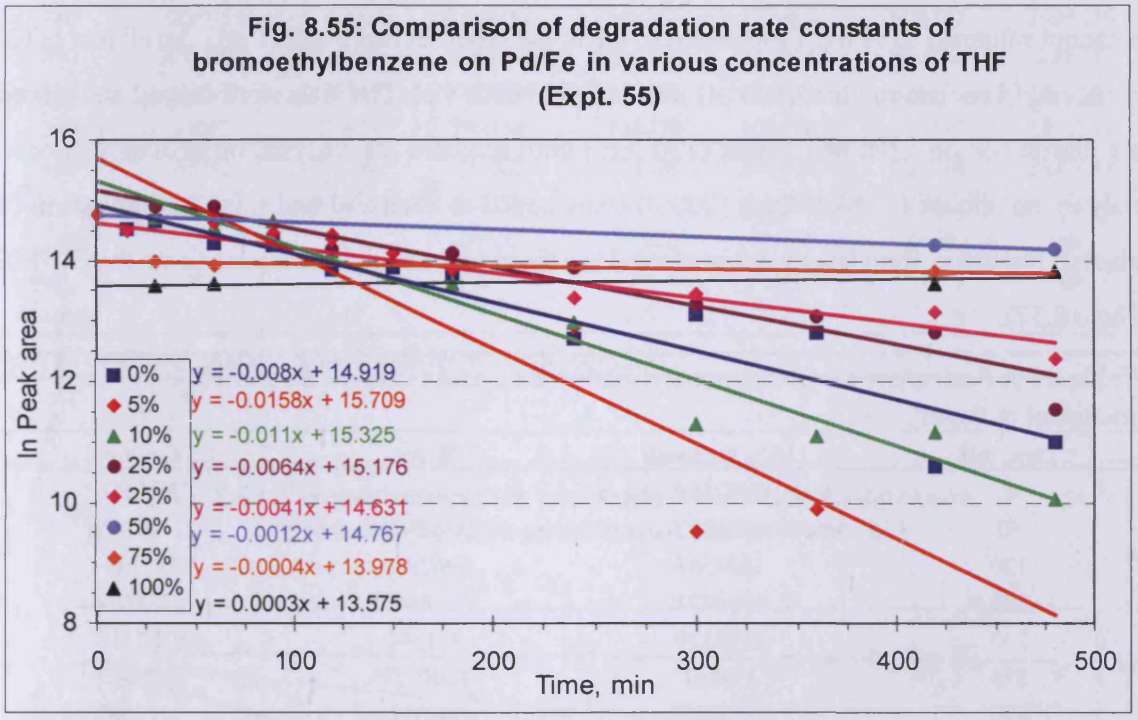

Degradation of (2-bromoethyl)benzene in 25 % THF solution (Expt. 56)

A stock solution of (2-bromoethyl)benzene (3 µl) in water (15 ml) was prepared. Pd/Fe (0.25 ± 0.02 g) was added to two sets of vials, one set had aqueous THF solution (25 % *v/v* THF/ water, 1 ml) added to them, the other set had water (1 ml). An aliquot of (2-bromoethyl)benzene solution (100 µl) was added to each vial which was shaken until required for analysis. Immediately prior to analysis, the samples were extracted with chloroform (200 µl), the aqueous layer decanted off and the chloroform layer (also containing the THF) transferred to a clean vial and an aliquot (1 µl) injected onto the GC-MS (Table 8.56).

Table 8.56: Peak areas for (2-bromoethyl)benzene degradation on Pd/Fe in 25% *v/v* THF or water

Time, min	25 % THF	Water	Control	Time, min	25 % THF	Water	Control
0	nm	nm	2918120	240	650304	332111	1644138
15	1988856	2056019	2372692	300	698551	491191	1931492
30	1200681	2280471	1856238	360	19924*	358586	1955974

60	2277008	1610925	1586556	420	516099	39668	2090625
90	1867634	1555942	2533817	480	238299	60109	2195360
120	1711771	1025313	1822046	k_1, min^{-1}	0.0041	0.0085	na
150	1367530	1085156	2831413	$t_{½}$, min	169.1	82	na
180	1064090	963857	2299184	Conv., %	88	97	na

nm = not measured, na = not applicable

Degradation of (2-bromoethyl)benzene in 10 % methanol solution (Expt. 57)

A stock solution of (2-bromoethyl)benzene (0.2 µl) in water (2 ml) was prepared as previously described. Pd/Fe (0.25 ± 0.02 g) was added to two sets of vials, one set had aqueous methanol solution (10 % *v/v*, 1 ml) added to them, the other set had water (1 ml). An aliquot of (2-bromoethyl)benzene solution (100 µl) was added to each vial. The vials were capped and placed in a plastic box on a flat bed shaker (120 rpm) until required for analysis. Immediately prior to analysis, an aliquot of chloroform (200 µl) was added to each vial and mixed by inversion (4 inverts). The chloroform layer was transferred to a clean vial, capped and injected onto the GC-MS (Table 8.57).

Table 8.57: Peak areas for (2-bromoethyl)benzene degradation on Pd/Fe in 10% *v/v* methanol or water

Time, min	10 % methanol	Water	Control
0	4902165	nm	27295661*
60	2491327	3784368	2449281
120	1634567	1968959	297143
165	1956723	1314641	5188809
240	2392139	874544	2832110
315	410867	1000779	2779247
390	4078205*	237912	1511582
k_1, min^{-1}	0.0059	0.007	na
$t_{½}$, min; Conv. %	118; 92	99; 94	na

nm = not measured, * = excluded, na = not applicable

Degradation of (2-bromoethyl)benzene in various concentrations of methanol (Expt. 58)

Pd/Fe (0.25 ± 0.02 g) was added to a series of vials which were were split into 6 sets. Aqueous methanol solutions (0, 10, 25, 50, 75, 100 % *v/v* methanol/ water) were prepared. Each set of vials had one concentration of methanol solution (1 ml) added and the control vials had water (1 ml) added to them. An aliquot of the (2-bromoethyl)benzene stock solution (100 µl) was added to each vial which was shaken until required for analysis. Immediately prior to analysis, the vials were extracted with chloroform (200 µl). The organic layer was transferred to a clean vial. The 75 %*v/v* samples were first filtered through a plug of silanised glass wool packed into a Pasteur pipette to break the emulsion. The chloroform was completely miscible with the 100 % *v/v* samples, and the methanol/chloroform layer was transferred in total to the clean vials. The vials

were capped and injected onto the GC-MS (Table 8.58, Fig 8.58).

Table 8.58: Peak areas for (2-bromoethyl)benzene degradation in varying concentrations of methanol

Time, min	0%	10 %	25 %	50 %	75 %	100 %	Control
0	2583202	3256677	3860442	2788822	1069079	711565	2583202
15	2191468	2865065	3356193	4376007	1191420	576284	3149519
30	1860241	2579531	2812924	4961269	1867850	611028	2637782
60	1327295	2355528	2778803	4217789	1234718	596681	2328749
90	870501	1826283	2267764	3554700	1417981	672672	1811001
120	1196210	1632127	2479100	4182962	1301328	606323	2231924
150	995039	1462129	1791863	6922057	1330359	620459	2779831
180	1007914	1050011	2168452	3440556	1426866	608777	2694876
240	253796	2317245	1983829	4466170	1160442	605567	2889751
300	212529	396549	1719976	4059086	1228394	626496	2700145
360	99067	121674	797155	3748773	1021592	573319	2591238
480	20082	23164	752529	3121335	3065095	591118	2872494
k_1, min^{-1}	0.0095	0.0093	0.0032	0.0003	0.0008*	0.0002	na
$t_{½}$, min	73.0	74.5	216.6	2310	886.4	3466	na
Conv., %	99	99	81	29	4.4	17	na
Multiple	129	141	5.1	1.4	0.35	1.2	na

nd = nil detected, * gradient of line is positive, na = not applicable

Fig. 8.58: Comparison of rate constants for bromoethylbenzene degradation in various methanol concentrations

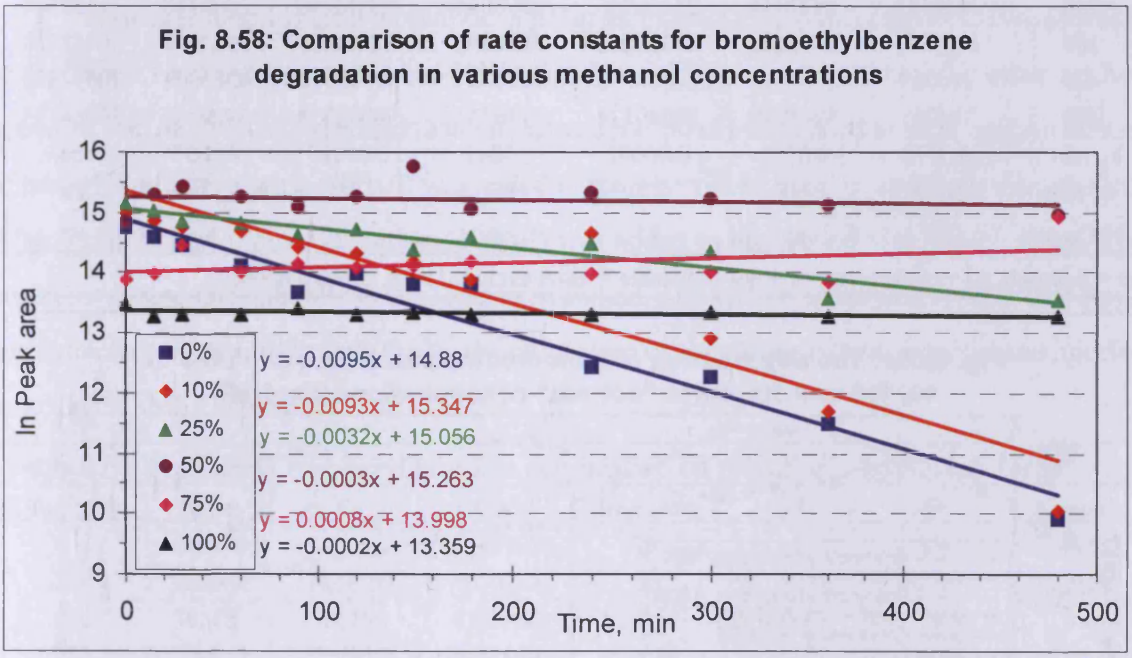

Degradation of 10, 100, 500 fold increase in (2-bromoethyl)benzene (Expt. 59)

Stock solutions of (2-bromoethyl)benzene (30 µl, 300 µl and 1500 µl) in methanol (15 ml) corresponding to 10, 100 and 500 fold increase respectively over the "normal" concentration were prepared. Pd/Fe (0.25 ± 0.02 g) was added to each of three sets of vials and water was added (900

µl) of to each vial. An aliquot of the appropriate stock solution (100 µl) was added to each vial. The vials were capped and placed on a flatbed shaker (120 rpm) until required for analysis. At the requisite time point, the vials were extracted with chloroform (500 µl) and the organic layer transferred to clean vials. A second chloroform extraction (500 µl) was performed on the 100 and 500 fold vials and combined with the first. The 500 fold organic layer was further diluted with chloroform (500 µl)(Table 8.59, Figs 8.59a, 8.59b). The samples were diluted as to avoid overloading the detector.

Table 8.59: Peak areas for 10, 100 and 500 fold increased (2-bromoethyl)benzene degradation and peak areas for the emergence of ethylbenzene

Time, min	10 Fold		100 Fold		500 Fold		Control
	Br-ethyl benzene	Ethyl benzene	Br-ethyl benzene	Ethyl benzene	Br-ethyl benzene	Ethyl benzene	Br-ethyl benzene
0	12001216	nd	27039482	nd	108475047	nd	nr
15	9815121	1050949	27828957	571264	108104351	nd	27505152
30	12568969	2229596	30632459	1512440	99722849	739283	29898504
60	11403604	3229856	31226146	2173486	105351936	1380062	29932645
90	9208286	4030115	28348107	2169981	101454755	1445246	31854903
120	9326228	4522649	1540545*	103222*	108296884	1936641	3139748*
150	7831714	4788935	27245132	3437825	107631381	2324908	31760472
200	8299164	4902746	28083911	3416676	107307997	2424466	28617950
240	3840132	6772884	25456936	4798044	103186902	2800748	31158544
360	1005903	7786685	22332103	5678396	110030995	3934098	30342184
420	716005	8054796	22008092	7290457	99555312	4385202	28044800
480	384745	8241179	17049124	7746751	98008558	5929667	29056175
k_1, min^{-1}	0.0073	0.0033	0.00092	0.0042	0.00010	0.0037	na
$t_{½}$, min	95.0	210	770	165	6931	187	na
% Conv.	96	na	37	na	10	na	na

nr = no result, nd = nil detected, na = not applicable * result excluded from all calculations

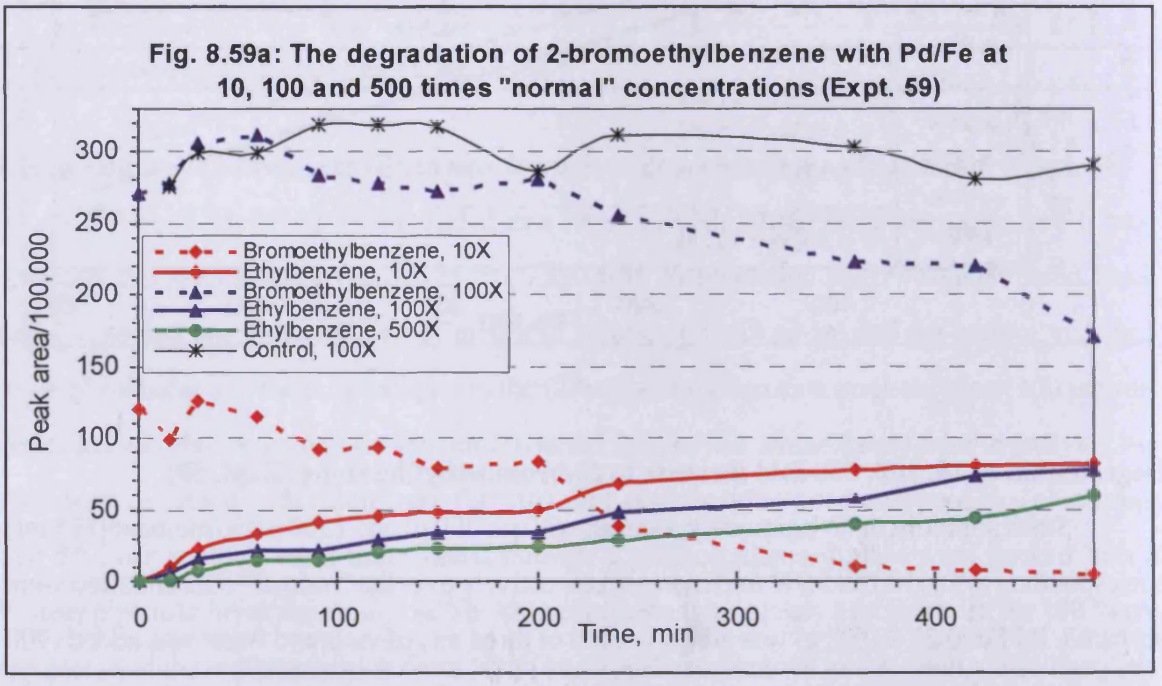

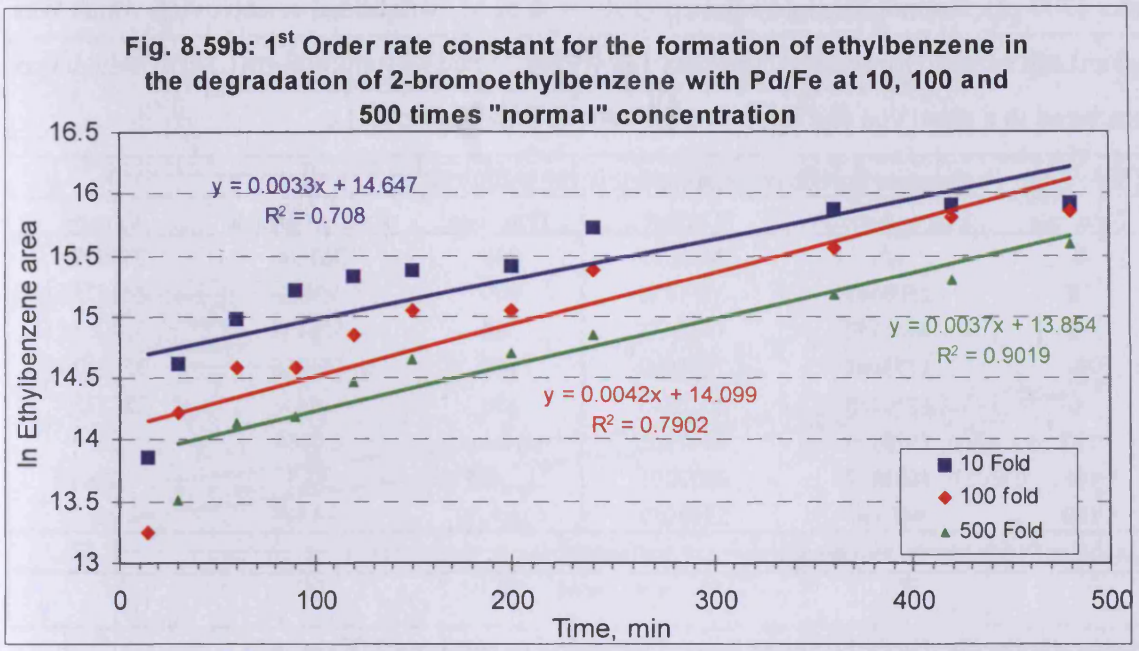

Comparison of the degradation of benzyl bromide on palladised and activated iron in methanol (Expt. 60)

A stock solution of benzyl bromide (3 µl) in methanol (15 ml) was prepared. Two identical sets of vials were taken, one set had Pd/Fe (0.25 ± 0.02 g) added to them, the other set had activated iron (0.25 ± 0.02 g) added to them and water (900 µl) was added to each vial. An aliquot of benzyl bromide solution (100 µl) was added to the first vial in each set and these vials shaken. After 5 min benzyl bromide solution (100 µl) was added to the second vial in each series. The process was repeated until all the vials had been spiked. The vials were shaken for a further 5 min and extracted with chloroform (200 µl). The chloroform was transferred to a clean vial and injected onto the GC-MS (Table 8.60).

Table 8.60: Peak areas for benzyl bromide degradation on palladised and activated iron

Time, min	Pd/Fe	Fe	Control	Time, min	Pd/Fe	Fe	Control
0	nm	nm	4048903	25	nd	18549	3744775
5	566349	1424760	4670252	30	nd	32267	3379310
10	30518	936190	4135984	k_1, min^{-1}	0.5842	0.1904	na
15	nd	217845	4371949	$t_{½}$, min	1.2	3.6	na
20	nd	15767	4300326	Conv., %	95	98	na

nm = not measured, nd = nil detected, na = not applicable

Degradation of bromophenetole (Expt. 61)

A stock solution of bromophenetole (15.01 mg) in methanol (15 ml) was prepared and sonicated (15 min) to aid dissolution. Pd/Fe (0.25 ± 0.02 g) was added to a series of vials followed

water (900 µl). Bromophenetole solution (100 µl, 0.5µM) was added to each vial, which was shaken until required for analysis. The samples were extracted with chloroform (200 µl) which was transferred to a clean vial and injected onto the GC-MS (Table 8.61).

Table 8.61: Peak areas for the bromophenetole degradation

Time, min	Bromophenetole	Control	Time, min	Bromophenetole	Control
0	nm	3030255	240	363206	2346791
10	2600408	3111136	300	99481	4435252
30	4661750	1863437	360	509497	5229155
60	1775081	2276869	420	164356	3782176
90	1736085	2020253	480	nd	2827357
120	1670025	2467925	k_1, min^{-1}	0.0084	na
165	1661487	2622271	$t_{½}$, min	82.5	na
180	441568	2593959	Conv. %	94 %[a]	na

[a] Multiple 1/15.8; nm = not measured, na = not applicable

Preparative scale degradation of benzyl bromide in methanol (Expt. 62)

A set of vials were charged with Pd/Fe (0.25 ± 0.02 g), aqueous methanol solution (10 % *v/v*, 1500 µl) and benzyl bromide (10 µl) and shaken until required for analysis (Table 8.62, Fig 8.62). The concentration of benzyl bromide (density, 1.44 g/ml) was 14.4 mg in 1.5 ml, ie circa 10 mg/ml.

Table 8.62: Peak areas for the degradation of benzyl bromide and formation of toluene and bibenzyl in 10 % methanol

Time, min	Benzyl bromide	Toluene	Bibenzyl	Control
0	nm	nd	nd	131773461
10	144302825	1000574	790983	146093241
20	156872058	1892552	1354635	139977562
30	148596058	2936902	1146931	132230260
45	150299534	3708223	2310390	142698389
60	125957590	5392211	6709455	122344299
k_1, min^{-1}	0.0028	0.0314	0.0395	na
$t_{½}$, min; Conv. %	248; 13	22; 81	18 ; 88	na; 16

nm = not measured, na = not applicable

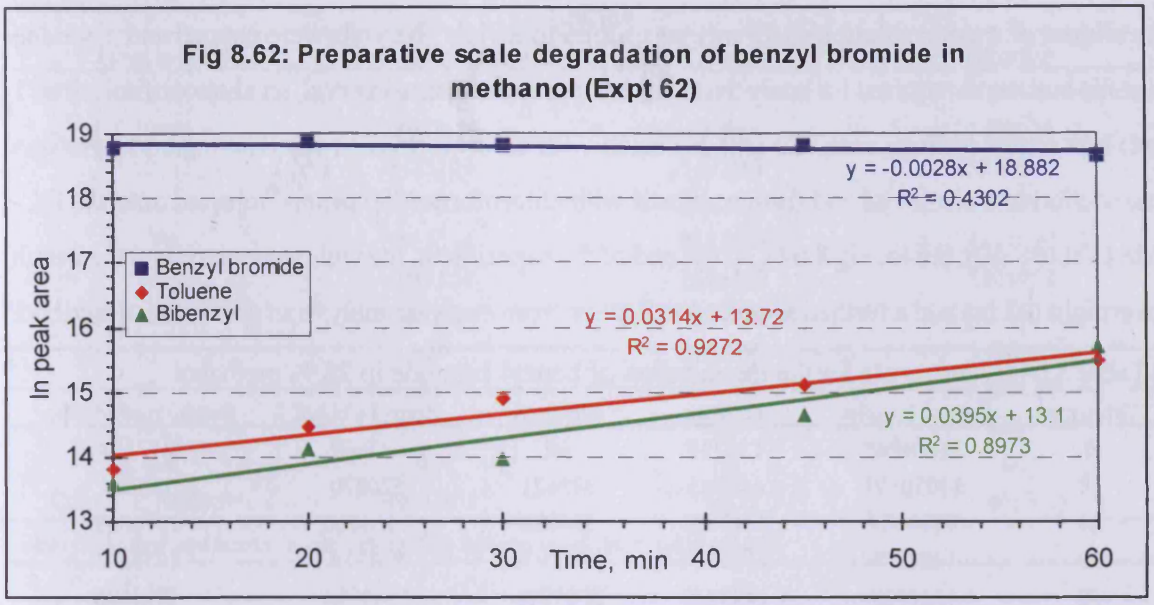

Preparative degradation of benzyl bromide, tentative conditions (Expt. 63)

Stock solutions of benzyl bromide (75 µl) in either aqueous methanol solution (25 % *v/v*, 15 ml) or aqueous THF solution (25% *v/v*, 15 ml) were sonicated. A series of vials charged with Pd/Fe (0.25 ± 0.02 g) and an aliquot of the appropriate stock solution (1500 µl) were shaken until required for analysis (Table 8.63). The last set of vials were placed in the sonic bath for an addition time period (30 min) prior to analysis. The samples were extracted with chloroform (200 µl) and the organic layer transferred to a clean vial. The extract was further diluted with chloroform (800 µl) and injected onto the GC-MS.

Table 8.63: Peak areas for the preparative degradation of benzyl bromide in either 25 % methanol or 25 % THF solutions

Time, min	Methanol			THF		
	Benzyl bromide[a]	Toluene	Bibenzyl	Benzyl bromide	Toluene	Bibenzyl
0	27252210	nd	nd	40059592	nd	nd
15	4653790	2842178	7206025	21810535	2412759	6488111
30	1995913	3692328	10368882	15737104	2369823	7892313
60	193507	3894582	9267227	11695768	3964556	14200527
90*	nd	1285873	2703344	2339058	4205787	12942724
k_1, min^{-1}	0.0778	na	na	0.0289	na	na
$t_{½}$, min	8.9	na	na	24.0	na	na

[a] 99 % conversion; nd = nil detected, nr = no result, na = not applicable * additional time in sonic bath

Large scale degradation of benzyl bromide in methanol and THF with use of a sonic bath (Expt. 64)

Stock solutions of benzyl bromide (75 µl) in methanol and THF (10 ml respectively) were

prepared. Pd/Fe (2.0 ± 0.05 g) was added to two vials. water (11.25 ml) was added to each vial, and an aliquot of a stock solution (3.75 ml) was added to a vial. The vials were capped and placed in a sonic bath until required for analysis. After an appropriate time interval, an aliquot of solution (1 ml) was removed from each vial and extracted with chloroform (250 µl). The organic layer was transferred to a clean vial and further diluted with chloroform (750 µl) and injected onto the GC-MS (Table 8.64a, 8.64b, Fig 8.64). At the end of the experiment, the vials were placed on the bench overnight (12 hr) and a further aliquot (1 ml) taken from each for analysis as previously described.

Table 8.64a: Peak areas for the degradation of benzyl bromide in 25 % methanol

Time, min	Benzyl bromide	Toluene	Bibenzyl	Benzyl alcohol	Benzyl methyl ether
0	11609845	155717	nd	137667	217258
10	11050503	644815	343621	520870	765956
20	9197485	1047401	536928	1066416	1526317
30	1438253	1189120	1042308	834310	1045121
40	1218729	1833812	2307976	1545712	1971620
50	568947	1891196	2831811	1743821	2196745
60	119752	1551866	2086929	1448080	1664163
75	nd	1280603	1973853	1338494	1514582
90	nd	1433288	1762813	1481632	1673562
k_1, min^{-1}	0.0774	0.0175	0.0202	0.020	0.016
$t_{½}$, min	9.0	40	34	35	43
R^2	0.92	0.46	0.53	0.55	0.46
% Conv.	99	89	81	91	87
Multiples	1/97	9	5	11	8

nd = nil detected, nr = no result

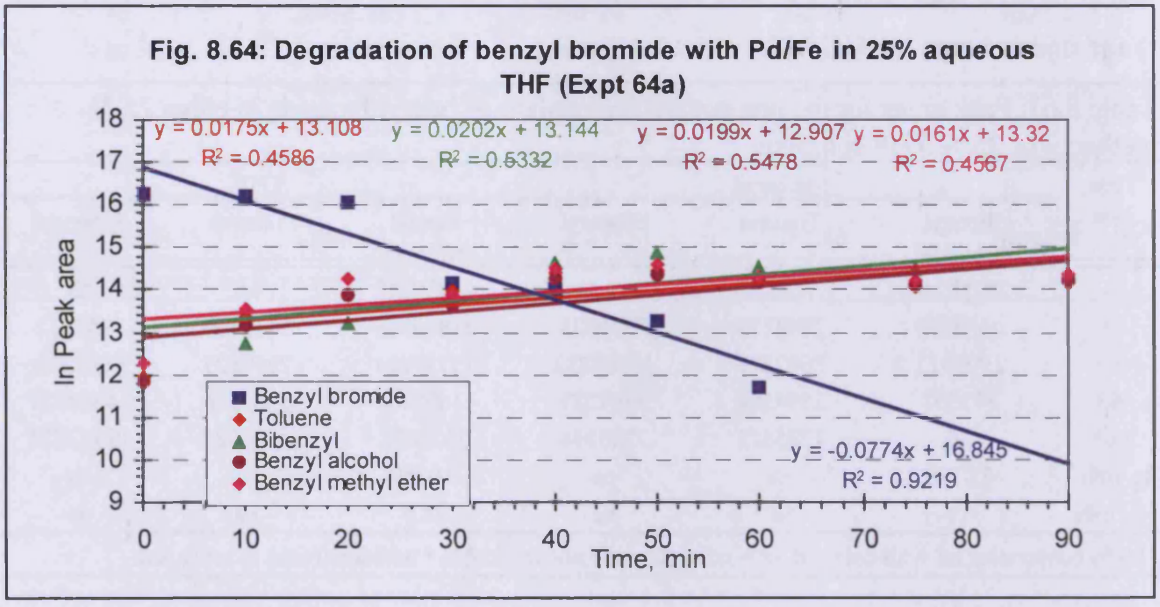

Fig. 8.64: Degradation of benzyl bromide with Pd/Fe in 25% aqueous THF (Expt 64a)

Table 8.64b: Peak areas for the large scale degradation of benzyl bromide in 25 % THF solutions

Time, min	Benzyl bromide	Toluene	Bibenzyl
0	16445461	88779	nd
10	12107657	734617	1359320
20	6423109	1492581	3316763
30	2709933	1950441	2959622
40	1865334	2177300	4411639
50	1047558	2326120	5801954
60	156399	2344128	4808501
75	nd	2155099	2570679
90	nd	2300952	3737615
k_1, min^{-1}	0.0718	na	na
$t_{½}$, min	9.7	na	na
Conv., %; Multiple	99; 1/105	96; 26	64; 3

Benzyl alcohol and benzyl methyl ether data not recorded, nd = nil detected

Phenol, ethoxybenzene and bromoethoxybenzene calibration (Expt. 65)

A commercially available stock solution of phenol (Sigma Aldrich, 500 µg/l) in methanol was obtained. A combined standard of ethoxybenzene (13.8 mg) and bromoethoxybenzene (10.5 mg) in methanol (10 ml) was prepared. A series of calibration standards was prepared by serial dilution with methanol (Table 8.65).

Table 8.65: Phenol, ethoxybenzene and bromoethoxybenzene calibration standards

Nominal concentration std	Volume phenol std, µl	Volume combined std, µl	Final volume, µl	[Phenol], µg/ml	[Ethoxy-benzene], µg/ml	[Bromo-ethoxy benzene], µg/ml
0	0	0	1000	0	0	0
2.5	5	2.5	1000	2.5	3.5	2.6
5	10	5	1000	5	6.9	5.3
10	20	10	1000	10	13.8	10.5
25	50	25	1000	25	34.5	26.3
50	50	25	500	50	69.0	52.5
75	75	37.5	500	75	103.5	78.8
100	100	50	500	100	138.0	105.0
150	150	75	500	150	207.0	157.5
200	200	100	500	200	276.0	210.0

The software on the data collection system was used to construct calibration curves for the three parameters. The calibration range used was 0 - 100 µg/ml. A linear fit was used and this gave correlation coefficients of 0.999, 0.994 and 0.991 for phenol, ethoxybenzene and bromoethoxybenzene respectively.

Quantification of bromophenetole degradation (Expt. 66)

The data generated from expt. no. 61 was quantified using the calibration curve data described in the previous experiment. These figures were converted to moles and the values compared (Table 8.66).

Table 8.66: Quantification of phenol, ethoxybenzene and bromoethoxybenzene

Time, min	Phenol		Ethoxybenzene		Bromoethoxy-benzene		Total	Ratio	Control	
	µg/ml	mMol	µg/ml	mMol	µg/ml	mMol	mMol	phenol :ethoxybenzene	µg/ml	mMol
0	nm	nm	nm	nm	nm	nm	na	na	58.54	0.293
10	1.85	0.02	0.60	0.005	50.52	0.253	0.278	4.0:1	59.73	0.299
30	3.30	0.035	1.46	0.012	86.52	0.431	0.478	2.9:1	37.27	0.186
60	6.11	0.065	1.85	0.015	35.31	0.177	0.257	4.3:1	44.49	0.222
90	4.77	0.051	1.32	0.011	34.17	0.171	0.237	4.6:1	39.74	0.199
120	8.67	0.092	2.69	0.022	32.45	0.162	0.276	4.2:1	47.58	0.238
165	9.52	0.101	2.81	0.023	33.64	0.168	0.292	4.4:1	50.30	0.252
180	10.76	0.114	2.76	0.023	9.17	0.046	0.183	5.0:1	49.34	0.247
240	14.03	0.149	3.92	0.032	7.14	0.036	0.217	4.7:1	45.46	0.227
315	17.19	0.183	5.39	0.044	2.58	0.013	0.240	4.2:1	84.80	0.424
360	16.79	0.179	5.63	0.046	11.02	0.055	0280	3.9:1	95.38	0.477
420	18.61	0.198	5.94	0.049	3.49	0.017	0.264	4.0:1	71.80	0.359
480	18.57	0.198	5.32	0.044	nd	nd	0.242	4.5:1	54.82	0.274
540	17.17	0.183	4.30	0.035	nd	nd	0.218	5.2:1	46.67	0.233
600	21.39	0.228	7.15	0059	nd	nd	0.287	3.9:1	56.11	0.281

nm = not measured, na = not applicable, nd = nil detected. The mean concentration of bromophenetole from the control values is 0.281 mMol. The total number of moles for the sum of the reactant and products is 0.268 mMole, a 95% recovery.

Degradation of benzyl bromide in D_2O (Expt. 67)

Iron filings (1 g) were activated and palladised in D_2O. Pd/Fe (0.25 ± 0.02 g), D_2O (1 ml) and benzyl bromide (10 µl) from a stock solution (0.2 µl in D_2O, 2 ml), were added to vials, which were shaken and extracted with chloroform (250 µl). The organic layer was transferred to vial and injected onto the GC-MS. Samples were analysed in duplicate (Table 8.67) after 5 min and 15 min.

Table 8.67: Ion abundances for toluene, in the degradation of benzyl bromide in D_2O with Pd/Fe prepared in D_2O (Expt. 67)

Sample	*m/z*							Ratio, CH_3Ph: CH_2DPh, error[a]
	89	90	91	92	93	94	95	
Library, toluene	404	518	9999	7256	539	0	0	100:0, 0.045[b]
5 min, No. 1	265	327	4221	10000	5492	388	0	23:77, 1
5 min, No. 2	317	350	5014	10000	5127	513	0	28,72, 2
15 min, No. 1	319	348	4962	10000	5250	585	27	28:72, 3
15 min, No. 2	298	333	5251	10000	5165	476	21	30:70, 3

[a] % Σ(abs errors)/Σ(counts) for *m/z* 91-94 [b] error reported to 2 significant figures, all others as integers

Degradation of benzyl bromide in the presence of CD_3OD (Expt. 68)

Iron filings (2 g) were palladised with either water or D_2O and portions of each (0.25 ± 0.02 g) added to two sets of vials. Stock solutions of benzyl bromide (0.2 µl) in water, D_2O, methanol or CD_3OD (0.5 ml) were prepared. The solutions in water and D_2O were placed in the sonic bath (10 min). D_2O (450 µl) was added to each of the deuterium Pd/Fe vials and water (450 µl) was added to each of the "normal" Pd/Fe vials. An aliquot (50 µl) of the appropriate stock solution was added to each vial, *i.e.* CD_3OD stock or D_2O stock to the D_2O vials. The vials were shaken for 10 min, extracted with chloroform (250 µl), the organic layer transferred to a clean vial and injected onto the GC-MS (Tables 8.68a, 8.68b, 6.68c, 8.68d, 8.68e).

The following combination of vials were analysed:

water, water, benzyl bromide stock (vials 16 - 18)

water, methanol, benzyl bromide stock (vials 10 - 12).

D_2O, D_2O, benzyl bromide stock (vials 13 - 16).

D_2O, CD_3OD, benzyl bromide stock (vials 7 - 9)

Benzyl methyl ether was detected in the runs in methanol, but the peak areas were below the integration threshold.

Table 8.68a: Peak areas for toluene, benzaldehyde, benzyl alcohol, bromomethylbenzene and bibenzyl degraded with either H_2O, H_2O/MeOH, D_2O or D_2O/MeOD (Expt. 68)

No.	Sample	Toluene	Benzaldehyde	Benzyl alcohol	Benzyl bromide	Bibenzyl
1	D_2O, CD_3OD control	-	-	-	103578075	-
2	H_2O, MeOH control	-	-	-	112044762	-
3	D_2O control	-	-	13244854	30505518	-
4	H_2O control	-	-	14547232	30804612	-
5	D_2O blank	-	-	-	-	-
6	H_2O blank	-	-	-	-	-
7	D_2O, CD_3OD, Pd/Fe 1	36280318	3624659	4217799	-	16708419
8	D_2O, CD_3OD, Pd/Fe 2	36285670	3120119	3944536	-	1676895
9	D_2O, CD_3OD, Pd/Fe 3	38124589	3257407	4208072	-	18056576
10	H_2O, CH_3OH, Pd/Fe1	57381699	7396913	7668229	-	16016045
11	H_2O, CH_3OH, Pd/Fe2	56070113	7115776	7080886	-	16526112
12	H_2O, CH_3OH, Pd/Fe3	58505815	8189661	7737468	-	17160851
13	D_2O Pd/Fe 1	18274895	-	13523067	-	4469649
14	D_2O Pd/Fe 2	19681536	-	10865272	-	2069328
15	D_2O Pd/Fe 3	18548553	-	12238964	-	3277436
16	H_2O Pd/Fe 1	19028235	2078353	17810868	-	2954954
17	H_2O Pd/Fe 2	18089694	1777331	16092241	-	2611388
18	H_2O Pd/Fe 3	17539439	1522307	15273797	-	2453544

Table 8.68b: % Product formation relative to control values and averages for experiment sets (Expt. 68)

No.	Sample	Toluene	Benzaldehyde	Benzyl alcohol	Bibenzyl
3	D_2O control			43	
4	H_2O control			47	
7	D_2O, CD_3OD, Pd/Fe 1	119	12	14	55
8	D_2O, CD_3OD, Pd/Fe 2	119	10	13	55
9	D_2O, CD_3OD, Pd/Fe 3	125	11	14	60
10	H_2O, CH_3OH, Pd/Fe1	186	24	25	52
11	H_2O, CH_3OH, Pd/Fe2	182	23	23	53
12	H_2O, CH_3OH, Pd/Fe3	190	26	25	56
13	D_2O Pd/Fe 1	60	-	44	15
14	D_2O Pd/Fe 2	64	-	36	7
15	D_2O Pd/Fe 3	60	-	40	11
16	H_2O Pd/Fe 1	62	7	58	10
17	H_2O Pd/Fe 2	59	6	52	9
18	H_2O Pd/Fe 3	57	5	50	8
3-4	D_2O or H_2O controls			45	
7-9	D_2O, CD_3OD, Pd/Fe	121	11	14	57
10-12	H_2O, CH_3OH, Pd/Fe	186	24	24	55
13-15	D_2O, Pd/Fe	61	0	40	9
16-18	H_2O, Pd/Fe	59	6	53	9

Table8.68c: Ion abundances and isotopomer ratios for toluene, in the degradation of benzyl bromide with Pd/Fe (Expt.68)

		m/z						Ratio, CH_3Ph:
No.	Sample	90	91	92	93	94	95	CH_2DPh, error[a]
7[b]	D_2O, CD_3OD, Pd/Fe 1	291	5639	10000	4985	357	12	32:68, 2
8	D_2O, CD_3OD, Pd/Fe 2	247	5511	10000	5031	383	16	31:69, 2
9	D_2O, CD_3OD, Pd/Fe 3	232	5640	10000	4972	377	17	32:68, 2
10	H_2O, CH_3OH, Pd/Fe 1	2	10000	6196	515	22	0	100:0, 6[c]
11	H_2O, CH_3OH, Pd/Fe 2	4	10000	6204	550	26	0	100:0, 6[c]
12	H_2O, CH_3OH, Pd/Fe 3	0	10000	6195	510	24	0	100:0, 6[c]
13	D_2O, Pd/Fe 1	314	4698	10000	5352	391	13	26:74, 3
14	D_2O, Pd/Fe 2	265	4949	10000	5235	400	17	28:72, 2
15	D_2O, Pd/Fe 3	312	4850	10000	5306	402	16	27:73, 3
16	H_2O, Pd/Fe 1	0	10000	6100	509	25	0	100:0,7[c]
17	H_2O, Pd/Fe 2	0	10000	6138	488	2	22	100:0,7[c]
18	H_2O, Pd/Fe 3	6	10000	6151	476	24	0	100:0,7[c]

[a] % Σ(abs errors)/Σ(counts) for *m/z* 91-94 [b]Controls 1-4 & blanks 5-6 nil determined [c] errors not minimised

Table 8.68d: Ion abundances and isotopomer ratios for benzyl alcohol, in the degradation of benzyl bromide with Pd/Fe (Expt. 68)

		m/z						
No.	Sample	105	106	107	108	109	110	111
	BnOH library	2711	2620	7862	10000	754	47	0
1	D_2O, CD_3OD control	706	499	3183	10000	6838	366	0
2	H_2O, MeOH control	640	421	5630	10000	3371	166	0
3	D_2O control	572	334	4149	10000	5461	439	33

4	H_2O control	584	338	5667	10000	2959	204	4
7	D_2O, CD_3OD, Pd/Fe 1	664	383	3946	10000	6143	745	23
8	D_2O, CD_3OD, Pd/Fe 2	690	438	3969	10000	6137	784	22
9	D_2O, CD_3OD, Pd/Fe 3	681	483	4036	10000	5914	734	0
10	H_2O, CH_3OH, Pd/Fe 1	661	365	5582	10000	2908	190	0
11	H_2O, CH_3OH, Pd/Fe 2	633	373	5680	10000	3008	211	0
12	H_2O, CH_3OH, Pd/Fe 3	622	355	5698	10000	2923	244	9
13	D_2O, Pd/Fe 1	618	382	4334	10000	5169	424	29
14	D_2O, Pd/Fe 2	617	387	4261	10000	5314	429	27
15	D_2O, Pd/Fe 3	591	373	4430	10000	5025	440	34
16	H_2O, Pd/Fe 1	613	370	5611	10000	2995	218	9
17	H_2O, Pd/Fe 2	590	314	5571	10000	3050	219	0
18	H_2O, Pd/Fe 3	616	342	5663	10000	3020	225	6

[a] All ratios indicate partial incorporation of one deuterium

Table 8.68e: Ion abundances and isotopomer ratios for benzaldehyde and bibenzyl in the degradation of benzyl bromide with Pd/Fe (Expt. 68)

		Benzaldehyde, *m/z*[a]		Bibenzyl, *m/z*[a]			
No.	Sample	105	106	180[b]	182	183	184
	BnBn library	-	-	25	2000	291	23
	Benzaldehyde library	10000	1000	-	-	-	-
1	D_2O, CD_3OD control	8612	9021	0	0	0	0
2	H_2O, MeOH control	9804	10000	nd	nd	nd	nd
3	D_2O control	9396	10000	nd	nd	nd	nd
4	H_2O control	9888	9762	nd	nd	nd	nd
7	D_2O, CD_3OD, Pd/Fe 1	9868	10000	23	2069	331	23
8	D_2O, CD_3OD, Pd/Fe 2	9466	10000	25	2046	319	25
9	D_2O, CD_3OD, Pd/Fe 3	9679	10000	24	2043	316	23
10	H_2O, CH_3OH, Pd/Fe 1	9588	10000	25	2066	312	22
11	H_2O, CH_3OH, Pd/Fe 2	9707	10000	24	2042	309	24
12	H_2O, CH_3OH, Pd/Fe 3	9749	10000	22	2004	310	23
13	D_2O, Pd/Fe 1	9917	10000	21	1967	299	21
14	D_2O, Pd/Fe 2	9765	10000	0	1931	317	11
15	D_2O, Pd/Fe 3	10000	9808	22	1992	309	20
16	H_2O, Pd/Fe 1	9519	10000	22	1976	313	21
17	H_2O, Pd/Fe 2	9573	10000	11	1983	311	22
18	H_2O, Pd/Fe 3	9546	10000	26	1948	302	16

[a] All ratios indicate natural abundance, within experimental error; [b] abundance *m/z* 181, 0; nd, not detected

Degradation of benzyl bromoethyl ether (Expt. 69)

Pd/Fe (0.25 ± 0.02 g), water (1 ml) and an aliquot (10 µl) of a stock solution of benzyl bromoethyl ether (0.2 µl in water 2 ml, sonicated) was added to each vial which was shaken until required for analysis. The vials were extracted with chloroform (250 µl) and the organic layer transferred to a clean vial for injection onto the GC-MS (Table 8.69).

Table 8.69: Peak areas for benzyl bromoethyl ether degradation and benzaldehyde, benzyl alcohol and ethoxymethylbenzene formation

Time, min	Benzylbromo ethyl ether	Benzaldehyde	Benzyl alcohol	Ethoxymethyl benzene	Control
0	nm	nd	nd	nd	6193387
10	5329287	nd	nd	143574	4934364
30	7291013	nd	630691	567941	10459122
60	3831174	nd	562670	535636	5743369
90	4435818	nd	687928	515861	8684902
120	4463378	nd	694706	525954	6974306
150	3723521	163986	819297	689011	8022234
180	1835887	nd	595978	480997	6312029
270	626885	211094	1220627	1115185	7191722
300	306851	nd	683273	599760	3508343
360	559213	189049	1257593	1203848	7743546
420	nd	nd	1210010	999122	4925995
480	nd	nd	913014	761877	4520731
k_1, min^{-1}	0.0087	na	na	na	na
$t_{1/2}$, min	79.7	na	na	na	na

nm = not measured, nd = nil detected

Degradation of two anion clocks, benzyl bromoethyl ether and bromoethoxybenzene (Expt. 70)

Combined stock solutions of benzyl bromoethyl ether (3 µl) and bromoethoxy-benzene (15 mg) in methanol and in water were sonicated (20 min) to aid dissolution. Pd/Fe (0.25 ± 0.02 g), water (900 µl) and an aliquot (100 µl) of the appropriate stock solution was added to each vial, which was shaken until required for analysis. The vials were extracted with chloroform (250 µl) and the organic layer transferred to a clean vial for injection onto the GC-MS (Table 8.70). The aqueous fractions were collected and the pH measured and found to be 5.65.

Table 8.70: Peak areas for benzylbromoethyl ether and bromoethoxybenzene combined degradation in methanol solution

Time, min	Pd/Fe		Control	
	Bromoethoxybenzene	Benzylbromoethyl ether	Bromoethoxybenzene	Benzyl bromoethyl ether
0	nm	nm	159263769	39251078
10	127704782	32475482	nm	nm
30	114698616	31644552	125836966	31665440
60	89994430	24675000	nm	nm
90	83594933	24655841	144830160	35778626
120	57980151	17924363	nm	nm
150	46462233	15351601	158816341	38844614
200	7013759	4576432	nm	nm
240	18526959	7236451	144168078	35266121
300	5087440	4754754	nm	nm
380	324146	319906	149198115	36000897
430	nd	nd	nm	nm

480	nd	nd	146937011	34668432
k_1, min^{-1}	0.0148	0.0108	na	na
$t_{½}$, min	46.8	64.2	na	na

nm = not measured, nd = nil detected, na = not applicable

Degradation of 1-bromo-2-*n*-hexyloxycyclohexane (Expt. 71)

A stock solution of 1-bromo-2-*n*-hexyloxycyclohexane (3 µl) in water (15 ml) was prepared. Pd/Fe (0.25 ± 0.02 g) was added to a series of vials and water (900 µl) was added. An aliquot (100 µl) of stock solution was added and the vials shaken (120 rpm) until required for analysis. The samples were extracted with chloroform (250 µl), the organic layer transferred to a clean vial and injected onto the GC-MS (Table 8.71).

Table 8.71: Peak areas and products for 1-bromo, 2-*n*-hexyloxycyclohexane degradation

Time, min	1-Bromo-2-*n*-hexyloxycyclohexane	Hexanol	Cyclohexane hexyl ether	Control, 1-Bromo-2-*n*-hexyloxycyclohexane
0	nm	nm	nm	68740478
10	49426372	399299	783551	72539056
30	35827383	1851145	2972778	78980442
60	25040880	2653652	4510385	82181493
90	29304044	2968270	7540308	87367018
120	13331885	3440883	6996485	74444806
165	19636819	4848233	13262050	75560828
205	5019994	7231187	16781177	86826629
240	2005471	6357855	14241122	63227578
300	1042720	8054754	15210566	81761316
360	1861603	8369286	17843768	74524648
420	251695	7880707	15634344	85509055
480	214686	8160650	18405112	72995211
k_1, min^{-1}	0.012	na	na	na
$t_{½}$, min	57.8	na	na	na

nm = not measured, na = not applicable

Degradation capacity of Pd/Fe with benzyl bromide(Expt.72)

Pd/Fe (32.7 mg) was placed in a round bottom flaskand aqueous methanol (10 % *v/v*, 200 ml) added. Portions of benzyl bromide (10, 10, 10, 20, 50, 20, 50, 50, 100 µl) were added to the flask over the course of the experiment (13 days). An aliquot of the reaction mixture (1 ml) was removed from the flask, extracted with chloroform (250 µl) and injected onto the GC-MS to monitor the consumption of the starting material (Table 8.72).

Table 8.72: Peak areas and products for repeated additions of benzyl bromide to Pd/Fe

Time, hrs	Toluene	Benzyl methyl ether	Benzyl alcohol	Bibenzyl	Benzyl bromide
0	nd	7752883	9411156	nd	75966672
14	219273	31577102	43754444	nd	197794
15	481029	34968880	48298444	211023	91116175
22	356610	34591274	48605940	ni	3583022

22.5	432608	40795485	61038977	440724	70056979
39	330445	54493441	84934458	478605	nd
39.25	425884	60093769	93932275	859931	78268446
44	628161	79664023	128812467	887646	43163048
46	581408	87064383	142621262	1020512	18748983
112.75	1133241	175325361	300096737	3401563	220872
137.5	ni	19155953	346617921	1377919	nd
157.5	ni	23595437	452103832	1108634	3038462
165.5	1933666	262034605	493141786	12228729	11798346
191.5	2565127	329755748	630558015	11824534	18109032
280.25	ni	42967206	ni	1124417	1853931
285	ni	45264885	967041923	ni	ni
307.5	2322857	438839611	898673728	1067661	1691543

nd = nil detected, ni = not integrated

Small scale degradation capacity of Pd/Fe, a small scale reaction (Expt.73)

Pd/Fe (2 ± 0.2 mg) was placed in a series of vials, water (900 µl) and an aliquot (100 µl) of benzyl bromide (20 µl in methanol 15 ml) added. The vials were shaken until required for analysis, and a portion of the chloroform (250 µl) extract injected onto the GC-MS (Table 8.73, Fig 8.73).

Table 8.73: Peak areas and products for benzyl bromide on Pd/Fe, small scale degradation capacity

Time, mins	Toluene	Benzyl methyl ether	Benzyl alcohol	Bibenzyl	Benzyl bromide
0	474347	1132004	1349194	304164	100329501
30	1337185	6061061	9443992	3474127	84854587
60	1439265	10020780	16537924	4706054	70542676
120	2060079	15144325	25540879	7093016	52671254
180	4791757	17587885	29634426	12265330	31538262
240	3738844	21699358	34075386	8839866	27548636
300	4070450	21821722	37369754	8791074	19112130
330	3182580	21996223	37326709	7640074	16695015

Fig 8.73: Small scale degradation of benzyl bromide on Pd/Fe (Table 8.73)

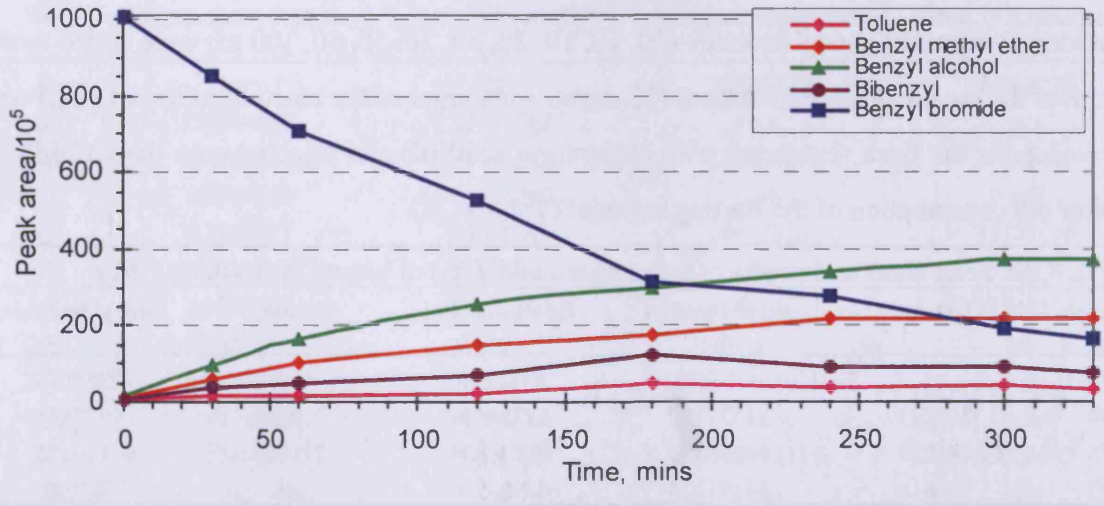

Repeated dosing of a small quantity of Pd/Fe with benzyl bromide and fresh solvent (Expt. 74)

Pd/Fe (2.5 mg) was weighed into a vial. Water (1 ml) and an aliquot (100 µl) of benzyl bromide (20 µl in methanol 15 ml) were added. The vial was capped shaken until required for analysis (1 hour), extracted with chloroform (250 µl) and the extract analysed by GC-MS. The aqueous layer was discarded, a further portion of water and stock solution was added and the vial returned to the shaker. The above procedure was repeated seven times. The starting material and the four degradation products were monitored (Table 8.74, Fig 8.74a, 8.74b) over an 8 hour time period.

Table 8.74: Peak areas and products for benzyl bromide on Pd/Fe, repeated additions

Time, mins	Toluene	Benzyl methyl ether	Benzyl alcohol	Bibenzyl	Benzyl bromide
60	338979	1095668	1639954	1330183	8329804
120	397305	1027165	1698460	1272441	8006286
180	216334	992047	1425177	827540	8909732
240	136082	1037854	1435334	655114	9133423
300	144845	1120894	1614244	385458	8079301
360	200939	1300611	1675390	1123705	8335815
420	80954	973054	1176257	333365	8204824
480	142538	1556973	1917997	570166	8888183

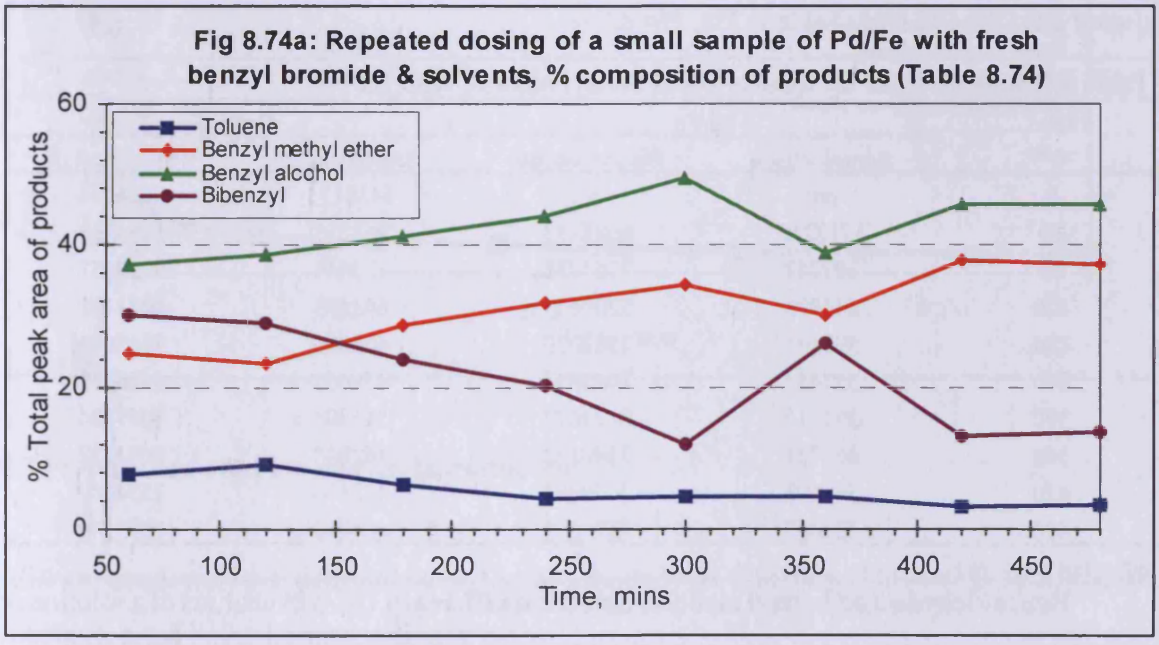

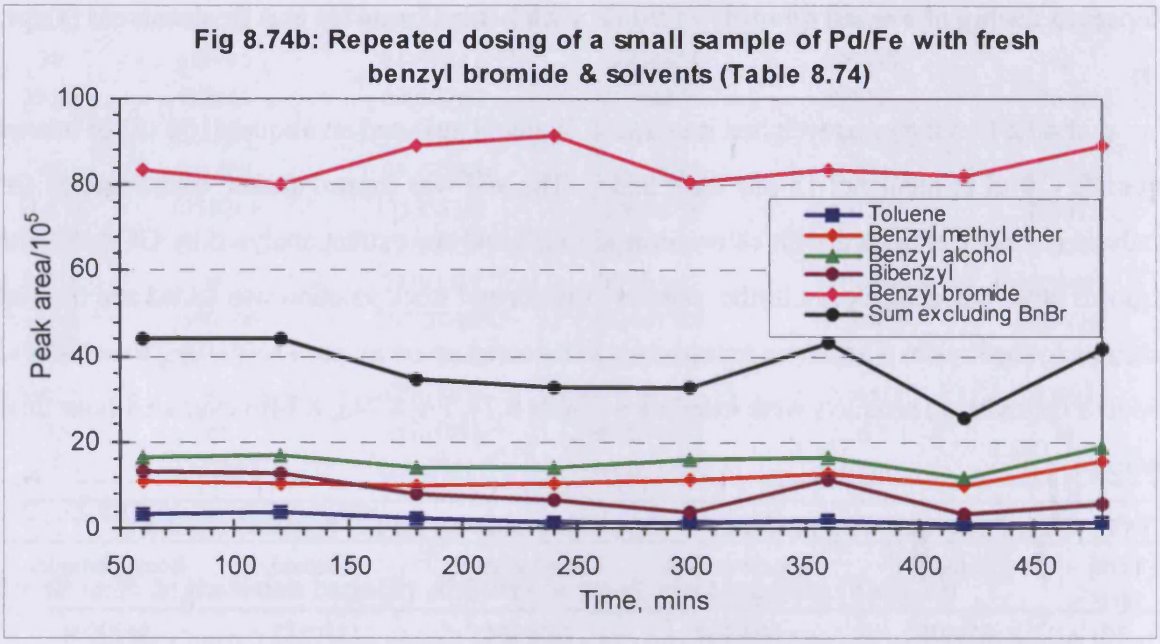

Incubation of alcohols with Pd/Fe and water (Expt. 75)

Benzyl alcohol: Pd/Fe (0.25 ± 0.02 g) was added to a series of vials. An aliquot (100 µl) of benzyl alcohol (20 µl in water 15 ml) and water (1 ml) was added to the vials, which were shaken until required for analysis. The vials were extracted with chloroform (250 µl) and the organic layer injected onto the GC-MS (Table 8.75a, Fig 8.75).

Table 8.75a: Peak areas for incubation of benzyl alcohol with Pd/Fe

Time, min	Pd/Fe		Control	
	Benzaldehyde	Benzyl alcohol	Benzaldehyde	Benzyl alcohol
0	nm	nm	1438175	6814674
10	1112210	6688453	968351	6954215
60	807247	7361738	772444	6926657
120	644978	7209679	643663	6941490
180	590141	7582233	600056	7545046
240	557453	7482634	459607	6416313
300	391917	6823672	511305	7041884
360	469721	7740192	462948	7093127
420	344893	7660762	412116	7534387
480	322687	7274591	404449	7895545

nm = not measured

Benzaldehyde and benzyl alcohol, detection efficiency GC-MS analysis of a solution of benzaldehyde (1.95 uM) and benzyl alcohol (2.05 uM) in dichloromethane (10 ml) gave only one integratable peak (peak area of 191397, Ret. time 11.45 min) which was library matched to benzaldehyde. Fragments at *m/z* 108, 105 were detected in SICs (Ret. time 13.43 min), which were tentatively identified as benzyl alcohol (conditions 35(50 x 10 to 140(0) x 25 to 200, inj 220 on a Zebron ZB5 column). Repetition of the analysis with benzaldehyde (0.49 mM) and benzyl alcohol (0.51 mM) gave two peaks (682699, 343191 counts and ratio 66:33 respectively).

Benzyl, hexyl and octyl alcohols with iron and water A combined stock solution of benzyl alcohol (10 µl), hexyl alcohol (20 µl) and octyl alcohol (20 µl) in water (15 ml) was prepared. Pd/Fe (0.25 ± 0.02g), water (1 ml) and stock solution (100 µl) was added to each vial and also to a set of control vials without the iron. The vials were shaken (360 min), extracted with chloroform (250 µl) and the organic layer injected onto the GC-MS (Table 8.75b).

Table 8.75b: Peak areas for incubation of benzyl, hexyl and octyl alcohols with Pd/Fe

Sample	Benzyl alcohol		Hexanol		Octanol	
	Peak area	µg/l	Peak area	µg/l	Peak area	µg/l
Pd/Fe 1	4218593	157.7	7601207	235.8	8788104	260.0
Pd/Fe 2	2767077	102.8	4887646	151.1	5626008	160.6
Pd/Fe 3	2867633	106.5	4931454	152.2	5842246	167.8
H_2O 1	4128741	153.9	7429750	231.6	8862653	261.5
H_2O 2	4459200	166.9	7972962	248.4	9235264	273.7
H_2O 3	3835912	143.1	6639628	206.6	7870646	226.5

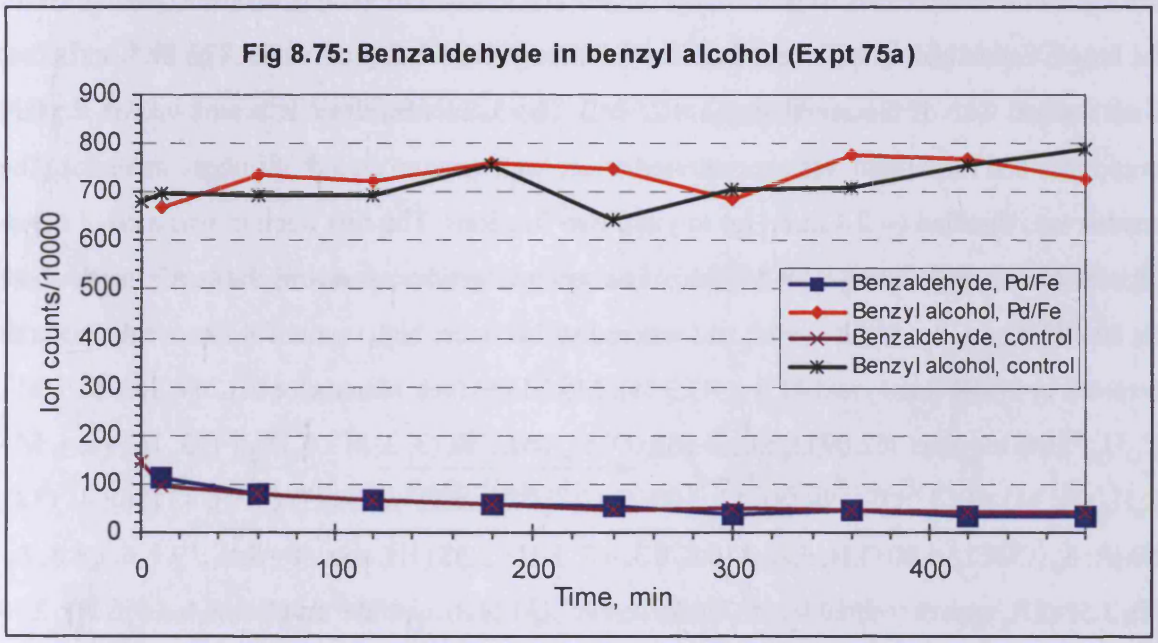

8.3 Preparation of anion clocks, Introduction

All compounds were purified until judged homogenous by ^{1}H-NMR and TLC or GC. Spectroscopic data is reported in the formats indicated below:

MS ionisation techniques (eg EI-(+)) *m/z* (abundance %, assignment, high resolution data);

NMR data: δ_H shift from TMS (integration, multiplicity and coupling constants, assignment);

δ_C (DEPT, $^1J^{13}$C-^{1}H COSY, $CDCl_3$) carbon shift (attached hydrogens, δ_H shift of $^1J^{13}$C-^{1}H coupled proton, carbon assignment);

J^1H-^{1}H COSY is reported as a contiguous sequences of correlations in order of assignment until

exhausted and then to next lowest numbered assignment, eg 1, 2, 3a, 3b, 2; 4, 5. In pairwise notation this would be written as 1, 2; 2, 3a; 2, 3b; 3a, 3b; 4, 5.

$^{2,3}J$ $^{1}H^{13}C$- COSY is reported as pairs of assignments in the order H assignment, C assignment and are assumed to be ^{3}J-correlations unless noted otherwise.

Preparation of *trans*-1-bromo-2-(*n*-hexyloxy)cyclohexane 105 (Expt. 76a DRK 832)

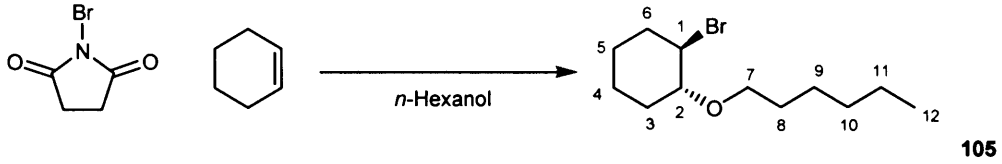

105

N-Bromosuccinimide (65 g, 365 mmoles) was added in portions (5.0 g, 28 mmoles) to a stirred solution of cyclohexene (40 g, 488 mmoles) and *n*-hexanol (325.6 g, 400 ml, 3192 mmoles) in a sealed flask in the dark at room temperature. The reaction mixture was stirred overnight until the brown colour had disappeared, then filtered through sand on a glass sinter. The flask and sinter were washed with dichloromethane (3 x 25 ml). The dichloromethane was removed on a rotary evaporator and the filtrate was concentrated under high vacuum on a cold finger evaporator. The residue was distilled (~ 0.4 mm Hg) to yield two fractions. The first fraction was a *cis*- / *trans*- mixture (40:60, 80 °C, 15 g, 15.6 % yield). The second fraction was mainly the *trans*- isomer(~ 90 %, 80 - 85 °C, 54.2 g, 56.5 % yield) and was redistilled under high vacuum to remove the hexanol detected by NMR (total yield 41.5 g, 43.3 %). MS EI-(+) (*m/z*, abundance %) 264, 262 (5, 5, M^+, $C_{12}H_{23}{}^{79}BrO$ requires 262.0933, found 262.0935); 180, 178 (3, 3, M - C_6H_{12}); 163, 161 (4, 4, M - $C_6H_{13}O$); 141 (9); 113 (9); 99 (8); 81 (100, C_6H_9 cyclohexenyl); 57 (57, C_4H_9); 43 (86); 41 (38); NMR: δ_H ($CDCl_3$) 4.00 (1 H, ddd, *J* 10.1, 8.3, 4.2, 1-H); 3.58 (1H, app. dt = ddd, *J* 9.1, 6.5, 6.5, 7a-H); 3.51 (1H, app. dt = ddd *J* 9.1, 6.7, 6.7, 7b-H); 3.31 (1H, app. td = ddd 8.4, 8.4, 4.3, 2-H); 2.30 (1H, m, 6_{eq}-H); 2.12 (1H, m, 3_{eq}-H); 1.9 - 1.2 (14 H, m); 0.9 (3H, t) 0.8, 12-H_3); H- H J-COSY 45; 1, 2, 3_{eq}; $1,6_{eq}$; 7-H_2, 8-H_2?; 11-H_2?, 12-H_3; δ_C (DEPT, $^{1}J^{13}C$-^{1}H COSY, $CDCl_3$) 82.05 (CH, δ_H 3.31, 2-C), 70.27 (CH_2, δ_H 3.58 & 3.51, 7-C); 56.28 (CH, δ_H 4.00, 1-C); 35.99 (δ_H 2.30 & 1.85), 32.06, 31.23, 30.44 (δ_H 2.12 & 1.60), 26.21, 25.2, 23.69, 23.03 (8 x CH_2, 3-6 & 8-11-C); 14.48 (CH_3, δ_H 0.90, 12-C)

Preparation of *trans*-1-bromo-2-(*n*-octyloxy)cyclopentane 107 (Expt. 76)

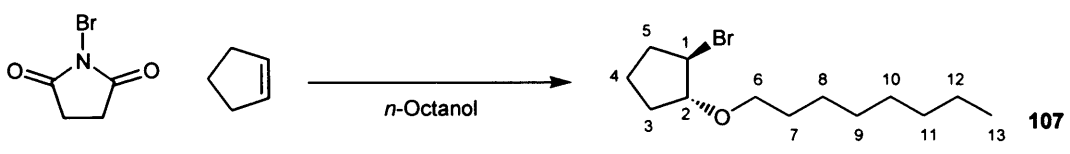

107

N-Bromosuccinimide (65 g, 365 mmoles) was added in portions (5 g, 28 mmoles) to a stirred solution of cyclopentene (45.6 g, 671 mmoles) and octanol (330 g, 400 ml, 2538 mmoles) in a sealed flask at room temperature. The reaction mixture was stirred overnight then filtered through sand on a glass sinter. The flask and sinter were washed with dichloromethane (3 x 25 ml). The dichloromethane was removed on a rotary evaporator. The filtrate was concentrated under high vacuum on a cold finger evaporator. The residue was distilled three times under high vacuum to yield three portions, *n*-octanol (< 100 °C), product **107** (100 - 110 °C, 49.6 g, 180 mmole, 49.3 % yield) and residue. MS EI-(+) (*m/z*, abundance %) 278, 276 (3, 3, M^+, $C_{13}H_{25}{}^{79}BrO$ requires 276.1085, found 276.1089); 193, 191 (2, 2, M - C_6H_{13}, alkoxy β-cleavage?) 166, 164 (22, 22, M - C_8H_{16}); 149, 147 (8, 8); 141 (12); 85 (10); 84 (12); 83 (14); 71 (42); 67 (68); 57 (100, C_4H_9); 56 (25, C_4H_8); 55 (32, C_4H_7); 43 (67); 41 (35); NMR data: δ_H ($CDCl_3$) 4.27 (1H, m, 1-H); 4.03 (1H, m, 2-H); 3.47 (2H, m, 6-H_2); 2.4-1.46 (8H, m, 3-H_2, 4-H_2, 5-H_2, 7-H_2); 1.32 (10H, m, 8-12H_2); 0.93 (3H, t, *J* 6.8, 13-H_3); δ_C (DEPT, $^1J^{13}C$-^1H COSY, $CDCl_3$) 88.0 (CH, δ_H 4.03, 2-C); 69.8 (CH_2 δ_H 3.47, 6-C); 54.6 (CH, δ_H 4.27, 1-C); 34.8; 31.8; 30.0; 29.9; 29.4; 29.3; 26.1; 22.7 (4-C); 21.8 (9CH_2); 14.1 (CH_3, δ_H 0.93, 13-C); J^1H-^1H COSY 1, 2, 3a, 3b, 2; 5a, 5b; 6a, 6b, 7, 6a; 12, 13; $^{2,3}J\,^1H^{13}C$- COSY 1, 3; 2, 5; 2, 6; 3a, 1; 3b , 1; 6, 2

Reduction of *trans*-1-bromo-2-(*n*-hexyloxy)cyclohexane <u>105</u> to *n*-hexyloxycyclohexane <u>106</u> (Expt. 77)

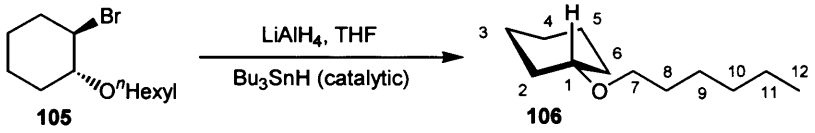

Lithium aluminium hydride (0.89 g, 23.4 mmole) was added to *trans*-1-bromo-2-(*n*-hexyloxy)-cyclohexane **105** (3.05 g, 11.6 mmole) dissolved in dry THF (60 ml). Tri-*n*-butyltin hydride (Bu_3SnH, 3 drops) was added to the flask and the reaction mixture refluxed under nitrogen overnight. The progress of the reaction was monitored using TLC. Ice was added until effervescence ceased. The mixture was filtered through silica and Celite supported on a sintered glass disk. The filter was washed with ether and combined with the filtrate. The solvent was removed on a rotary evaporator. The resulting liquid was subject to high vacuum filtration (50 - 60 °C, 0.7 millibar). Three fractions were collected. The first fraction contained hexanol and was discarded. The final residue fraction was also discarded. The second fraction was redistilled under high vacuum (56 - 58 °C, 0.7 millibar) and a further three fractions collected. The first and last fractions were discarded and the second fraction retained (56 - 58 °C, 1.97 g, 10.7 mmole, 92 % yield). NMR

analysis of all fractions confirmed the reduced hexyl compound **106** to be retained in the second fraction. MS EI-(+) (*m/z*, abundance %) 184 (10, M^+, $C_{12}H_{24}O$ requires 184.1827, found 184.1824); 155 (3); 141 (17); 113 (16); 100 (18); 83 (76); 82 (65); 69 (15); 67 (19); 57 (88, C_4H_9); 56 (24, C_4H_8); 55 (70, C_4H_7); 43 (100); 41 (81); NMR data: δ_H ($CDCl_3$) 3.45 (2H, t *J* 6.8, 7-H_2); 3.22 (1H, m, 1-H); 1.95 (2H, m, 2a, 6a); 1.75 (2H, m, 3a, 5a); 1.55 (3H, m, 8-H_2 + ?); 1.27 (11H, m, 2b-H, 3b-H, 6b-H, 11-H_2 +?); 0.9 (3H, t *J* 6.9, 12-H_3); δ_C (DEPT, $^1J^{13}$C-^{1}H COSY, $CDCl_3$) 77.2 (CH, δ_H 3.22, 1-C); 68.0 (CH_2 δ_H 3.45, 7-C); 32.4, 31.8, 30.2, 25.95, 25.88, 24.3, 22.7 (7CH_2); 14.1 (CH_3, δ_H 0.90, 12-C); J^1H-^{1}H COSY 1, 2a/6a, 2b/6b, 1; 2a/6a, 3a/5a, 3b/5b; 7, 8; 11, 12; $^{2,3}J^1H^{13}C$- COSY 7,1; ^2J 8,7;

Reduction of *trans*-1-bromo-2-*(n*-octyloxy)cyclopentane 107 to octyloxycyclopentane 108(Expt. 78)

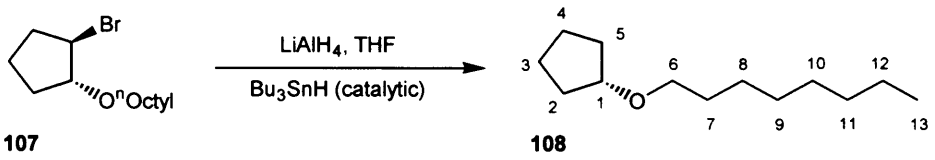

107 108

Lithium aluminium hydride ($LiAlH_4$, 0.89 g, 23.4 mmole) was added to *trans*-1-bromo-2-(*n*-octyloxy)cyclopentane **107** (3.1 g, 11.2 mmole) dissolved in dry THF (60 ml). Tri-*n*-butyltin hydride (Bu_3SnH, 3 drops) was added to the flask and the reaction mixture refluxed under nitrogen overnight. The progress of the reaction was monitored using TLC. Ice was added until effervescence ceased. The mixture was filtered through silica and Celite supported on a sintered glass disk. The filter was washed with ether and combined with the filtrate. The solvent was removed on a rotary evaporator. The resulting liquid was subject to high vacuum distillation (60 - 64 °C, 0.4 millibar). Three fractions were collected. The first fraction contained octanol and was discarded. The final residue fraction was also discarded. The second fraction was redistilled under vacuum (105 -120 °C, 15 mm Hg) and a further three fractions collected. The first and last fractions were discarded and the second fraction retained. NMR analysis of all fractions indicated the reduced octyl compound **108** (2.28g, 11.5 mmole, 102 % yield) in the second fraction. MS EI-(+) (*m/z*, abundance %) 198 (3, M^+, $C_{13}H_{26}O$ requires 198.1984, found 198.1980); 169 (7, M - C_2H_5); 141 (9 M - C_4H_9); 112 (9); 99 (10); 86 (34); 69 (100, C_5H_9); 57 (85, C_4H_9); 43 (48); 41 (74); NMR δ_H ($CDCl_3$) 3.88 (1H, m, 1-H); 3.45 (2H, t, 6-H_2); 1.79-1.43 (10H, m, 2-5H_2); 1.28 (10H, m, 8-12H_2); 0.90 (3H, t *J* 6.6, 13-H_3); δ_C (DEPT, $^1J^{13}$C-^{1}H COSY, $CDCl_3$) 81.2 (CH, δ_H 3.88, 1-C); 69.0 (CH_2 δ_H 3.45, 6-C); 32.3 (CH_2, double intensity, 2-C & 5-C?), 31.9, 30.1, 29.5, 29.3, 26.3 (5CH_2), 23.6 (CH_2, double

intensity, 3-C & 4-C?), 22.7 (CH_2); 14.1 (CH_3, δ_H 0.90, 13-C);J^1H-^{1}H COSY 1, 2a, 2b, 1; 6,7; 12, 13; $^{2,3}J$ ^{1}H^{13}C- COSY 6,1.

Degradation of *trans*-1-bromo-2-(*n*-hexyloxy)cyclo-hexane 105 and *trans*-1-bromo-2-(*n*-octyloxy)cyclopentane 107 (Expt. 79)

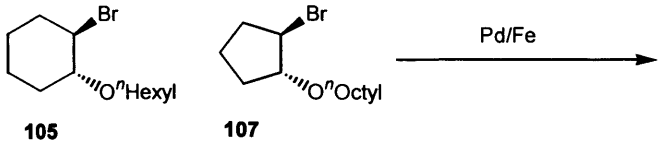

105 107

Pd/Fe (0.25 ± 0.02 g) was added to a series of vials. Stock solutions of *trans*-1-bromo-2-(*n*-hexyloxy)-cyclohexane **105** (3 µl), *trans*-1-bromo-2-(*n*-octyloxy)cyclopentane **107** (3 µl) and *trans*-1-bromo-2-(*n*-hexyloxy)-cyclohexane **105** plus *trans*-1-bromo-2-(*n*-octyloxy)cyclopentane **107** (3 µl respectively) in methanol (3 x 15 ml) were prepared. Water (900 µl) was added to the vials, then an aliquot (100 µl) of the appropriated stock solution. The vials were capped and shaken until required for analysis. The vials were extracted with chloroform (250 µl), which was injected onto the GC-MS (Tables 8.79a, 8.79b).

Table 8.79a: Peak areas for *trans*-1-bromo-2-(*n*-hexyloxy)-cyclohexane **105** and *trans*-1-bromo-2-(*n*-octyloxy)cyclopentane **107** single component degradation

Time, min	*trans*-1-bromo-2-(*n*-hexyloxy)-cyclohexane **105**	Hexanol	*n*-Hexyloxy-cyclohexane **106**	*trans*-1-bromo-2-(*n*-octyloxy) cyclopentane **107**	Octanol	*n*-Octyloxy-cyclopentane **108**
0	1853499	nd	nd	1186058	nd	nd
10	2981246	nd	nd	2068303	nd	nd
70	2969173	135202	52262	3244148	121533	240664
95	2860126	nq	126412	2628017	nq	143087
120	3017976	89102	257985	3099958	95712	196656
150	3406903	77160	355227	2428849	122272	256824
180	2924691	86634	286391	2152822	202488	497582
210	2536571	84611	273218	1757703	144299	282802
280	2813008	118444	480284	1906777	204133	376507
315	1800189	73263	218975	2206821	214111	550196
360	1981745	171944	785673	1114201	224104	419974
420	2188366	79309	378746	1061061	141125	378210
480	1685293	137056	783298	1150287	165829	484436
k_1, min^{-1}	0.0015	na	na	0.0027	na	na
$t_{½}$	462	na	na	257	na	na

nd = nil detected, nq = not quantified, na = not applicable

Table 8.79b: Peak areas for *trans*-1-bromo-2-(*n*-hexyloxy)-cyclohexane **105** and *trans*-1-bromo-2-(*n*-octyloxy)cyclopentane **107** mixed component degradation

Time, min	*trans*-1-Bromo-2-(*n*-hexyl oxy)cyclo hexane **105**	Hexanol	Hexyloxy cyclo hexane **106**	*trans*-1-Bromo-2-(*n*-octyloxy) cyclopentane **107**	Octanol	Octyloxy-cyclo-pentane **108**	Control *trans*-1-bromo-2-(*n*-hexyl oxy)-cyclohexane **105**	Control *trans*-1-bromo-2-(*n*-octyloxy)cyclopentane **107**
0	nm	nd	nd	nm	nd	nd	2205159	1943769
10	3388873	nq	nq	3083119	nq	nq	2266980	1654491
70	3769770	nq	169657	3316219	nq	112403	4159404	3459131
95	3827286	nq	230586	3441576	nq	188275	4968754	4909689
120	3517795	nq	244020	3337781	123955	255381	3967030	4120261
150	3411167	nq	198517	2951184	107548	221063	4520210	4628076
180	3430936	nq	359923	3322812	138007	359923	4617556	4414361
210	2887050	82060	400216	2608630	198417	512124	3690115	3581595
280	3151348	100886	469313	3066762	198663	418453	4582890	4640806
315	2995338	81521	427004	2872369	161634	363656	4702697	4943470
360	2208678	65955	345483	1938574	112211	243603	3756520	3895825
420	2675633	nq	388947	2591022	76233	327089	4243896	4362572
480	2777755	nq	616717	2750412	120642	512004	4098354	4277830
k_1, min^{-1}	0.0009	na	na	0.0007	na	na	na	na
$t_{½}$	770	na	na	990	na	na	na	na

nm = not measured, nd = nil detected, nq = not quantified, na = not applicable

Combined degradation of *trans*-1-bromo-2-(*n*-hexyloxy)-cyclohexane 105 and *trans*-1-bromo-2-(*n*-octyloxy)cyclopentane 107 (Expt. 80)

Pd/Fe filings (25 g) were placed in a round bottomed flask. A stock solution of *trans*-1-bromo-2-(*n*-hexyloxy)-cyclohexane **105** (11.6 mg) and *trans*-1-bromo-2-(*n*-octyloxy)cyclopentane **107** (14.8 mg) in methanol (15 ml) was prepared. water (185 ml), methanol (15 ml) and stock solution (5 ml) was added to the flask. The flask was fitted with a glass stopper and placed on a flatbed shaker (120 rpm) until required for analysis. Aliquots (2 x 1ml) were removed at the appropriate time points, extracted with chloroform (250 µl) and analysed by GC-MS (Table 8.80). A control of stock solution (2.5 ml) in methanol (7.5 ml) and water (90 ml) was also prepared and analysed in duplicate.

Table 8.80: Combined *trans*-1-bromo-2-(*n*-hexyloxy)-cyclohexane **105** and *trans*-1-bromo-2-(*n*-octyloxy)cyclopentane **107** degradation peak areas

Time,	Pd/Fe **105**		Pd/Fe **107**		Control **105**		Control **107**	
min	1	2	1	2	1	2	1	2
0	200635	nm	145085	nm	80522	86051	24245	25052
10	169344	269552	114917	247073	61188	nm	19999	nm
30	457166	504028	432520	512160	107664	nm	35195	nm
60	574876	642164	626129	673059	214782	nm	90602	nm
100	514727	514863	529392	500805	259672	nm	157189	nm

140	393916	458481	374892	458322	76918	nm	24861	nm
160	492396	440189	500311	380382	169477	nm	88952	nm
180	307113	438829	228805	418872	203192	nm	102903	nm
240	334510	397648	266976	345951	142502	nm	80539	nm
300	254604	281098	170551	201187	259634	nm	201801	nm
390	203546	165660	102250	60530	155393	nm	147660	nm
420	144687	185271	60420	115959	151713	113631	147717	86639
480	138211	169793	56268	71348	116764	1147592	111061	127406
540	65897	71407	15241	18002	84965	64232	66798	43457

nm = not measured

Calibration curve for hexanol, octanol, *trans*-1-bromo-2-(*n*-hexyloxy)-cyclohexane 105, *trans*-1-bromo-2-(*n*-octyloxy)cyclopentane 107, 2-*n*-hexyloxycyclohexane 106 and 2-*n*-octyloxycyclopentane 108 using naphthalene as internal standard (Expt. 81)

A stock solution of naphthalene (14.8 mg) in methanol (25 ml) was prepared. A working solution was prepared by dilution of the stock solution (2.5 ml) with methanol (22.5 ml). The naphthalene solution was used as an internal standard (IS). A combined stock solution of *trans*-1-bromo-2-(*n*-hexyloxy)-cyclohexane **105** (13.7 mg), *trans*-1-bromo-2-(*n*-octyloxy)cyclopentane **107** (20.5 mg), 2-*n*-hexyloxycyclohexane **106** (9.7 mg), 2-*n*-octyloxycyclopentane **108** (9.6 mg), hexanol (14.4 mg) and octanol (12.2 mg) in methanol (15 ml) was prepared. A working standard was prepared by dilution of the stock standard (5 ml) to volume with chloroform (10 ml). A series of calibration standards (1 ml) was prepared by serial dilution of the stock standard (Table 8.81)

Table 8.81: Calibration standard volumes

Standard identity	Volumes			Standard identity	Volume		
	Int. Std., µl	Stock solution, µl	$CHCl_3$, µl		Int. Std., µl	Stock solution, µl	$CHCl_3$, µl
0	100	0	900.0	6	100	300.0	600.0
1	100	9.4	890.6	7	100	450.0	450.0
2	100	18.8	881.25	8	100	600.0	300.0
3	100	37.5	862.5	9	100	750.0	150.0
4	100	75.0	825.0	10	100	900.0	0.0
5	100	150.0	750.0				

Under normal experimental conditions, an aliquot of test sample is taken and extracted with chloroform. This is done for two reasons. The main reason is that the reaction solvent which is always water based, is incompatible with the mass spectrometer, so conversion to an acceptable solvent must take place. The other, minor reason is that some concentration can also take place. Routinely, extraction from 1 ml aqueous methanol to 250 µl chloroform is performed. This must be taken into account when the calibration curve is constructed. For example, the ABSOLUTE concentration of the top standard is different from the EQUIVALENT concentration of the starting conditions. The calculation for the conversion is shown below:

Molecular mass 1-bromo-2-*n*-hexyloxycyclohexane	262
Mass of 1-bromo-2-*n*-hexyloxycyclohexane taken	13.7 mg
Moles of 1-bromo-2-*n*-hexyloxycyclohexane taken	13.7/262 = 0.0523 mM
Moles per ml in stock solution	0.0523/15
	0.003486 mM/ml
Moles per ml in working standard	5 x 0.003486/15
	0.001162 mM/ml
Converting to μM/ml	0.001162 x 1000
	1.162 μM/ml
Thus, the initial concentration of 1-bromo, 2-*n*-hexyloxycyclohexane in the reaction flask is	1.162 μM/ml

Transfer to chloroform concentrates the 1-bromo-2-*n*-hexyloxy-cyclohexane:

Amount of 1-bromo-2-*n*-hexyloxycyclohexane in 1 ml	1.162 μM
Assuming 100 % recovery, amount of 1-bromo-2-*n*-hexyloxycyclohexane in 250 μl chloroform is	1.162 x 0.25
	4.648 μM

Thus, in ABSOLUTE concentration terms, the final concentration is 4.648 μM/ml. This is EQUIVALENT to a starting concentration of 1.162 μM/ml. When the calibration curve was constructed, the standards were prepared at ABSOLUTE concentrations, but the graph axes were annotated in EQUIVALENT concentrations. This relates all results back to the initial concentration in the reaction vessel.

Degradation of *trans*-1-bromo-2-(*n*-hexyloxy)-cyclohexane 105, and *trans*-1-bromo-2-(*n*-octyloxy)cyclopentane 107 with naphthalene internal standard (Expt. 82)

Pd/Fe (12.5 g) was placed in a conical flask. A stock solution of *trans*-1-bromo-2-(*n*-hexyloxy)-cyclohexane **105** (14.1 mg) and *trans*-1-bromo-2-(*n*-octyloxy)cyclopentane **107** (18.7 mg) in methanol (15 ml) was prepared. water (90 ml), naphthalene working internal standard solution (Expt. 81, 2.5 ml), methanol (2.5 ml) and stock solution (5 ml) was added to the Pd/Fe. At predetermined time points the reaction mixture was subsampled (1 ml) in duplicate. The aqueous samples were extracted with chloroform (250 μl) and the organic layer injected onto the GC-MS. The raw data was converted into concentration results using the quantification package within the instrument software (Tables 8.82a, 8.82b). Repetition of this experiment confirmed the results (Expt. 83).

The results of this experiment confirmed that of the previous experiment. As the experiment was repeated with increased injector temperature, the results are not reported here.

Table 8.82a: Concentrations of products in nM/ml from combined degradation using MSD software

Time, min	Hexanol	Octanol	*n*-Hexyloxycyclohexane **106**	*n*-Octyloxycyclopentane **108**
0	0	0	0	0
10	0	0	0	0
30	0	0	0	0
60	2.32	0	0	0
90	2.4	6.55	0	0
120	2.71	8.15	nq	0
180	2.62	7.08	0	0
240	3.18	8.86	2.15	1.22
300	3.34	9.01	3.63	2.94
385	3.50	8.8	nq	0
420	3.61	9.7	5.80	1.81
480	3.50	9.05	2.83	0
540	3.88	9.97	5.85	0.55

nq = not quantifiable

Table 8.82b: Concentrations of starting materials in nM/ml from combined degradation using MSD software

Time, min	*trans*-1-Bromo-2-(*n*-hexyloxy)-cyclohexane **105**	*trans*-1-Bromo-2-(*n*-octyloxy)cyclopentane **107**	Control *trans*-1-bromo-2-(*n*-hexyloxy)-cyclohexane **105**	Control *trans*-1-bromo-2-(*n*-octyloxy)cyclopentane **107**
0	217.44	111.57	71.55	25.01
10	128.39	58.3	96.19	42.62
30	149.11	71.86	105.65	42.39
60	387.52	220.23	78.36	30.15
90	214.63	127.84	152.65	79.27
120	351.62	207.72	72.88	26.02
180	58.16	19.67	64.65	29.29
240	362.13	218.52	74.81	36.31
300	384.87	220.17	81.09	39.50
385	74.36	25.01	22.64	8.40
420	229.05	136.01	85.81	58.41
480	135.38	67.16	98.12	58.61
540	181.15	99.14	165.87	153.04

Degradation of *trans*-1-bromo-2-(*n*-hexyloxy)-cyclohexane 105, and *trans*-1-bromo-2-(*n*-octyloxy)cyclopentane 107 with naphthalene internal standard (Expt. 84)

Hyper-Pd/Fe (20.0 g iron, 50.0 mg palladising agent) was placed in a conical flask. A stock solution of *trans*-1-bromo-2-(*n*-hexyloxy)-cyclohexane **105** (14.8 mg) and *trans*-1-bromo-2-(*n*-octyloxy)cyclopentane **107** (14.8 mg) in methanol (15 ml) was prepared. water (90 ml), naphthalene working internal standard solution (Expt. 81, 2.5 ml), methanol (2.5 ml) and stock solution (5 ml) was added to the Pd/Fe. At predetermined time points the reaction mixture was subsampled (1 ml) in duplicate. The aqueous samples were extracted with chloroform (250 µl) and the organic layer

injected onto the GC-MS. The GC parameters were identical to those used previously with the exception that the injector temperature was increased to 280 °C. The results were converted to nM/ml, comparison of the duplicates showed good agreement, so a mean value was calculated (Table 8.84).

Table 8.84: Concentrations in nM/ml for reactants and products in 1-bromo, 2-*n*-hexyloxycyclohexane and 1-bromo, 2-*n*-octyloxycyclopentane degradation

Time, min	Hexanol	Octanol	2-*n*-Hexyloxy-cyclohexane **106**	2-*n*-Octyloxy cyclo-pentane **108**	*trans*-1-bromo-2-(*n*-hexyl oxy)-cyclo hexane **105**	*trans*-1-bromo-2-(*n*-octyloxy)cyclopentane **107**	Control *trans*-1-bromo-2-(*n*-hexyl oxy)-cyclo hexane **105**	Control *trans*-1-bromo-2-(*n*-octyloxy)cyclopentane **107**
0	0	1.40	0	1.88	97.40	123.31	13.51	11.37
10	0	3.43	0	2.93	98.48	128.34	13.91	10.64
30	0	2.93	1.82	2.94	89.25	119.31	19.77	15.56
60	3.24	3.22	2.35	2.38	56.85	80.18	17.68	12.47
90	3.97	2.98	2.47	2.22	44.44	62.04	15.34	11.28
120	4.79	4.48	5.81	4.74	45.35	62.24	17.34	13.31
150	6.16	5.58	11.45	10.75	91.77	133.01	32.41	34.54
180	7.16	5.83	15.08	13.28	91.50	137.08	18.28	13.70
240	9.20	5.92	8.70	13.4.55	27.30	32.75	14.39	9.99
300	12.75	8.57	16.81	10.59	45.11	64.99	25.06	18.00
360	15.77	10.04	14.36	5.22	17.61	18.91	23.66	20.95
420	16.56	11.14	33.82	23.09	61.55	102.88	41.09	36.79
480	19.10	13.09	26.56	14.35	37.14	58.46	32.40	35.28
540	19.87	12.88	31.60	17.60	40.79	70.83	15.24	14.48
600	23.06	15.16	33.29	15.43	31.76	56.04	28.88	31.04

Examination of the raw data revealed that the internal standard peak area was gradually decreasing during the course of the experiment. The fluctuating results are seen in both duplicates, which suggests that it is the samples rather than the instrument. This was confirmed by repeated analysis of a single sample six times throughout the course of the analysis which showed a variation of less than 2% (data not shown).

Degradation of benzyl bromide on Pd/Fe using hexane as the bulk solvent (Expt. 86)

Pd/Fe (1.0 g) was added to each of two amber glass vials (15 ml). water (1 ml) was added to one of the vials. The vials were filled to the brim with hexane. A stock solution of benzyl bromide (3 µl) in hexane (15 ml) was prepared and an aliquot (500 µl) added to each vial. At the appropriate time points, hexane (200 µl) was withdrawn and injected onto the GC-MS. No degradation products were detected in either vial, although the peak area of benzyl bromide was seen to decrease (Table 8.86).

Table 8.86: Benzyl bromide degradation using hexane as the solvent

Time, min	Water & hexane	Hexane only	Time, min	Water & hexane	Hexane only
0	704982	647486	60	627091	544298
5	690607	664721	90	602010	547276
10	734196	635658	120	588319	522393
15	662542	630154	150	567943	521883
30	645129	581176	180	502325	566344
45	641563	557271			

Chapter 9, Halo-compound Degradation on Iron and Palladium/Iron Surfaces, Discussion and Conclusions

9.0 Introduction

It has been known for many years that chlorinated solvents in steel drums, undergo degradation predominantly by reductive dehalogenation[152]. For polychlorinated solvents, sequential chlorine loss occurs with declining reaction rates and the rate is up to an order of magnitude faster with bimetallic Pd/Fe systems. The purpose of this project was to investigate the mechanism of degradation and to discover if the reaction might be synthetically useful. The initial targets were to assess the benefits of the bimetallic Pd/Fe system over iron alone, and to confirm the selectivity with polyhalocompounds. The longer term goals were to elucidate the mechanism of degradation and to expand the scope of the reaction. Such a study would have benefits for the optimisation of both soil buried iron barriers and synthetic applications[206].

9.1 Degradation of chlorinated compounds

The conditions for our experiments were broadly intended to mimic the conditions for the degradation of polyhalo-compounds in iron barriers. These have ranged from iron filings to buried old cars! In the current study standard iron filings were used. These have a surface layer of oxide which was removed by washing with hydrochloric acid to give "activated" iron as the "surface active" sites have been liberated. This is referred to as "activated iron" in the text or just "Fe" in tables. When the iron filings were treated with 6 M hydrochloric acid until nothing more dissolved, the remaining dried insoluble material weighed 6.46% of the original mass of iron. This insoluble material was assumed to consist of carbon/carbides and insoluble oxides.

Some hydrocarbons are produced during the degradation of halocarbons by iron filings. Labelling studies excluded carbon dioxide as the source and it seems more likely that inactive graphite or active carbide in the iron surface, which are reduced by a Fischer-Tropsch type process are responsible[198].

9.1.1 Comparison of activated and Pd/Fe and pH on the degradation rate of chloroform.

Chloroform was added to activated iron filings and the reduction in chloroform was determined by GC-MS. The rate constant k_1 and half life were calculated using the peak areas tabulated in (Table 8.1) and were found to be 0.04 hr^{-1} and 17.4 hr respectively (Table 9.1). The data is represented graphically (Fig. 9.1) to show the reduction in chloroform with time by plotting the peak areas, as a measure of concentration. The relationship is not linear when absolute areas

are used, but when ln peak area (or $\log_{10}$) is used, an approximately linear fit is obtained indicating a pseudo first order degradation (Fig. 9.2). This experiment clearly shows that the concentration of chloroform decreases in the presence of iron, but remains constant when only water is present. However there are considerable variations in the amount of chloroform detected, and the effect of this on the rate is exacerbated by the slow rate of the reaction, therefore we turned to the palladised iron degradation of chloroform.

Fig 9.1: Peak areas of chloroform incubated with activated iron (cf.Table 8.1)

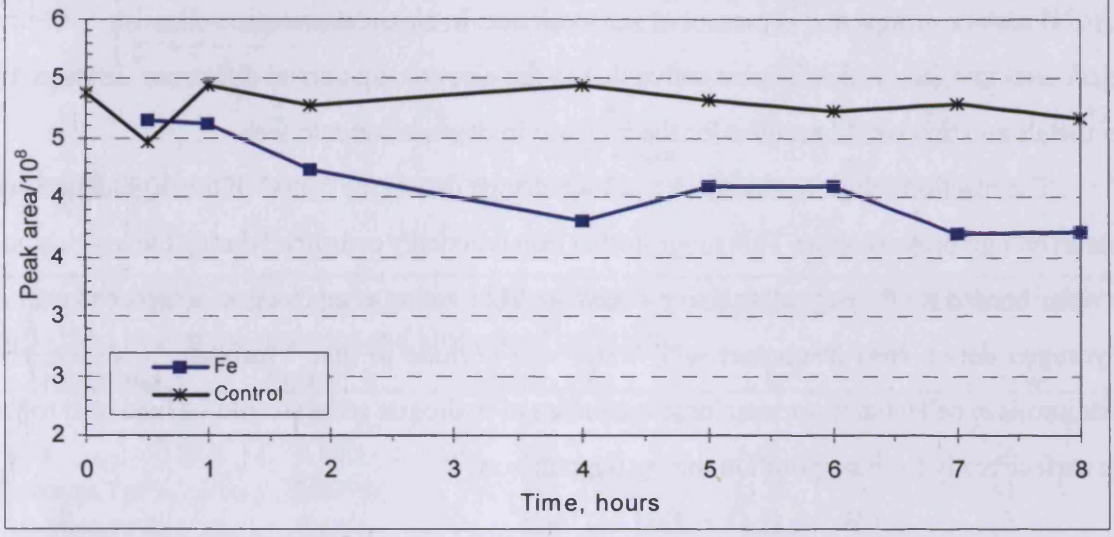

Fig 9.2: ln Peak areas of chloroform incubated with activated iron

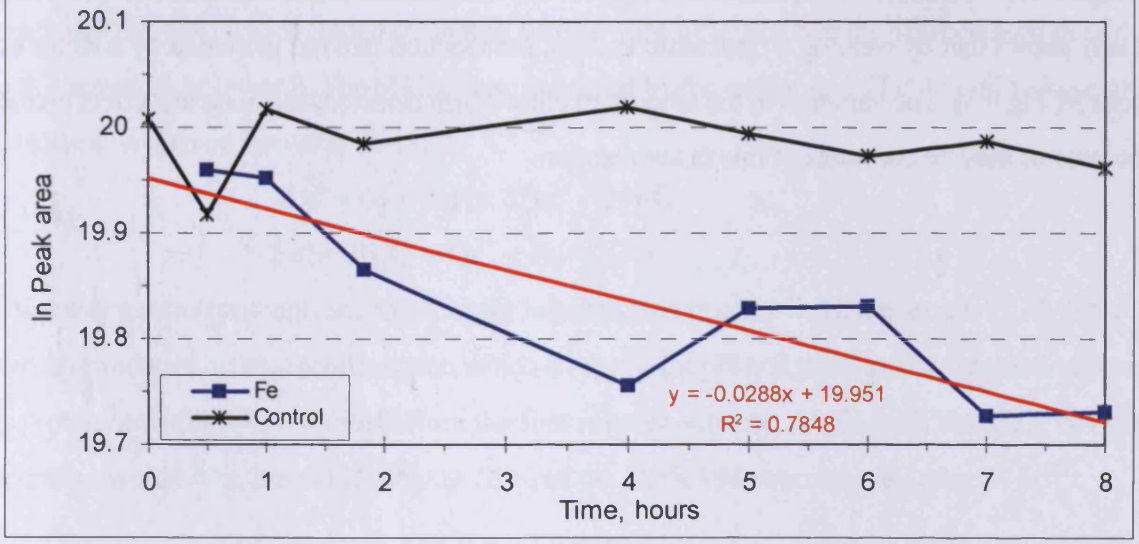

After the standard activation process for iron, potassium hexachloropalladate solution was added. The reaction mixture immediately changed from orange to black as palladium was deposited on the iron surface. Surface studies have shown that the palladium is deposited in its

elemental state on the surface, but have not identified if the palladium is present in monolayer patches or in clustered deposits[173]. Palladium is deposited onto the iron surface *via* a redox reaction and the relatively small amount of palladium compared to iron ensures that all the palladium is removed from solution:

$$PdCl_6^{2-} + 2\,Fe^0 \rightarrow 2\,Fe^{2+} + Pd^0 + 6Cl^-$$

The surface of the iron is covered in a layer of complex hydroxylated species (rust!) and is likely to be the source of protons which exchange with the halogens during degradation. This hypothesis is supported by work detailed later in this thesis. The palladium is unaffected by the oxide and hydroxyl surface groups and is present at zero-valence. In classical corrosion chemistry, it is the metal/metal interface which is most active due to the electronic potential difference between the two metals and this would account for the increase in degradation rate seen.

The reaction solution undergoes a colour change during the course of the degradation and turns an orange-brown colour. This suggests that iron is actually consumed during the reaction and the water needed for the degradation to proceed could be acting as an electron acceptor as well as a hydrogen donor. Iron in contact with water will corrode to give hydrogen as shown, and palladium is excellent at absorbing large quantities of hydrogen which would be held next to the iron surface ready for incorporation during degradation[172]:

$$Fe^{2+} + H_2O \rightarrow Fe(OH)^+ + H^+$$

$$Fe^0 + 2H^+ \rightarrow Fe^{2+} + H_2$$

Comparison of the half life on palladised iron (6.63 hr) with the half life on activated iron (17.4 hr), clearly shows that by creating a bimetallic system, the reaction rate has increased by a factor of about 3 (Fig 9.3). The variation in the amount of chloroform detected has much less effect on the accuracy of the rate constants of this faster reaction.

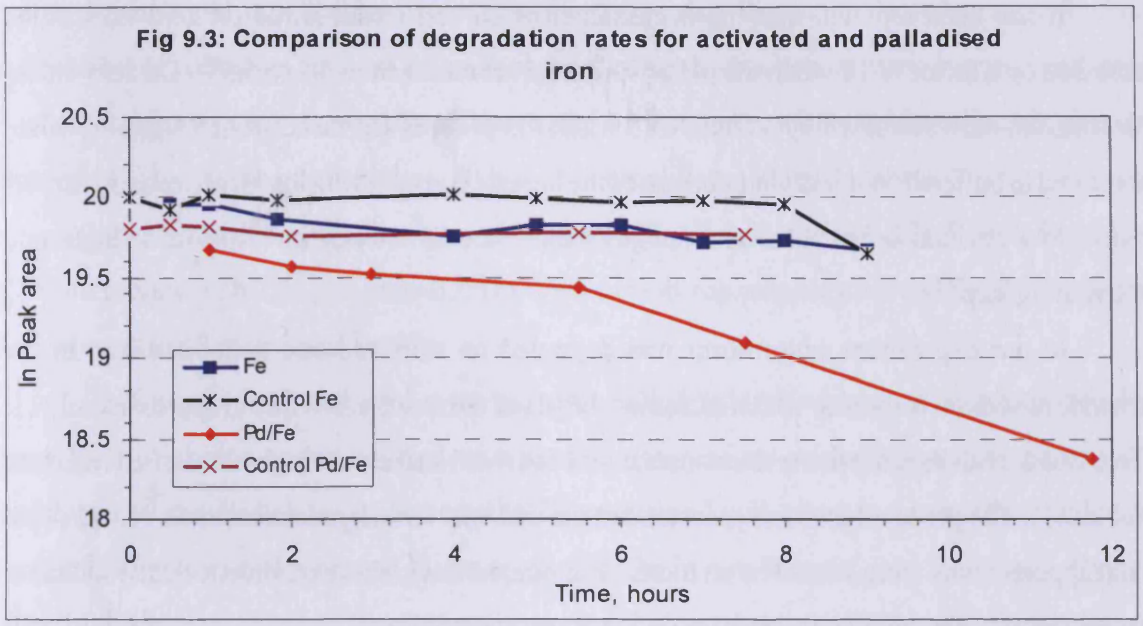

Table 9.1: Comparison of degradation rates and half lives of chloroform on activated, and palladised iron in the presence and absence of carbonate.

Iron System	Mean k_1, hr^{-1}	Mean k_1 ratio	$t_{1/2}$, hr	$t_{1/2}$, ratio
Fe	0.03978	100	17.4	100
Pd/Fe	0.1045	263	6.63	38
Carbonate, Fe	0.04395	110	15.77	91
Carbonate, Pd/Fe	0.1292	325	5.36	31

If the reaction consumes hydrogen derived from protons in the water, the rate should be decreased by an increase in pH. It has been reported that when hexahydro-1,3,5-trinitro-1,3,5-triazine (RDX **104**) was degraded on an iron surface during the first 8 hr the pH increased from 6.2 to 8.3 and at 24 hr it was 9. The pH increase is caused by the oxidation of Fe^0 to Fe^{2+} using either dissolved oxygen or the water itself ;

$$2Fe^0 + O_2 + 4H^+ \rightleftarrows 2Fe^{2+} + 2H_2O$$

$$Fe^0 + 2H_2O \rightleftarrows Fe^{2+} + H_2 + 2OH^-$$

This latter reaction probably accounts for the bubbles seen in some literature reports[195]. Hydroxide ions are produced in the second reaction which drives up the pH and should slow the reaction down as protons are effectively withheld from the first reaction scheme. At pH 2, all the RDX **104** was degraded within 4 hr, but at pH 10 only 76 % of the RDX **104** was removed after 24 hr[207].

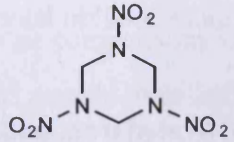

Hexahydro-1,3,5-trinitro-1,3,5-triazine, RDX **104**

It has been reported that the degradation of carbon tetrachloride on zero-valent zinc decreased by a factor of 10 when the pH of solution was raised from 3.5 to 5.5[167]. On zero-valent iron, the rate only decreased by a factor of 5 when the pH was increased from 5.0 to 10.0 when monitored in buffered solution. Comparison of the log rate constant with log H^+ concentration (pH) gave a low reaction order value and suggests that protons are not involved in a single rate determining step[194].

In our experiment, chloroform was degraded on activated and palladised iron in the presence of sodium carbonate which increased the pH of the reaction mixture to approximately 11. There was a small increase in the rate constant for both reactions relative to the unbasified reactions (Table 9.1). The pH of all the vials measured at the end was virtually identical at 11.46 - 11.47. It is not apparent why there should be an increase in rate, however this experiment clearly indicates that proton concentration is not rate limiting under our conditions.

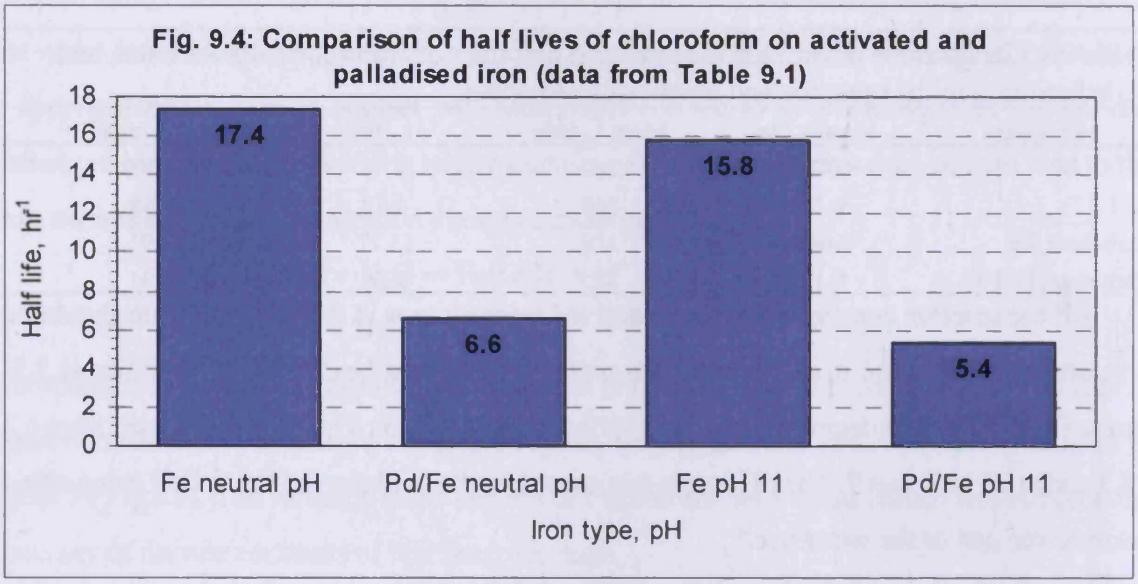

In summary, comparison of the reaction rates (Table 9.1, Fig 9.4) confirms that the bimetallic system is three times faster than iron alone and that pH only has a minor effect on the rate of degradation. The concentration of chloroform was five times higher in the Fe neutral pH experiment than that in the others, but the rate constant and half life was virtually the same in all experiments, in line with a pseudo first order degradation with respect to chloroform. The concentration effects are examined in more detail in later experiments.

9.1.2 Comparison of the activity of activated iron, palladised iron, aged palladised iron and hyper-palladised iron (Expt. 50, 51, 52)

Having demonstrated that chloroform could be degraded on an iron surface and that adding

even small amounts of palladium could significantly increase the rate of degradation, we looked at the effect of palladium and oxides on the iron surface. Bromohexane was selected because it would react more quickly than a chloroalkane and the reduction would be achieved in a single step, presumably by a single mechanism, which would simplify the kinetic analysis.

Initially suitable conditions were investigated (Table 9.2, entries 1 &2). Both 0.5 and 1 nl of bromohexane with 0.25 g of palladised iron gave easily measurable rates and the 0.5 nl variant was selected for further investigation.

To compare fresh and aged systems, some palladised iron which had been stored under water for a week in a beaker covered with parafilm (air was not excluded) was compared with freshly prepared palladised iron. The aged Pd/Fe was rinsed with water to remove the buildup of orange (sludgy) material produced by the reaction of the iron with water used for storage. Hyper-palladised iron was prepared by adding an orange solution of potassium hexachloropalladate to activated iron and stirring with a glass rod. When the colour was discharged, the aqueous layer was decanted and a fresh batch of potassium hexachloropalladate was added. This procedure was repeated until no colour change occurred. This material was visibly much darker than the usual palladised iron. When the solutions were left on the shaker, the vials containing hyper-palladised iron vials were almost black as compared to the orange colour of the normally palladised iron.

Table 9.2: Comparison of the rate constants for degradation of bromohexane by fresh, aged and hyper-palladised iron (*components of the average reported in the last row). Horizontal lines separate different batches of activated iron.

Iron status	Rate constant, k_1		$t_{½}$	
	min^{-1}	Ratio	min	Ratio
Pd/Fe-1*	0.0044	94	157.5	107
Pd/Fe-2, 1nl	0.0089	189	77.9	52
Activated Fe	0.0047	100	147.5	100
Pd/Fe-3*	0.0118	251	58.7	40
Pd/Fe-4*	0.0038	81	182.4	124
Aged Pd/Fe	0.0046	98	150.7	102
Pd/Fe-5*	0.0052	111	133.3	90
Hyper Pd/Fe	0.0171	364	40.5	27
Average* Pd/Fe	0.0074	157	124	84

The rate constants for the degradation of bromohexane by individual batches of palladised iron differ almost three fold from the least to most reactive. This is due to differences in the degree of activation in each batch, so only pairwise comparisons are possible, but this almost means that there is no direct comparison for the aged sample of palladised iron.

As shown previously palladised iron is more active than activated iron. Aged palladised iron has activity which is comparable to two of the other batches of fresh palladised iron and about two-thirds the mean activity. When the data is presented in a graphical form (Fig 9.5), it may be

seen that the two degradation slopes run almost parallel, with the fresh Pd/Fe line always below the aged Pd/Fe line. Towards the end of the experiment, the lines appear to merge together, but the bromohexane in the fresh Pd/Fe experiment became undetectable after 300 minutes. It is difficult to be certain that the aged Pd/Fe reaction proceeds at the same rate throughout this experiment. It is possible that initially, the rate on the aged surface is considerably slower because the active sites are blocked by the oxide formed in storage. As the degradation proceeds, more and more of the active sites become unblocked and therefore available for binding the bromohexane. With the inherent problem with creating a matching control, the best conclusion that can be reached is that aging does not greatly reduce activity. In a practical application, such as a ground water barrier, the fact that an old iron surface is effective is important because it means that the material can be generated and stored off site until required. It also means that no costly or damaging materials are needed to generate an active barrier *in situ*.

The hyperpalladised iron has more than three times the activity of the palladised iron prepared at the same time and about 50% more activity than the most active sample of palladised iron used in this study. Without some surface analysis, it is not possible to guarantee the amount of surface coverage attained by this method. It does seem likely that 100 % coverage was not obtained. The reaction is thought to take place at the metal/metal interface and is accelerated with this bimetallic system because of the differences in potential. This constitutes classical corrosion chemistry. If the coverage was 100 %, then an increase in the rate of reaction of this magnitude would be most likely not be seen as the bimetallic interfaces would not exist. This is analogous to the iron only surface described in the first experiment in this sequence.

Fig. 9.5: Comparison of the degradation rate constants for bromohexane on activated iron, fresh, aged and hyper-palladised iron

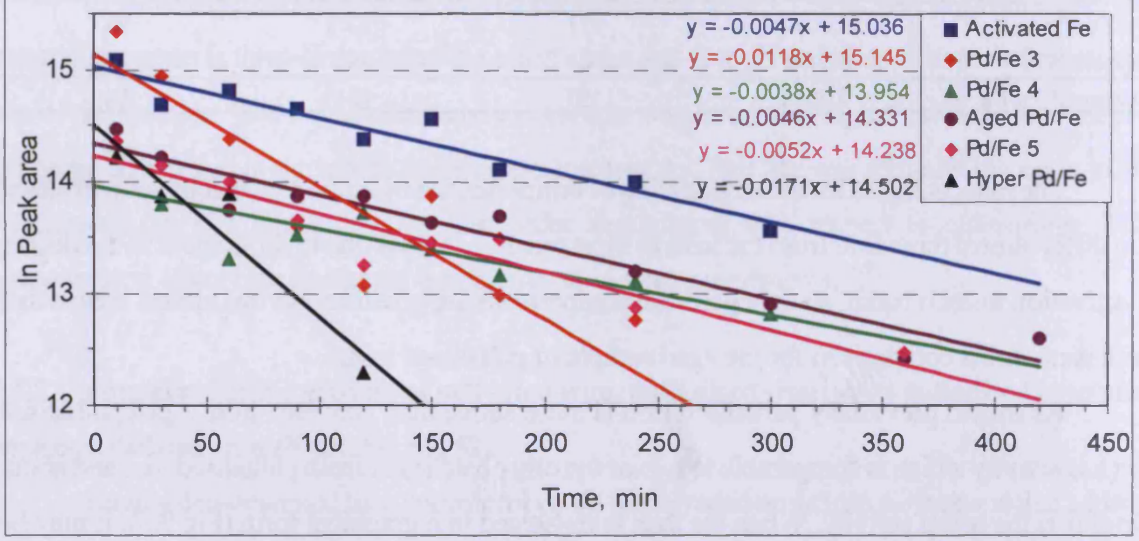

9.1.3 Degradation capacity of palladised iron (Expt. 60, 72-74)

Bromohexane was degraded at a satisfactory rate, but a more reactive substrate was required to investigate a wider range of conditions. Ideally this would have a higher solubility in water than bromohexane, a higher boiling point product, so that it could be analysed without resorting to thick film columns, and most importantly, a higher ionisation efficiency in the source of the mass spectrometer so that the lower limit of detection could be increased. Benzyl bromide appeared to satisfy all these criteria. When it was treated with activated and palladised iron, the rate constants and half lives were 0.1904 min^{-1}, 3.6 mins and 0.5842 min^{-1}, 1.2 min respectively. However the reaction rate was so fast that only two data points could be measured for the palladised iron reaction, before benzyl bromide fell below the limits of detection (Fig. 9.6). However despite the inaccuracies that this causes, it is apparent that as seen previously with chloroform and bromohexene, palladised iron was some three times more active than activated iron.

Fig. 9.6: Comparison of the degradation rate constants for benzyl bromide on activated and palladised iron

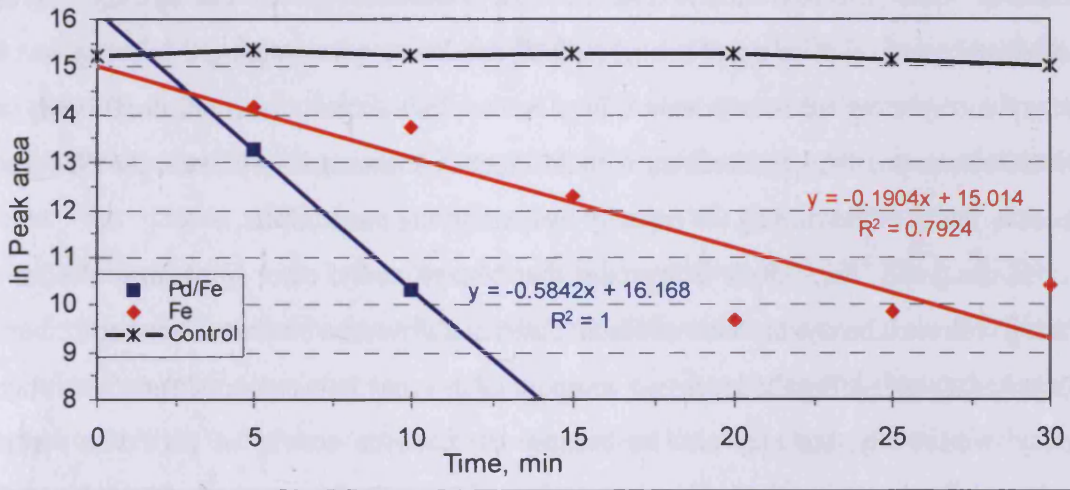

However the high reactivity of benzyl bromide enabled a study of the total degradative capacity of the system and might enable a distinction to be made between the Pd/Fe acting as a catalyst or a reagent. A small quantity of palladised iron (32.7 mg) was taken with the intention it should all be consumed. Nine portions of benzyl bromide solution in aqueous methanol were added to the palladised iron over the course of the experiment (13 days) and the increase in products monitored by GC-MS. The main challenge in this experiment was the solubility of benzyl bromide. Aqueous methanol was used to boost the solubility and 20 µl would just dissolve in methanol if sonication was used. In the latter stages of the experiment, larger volumes were used because as the starting material was consumed, more benzyl bromide would dissolve to keep a saturated

solution.

A colour change to pale yellow was noted in the first 24 hr, but there was no noticeable change after this and black magnetic filings could be seen. Thus, not all the iron was transferred into solution, which is probably due to a protective oxide layer. If the reduction was the sole reaction occurring, and all the iron was converted to $FeBr_3$ the maximum volume of benzyl bromide consumed would be 209 µl, but over 320 µl benzyl bromide was consumed and filings could still be seen.

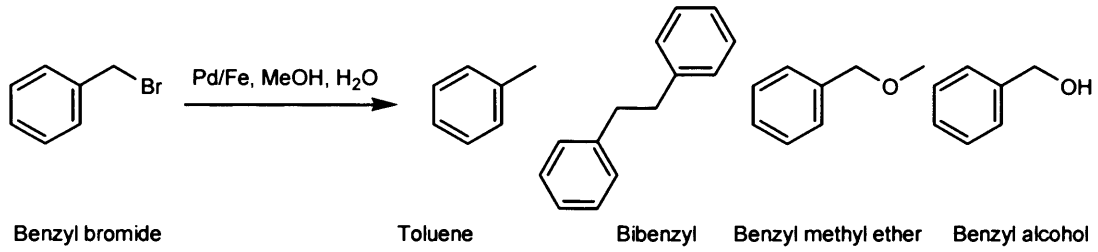

Fig. 9.7: Benzyl bromide is reduced to toluene but bibenzyl, benzyl alcohol and benzyl methyl ether are side products.

Examination of the GC-TIC trace revealed that reduction to toluene was accompanied by formation of bibenzyl, benzyl methyl ether and benzyl alcohol (Fig 9.7). The bibenzyl might be formed either by radical coupling of benzyl radicals or a Wurtz type coupling. The benzyl alcohol and benzyl methyl ether are clearly derived from nucleophilic substitution reactions. Bibenzyl can be formed by two possible mechanisms, with different stoichiometries relative to the Pd/Fe, so it was not worthwhile determining the capacity by quantifying the products.

In the graph (Fig. 9.8) it is apparent that benzyl methyl ether and benzyl alcohol are increasing with each benzyl bromide addition, albeit at a slow rate, but that toluene and bibenzyl have reached a plateau. For the latter two compounds this may be a consequence of volatility or solubility respectively, but may also be because the catalytic activity of the Pd/Fe for their formation has been exhausted. However benzyl bromide continues to be consumed.

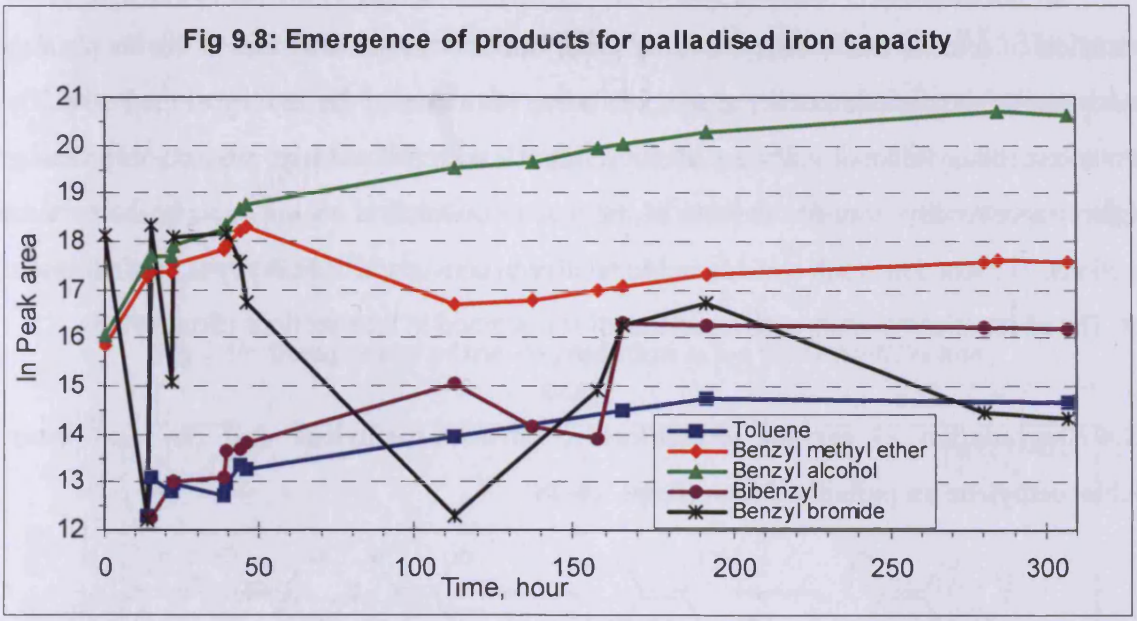

A reduced amount of iron (2.5 mg) was used in the next experiment, as it was not exhausted in the previous one. However in this experiment, both the aqueous layer and the organic layer were discarded after each measurement and replaced with fresh solvents and benzyl bromide. This was intended to minimise the effect of soluble byproducts (eg $FeBr_3$). The first analysis was done at 60 min. and seven further doses of benzyl bromide and measurements were made over the course of the 8 hours of the experiment. Benzyl bromide had the largest peak area and the relative amount was largely unchanged during the course of the reaction, but the ratio toluene:bibenzyl:benzyl methyl ether:benzyl alcohol changed from 8:30:25:37: to 3:14:37:46, thus toluene and bibenzyl are decreasing relative to benzyl methyl ether and benzyl alcohol. Therefore the catalyst/reagent for the latter two products is not wholly soluble and the amounts formed increase towards the end of the reaction. In this experiment the large excess of palladised iron (2.5 mg) would be potentially capable of degrading 15.5 µl benzyl bromide (23 mg) to $FeBr_3$, but only 1.07 µl benzyl bromide (1.53 mg) was used.

The degradation was rerun with a single dose of benzyl bromide,(0.133 µl,0.192 mg) and sufficient palladised iron (2 mg) to degrade 13 µl (18.4 mg) of benzyl bromide to $FeBr_3$. There was a six fold decrease in benzyl bromide during the experiment (330 minutes) and a rapid initial increase in the formation of products until a plateau was reached. The peak area ratios of the products, toluene:bibenzyl:benzyl methyl ether:benzyl alcohol were approximately 5:14:30:50 from 30 - 330 minutes, with standard deviations of 1.2, 1.4, 2.7 and 2.8 respectively. The toluene and bibenzyl did show a slight apparent decrease after the mid-time of the reaction (180 minutes), but as the standard deviations indicate this was barely significant.

In conclusion it is apparent that there is a limited capacity of the palladised iron for the formation of toluene and bibenzyl as measured, but it is not clear if this is due to physical constraints on the detection of the analytes or a true limitation of the activity of the Pd/Fe. The formation of benzyl alcohol and benzyl methyl ether is less limited and these products are produced slightly more readily towards the end of the reaction, which is not apparent in shorter term reactions. The reaction is sub-stoichiometric relative to conversion to $FeBr_3$ by at least a factor of ten. The effect of co-solvents such as methanol is discussed in later sections (Section 9.5)

9.1.4 Degradation of carbon tetrachloride, tetrachloroethylene and *cis*- and *trans*-dichloroethylene on palladised iron (Expt. 46-48).

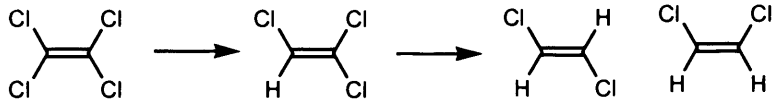

Fig 9.9: Tetrachloroethylene, trichloroethylene and *cis*- and *trans*-dichloroethylene

Carbon tetrachloride and tetrachloroethylene are both reported to be degraded by iron *via* reduction and intriguingly tetrachloroethylene is reported to yield only *cis*-dichloroethylene. (Fig. 9.9). But it was not apparent if this this was due to a single pathway or fast preferential degradation of *trans*-dichloroethylene. Carbon tetrachloride, tetrachloethylene, *cis*- and *trans*- dichloroethylene were degraded on a palladised iron and the reaction components monitored by GC-MS (Table 9.3, Fig. 9.10)

Table 9.3: Comparison of degradation rates and half lives for carbon tetrachloride, tetrachloroethylene, *cis*-dichloroethylene and *trans*-dichloroethylene.

System	Mean k_1, min^{-1}	Mean k_1, ratio	$t_{½}$, min	$t_{½}$, ratio
Carbon tetrachloride	0.0730	100	9.5	100
Tetrachloroethylene	0.0073	10	95.0	1000
cis-Dichloroethylene	0.0035	5	198.8	2093
trans-Dichloroethylene	0.0078	11	88.5	932

The rate of degradation of carbon tetrachloride was 10 times faster than tetrachloroethylene and the appearance of the chloroform peak was almost instantaneous. Chloroform also degrades in this system, but this reaction is reported in more detail later (Section 9.2). *Trans*-dichloroethylene is degraded at similar rate to tetrachloroethylene and about twice as fast as *cis*-dichloroethylene. Therefore it is likely that either of the dichloroethylenes would have been apparent in the degradation of tetrachloroethylene if they had been free intermediates. Surprisingly, no products were detected at all with tetrachloroethylene or the dichloroethylenes.

Studies looking at the degradation of trichloroethene on zero-valent iron have reported the

presence of *cis*-dichloroethene as a product, but not when using palladised iron. Vinyl chloride was a product in both systems, but at an order of magnitude less with palladised iron[174,172]. The reason for the absence of *cis*-dichloroethylene in the palladised iron system has not been investigated, but studies looking at zero-valent metal systems suggest that the π bonding between trichloroethylene or tetrachloroethylene and the iron surface is so strong that all the chlorines are removed before desorption back into solution[195].

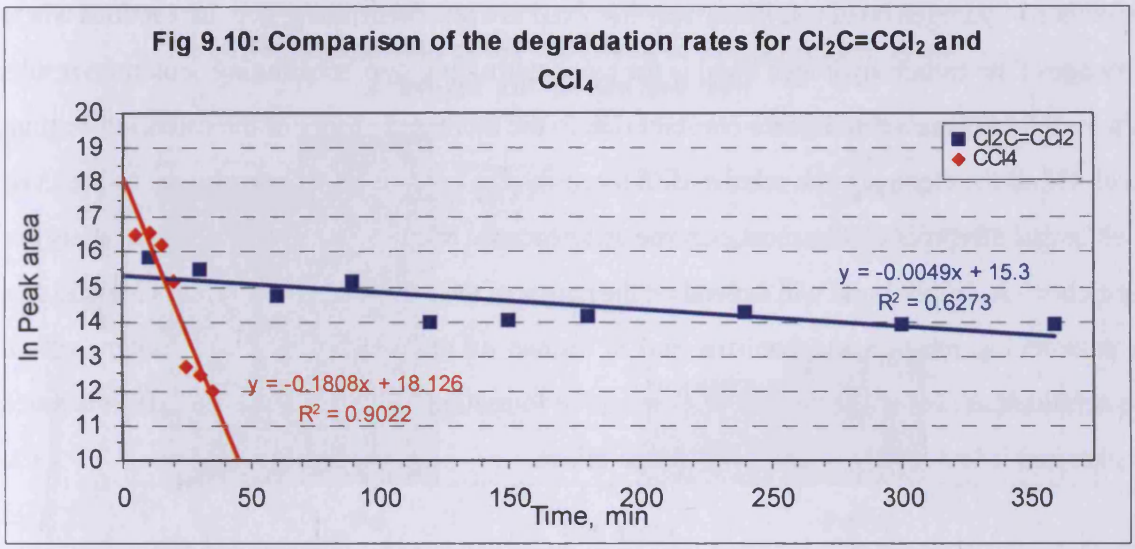

Fig 9.10: Comparison of the degradation rates for $Cl_2C=CCl_2$ and CCl_4

9.1.5 Degradation of bromoform on palladised iron (Expt 42,43)

The majority of the work initially examined the degradation of chloroform on a variety of surfaces and under different experimental conditions, and as a final comparison, we looked at the brominated analogue, which was anticipated to be more reactive. Aqueous bromoform solution was shaken over palladised iron and the degradation monitored by GC-MS. The degradation was found to proceed fifteen times faster than that of chloroform, with a rate constant of 0.074 min^{-1} as compared to 0.005 min^{-1} for chloroform.

The bromoform peak rapidly decreased, but despite the use of SIC no trace of dibromomethane or bromomethane could be detected. In other studies using palladised iron, reaction internediates have not been detected[172], and it has been postulated that they never desorb from the iron surface, but remain bound until all the halogens have been cleaved. This, coupled with the faster rate of degradation of bromo-compounds explains why we were not able to detect any dibromomethane or bromomethane in this system.

9.2 Degradation of deuterated compounds - isotopic composition of products

Much of the work recently published has centred around the use of iron as a means for VOC removal from contaminated ground water sources. Whilst this is of enormous importance

environmentally, most of the emphasis is on complete removal of all VOCs and little attention has been focussed on the actual mechanism of chlorine removal. In this series of experiments, we investigated the isotopic composition of the degradation products using various combinations of chloroform, deuterated chloroform, water and deuterium oxide to try and establish the source of the protons that replace the chlorine. We also compared the reaction rates of deuterated chloroform with "normal" chloroform to see if there was any significant difference which might indicate that the carbon - hydrogen bond was in any way involved in a rate determining step. In reactions where cleavage of the carbon-hydrogen bond is the rate determining step, substituting deuterium results in a 5 - 8 fold decrease in the rate constant due to the increased energy of the carbon-deuterium bond. Of all the elements, the relative difference in size is the largest for hydrogen as the mass doubles and this produces the most extreme differences in reaction rate The actual bond energy of the carbon - hydrogen bond will depend on the nature of the compound itself. This is a useful tool in determining reaction mechanisms and is known as the primary hydrogen isotope effect. Deuteration can also affect the rate of cleavage or formation of other bonds. This effect is much weaker and is known as a secondary isotope effect.

9.2.1 Degradation of deuterated chloroform on activated and palladised iron (Expt. 4)

Table 9.4: Comparison of the degradation rates and half lives of chloroform and deuterated chloroform on activated and palladised iron.

Expt.	System	k_1, hr^{-1}	k_1 ratio	$t_{1/2}$, hr	$t_{1/2}$ ratio
4	$CDCl_3$, Fe	0.04614	100	15.02	100
4	$CDCl_3$, Pd/Fe	0.1346	292	5.15	34
1	$CHCl_3$, Fe	0.0398	86	17.4	116
2	$CHCl_3$, Pd/Fe	0.1045	226	6.63	44
3	$CHCl_3$, Fe, carbonate,	0.0440	95	15.77	105
3	$CHCl_3$, Pd/Fe, carbonate,	0.1295	281	5.36	36

Comparison of the rate constants (Table. 9.4) for this and previous experiments (Fig 9.11), clearly show that the degradation rates on activated iron are three times slower than on palladised iron. The degradation rate of $CDCl_3$ is not significantly different from $CHCl_3$ and hence cleavage of the carbon - deuterium bond is not the rate limiting in this reaction. This means that during the degradation, the carbon hydrogen bond is either broken and is not the slowest step, or is not broken and the atom is retained. This experiment excludes a substantial primary deuterium isotope effect, but is not sufficiently sensitive to detect a secondary isotope effect (cf Section 9.2.6).

There are four possible products from the degradation of deuterated chloroform with palladised iron: chloroform, dichloromethane, monodeuterated dichloromethane and dideuterated

dichloromethane. The products in which protons are incorporated, would be derived from "H" produced on the surface of the palladised iron formed during the activation. The term "H" is intended to indicate an unspecified hydrogen species (H^+, H^- or H_2), which is capable of participating in the reaction. However considerable care needs to be taken with control experiments before assigning dichloromethane as a product because this is a common laboratory contaminant and is formed in extremely small amounts in the degradation of chloroform.

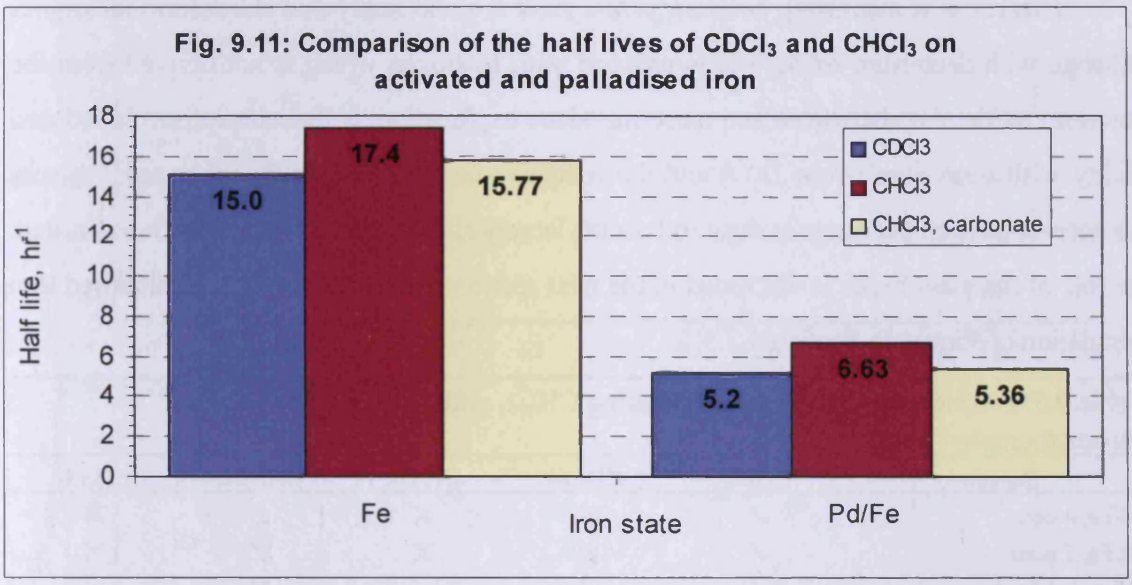

9.2.2 Degradation of chloroform in deuterium oxide on a palladised iron in the presence of chromatography glass beads (Expt 5)

Having demonstrated that the degradation rate for deuterated chloroform in water was approximately the same as for "normal" chloroform, the reverse experiment was performed to determine if the the rate determining step involved the cleavage of aqueous hydrogen - oxygen bonds.

Contamination of the degradations with dichloromethane from other work in the laboratory was a persistant problem in the studies of the degradation of chloroform. Dichloromethane is much less reactive than chloroform with activated or palladised iron, but its presence means that quantification of the products is more difficult.

Chromatography glass beads (80 mesh) were added to the reaction vials to reduce the volume of deuterium oxide required for the experiment. The beads were chosen as in normal usage they are an inert support and therefore thought to be unreactive. This was a qualitative experiment designed to see what types of products were obtained and to discover if a quantitative experiment would be worthwhile. The spectra of the peaks generated from the experiment were examined and the following results noted; at this stage peak areas and relative compositions were not of

paramount importance, these were examined in greater detail in subsequent experiments.

Incubation of deuterium oxide with chloroform and glass beads (the control) resulted in incorporation of deuterium in chloroform, but not the contaminating dichloromethane which was only present at trace levels (Table 9.5). Whereas in the presence of palladised iron, both deuterated chloroform and a trace of monodeuterated dichloromethane are formed and in neither reaction is dideuterated dichloromethane formed.

This result is interesting because, *prima facie* it could imply that chloroform undergoes exchange with deuterium oxide, but is reduced with hydrogen which is not derived from the deuterium oxide. An alternative and more mundane explanation, is that chloroform is reduced quickly with deuterium (from D_2O) and the reductive capacity is quickly exhausted, whereas hydrogen-deuterium exchange is slow and occurs largely after the reducing capacity is exhausted. The role of the glass beads is discussed in the next section and discussion of the palladised iron degradation continues in Section 9.2.5.

Table 9.5: Products identified from incubating $CHCl_3$ with D_2O, Pd/Fe and glass chromatography beads

Sample	$CHCl_3$	$CDCl_3$	CH_2Cl_2	$CHDCl_2$	CD_2Cl_2
Pd/Fe, 4 hour	✓	✓	×	✓	×
Pd/Fe, 7 hour	✓	✓	×	✓	×
Control, 4 hour	✓	✓	✓	×	×
Control, 7 hour	✓	✓	✓	×	×

9.2.3 Chloroform and deuterated chloroform hydrogen exchange with deuterium oxide or water in the presence of glass chromatography beads (Experiment 9, 10)

In a mass spectrometer with an EI-(+)-source, chloroform gives a very low abundance molecular ion cluster. The base peak is *m/z* 83, which results from loss of a single chlorine. The ion cluster for M - Cl consists of the following ions (% abundances): 83 (100), 84 (1.1) 85 (64), 86 (0.7), 87 (10.2), 88 (0.1); 89 (1.5×10^{-5}) which range from $^{12}C^{35}Cl_2{}^{1}H$ to $^{13}C^{37}Cl_2{}^{2}H$. The even *m/z* ions are predominantly due to ^{13}C. In the mass spectrum, there is also a peak at *m/z* 82, which is due to M - HCl, which typically has an abundance of about 3 %, this has isotope peaks at *m/z* 84, 86 etc, but the largest of these at *m/z* 84 only has an abundance of 2 % (Fig 9.12).

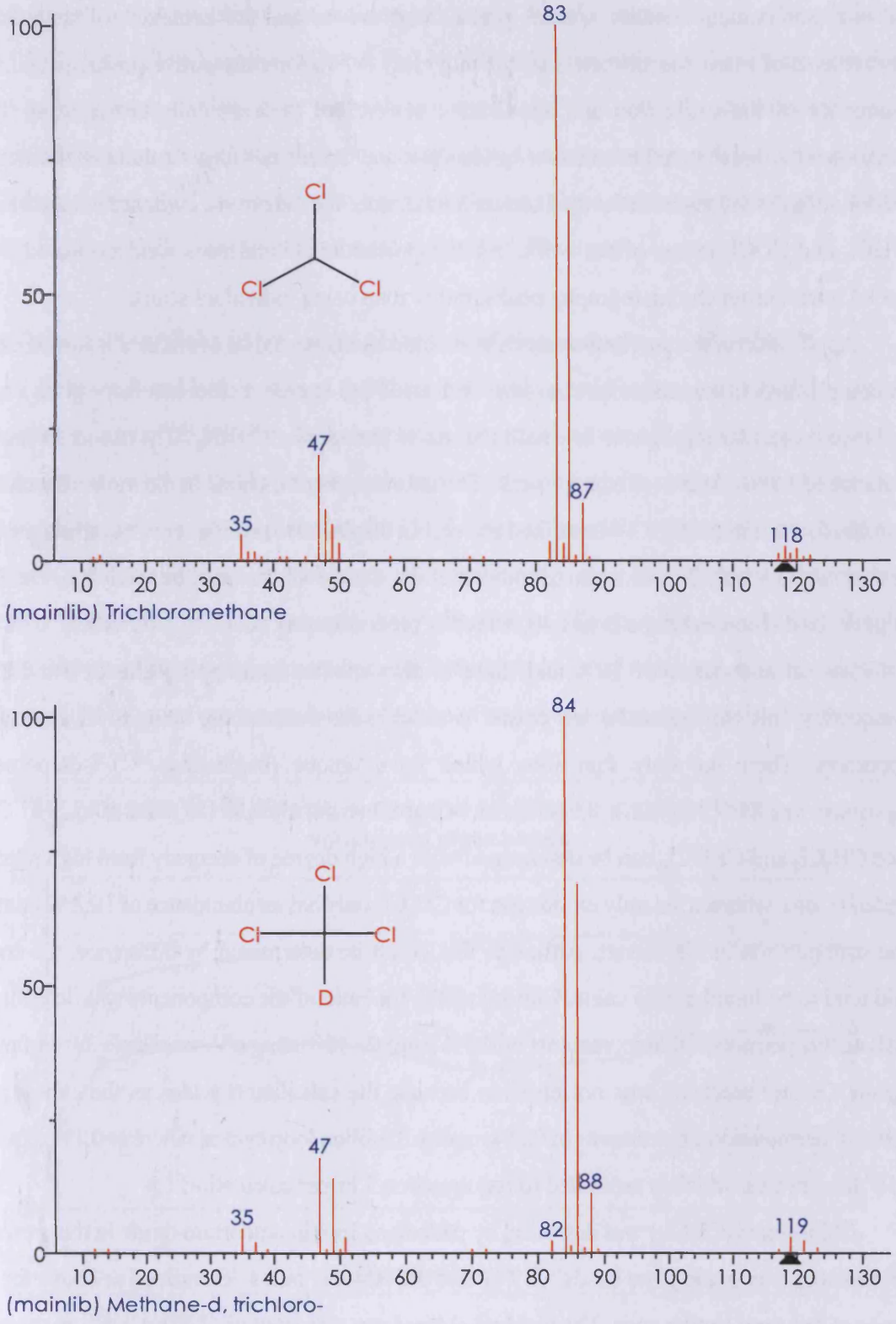

Fig 9.12 Mass spectra of chloroform and deuterated chloroform

Deuterated chloroform has a similar M - Cl cluster at one *m/z* unit higher than chloroform and because there is no overlap, between the two clusters the ratio of chloroform to deuterated chloroform can be determined with practical degree of accuracy by determining the ratio of odd:

even *m/z* isotopomers. Unless special precautions are taken, the accuracy of abundance measurements of mass spectrometers is typically only ± 5% for consecutive peaks, which is a consequence of the calibration and apodisation settings of the data collection system. This calculation was implemented in an Excel spreadsheet and the errors were calculated as the sum of the absolute % deviations from the total cluster abundance. We did not see evidence for separation of $CHCl_3$ and $CDCl_3$ in any of our work, but as a precaution, abundances were measured from summed scans across chromatography peaks, rather than using individual scans.

Application of the previous analysis to dichloromethane and its deuterated isotopomers is more complicated. In the a mass spectrometer with an EI-(+)-source, dichloromethane gives a high abundance molecular ion cluster in which the major isotopomer ($^{12}C^1H_2{}^{35}Cl_2$) at *m/z* 84 has an abundance of 64 % relative to the base peak. The abundances of the ions in the molecular cluster are similar to those of the $CHCl_2^+$ described above, but displaced to one higher *m/z* unit and the M - H peak at *m/z* 83 is only 2 %, so again the other members of this cluster may be safely ignored. The base peak for dichloromethane is *m/z* 49, which is predominantly $^{12}C^1H_2{}^{35}Cl$, however $^{12}C^{35}Cl$ at *m/z* 47 has an abundance of 10% and there is also another overlapping cluster for CHCl. Consequently only the molecular ion cluster is suitable for determining the ratio of deuterated isotopomers. There are only four ions which have unique (neglecting ^{13}C) isotopomeric composition *m/z* 84 ($C^1H_2{}^{35}Cl_2$); 85 ($C^1H_1{}^2H_1{}^{35}Cl_2$); 87 ($C^1H_1{}^1H_2{}^{35}Cl^{35}Cl^{37}$) and 90 ($C^2H_2{}^{37}Cl_2$). Hence CH_2Cl_2 and $CHDCl_2$ can be determined with a high degree of accuracy from high relative abundance ions, whereas the only unique ion for CD_2Cl_2 only has an abundance of 10.2 % relative to the strongest ion in the cluster. Although this could be determined by difference, the errors would tend to be found in this value. Consequently, the ratio of the components was determined by exhaustive permutation in increments of 0.5% from 0 - 100 using a Visual Basic 3.0 computer program. Greater precision was not possible because the calculation scales as the cube of the number of permutations. Increments of 0.5% require 8 million loop cycles, where as 0.1% requires 1×10^9 loop cycles, which is estimated to require circa 3 hr per calculation.

Chloroform ($CHCl_3$) was degraded by palladised iron in deuterium oxide in the presence of chromatography grade glass beads for 7 hr and the isotopic ratios determined as above for the average of two very similar runs. The residual chloroform consisted of $CHCl_3$:$CDCl_3$ in the ratio 29:71 and the dichloromethane, consisted of CH_2Cl_2:$CHCCl_2$:CD_2Cl_2 in the ratio 13:54:32. This clearly indicates that chloroform is undergoing exchange and that a combination of chloroform and deuterated chloroform undergoes degradation to dichloromethane. In the control vial, which contains no palladised iron, the residual chloroform consisted of $CHCl_3$:$CDCl_3$ in the ratio 19:81, which is comparable to the reaction vials. In both the control and blank (no $CHCl_3$) vials, there

were traces of contaminating dichloromethane, which surprisingly was deuterated (CH_2Cl_2:$CHCCl_2$:CD_2Cl_2) in the ratios 68:21:11 and 78:22:0 respectively. These were determined from low ion counts and hence are probably not significant. The virtually equal exchange in the control and reaction vials clearly suggests that the glass beads were responsible for the exchange. Accordingly, deuterated chloroform was treated with water alone and two replicates gave identical results; $CHCl_3$:$CDCl_3$ was formed in the ratio; 74:26 (1.5% error).

9.2.4 Examination of the effect on the pH water of chromatography glass beads

Initially, it had been assumed that the glass beads would act as an inert bulking agent to reduce the amount of (expensive) deuterium oxide required for the reactions, but from the previous experiments, it was clear that hydrogen exchange occurred in both the reactant and product. Beads were measured by volume and placed in the 15 ml degradation vials which were then filled to the brim with water. As little as 2 mls of beads were sufficient to raise the pH close to the maximum observed (Fig. 9.13) and this occurred over the course of about an hour. It is difficult to quantitatively analyse this experiment because both the volume of water and volume of beads are changing. In the second measurement the volume of water was constant (20 mls), but the volume

Fig 9.13: pH of differing volumes of deionised water with various volumes of glass beads

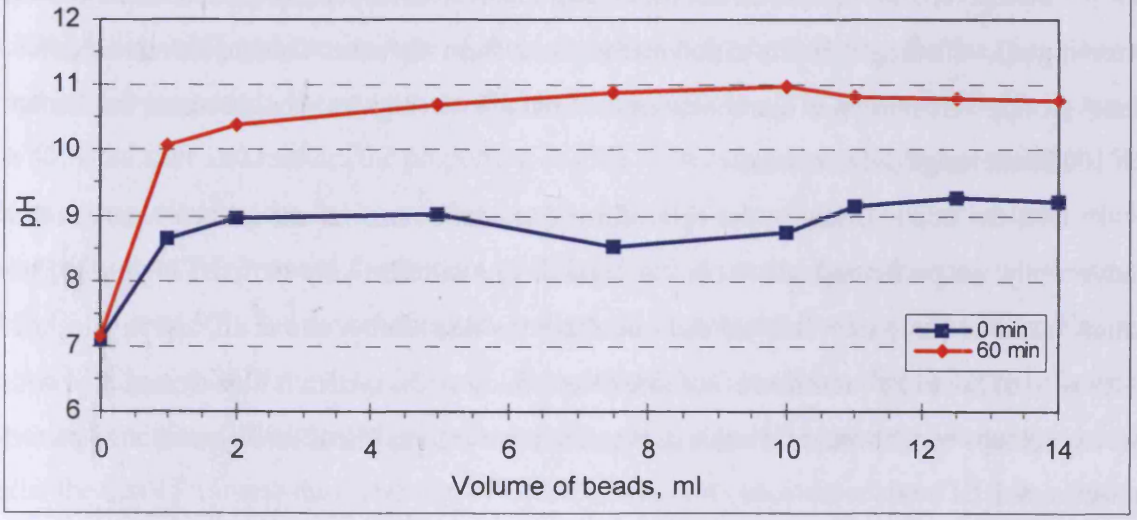

of beads was varied. Less than 5 mls of beads are sufficient to achieve the maximum: pH 11 (Fig. 9.14)

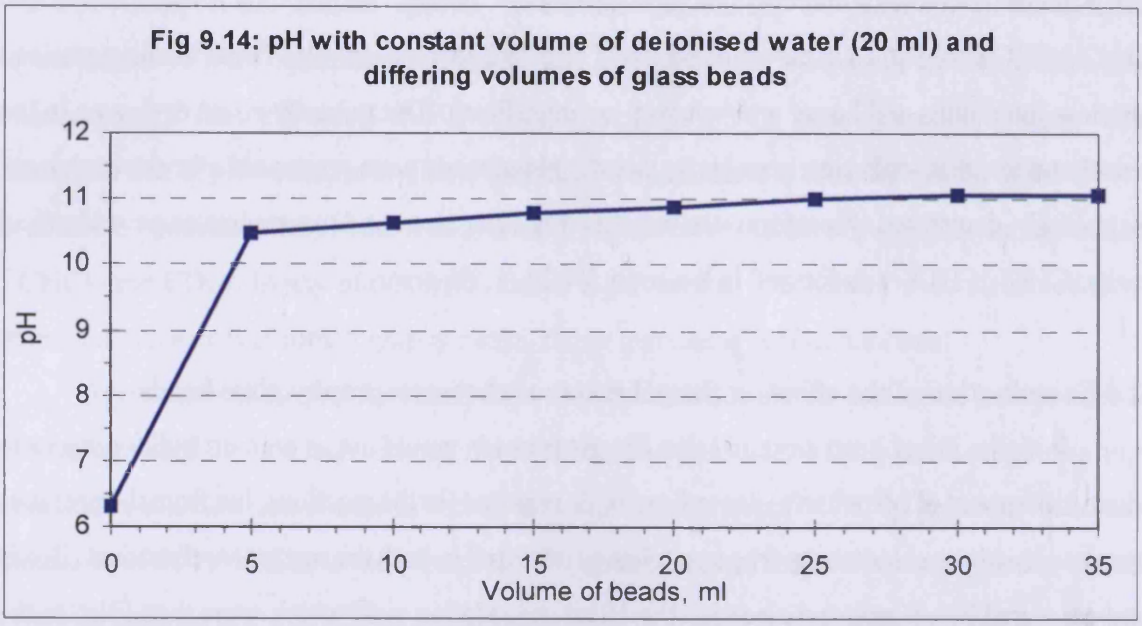

The beads are 80 - 100 mesh (the same size as the iron filings used) and consequently have a high surface area. The basicity is presumably due to surface metal (presumably sodium) silanoxides. Recent work[208] has shown that water reacts with the surface silanol groups to release hydrogen via a hydroxyl exchange reaction between water and the surface hydroxyl. Two types of complex are formed, in the first, water molecules adsorb to the surface and act as proton donors and in the second, the water molecules adsorb and act as proton acceptors.

Another report[209] has shown that the concentration of surface silanol groups decreases with increasing pH, with the possibility of polymerization to form siloxanes. This should mean that few silanol groups were present in our system as the final pH was high and could account for the fact that 100 % exchange did not occur.

The use of the beads in the chloroform degradation had an unexpected bonus in that inadvertently we performed some of our degradations at effectively buffered high pH. This demonstrated in our system that pH did not affect the degradation rate at all, and implies that conversion of Fe^0 to Fe^{2+} reaction is not rate determining as the system is already saturated with hydroxyl groups which would slow this conversion relative to an unbuffered system, as discussed in Section 9.1.1.

9.2.5 Comparison of the products of degraded deuterated chloroform in water and chloroform in deuterium oxide (Expt 16, 17, 8, 31, 6)

Having determined that the chromatography beads were causing hydrogen exchange in chloroform and possibly dichloromethane, we reinvestigated the degradation without the

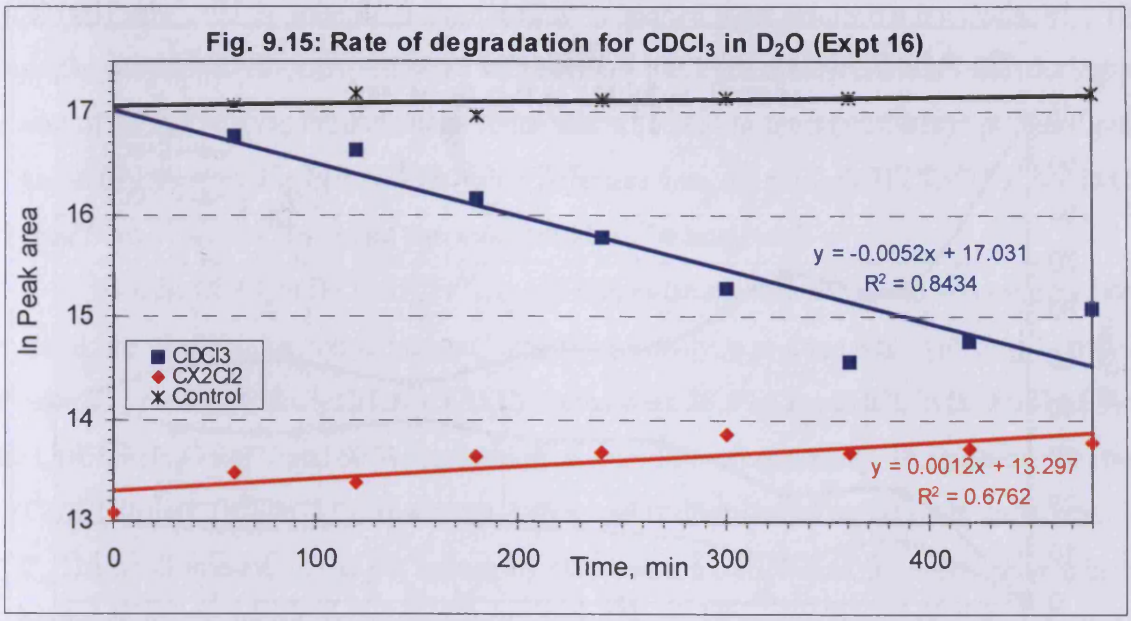

chromatography beads. The issue of dichloromethane contamination was a severe problem, so we looked at the degradation of $CDCl_3$ in D_2O first, because this was the experiment least likely to give CH_2Cl_2 and hence the one in which contamination would be most apparent. However, it is possible that $CDCl_3$ is converted to CH_2Cl_2, by "H" formed on the surface of the iron during activation, or that it is converted to $CHDCl_2$ in a similar way. About 80% of the $CDCl_3$ (0.125 nl/ml) was degraded and the rate of degradation (k_1 0.0052 min^{-1}, $t_{½}$, 133 min, Fig. 9.15) was comparable to previous runs. All of the dichloromethane present at the start of the reaction was CH_2Cl_2 (Fig 9.15) and the amount of dichloromethane doubled during the reaction. As the degradation progressed, the proportion of CH_2Cl_2 decreased to 40 %, whereas CD_2Cl_2 increased to 40% and after 180 minutes the proportion of CHDCl remained more or less constant at 15%. In an attempt to reduce the dichloromethane contamination, the reaction was repeated using helium sparged water. This reduced the amount of CH_2Cl_2 and in consequence the final proportion of CD_2Cl_2 reached 50%, but the benefits were mitigated by a comparatively poor batch of palladised iron ($CDCl_3$, k_1 0.0029 min^{-1}, $t_{½}$, 239 min, 70 % degradation) and there was no overall change in the small amount of dichloromethane present during the course of the reaction. As seen previously, after the first 15 minutes the proportion of $CHDCl_2$ was fairly constant at about 15%. In all of the controls (and the Pd/Fe vials), the isotopic composition of the $CDCl_3$ was unchanged and all the dichloromethane was CH_2Cl_2, hence all changes are a consequence of the palladised iron.

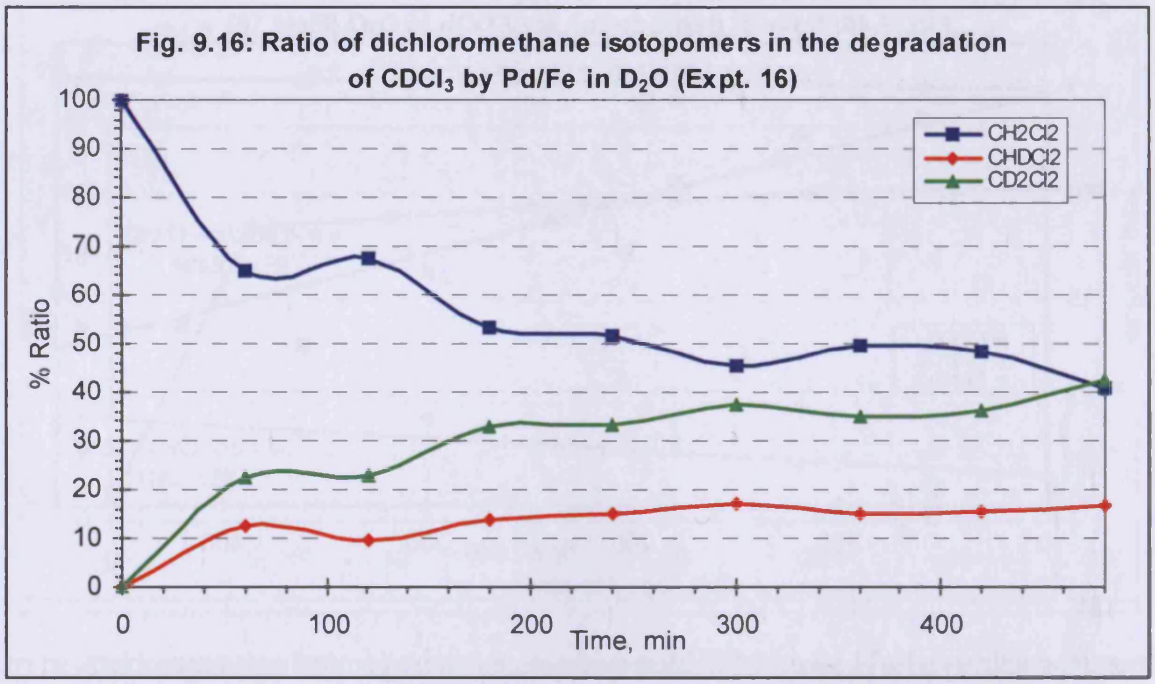

In both of these experiments the degradation curves (Fig 8.17 for Expt 17, Fig 9.16) are not smooth. This is due in part to the small amounts of dichloromethane detected and also because the variables are not independent because they are ratios.

The isotopic composition of the $CDCl_3$ was measured in both the controls and the degradation vials, there was no change whatsoever and hence surface exchange with bound "H" and release of $CHCl_3$ into solution can be definitively excluded. Deuterium derived from D_2O is clearly incorporated into dichloromethane and the proportion of CD_2Cl_2 increases as the reaction progresses. The results are consistant with initial reduction of chloroform by surface bound "H", followed by H/D exchange at the surface and subsequent reduction of dichloromethane to give an undetectable product (eg. methyl chloride or methane)

When $CDCl_3$ (0.125 nl/ml) was degraded in H_2O with palladised iron, for a protracted period (15 hr), the degradation of $CDCl_3$ ranged from 59 - 77% for three replicates and the ratio CH_2Cl_2:$CHDCl_2$:CD_2Cl_2 was 58/55/55:42/38/45:0/7/0. The longer run time enabled the peak areas of the dichloromethane to be measured in both the controls and the degradation vials. As the dichloromethane in the control vials is all CH_2Cl_2 and assuming that the sampling bias and ionisation efficiency are identical for all isotopomers, the % of contaminating CH_2Cl_2 in the degradation vials was calculated to be 65%. This is slightly higher than observed and hence it is reasonable to suppose that the vast majority of the CH_2Cl_2 in the reaction vials is due to contamination and that reduction gives $CHDCl_2$. Repetition of the degradation with palladised iron in H_2O with an increased concentration of $CDCl_3$ (0.25 nl/ml), but as a kinetics run over 420 mins

(k_1 0.0051 min^{-1}, $t_{½}$, 136 min, 86 % degradation) supported these results but not decisively. The isotopic composition of $CDCl_3$ remained unchanged in the degradation and control vials during the course of the reaction, but the dichloromethane was at such a low level that the isotopic ratio could not be determined reliably from 60 - 180 mins. After that time, the ratio of CH_2Cl_2:$CHDCl_2$:CD_2Cl_2 ranged from 27-41:55-73:0-5, but the peaks could not be integrated.

Both the $CDCl_3$ in D_2O and $CHCl_3$ in H_2O degradations with palladised iron were repeated in duplicate at still higher concentration (1.25 nl) with analysis at 4 and 6 hr, with largely similar results. The average CH_2Cl_2:$CHDCl_2$:CD_2Cl_2 ratios were 38:59:4 for $CHCl_3$ in D_2O and 14:86:1 for $CDCl_3$ in H_2O for 71 and 60 % degradation of chloroform respectively. The higher proportion of CH_2Cl_2 in the $CHCl_3$ in D_2O experiment is presumably due to initial reduction by surface bound "H". The small amounts of CD_2Cl_2 apparently observed are zero, within the errors inherent in the experiment. The standard deviations for the four values which contributed to each average for CH_2Cl_2 and $CHDCl_2$ were all 2.5 ± 0.15.

In summary, the water controls containing deuterated chloroform do not undergo proton exchange and any dichloromethane present (contaminant) is fully protonated. The deuterium oxide controls contain only protonated chloroform, so no exchange, and the dichloromethane present is also protonated suggesting again that this is contamination. Deuterated chloroform incubated with water and palladised iron produced only deuterated chloroform, so no exchange with the bulk solvent, and the majority of the dichloromethane detected contained one deuterium. This suggests that there is no exchange with the solvent and that the degradation proceeds with the chlorine being replaced with a proton from the solvent, probably the protons on the iron surface being used first and then those in the solvent moving onto the surface to replace those that are lost. This scenario is supported by the results from the protonated chloroform in deuterium oxide degradation where the dichloromethane produced is a mixture of singly deuterated and protonated dichloromethane. In this case, the iron surface initially contained protons from the activation process so protonated dichloromethane was formed. As these protons were replaced with deuterium, mono-deuterated dichloromethane was formed, thus resulting in the mixed dichloromethane detected.

9.2.6 Comparison of the degradation rates of chloroform in deuterium oxide and deuterated chloroform in water (Expt, 14, 16, 17, 31, 7)

Table 9.6 shows kinetics data for the four possible combinations of $CHCl_3$, $CDCl_3$, H_2O, D_2O degrdations with palladised iron. As seen previously, there are a wide range of values due to different degrees of activation of palladised iron. To minimise these problems, $CHCl_3$ and $CDCl_3$ were degraded in D_2O and H_2O respectively using the same batch of palladised iron (Expt 14.).

Table 9.6: Comparison of rate constants and half lives for the degradation of $CHCl_3$ in D_2O and $CDCl_3$ in H_2O with Pd/Fe.

Expt.	System	Graphical values			
		k_1, min^{-1}	k_1 ratio	$t_{½}$, min	$t_{½}$ ratio
2	$CHCl_3$, H_2O	0.0017	50	398	195
14	$CHCl_3$, D_2O	0.0034	100	204	100
4	$CDCl_3$, H_2O	0.0022	64	309	151
31	$CDCl_3$, H_2O	0.0051	150	136	67
14	$CDCl_3$, H_2O	0.0034	100	204	100
16	$CDCl_3$, D_2O	0.0052	153	133	65
17	$CDCl_3$, D_2O	0.0029	85	239	117

The kinetics plots (Fig 9.17) show equal gradients for the two transformations and hence equal rate constants (0.0034 min^{-1}), although the intercepts are quite different, due to systematic differences in the amounts of chloroform detected, however the percentage degradation for $CDCl_3$ and $CHCl_3$, (74%; 68%) were comparable.

Fig. 9.17: Comparison of degradation rates of $CHCl_3$ and $CDCl_3$ on Pd/Fe

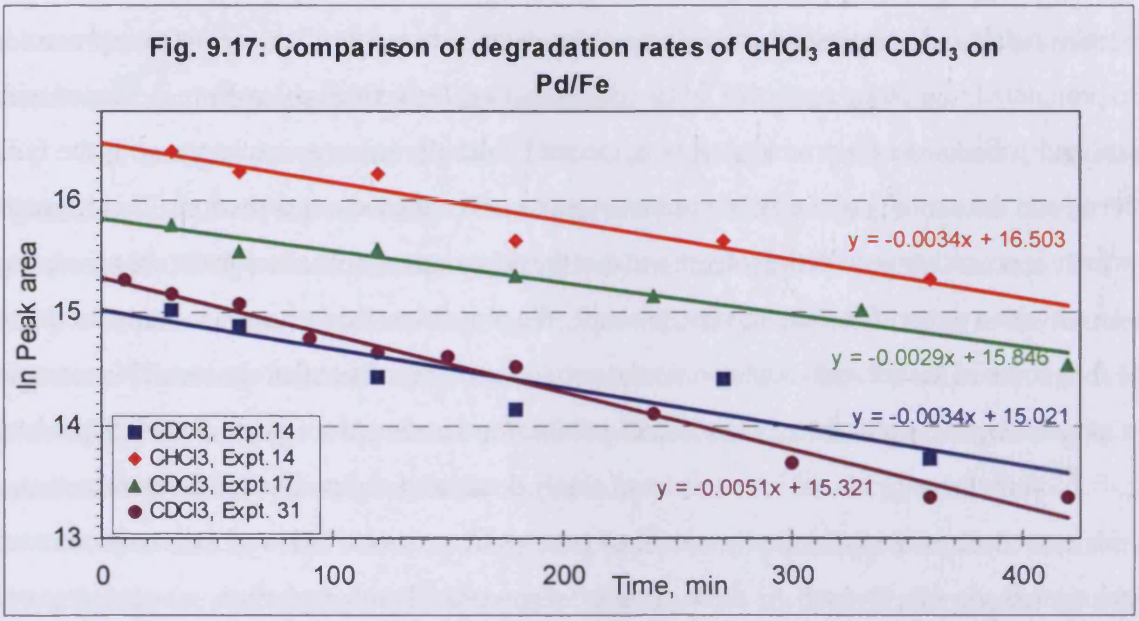

It has clearly been shown that $CHCl_3$ degrades in D_2O at a similar rate to $CDCl_3$ in H_2O, but nevertheless these "parallel" experiments, even with the same batch of palladised iron are insufficiently sensitive to detect small isotope effects. Accordingly, a mixture of $CDCl_3$ and $CHCl_3$ was degraded in the same vial, in either D_2O or H_2O, in duplicate. If an isotope effect occurs, the $CHCl_3$ will react in preference to the $CDCl_3$ and the change can be detected by measuring the ratio of the isotopomers. Both the control and degradation vials had $CHCl_3$:$CDCl_3$ ratios in the range 44-48: 56-52, with errors ranging from 1 - 3 %. This absolutely excludes a deuterium isotope effect, within the limits of the accuracy of the abundances of the ions in the ion cluster. The isotope

composition of dichloromethane was adequately reproducible between the duplicates and in accordance with expectations, albeit the errors were higher (1 - 5%) than with chloroform, because of the lower abundance. In the degradation in D_2O, the average ratio CH_2Cl_2:$CHDCl_2$:CD_2Cl_2 was 26:40:34 and hence there were nearly equal amounts of $CHDCl_2$ and CD_2Cl_2 derived from $CHCl_3$ and $CDCl_3$ respectively. The 6 % excess of $CHDCl_2$ over CD_2Cl_2 presumably results from reduction of $CDCl_3$ by active "H" on the surface. If the same contribution occurs in the formation of CH_2Cl_2, then the contaminating CH_2Cl_2 is 20%.

In the degradation in H_2O, the average ratio CH_2Cl_2:$CHDCl_2$:CD_2Cl_2 was 60:40:0, which indicates 20% contamination from exogenous CH_2Cl_2, which is identical to that seen in the D_2O degradation. The absence of CD_2Cl_2 excludes metathesis of deuterium with the palladised iron.

9.2.7 Degradation of benzyl bromide in deuterium oxide (Expt. 67,68, 75a)

The presence of active "H" on the surface of the palladised iron confounds unambiguous determination of the course of the reaction and moreover the problems in detecting adequate amounts of dichloromethane also compromises the accuracy of the experiment. Therefore it seemed worthwhile to investigate the incorporation of deuterium during the reduction of benzyl bromide, using iron filings which were activated (by hydrochloric acid) and palladised in deuterium oxide. The samples were analysed in duplicate after 5 minutes and 15 minutes. The benzyl bromide was completely degraded and gave toluene as the only product. In the experiments using methanol as a co-solvent, bibenzyl was also formed but it was not detected in this experiment, even in SICs.

Determination of the isotopomer ratio for toluene and toluene-d_1 is not straightforward, because in the EI-(+)-mass spectrum the only high abundances ions are *m/z* 92 (73 %) and *m/z* 91 (100% M - H) and hence there is an overlap between the ions for the two isotopomers. The ion abundances were modelled by assuming that *m/z* 92 consists of 8 % $^{12}C_6{}^{13}C_1H_8$ and the remainder (65 %) is due to $^{12}C_7H_8$. Hence the M - 1 ions (*m/z* 91-93) have the abundances, 100, 8, 0.3%, whereas the M ions (*m/z* 92 - 94) have the abundances 65, 5, 0.2%. If we assume that only benzylic hydrogen is lost during ionisation and that there is no deuterium isotope effect, then the abundances can be modelled as the sum of two times the M and M - 1 ions derived from C_7H_8, plus C_7H_7D, which reflects the ratio of hydrogen to deuterium in the benzylic methyl group. The sums of the six ion series were manually iterated in Excel, to match the data.

Application of this methodology to the toluene produced in the two replicates at 5 and 15 minutes, showed that the ratio of C_7H_8:C_7H_7D was 23-30:70-77 (< 3% error) for all four runs. The palladised iron was activated using hydrochloric acid, but washed and palladised in deuterium

oxide. The presence of C_7H_8 indicates that the active "H" is produced during activation by hydrochloric acid. Thus "H" does not undergo appreciable exchange during four washes with deuterium oxide or palladisation, but seemingly does undergo exchange as the reaction proceeds.

The success of this exploratory experiment, motivated a repeat with more replicates and using methanol as a co-solvent. The low solubility of typical organic halides in water is an impediment to the use of palladised iron as a reduction technique and it appeared possible that the reduction would proceed in methanol. Four variants were investigated: palladised iron in water or methanol:water (10:90) and palladised iron prepared in deuterium oxide with D_2O or CD_3OD:D_2O, plus the corresponding controls and blanks.

Table 9.7: % Average product formation relative to control values for experiment sets (Expt. 68, cf. Table 8.68b, Fig. 9.17). * indicates deuteration.

No.	Sample	Toluene	Benzaldehyde	Benzyl alcohol	Bibenzyl
3-4	D_2O or H_2O controls			45*	
7-9	D_2O, CD_3OD, Pd/Fe	121*	11	14*	57
10-12	H_2O, CH_3OH, Pd/Fe	186	24	24	55
13-15	D_2O, Pd/Fe	61*	0	40*	9
16-18	H_2O, Pd/Fe	59	6	53	9

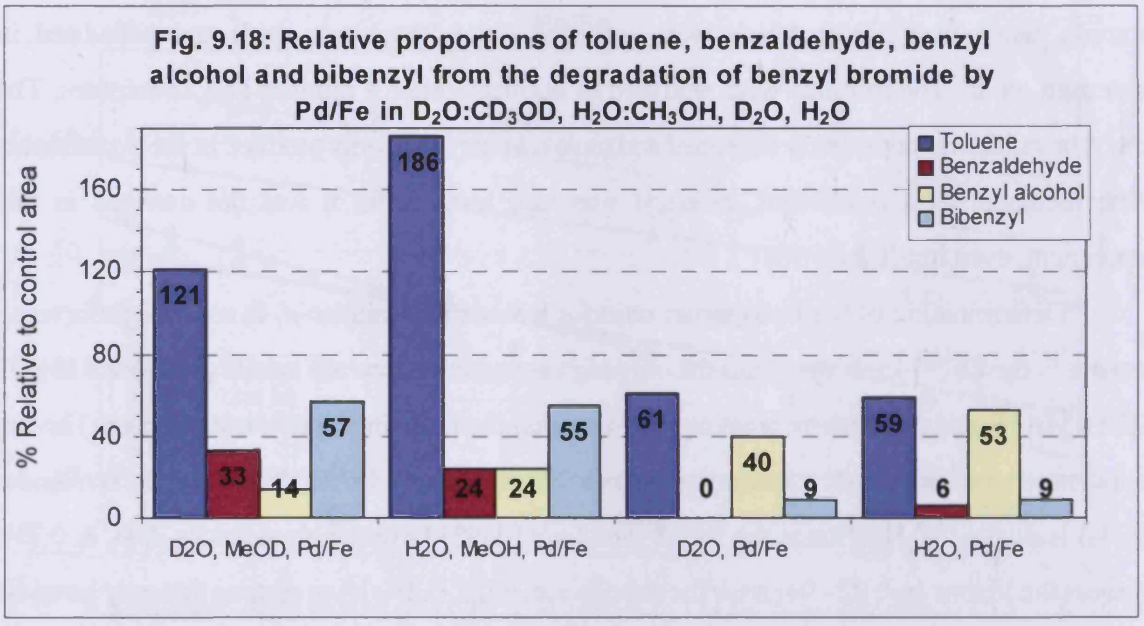

All of the benzyl bromide was consumed as seen in the previous experiment and the relative proportions of the products are shown in Table 9.7 and Fig 9.18. Benzyl alcohol in the control vials is presumably due to spontaneous hydrolysis, but all other products were only present in the vials containing palladised iron. The proportion of toluene and bibenzyl produced are greatly increased in the reactions in aqueous methanol, whereas the amount of benzyl alcohol is increased 2-3 fold in water relative to aqueous methanol. Clearly the latter is due to the higher concentration

of water, but why methanol should promote the formation of toluene and bibenzyl is not obvious. In deuterium oxide, the toluene produced consisted of CH_3Ph and CH_2DPh in the ratio 27:73 ± 1 (2-3 % error) for the three replicates, whereas in CD_3OD, D_2O the ratio was 32:68±< 1 (2 % error) for the three replicates. Given the close agreement between the data from the replicates this difference is real, albeit small. No deuterium was detected in bibenzyl or benzaldehyde in any of the runs and the benzyl alcohol from the deuterated runs only contained a single deuterium which is presumably hydroxylic.

The benzaldehyde is likely formed from oxidation of benzyl alcohol and the proportion detected is increased in the runs in methanol. In control experiments, when benzyl alcohol was shaken over palladised iron or in water alone, some 7 % of benzaldehyde relative to benzyl alcohol (peak area ratios) was detected. When the detection efficiency was checked at 50 μM, the peak area for benzaldehyde was twice that of benzyl alcohol and the ratio was higher at lower concentration, consequently the benzaldehyde detected in the degradation represents no more than 3% of the benzyl alcohol present. There was a slight decrease in benzaldehyde peak area during the course of the experiment (480 min), but this was also detected in the controls and the benzyl alcohol peak area was unchanged. This experiment excludes conversion during the run time and irreversible binding to the surface. The data is most consistant with aerial oxidation, which is independent of the presence of the Pd/Fe catalyst.

9.3 Factors affecting reaction rates

There are various factors which can affect the rate of degradation, some of which have already been examined, such as the introduction of the second metal and pH of the system. We have also demonstrated that the rates for sequential chlorine loss decrease; this is likely to be due to a combination of structure and bond strength, that is, the molecule must bind to the surface in the correct orientation and attacking species have sufficient energy to force the exchange.

In this section, we looked at other factors which could influence the rates of degradation, including initial concentration, use of internal or surrogate standards and solvent in the reaction matrix. We have already shown that using either deuterochloroform, deuterium oxide or a combination of the two does not affect the rate, thus eliminating the carbon - hydrogen and oxygen - hydrogen bond breakage as the rate determining step.

9.3.1 Comparison of reaction rates for differing initial concentrations (Expt 15, 59)

The degradation of halogenated organic compounds on both zero-valent and bimetallic systems is first order, which means that the substrate concentration does not affect the rate constant

and half lifes are constant. This holds true for very low substrate concentrations, but as it increases, the rate increases and eventually reaches a constant value, because the active sites are saturated and the time for the products to be released back into solution becomes rate limiting. Under these circumstances the reaction becomes zero-order because the rate is independant of substrate concentration. A study examining the degradation of carbon tetrachloride over a wide concentration range found that the rate of degradation increased as the concentration of carbon tetrachloride increased until it appeared to reach a constant value at about 0.09 g/l. This situation is assumed to show that both surface association, either by diffusion to and from the surface or by adsorption to form a surface complex, and reaction of the surface complex both affect the reaction rate[203].

The solubility of chloroform in water is 1 ml in 200 ml water at 25° C[210] giving a concentration of 0.74 g/100ml and our experiments were performed at relatively low concentration, with the stock solution at 0.015g/100ml (0.15 mg/ml). Having found some differences in calculated values for k_1, we decided to investigate concentration effects more fully. Chloroform degradation on palladised iron was performed with three chloroform concentrations, 5, 10, 15µl per vial, (0.375µg/ml, 0.75 µg/ml and 1.125 µg/ml), and the rate was monitored by GC-MS (Table 9.8).

Table 9.8: Comparison of rate constants and half lives for different concentrations of chloroform by analysis of the complete reaction.

Chloroform volume, µl (% conversion)	Full range				Initial rate			
	k_1		$t_{½}$		k_1		$t_{½}$	
	min^{-1}	Ratio	min	Ratio	min^{-1}	Ratio	min	Ratio
5 (86)	0.0031	100	224	100	0.0034	100	203	100
10 (90)	0.0035	113	198	88	0.0041	121	169	89
15 (96)	0.0050	161	139	62	0.0041	121	169	89

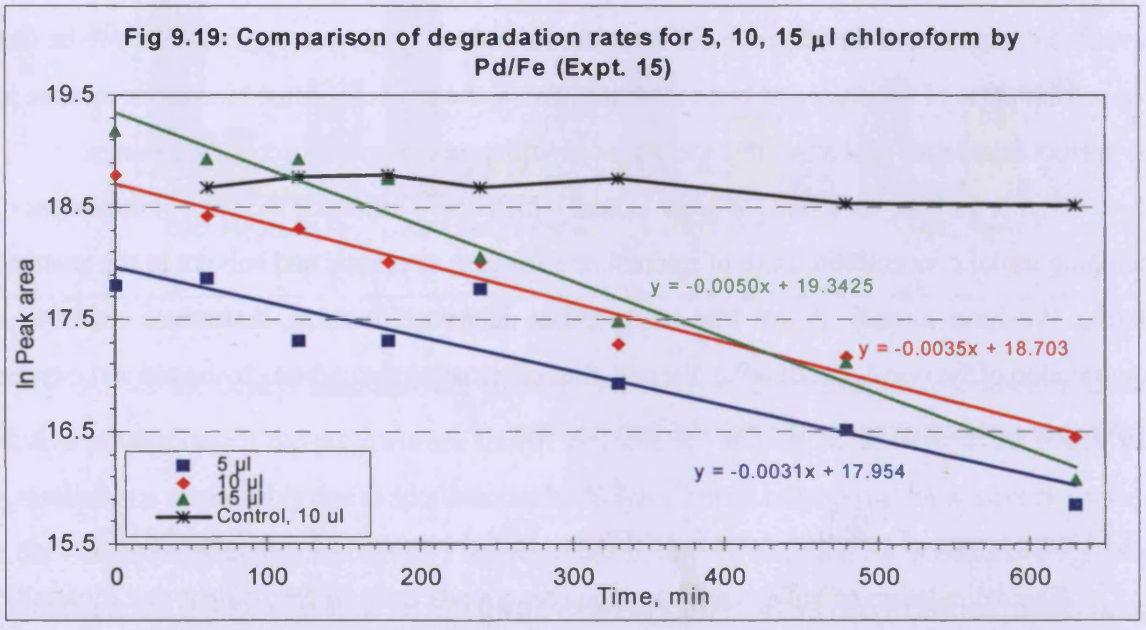

When the full data set is plotted (Fig. 9.19), the rate constants calculated graphically for the

5 and 10 µl solutions are identical, whereas the 15 µl solution appears to degrade faster, particularly towards the end of the degradation. The reason for this is that the rate constants should be determined from rates measured at close to the initial concentration when there is a small degree of conversion. It is not practical (particularly in parallel runs) to make a sufficient number of measurements in a short time (say 10% conversion) and so measurements at a higher degree of conversion need to be included. A trade off needs to be made been the number of measurements (with their inherent variability) and the degree of conversion. This can be seen by looking at the regression lines for the initial measurements (Fig 9.20).

For the initial rate measurements, the rate constants for the 10 and 15µl runs are now identical and that for the 5 µl run is now slightly higher. It is apparent that within the limitations of the experimental technique and within the three fold range investigated, the rate constants are independent of initial concentration.

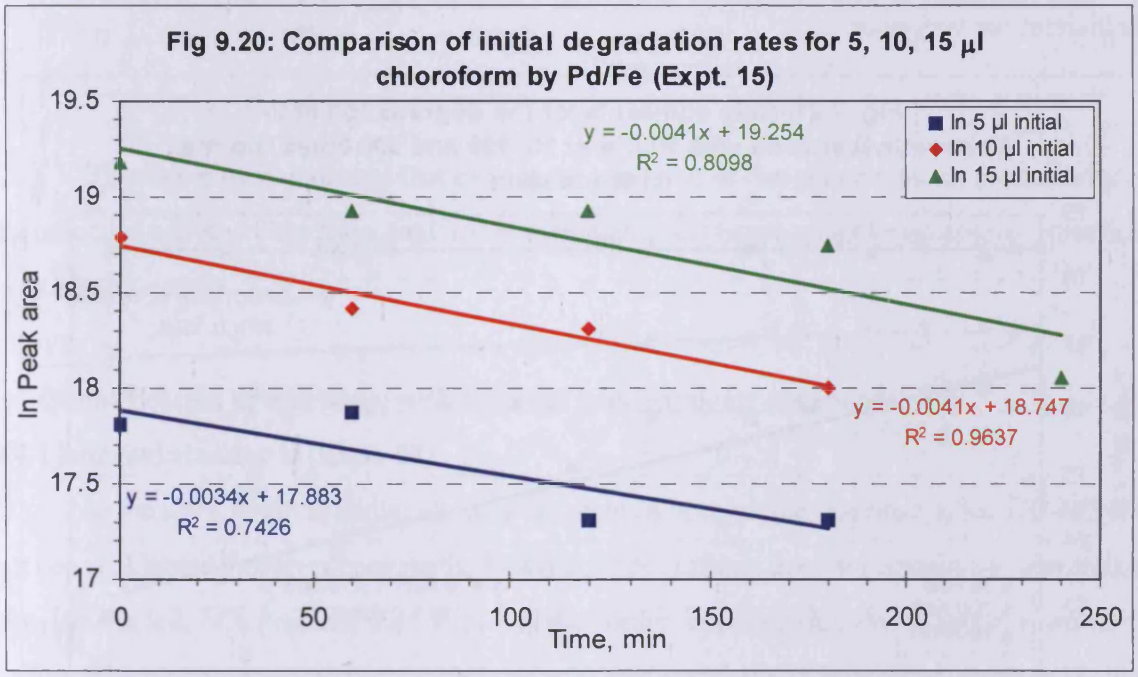

Fig 9.20: Comparison of initial degradation rates for 5, 10, 15 µl chloroform by Pd/Fe (Expt. 15)

The limited range of concentration achievable with chloroform and the difficulties in quantifying the dichloromethane formed prompted us to repeat the experiment with (2-bromoethyl)benzene. (2-Bromoethyl)benzene was degraded in water and methanol with palladised iron at 10, 100 and 500 fold times "normal" concentrations. The samples were extracted at the appropriate time points with chloroform and further diluted if necessary to avoid overloading the column and GC-MS. At the 100 fold level, the addition of the methanolic solution of (2-bromoethyl)benzene caused the formation of an emulsion whilst at the 500 fold level, drops of the liquid were clearly seen resting on top of the iron layer.

Table 9.9: Rate constants for 10, 100 and 500 fold increased (2-bromoethyl)benzene degradation and peak areas for the emergence of ethylbenzene (na, not applicable)

Time, min	10 Fold		100 Fold		500 Fold	
	2-(Bromo-ethyl)benzene	Ethyl benzene	2-(Bromo-ethyl)benzene	Ethyl benzene	2-(Bromo-ethyl)benzene	Ethyl benzene
k_1, min^{-1}	0.0073	0.0033	0.00092	0.0042	0.00010	0.0037
$t_{½}$, min	95.0	210	770	165	6931	187
% Conv.	96	na	37	na	10	na

The rate constant for the degradation of (2-bromoethyl)benzene under "normal" conditions is 0.0088 min^{-1} (sections 9.5.1, 9.5.2) and a comparable value (0.0073 min^{-1}) was found in the 10 fold higher concentration run, although the rate constant increases towards the end of the run (Fig 9.21). The apparent rate constants for the 10 fold and 500 fold runs are 3.5 and 33 times lower, but the data is based on a low degree of conversion and highly concentrated samples and hence these values are not reliable. The visual appearance of this data is very good, but the correlation coefficients are very poor.

Fig. 9.21: Rate constants for the degradation of 2-bromoethylbenzene with Pd/Fe at 10, 100 and 500 times "normal" concentration

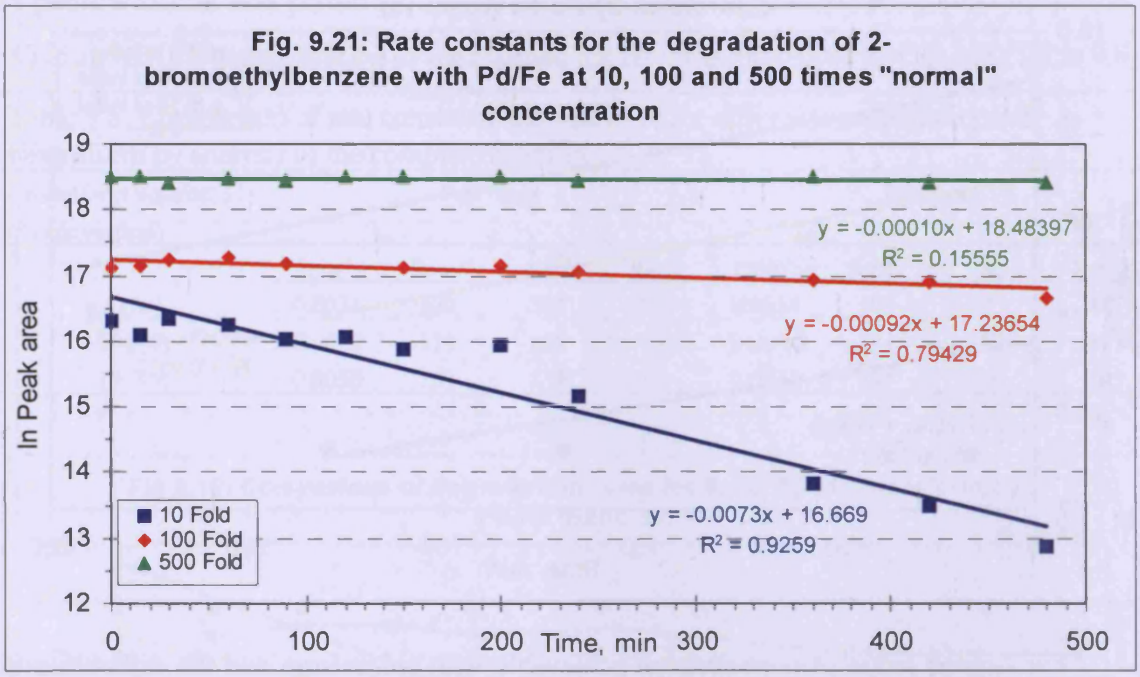

The rate of appearance of ethylbenzene increases rapidly at the beginning of the run and then slows down, regression over the whole data set gives the values reported in Table 9.9. Given that the 100 and 500 fold reactions were not homogenous, the range of the rate constants (0.0033-0.0042 min^{-1}) is small. If the data prior to 60 mins is excluded from the regression analysis, (Fig 9.22) the rate constants are 0.0021, 0.0031 and 0.0037 for 10, 100, 500 fold respectively with R^2 > 0.90. Overall the data indicates that there is at most, a modest increase in rate constant with concentration. Although the rate constants are comparable, because of the initial "burst" in the production of ethylbenzene, the 10 fold run contains the most ethylbenzene, followed by the 100

fold and lastly the 500 fold run. Throughout the run, the 10 fold vial contains about twice as much ethylbenzene as the 500 fold vial.

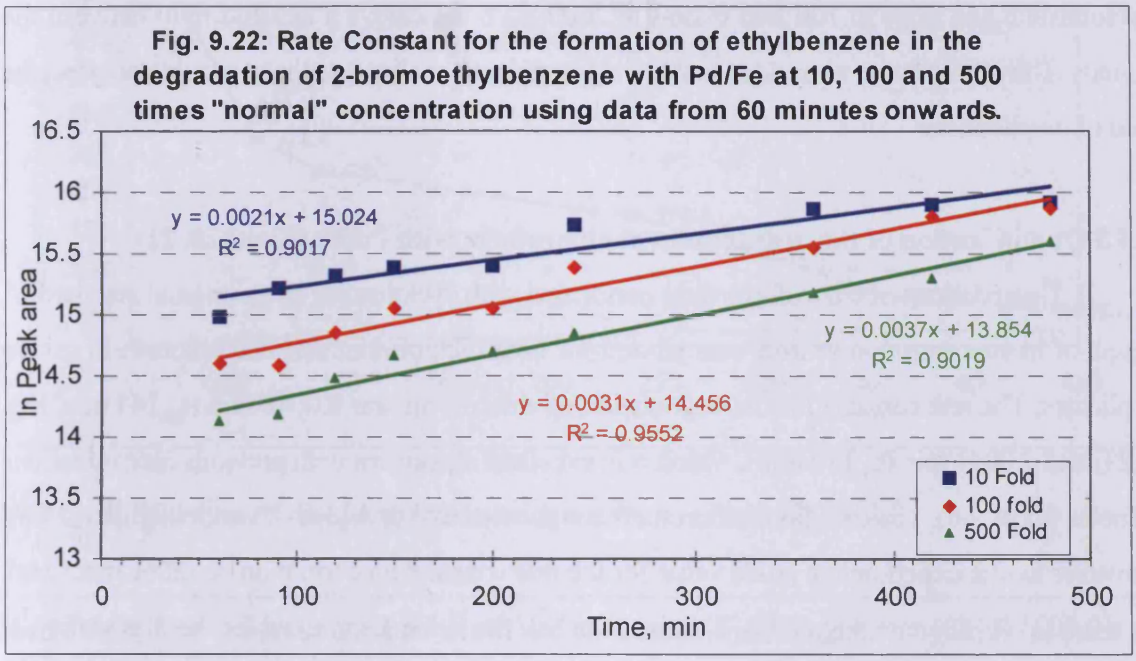

Fig. 9.22: Rate Constant for the formation of ethylbenzene in the degradation of 2-bromoethylbenzene with Pd/Fe at 10, 100 and 500 times "normal" concentration using data from 60 minutes onwards.

This experiment indicates that even in an emulsion or two phase system, the majority of the reductive activity of the palladised iron is maintained and hence might be usuable as a practical synthetic procedure.

9.4 Quantification of reactions, with internal and surrogate standards.

9.4.1 Internal standards (Expt. 18)

In the work reported so far, all rates are relative because the response of the GC-MS has not been calibrated, however because the first order rate constant does not contain a concentration term, this is less of a problem than with a higher order reaction. However it is not possible to compare the proportions of materials degraded with those produced. The most appropriate internal standard is a compound similar in nature to the compound to be quantified, so deuterated analogues are frequently used in mass spectrometry as the ions will have different masses although the retention times and response should be virtually identical. However, in this instance it is not possible to use a deuterated isotope because the degradation would still occur.

9.4.2 Calibration using MSD software and cyclohexane as internal standard (Expt. 19)

Table 9.10: Chloroform and dichloromethane calibration with cyclohexane internal standard.

Parameter	Response (counts)	R^2
Dichloromethane	$3.48 \times 10^3 \times$ [ug/l] + 6.02×10^4	0.999
Chloroform	$1.03 \times 10^4 \times$ [ug/l] + 3.05×10^4	0.999

A calibration curve using cyclohexane as an internal standard was constructed. A straight line response was recorded for both chloroform and dichloromethane (Table 9.10), although cyclohexane had to be in 100 fold excess at 2000 µg/l, to achieve a usuable ratio between the signals. The cyclohexane was added to the vial just prior to analysis, so that it would not affect the rate of degradation.

9.4.3 Quantification of the degradation of chloroform with Pd/Fe (Expt. 20, 21)

Degradations of chloroform were performed with cyclohexane as an internal standard. A graph of ln concentration *vs* time was plotted for both dichloromethane and chloroform in two replicates. The rate constant for the degradation of chloroform was 0.0048 min ($t_{½}$ 144 min, Fig. 9.23) and 0.0041 min ($t_{½}$ 170 min), which is in excellent agreement with previous determinations (Tables 9.1 & 9.6). The data for dichloromethane showed a high degree of variability (R^2 0.458), however in one experiment a crude value for the rate constant for formation could be measured, $k_1 = 0.0023$ ($t_{½}$ 301 min, Fig. 9.23). This is about half the value determined for the degradation of chloroform and within the errors of the experiment plausibly could be the same value. However there is still a mismatch between the amount of chloroform degraded, 89 or 72 % and the amount of dichloromethane detected 6 & 11 % respectively. This is apparent from the concentration time plot (Fig 9.24), which also shows the early burst in degradation, followed by comparatively linear degradation. One explanation for the small amount of dichloromethane detected is that, it in turn is degraded by the palladised iron, consequently this was investigated next.

Fig. 9.23: Quantified comparison of $CHCl_3$ degradation with Pd/Fe and CH_2Cl_2 formation (Expt. 20)

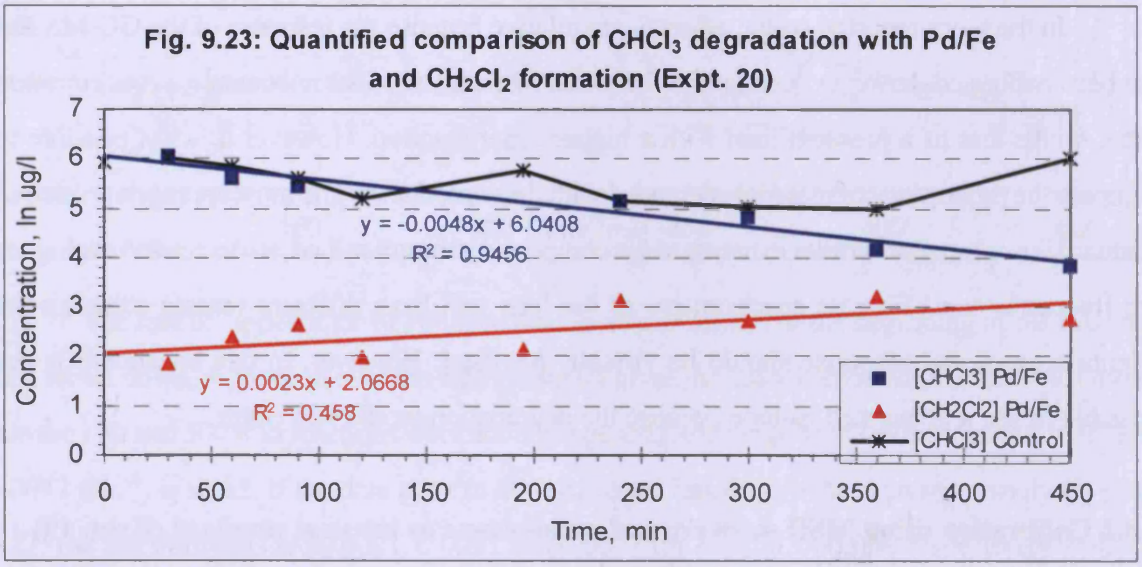

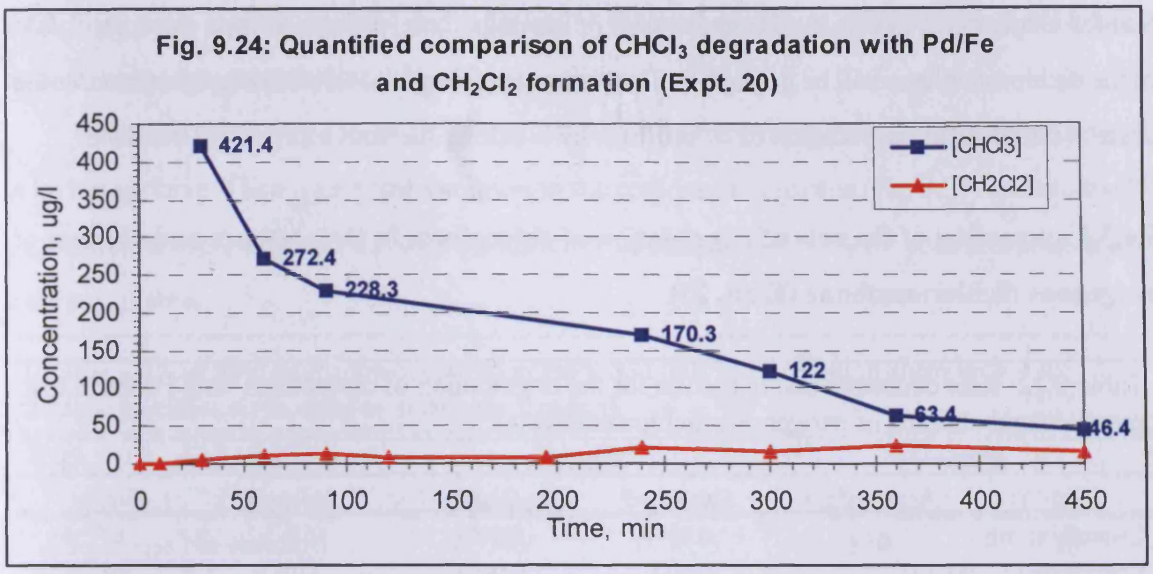

9.4.4 Quantification of dichloromethane degradations (Expt 22, 23, 24)

Table 9.11: Rate constants and half lives for dichloromethane degradation on Pd/Fe in three replicates

	k_1		$t_{½}$	
	min^{-1}	Ratio	min	Ratio
Expt. 22	0.00055	100	1260	100
Expt. 23	0.00021	38	3300	262
Expt. 24	0.00093	170	745	59

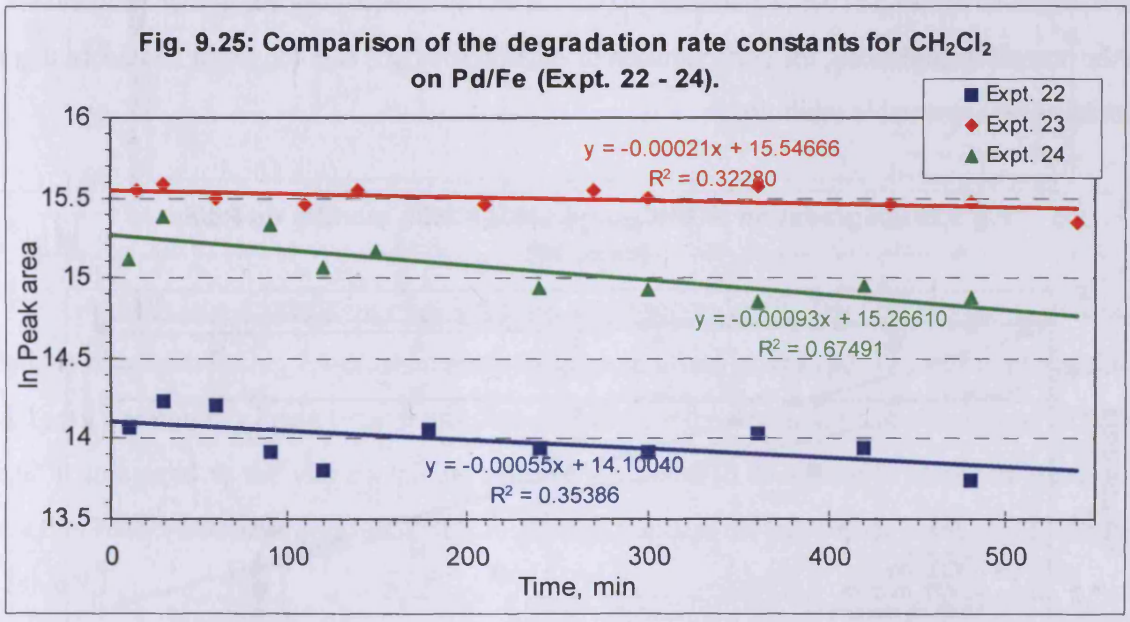

Dichloromethane was degraded in three replicates, the rate constants vary from 0.00021-0.00093, with very poor coefficients of determination. This is due to the slow rate of reaction and the scatter of the measurements (Fig. 9.25). The median rate constant is about ten times lower than

that for chloroform, therefore, over the course of the degradation of chloroform, the degradation of the dichloromethane will be negligible. The slow rate of degradation of dichloromethane, could act as a block to the degradation of chloroform by blocking the active sites on the surface.

9.4.5 Comparison of the rate of degradation of chloroform in the presence and absence of exogenous dichloromethane (Expt. 25)

Table 9.12: Rate constants and half lives for the degradation of chloroform with Pd/Fe in the presence and absence of exogenous dichloromethane.

System	k_1, min^{-1}		$t_{½}$, min	
	Calculated[a]	Graph	Calculated[a]	Graph
Chloroform only	0.0104	0.0103	67	67
Chloroform (+ CH_2Cl_2)	0.0063	0.0081	110	86
Dichloromethane (+ $CHCl_3$)	0.0017	nd	407	nd

[a] Calculated from the data at 10 min; nd not determined due to scatter of data.

The degradation of chloroform with palladised iron was performed in the presence and absence of an equal volume of dichloromethane. The rate constant for chloroform alone is twice the value for chloroform in the mixture, but the data for the chloroform alone run shows a high degree of variability ($R^2 = 0.78$). Consequently, the data was also analysed using the 10 min. data points (Table 9.12), which gave comparable results. The degree of conversion of chloroform was 95% and 93% in the single and mixed runs. Overall the data (Fig 9.26) indicates that there is, at most, a small inhibition of the degradation of chloroform by an equal volume of dichloromethane. In the normal degradations, the concentration of dichloromethane is much lower and hence there should be no appreciable inhibition.

Fig 9.26: Degradation of $CHCl_3$ and $CHCl_3/CHCl_2$ mixture on Pd/Fe (Expt. 25)

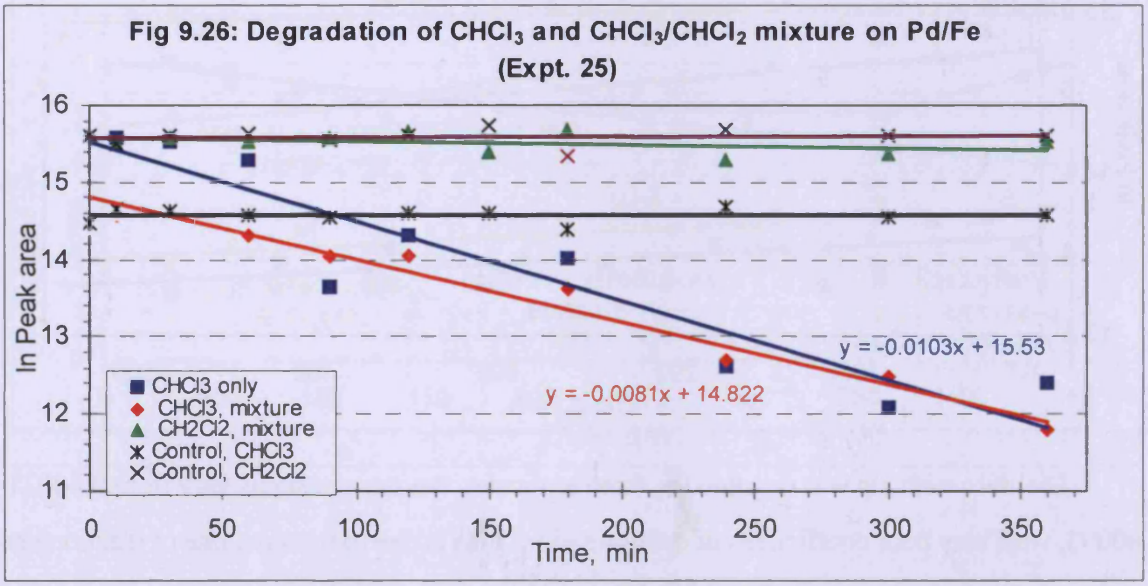

9.4.6 Comparison of the rate of degradation of chloroform (Expt. 28, 29) with 1,4-dioxane as a surrogate standard (Expt. 26, 27)

The use of 1,4-dioxane as an internal standard was reinvestigated as cyclohexane proved to be too variable. There was some variation in the response to dioxane (Fig 9.27) and relatively large amounts were required, but with a coefficient of variation of 5.7% for peak area, the results were acceptable.

Table 9.13: Comparison of the degradation rates and half lives of chloroform with 1,4 dioxane as either an internal or surrogate standard.

Expt.	System	k_1, min^{-1}		$t_{½}$, min	
		Calculated	Graph	Calculated	Graph
28	No standard	0.0046	0.0035	150	198
28	Surrogate standard	0.0043	0.0024	161	289
29	Internal standard		0.0033		210
29	Surrogate standard		0.0038		182

Fig. 9.27: Variation in 1,4-dioxane peak area when used as internal standard for $CHCl_3$ degradation on Pd/Fe (Expt. 27). Error bars ± 5 %.

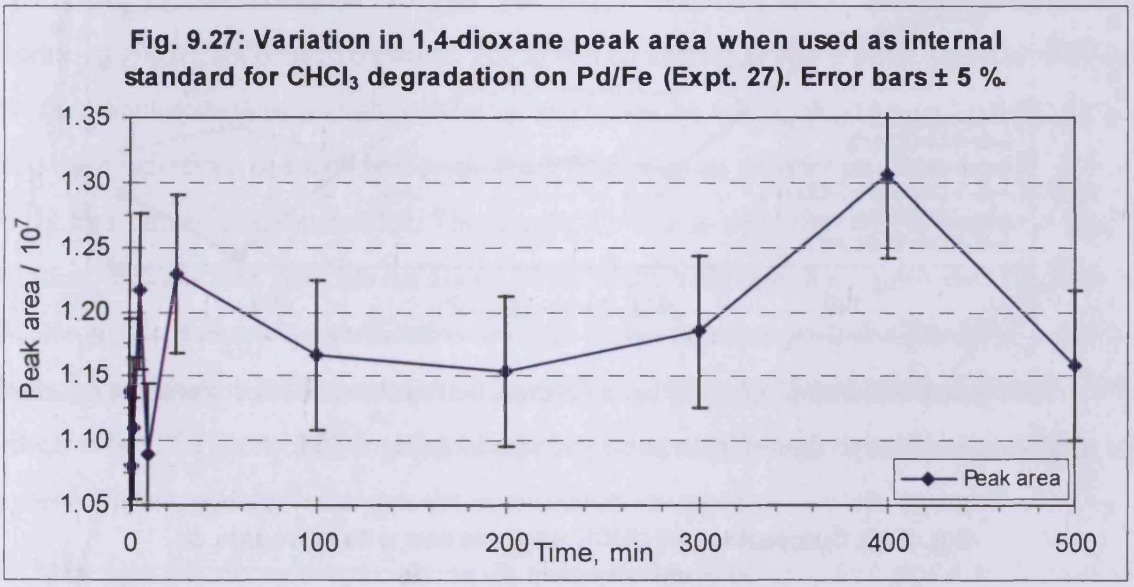

Initially, the degradation of chloroform was analysed with two sets of vials containing palladised iron and using 1,4-dioxane as a surrogate standard in one vial. The surrogate standard vial gave a marginally lower value for the rate constant for the degradation of chloroform (0.0024 min^{-1}), compared to the vial containing chloroform alone (0.0036 min^{-1}). However when the reaction was repeated and compared with an internal standard the rate constant was slightly higher (Table 9.13).

In the first run the curve for chloroform alone is just below that of the surrogate standard (Fig 9.28). The chloroform and dioxane controls and the dioxane surrogate standards show little change during the run, which indicates good reproducibility, and in the case of the dioxane surrogate standard, that it is not being affected by the palladised iron.

A surrogate standard is intended to check for differential losses of the analyte during the procedure, whereas an internal standard added at the end of the reaction is intended to be used for quantification. To counter systematic measurement errors in the surrogate standard runs, the peak areas for each chloroform peak area measurement were multiplied by the average peak area for all the dioxane measurements divided by the peak area of dioxane for the individual run. However when the data was plotted, there was no significant improvement in the coefficient of determination of the regression line and the rate constants were largely unchanged. The same methodology applied to the internal standard equally had no effect.

Fig. 9.28: Comparison of ln peak areas for $CHCl_3$ and 1,4-dioxane (Expt. 28)

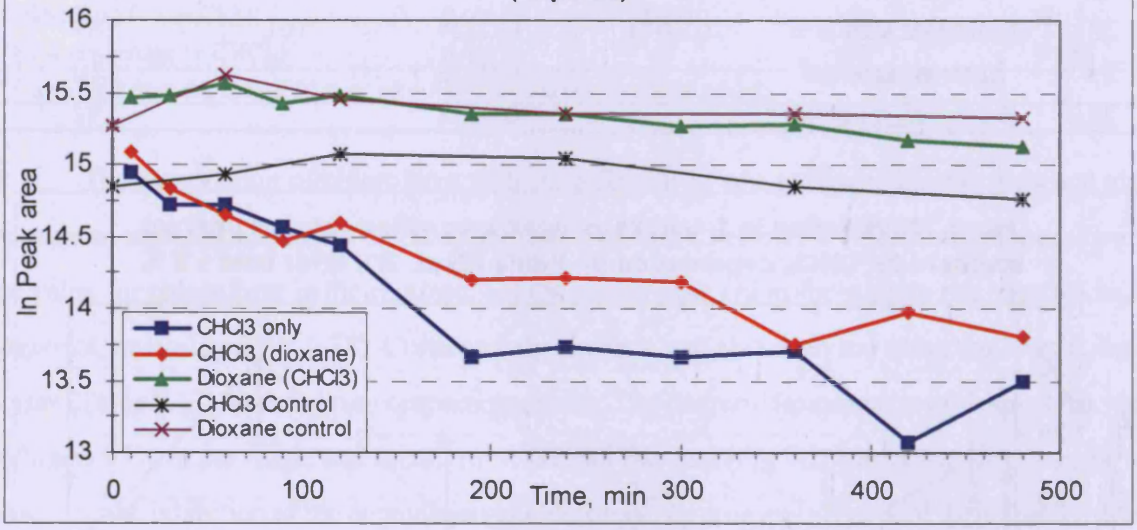

The internal standard added at the end of the reaction can have no effect on the degradation. The results were similar to those for the surrogate standard (Fig. 9.29).

Fig. 9.29: Comparison of $CHCl_3$ degradation with surrogate or internal standard (Expt. 29)

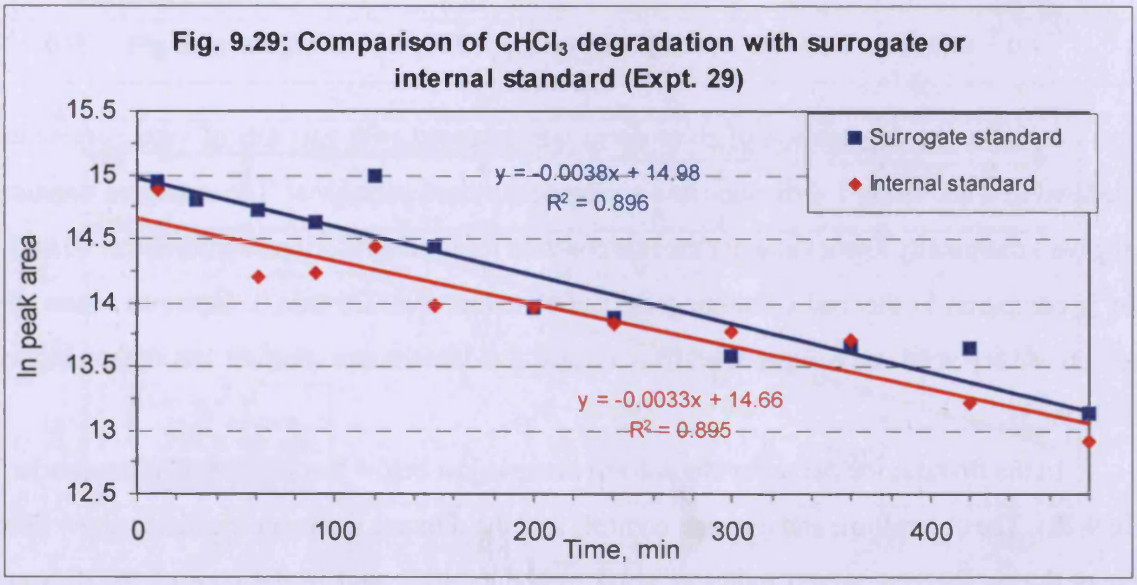

In summary, both the surrogate and internal standards had no more than a marginal effect on the rate of degradation of chloroform by palladised iron. This indicates that they do not efficiently compete for the surface active sites.

9.4.7 Quantification of the degradation of chloroform and formation of dichloromethane using dioxane as an internal standard (Expt 30)

Chloroform was degraded with palladised iron, using dioxane as an internal standard, together with a full set of controls. The degradation of chloroform was comparatively fast (k_1 0.0098 min^{-1}; $t_{½}$, 71 min; 85 % conversion, Fig. 9.30) and the amount of dichloromethane rose rapidly from zero to about 15 ug/l at the end of the experiment. The nominal dichloromethane concentration in the controls was calculated to be 8.8 µg/l. Except for one measurement, this remained constant at a slightly lower level (6.1 - 8.2 µg/l) throughout the experiment (Fig. 9.31). During the course of the experiment, the amount of chloroform was reduced from at least 478.5 µg/l (10 min measurement) to 70 µg/l. 408.5 ug/l of chloroform is theoretically capable of producing 290 µg/l of dichloromethane. The lowest control measurement indicates that at least 70 % of the dichloromethane should be detected and hence the "yield" should be at least 200 µg/l. In fact the maximum amount of dichloromethane detected was circa 20 µg/l, hence some 90 % of the chloroform is unaccounted for. This cannot be due to degradation of dichloromethane in solution, because the half life is about 1260 mins, although the initial concentration of dichloromethane in those experiments was much higher than that produced here. One possibility that was considered was that some form of hydrolysis to formaldehyde might occur. However the detection limit for formaldehyde using Nessler's reagent was too high to make this possible. It is possible that some is converted into the hydrocarbons as reported by other workers.

Fig. 9.30: Degradation of chloroform with palladised iron. Quantification of chloroform with a dioxane internal standard (Expt. 30)

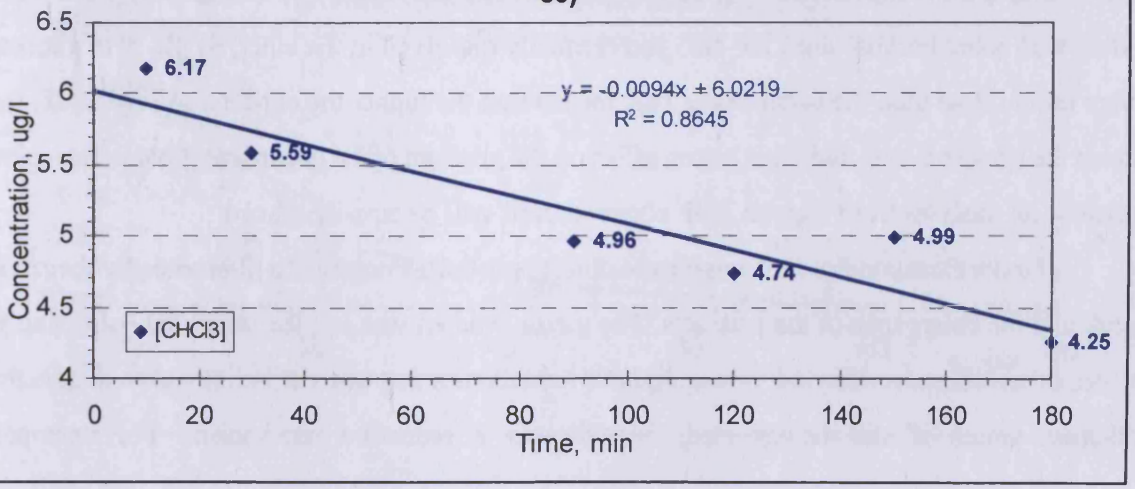

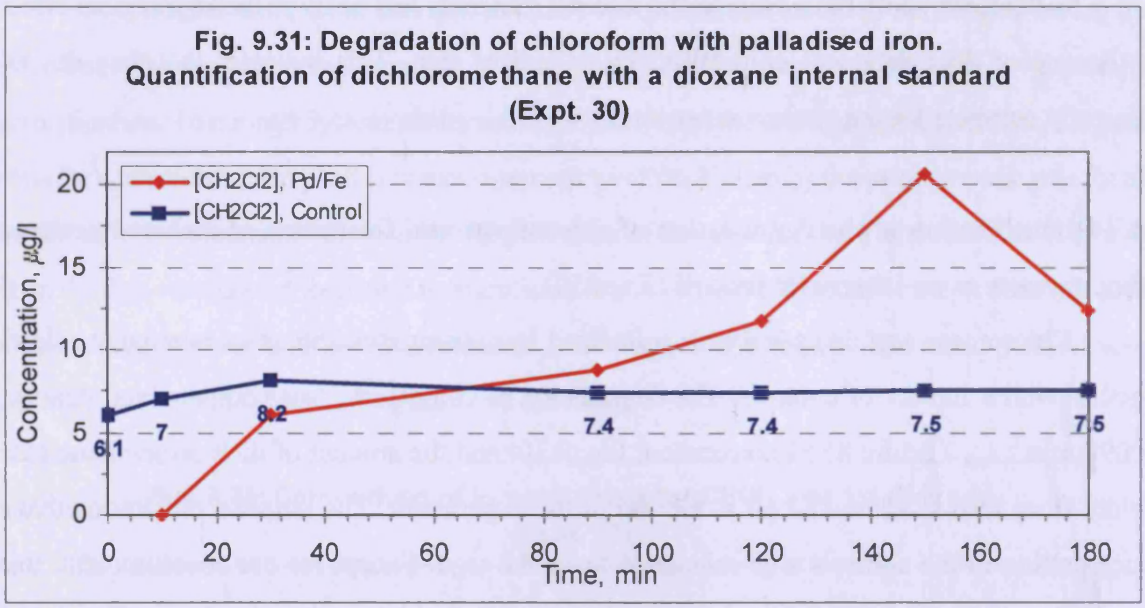

Fig. 9.31: Degradation of chloroform with palladised iron. Quantification of dichloromethane with a dioxane internal standard (Expt. 30)

9.5 Use of solvent

9.5.1 Degradation of (2-bromoethyl)benzene in various concentrations of aqueous THF (Expt. 54, 55, 56)

The solubility of halogenated organic compounds tends to be low, and adding a suitable solvent can increase the amount of VOC in solution. We attempted to perform the degradation of (2-bromoethyl)benzene in THF/water with a view to using this as a synthetic method. Instead of the previously used purge and trap technique we moved to solvent extraction and liquid injection, which is more suitable for less volatile analytes.

A solvent extraction step was necessary for several reasons. The main reason was to convert the analytes of interest from an aqueous medium to an organic one and both the starting material and the potential products preferentially dissolve in organic solvents. Diethyl ether was chosen because it is less dense than water and therefore was the top layer, making the separation easier than with a solvent layer at the bottom. The solvent extraction also had the benefit of concentrating the compounds of interest, making lower detection levels possible. A slight dilution effect was noted because the THF also preferentially dissolved in the ether, so the THF extracts were more dilute than the water ones. This means that the higher the concentration of THF, the lower the peak area detected. This has no effect on the gradient of the ln concentration *vs* time plot, because all analytes from a given THF concentration will be equally diluted.

Under these conditions it was easy to detect both the decrease in the (2-bromoethyl)benzene peak and the emergence of the products. The major product was ethylbenzene, but surprisingly, traces of styrene were detected. Some aliphatic haloalkanes degrade via β-elimination to give the alkenes, which if still halogenated, degrade *via* a reduction mechanism. For example,

hexachloroethane degrades to give tetrachloroethene which in turn give *cis*-dichloroethene.

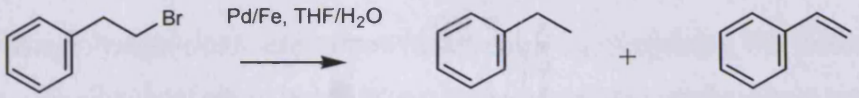

Fig. 9.32: 2-bromoethyl benzene degrades to give ethyl benzene as the major product and styrene as a minor product

The rate of degradation of (2-bromoethyl)benzene was measured at a range of concentrations of THF (Table 9.14, Fig. 9.33). The maximum rate was achieved with 5 % THF. At 50 % THF and beyond the rates became too slow to measure accurately and the measured values are not reliable. Indeed at 100% THF, there was a slight increase in 2-bromo-ethylbenzene, which indicates there was no transformation and the likely error in measurement. The difference between the duplicate determination at 25 % THF was used to give a range for the error bars and even by this extreme measure the rate differences are significant. From 0 - 25 % THF, with one exception, all the conversions were 98 ± 1 %, hence this represents a reasonable range for a synthetically useful procedure.

Table 9.14: Rate constants for the degradation of (2-bromoethyl)benzene on Pd/Fe in aqueous THF solution

% THF *v/v* in H_2O	k_1		$t_{½}$		Conversion
	min^{-1}	Ratio	min	Ratio	%
0	0.0080	100	86.6	100	98
5	0.0158	198	43.9	51	99
10	0.0110	138	63.0	73	99
25	0.0064	80	108.3	125	97
25*	0.0041	51	169.1	195	88
50	0.0012	15	577.6	667	7
75	0.0004	5	1732.9	2001	16
100	+0.0003†	-4	-2310.5	-2668	-26

* = duplicate experiment; † Gradient of line is positive

Fig. 9.33: Variation in rate constant with %THF in the degradation of bromoethylbenzene with Pd/Fe (Expt 55)

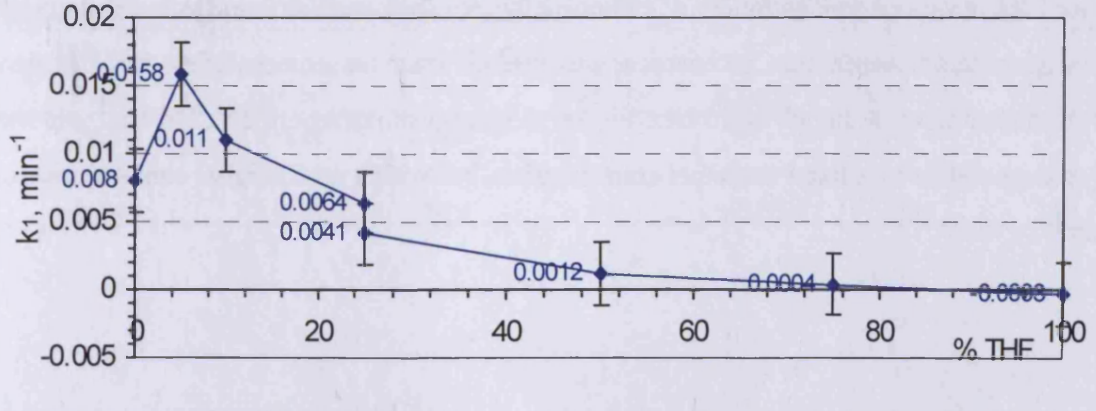

9.5.2 Degradation of (2-bromoethyl)benzene in various aqueous methanol concentrations (Expt. 57, 58)

25 % aqueous THF is adequate for more reactive substrates, but a higher organic content would be beneficial for less polar substrates, moreover THF has limited solubility in water and tends to form a separate phase more easily if non-polar species are present. We therefore turned to methanol which is miscible with water in all proportions. (2-Bromoethyl)benzene was degraded with palladised iron in mixtures of methanol and water. Rates and products were determined as before (Table 9.15). The major product was ethylbenzene as seen previously together with traces of styrene. The results were remarkably similar to those achieved with THF. The reaction proceeded well up to 25 % methanol, but with more than 50% methanol the rate dropped dramatically.

Table 9.15: Rate data for the degradation of (2-bromoethyl)benzene by Pd/Fe in aqueous methanol solution.

% Methanol	k_1		$t_{1/2}$		Conv.	Multiple
v/v	Min^{-1}	Ratio	Min	Ratio	%	
0	0.0095	100	73.0	100	99	129
10	0.0093	98	74.5	102	99	141
25	0.0032	35	216.6	297	81	5.1
50	0.0003	3	2310	3164	29	1.4
75	0.0008†	8	866.4	1187	4	0.35
100	0.0002	2	3466	4748	17	1.2

† Gradient of line is positive

These degradations used a relatively low concentration of (2-bromoethyl)benzene, the reaction vials contained only 13.6 μg (6.8 μg/ml, 0.037 μM), which is too dilute to be of much interest synthetically. The use of solvents to speed up degradations on both zero-valent and palladised iron has been reported; in the case of zero-valent iron, methanol, ethanol and iso-propanol at 57 % *v/v* were found to decrease the degradation rate constants for trichloroethylene and tetrachloroethylene, only ethanol at 28 % *v/v* was found to give a comparable rate constant to that using water. The effect on product formation was not reported[205]. The dechlorination of Aroclor 1260 in various concentrations of ethanol or isopropanol was also found to be reduced with increasing solvent concentration, with isopropanol giving slower rate constants than the equivalent ethanol concentration, although again the effect on products was not reported[211]. The next step was to try a degradation in a fixed methanol concentration, but with a much higher concentration of reactant.

9.5.3 Degradation of benzyl bromide in aqueous methanol and THF solutions (Expt. 62, 63, 64)

The 25 % limit for cosolvents achieved so far is useful, but not sufficient for a robust procedure. We turned to benzyl bromide as our most reactive monohalo-substrate to determine if we could achieve a useful degree of degradation at higher concentrations of co-solvent and substrate. Initially we held the solvent concentration at 10 % methanol which gives a reasonably quick degradation, and used a higher initial reactant concentration. In the first experiment, neat benzyl bromide was used at 9.6 mg/ml (42 μM) and the degradation was monitored over one hour. The major problem encountered was the solubility of the benzyl bromide. When the benzyl bromide was added to the aqueous iron filings, it only partially dissolved. Therefore, although the initial concentration was approximately 10 mg/ml, the final concentration was unknown, although a saturated solution was formed. The effect of concentration on the degradation rate is discussed in Section 9.3.1.

As seen previously, toluene was produced together with bibenzyl, benzyl alcohol and benzyl methyl ether (Fig. 9.7). The amount of benzyl methyl ether formed is in direct proportion to the concentration of methanol, so more was formed in the 25 % *v/v* systems than in the 10 % *v/v* system. When the degradation of benzyl bromide is carried out in water, no bibenzyl is formed.

The experiment was repeated using 25 % *v/v* methanol or 25 % *v/v* THF and 7.2 mg/ml benzyl bromide to check conditions to see if either would be suitable for preparative scale degradation. The degradation was monitored by GC-MS and again, the formation of products was also monitored. Some problems were encountered with the solubility of the benzyl bromide, so a further experiment was performed where the 7.2 mg/ml benzyl bromide solution was made up in either methanol or THF to give approximately 10 mg/ml, then 40 mg added to water giving a final reaction volume of 15 ml and a solvent concentration of 25 % *v/v* with the benzyl bromide at 2.7 mg/ml (Table 9.16, Fig 9.34).

Table 9.16: Comparison of the degradation rate constants for benzyl bromide in aqueous methanol or THF, with Pd/Fe. (na not applicable)

Solvent	Methanol,			THF		
% *v/v*	k_1, min^{-1}	k_1, Ratio	Conv. %	k_1, min^{-1}	k_1, Ratio	Conv. %
0%	0.5842	20864	95	-	-	-
10 %	0.0028	100	13	na	na	na
25 %	0.0778	2779	99	0.0718	2564	99

Fig. 9.34: The degradation of benzyl bromide with Pd/Fe at high concentration in methanol or THF solution

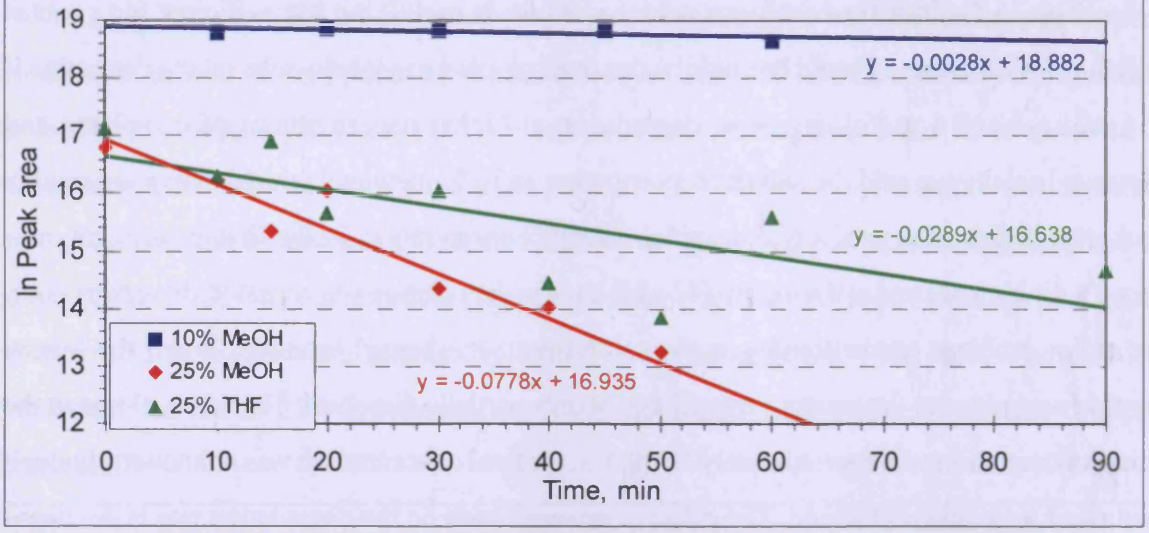

The reactions in 25 % methanol and THF proceed at about 10 % of the rate in water alone, but despite this the degree of conversion was similar. The reaction in 10 % methanol is not directly comparable with the others because it was performed with a different concentration of benzyl bromide. Although the conversion of benzyl bromide was high in both the 25 % aqueous methanol and THF degradation, the formation of products had high variability (Fig. 9.35), which is partially due to the division of a slow rate of degradation amongst four products.

Fig. 9.35: Formation of toluene in 10 % *v/v* methanol and toluene, benzyl alcohol and benzyl methyl ether from benzyl bromide in 25 % *v/v* methanol (Expt. 64).

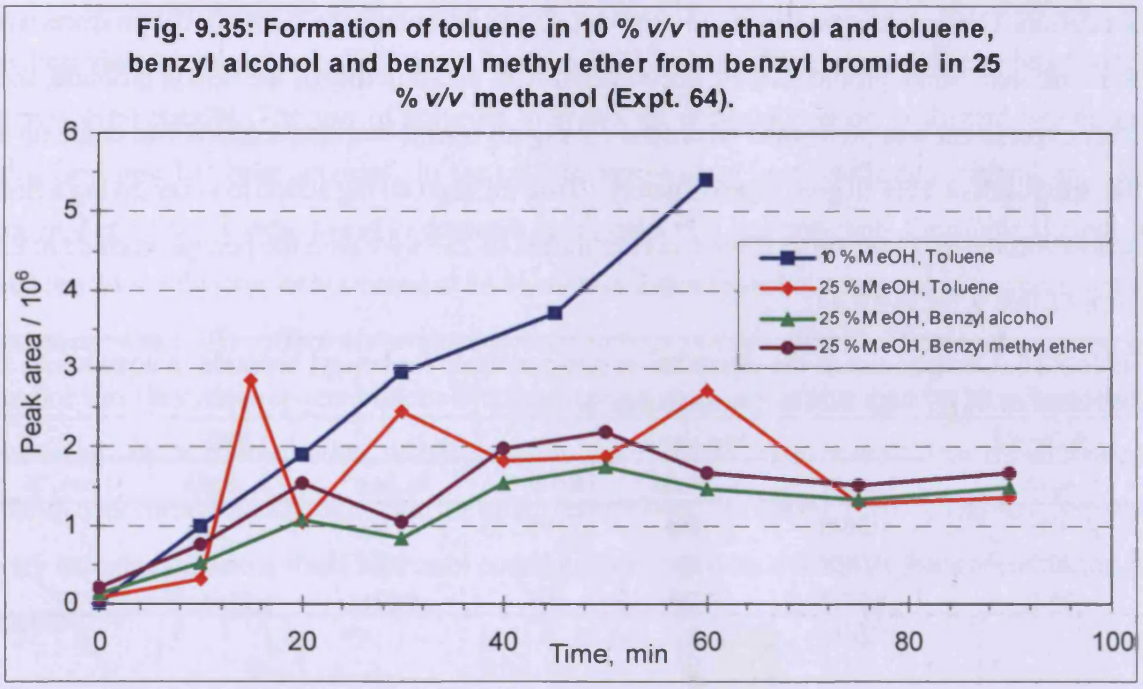

The kinetics for the formation of products were unreliable due to the variability of the measurements, but the data for the 25 % aqueous methanol was capable of interpretation, albeit

with some caveats (Table 9.17).

Table 9.17: Peak areas for the degradation of benzyl bromide in 25 % methanol

Time, min	Benzyl bromide	Toluene	Bibenzyl	Benzyl alcohol	Benzyl methyl ether
k_1, min^{-1}	0.0774	0.0175	0.0202	0.020	0.016
$t_{½}$, min	9.0	40	34	35	43
R^2	0.92	0.46	0.53	0.55	0.46
% Conv.	99	89	81	91	87
Multiples	1/97	9	5	11	8

The sum of the rate constants for the formation of toluene, bibenzyl, benzyl alcohol and benzyl methyl ether (0.0737 min^{-1}) is comparable to the rate of degradation of benzyl bromide (k_1 0.0774 min^{-1}). The quality of the rate constant measurements are poor as judged from the coefficient of determination (R^2), but the trend is valid.

From a synthetic viewpoint, this reaction is interesting, but not particularly useful as it gives a range of products. The main issues with these experiments are compound solubility. Benzyl bromide at experimental concentration forms a suspension when added to water. The reaction runs more slowly in high organic solvent systems but insufficient material is soluble in low organic solvent systems to make it viable.

The differences in products under different conditions *via* different mechanisms had already produced some interesting findings, as detailed above. We decided to examine the reaction mechanism in more detail using specific compounds designed to give one product over another if a particular pathway was predominant, these are known as radical clocks.

9.6 Radical clocks

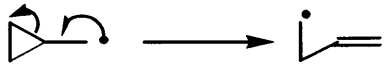

Fig. 9.36: The methylcyclopropane radical undergoes ring cleavage to give the 4-butenyl radical, k_1 1.3 x 10^8 s^{-1}

The rates of radical reactions can be measured by rotating sector methods, flash photolysis (for light induced reactions[212]) and pulse radiolysis. However these methods require specialised equipment and in many cases the relative rate of a reaction is more important than the absolute rate. Relative rates can be measured by creating competing reactions which can give two possible outcomes and if the rate of one process is known the other can be deduced from a measurement of the relative amounts of the two products from the competing pathways. The use of certain organic molecules as mechanistic and rate probes has been in regular use since the 1980s; the reaction needs to be unimolecular and *via* a radical intermediate which undergoes a characteristic

rearrangement and competes with a bimolecular reaction. The spread of products is then analysed to determine rate constants. This is termed a "radical clock". Accurate rate constants covering both fast and slow radical reactions in solution have been obtained and a number of reactions have been "calibrated" using EPR spectroscopy and lists of the radicals, their rearrangements and rate constants have been published[213].

The use of bromomethylcyclopropane as a radical clock was first reported in 1976. It is a fast clock with a rate constant of $1.3 \times 10^8\ s^{-1}$, which is capable of detecting short lived radicals and seemed ideally suited to our investigations. A liquid injection of commercial bromomethylcyclopropane in dichloromethane was run by GC-MS to confirm the identity of the starting material. Two peaks were observed in the TIC, the earlier eluting and minor peak matched the library entry for bromocyclobutane, and the later peak bromomethylcyclopropane (peak area ratio 12:88).

An aqueous solution of bromomethylcyclopropane was added to two sets vials, one set containing palladised iron and the second set without palladised iron which would act as controls. The samples were extracted by purge and trap and monitored by GC-MS. The first sample analysed was the zero time control solution, which yielded two peaks of almost the same area. These were identified by comparison with the reference spectrum from the liquid injection as bromocyclobutane and bromomethylcyclopropane in the ratio 56:44. In all subsequent samples, the bromomethylcyclopropane peak disappeared and the bromocyclobutane peak also rapidly diminished (Fig 9.38). The rate of degradation in the control vials was comparable to that in the vials containing palladised iron and bromocyclobutane could not be detected in either series of vials after 90 minutes.

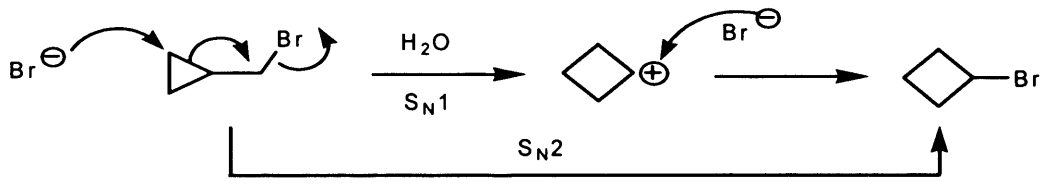

Fig. 9.37: Bromomethylcyclopropane rearrangement to bromocyclobutane

The commercially supplied material gave two peaks on initial analysis which raises questions over the purity and what effect these might have on the degradation conditions. Under our experimental conditions, the bromomethylcyclopropane spontaneously rearranged to give bromocyclobutane (Fig. 9. 37), which is also unstable and degrades to an unknown species even in the absence of palladised iron. The undetected species are most likely cyclopropylmethanol and cyclobutanol formed by hydrolysis, but as no useful radical clock data could be obtained from this

experiment the matter was not persued.

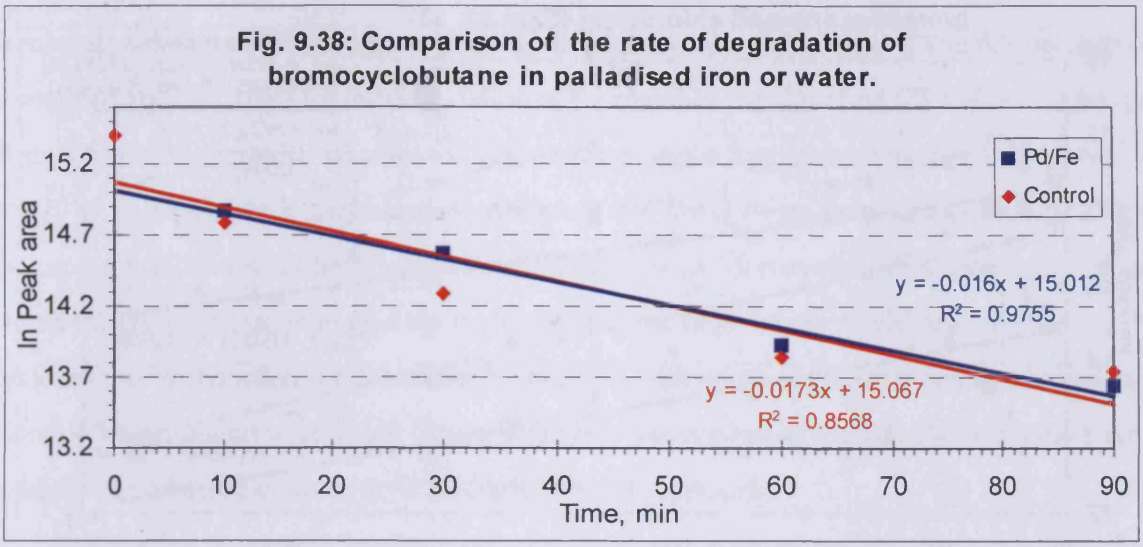

9.6.2 Degradation of 6-bromohex-1-ene alone and mixed with chloroform on a palladised iron (Expt. 32, 33)

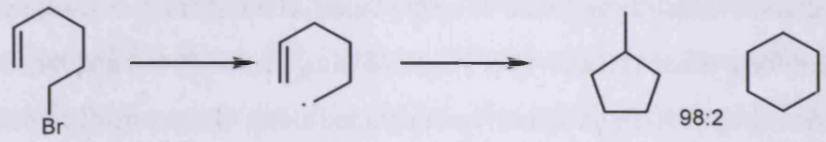

Fig. 9.39: The cyclisation of 5-hexenyl to methylcyclopentane and cyclohexane, k_1 1.0 x 10^5 s^{-1}

The cyclisation of the 5-hexenyl radical to methylcyclopentane is the oldest example of a radical clock. If the radical trapping reaction is fast hexene is formed because the radical does not have time to cyclise, however if the reaction proceeds more slowly, then methylcyclopentane is formed. The rate constant for the formation of methylcyclopropane radical was first determined in 1968. It is 1.0 x 10^5 s^{-1} at 25° C[213], which is regarded as a moderately fast clock. Aqueous solutions of 6-bromo-1-hexene, and a mixture of 6-bromo-1-hexene and chloroform were degraded on palladised iron and monitored by GC-MS (Table 9.18, Fig. 9.40). The co-degradation was intended to determine if both chloroform and 6-bromohexene are degraded at the same site.

Table 9.18: Comparison of the degradation rate constant for 6-bromohexene and 6-bromohexene plus chloroform

Parameter	Rate constant, k_1, min^{-1}	Ratio	$t_{½}$, min	Ratio
6-Bromohexene alone	0.0023	100	301	100
6-Bromohexene* (+ $CHCl_3$)	0.0032	139	217	72
Chloroform* (+ 6-bromohexene)	0.0039	170	178	59

* data from co-degradation of 6-bromohexene and chloroform

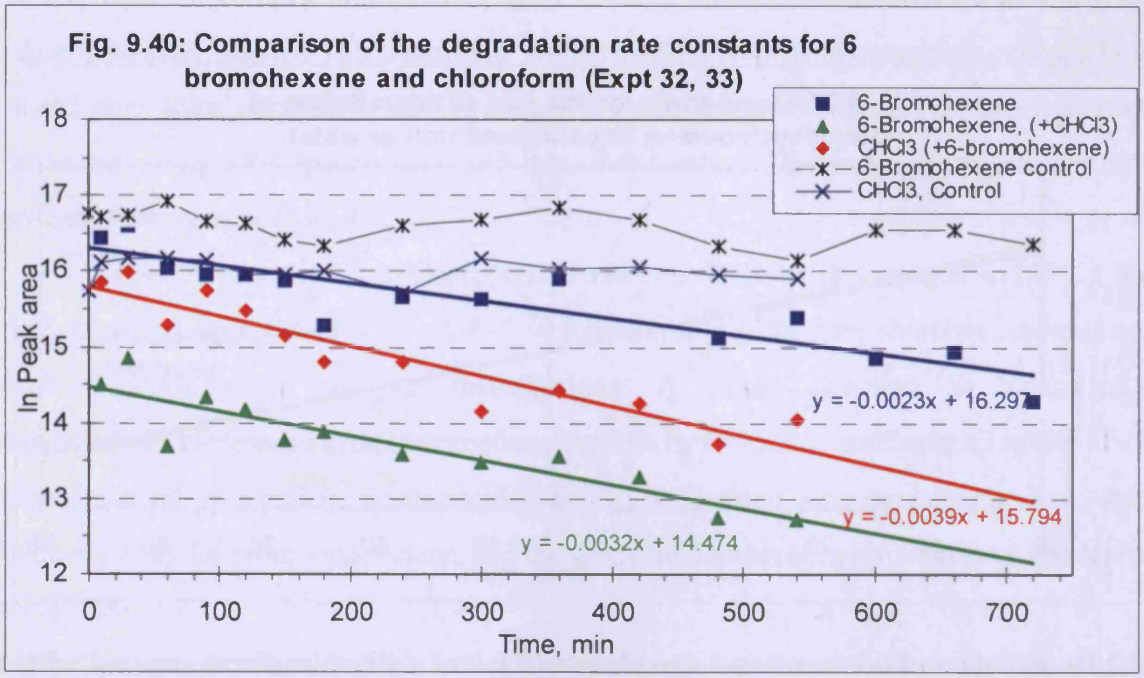

The degradation half life and k_1 for 6-bromohexene are in the same range (allowing for experimental error) as that for chloroform. In the co-degradation, chloroform is degraded slightly more quickly than chloroform alone (0.0031 min^{-1}, $t_{½}$, 224 min, Expts 15, 59) and similarly 6-bromohexene is degraded circa 40% faster than when degraded alone. These rate differences are likely due to variation in the batches of palladised iron, but the co-degradation is immune to this problem and hence the rate ratios for these substrates are reliable; k_1(6-bromohexene):k_1 (chloroform) 0.82.

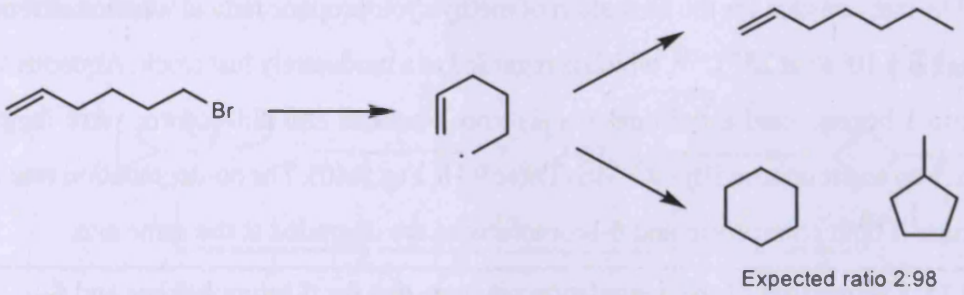

Fig. 9.41: 6-Bromohexene gives hexene rather than cyclohexane or methyl-cyclopentane, which indicates either that the putative radical intermediate is captured before ring closure, or that the intermediate has anionic character.

The major product produced from this degradation was found to be hex-1-ene (Fig 9.41). There were traces of other hexenes and hexane, but these were present as a result of impurities in the original starting material (95 % from Aldrich). After 8 hours, traces of methylcyclopentane were detected, but no cyclohexane. Examination of the chromatogram by selected ions (*m/z* 84 for

cyclohexane) revealed only a very small peak, and this was attributed to background noise. By contrast, the hexene peak is substantial and very stable; even after almost 24 hours, it is still the dominant peak in the chromatogram. Expression of the rate constant data in Table 9.17 in units of seconds gives 3.8 x $10^5 s^{-1}$ for the degradation of 6-bromohexene alone and 5.3 x $10^5 s^{-1}$ for the co-degradation. The literature value for the rate constant for the formation of methylcyclopentane is 1 x $10^5 s^{-1}$ at 25 °C, hence the reduction reaction is 3.8 to 5.3 times faster than cyclisation. This indicates that if there is a radical intermediate it is short-lived. Moreover a carbocation intermediate would undergo cyclisation to give the cyclohexyl carbocation, which would react further to give cyclohexane by reduction, cyclohexanol by reaction with water or cyclohexene by elimination. None of these products were found. Consequently the reaction must proceed either *via* a short lived radical or a carbanion equivalent (ie an organometallic species).

Recently, a question has been raised over the accuracy of radical clocks when used in organo-metallic reactions. Calculations of *ab initio* molecular orbitals and density functions have found that the rate of ring closure of the 5-hexenyl radical may be increased by as much as four orders of magnitude in the presence of various metals, due to the metal cations forming a complex with the hexenyl double bond[214]. Hence at the limit of these values, the 6-hexenyl radical would be captured at rates greater than 1.0 x 10^9 s^{-1}. The only common radical clock which approaches this rate is methylcyclopropane radical (1.3 x 10^8 s^{-1}).

9.7 Anion clocks

The use of free radicals in synthetic organic chemistry is an important method for the addition of carbon atoms to a chain, often used in polymerisation reactions. Typically, an oxygen centred radical is added to a carbon-carbon double or triple bond and forms a carbon-oxygen bond which effectively substitutes oxygen in the β position of the alkyl radical. A variety of alkoxy radicals were studied and similar stabilities found for both alkyl and β-alkoxyethyl radicals although the rates of reaction of *tert*-butoxy radical was significantly slower than the other alkoxy radicals studied. It is therefore thermodynamically favourable for the addition of the alkoxy radical to an alkene[215], which is the reverse reaction to the theoretical radical VOC degradation pathway (Fig 9.42).

Fig 9.42: The formation of alkoxy radicals is thermodynamically unfavourable

Unexpected experimental results gave rise to the hypothesis that there is β- bond

stabilisation by oxygen of alkyl radicals[216]. This was confirmed by studies using esr spectroscopy which looked at halogen atom abstraction from metalloid centred radicals and found that for β-methoxy substituents, the rate of reaction was increased. This rate increase was attributed to a polar effect in the transition state and involves charge transfer from the metal centre to the alkyl-halo group and is supported by *ab initio* calculations[217].

The stabilisation effect described above should mean that if a radical intermediate is involved in the degradation mechanism on palladised iron, we should be able to detect the radical products as the radicals should be more long lived than under other conditions. As we do not detect these products in significant quantities, our hypothesis that the mechanism is anion based is enhanced. As the radical clocks pointed towards either a slow radical or anion intermediate, we decided to look at a series of compounds which could be termed anion clocks. These clocks are direct analogues of the radical clocks and again, the products from the reaction indicate whether an anion or radical pathway is dominant. To date, there is no published literature which looks at these types of anion reactions or gives any rate constants for the reactions.

9.7.1 Degradation of bromophenetole, anion clock 1 (Expt. 61, 66)

In our initial test of an anion clock candidate we used commercially available bromophenetole, because prior experience with (2-bromoethyl)benzene, bromohexane and 6-bromohexene suggested it would have sufficient reactivity with palladised iron. Bromophenetole was expected to undergo facile elimination by either a radical or anion mechanism, and thus it acted as a test for the concept, albeit with ambiguity over the actual mechanistic pathway (Fig. 9.43). However, if ethoxybenzene was formed as the sole product, it would indicate that the anion or radical intermediates were being trapped very quickly and efficiently, and would require the design of anion clocks which could act more quickly, (*e.g.* carboxylate leaving groups). An aqueous solution of bromophenetole was shaken over palladised iron and the degradation and emergence of products was monitored by GC-MS. The rate constants for the formation of the products will also give an indication of the dominant pathway; this may be useful where there are highly water soluble products (phenol) which are difficult to extract from the water matrix and hence recovery may be significantly less than 100 % and hence comparison of amounts of products would give a false result.

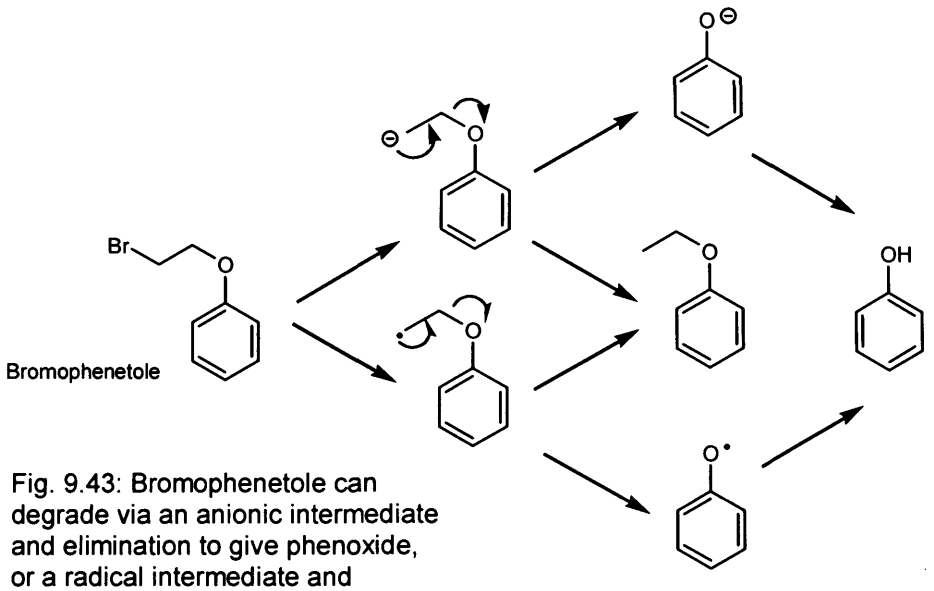

Fig. 9.43: Bromophenetole can degrade via an anionic intermediate and elimination to give phenoxide, or a radical intermediate and elimination to give phenoxy radical, and either intermediate may be reduced to ethoxybenzene

The rate constant for the degradation of bromophenetole was found to be 0.0084 min^{-1} and the rate constants for the formation of phenol and ethoxybenzene were found to be 0.0023 and 0.0026 min^{-1} respectively, slightly in favour of phenol production, but it is not enough to be a conclusive result. The mixture of both products was formed at such similar rates. By performing a quantification on the amounts of products formed, it should be possible to determine the major product and hence the dominant pathway. Bromophenetole was present at 0.5 μM in the reaction vials and declined until it could not be detected at 420 minutes. Phenol and ethoxybenzene were first detected at 10 minutes and increased during the entire duration of the experiment (Table 9.19)

Table 9.19: Formation of phenol and ethoxybenzene from the degradation of bromophenetole

Time, min	Phenol		Ethoxybenzene		Ratio
	μg/ml	μMol	μg/ml	μMol	phenol:ethoxybenzene
10	1.85	0.02	0.6	0.00	4.00
30	3.3	0.04	1.5	0.01	2.86
60	6.1	0.06	1.8	0.01	4.40
90	4.8	0.05	1.3	0.01	4.79
120	8.7	0.09	2.7	0.02	4.18
165	9.5	0.10	2.8	0.02	4.40
180	10.8	0.11	2.8	0.02	5.01
240	14	0.15	3.9	0.03	4.66
300	17.2	0.18	5.4	0.04	4.13
360	16.8	0.18	5.6	0.05	3.89
420	18.6	0.20	5.9	0.05	4.09
480	18.6	0.20	5.3	0.04	4.56
540	17.2	0.18	4.3	0.04	5.19
600	21.4	0.23	7.2	0.06	3.86

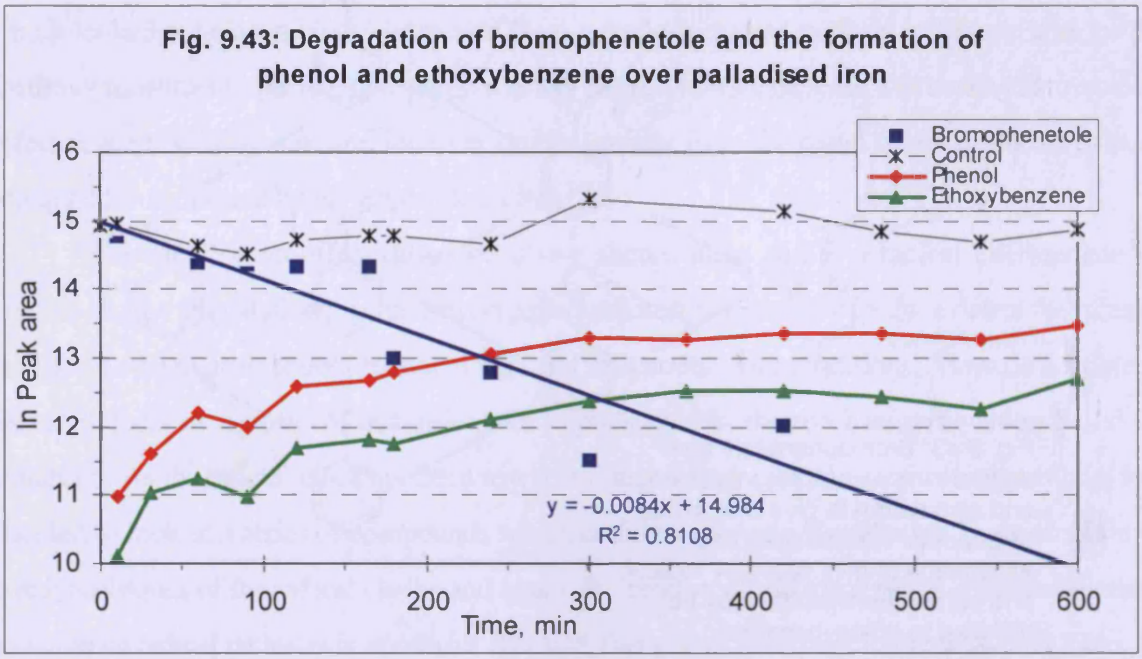

Fig. 9.43: Degradation of bromophenetole and the formation of phenol and ethoxybenzene over palladised iron

The mean ratio of phenol concentration to ethoxybenzene concentration is 4.3, indicating a bias towards phenol. From the graph (Fig 9.43) it may be seen that the lines for the formation of phenol and ethoxybenzene are curved rather than straight, indicating that the formation is not first order, but second order. The equation for a second order reaction is given as

$$k_2 = \frac{1}{at}\left\{\frac{x}{a-x}\right\}$$

where a is some measure of initial concentration and x is some measure of concentration at time t[218]. If a plot of product peak area divided by total peak area of reactant plus all products is obtained, the relationship for the products is found to be linear with the gradient being the rate constant, confirming a second order reaction. This only applies whilst reactant is present in the system, thereafter a steady state is reached and the lines plateau. From the graph (Fig 9.44) it may be seen that the rate constant for the formation of phenol is 0.0022 min^{-1} and for ethoxybenzene is 0.0009 min^{-1}, a ratio of 2.5 towards the formation of phenol.

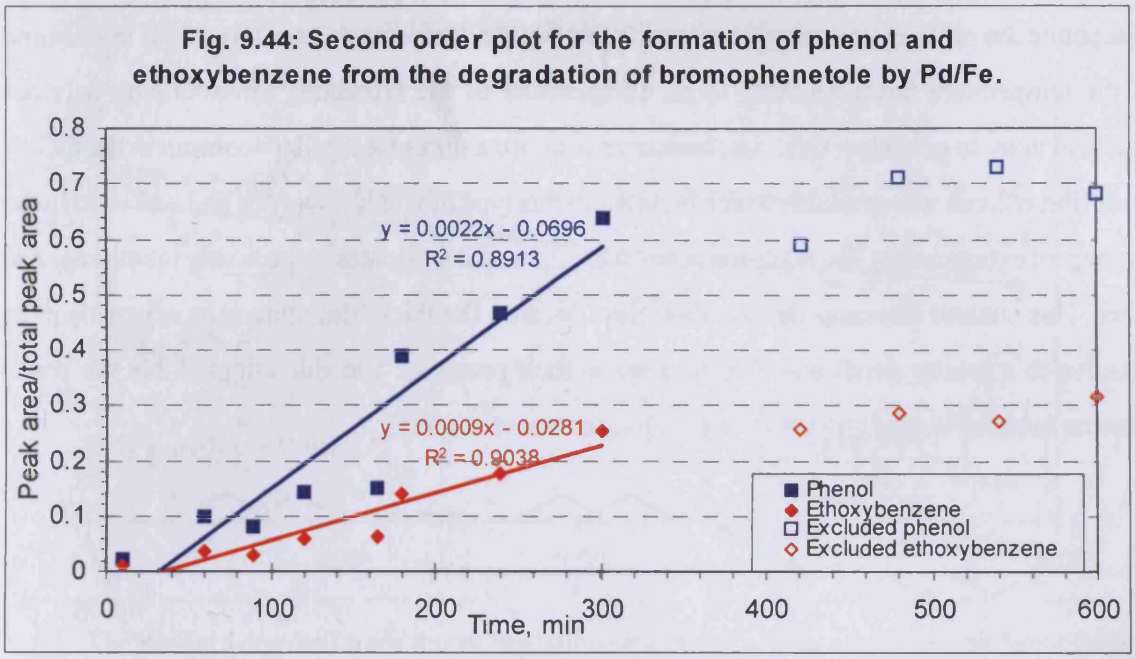

The use of bromophenetole is of no value as an anion (or radical clock) because of mechanistic ambiguities, nevertheless these experiments demonstrated that an elimination based anion clock would be viable. Both phenoxy radical and phenoxide are relatively stable due to the effect of the benzene ring, hence the mixed products reported. This lead us to consider the use of another compound, bromoethyl ethyl ether as an anion clock which does not have this ring stabilisation effect and which would be compatible with purge and trap injection.

9.7.2 Degradation of bromoethyl ethyl ether on palladised iron, anion clock 2 (Expt. 34, 36, 39)

An aqueous solution of bromoethyl ethyl ether was shaken over palladised iron with the degradation and emergence of products was monitored by GC-MS. The experiment was initially run on a small scale, but the high detection limit of ethanol meant that if it had been formed, it would be too low to be detected, so the experiment was repeated, once at the same level mixed with chloroform to check the kinetics and then again alone on at a higher concentration of 907 µg/l, a 7.5 fold increase over the 120 µg/l in the small scale work. The relative amount of iron remained the same, with 0.25 g in 2 ml for the small scale and 2.0 in 15 ml for the large scale work.

Bromoethyl ethyl ether can degrade to give either ethanol or diethyl ether, depending whether a radical or anion mechanism is dominant (Fig. 9.45). The ether/ethanol standard run under the initial conditions showed that the retention times of the two compounds was very close at 2.1 and 2.0 minutes respectively, so close that they were almost co-eluting. Whilst this is not a problem in mass spectrometry as quantitation may be performed by monitoring selected ions

unique to each compound, it makes the TIC trace difficult to interpret by eye. It may be possible to separate the peaks by lowering the temperature, but the temperature was only 35° C at this time in the temperature ramp, and due to the temperature of the laboratory environment, it is not practical to try to get below this. An alternative is to use a different capillary column in the GC. A thick film column was available which is suited to this type of volatile analysis and was used in the two repeat experiments. The retention times were 2.8 and 2.9 minutes respectively for ethanol and ether. This column increases the retention time because the thick film allows the components to dissolve to a greater depth and therefore slows their progress. The side effect is that the peaks become broader, so the limit of detection may increase slightly.

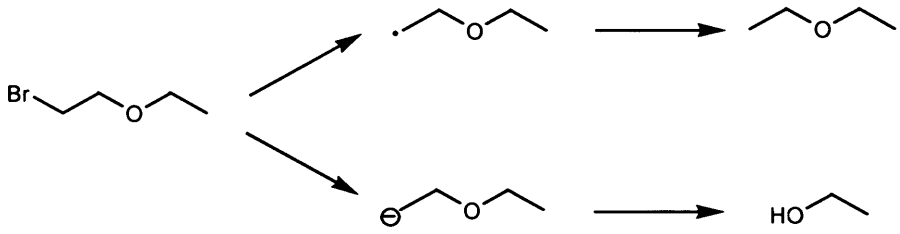

Fig. 9.45: 2-Bromoethyl ethyl ether gives either ethanol or diethyl ether by anionic or radical mechanisms respectively.

In the first experiment, the disappearance of the bromoethyl ethyl ether was slow but steady, however, no products were detected during the early stages of the degradation and only towards the latter stages of the reaction were traces of ether were detected.

In the second experiment where a mixed system of chloroform and bromoethyl ethyl ether was used, the degradation of bromoethyl ethyl ether was again shown to be significantly slower than that of chloroform. The half life for chloroform in this system is longer than has been previously reported, probably as a result of the presence of the bromoethyl ethyl ether. This can be compared to the slowing of the rate of degradation in the presence of 1,4-dioxane when used as a surrogate standard. Again, the reaction is slowed because the active sites on the iron/palladium surface are being blocked and are therefore not available for chloroform binding and reduction (not shown in Fig 9.46).

Fig 9.46: Degradation of 2-bromoethyl ethyl ether singly and with chloroform on palladised iron

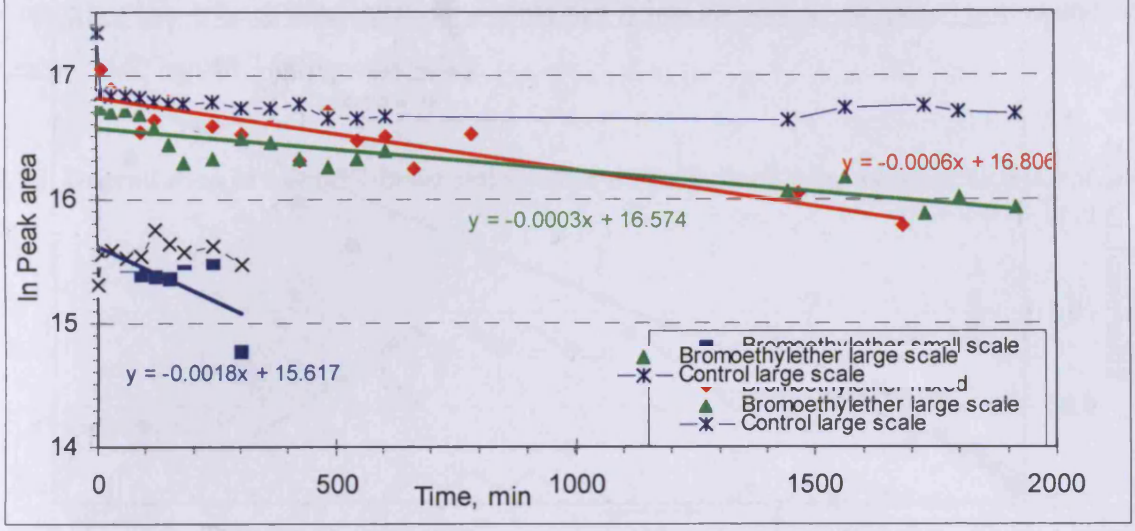

The product detected from this degradation was ether, which confirmed the first finding. Even though the reaction was left for 28 hours, no ethanol was detected, even by selected ion monitoring. This may be for two reasons, no ethanol is being produced from the reaction, or the amount of ethanol production is so small it cannot be detected by this technique. Ethanol is very water soluble and is difficult to purge from solution at the levels likely to be formed. The limit of detection was determined by a series of calibration standards prepared in water and run under identical conditions which gave a limit of detection of 500 µg/l. This is a serious problem because if the reaction proceeds *via* the anion mechanism, we will not be able to detect the ethanol formed at the concentration levels we are working at. This formed the basis for the large scale experiment were we hoped to have a sufficiently high starting concentration of bromoethyl ethyl ether to be able to detect any ethanol formed. The bromoethyl ethyl ether experiment was run on a larger scale to see if any more products at a very low concentration could be detected. Although overall the concentrations remained the same as in the small scale reaction, the net effect is to increase the amount of material being injected onto the system because the amount of sample is larger.

The rate constant for the degradation of bromoethyl ethyl ether in s^{-1} was found to be 3 x 10^6 s^{-1}, and the rate constant for the formation of ether was 2 x 10^6 s^{-1} (Fig. 9.47). Although the coefficient of determination is acceptable (R^2 = 0.946), the plot shows some curvature at the beginning; the formation is second order.

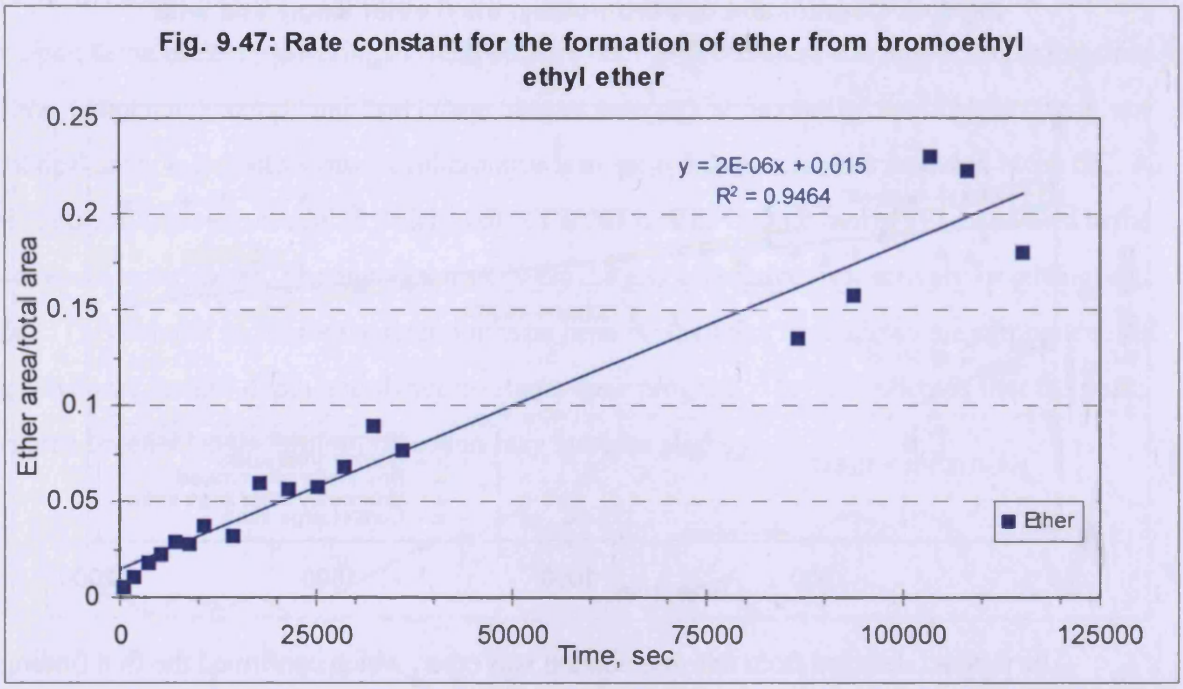

Using the calibration curves from the instrument software, the degradation produced approximately 90 µg/l ether after 10 hours and hence some 50% of the material in the system is unaccounted for. To determine if the products of the degradation were being adsorbed onto the iron surface, a calibration curve in the presence of iron was measured, and this proved that the missing reactants and products were retained on the surface, hence our low recoveries. This in part also explains why we may be unable to detect ethanol in this reaction as it effectively doubles our detection limit.

When we ran a series of standards containing methylcyclopentane, cyclohexane and hexene, we found the greatest loss appears was for hexene, with very poor recovery and detection below the 500 µg/l level. Even at this high level, there is on average a 20% loss of hexene when incubated with the iron filings. This loss at the high standard level is mirrored in both the methylcyclopentane and the cyclohexane, at approximately 20% and 10% respectively. However, this loss is not detected at the lower levels, which is something of a surprise. It would be expected that the loss would be less noticeable at the higher concentrations because if a finite quantity of material could be adsorbed onto the iron surface, the proportion of the total becomes less as the total concentration increases. This apparent effect may be explained if the increasing concentration is in some way forcing the components onto the surface.

As these components are formed on the surface of the iron during degradation, and assuming that similar amounts of material are bound as demonstrated in the above experiment, the maximum quantity of recoverable material will be 80% of the starting concentration of the

degrading component.

We were not able to get a conclusive result from this experiment as we could not detect ethanol at a low enough concentration to show that it was formed, so we looked next at another radical clock, benzyl 2-bromoethyl ether.

9.7.3. Degradation of benzyl 2-bromoethyl ether on palladised iron, anion clock 3 (Expt. 69, 70)

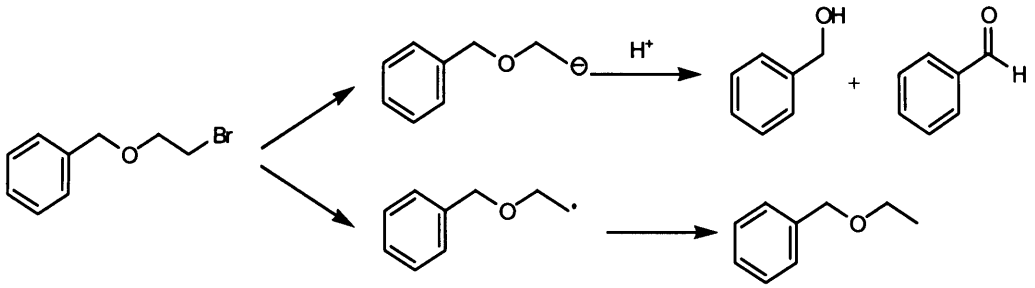

Fig. 9.48: Benzyl 2-bromoethyl ether gives benzyl alcohol and benzaldehyde via elimination from anion or benzyl ethyl ether from a radical

An aqueous solution of benzyl 2-bromoethyl ether was shaken over palladised iron and the degradation and emergence of products was monitored by GC-MS. Benzyl 2-bromoethyl ether is another example of an anion clock (Fig. 9.48). The expected products were benzyl alcohol from an anionic intermediate and benzyl ethyl ether from a free radical intermediate.

We had previously observed benzaldehyde as a contaiminant in benzyl alcohol, but it was not found in this degradation. Examination of the peak areas of benzyl alcohol to benzyl ethyl ether gave an average ratio of 1.16:1 respectively. This does NOT take into account any difference in response of the compounds. In each case, the peak area of the benzyl alcohol was larger. This is significant because (assuming the response is identical for both compounds) it indicates that the benzyl alcohol formation is slightly more facile than the benzyl ethyl ether reaction.

If the rates of formation for the benzyl alcohol and benzyl ethyl ether are compared, it is found that the rate constants are 0.0013 min^{-1} and 0.0012 min^{-1} respectively in the single system (Fig 9.49). Effectively both reactions have the same rate constant and we are therefore not able to distinguish which pathway predominates.

Fig. 9.49: Rate constants for the formation of products from the degradation of bromoethoxybenzene and benzyl bromoethyl ether with Pd/Fe

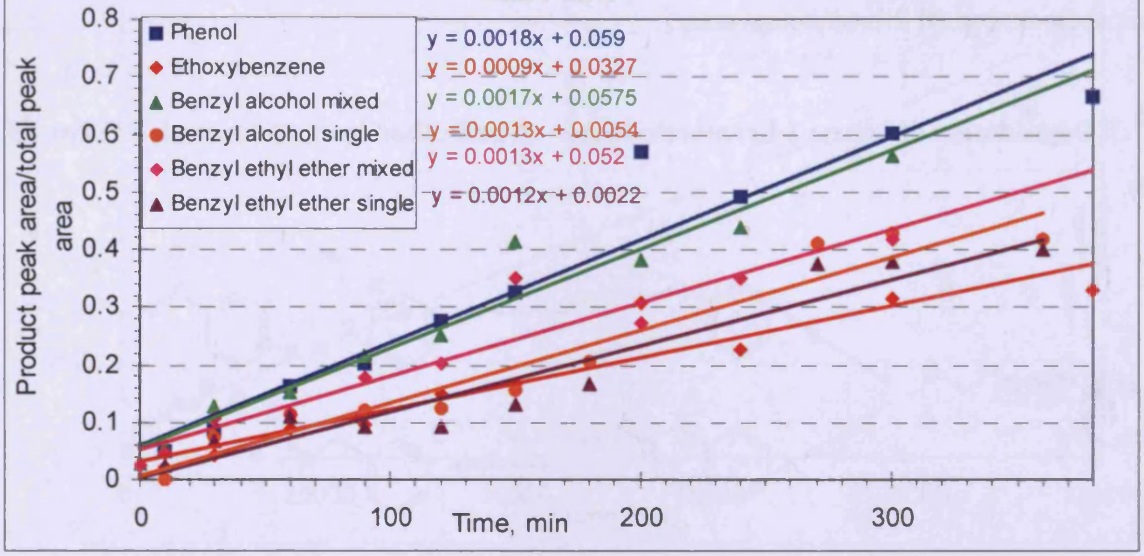

Fig. 9.50: Rate of degradation of benzyl bromoethyl ether in single and mixed system plus formation of benzyl alcohol and benzyl ethyl ether

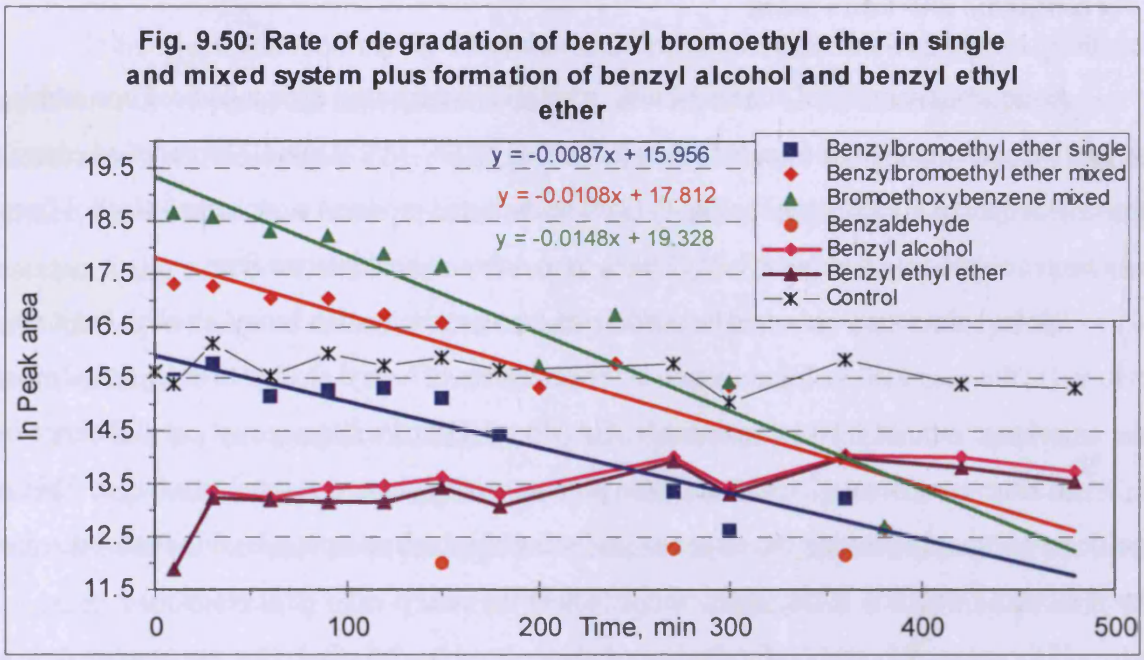

The experiment was repeated in a mixed system with bromophenetole which is another example of an anion clock. This compared two anion systems. In this experiment, a mixed aqueous solution of benzyl 2-bromoethyl ether and bromophenetole and a mixed solution in a 10 % *v/v* methanol solution were shaken over palladised iron with the degradation and emergence of products monitored by GC-MS. The methanol solution was used as it slows the proton donation required to form benzyl alcohol and also stabilises some intermediates so that dimers can form, as in the case of bibenzyl from benzyl bromide.

A graph comparing rate of degradation (Fig 9.50) of the reactants shows two lines which run almost parallel with rate constants of 0.0108 min^{-1} and 0.0148 min^{-1} for benzyl 2-bromoethyl ether and bromoethoxybenzene respectively. This indicates that the rate of degradation is approximately the same for both systems. The implication from this finding is that the leaving group does not significantly affect the rate of reaction under these conditions and hence the rate determining step does not involve the loss of the leaving group. The slowest step may involve either diffusion to/from the metal surface or binding to the surface. If this is sufficiently slow, the actual rate at which the compounds degrade will be unmeasurable. The same result was obtained with the water system and confirm the difference in the rates of reaction indicate a difference in stability of the anion. As the rates are similar, it suggests that the stability of the anion and the leaving group are not the rate determining step.

The experiments with radical clocks have failed to show a radical intermediate, whereas the experiments with anion clocks are consistant with an anionic mechanism. However the work with 2-bromophenetole is ambiguous because there are two possible modes of elimination *via* radical and anionic intermediates. In the case of 2-bromoethyl ethyl ether the results are equally inconclusive because the limit for detection of ethanol was too high. However with benzyl 2-bromoethyl ether there is no ambiguity because benzyl alcohol can only be formed *via* an anionic intermediate. The formation of almost equal amounts of benzyl alcohol and benzyl ethyl ether is due to interception of the anion before elimination. In this context the formation of even a trace of benzyl alcohol indicates an anionic intermediate.

Elimination requires that the orbital containing the anion is able to overlap with the antibonding orbital of the nucleofuge. In the acyclic systems described thus far, there is free rotation and hence elimination depends on a time averaged conformational constraints. It appeared possible that if we could free out the rotation by placing the anion and the nucleofuge in a ring, elimination would be more rapid and the results would be more decisive.

9.7.4 *trans*-1-Bromo-2-(*n*-hexyloxy)-cyclohexane 105 and *trans*-1-bromo-2-(*n*-octyloxy)cyclopentane 107, anion clocks 4 and 5

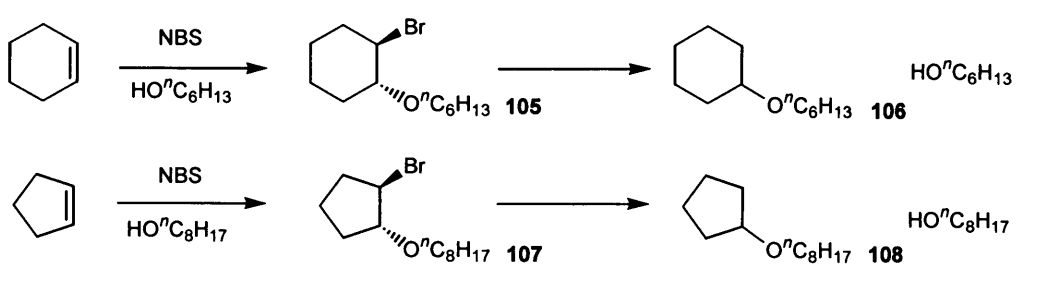

Fig 9.51: Anion clocks

Two compounds were synthesised to act as cyclic anion clocks, *trans*-1-bromo-2-(*n*-hexyloxy)-cyclohexane **105** and *trans*-1-bromo-2-(*n*-octyloxy)cyclopentane **107**. These were prepared by electrophilic addition to cyclohexene and cyclopentene using NBS and the appropriate alcohol. Both compounds were reduced with a catalytic amount of tri-*n*-butyltin hydride regenerated with lithium aluminium hydride to give the ethers **106**, **108**, as authentic compounds for the degradative work. The use of the catalytic procedure was essential, because there was little prospect that the non-polar ethers **106**, **108** could be separated from a stoichiometric amount of tri-*n*-butyltin bromide in acceptable yield. The bromoethers **105**, **107** and the ethers **106**, **108** are all new compounds and were fully characterised by NMR and MS and the homogeneity demonstrated using TLC and GC.

The byproducts from elimination are cyclopentene and cyclohexene, but these are too volatile to analyse by conventional injection GC and they ionise too poorly to be determined at a low level by MS. We intended to measure the elimination by measuring the amounts of alcohols produced. Therefore the alcohols were chosen so that they could be conveniently determined by GC. Hexanol was chosen for the cyclohexyl bromoether **105** and octanol for the cyclopentyl bromoether **107** (rather than the other way round) to roughly match the molecular weights. It was anticipated that the cyclopentyl bromoether **107** would eliminate more quickly than the cyclohexyl bromoether **105**, because the latter would need to adopt the diaxial conformation **111**, which is the least favourable of three chair conformers **109**, **110**, **111** (Fig. 9.52).

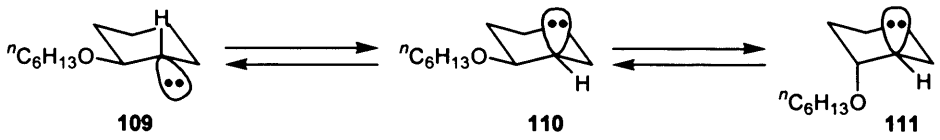

109 **110** **111**

Fig 9.52: Conformational constraints on elimination

trans-1-Bromo-2-(*n*-hexyloxy)-cyclohexane **105** and *trans*-1-bromo-2-(*n*-octyloxy)cyclopentane **107** were degraded on palladised iron in water with the degradation and product formation monitored by GC-MS. In the first instance, the degradation was carried out with both single compounds and a mixed component system for the degradation rate constants to be calculated (Table 9.19).

Table 9.19: Comparison of the various rate constants calculated for the degradation of the cyclohexyl and cyclopentyl compounds

Experiment no	*trans*-1-Bromo-2-(*n*-hexyloxy)-cyclohexane **105**, Rate constant, min^{-1}				*trans*-1-Bromo-2-(*n*-octyloxy) cyclopentane **107**, Rate constant, min^{-1}			
	Calcul.	Ratio	Graph	Ratio	Calcul.	Ratio	Graph	Ratio
79, single component	0.0021	100	0.0015	100	0.0030	100	0.0027	100
79, mixed component	0.00097	46	0.0009	60	0.00138	46	0.0007	26
80, mixed component	0.0037	176	0.0039	260	0.0055	183	0.0069	256

This reaction is considerably slower than some of those examined recently. Although a gradual decrease in starting material can be seen when the data is examined graphically (Fig 9.53), it is more difficult to detect any trend with the degradation products. The rates for the degradation are slower in the mixed component system than the single system, as has already been seen for other mixed component and internal standard systems, probably because of competition for the active sites.

When the rate constant plot for the formation of products is drawn (Fig 9.54), assuming that this is first order kinetics, it can clearly be seen that the rate constants for the formation of the reduced hexyl and octyl compounds are much larger at 0.0005 min^{-1} and 0.0006 min^{-1} respectively than for the corresponding alcohols, as predicted for an anion mechanism and the production of hexanol with a rate constant of 0.00009 min^{-1} is slower than for octanol at 0.0002 min^{-1}, again as predicted by an anion mechanism. This means that reduction is the dominant pathway for this degradation and some rate limiting step (probably diffusion to and from the surface) holds back the elimination reaction.

Fig 9.53: Comparison of the degradation rate constants for *trans*-1-bromo-2-(n-hexyloxy)-cyclohexane 105 and *trans*-1-bromo-2-(n-octyloxy)cyclopentane 107 with Pd/Fe

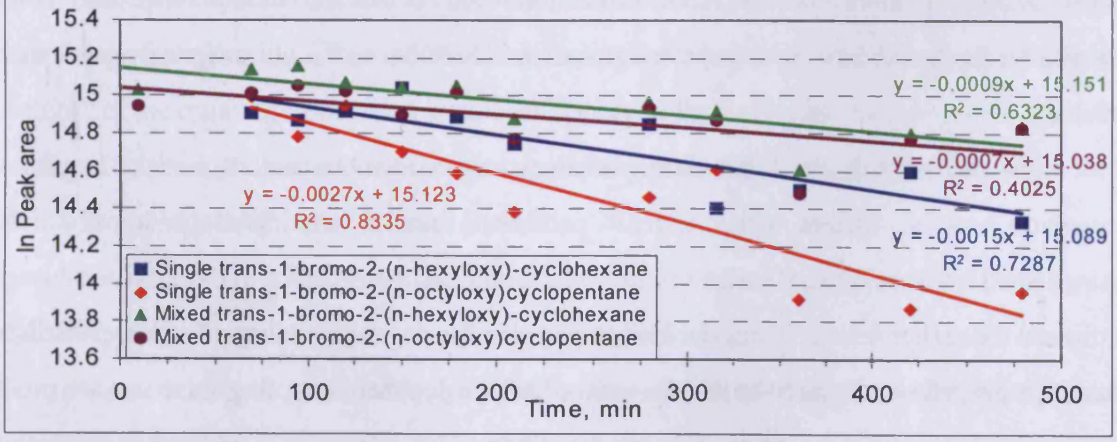

The reason that octanol is produced more readily than hexanol is due to the conformation of the cyclohexane ring. It is assumed that the hexyl ether-substituent of the cyclohexane derivative

must enter the less favourable axial position for elimination to occur so that electrons from the anion can feed into the antibonding orbital of the C-O bond (Fig. 9.52). Whereas the octyl ether substituent of the cyclopentane derivative is already close to the optimum position for elimination.

Fig. 9.54: Rate constants for the formation of the alcohols and ethers from synthesised anion clocks in single systems

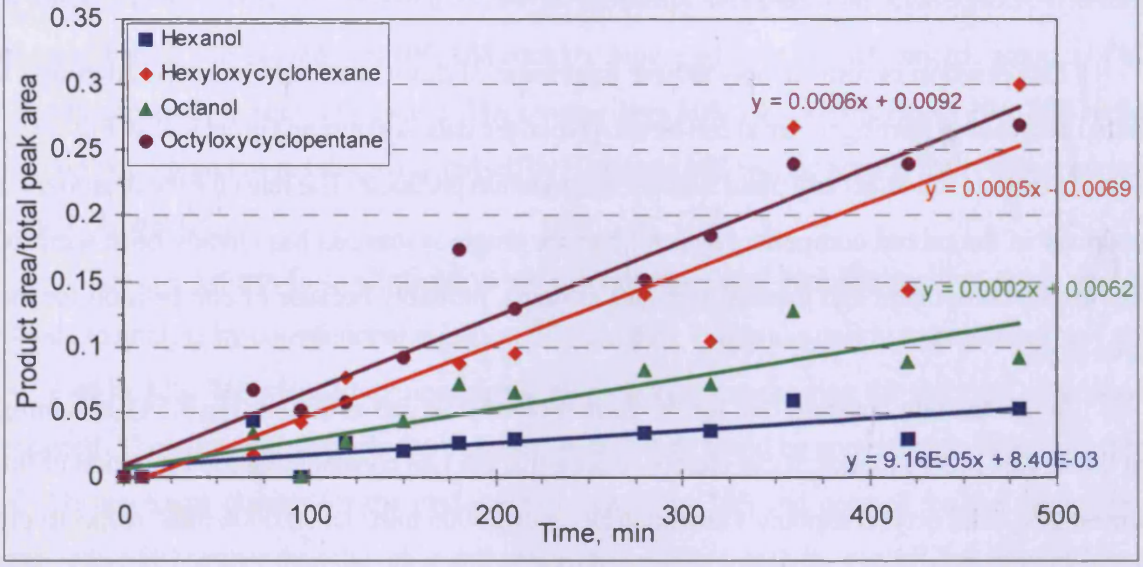

A large scale combined degradation was undertaken in which the stock solutions were shaken over palladised iron and at the appropriate time points, two aliquots of the aqueous phase were removed, extracted with chloroform and analysed by GC-MS. The samples were analysed in duplicate and from a single reaction vessel to remove individual vial variations. The results for the degradation confirm the first experiment, with the *trans*-1-bromo-2-(*n*-octyloxy)cyclopentane **107** degrading faster than the *trans*-1-bromo-2-(*n*-hexyloxy)-cyclohexane **105** (fig not shown). The formation of products was not followed as the peak areas were too low to give enough data points for any meaningful calculation. It was also found that when octanol and hexanol were shaken over palladised iron, the extracted recovery was approximately 80 %, so this also affects the peak areas detected.

The degradation was run with naphthalene as an internal standard, but the degree of conversion was insufficient with "normal" palladised iron to give results which could be distinguished from background variation and whilst graphical interpretation of the data (not shown) confirmed the earlier results, it was decided to perform the degradation using "hyper" palladised iron as this gives faster degradation rate constants. Despite duplicate sampling, there was too much variation in the results for any degradation constants to be calculated. The product formation suffered from less variation but, as determining rates of formation also relied on the use of the degradation data, was found to be meaningless.

From this series of experiments, we can see that the formation of octanol occurs at a faster rate than the formation of hexanol and the formation of the ethers is faster than the formation of alcohols which supports our anion mechanism hypothesis.

9.8 Conclusions

The series of experiments described here clearly demonstrates that degradation of halogenated compounds by iron is enhanced when the iron is freshly activated by acid washing and by the addition of a second metal, palladium, to the surface. We have also confirmed the surface reaction theory by demonstrating that protons created during the activation process are consumed before protons from the bulk solvent. The solvent must also be capable of easily donating protons for the reaction as increasing organic solvent concentration slows and eventually inhibits the degradation completely. We have shown that the leaving group also has an effect on the reaction rate as bromine compounds were found to degrade faster and without detectable intermediates.

Examination of the reaction mechanism by the use of radical clocks such as 6-bromohexene, gave strong evidence that radicals were not generated by the surface bound species which in turn led us to examine "anion clocks". Initially, we looked at commercially available compounds which gave us ambiguous results, so we examined benzyl 2-bromoethyl ether and the synthesised anion clocks 4 & 5 **105**, **107**. The formation of alcohols by these novel clocks also supported an anion mechanism. We therefore conclude that the reaction mechanism for the degradation of halogenated compounds with zero-valent metals proceeds *via* an anionic species, but this is an incomplete designation, because the cationic counterion has not been specified. The degree of covalency or ionic character in the metal cation-carbanion bond is the predominant feature, which controls elimination or protonation (and hence overall reduction) from an anion clock. This is an important distinction between free radical clocks and the anion clocks, because the outcome from starting a free radical clock depends predominantly on the concentration and reactivity of the trapping agent. This is also an important factor for anion clocks, but it is further modulated by the metal and so for example we might expect that elimination will be a more facile process for an organolithium than an organozinc.

9.8.1 The catalytic cycle

The generally accepted redox cycle for the degradation of haloorganics by palladised iron is shown in Fig. 9.55. The direction of reaction is dictated by the electrode potentials and the difference is close to the maximum that can be achieved with transition metals. Hence we can be assured that any palladium that is present in a redox active form will be in the Pd^0 form.

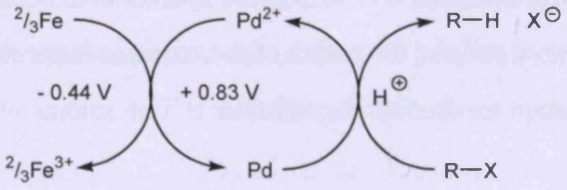

Fig. 9.55: The redox cycle for the degradation of haloorganics by Pd/Fe

The crucial issue with regard to our work is the nature of the interaction between palladium and the organohalide. Our data is most consistant with oxidative addition into the carbon-halogen bond, followed by displacement or elimination.

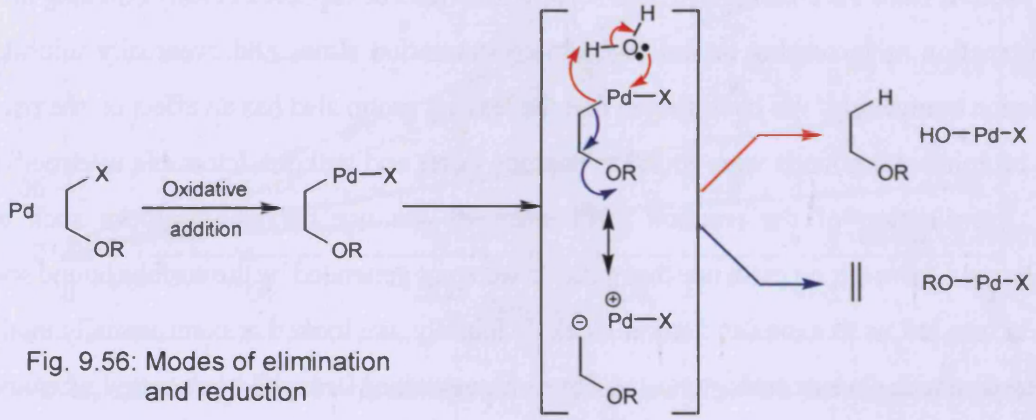

Fig. 9.56: Modes of elimination and reduction

The presence of a polarised carbon-palladium bond is consistant with the greater rates observed in the degradation of polyhaloorganics because the anionic character is stabilised by the halosubstituents. The decreased rate of reaction in THF and to a lesser extent methanol may be due to a lower concentration of free protons which are required for the cleavage of the Pd-C bond.

9.8.2 Future work

The study of the palladised iron degradation of 6-bromohexene conclusively demonstrated that a long lived radical is not an intermediate, because methylcyclopentene was not detected. The anionic clocks indicated that a short lived anionic species was present, such that anion capture by a proton was competitive with elimination of the ether substituent as alkoxide. Observation of elimination is incompatible with a radical, but the result would be would be more persuasive if the clock were also able to give positive evidence for a long lived radical. To this end we propose the dual clock **110** below which would act as a radical and anion clock, with a fast radical giving one product **111**, a slow radical producing a second product **112** and an anion intermediate giving a third distinct product **109**.

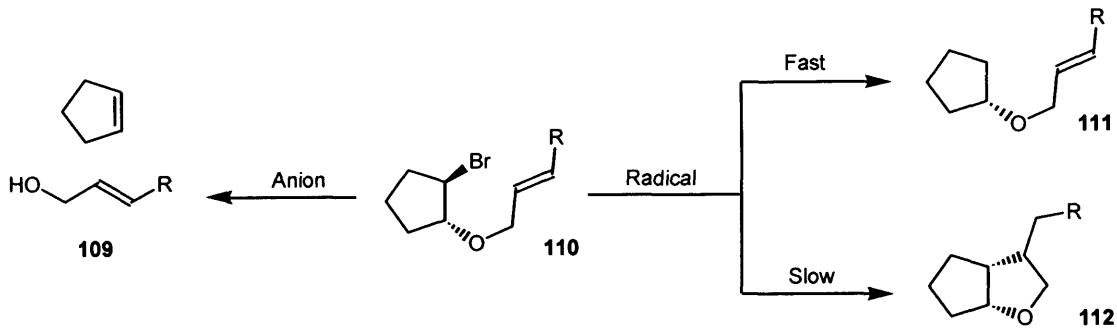

Fig. 9.57: Suggested candidate compound for dual anion and radical clock

1. Agosta, W., Chemical Communication - The Language of Pheromones, Scientific American Library, W. H. Freeman, New York, Oxford, 1992, 1 - 11.

2. Shorey, H. H., Animal Communication by Pheromones, Academic Press, New York, London, 1976, 1 - 6.

3. Lewis, R. J. (ed.), Hawley's Condensed Chemical Dictionary, 12th edition Van Nostrand Reinhold, New York, 1993, 607.

4. Karlson, P., Lüscher, M., `Pheromones': a new term for a class of biologically active substances, *Nature*, 1959, **183**, 55-56.

5. Bishop R.J., Aggregation of Sap Beetles, http://www.colostate.edu 1996

6. Coghlan, A., Sensitive flower, Sept 26 1998, *New Scientist*, pages 24 - 28.

7. Kelly, D. R., Insect Semiochemicals, *Chemistry in Brit.*, 1990, 124-127.

8. Scott A. P., Vermeirssen E. L. M., Production of conjugated steroids by teleost gonads and their role as pheromones, *Perspect. Comp. Endocrinol.*, 1994, **13,** 645 - 654.

9. Søresen P. W., Scott A. P., The evolution of hormonal sex pheromones in teleost fish: poor correlation between the pattern of steroid release by goldfish and olfactory sensitivity suggests that these cues evolved as a result of chemical spying rather than signal specialisation, *Acta Physiol. Scand.*, 1994, **152**, 191 - 205.

10. Hecker, E., Butenandt, A., Bombykol revisited- Reflections on a pioneering period and on some of its consequences in *Techniques in Pheromone Research* (eds. Hummel, H. E., Miller, T. A.), Springer-Verlag, New York, 1984, 1 - 44.

11. Attygalle, A. B., Morgan, E. D., Pheromones in nanogram quantities - Structure determination by combined microchemical and gas chromatographic methods, *Angew. Chem. Int. Ed., Engl*,.1998, **27**, 460 - 478.

12. Caplan, S., Kurjan, J., Role of alpha-factor and the mf-alpha-1 alpha-factor precursor in mating in yeast, *Genetics*, 1991, **127**, 299 - 307.

13. Bender, A., Sprague, G. F., Yeast peptide pheromones, a-factor and alpha -factor, activate a common response mechanism in their target cells, *Cell*, 1986, **47**, 929 - 937.

14. Lui, S., Henry, L. K., Lee, B. K., Wang, S. H., Arshava, B., Becker, J. M., Naider, F., Position 13 analogs of the tridecapeptide mating pheromone from *Saccharomyces cerevisiae*: design of an iodinatable ligand for receptor binding, *J. Peptide Res.*, 2000, **56**, 24 - 34.

15. Manfredi, J. P., Klein, C., Herrero, J. J., Byrd, D. R., Trueheart, J., Wiesler, W. T., Fowlkes, D. M., Broach, J. R., Yeast alpha mating factor structure-activity relationship derived from genetically selected peptide agonists and antagonists of Ste2p, *Mol. Cell. Biol.*, 1996, **16**, 4700 - 4709.

16. Butty, A. C., Pryciak, P. M., Huang, L. S., Herskowitz, I., Peter, M., The role of Far1p in linking the heterotrimetric G protein to polarity establishment proteins during yeast mating, *Sci.*, 1998, **282**, 1511 - 1516.

17. Xie, H. B., Shao, Y., Becker, J. M., Naider, F., Gibbs, R. A., Synthesis and biological activity if the geometric farnesylated analogues of the a-factor mating peptide of *Saccharomyces cerevisiae*, *J. Org. Chem.*, 2000, **65**, 8552 - 8563.

18. Caldwell G. A., Naider F., Becker J. M., Fungal lipopeptide mating pheromones - a model system for the study of protein prenylation, *Microbiol. Review*, 1995, **59**, 406 - 422.

19. Nahon, E., Atzomony, D., Zahavi, A., Granot, D., Mate selection in yeast - a reconsideration of the signals and messages encoded by them, *J. Theoret. Biol.*, 1995, **172**, 315 - 322.

20. Kelly, D. R., Insect semiochemicals, *Chem. In Brit.*, 1990, **26**, 124 - 127.

21. Kelly, D. R., Sex and scents in the natural world, *Chem. Rev.*, 1997, **6**, 2 - 6.

22. Kelly, D. R., When is an elephant like a butterfly? Coincidences in pheromone structures, *Chem. Biol.*, 1996, **3**, 595 - 602.

23. Pfeiffer, W., Chemical signals in communication, *Chemoreception in Fishes*, 1982, Hara, T. J. (ed.), Elsevier, Amsterdam, 307 - 325.

24. Pfeiffer, W., Pheromones in fish and amphibia, *Pheromones*, 1974, Birch, M. C. (ed.), Elsevier, Amsterdam, London, 269 - 296.

25. Cooper, J. C., Hirsch, P. J., The role of chemoreception in salmonid homing, *Chemoreception in Fishes*, 1982, Hara, T. J. (ed.), Elsevier, Amsterdam, 343 - 361.

26. Nordeng, H., A pheromone hypothesis for homeward migration in anadromous salmonids, 1977, *Oikos*, **28**, 155 - 159.

27. Matty, A. J., Fish Endocrinology, 1985, Croom Helm, Timber Press, Portland, Oregon, 198 - 219.

28. Smith, R. J. F., The adaptive significance of the alarm substance - fright reaction system, *Chemoreception in Fishes*, 1982, Hara, T. J. (ed.), Elsevier, Amsterdam, 327 - 341.

29. Smith, R. J. F., The evolution of chemical alarm signals in fishes, *Chemical Signals in Vertebrates vol. IV*, 1986, Duvall, D., Muller-Schwarze, D., Silverstein, R. M. (eds.), Plenum Press, New York, 99 - 115.

30. Brown, G. E., Adrian, J. C., Smith, E.,. Leet, H., Brennen, S., Ostariphysan alarm pheromones: laboratory and field tests of the functional significance of nitrogen oxides, *J. Chem. Ecol.*, 2000, **26**, 139 - 154.

31. Brown, G. E., Adrain, J. C., Shih, M. L., Behavioural responses of fathead minnows to hypoxanthine-3-*N*-oxide at varying concentrations, *J. Fish Biol.*, 2001 **58**, 1465 - 1470.

32. Wisenden, B. D., Chivers, D. P., Smith, R. J. F., Risk-sensitive habitat use by brook stickleback (*Culaea inconstans*) in area associated with minnow alarm pheromone, *J. Chem. Ecol.*, 1994, **20**, 2975 - 2983.

33. Mathias, A., Smith, R. J. F., Intraspecific and cross-superorder responses to chemical alarm signals by brook stickleback, *Ecol.*, 1993, **74**, 2395 - 2404.

34. Mathias, A., Smith, R. J. F., Chemical labelling of the Northern pike (*Esox lucius*) by the alarm pheromone of Fathead minnows (*Pimephales promelas*), *J. Chem. Ecol.*, 1993, **19**, 1967 - 1979.

35. Chivers, D., Smith, R. F. J., The role of olfaction in chemosensory-based predator recognition in the Fathead minnow, *Pimephales promelas*, *J. Chem. Ecol.*, 1993, **19**, 623 - 633.

36. Hara, T., Olfaction and gustation in fish: an overview, *Acta Physiol. Scand.*, 1994, **152**, 207 - 217.

37. Nevitt, G. A., Do fish sniff? A new mechanism of olfactory sampling in pleuronectid flounders, *J. Exp. Biol.*, 1991, **157**, 1 - 18.

38. Fisknes, B., Døving, K., Olfactory sensitivity to group-specific substances in Atlantic salmon (*Salmo salar* L.), *J. Chem Ecol.*, 1982, **8**, 1083 - 1092.

39. Kawabata, K., Induction of sexual behaviour in male fish (*Rhodeus ocellatus ocellatus*) by amino acids, *Amino Acids*, 1993, **5**, 323 - 327.

40. Rosenblum, P. M., Sørensen, P. W., Stacey, N. E., Peter, R. E, Binding of the steroidal pheromone 17α,20β-dihydroxy-4-pregnen-3-one to goldfish (*Carassius auratus*) olfactory epithelium membrane preparation, *Chemical Senses*, 1991, **16**, 143 - 154.

41. Sørensen, P. W., Hara, T., Stacey, N. E., Sex pheromones selectively stimulate the medial olfactory tracts of male goldfish, *Brain Res.*, 1991, **558**, 343 - 347.

42. Teeter, J., Pheromone communication in sea lampreys (*Petromyzon marinus*): implications for population management, *Can. J. Fish. Aquat. Sci.*, 1980, **37**, 2123 - 2132.

43. Resink, J. W., Voorthuis, P. K., Van den Hurk, R., Vullings, H. G. B., Pheromone detection and olfactory pathways in the brain of the female African catfish, *Clarias gariepinus*, *Cell Tissue Res.*, 1989, **256**, 337 - 345.

44. Stacey, N., Hormones and pheromones in fish sexual behaviour, *Bioscience*, 1983, **33**, 552 - 556.

45. Liley, N. R., Cardwell, J. R., Rouger, Y., Current status of hormones and sexual behaviour in fish, 1987, *Proceedings of the Third International Symposium on the Reproductive Physiology of Fish*, Idler, D. R., Crim, L. W., Walsh, J. M. (eds.), Plenum Press, St John's, Canada, 141 -165.

46. Van Weerd, J. H., Richter, C.J.J., Sex pheromones and ovarian development in teleost fish, *Comp. Biochem. Physiol.*, 1991, **100a**, 517 - 527.

47. Scott A. P., Vermeirssen E. L. M., Research on reproductive priming pheromones in fish, 1995, *Unpublished data.*

48. Lambert, J., Resink, J., Steroid glucuronides as male pheromones in the reproduction of the African catfish *Clarias gariepinus* - a brief review, *J. Steroid Biochem. Molec. Biol.*, 1991, **40**, 549 - 556.

49. Stacey, N. E., Cardwell, J. R., Liley, N. R., Scott, A. P., Sørensen, P. W., Hormones as sex pheromones in fish, *Persp. Comp. Endocrinol.*, 1993, **12**, 438 - 448.

50. Stacey, N. E., Sørensen, P. W., Function and evolution of fish hormonal pheromones, *Biochemistry and Molecular Biology of Fishes, vol. 1*, 1991, Hochachka, Mommsen (eds.) Elsevier Science Publishers, 109 -135.

51. Stacey, N. E., Kyle, A. L., Liley, N. R., Fish reproductive pheromones, *Chemical Signals in Vertebrates vol IV*, 1986, Duvall, D., Muller-Schwarze, D., Silverstein, R. M., (eds.), Plenum Press, New York, 117 - 133.

52. Stacey, N. E., Sørensen, P. W., Dulka, J. G., Van Der Kraak, G. J., Hara, T. J., Teleost sex pheromones: recent studies on identity and function, *Proceedings of the Third International Symposium on the Reproductive Physiology of Fish*, 1987, Idler, D. R., Crim, L. W., Walsh, J. M., (eds.) Memorial University Press, St. John's, Canada, 150 - 154.

53. Partridge, B., Liley, N. R., Stacey, N. E., The role of pheromones in the sexual behaviour of the goldfish, *Anim. Behav.*, 1976, **24**, 291 - 299.

54. Liley, N. R., Chemical communications in fish, *Can. J. Fish Aquat. Sci.*, 1982, **39**, 22 - 35.

55. Solomon, D., A review of chemical communication in fresh water fish, *J. Fish Biol.*, 1977, **11**, 363 - 376.

56. Scott, A. P., Sørensen, P. W., Time course release of pheromonally active gonadalsteroids and their conjugates by ovulatory goldfish, *Gen. Comp. Endocrinol.*, 1994, **96**, 309 - 323.

57. Sørensen, P. W., Stacey, N. E., Naidu, P., Release of spawning pheromone(s) by naturally-ovulated and prostaglandin-injected , nonovulated female goldfish, *Chemical Signals in Vertebrates vol. IV*, 1986, Duvall, D., Muller-Schwarze, D., Silverstein, R. M., (eds.), Plenum Press, New York, 149 - 154.

58. Stacey, N. E., Liley, N. R., Regulation of spawning behaviour in the female goldfish, *Nature*, 1974, **247**, 71 - 72.

59. Dulka, J., Stacey, N., Sørensen, P. W., Van Der Kraak, G., A steroid sex pheromone synchronises male-female spawning readiness in goldfish, *Nature*, 1987, **325**, 215 - 253.

60. Stacey, N. E., Sørensen, P. W., 17α,20β-dihydroxy-4-pregnen-3-one: a steroidal primer pheromone increasing milt volume in the goldfish, *Carassius auratus*, *Can. J. Zool.*, 1986, **64**, 2412 - 2417.

61. Dulka, J. G., Sloley, B. D., Stacey, N. E., Peter, R. E., a reduction in pituitary dopamine turnover is associated with sex pheromone - induced gonadotropin secretion in male goldfish, *Gen. Comp. Endocrinol.*, 1992, **86**, 496 - 505.

62. Kime, D. E., Scott, A. P., Canario, A. V. M., *In vitro* biosynthesis of steroids, including 11-deoxyxortisol and 5α-pregnane-3β,7α,17,20β-tetrol, by ovaries of the goldfish, *Carassius auratus* during stage of oocyte final maturation, *Gen. Comp. Endocrinol.*, 1992, **87**, 375 - 384.

63. Defraipont, M., Sørensen, P. W., Exposure to the pheromone 17α,20β-dihydroxy-4-pregnen-3-one enhances the behavioural spawning success, sperm production and sperm motility of male goldfish, *Anim. Behav.*, 1993, **46**, 245 - 256.

64. Stacey, N. E., Goetz, F. W., Role of prostaglandins in fish reproduction, *Can. J. Fish. Aquat. Sci.*, 1982, **39**, 92 - 98.

65. Sørensen, P. W., Hara, T., Stacey, N. E., Goetz, F., F prostaglandins function as potent olfactory stimulants that compromise the postovulatory female sex pheromone in goldfish, *Biol. Reprod.*, 1988, **39**, 1039 - 1050.

66. Sørensen, P. W., Chamberlain, K. J., Stacey, N. E., Hara, T. J., Differing roles of prostaglandin $F_{2\alpha}$ and its metabolites in goldfish reproductive behaviour, *Proceedings of the Third International Symposium on the Reproductive Physiology of Fish*, 1987, Idler, D. R., Crim, L. W., Walsh, J. M., (eds.) St. John's, Canada, Plenum Press, page.

67. Irvine, L. A. S., Sørensen, P. W., Acute olfactory sensitivity in wild common carp, Cyprinus carpio, to goldfish hormonal sex pheromones in influenced by gonadal maturity, *Can. J. Zool.*, 1993, **71**, 2199 - 2210.

68. Stacey, N. E., Zheng, W. B., Cardwell, J. R., Milt production in common carp (*Cyprinus carpio*): stimulation by a goldfish steroid pheromone, *Aquaculture*, 1994, **127**, 265 - 276.

69. Lambert, J. G. D., Van Den Hurk, R., Schoonen, W. G. E. J., Resink, J. W., Van Oordt, P. G. W. J., Gonadal steroidogenesis and the possible role of steroid glucuronides as sex pheromones in two species of teleosts, *Fish Physiol. Biochem.*, 1986, **2**, 101 - 107.

70. Schoonen, W. G. E. J., Lambert, J. G. D., Gas chromatographic-mass spectrometric analysis of steroids and steroid glucuronides in the seminal vesicle fluid of the African catfish, *Clarias gariepinus*, *Gen. Comp. Endocrinol.*, 1987, **68**, 375 - 386.

71. Schoonen, W. G. E. J., Lambert, J. G. D., Van Oordt, P. G. W. J., Quantative analysis of steroids and steroid glucuronides in the seminal vesicle fluid of spawning and feral and cultivated nonspawning African catfish, *Clarias gariepinus*, *Gen. Comp. Endocrinol.*, 1987, **68**, 91 - 100.

72. Van Weerd, J., Sukkel, M., Lambert, J., Richter, C., GC-MS identified steroids and steroid glucuronides in ovarian growth-stimulating holding water from adult African catfish *Clarias gariepinus*, *Comp. Biochem. Physiol.*, 1991, **988**, 303 - 311.

73. Moore, A., Scott, A. P., Testosterone is a potent odorant in precocious male Atlantic salmon parr, *Phil. Trans. R. Soc. Lond. B.*, 1991, **332**, 241 - 244.

74. Scott, A. P., Canario, A. V. M., 17α,20β-dihydroxy-4-pregnen-3-one 20-sulphate: a major new metabolite of the teleost oocyte maturation-inducing steroid, *Gen. Comp. Endocrinol.*, 1992, **85**, 91 - 100.

75. Moore, A., Scott, A. P., 17α,20β-dihydroxy-4-pregnen-3-one 20-sulphate is a potent odorant in precocious male Atlantic salmon parr which have been pre-exposed to the urine of ovulated females, *Proc. R. Soc. Lond. B*, 1992, **249**, 205 - 209.

76. Newcombe, C., Hartman, G., Some chemical signals in the spawning behaviour of rainbow trout, *J. Fish Res. Board Can.*, 1973, **30**, 995 - 997.

77. Emanuel, M. A., Dodson, J. J., Modification of the rheotropic behaviour of male rainbow trout (*Salmo gairdneri*) by ovarian fluid, *J. Fish Res. Board Can.*, 1979, **36**, 63 - 68.

78. Honda, H., Female sex pheromone of rainbow trout, *Salmo gairdneri*, involved in courtship behaviour, *Bull. Jap. Soc. Fish*, 1980, **46**, 1109 - 1112.

79. Liley, N. R., Fostier, A., Breton, B., Tan, E. S. P., Endocrine changes associated with spawning behaviour and social stimuli in a wild population of rainbow trout (*Salmo gairdneri*):II females, *Gen. Comp. Endocrinol.*, 1986, **62**, 157 - 167.

80. Scott, A. P., Baynes, S. M., Plasma levels of sex steroids in relation to ovulation and spermination in rainbow trout (*Salmo gairdneri*), *Reproductive physiology of fish, Proc.2nd International Symposium*, 1982, pages.

81. Baynes, S. M., Scott, A. P., Seasonal variations in parameters of milt production and in plasma concentration of sex steroids of male rainbow trout (*Salmo gairdneri*), *Gen. Comp. Endocrinol.*, 1985, **57**, 150 - 160.

82. Schulz, R., Blüm, V., Steroid secretion of rainbow trout testis *in vitro*: variation during the reproductive cycle, *Gen. Comp. Endocrinol.*, 1990, **80**, 189 - 198.

83. Rouger, Y., Liley, N. R., Effects of social environment on plasma hormones and availability of milt in spawning male rainbow trout (*Oncorhynchus mykiss* Walbaum), *Can. J. Zool.*, 1993, **71**, 280 - 285.

84. Olsén, K. H., Liley, N. R., The significance of olfaction and social cues in milt availability, sexual hormone status, and spawning behaviour of male rainbow trout (*Oncorhynchus mykiss*), *Gen. Comp. Endocrinol.*, 1993, **89**, 107 - 118.

85. Scott, A. P., Turner, R. J., 17α,20β-dihydroxy-4-pregnen-3-one 2-sulphate a major metabolite of the oocyte maturation-inducing steroid in plaice (*Pleuronectes platessa*) and rainbow trout (*Oncorhynchus mykiss*), *4th Int. Symp. Reprod. Physiol. Fish*, 1991, 92 - 94.

86. Scott, A. P., Liley, N. R., Vermeirssen, E., Urine of reproductively mature rainbow trout, *Oncorhynchus mykiss* (Walbaum), contains a priming pheromone which enhances plasma levels of sex steroids and gonadotropin II in males, *J. Fish Biol.*, 1994, **44**, 131 - 147.

87. Scott, A. P., Liley, N. R., Dynamics of excretion of 17α,20β-dihydroxy-4-pregnen-3-one 20-sulphate, and the glucuronides of testosterone and 17β-oestradiol, by urine of reproductively mature male and female rainbow trout (*Oncorhynchus mykiss*), *J. Fish Biol.*, 1993, **44**, 117 - 129.

88. Vermeirssen, E. T. L., Scott, A. P., Liley, N. R., Female rainbow trout (*Oncorhynchus mykiss*) urine is the main source of a pheromone which causes a rapid rise in plasma 17α,20β-dihydroxy-4-pregnen-3-one levels and milt amounts in males, *J. Fish Biol.*, 1997, **50**, 107 - 119.

89. Adams, M. A., Teeter, J. H., Katz, Y., Johnsen, P. B., Sex pheromones of the sea lamprey (*Petromyzon marinus*): steroid studies, *J. Chem. Ecol.*, 1987, **13**, 387 - 396.

90. Katsel, P., Dmitrieva, T., Valeyev, R., Kozlov, Y., Sex pheromones of the male yellowfin Baikal sculpin (*Cottocomaphorus grewingki*): isolation and chemical studies, *J. Chem. Ecol.*, 1992, **18**, 2003 -2010.

91. Degani, G., Schreibman, M. P., Pheromone of male blue gourami and its effect on vitellogenesis and gonadotropin cells in pituitary of the female, *J. Fish Biol.*, 1993, **43**, 475 - 485.

92. Matsubara, T., Role of urine in the spawning of female rose bitterling, *Rhodeus ocellatus ocellatus*, *Fish Physiol. Biochem.*, 1994, **13**, 399 - 405.

93. Ogata, H., Kitamura, S., Takashima, F., F-prostaglandins in the holding water of female loach, *Nippon Suisan Gakkaishi*, 1993, **59**, 1259.

94. Ogata, H., Kitamura, S., Takashima, F., Release of 13,14-dihydro-15-keto-prostaglandin $F_{2\alpha}$, a sex pheromone, to water by cobitid loach following ovulatory stimulation, *Fish. Sci.*, 1994, **60**, 143 - 148.

95. Villars, T. A., Burdick, M.., Rapid decline in the behavioural response of paradise fish (*Macropodus opercularis*) to prostaglandin $F_{2\alpha}$ treatment, *Gen. Comp. Endocrinol.* 1986, **63**, 157 - 161.

96. Liley, N. R., Tan E. S. P., The induction of spawning behaviour in *Puntius gonionotus* (Bleeker) by treatment with prostaglandin $PGF_{2\alpha}$, *Fish Biol.*, 1985, **26**, 491 - 502.

97. Scott, A. P., Canario, A. V. M., Sherwood, N. M., Warby, C. M., Levels of steroids including cortisol and 17α,20β-dihydroxy-4-pregnen-3-one, in plasma, seminal fluid, and urine of Pacific herring (*Clupea harengus pallasi*) and North Sea plaice (*Pleuronectes platessa* L.), *Can. J. Zool.*, 1991, **69**, 111 - 116.

98. Scott, A. P., Sherwood, N. M., Canario, A. V. M., Warby, C. M., Identification of free and conjugated steroids, including cortisol and 17α,20β-dihydroxy-4-pregnen-3-one, in the milt of Pacific herring, *Clupea harengus pallasi*, *Can. J. Zool.*, 1991, **69**, 104 - 110.

99. Canario, A. V. M., Scott, A. P., Plasma levels of ovarian steroids, including 17α,20β-dihydroxy-4-pregnen-3-one and 3β,17α,20α-trihydroxy-5β-pregnane, in female dabs (*Limanda limanda*) - marine flatfish induced to mature and ovulate with human chorionic gonadotropin, *Gen. Comp. Endocrinol.*, 1990a, **77**, 177 - 191.

100. Canario, A. V. M., Scott, A. P., Levels of 17α,20β-dihydroxy-4-pregnen-3-one, 3β,17α,20α-trihydroxy-5β-pregnane, and other sex steroids , in blood plasma of male dab, *Limanda limanda* (marine flatfish) injected with human chorionic gonadotropin, *Gen. Comp. Endocrinol.*, 1991, **83**, 258 - 264.

101. Becker, D., Galili, N., Degani, G., GC-MS identified steroids and steroidal glucuronides in gonads and holding water of *Trichogaser trichapterus* (Anabantidae Pallas 1770), *Comp. Biochem. Physiol.*, 1992, **103b**, 15 - 19.

102. Venkatesh, B., Tan, C. H., Lam, T. J., Blood steroid levels in the goldfish: measurement of six ovarian steroids in small volumes of serum by reverse-phase high-performance liquid chromatography and radioimmunoassay, *Gen. Comp. Endocrinol.*, 1989, **76**, 398 - 407.

103. Personal communication, Mrs J Watson, JT Baker Ltd. 1994.

104. Schoonen, W. G. E., Lambert, J. G. D., Van Oordt, P. G. W. J., Quantitative analysis of steroids and steroid glucuronides in the seminal vesicle fluid of feral spawning and feral and cultivated nonspawning African Catfish, *Clarias gariepinus, Gen. Comp. Endocrinol.*, 1987, **68**, 91 - 100.

105. Yoon, J. M., Lee, K. H., Gas chromatographic and mass spectrametric analysis of conjugated steroids in urine, *J. Biosci.*, 2001, **26**, 627 - 634.

106. Sasaki, S., Ota, T., Yamaguchi, H., Takagi, T., Hydrocarbon components of salmons in Gulf of Alaska, *Nippon Suisan Gakkaishi*, 1991, **57**, 111 - 117.

107. Satué, M. T., López, M. C., Sex-linked differences in fatty acid composition of rainbow trout (*Oncorhynchus mykiss*) liver oil, *Food Chemistry*, 1996, **57**, 359 - 363.

108. Pritchard, J. B., Bend, J. R., Relative roles of metabolism and renal excretory mechanisms in xenobiotic elimination by fish, *Environ. Health Perspect.*, 1991, **90**, 85 - 92.

109. Http://www-eaos.mit.edu/geobiology/biomarkers/hopanoids.html

110. Cravatt, B. F., Lerner, R. A., Boger, D. L., Structure determination of endogenous slepp-inducing lipid, *cis*-9-octadecenamide (oleamide): a synthetic approach to the chemical analysis of trace quantities of a natural product, *J. Am. Chem. Soc.*, 1996, **118**, 580 - 590.

111. Patterson, J. E., Ollmann, I. R., Cravatt, B. F., Boger, D. L., Wong, C. H., Lerner, R. A., Inhibition of oleamide hydrolase catalyzed hydrolysis of the endogenous sleep inducing lipid *cis*-9-octadecenamide, *J. Am. Chem. Soc.*, 1996, **118**, 5938 - 5945.

112. Vermeirssen E. L. M., Scott, A. P., Excretion of free and conjugated steroids in rainbow trout (*Oncorhynchus mykis*): Evidence for branchial excretion of the maturation-inducing steroid, 17,20 β-dihydroxy-4-pregnen-3-one, *Gen. Comp. Endocrinol.*, 1996, **101**, 180 - 194.

113. Vainikka A., Jokinen, E. I., Kortet, R., Taskinen, J., Gender- and season-dependent relationships between testosterone, oestradiol and immune functions in wild roach, *J. Fish Biol.*, 2004, **64**, 227 - 240.

114. Kestemont, P., Rinchard, J., Feys, V., Fostier, A., Spawning migrations, sexual maturity and sex steroid levels in female roach *Rutilus rutilus* from the River Meuse, *Aquat. Sci.*, 1999, **61**, 111 - 121.

115. Kortet, R., Vainikka, A., Rantala, M. J., Jokinen, I., Taskinen, J., Sexual ornamentation, androgens and papillomatosis in male roach (*Rutilus rutilus*), *Evol. Ecol. Res.*, 2003, **5**, 411 - 419.

116. Gonçalves, F., Ribeiro, R., Soares, A. M. V. M., *Rhithroanopeus harrisii* (Gould), an American mud crab in the estuary of the Mondego River, Portugal, *J. Crustacean Biol.*, 1995, **15**, 756-762.

117. Goy, J. W., Morgan, S. G., Costlow, J. D. Jr., Studies on the reproductive biology of the mud crab *Rhithropanopeus harrisii* (Gould): induction of spawning during the non-breeding season (Decapoda, Brachyura), *Crustaceana*, 1985, **49**, 83-87.

118. Keith, D. E., Richey, H. http://twri.tamu.edu/twripubs/NewWaves/v13n2/research-1.html. This work has not been published in the referred scientific literature.

119. Directory of non-native marine species in British waters, Eno, N. C., Clark, R. A., Sanderson, W. G. (eds.), http://www.jncc.gov.uk/marine/dns/d2_2_5_7.htm

120. Morgan, S. G., Goy, J. W., Costlow, J. D. Jr., Effect of density, sex ratio, and refractory period on spawning of the mud crab *Rhithropanopeus harrisii* in the laboratory, *J. Crustacean Biol.*, 1988, **8**, 245-249.

121. Morgan, S. G., Goy, J. W., Costlow, J. D. Jr., Multiple ovipositions from single matings in the mud crab *Rhithropanoeus harrisii*, *J. Crustacean Biol.*, 1983, **3**, 542-547.

122. Forward, R. B.Jr., Lohmann, K. J., Control of egg hatching in the crab *Rhithropanopeus harrisii* (Gould), *Biol. Bull.*, 1983, **165**, 154-166.

123. Forward, R. B. Jr., Lohmann, K. J., Cronin, T. W., Rhythms in larval release by an estuarine crab (*Rhithropanopeus harrisii*), *Biol. Bull.*, 1982, **163**, 287-300.

124. Cronin, T. W., Estuarine retention of larvae of the crab *Rhithropanopeus harrisii*, *Estuarine, Coastal and Shelf Science*, 1982, **15**, 207-220.

125. Cronin, T. W., Forward, R. B. Jr., Vertigal migration rhythms of newly hatched larvae of the estuarine crab, *Rhithropanopeus harrisii*, *Biol. Bull.*, 1983, **165**, 139-153.

126. Forward, R. B. Jr., Behavioral responses of larvae of the crab *Rhithropanopeus harrisii* (Brachyura: Xanthidae) during diel vertical migration, *Marine Biology*, 1985, **90**, 9-18.

127. Gerhart, D. J., Clare, A. S., Eisenman, K., Rittschof, D., Forward, R. B. Jr., Eicosanoids in corals and crustaceans: primary metabolites that function as allelochemicals and pheromones in *Progress in Comparative Endocrinology*, Epple, A., Scanes, C. G., Stetson, M. H. (eds.), Wiley-Liss. New York, 1990, 598-602.

128. Hill, E. M., Holland, D. L., Gibson, K. H., Clayton, E., Identification and hatching factor activity of monohydroxyeicosapentaenoic acid in homogenates of the barnacle *Elminius modestus*, *Proc. R. Soc. Lond. B*, 1988, **234**, 455-461.

129. Shing, T. K. M., Gibson, K. H., Wiley, J. R., Watt, C. I. F., First total synthesis of a barnacle hatching factor 8(*R*)-hydroxy-eicosa-5(*Z*),9(*E*),11(*Z*),14(*Z*),17(*Z*)-pentaenoic acid, *Tetrahedron Lett.*, 1994, **35**, 1067-1070.

130. Clare, A. S., Walker, G., Holland, D. L., Crisp, D. J., Barnacle egg hatching: a novel rôle for a prostaglandin-like compound, *Marine Biol. Lett.*, 1982, **3**, 113-120.

131. Holland, D. L., East, J., Gibson, K. H., Clayton, E., Oldfield, A., Identification of the hatching factor of the barnacle *Balanus balanoides* as the novel eicosanoid 10,11,12-trihydroxy-5,8,14,17-eicosatetraenoic acid, *Prostaglandins*, 1985, **29**, 1021-1029.

132. Dembitsky, V. M., Rezanka, T., Furan fatty acids of some brackish invertebrates from the Caspian Sea, *Comp. Biochem. Physiol.*, 1996, **114B**, 317-320.

133. DeVries, M. C., Rittschof, D., Forward, R. B. Jr., Response by rhizocephalan-parasitized crabs to analogues of crab larval-release pheromones, *J. Crustacean Biol.*, 1989, **9**, 517-524.

134. Forward, R. B. Jr., Rittschof, D., De Vries, M. C., Peptide pheromones synchronize crustacean egg hatching and larval release, *Chem. Senses*, 1987, **12**, 491-498.

135. Rittschof, D., Forward, R. B. Jr., Mott, D. D., Larval release in the crab *Rhithropanopeus harrisii* (Gould): chemical cues from hatching eggs, *Chem. Senses*, 1985, **10**, 567-577.

136. Rittschof, D., Peptide mediated behaviors in marine organisms evidence for a common theme, *J. Chem. Ecol.*, 1990, **16**, 261-272.

137. DeVries, M. C., Rittschof, D., Forward, R. B. Jr., Chemical mediation of larval release behaviors in the crab *Neopanope sayi*, *Biol. Bull.*, 1991, **180**, 1-11.

138. Adron, J., W., Mackie, A. M., Studies on the chemical nature of feeding stimulants for rainbow trout, *Salmo gairdneri* Richardson, *J. Fish Biol.*, 1978, **12**, 303-310.

139. Carr, W. E. S., Blumenthal, K. M., Netherton III, J. C.,Chemoreception in the pigfish, *Orthopristis Chrysopterus*: the contribution of amino acids and betaine to stimulation of feeding behavior by various extracts, *Comp. Biochem. Physiol. A*, 1977, **58A**, 69-73.

140. Rittshof, D., Bonaventura, J., Macromolecular cues in marine systems, *J. Chem. Ecol.*, 1986, **12**, 1013 - 1023.

141. Rittschof, D., Enzymatic production of small molecules attracting hermit crabs to simulated gastropod predation sites, *J. Chem. Ecol.*, 1980, **6**, 665-675.

142. Rittschof, D., Bonaventura, J., Macromolecular cues in marine systems, *J. Chem. Ecol.*, 1986, **12**, 1013-1023.

143. Rittschof, D., Forward, R. B. Jr., Simons, D. A., Reddy, P. A., Erickson, B. W., Peptide analogs of the mud crab pumping pheromone: structure-function studies, *Chem. Senses*, 1989, **14**, 149-162.

144. Pettis, R. J., Erickson, B. W., Forward, R. B. Jr., Rittschof, D., Superpotent synthetic tripeptide mimics of the mud crab pumping pheromone, *Int. J. Peptide Protein Res.*, 1993, **42**, 312-319.

145. Farrant, T., Practical statistics for the analytical chemist, *R. S. C. (L. G. C.)*, Teddington, 1997.

146. Rittschof, D., Forward Jr., R. B., Erickson B. W., Larval release in brachyuran crustaceans: Functional similarity of the peptide pheromone receptor and the catalytic site of trypsin, *J. Chem. Ecol.*, 1990, **16**, 1359 - 1370.

147. Walker, J. M. (ed.), Basic protein and peptide protocols, *Methods in molecular biology*, 1994, **32**, Humana Press, Totowa, N.J. chapter 31.

148. Personal communication from D. Rittschof, Duke University, Department of Zoology, Beaufort, NC 28516, USA, to J Hardege, 1997.

149. Personal communication from D. Rittschof, Duke University, Department of Zoology, Beaufort, NC 28516, USA, to J Hardege, 1997.

150. De Hoffmann, E., Charette, J., Stroobant, V., Mass spectrometry principles and applications, John Wiley & Sons, Chichester, 1996, 218 - 221.

151. Reynolds, G. W., Hoff, T. J., Gillham, R. W., Sampling bias caused by materials used to monitor halocarbons in groundwater, *Environ. Sci. Technol.*, 1990, **24**, 135 - 142.

152. Schreir C.G., Reinhart M., Transformation of chlorinated organic compounds by iron and manganese powders in buffered water and in landfill leachate, *Chemosphere*, 1994, **29**, 1743 - 1753.

153. Gillham, R. W., O'Hannesin, S. F., Enhanced degradation of halogenated aliphatics by zero-valent iron, *Ground Water*, 1994, **32**, 958 - 967.

154. Grittini, C., Malcolmson, M., Fernando, Q., Korte, N., Rapid dechlorination of polychlorinated biphenyls on the surface of a Pd/Fe bimetalllic system, *Environ. Sci. Technol.*, 1995, **29**, 2898 - 2900.

155. Agrawal, A., Tratnyek, P. G., Reduction of nitro aromatic compounds by zero valent iron metal, *Environ. Sci. Technol.*, 1996, **30**, 153 - 160.

156. Burris, D., R., Hatfield, K., Wolfe, N. L., Laboratory experiments with heterogeneous reactions in mixed porous media, *J. Environ. Engineering*, 1996, **122**, 685 - 691.

157. Juršić, B., Galoši, A., The hydrogenolysis of organic halides with zinc dust in micelle, *Syn. Commun.*, 1989, **19**, 1649 - 1653.

158. Choudhury, P.K., Foubelo, F., Yus, M., Direct indium-promoted preparation of α-methylene-γ-lactones from 2-(bromomethyl)acrylic acid and carbonyl compounds, *Tetrahedron*, 1999, **55**, 10779 - 10788.

159. Gao, J.M., Harter, R., Gordon, D. M., Whitesides, G. M., Synthesis of KDO using indium-mediated allylation of 2,3/4,5-di-*O*-isopropylidene-D-arabinose in aqueous media, *J. Org. Chem.*, 1994, **59**, 3714 - 3715.

160. Gordon, D. M., Whitesides, G. M., Indium-mediated allylations of unprotected carbohydrates in aqueous media - a short synthesis of sialic acid, *J. Org. Chem.*, 1993, **58**, 7937 - 7938.

161. Li, C. J., Aqueous Barbier-Grignard type reactions: scope, mechanism, and synthetic applications, *Tetrahedron*, 1996, **52**, 5643 - 5668.

162. Zhang, W. C., Li, C. J., Magnesium-mediated carbon-carbon bond formation in aqueous media; Barbier-Grignard allylation and pinacol coupling of aldehydes, *J. Org. Chem.*, 1999, **64**, 3230 - 3236.

163. Kochany, J., Effects of iron (III) and manganese (II) ions on the aquatic photodegradation rate of bromoxynil (3,5-dibromo-4-hydroxybenzonitrile) herbicide, *Chemosphere*, 1992, **25**, 261 - 270.

164. Gillham, R. W., O'Hannesin, S. F., Metal-catalysed abiotic degradation of halogenated organic compounds, *Modern Trends in Hydrogeology* 1992, International Association of Hydrogeologists, Hamilton, Ontario, Canada, 94 - 103.

165. Yang, M. X., Kash, P. W., Sun, D. H., Flynn, G. W., Bent, G. E., Holbrook, M. T., Bare, S. R., Fischer, D. A., Gland, J. L., Chemistry of chloroethylenes on Cu(100): bonding and reactions, *Surface Sci.*, 1997, **380**, 151 - 164.

166. Lien, H. L., Zhang, W. X., Enhanced dehalogenation of halogenated methanes by bimetallic Cu/Al, *Chemosphere*, 2002, **49**, 371 - 378.

167. Warren, K. D., Arnold, R. G., Bishop, T. L., Lindholm, L. C., Betterton, E. A., Kinetics and mechanism of reductive dehalogenation of carbon tetrachloride using

zero-valence metals, *J. Haz. Mat.*, 1995, **41**, 217 - 227.

168. Roberts, A. L., Totten, L. A., Arnold, W. A., Burris, D. R., Campbell, T. J., Reductive elimination of chlorinated ethylenes by zero-valent metals, *Environ. Sci. Technol.*, 1996, **30**, 2654 - 2659.

169. Atwater, J. E., Akse, J. R., McKinnis, J. A., Thompson, J. O., Aqueous phase heterogeneous catalytic oxidation of trichloroethylene, *App. Cat. B. Environ.*, 1996, **11**, L11 - L18.

170. Cheng, I. F., Fernando, Q., Korte, N., Correction in: "Electrochemical dechlorination of 4-chlorophenol to phenol" *ES&T*, **31**, 1074 - 1078., *Environ. Sci. Technol.*, 1997, **31**, 2443.

171. Schreier, C. G., Reinhard, M., Catalytic dehydrohalogenation and hydrogenation using H_2 and supported palladium as a method for the removal of tetrachloroethylene from water, 209th National Meeting, American Chemical Society. Abaheim, CA., Preprint Extended Abstracts, Division of Environmental Chemistry, 1995, **35**, 749 - 754.

172. Korte. N., Liang. L., Muftikian, R., Grittini, C., Fernando, Q., The dechlorination of hydrocarbons: Palladised iron utilised for ground water purification, *Platinum Metals Rev.*, 1997, **41**, 2 - 7.

173. Muftikian, R., Nebesny, K., Fernando, Q., Korte, N., X-ray photoelectron spectra of the palladium-iron bimetallic surface used for the rapid dechlorination of chlorinated organic environmental contaminants, *Environ. Sci. Technol.*, 1996, **30**, 3593 - 3596.

174. Liang, L., Korte, N., Goodlaxson, J. D., Clausen, J., Fernando, Q., Mufitikan, R., Byproduct formation during the reduction of TCE by zero-valent iron and palladised iron, *Ground Water Monitoring & Remediation.*, 1997, **17**, 122 - 127.

175. Schüth, C., Disser, S., Schüth, F., Reinhard, M., Tailoring catalysts for hydrodechlorinating chlorinated hydrocarbon contaminants in groundwater, *App. Cat. B. Environ.*, 2000, **28**, 147 - 152.

176. http://www.gsw.edu/~tjw/minweb2.htm

177. Kriegman-King, M. R., Reinhard M., Reduction of hexachloroethane and carbon tetrachloride at surfaces of biotite, vermiculite, pyrite, and marcasite, *Organic substances and sediments in water*,1990, Baker, R. A., **2**, Lewis Publishers, 349 - 364.

178. Kriegman-King, M. R., Reinhard, M., Transformation of carbon tetrachloride in the presence of sulfide, biotite and vermiculite, *Environ. Sci. Technol.*, 1992, **26**, 2198 - 2206.

179. Hwang, I., Batchelor, B., Reductive dechlorination of chlorinated methanes in cement slurries containing Fe(II), *Chemosphere*, 2002, **48**, 1019 - 1027.

180. Cervini-Silva, J., Larson, R. A., Wu, J., Stucki, J. W., Dechlorination of pentachloroethane by commercial Fe and ferruginous smectite, *Chemosphere*, 2002, **47**, 971 - 976.

181. Chen, G., Hoag, G. E., Chedda, P., Nadim, F., Woody, B. A., Dobbs, G. M., The mechanism and applicability of in situ oxidation of trichloroethylene with Fenton's reagent, *J. Haz. Mat.*, 2001, **B87**, 171 - 186.

182. Turk E., Phosgene from chloroform, *Chem. Eng. News*, 1998, **76**, 6.

183. Williams, R. A., Shuttle, K. A., Kunkler, J. L., Madsen, E. L., Hooper, S. W., Intrinsic bioremediation in a solvent-contaminated alluvial groundwater, *J. Ind. Microb. Biotech.*, 1997, **18**, 177 - 188.

184. Warith, M. A., Feretner, R., Fernandes, L., Bioremediation of organic contaminated soil, *Haz. Waste & Haz. Mat.* 1992, **9**, 137 - 147.

185. Beeman, R. E., Bleckmann, C. A., Sequential anaerobic-aerobic treatment of an aquifer contaminated by halogenated organics: field results, *J. Contaminant Hydrology*, 2002, **57**, 147 - 159.

186. http://www.biologie.uni-hamburg.de/b-online/e19/19d.htm

187. Furukawa, K., 'Super bugs' for bioremediation, *Trends in Biotech.* 2003, **21**, 187 - 190.

188. Glod, G., Angst, W., Holliger, C., Schwarzenbach, R. P., Corrinoid-mediated reduction of tetrachloroethene, trichloroethene, and trichlorofluoroethene in homogeneous aqueous solution; reaction kinetics and reaction mechanisms, *Environ. Sci. Technol.*, 1997, **31**, 253 - 260.

189. Maymó-Gatell, X., Nijenhuis, I., Zinder, S. H., Reductive dechlorination of *cis*-1,2-dichloroethene and vinyl chloride by "*Dehalococcoides ethenogenes*", *Environ. Sci. Technol.*, 2001, **35**, 516 - 521.

190. Karpouzas, D. G., Walker, A., Factors influencing the ability of *Pseudomonas putida* epI to degrade ethorophos in soil, *Soil Biol. & Biochem.*, 2000, **32**, 1753 - 1762.

191. Doong, R. A., Wu, Y, W., Enhanced biodegradation of 1,1,1-trichloroethane under low biomass conditions, *Chemosphere*, 1997, **34**, 1653 - 1662.

192. Zhuang, P., Pavlostathis, S. G., Effect of temperature, pH and electron donor on the microbial reductive dechlorination of chloroalkenes, *Chemosphere*, 1995, **31**, 3537 - 3548.

193. Andrews, E., Novak, P. J., Influence of ferrous iron and pH on carbon tetrachloride degradation by *Methanosarcina thermophila*, *Wat. Res.*, 2001, **35**, 2307 - 2313.

194. Matheson, L. Tratnyek, P. G., Reductive dehalogenation of chlorinated methanes by iron metal, *Environ. Sci. Technol.*, 1994, **28**, 2045 - 2053.

195. Orth, W. S., Gillhan, R. W., Dechlorination of trichloroethene in aqueous solution using Fe^0, *Environ. Sci. Technol.*, 1996, **30**, 66 - 71.

196. Hawley's Condensed Chemical Dictionary, 12^{th} edition, Lewis, R. J. (ed), Van Nostrand Reinhold Company, New York, 1993, 523.

197. Hardy, L. I., Gillham, R. W., Formation of hydrocarbons from the reduction of aqueous CO_2 by zero-valent iron, *Environ. Sci. Technol.*, 1996, **30**, 57 - 65.

198. Deng, B., Campbell, T. J., Burris, D. R., Hydrocarbon formation in metallic iron/water systems, *Environ. Sci. Technol.*, 1997, **31**, 1185 - 1190.

199. Vogel, T. M., Criddle, C. S., McCarthy, P. L., Transformations of halogenated aliphatic compounds, *Environ. Sci. Technol.*, 1987, **21**, 722 - 736.

200. Arnold, W. A., Ball, W. P., Roberts, A. L., Polychlorinated ethane reaction with zero-valent zinc: pathways and rate control, *J. Contaminant Hydrology*, 1999, **40**, 183 - 200.

201. Nonnenberg, C., van der Donk, W. A., Zipse, H., Reductive dechlorinationn of trichloroethylene; a computational study, *J. Phys. Chem.*, 2002, **106**, 8708 - 8715.

202. Kanakaraju, R., Senthilkumar, K., Kolandaivel, P., Origin of the *cis* effect - nonbonded intramolecualr interactions: quantum chemical studies on 1,2 dihaloethylene molecules, *J. Mole. Struct. (Theochem)*, 2002, **589 - 590**, 95 - 102.

203. Johnson, T. L., Scherer, M. M., Tratnyek, P. G., Kinetics of halogenated organic compound degradation by iron metal, *Environ. Sci. Technol.*, 1996, **30**, 2634 - 2640.

204. Wang, C. B., Zhang, W. X., Synthesizing nanoscale iron particles for rapid and complete dechlorination of TCE and PCBs, *Environ. Sci. Technol.*, 1997, **31**, 2154 - 2156.

205. Loraine, G. A., Effects of alcohols, anionic and nonionic surfactants on the reduction of PCE and TCE by zero-valent iron, *Wat. Res.*, 2001, **35**, 1453 - 1460.

206. Vogan, J. L., Focht, R. M., Clark, D. K., Graham, S. L., Performance evaluation of a permeable reactive barrier for remediation of dissolved chlorinated solvents in groundwater, *J. Hazardous Mat.*, 1999, **68**, 97 - 108.

207. Singh, J., Comfort, S. D., Shea, P. J., Iron-mediated remediation of RDX-contaminated water and soil under controlled Eh/pH, *Environ. Sci. Technol.*, 1999, **33**, 1488 - 1494.

208. Nakazawa,, T., Yokoyama, K., Grismanovs, V., Katano, Y., Jitsukawa, S., Ab initio study on the mechanism of hydrogen release from the silicate surface in the presence of water molecule, *J. Nuclear Mat.*, 2002, **302**, 165 - 174.

209. Carroll, S. A., Maxwell, R. S., Bourcier, W., Martin, S., Hulsey, S., Evaluation of silica-water surface chemistry using NMR spectroscopy, *Geochimica et Cosmochimica Acta*, 2002, **66**, 913 - 926.

210. The Merck Index, eleventh edition, Budavari, S., O'Neil, M. J., Smith, A., (eds.) 1989, Merck & Co., Inc., Rahway, New Jersey

211. Korte N. E., West, O. R., Liang, L., Gu, B., Zutman, J. L., Fernando, Q., The effect of solvent concentration on the use of palladised-iron for the stepwise dechlorination of polychlorinated biphenyls in soil extracts, *Waste Management*, 2002, **22**, 343 - 349.

212. Chatgilialoglu, C., Ingold, K. U., Scaiano, J. C., Rate constants and Arrhenius parameters for the reactions of primary, secondary and teriary alkyl radicals with tri-*n*-butyltin hydride, *J. Am. Chem. Soc.*, 1981, **103**, 7739 - 7742.

213. Griller, D., Ingold, K. U., Free radical clocks, *Acc. Chem. Res.*, 1980, **13**, 317 - 323.

214. Horn, A. C. H, Clark, T., Does metal ion complexation make radical clocks run fast? *J. Am. Chem. Soc.*, 2003, **125**, 2809 - 2816.

215. Elson, I. H., Mao, S.W., Kochi, J. K., Electron spin resonance study of addition of alkoxy radicals to oelfins, *J. Am. Chem. Soc.*, 1975, **97**, 335 - 341.

216. Barton, D. H. R., Hartwig, W., Motherwell, W. B., Oxygen-carbon β- bond effects in radical reactions, *J. Chem. Soc. Chem. Commun.*, 1982, **8**, 447 - 448.

217. Roberts, B. P., Steel, A. J., The effects of β-alkoxy substituents on radical reactions: halogen-atom abstraction from alkyl chlorides, *J. Chem. Soc. Perkin Trans.*, 1994, **12**, 2411 - 2422.

218. Griffiths, P. J. F., Thomas, J. D. R., Calculations in advanced physical chemistry, 3rd edition, 1983, Edward Arnold (pubs.), London, 174 - 177.